Ram K. Gupta *Editor*

Organic Electrodes

Fundamental to Advanced Emerging Applications

Springer

Engineering Materials

This series provides topical information on innovative, structural and functional materials and composites with applications in optical, electrical, mechanical, civil, aeronautical, medical, bio- and nano-engineering. The individual volumes are complete, comprehensive monographs covering the structure, properties, manufacturing process and applications of these materials. This multidisciplinary series is devoted to professionals, students and all those interested in the latest developments in the Materials Science field, that look for a carefully selected collection of high quality review articles on their respective field of expertise.

Indexed at Compendex (2021)

More information about this series at https://link.springer.com/bookseries/4288

Ram K. Gupta
Editor

Organic Electrodes

Fundamental to Advanced Emerging
Applications

🐎 Springer

Editor
Ram K. Gupta
Department of Chemistry
Kansas Polymer Research Center
Pittsburg State University
Pittsburg, KS, USA

Contents

Organic Electrodes: An Introduction

Tanvir Arfin, Priya Ranjan, Sudhakar Bansod, Reena Singh, Shaz Ahmad, and Krishna Neeti

Abstract The world is moving for electromobility as well as associated decarbonization. The era and community related to it are moving towards the fourth industrial revolution comprising of digital technology and electronic devices. The organic electrode materials (OEMs) obtained from biomass serve to be the best option for sustainable and green lithium batteries due to various features such as low costing, availability in large amounts, high sustainability, environmental compassion, and recyclability. The research on organic electrodes is mainly based on material level despite the performing ability of batteries. The current chapter focuses on the history of organic electrode materials and prospects of elevation, and the challenges faced by organic electrode materials for practical use in the form of density of OEMs and intrinsic electronic conductivity. Later the comprehensive optimization is performed. Finally, we have focused on developing high-quality stimulation for research to obtain future commercialization of OEMs.

Keywords Electrode reaction · Electrode process · Organic electrodes · Lithium-ion batteries · Electrochemical energy storage

1 Introduction

In the present situation, the development and acceptance of new creative material are advancing faster [1]. In sophisticated ways, essential raw materials are employed in many sub-branches of analytical chemistry to achieve precise data and statistical evaluations of hazardous and small amounts of critical compounds [2]. Materials

T. Arfin (✉) · P. Ranjan
Hyderabad Zonal Centre, CSIR-National Environmental Engineering Research Institute (NEERI), IICT Campus, Tarnaka, Hyderabad, Telangana 500007, India

S. Bansod
Fluoro-Agrochemicals Department, CSIR-Indian Institute of Chemical Technology, Tarnaka, Hyderabad, Telangana 500007, India

R. Singh · S. Ahmad · K. Neeti
Civil Engineering, National Institute of Technology, Patna, Patna, Bihar 800005, India

science is regarded as the most critical factor in increasing human life, as it leads to technological advancement and the creative improvement of substances using a variety of resources [3]. Human beings' vital lifestyle and existence have given contemporary materials new specialized standards in the current age of expansion [4]. The substance is highly valued for its potential to impact people's living standards and global growth since life cannot exist without obstacles [5]. As a result, people's whole existence now relies only on the various materials and their fundamental properties [6]. It provided convenience, ease, and outstanding life-sustaining modules, and it met the acceptable criterion overall [7]. Most industrialized nations' economic development and long-term growth have benefited from such material [8]. The usage of raw resources and lively compounds is investigated [9]. Several methods, tools, and strategies are applied as a developmental component. It is considered a vital vantage point for advancing current science, and it may later be applied to a variety of subjects [10].

2 Electrodes

At the onset of novel electrochemistry, the demand for advanced electrodes is brought into interest and is installed. In the recent era, arrangements of an electrochemical cell with three electrodes are acknowledged, such as a reference electrode, a counter electrode, and a working electrode.

2.1 Working Electrodes

The main point of consideration is that working materials should be made of materials capable enough to yield a higher signal for the noise ratio. Hence, two factors need to be fulfilled such as:

(a)   Target analytic behavior
(b)   The need for current for measuring the potential.

Different types of working electrodes are given in Fig. 1.

On a minor basis, there are other factors such as price, toxic nature, conductivity, reproducibility of the surface, mechanical properties, and availability.

2.2 Chemically Modified Electrode

Despite the traditional modified electrode, the chemically modified electrode is regarded as the modern type. The surface of the electrode is modified separately as the electrode responds towards the reagent or the chemical in which it to dipped.
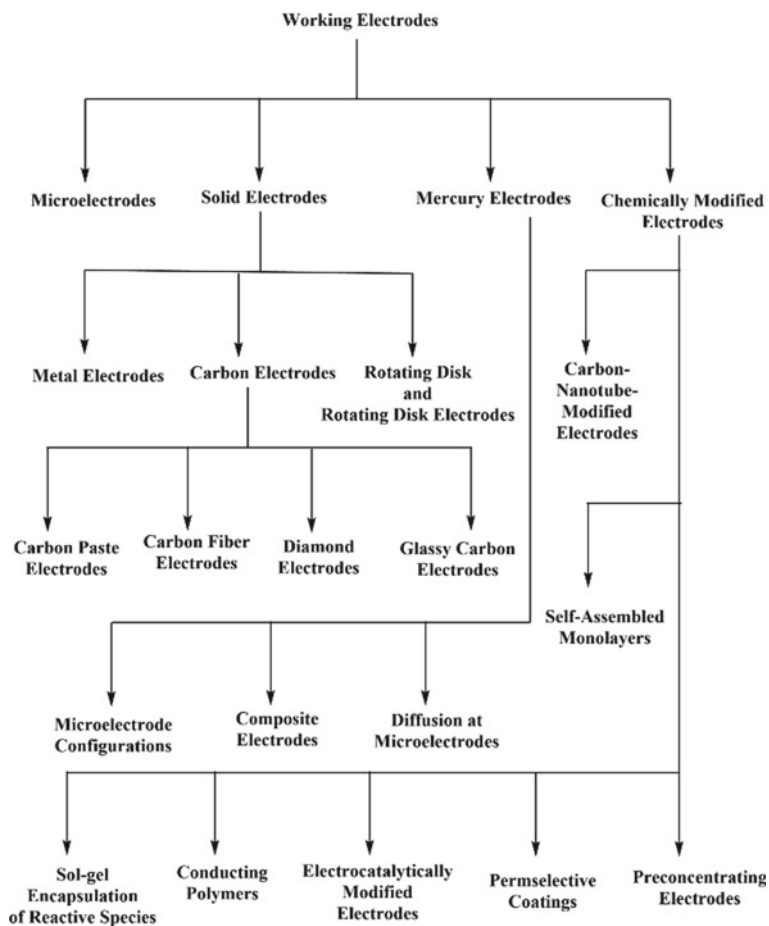
Fig. 1 Different types of working electrodes

The chemically modified electrode (CME) is supportive during the problem related to electrochemical analysis, finally increasing the utility in different sensing devices and the electrochemical field.

The uses include producing material by the electrochemical reaction to convert and is also used in devices such as microelectronic. Other applications are accumulation, membrane permeation, and electron transfer rate. All the applications, as well as the information, are reviewed [11]. It is applied in the medical sector, such as drug delivery to control the releasing steps, it is also applied in devices for display, protection against corrosion, in the fuel, and finally as synthesis to design the surface of the electrode. The polymer films coating improves the efficiency of the surface by the process of casting. The solvent is added to the polymer. The solution is placed as droplets on the electrode. Finally, the solvent is evaporated. The entire process occurs as a monomer by the process of electropolymerization. Here the primary

consideration is that the thickness is maintained correctly for relevant results. Modifier such as DuPont Nafion perfluorinated sulfonated cation exchanger is used for better results. The mild form of the polymer is more advantageous for its application. There are several modes to adjust the electrode making, namely chemical modification, adsorption method, and so on.

2.3   Self-assembled Monolayer

On the surface of gold, a layer is observed to maintain the reactivity of sulfur and gold. The layer is an ethanolic solution containing alkane-thiols $[X(CH_2)_nSH]$, with $n > 10$. The monolayer is self-assembled and even shows different applications from several years [12]. Because of monolayer formation, it is used as various application.

2.4   Carbon Nano-tube Modified Electrodes

Carbon nanotubes refer to the most acceptable multifunctional properties [13]. Carbon nanotubes are of two types like single-walled nanotubes (SWCNT) and multi-walled nanotubes (MWCNT). SWCNT have graphite sheets in rolled form. MWCNT exhibit a structure like a tree trunk appearing as a concentrically arranged form. It has the properties used to modify surfaces and electrochemical detection reactions. The respective electrodes are responsible for increasing the efficiency of the analyte and reducing the fouling [14]. The electrodes are inbuilt with properties so that they have end caps showing any defects in the surface of edge planes [15].

2.5   Sol–Gel Encapsulation of Reactive Species

Sol–gel encapsulation is a significant way of modifying the electrode, which serves at low temperatures [16]. The film is prepared by incorporating the polycondensation of the hydroxyl monomer by utilizing the precursor of alkoxide, namely $Si(OCH_3)_4$. The process of sol–gel encapsulation forms a porous glass-like network like the permeable towards the analyte. The respective method possesses various properties, namely the physical characteristics, mechanically rigid and thermally stability, and entrapping modifier. The material, namely the carbon powder and gold powder, is employed for dispersing within the sol–gel mixture [17]. Molecular imprinting is used for the preparation of selective binding [18].

2.6 Electrocatalytically Modified Electrodes

It is noticed that the preferred redox reaction at the naked electrode has the deliberate transfer of electron kinetics. Therefore, it occurs at a favorable potential rate which is more than that of thermodynamic redox potential. The reaction is catalyzed by attaching a suitable electron transfer mediator on the surface [19]. The mediator's primary function is to assist the mechanism of charge transfer among the electrode and analyte. The mediated reaction mechanism is explained by the equation given below:

$$M_{ox} + ne^- \longrightarrow M_{red}$$

$$M_{ox} + A_{red} \longleftarrow M_{red} + A_{ox}$$
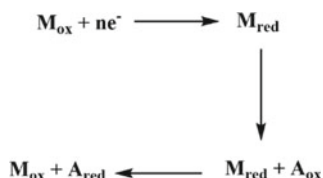
In this reaction, M is known as a mediator and A is known as analyte.

2.7 Pre-concentrating Electrodes

The pre-concentrating CMEs and the surface react and bind the target analyte, showing various prospects in chemical sensing [20]. The respective concept reflects stripping voltammetric arrangements where the target analyte gets detached from the dilute material on the surface layer on the preconcentrating electrode, finally reducing and oxidizing during the scanning period.

2.8 Permselective Coatings

The permselective coatings advance the stability and selectivity of the electrochemical devices. It is attained by rejecting the additional matrix content available on the surface of the electrode. It also allows the immigration of the target analyte.

2.9 Conducting Polymers

The conducting polymer is an attractive topic because of the underlying characteristics, such as the ability to be modified reversibly among the conductive state of positively charged and neutral ones. The anionic class shows the ability to be integrated and ejected during oxidation and reduction [21]. At different groups of the

conducting polymer, the delocalization of the redox alteration takes place [22]. Due to the conjugation of π-electron, molecular orbitals are formed, which helps in the elongation of the polymer chain [23].

3   Synthesis of Conjugated Polymers in General

The adequate graphite single covalent bonding between two saturate carbons in the phenyl units is crucial to building conjugated polymers. Transition-metal-catalyzed cross-coupling processes, in addition to electromechanical [24] or chemical oxidant polymerizations, offer a particularly potent armament for $Csp–Csp^2$ and $Csp^2–Csp^2$ formation of the bond [25]. The reaction entails an oxidative conversion across an electrophile's CsX bond, followed by transmetalation with the leading group organometallic positive ion and a reductive elimination step that leads to the synthesis of carbon bonds. Nickel or palladium-based complexes are the most often utilized transition-metal catalysts. However, other elements have also been used. Grignard reagents, stannyl, borate reagents, or copper may be used as organometallic nucleophiles. Consecutive transformation in the catalytic cycle may therefore lengthen conjugation durations. Region regularity of the polymers may be easily accomplished as electrophilic substitution interiors of substrates of membrane protein are conveniently used. Another benefit is that these reactions are often moderate and may withstand a wide range of functional groups. This is especially critical for creating sophisticated functional conjugated polymers. Using two monomers, the most common coupling processes are Stille and Suzuki pairing reactions. Methods for making alternating copolymers that are both efficient and extensively are utilized. Under Stille coupling conditions, stannyl groups substitution on the monomer substrate's aromatic ring invariably produces weak reactivity with aryl halides [26].

4   Electrochemical Behavior

Electrochemistry holds an extraordinary place because of the high controlling rate, dynamic forces, and the specified electron-transfer mechanism. Such unique features provide advantages in terms of sustainability and selectivity to prepare organic compounds. Synthetic organic electrochemistry has gathered attention from last decades owing to the realization by the academic as well as industrial research sectors on a world basis [27].

The innovative and synthetic methods and reactivity techniques were enhanced along with the cost-effective, safe, producing minimum amount of waste compared to the classical mechanism. Various organic electrochemical approaches were advanced to cope with the easiness of scaling the technique.

The transfer of electrons among the solution-phase electrolyte and electrode are heterogeneous; hence the reaction of synthetic organic electrochemical needs more

consideration towards the parameters which are non-traditional to be faced through the organic chemists. The electrochemical reactions need to be executed in batch cells or the flows cells, or they can be in divided or undivided cells to optimize the potential difference through a cell and application of current density. Moreover, the electrodes are responsible for presenting the significant difference because the selectivity of specific transformation depends on the materials. Various factors are responsible for determining the specific parameter, such as electrode material determining the mechanism of electron transfer; shape, size, and separation distance of electrode determines the field homogeneity, resulting in current density and submerged surface area. All these factors are responsible for disturbing the outcome of the reaction.

The electrode material is oppressed for controlling and altering the selectivity of the reaction, which on the other hand, offers an opportunity to change the reactivity by the process of electrocatalysis or chemically-modified electrocatalysis. It was observed that the ability of respective materials was taken into account to yield extraordinary outcomes and also to determine the selectivity towards synthetic electrochemical reactions [28].

It is also observed and renowned that the optimum electrode cannot be selected for the respective process theoretically. Despite it, an empirical method should be used. In the present book chapter, the summarization of highly significant practical and reactivity deliberations of electrode material is focussed on organic electrochemistry. The next target is to highlight the examples where the behavior of the corresponding electrode material is extraordinary and significant. Although electrodes are composed of conducting material, various mechanical and electrochemical features are taken into account to attain a better result. For an electrode to be ideal, it has different features such as non-toxic, cost-effective, stable at varied ranges of pressure, solvents, and temperature. It should also get manipulated into various forms for the construction of electrodes, namely into meshes, plates, rods, foams, and wires.

5   Energy Storage Devices

Organic material is considered an encouraging material for all the sustaining and multipurpose energy storage devices despite the conventional inorganic intercalation electrode materials. Based on the various organic materials such as *n*-type, *p*-type, and bipolar, the researcher analyzed their reaction mechanism, challenges, working principles, advantages, and electrochemical behavior for the first time. Along with the extraordinary features, namely processibility, structural diversity, and higher electrochemical behavior, the material enables a higher perspective for energy storage devices like super-capacitor, rechargeable Li/Na batteries, aqueous rechargeable batteries, redox flow, thin-film batteries, and also all other organic batteries. The theoretical redox reactions are enclosed for various electroactive organics, which is insufficient to develop the new innovative OEM. The researcher needs to work out the type of organic structure and the redox approach that have to be applied in

Table 1 The structure and redox mechanism of numerous types of OEMs

S. No.	Structure	Redox mechanism	References
1	Conjugated carbonyl		[29]
2	Conjugated hydrocarbon		[30]
3	Organodisulfide	R-S-S-R ⟷ R-S⁻ + ⁻S-R	[31]
4	Conjugated thioether	R-S-R ⟷ R-S-R	[32]
5	Thioether (4e)	R-S-R ⟷ R-S-R ⟷ R-S-R	[33]

the electrode materials. The OEMs are divided into seven different types covering research studies in the past ten years, as shown in Table 1.

5.1 Advantages

A tendency of development was noticed in different photoelectric materials that organic material was replaced with the inorganic material. Many organic photo-electric materials were used in the photoelectric devices namely the photovoltaic (PV) devices, field-effect transistor (EFTs), and light-emitting diodes (OLEDs). Such observation could be possible as the behavior of organic material was superior to the conventional inorganic material and it also has several advantages in comparison to the inorganics. For most of the energy storage devices, it was suggested that it was applicable based on the advantages the OEM exhibits as shown in Fig. 2.

At present, most of the OEMs are yet to be recognized, which are even occupied of several contests in the investigation and commercialization of different organic electrode materials, as reflected in Fig. 3.

5.2 Energy Storage Materials

It is noteworthy that three categories of conjugated structures, as shown in Table 1, such as thioethers, and organodisulfide, are recognized as the conducting polymers as they occur in the redox method and even infer the same properties. The other feature is that chronological demand is mainly based on when one specific form of
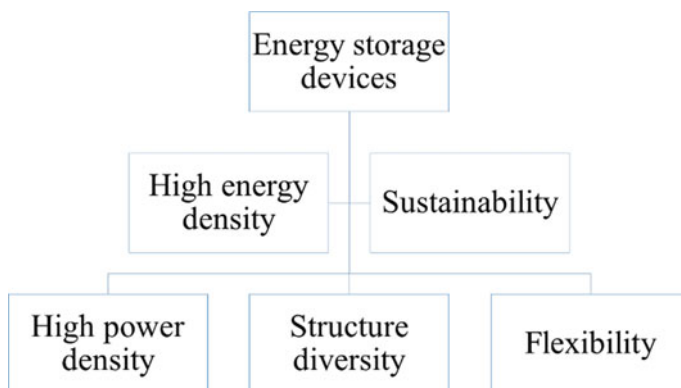
Fig. 2 Advantages of energy storage devices
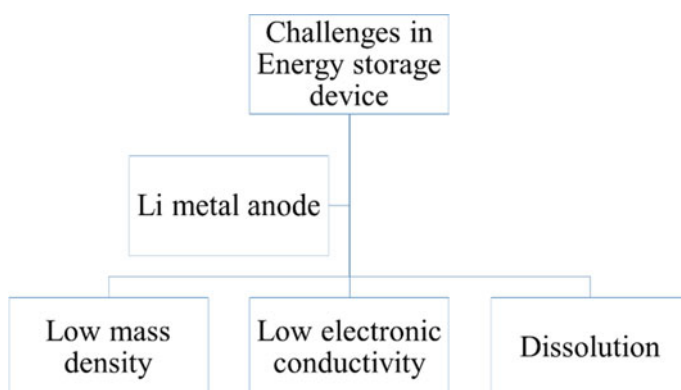
Fig. 3 Challenges in the energy storage device

OEM is brought to study and is considered the best option for understanding the history of development and its tendency. The conjugated carbonyl compounds are the earliest and most attractive and are currently the productive research material in Fig. 4.

6   Organic Solid Electrodes for Advanced Batteries

A future breed of environmentally friendly and long-term energy storage systems is available. They have a reduced environmental impact and toxicity than inorganic metallic nanoparticles, are made up of various elements, are synthesized using more environmentally responsible methods and needless energy-intensive recycling
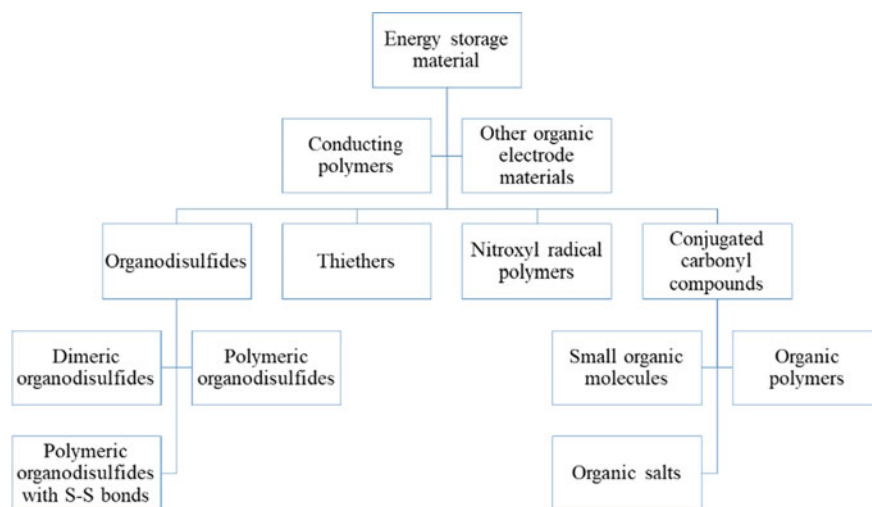
Fig. 4 Various types of energy storage material

processes. Aside from the due to the structural designability, two battery management methods may be used: "n-type" electrodes react with that of cation discharge following oxidization, whereas "p-type" electrodes react with anion absorption. Organic batteries have been the subject of many studies over the last decade. This covers, among other things, the synthesis and research of organic electrode material, as well as electrode building, the realization among all batteries, and sustainability concerns [34]. Both oxidative polymer and small-molecule electroactive chemicals make up the organic electroactive materials' makeup. Different ways for obtaining good electrocatalytic activity of organic molecules in batteries have been found. Their start charging potential, rate capability, and cycle stability are the most important factors. The redox-active groups' start was charging potential, and unique ability is determined by the molecular weight and number of electrons involved within the redox process. The appearance and ion-transfer operations in and out of the electrodes determine the rate capability. It is controlled by the redox-active group's electron-transfer rate constant and the shape of the composite electrode, which is typically made of the concentration of natural material, conductivity carbon, and a polymeric binder. Either dissolving of the active ingredient typically limits cycling stability into the battery electrolytes or breakdown processes. In non-aqueous electrolyte media, various protocols have been proposed to overcome this issue, including incorporating redox-active units in the structure of polymer [35]. Computational modeling is becoming more critical in organic batteries as computational power, quality, and software improvement. Predicting characteristics like the redox chemistries of organic conductive polymers, as well as a mechanical knowledge of charge/discharge processes at the molecule and microscopic levels, are all part of this.

As previously stated, most battery electrodes are made by combining organic electrocatalyst materials with additional components. Among the characteristic of

different organic materials, the interface with additives is critical. Because they are frequently added in substantial proportions, ranging from 30 to 70 weight percent, organic conductive filler's efficiency and power density are primarily decreased. It might be the primary cause for the organic battery's lack of commercialization so far. As a result, the electrode structure is critical for organic batteries.

Besides being the only electroactive material, organic redox-active molecules are also promising possibilities for sustainably grown hybrid electrodes. These materials can combine the best technologies, namely the inorganics' limited functionality and power performances and organic electroactive materials' minimum energy density, to unleash more excellent and high-energy performances.

Finally, since one of the primary goals for creating organic electrocatalyst materials is to improve sustainability, it is critical to stress-producing self-sustaining electrode materials for new energy storage applications.

7 Organic Electroactive Compounds with Small Molecular Structures

OEMs are molecular or crystalline materials that have most of the desirable properties of organic materials, including significant design freedom at the protein interaction levels and a very sound redox signature. Because they lack an electrochemically inert polymeric backbone, they have larger volumetric and gravimetric capacities than the redox-active polymers. Their molecular architectures make adequate packing possible. However, they frequently suffer from the inherent problems of OEMs, such as extraordinary solubility throughout most electrolytes, resulting in deprived cyclability. Highly energetic density and extended life materials are essential if OEMs are utilized. On the other hand, organic matter provides unrivaled prospects for molecule engineering and property enhancement [36].

8 Conjugated Polymers as Organic Electrodes for Photovoltaics

Designing and synthesizing a conjugated polymer with superior film-forming capabilities, robust absorbance facility, significant hole motion in addition to appropriate HOMO–LUMO levels are the most challenging issues in generating perfect p-type materials. A basic grasp of protein engineering and the advantages of flexible polymer synthesis enables practical customization of the inherent characteristics of conductive polymers to serve the intended purpose and meet application requirements.

The donor–acceptor interfaces allow for the visualization profile and complex nonlinear relationships parameters illustrated. The donors with the lesser Lumo will achieve the Voc more easily. A decrease in the bandgap of a polymer to extend the

absorbance coverage by raising the HOMO level would ultimately lead to a loss of Voc. Lowering a conjugated polymer's LUMO level to produce a small bandgap may cause the LUMO level to ultimately fall below that of the graphene, preventing effective electron transmission. Cooperation is required to resolve the trade-off between the donor's small bandgap and the acceptor's favorable energy HOMO–LUMO bond. Consequently, the search for novel p-type polymers for PSC is focused on achieving low band gaps and managing the bandgap by adjusting the HOMO–LUMO values to their optimum levels. Conjugated polymers have a backbone with delocalized electrons that may be electrically conductive by adding or subtracting an electron by doping. These electrically and visually active materials have high light-harvesting activity and significant extinction coefficients. It has been shown that a mixture of materials can absorb incoming radiation with relatively high quantum efficiencies and extract mobile charge carriers from the device, resulting in power conversion efficiencies of more than 8%. Individual donor and recipient components have been linked to devise performance.

9   Conjugated Polymers as Organic Electrodes for Fuel Cells

Covalently polymer-based nanocomposites have sparked much interest in energy storage and generation. They are developing polymeric nanocomposites for energy-producing devices such as solar cells, sensor and transistors materials, medical imaging, and other electronic and fuel-cell technologies. Nanocomposites have also been discussed in energy storage systems such as lithium energy storage devices. Polyaniline, polypyrrole, conducting polymers, poly(N-vinyl carbazole), and other carbon-containing and steel nanoparticles in mixture with polymer electrolytes (polyaniline, polypyrrole, conducting polymers), durability, cyclability, photovoltaic properties, and solar cell efficiency of energy devices are all affected by interactions in nanostructured composites. In addition, the linked polymer-based nanocomposites meet the mechanical mobility and thermal stability criteria of energy devices. Prospects for the creation of energy-efficient technologies have also been highlighted.

10   Conjugated Polymers as Organic Electrodes for Batteries

A polymer-based battery is made out of organic components rather than bulk metals. Due to limited resources, severe environmental effects, and the nearing limit of advancement, already accepted metal-based batteries face several hurdles. Redox-active polymers are promising electrodes in storms because of their chemical accessibility, high capacity, versatility, lightweight, cheap cost, and toxicity.

Conjugated polymers with nanostructures are an electroactive organic material with excellent electronic conductivity, solid electrochemical stability, and great flexibility. Because of these benefits, there has been a surge in interest in using nanostructured linked polymers as sustainable and eco-friendly resources for high-performance power storage and power electronics. Many polymers, notably conducting, non-conductive, and radical polymers, are being investigated. Compared to contemporary metal-based batteries, batteries with the electrode (one metallic electrode and one polymer electrode) are easy to test and compare. However, polymer anode and anode batteries are a hot topic in the study. Metal/polymer electrode combinations should be differentiated from steel batteries, such as a rechargeable battery, which frequently uses a polymeric electrolyte instead of active polymer composites.

11   Non-aqueous Multivalent Rechargeable Batteries

As the multivalent metallic resources are available in abundance and at low cost, namely the Mg, Al, Zn, and Ca, the multivalent rechargeable batteries (MRBs) serve as the best-suited alternatives for Pb-acid batteries (LAB) and Li-ion batteries (LIB) be applied in the grid-scale motionless energy storage application. However, the higher act of inorganic electrodes in the Li-ion batteries is not extended to the MRBs as the high charge density of the respective cations tends to reduce the diffusivity in the inorganic material's crystal lattice. For higher act in MRBs, organic materials provide the best option due to the high structural tenability and sizeable structural diversity. It also explains the rationale structure plan and optimization of the enhanced OEMs within the MRBs. Different kinds of OEMs in the non-aqueous MRBs are exhibited in Fig. 5.

11.1   Non-aqueous Rechargeable Magnesium Batteries

Non-aqueous rechargeable magnesium batteries (RMBs) are the most appropriate substitutes to the LABs and LIBs specific grid-scale immobile energy storage due to the features such as being available in large quantities, high volumetric and specific capacity of anode of Mg, as well as it is cost-effective. To attain the extraordinary non-aqueous RMBs, OEM of supple and tunable properties are considered outstanding cathodes.

11.2   Non-aqueous Rechargeable Aluminum Batteries

Aluminum is the metallic element available in plentiful within the earth crust with the high volumetric capacity value of 8046 mAh/mL and a low reaction potential value

of -1.66 V compared to a standard hydrogen electrode (SHE), the high gravimetric value of 2980 mAh/g, and highly safe in the air.

Based on the above reading, Al is the encouraging anode for the upcoming group due to safety and low-cost rechargeable batteries. At the same time, the deprived electrochemical behavior of inorganic electrode materials obstructs the growth of the non-aqueous rechargeable aluminum batteries (RABs). OEM is available in large amounts and at a low cost, but the versatile electrode material is available in less quantity.

11.3 Non-aqueous Rechargeable Zinc Batteries

Researchers attract rechargeable zinc batteries (RZBs) as it also poses features the same as RABs and RMBs, the name, the high volumetric capacity of Zn, and lower cost. Because of the higher reaction potential of Zn/Zn^{2+} (-0.76 V) against SHE, the ability of the non-aqueous RZBs is lower in comparison to the non-aqueous rechargeable Li/Mg/Al batteries [37].

12 Aqueous Multivalent Rechargeable Batteries

Aqueous batteries are considered the best option to develop sustaining, environment-friendly, and inexpensive energy storage devices owing to the features such as being non-inflammable, reasonable, and safe among the aqueous electrolyte. The aqueous electrolyte's electrochemical stability window is narrow because of the electrochemical water splitting at lower and higher potentials. Figure 6 shows the different types of aqueous MRBs.

12.1 Aqueous Rechargeable Magnesium Batteries

Aqueous RMBs are recognized as suitable energy storage devices due to their reasonable price, high quantity, high sustaining ability, environmentally friendly magnesium resources, and even aqueous electrolytes.

Fig. 6 Different types of aqueous MRBs
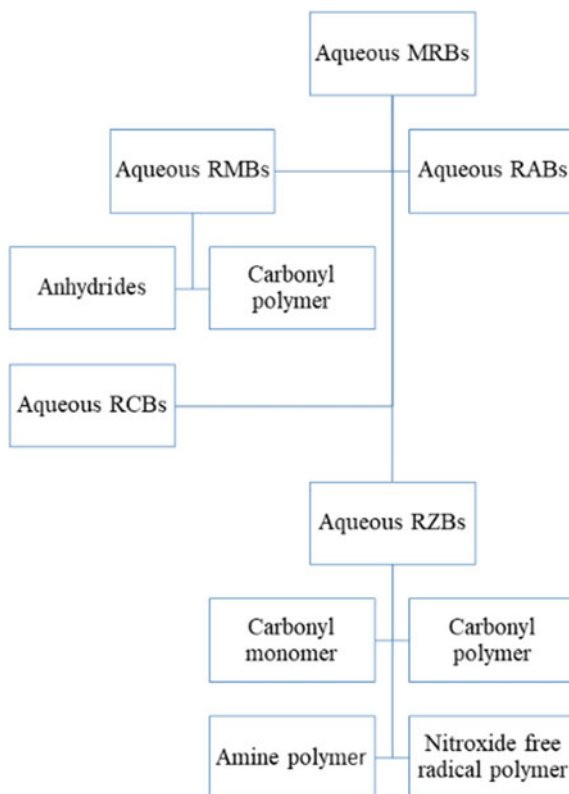
12.2   Aqueous Rechargeable Aluminum Batteries

Aqueous RABs is also one of the other substitutes to LIBs as it also has low costing charge, present in higher amount, aqueous electrolyte, and ecological benevolence of aluminum possessions. To date, most of the investigation study on OEM within aqueous RABs mainly emphasizes anode as the higher capacity Aluminium anode is not found to be well-matched to the aqueous electrolyte.

12.3   Aqueous Rechargeable Calcium Batteries

Same as MRBs, aqueous RCBs are also favorable replacements to the LIBs due to their inexpensive and availability in large quantities of calcium resources. The redox potential of calcium metal is -2.87 V against SHE, which is very close to Li metal -3.04 V against SHE. Aqueous RCBs even have an extraordinary theoretical volumetric capacity value of 2073 mAh/cm^3 [38].

12.4   Aqueous Rechargeable Zinc Batteries

Contrasting to metals such as Al, Mg, Ca, and Li, Zn is stable in the electrolyte at the discharge and charge of aqueous RZBs because of the extraordinary reaction potential Zn/Zn^{2+} against SHE. Therefore, Zn metal is also employed as an inexpensive and high-capacity anode in RZBs, posing higher benefits for this specific battery system.

13   Sustainable Supercapacitors

Organic redox polymers are suitable for the inorganic electrode materials showing high-performance supercapacitors because of their economic value, extensive resources, structural versatility, good processability, and higher electrochemical activity. The soft mechanical properties and the chemical diversity of the organic material permit the manufacture of flexible and stretchable supercapacitor (SC) electrodes. The application of conducting polymers in the form of pseudocapacitive materials is highly studied nowadays, and it has also gained interest. However, it is still observed that problems such as low power density and low cycling stability arise, and they must be formulated before the profitable viability of the particular organic electrodes. The primary process to remove such barriers comes under the branch, such as structural engineering of materials. As a result, a class of redox-active organic material is developed and improved, showing numerous implementations of SC. Zhang et al. [39] illustrated the improvement in the organic polymers

Fig. 7 Various types of
redox polymers
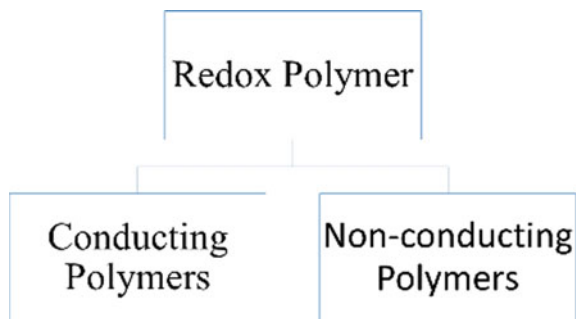
for supercapacitors and focused on the diversity of redox-active materials and their characteristic and working modes. At present, studies performed on the SC have made consequent development in theory and practice form, but high production cost and inferior energy density ability is still a challenging task that causes problems for the technological study of SC. The capability of energy storage of SC is dependent on the electrode materials. The commercialized SC electrode contains carbon materials such as activated carbon (AC), graphene and carbon nanotubes (CNTs). It possesses varied features good conductivity, non-toxicity, etc.

13.1   Redox Polymers

The redox polymer shows much more capacitance in comparison to the carbon material. Several forms of metals are located inside the metal oxides lattices with the redox centers.

The redox polymers possess various benefits for organic supercapacitor technology, but an essentially low electrical conductivity phenomenon is a significant issue causing the minor use of the active sites and showing a reduced performance rate. The studies carried out further illustrated that the creative designing of the molecules can lessen low electrical conductivity. The specific type of polymer backbone shows a higher impact on the π-electron delocalization and later influences the transfer capacity of electrons during the entire polymer structure. The design of the redox polymer structure is of utter importance due to the ironic redox-active functionalities and noble electron conductor essential. Different types of redox polymers are exhibited in Fig. 7.

13.2 π-Conjugation Polymers

π-conjugation polymers are a typical organic electrode material used for developing higher behavior in different implementations, namely supercapacitor. Many reviews

Table 2 A rapid of conducting polymers as supercapacitor electrode

S. No.	Electrode composition	Electrolyte	Specific capacitance (F g^{-1})	References
1	PTTA	TBABF$_4$	950	[40]
2	PCDT film	Et$_4$NBF$_4$/ACN	70	[41]
3	PEDOT/Pt	KCl	92	[42]
4	PANI/SS	H$_2$SO$_4$	608	[43]
5	PTFu on Pt	LiClO$_4$	249	[44]
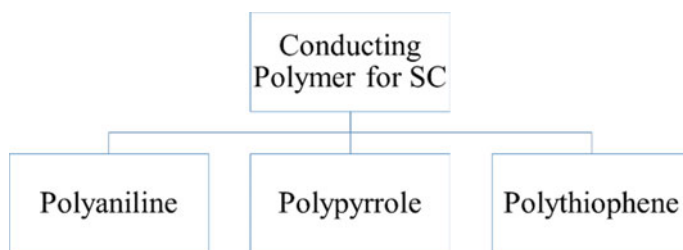
Fig. 8 Various types of conducting polymer for SC application

have been published summarising the use of conducting polymer in the energy storage system as referred to in Table 2. Figure 8 exhibits the different types of conducting polymer posing the potential towards SC.

13.3   Polyaniline

Polyaniline (PANI) occurs in different arrangements with distinct physical as well as chemical properties. There are three structures of PANI, namely emeraldine (EB), pernigraniline (PB), and leucoemeraldine (LEB), and they are related to each other through their synthesis approaches [45]. PANI has various physicochemical properties, enabling it to be used in different fields such as sensors, actuators, and organic electrodes [46].

PANI is an extraordinary innovative conducting polymer having an electrical conductivity value of 0.1–5 S/cm. It has become the choice of interest for the SC application due to stability towards the environment, facile synthesis, and easiness of doping or de-doping. The electrochemical performance was also firstly proposed [47]. The use of PANI as the SC electrode is yet found to be limited because of low practical capacitance, restriction in the electrolyte, and deprived cycling stability.

13.4 Polypyrrole

Polypyrrole (PPy) is the conducting polymer showing ecological stability, cost-effective, simple synthesis method, good thermal stability, higher electrochemical behavior, high conductivity as 10–50 S/cm, which enables it to be posing the higher potential for the use as SC.

13.5 Polythiophene

Polythiophene (PTh), conducting polymer, infers a high electrical conductivity value between 300 and 400 S/cm, which has gathered interest in the use as SC since the last 10 years. In contrast, p-doped PTh is more stable and is employed in the form of an SC electrode.

13.6 Non-conducting Polymer

Non-Conducting redox polymers are the characteristic organic electrode materials for developing the SC of higher performance. It provides a portrait of the recent progress made in conservative non-conducting redox polymers in the application of SC. Figure 9 exhibits the different types of non-conducting redox polymer.
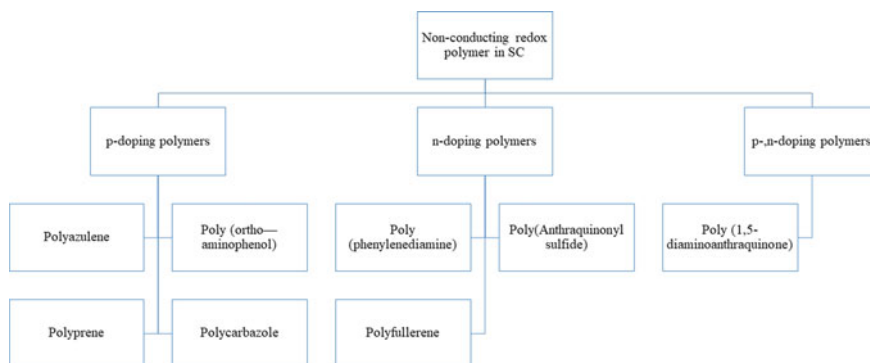
Fig. 9 Different types of non-conducting redox polymers

14　Lithium-ion Batteries

In most energy conversion devices, the chemical electrode is employed. As the name implies, Electrochemical devices transform chemical energy into electricity or vice versa. The use of organic electrocatalysts in lithium-ion batteries (LIBs) has piqued researchers' interest as a means of developing sophisticated electrochemical storage technology that does not rely on rare lithium and nucleophiles (cobalt, nickel, manganese, etc.). For example, sizable stationary energy storage facilities might benefit from such batteries since they are economical and environmentally beneficial.

LIBs are the chief power supply device for smart grids and electric vehicles, and it is also the leading energy storage batteries for portable electronic items. LIBs are used in large quantities in electric vehicles, encouraging the consumption-ability of the electrode materials. The conventional LIBs contain graphite, inorganic electrode materials. Manufacturing and recycling liberate large quantities of CO_2 and need enormous energy consumption [48]. Hazardous environmental pollution can be caused by the toxic heavy metal, namely Co formed in the LIB cathode. Hence, to avoid the negative impact on the environment, it is necessary to develop green and sustaining material to substitute the inorganic electrode material within the rechargeable batteries.

The OEM, resultant of the biomass, can serve as the best alternative to the green and sustaining LIBs due to significant features such as being available in large amounts, high sustaining ability, inexpensive, recyclability of the organic compound, and ecological benignity. The OEM has gathered interest in the research field in batteries, where extraordinary efforts are being made to synthesize and design the improved OEMs. Along with success accomplished, the OEM still faces many challenges in the organic batteries. The electronic conductivity of OEM limits the reaction kinetics of organic batteries; within the electrolyte, the high solubility of OEM results in rapid capacity fading.

14.1　Mechanism Phenomena in Organic Batteries

OEM is announced as positive electrode material in the case of rechargeable batteries. The unique application reveals the significance of both polymers and organic material in rechargeable batteries. Different types of mechanisms in the organic batteries are exhibited in Fig. 10.
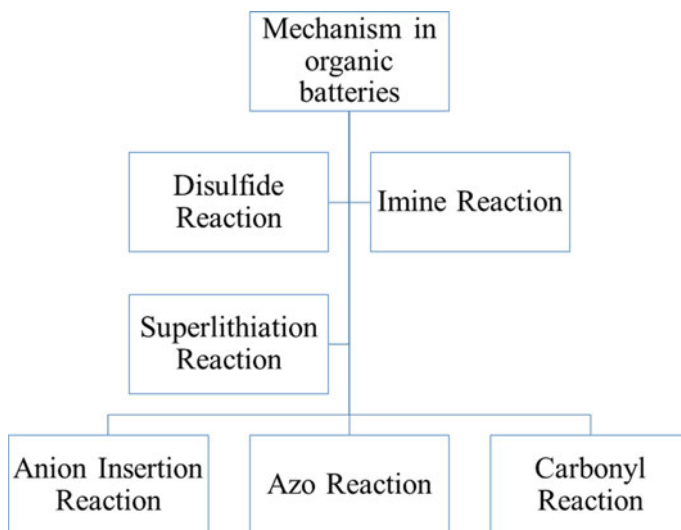
Fig. 10 Different types of mechanisms in the organic batteries

14.2 An Application Under Thrilling Situation

To date, the study reveals that organic electrode materials are employed in energy storage device fields. The application illustrates the position of both polymer and organic materials within the rechargeable batteries. Different applications under extreme conditions for the materials are inferred in Fig. 11.

14.3 Organic Electrodes Materials

For 20 years, the immediate attention of the researchers for designing the alternative electrode material has been centered on polymer and organic molecules. Organic materials are advantageous due to their large quantities, cost-effectiveness, low toxic nature, tunability, and potential for being recycled [49]. The organic material shows higher structural flexibility, which on the other hand, sustain facile ion diffusion. It permits the energy to be scattered rapidly and with the least polarization, whereas some organic batteries have attained extreme charge in just minutes or seconds instead of hours [50]. All such properties of OEM are striking for the great power utility.

Most OEMs are insulators and use many conductive extracts to provision rapid charge transport inside the batteries. In the electrode composite, the carbon additives give healthy ways for electron transport. It is predicted that the carbon extracts resistance is minute where just additional polarization is gained which is related
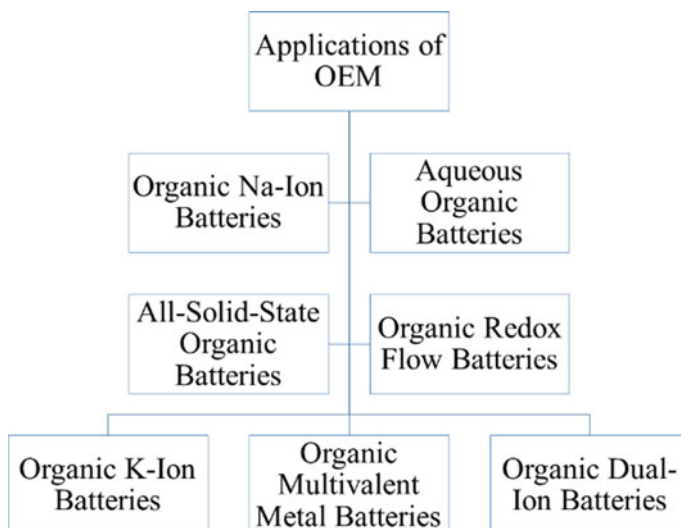
Fig. 11 Different applications under extreme conditions

to the heterogeneous transfer of charge between conductive additive and the active material.

14.4 Characterization Techniques for Organic Electrodes Materials

The characterization technique provides the electrochemical methods to determine the critical parameters based on the rate presentation in the battery electrode materials. These factors should permit high systematics. Various techniques for OEM are exhibited in Fig. 12.

Fig. 12 Various techniques for OEM
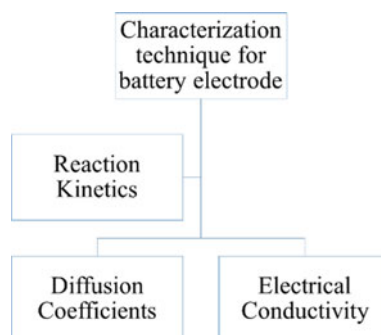
15 Conclusion and Future Perspectives

In conclusion, the outline of an organic electrode is delivered, which involves the history of development, fundamental understanding, and future application. After many years of research, the understanding and knowledge based on the organic electrode material are yet in the early stage. Nevertheless, they are urging to meet with various opportunities due to growth in resources and environmental problems in terms of the electrochemical behavior and energy density limitation of the materials. Compared to the other types of organic material, the conjugated carbonyl compounds are regarded as the best suitable ones in recent years due to the features that they are capable of attaining instantaneously higher energy density, higher power density, and cycling stability. With the view to overcoming the circumstances, still many opportunities are present for enhancing the electrochemical behavior of the organic electrode materials. The organic electrode material has a higher diversity of application owing to the features such as fast kinetics, processability, structure diversity, and flexibility. When ECs materials are employed eventually as the more considerable resistance, defects may arise in the process. Hence, two varied facets were considered in the research field, such as for developing the novel conducting material and enhancing the capacitance of ESC electrode material. Another one is related to the conductive polymer employed in the form of the modified membrane is coated enthusiastically on active carbon for reducing the resistance, in a combined way as organic and inorganic hybrid ESC electrode, which is completely capable of using the benefits of the materials.

References

1. Mohammad, F., Arfin, T., Al-Lohedan, H.A.: Biocompatible polylactic acid-reinforced nickel-arsenate composite: studies of electrochemical conductivity, mechanical stability, and cell viability. Mater. Sci. Eng. **C102**, 42–149 (2019)
2. Arfin, T.: Emerging trends in lab-on-a-chip for biosensing applications. In: Hussain, C.M., Shukla, S.K., Joshi, G.M. (eds.) Functionalized Nanomaterials Based Devices for Environmental Applications, pp. 199–218. Elsevier, Netherlands (2021)
3. Mohammad, F., Arfin, T., Al-Lohedan, H.A.: Enhanced biological activity and biosorption performance of trimethyl chitosan-loaded cerium oxide particles. J. Ind. Eng. Chem. **45**, 33–43 (2017)
4. Sophia, A.C., Arfin, T., Lima, E.C.: Recent developments in adsorption of dyes using graphene-based nanomaterials. In: Naushad, M. (ed.) A New Generation Material Graphene: Applications in Water Technology, pp. 439–471. Springer International Publishing, Cham (2019)

5. Arfin, T., Bushra, R., Mohammad, F.: Electrochemical sensor for the sensitive detection of o-nitrophenol using graphene oxide-poly(ethyleneimine) dendrimer-modified glassy carbon electrode. Graph. Technol. **1**(1), 1–15 (2016)
6. Arfin T, Rafiuddin: Transport studies of nickel arsenate membrane. J. Electroanal. Chem. **636**(1), 113–122 (2009)
7. Arfin, T., Jabeen, F., Kriek, R.J.: An electrochemical and theoretical comparison of ionic transport through a polystyrene based titanium-vanadium (1:2) phosphate membrane. Desalination **274**(1–3), 206–211 (2011)
8. Obulapuram, P.K., Arfin, T., Mohammad, F., Khiste, S.K., Chavali, M., Albalawi, A.N., Al-Lohedan, H.A.: Adsorption, equilibrium isotherm, and thermodynamic studies towards the removal of reactive orange 16 dye using Cu(I)-polyaniline composite. Polymers **13**(20), 3490 (2021)
9. Obulapuram, P.K., Arfin, T., Mohammad, F., Kumari, K., Khiste, S.K., Al-Lohedan, H.A., Chavali, M.: Surface-enhanced biocompatibility and adsorption capacity of a zirconium phosphate-coated polyaniline composite. ACS Omega **6**(49), 33614–33626 (2021)
10. Arfin, T., Tarannum, A.: Rapid determination of lead ions using polyaniline-zirconium (IV) iodatebased ion selective electrode. J. Environ. Chem. Eng. **7**(1), 102811 (2019)
11. Wang, J.: Organic-phase biosensors-new tools for flow analysis: a short review. Talanta **40**(12), 1905–1909 (1993)
12. Wang, J., Lin, M.S.: Mixed plant tissue carbon paste bioelectrode. Anal. Chem. **60**(15), 1545–1548 (1988)
13. Kaku, S., Nakanishi, S., Horiguchi, K.: Enzyme immunoelectrode for insulin incorporating a membrane partially treated with water vapor plasma. Anal. Chim. Acta **225**, 283–292 (1989)
14. Warsinke, A., Benkert, A., Scheller, F.W.: Electrochemical immunoassays. Fresen. J. Anal. Chem. **366**, 622–634 (2000)
15. Sadik, O.A., John, M.J., Wallace, G.G., Barnett, D., Clarke, C., Laing, D.G.: Pulsed amperometric detection of thaumatin using antibody-containing poly(pyrrole) electrodes. Analyst **119**, 1997–2000 (1994)
16. Bagel, O., Limoges, B., Schollhorn, B., Degrand, C.: Subfemtomolar determination of alkaline phosphatase at a disposable screen-printed electrode modified with a perfluorosulfonated lonomer film. Anal. Chem. **69**(22), 4688–4694 (1997)
17. Scheller, F.W., Bauer, C.G., Makower, A., Wollenberger, U., Warsinke, A., Bier, F.F.: Coupling of immunoassays with enzymatic recycling electrodes. Anal. Lett. **34**(8), 1233–1245 (2007)
18. Kojima, K., Hiratsuka, A., Suzuki, H., Yano, K., Ikebukuro, K., Karube, I.: Electrochemical protein chip with arrayed immunosensors with antibodies immobilized in a plasma-polymerized film. Anal. Chem. **75**(5), 1116–1122 (2003)
19. Zak, J., Kuwana, T.: Chemically modified electrodes and electrocatalysis. J. Electroanal. Chem. Interfacial Electrochem. **150**(1–2), 645–664 (1983)
20. Ugo, P., Moretto, L.M.: Ion-exchange voltammetry at polymer-coated electrodes: principles and analytical prospects. Electroanalysis **7**(12), 1105–1113 (1995)
21. Mohammad, F., Arfin, T., Saba, N., Jawaid, M., Al-Lohedan, H.A.: Electrical conductivity and biological efficacy of ethyl cellulose and polyaniline-based composites. In: Khan, A., Jawaid, M., Khan, A.A.P., Asiri, A.M. (eds.) Electrically Conductive Polymers and Polymer Composites: From Synthesis to Biomedical Applications, pp. 181–197. Wiley-VCH Verlag, Germany (2018)
22. Arfin, T., Bushra, R., Kriek, R.J.: Ionic conductivity of alkali halides across a polyaniline-zirconium(IV)-arsenate membrane. Anal. Bioanal. Electrochem. **5**(2), 206–221 (2013)
23. Arfin, T., Sonawane, K., Tarannum, A.: Review on detection of phenol in water. Adv. Mater. Lett. **10**(111), 753–785 (2019)
24. Sadki, S., Schottland, P., Brodie, N., Sabouraud, G.: The mechanism of pyrrole electropolymerization. Chem. Soc. Rev. **29**, 283–293 (2000)
25. Cheng, Y.-J., Luh, T.-Y.: Synthesizing optoelectronic heteroaromatic conjugated polymers by cross-coupling reactions. J. Organomet. Chem. **689**(24), 4137–4148 (2004)

26. Bao, Z., Chan, W.K., Yu, L.: Exploration of the stille coupling reaction for the synthesis of functional polymers. J. Am. Chem. Soc. **117**(50), 12426–12435 (1995)
27. Arfin, T., Rangari, S.N.: Graphene oxide-ZnO nanocomposite modified electrode for the detection of phenol. Anal. Methods **10**(3), 347–358 (2018)
28. Arfin, T.: Functional graphene-based nanodevices: emerging diagnostic tool. In: Kanchi, S., Sharma, D. (eds.) Nanomaterials in Diagnostic Tools and Devices, pp. 85–112. Elsevier, Netherlands (2020)
29. Oyama, N., Sarukawa, T., Mochizuki, Y., Shimomura, T., Yamaguchi, S.: Significant effects of poly(3,4-ethylenedioxythiophene) additive on redox responses of poly(2,5-dihydroxy-1,4-benzoquinone-3,6-methylene) cathode for rechargeable Li batteries. J. Power Sources **189**(1), 230–239 (2009)
30. Nigrey, P.J., MacInnes, D., Nairns, D.P., MacDiarmid, A.G., Heeger, A.J.: Lightweight rechargeable storage batteries using polyacetylene, $(CH)_x$ as the cathode-active material. J. Electrochem. Soc. **128**(8), 1651 (1981)
31. Oyama, N., Tatsuma, T., Sato, T., Sotomura, T.: Dimercaptan-polyaniline composite electrodes for lithium batteries with high energy density. Nature **373**, 598–600 (1995)
32. Sakaushi, K., Hosono, E., Nickerl, G., Gemming, T., Zhou, H., Kaskel, S., Eckert, J.: Aromatic porous-honeycomb electrodes for a sodium-organic energy storage device. Nat. Commun. **4**, 1485 (2013)
33. Zhan, L., Song, Z., Zhang, J., Tang, J., Zhan, H., Zhou, Y., Zhan, C.: PEDOT: cathode active material with high specific capacity in novel electrolyte system. Electrochim. Acta **53**(28), 8319–8323 (2008)
34. Poizot, P., Dolhem, F.: Clean energy new deal for a sustainable world: from non-CO_2 generating energy sources to greener electrochemical storage devices. Energy Environ. Sci. **4**(6), 2003–2019 (2011)
35. Gracia, R., Mecerreyes, D.: Polymers with redox properties: materials for batteries, biosensors and more. Polym. Chem. **4**(7), 2206–2214 (2013)
36. Liang, Y., Yao, Y.: Positioning organic electrode materials in the battery landscape. Joule **2**(9), 1690–1706 (2018)
37. Selvakumaran, D., Pan, A., Liang, S., Cai, G.: A review on recent developments and challenges of cathode materials for rechargeable aqueous Zn-ion batteries. J. Mater. Chem. A **7**, 18209–18236 (2019)
38. Li, H., Ma, L., Han, C., Wang, Z., Liu, Z., Tang, Z., Zhi, C.: Advanced rechargeable zinc-based batteries: recent progress and future perspectives. Nano Energy **62**, 550–587 (2019)
39. Zhang, X., Xiao, Z., Liu, X., Mei, P., Yang, Y.: Redox-active polymers as organic electrode materials for sustainable supercapacitors. Renew. Sustain. Energy Rev. **147**, 111247 (2021)
40. Mo, D., Zhou, W., Ma, X., Xu, J.: Facile electrochemical polymerization of 2-(thiophen2-yl)furan and the enhanced capacitance properties of its polymer in acetonitrile electrolyte containing boron trifluoride diethyl etherate. Electrochim. Acta **155**, 29–37 (2015)
41. Fusalba, F., El Mehdi, N., Breau, L., Bélanger, D.: Physicochemical and electrochemical characterization of polycyclopenta[2,1-b;3,4-b′]dithiophen-4-one as an active electrode for electrochemical supercapacitors. Chem. Mater. **11**, 2743–2753 (1999)
42. Snook, G.A., Chen, G.Z.: Polythiophene-based supercapacitors. J. Electroanal. Chem. **612**, 140–146 (2008)
43. Li, H., Wang, J., Chu, Q., Wang, Z., Zhang, F., Wang, S.: Theoretical and experimental specific capacitance of polyaniline in sulfuric acid. J. Power. Sources **190**(2), 578–586 (2009)
44. Mo, D., Zhou, W., Ma, X., Xu, J., Jiang, F., Zhu, D.: Alkyl functionalized bithiophene endcapped with 3,4-ethylenedioxythiophene units: synthesis, electropolymerization and the capacitive properties of their polymers. Electrochim. Acta **151**, 477–488 (2015)
45. Arfin, T., Bhaisare, D.A., Waghmare, S.S.: Development of a $PANI/Fe(NO_3)_2$ nanomaterial for reactive orange 16 (RO16) dye removal. Anal. Methods **13**(44), 5309–5327 (2021)
46. Bushra, R., Arfin, T., Oves, M., Raza, W., Mohammad, F., Khan, M.A., Ahmed, A., Azam, A., Muneer, M.: Development of PANI/MWCNTs decorated with cobalt oxide nanoparticles towards multiple electrochemical, photocatalytic and biomedical application sites. New J. Chem. **40**, 9448–9459 (2016)

47. Diaz, A.F., Logan, J.A.: Electroactive polyaniline films. J. Electroanal. Chem. Interfacial Electrochem. **111**(1), 111–114 (1980)
48. Shea, J.J., Luo, C.: Organic electrode materials for metal ion batteries. ACS Appl. Mater Interfaces **12**(5), 5361–5380 (2020)
49. Larcher, D., Tarascon, J.M.: Towards greener and more sustainable batteries for electrical energy storage. Nat. Chem. **7**, 19–29 (2015)
50. Otteny, F., Perner, V., Wassy, D., Kolek, M., Bieker, P., Winter, M., Esser, B.: Poly(vinylphenoxazine) as fast-charging cathode material for organic batteries. ACS Sustain. Chem. Eng. **8**(1), 238–247 (2020)

Materials and Synthesis of Organic Electrode

Monojit Mondal, Arkaprava Datta, and Tarun K. Bhattacharyya

Abstract The ameliorating urge for energy in consonance with the descending environment and attenuation of natural resources leads to the development of alternate energy storage. Furthermore, they suffer few boundaries like a thermal runaway, safety concerns, high carbon footprint, cost, and less metal content. Those hurdles were the incentive for immense exploration to substitute the electrodes of inorganic with organic. The long cycle stability and rapid kinetics recommend their usage in power regulation, grid storage, and probably in hybrid electric vehicles. An organic electrode material depicts potential for electrochemical energy storage devices for structural diversity, high theoretical capacity, and flexibility. Organic disulfides, polymers of nitroxyl radical, carbonyl compounds conjugated, and conducting polymers are organic materials analyzed as electrode materials. Their compounds have been broadly explored as electrode materials for rapid redox kinetics, higher theoretical capacity, and structural diversity. Tetrahydroxyphenazine, tetraazopentacene, octahydroxytetraazapentacene, cyclic polyketones, triquinoyl are specific compounds for active activity electrode materials delineating higher charge and discharge attributes in aqueous ion batteries with higher theoretical specific capacity. Organic materials are plentiful, flexible, cost-effective, and their fabrication can yield minimal waste and high storage capabilities. There are dianhydrides, phthalocyanines, and quinones, poly(acetylene) was worked as a cathode material followed by many different conjugated polymers such as polythiophene, polypyrrole, polyaniline. Redox and conducting polymers such as sulfur-containing polymers, carbonyl, and nitroxyl radical polymers possess several benefits: abundant resources, film-forming ability, versatile chemical structures, flexibility recyclability, and tunable redox properties all have conversed in this chapter.

Keywords Organic electrode · Energy storage · MOF · COF · Organic polymer · Conducting polymer

M. Mondal · A. Datta
School of Nanoscience and Technology, IIT Kharagpur, Kharagpur, West Bengal 721302, India

T. K. Bhattacharyya (✉)
Department of Electronics and Electrical Communication Engineering, IIT Kharagpur, Kharagpur, West Bengal 721302, India
e-mail: tkb@ece.iitkgp.ac.in

1 Introduction

Environmental and energy matters are documented as the two initial encounters to human civilizations in this present era. Concerning the desire for a proficient and clean source of power that can ameliorate the advancement of peoples' daily lives, the potential scientists have always involved them in escalating the electrochemical performance of prevailing battery performances and hunting for innovative battery storage techniques [1, 2]. However, in the expeditious expansion of consumer usage of electric-driven vehicles, electronics, and storage of energy platforms, the moderately poorer response of battery turns into the chief bottleneck. They introduced high necessities of the state-of-the-art lithium rechargeable batteries and supercapacitors with the performance of charge and discharge aspect and security, economic, and environmental friendliness with sustainability afford excellent prospects and challenges to the investigation and application of innovative active materials of the electrode with novel battery storage techniques [3]. Safety, sustainability, and higher cost, rechargeable Li-batteries are conventionally unable to placate the ever-enhancing mandate for energy storage in firm application zones of the challenges in storage abilities, e.g., electric power grid and electro-mobility.

Organic batteries are observed as potential candidates of the forthcoming generation energy storage electrochemically for their economic, resource sustainability, recyclability, and environmental approachability with flexible structural diversity. As a substitute to electrode materials inorganically connecting with reactions of intercalation (e.g., $LiFePO_4$, $LiCoO_2$, $Li_4Ti_5O_{12}$, graphite, and silicon) or reactions of conversion like as transition metal sulfides and oxides, along with electroactive polymers or organics linking reactions of redox reversibly are auspicious for materials of electrode for the innovation of "green lithium batteries" for the higher theoretical capacity, sustainability, safety, and environmental approachable with very economical [4, 5]. The Li^+ ion charge function of compensation may be replaced with alternative ions of reactions of redox electrochemically of numerous electrode materials of organic. Those possess diverse advantages over materials of the inorganic electrode in structure diversity, reaction kinetics, processability, and flexibility, also exhibiting superior implication in variational battery performances, like as supercapacitors, sodium rechargeable batteries, batteries of thin-film, redox flow batteries, rechargeable aqueous batteries, along with all-organic batteries. In several cases, the counter-ion is precise to the crystal construction of the inorganic compound for the size limitations of the ionic conductivity, crystal lattice, and reversible redox reaction. This integrally hinders the inorganic compounds' adaptability, like as similar material of cathode cannot be worked for dissimilar metal alkali battery series like as sodium and lithium-ion.

One of the most significant challenges of the complexes of inorganic is naturally needed synthesis procedures, and abstraction and those are environmentally destructive. The fabrication can generate huge amounts of waste of heavy metal and sometimes needed processing of energy-intensive. To comprehend the forecasted general

EESSs use, those encounters should be conquered. Materials of the organic electrode have gained less consideration in comparison to inorganic electrode materials, for there relatively less performance of electrochemical and the huge advancement in materials of inorganic electrode application. However, their performance of the battery is still away from real work. The researchers steadily focused on polymers of nitroxyl radicals and carbonyl conjugated compounds and attained huge development in those fields [6, 7].

2 Materials of Organic Electrode

2.1 Conducting Polymer
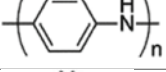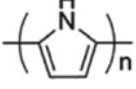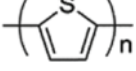
The prime organic configuration and process of redox have been segregated into several categories and denoted in Table 1. The three primaries of conjugated configuration containing amines, hydrocarbons, and thioethers are accredited to conducting polymers. It is depicted those forms and delineated a few similar features. Moreover,

Table 1 The redox mechanism and structure of several types of materials of the organic electrode

Structure	Redox mechanism	Examples	References
Conjugated hydrocarbon		PAc PPP	[8]
Conjugated amine		PAn PPy	[9]
Conjugated thioether		PTh TA	[10]
Organodisulfide		PDMcT PDTTA	[11]
Thioether (4e)		PEDOT PTBDT	[12]
Nitroxyl radical			[13]
Conjugated carbonyl		AQ NTCDA	[14]

Adapted with permission from Ref. [15], Copyright 2013 Energy and Environmental Science, RSC

Table 2 The conducting polymers parameters (electrochemical)

Name	Structure	Doping level (X_{max})	Theoretical capacity (mAh/g)	Redox potential (V vs. Li$^+$/Li)
Polyacetylene (PAc)		0.07	144	0–2.0 (n) 3.5–4.0 (p)
Polyparaphenylene (PPP)		0.4	141	0–1.0 (n) 4.0–4.5 (p)
Polyaniline (PAn)		1	295	3.0–4.0
Polypyrrole (PPy)		0.33	136	3.0–4.0
Polythiophene (PTh)		0.25	82	3.0–4.2

Adapted with permission from Ref. [15], Copyright 2013 Energy and Environmental Science, RSC

the chronological order is depended on the organic electrode's types and intensive material analysis, and those are more suitable for us to comprehend the tendencies and development history. However, the compounds of conjugated carbonyl are the most primitive materials for organic electrodes and the utmost potential and attractive study area in the present-day time. In the innovation of conducting polymers, the scientific community has invented that they can escalate the semiconductors' conductivity or metals. Furthermore, the electrode materials' redox activity is analyzed and enhanced. Thus since 1981, the conducting polymer has become the potential material of electrode for rechargeable batteries, and those are extensively analyzed. However, typically there are five organic polymer matrixes comprising polythiophene (PTH), polyparaphenylene (PPP), polyacetylene (PAC), polypyrrole (PPy), and polyaniline (PAn) (Table 2) [16–18]. The PPy, PAn, and PTH are considered organics of p-type, while PPP and PAC belong to organics of bipolar. Those materials used as the cathode, PPP and PAC were accredited to organics of p-type. Concerning the different p-type organic materials, the conducting polymers belong to the state of p-doping in electro neutralization. The polymers are electroneutral generally insulators; conversely, the polymers that are doped depicted superior enhanced ionic conductivity. The rest of conducting polymers are in a state of p-doped pristinely except for PAC, and those are fabricated by electrochemical oxidation or either chemical polymerization methods. The doping ratio units corresponding to the morphological units are elucidated as the degree of doping or level of doping, delineated as x in $(P^{x+}.xA^-)_n$, where $0 \leq x \leq 1$. P denotes an element of the structure of the polymer conducting that is equivalent to the C.H. of PAC. It is delineated in Fig. 1a that the distinctive redox electrochemically procedures of conducting polymer of p-type working as a material of the cathode. The cathode material's voltage of open-circuit (OCV) intensely relies on the level doping. The voltage profile gradient is
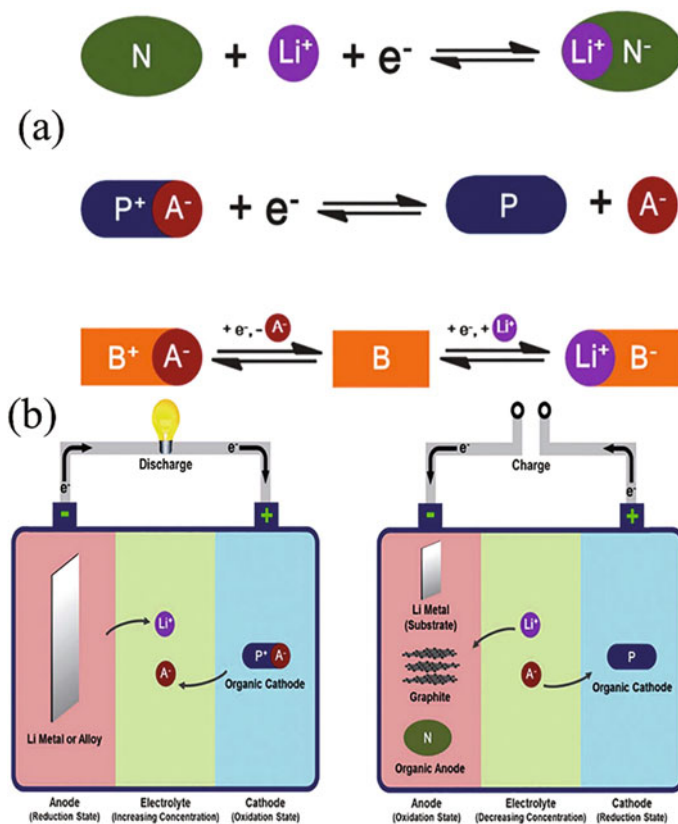
Fig. 1 **a** The three types redox reaction organics electroactive: p-type; n-type; and bipolar. A^- denotes electrolyte anion and other alkali ions can Li^+. **b** The cell assembles and process of charge transport of several kinds of batteries. The Bipolar organic may be recharged as P or N in the formations following the real reaction of the electrode. Adapted with permission from Ref. [15], Copyright 2013 Energy and Environmental Science, RSC

steadily decreased for the as-fabricated polymer conducting is present in the form of an intermediary, firstly, it can charge to the state of semi-oxidation, or either to the state of full-reduction form discharged at the time Li metal is working as anode depicted in Fig. 1b.

Moreover, this is improbable to charge the entire state of oxidation. The oxidation in the state of totality is perilous for most conducting polymers. It initiates to decompose after the state of semi-oxidation is generally involved in the electrolytic reaction, and this is for the significant alteration repulsion between the construction units. V_{max} is depicted as the higher voltage of cut-off of conducting polymers to accomplish huge capacity with higher stable long cycle response. The doping level X_{max} is noted as highest accordingly. Furthermore, this is a crucial aspect of evaluating the conducting polymer's theoretical capacity. Moreover, for a specific

type of conducting polymer, that X_{max} factor was considerably different from the earlier analysis. The X_{max} rely on the conditions of fabrication, electrochemical test ambience and type of anion. Furthermore, for comparing the performance of electrochemical analysis in between variational conducting polymers, the higher reliable X_{max} factor value is adopted and investigated the value of theoretical capacity and depend on the data (Table 2). The value of theoretical capacity is dependent only on the P unit's molecular weight in $(P^{x+}.xA^{-})_n$.

On the contrary, the specific capacity from the experiment is largely relying on the total molar mass of $P^{x+}.xA$ in the primaeval form. The theoretical capacity of PPP, PAC, PTH, and PPy is less than 150 mAh/g for the lesser doping level, and also the practical capacity is much lesser. PAn can accomplish a state of full-oxidation ($X_{max} = 1$) in the electrolyte of not aqueous. Moreover, it contains the optimum theoretical capacity of 295 mAh/g. However, it is challenging for the real capacity to depend on the entire P's and A's mass in the primaeval formal to surpass 150 mAh/g. As discussed earlier, the p-type organics system attributed comparatively high redox potential compared to the n-type organic system. The potentials of redox are more than 3.0 V of the polymers conducting illustrated in Table 2. Furthermore, the redox potential for PPP is 4.0–4.5 V, comparatively advanced in comparison to the materials of the inorganic electrode. However, the conducting polymer's energy density is not analogous to the inorganics system for possessing a huge, less specific capacity. Furthermore, the perilous disadvantage of conducting polymers is scanty in long cycle stability and self-discharge phenomenon and lesser Coulombic efficiency, considerably when the voltage of cut-off is increased for high capacity. Furthermore, considering the above-said difficulties, the utmost strong point of conducting polymers is the higher conductivity electronically. Consequently, the best suitable field for energy storage is a supercapacitor's cathode or an additive composite cathode's conductive material [19]. PPy and PAn are the two potential materials in those applications for their comparatively higher energy density, facile synthesis, and the stability of long cycles. The pseudo capacitor relying on a cathode of conducting polymer may allow rapid reaction of redox in the bulk scale material to acquire an abundant bigger capacitance. Meanwhile, the electrochemical responses may be endorsed by enlightening the electronic conductivity, surface area, and ion conductivity. In recent times, there has been researched on the nanostructured fabrication of conducting polymers and nanocomposites with graphene or CNT [8, 20]. Specifically for PAn, there are several efforts to formulate a composite of PAn/graphene and its thin films that may acquire higher flexibility with the higher electrochemical response (Fig. 2c, d) [9].

2.2 Organodisulfides

This is familiar that the sulfur bond may be reversibly fragmented and reconstructed. The redox reaction of the two-electron (Table 1) is corroborated a higher capacity compared to the conducting polymers' undoing and doping reaction. Furthermore,
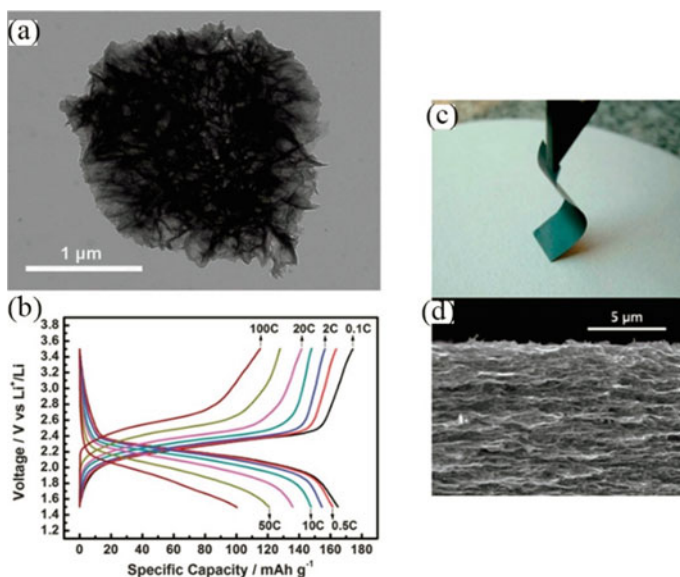
Fig. 2 **a** Image of HRTEM of composite graphene-PAQS fabricated by polymerization. **b** Outlines of voltage of a composite of graphene-PAQS (graphene: PAQS = 26:74) at variational C rates. The capacity is analyzed depending on the entire mass of composite. **c** Images and **d** SEM cross-section image of a composite of PAN-graphene thin film. **a**, **b** is adapted with permission from Ref. [21], Copyright 2012 Nano Letters, ACS. **c**, **d** is adapted with permission from Ref. [22], Copyright 2010 ACS Nano, ACS

a huge amount of analysis has gained more attention on cathode materials of organodisulfide (Fig. 3c), conducted by Visco et al. and also Oyama et al. [10]. To comprehend the electrochemical response of organodisulfide cathode materials, the improvement is delineated into the three stages as follows.

2.2.1 Dimeric Organodisulfides

Visco et al. initially integrated TETD in 1988 work as the material of cathode in the application of sodium battery of high-temperature [23]. Then, they analyzed different dimeric organodisulfides with a detailed study of the kinetics of the reaction. Those types of organodisulfides may be incorporated in rechargeable lithium batteries for possessing a significantly higher solubility of R.S. and RSSR in electrolytes of organic.
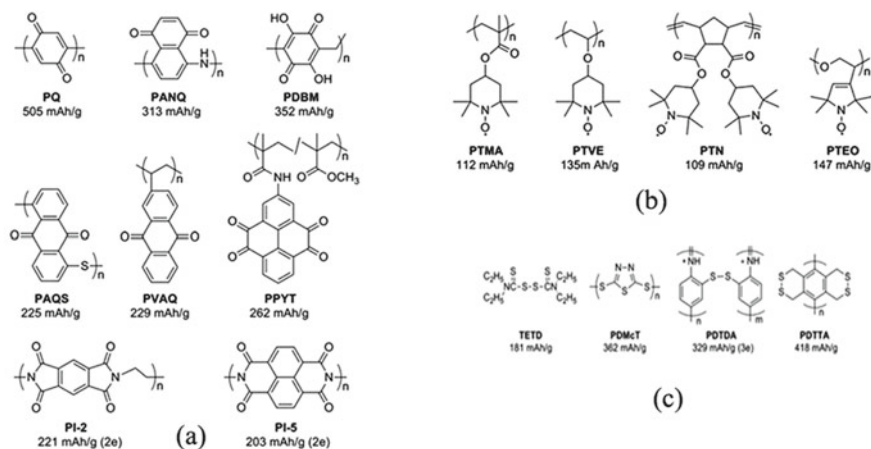
Fig. 3 a General materials of polymer electrode rely on carbonyl conjugated forms and its theoretical capacity: poly(2-vinylanthraquinone) (PVAQ), polymeric quinone (PQ), polyimide (PI-2 and PI-5), polymer-bound pyrene-4,5,9,10-tetraone (PPYT). The theoretical capacity is analysed rely on the number of carbonyl group. **b** Typical polymers of nitroxyl radical and their theoretical capacity: poly (2,2,6,6-tetramethylpiperidine-1-oxyl-4-yl vinyl ether) (PTVE), poly (2,2,6,6-tetramethylpiperidine-1-oxyl-4-yl methacrylate) (PTMA), poly (2,2,5,5-tetramethylpyrroli-dine-1-oxyl-3-yl ethylene oxide) (PTEO), poly-(TEMPO-substitued norborene) (PTN). **c** General organosulfides and their theoretical capacity: poly(2,5-dimercapto-1,3,4-thiadiazole) (PDMcT), tetraethylthiuram disulfide (TETD), poly(5,8-dihydro-1H,4H-2,3,6,7-tetrathia-anthracene) (PDTTA), poly(2,2'-dithiodianiline) (PDTDA). The PDTDA capacity is depend on the postulation that every aniline unit can donate 0.5 e^- and disregards the mass of A^-. Adapted with permission from Ref. [15], Copyright 2013 Energy and Environmental Science, RSC

2.2.2 Polymeric Organodisulfides

This polymer matrix is present with bonds of sulfur in the primary chain is mostly fabricated from multimercaptan or dimercaptan with the help of oxidation polymerization. The PDMcT is the most distinctive example, enticing the utmost consideration between the organodisulfides for corroborating higher theoretical specific capacity (362 mAh/g). The PDMcT depicted an oxidized state of the polymer. The DMcT is a discharged product that exhibits minor organic molecules. DMcT is often working as active material directly in the form of a reduced state. The long cycle stability of polymer cathode is poorer till now as it holds huge dissolution of smaller molecules of organic in the electrolyte. Furthermore, the slower reaction kinetics of the sulphur bond is creating a huge problem that leads to lower consumption of active material at the normal room temperature. Oyama et al. revealed in 1995 the consequence of electrocatalysis of PAn in the process of reaction of redox mechanism of DMcT. Furthermore, they also revealed that the Cu^{2+} incorporation could enhance the response of the battery of DMcT for the stabilization and electrocatalysis effect. Afterwards, the DMcT/PAn/Cu(II) and DMcT/PAn composite materials have

been explored extensively [11]. This polymer entails polymer conducting as the foremost chain with bonds of sulphur present within the chain; two distinctive samples are PDTTA and PDTDA. The PDTDA comprises an electronically conductive and insoluble main chain, and the performance of long cycling is insufficient for the disarticulation of the two principal chains next to discharging impedes the reconstruction of the sulphur bond. Furthermore, the researchers projected different variations of polymer with sulphur bonds in a similar chain sideways, like PDTTA. That strategy can resolve the problem together of dissolution and dislocation, though the electrochemical analysis of PDTTA is not up to the mark, mostly for the slower kinetics. In summary, organodisulfides were documented as potential materials of the organic cathode in the application of rechargeable batteries of lithium. To attuned slower kinetics and dissolution, the scientists have created substantial efforts in enhancing the polymer construction and additives of integrating electrocatalytic [24].

2.2.3 Thioethers

In exploring materials of organosulfide cathode, Zhan et al. developed that the material may exhibit an abundant advanced capacity compared value of theoretical in electrolytes like as DOL/LiTFSI with DME and consisting higher voltage of cut-off is more than 4.2 V is introduced. It is ventured that it is linked to the response of four-electron of thioether-sulphone-sulfoxide. Numerous thioethers are investigated as materials of the cathode, both in the conjugated and unconjugated form. PEDOT (Poly (3,4-ethylene dioxythiophene) and PDBDT poly-(tetrahydro-benzodithiophene) can attain a superior discharge capacity of 500–800 mAh/g, along with a voltage of discharge in the window of 1.5–2.5 V. Moreover, the cells' performance is lessened after huge long discharge/charge cycles. Perhaps for the uncommon response methodologies, the electrolyte is proficient in providing oxygen atoms to fabricate sulphone and sulfoxide groups [25].

2.2.4 Nitroxyl Radical Polymers

Nakahara et al., in 2002, anticipated a steady polymer of nitroxyl radical, i.e., PTMA, work as the material of cathode for lithium batteries rechargeable. The electrode materials on radical polymer, typically rely on radicals of nitroxyl, like as 2,2,5,5-tetramethylpyrrolidine-1-oxyl (PROXYL) and with 2,2,6,6-tetramethylpiperidine-1-oxyl (TEMPO). The maximum investigation is conducted on that subject by Nishide et al. and Nakahara et al. Even though the other radicals are segregated as electrode materials of radical polymer. The batteries were denoted as ORBs, i.e., batteries of radical organic; only in radical polymers of nitroxyl are conferred. The methodologies of reaction of radical nitroxyl designate are organic of bipolarity. Several cases worked as polymers of p-type to attain higher voltage of discharge and long steady cycle response. Thus, the arrangement is assumed to accumulate a cell for a polymer of nitroxyl radical.

Although the expended from the electrolyte, the nitroxyl radical polymers' capacity theoretically is firmly restricted by the reaction of one-electron with their high molecular weight. The typical examples' constructions and theoretical capacities include PTMA, PTN, PTV, and PTEO. The maximum theoretical capacity of polymers is 147 mAh/g, and it will further be enhanced by optimizing the morphology. PTMA is the maximum analyzed between different nitroxyl radical polymers for having relatively high capacity and adequate stability. The plateau of charge/discharge is at 3.5 V, with the application ratio nearer to 100%. The rate performance and cycling of PTMA are too outstanding for the steady polymer morphology and faster kinetics of the radical reaction. The polymers based on TEMPO depicted alike electrochemical performances but dissimilar specific capacities. The utmost firmness of nitroxyl radical polymers is a higher rate of response. Though the condition of the electrode is fine configured, then TEMPO is effortlessly withstanding a rate of current of 50°C or 20°C. This ascends mostly from the reaction of faster self-exchange of an electron between head-to-head units of TEMPO that delineated in the effectual transportation of electron contemplating the main chain of polymer insulating [14, 26].

2.2.5   Conjugated Carbonyl Compounds

Quinone is a very renowned organic material with higher electroactivity. The mechanism of a redox reaction is specified by the reaction of enolization and with the carbonyl group's reverse reaction that may be upheld by a conjugate configuration. As well as quinone, there are additional carbonyl conjugated composites that can delineate redox reactions electrochemically. Depending on the value of theoretical capacity is high, the structural diversity and fast reaction kinetics are the most favorable organic electrode materials. A.Q. and NTCDA are considered for depicting the usual dianhydride and quinone redox reaction; these are the two important morphological units in the compounds of conjugated carbonyl. The revocable two-step redox procedure involves a radical anion, i.e., A.Q.$^{-}$ in the state of transition, which is vastly researched. Moreover, when working as rechargeable batteries materials of the electrode, there is a charge/discharge plateau in the flat. Also, the subsequent reduction step (AQ^-/AQ_2) is rapid, with the voltage difference in the two consecutive steps being too small to differentiate the plateaus. However, NTCDA holds carbonyl groups of four to employ all of them completely. The two-electron performance is typically assumed for batteries rechargeable. Though lessening the cut-off voltage may also decrease NTCDA and attain a higher capacity of discharge, the morphology may be demolished for the interaction of huge charge repulsion, like conducting polymers at higher voltage of charging. A huge number of elements work as materials of the electrode, and those are divided into groups as organic polymers, small organic molecules, and organic salts [27].

2.2.6 Small Organic Molecules

Williams et al. conveyed in 1969 a main lithium-ion battery with DCA, i.e., dichloro-iso-cyanuric acid as the cathode. This analysis is perhaps the initial materials of the organic electrode. Numerous scientists endeavored to introduce smaller organic molecules from then on work as cathodes electrodes to configure batteries of rechargeable with the electrolyte of aqueous and nonaqueous. The distinctive assemblies with theoretical capacity mostly depend on dianhydride and quinone. However, many researchers can realize higher discharge capacity and energy density are the prime features. Also, using LISICON as a solid electrolyte or electrolyte of polymer-like as PEO/LiTFSI can entirely avoid liquefaction. The immobilization technique cannot fundamentally evade the dissolving and may perhaps decrease the entire electrode capacity. A polymer or solidified electrolyte will transport lower conductivity of ions at room temperature with substantial interfacing resistance. Recent work delineates an electrolyte of high-salt-concentration assistances to constrain Li–S batteries [28].

2.2.7 Organic Polymers

Foos et al. in 1986 endeavored to fabricate P.Q., i.e., quinone polymeric form as prepared poly(l,4-dimethoxybenzene) electrochemically. They investigated its electrochemical response work as a cathode electrode of lithium-ion batteries. Polymeric quinone appears as a seamless assembly for polymeric cathode relies on carbonyl conjugated for comparatively higher discharge voltage along with higher theoretical capacity. Researchers have fabricated and analyzed variational polymer electrode materials depending on dianhydride and quinone after 1999. Specifically, in current times, numerous polymers like PVAQ, PAQS, PI-5, and PPYT have exhibited outstanding inclusive electrochemical response associated to outcomes above, together with higher capacity adjacent to the theoretical value, higher Coulombic efficiency and higher long cycle stability, with higher rate capability. After 500 cycles, PPYT can hold 83% of its preliminary capacity, at 30 C 90% of its capacity associated to 1 C (Fig. 4d). Whether nonaqueous or aqueous, the polymer is completely not soluble in the electrolyte, is associated with a monomeric form. Consequently, the greatest method to resolve the problem of dissolution is by building materials of polymer electrodes with a steady and proficient electroactive organic moiety. PAQS can accomplish meaningfully upgraded long cycle stability with a somewhat decreased degree. The discharge/charge plots depicted more slanted, with a decreased average voltage of discharge to some extent. This is perhaps correlated to the revulsion of charge interface within A.Q. elements in between the chain of the polymer, moreover, with the polymer electronic insulation. However, the increasing capacity for the polymeric electrode is recognized as a process of activation. It is accredited to the inadequate interaction of the electrolyte with a polymer that will be progressively upgraded in the methods of charge and discharge [21, 29].
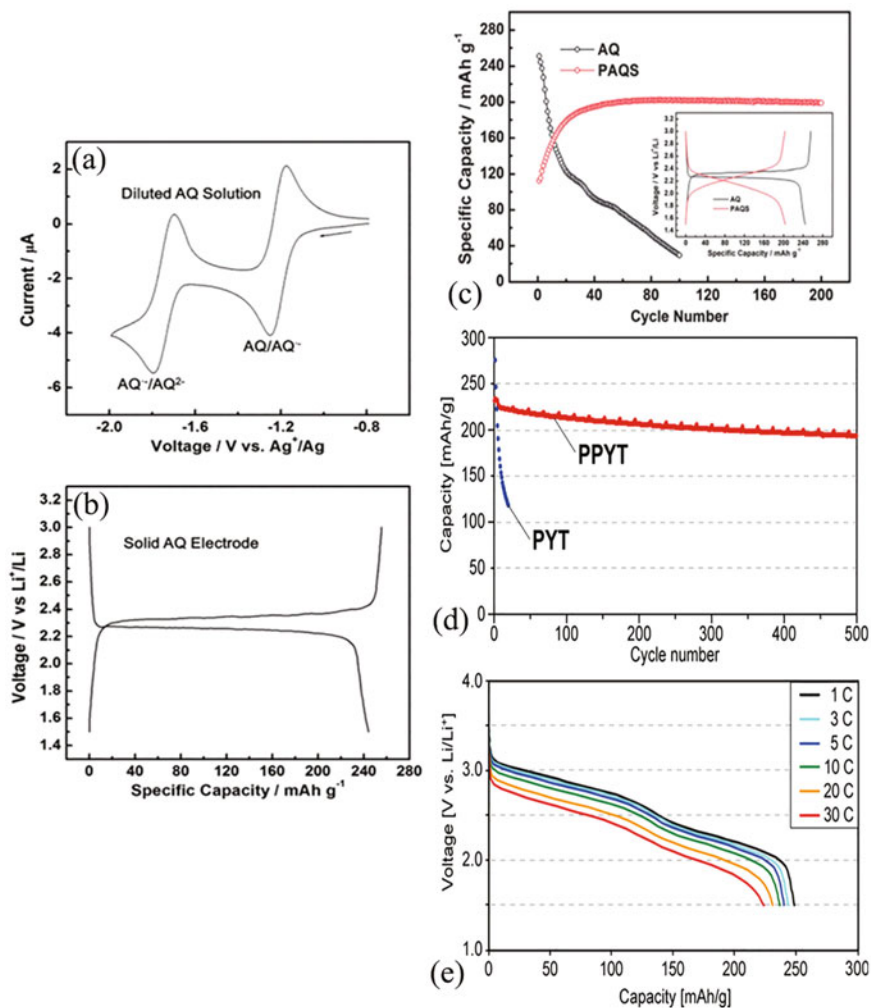
Fig. 4 **a** Cyclic voltammogram plot of a scan rate of $100\,mV\,s^{-1}$ of 2 mM A.Q. in 0.1 M electrolyte of TBAP/CH3CN. **b** Charge and discharge response in the current rate of 0.2C of electrode of A.Q. (PTFE: A.Q.:C: = 1:6:3) in electrolyte of 1 M DME + LiTFSI/DOL. **c** The electrochemical response comparison of PAQS and A.Q. as materials of cathode for rechargeable lithium batteries. The cathode (PTFE: A.Q.:C: = 1:6:3) is verified at a 0.2 C current rate in 1 M electrolyte of DME + LiTFSI/DOL. **d** Cycling response and rate analysis of PPYT. The cathode (PPYT or PYT:PVDF:AB: = 3:2:8) is verified at 45 °C in electrolyte of LiTFSI-tetraglyme. **a**, **b** is adapted with permission from Ref. [27], Copyright 2005, The Journal of Physical Chemistry B, ACS. **d** is adapted with permission from Ref. [30], Copyright 2012 Journal of the American Chemical Society, ACS

2.2.8   Other Organic Electrode Material

The -ve organic electrode materials, like organic triazine bipolar, poly(galvinoxyl-styrene), and TCNQ, all are fit into the organics of n-type; on the other hand, all are p-type. Triquinoxalinylene, PVK with PTPAn, all possess amine conjugated formation, so their process of redox is alike to PPy and PAn. Furthermore, the PTPAn lower capacity theoretically exhibited an excellent rate of ability at 20 °C and stability of long cycle after 1000 cycles. However, amine conjugated formation is triazine, but its bipolar attributes can deliver much bigger reversible capacity versus Li^+/Li in between 1 and 5 V. Also, Poly(S-TTN) comprises both thianthrene (T.A.) and sulfur bond configurations having distinct mechanisms from different organodisulfides. It is analogous to the response of p-type PTH. However, the high specific capacity and stability of long cycles corroborated. Poly (vinyl ferrocene) is a potential sample of the electrode of organometallic type concerning the renowned moiety of ferrocene redox. It delineated a redox potential of 3.5 V nearer to the 126 mAh/g theoretical value of specific capacity. It is predictable as a proficient candidate for high power cathode for the faster kinetics reaction of ferrocene unit [31].

Moreover, TCNQ90 has exhibited the same behavior of electrochemical to quinone and showed a higher potential of redox is 2.8–3.2 V compared to B.Q., for the substantial consequence of four electron-withdrawing groups of C.N. On the other side, the nitroxyl radical as electrode materials like PDBDAB and poly(galvinoxylstyrene), many other types of steady radicals have been explored. An n-type radical is galvinoxyl is depicting a redox potential of 3.0 V. A p-type organic is dialkoxyaryl possesses redox potential of 4.0 V. Though many organics indicate the several morphological multiplicities of materials of the organic electrode shows a higher electrochemical response [32].

2.2.9   Porphyrin

The porphyrins are broadly systems of planar macrocyclic in conjugated and depicted admirable harvesting of light and proficient transporting capabilities of an electron. Subsequently, the porphyrins corroborate a great response to the applications of the photovoltaic field. Due to their gaps within the HOMO–LUMO that permit faster acceptance and release of the electron, porphyrins delineated a higher redox response. They can be worked proficiently as devices of energy storage and gained huge consideration as a novel class of working material of organic electrode for batteries, super-capacitors, and batteries of redox-flow [33, 34]. The Porphyrin with derivatives of that, consisting of extremely macrocycles with π-electron conjugated with exclusive features of redox, has been delineated as prevailing molecular structure units for constructing new materials of the electrode by organic. The outstanding electrochemical/chemical features anticipated inorganic electrode materials, higher electric conductivity, lower insolubility, faster ion movement and charge transportation, and capabilities of effectual storage that may be apprehended in materials derived from porphyrin by appropriate engineering of molecular. The COFs built porphyrin

exhibited rapid ion transportation and higher conductivity electronically owed to the structures of exposed framework and the exclusive interaction of π–π within the units of porphyrin. The CuDEPP is a precursor of porphyrin has been revealed to work as favorable material of electrode molecular in different systems of battery. The porphyrins work as materials of the electrode, and their potential attribution explored novel trails for the fabrication of batteries of thin-film, faster supercapacitors, batteries of redox flow, all flexible organic batteries, and even aqueous rechargeable batteries. Also, organic-framework based on porphyrin corroborates spheres like hollow formation have been worked as cathode electrodes to physically entrap and adsorb chemically sulfur in lithium-sulfur batteries and carbon nanotubes composites working as a zinc-air batteries catalyst [35].

3 Synthesis of Organic Electrode Material

3.1 Synthesis of Cobalt- and Manganese-Based MOF

Kazemi et al. have fabricated manganese and cobalt-based MOF with the help of a typical method of synthesis. In the facile Co–Mn MOF synthesis, 0.08 g of terephthalic acid (p-benzene dicarboxylic acid, H2BDC) along with cobalt (II) chloride of 0.04 g were liquified in N,N dimethylformamide (DMF) of 10 mL in the extensive stirring in the ambient temperature. Afterward, manganese (II) nitrate 0.04 g was mixed in the solution, and the subsequent reaction blend relocated to a stainless-steel Teflon-lined autoclave. Furthermore, a 1 cm × 1 cm sized Ni-foam electrode was incorporated in the autoclave solution, and after that, the whole system temperature is targeted at 120 °C up to 24 h. Furthermore, when the autoclave setup is cooled at ambient temperature, the sediment of violet tone and the electrode were rinsed with ethanol three times. Lastly, it was desiccated for 12 h at 120 °C in an oven. Moreover, various cobalt (II) chloride quantities were synthesized by similar methodologies to equivalence the combined metal MOF, Mn-based MOF, Co–Mn MOF, and Co-based MOF [36].

3.2 Covalent Organic Frameworks and Graphene Composite

Wang et al. delineated a facile procedure to produce the composite of graphene-COFs by the aldehyde group reaction in amine and 1,3,5-triformylbenzene group in 1,4-diaminobenzene and NH_2–graphene in a single step to the graphene surface of amino-functionalized. Covalent organic frameworks and graphene composite fabrication is conjugated and depicted enhanced super capacitance to the graphene and COFs. The reduced graphene oxide with amine-modified (NH_2–rGO) was dispersed in 1,4-dioxane. Afterward, it is stirred vigorously for half an hour, afterward aqueous acetic
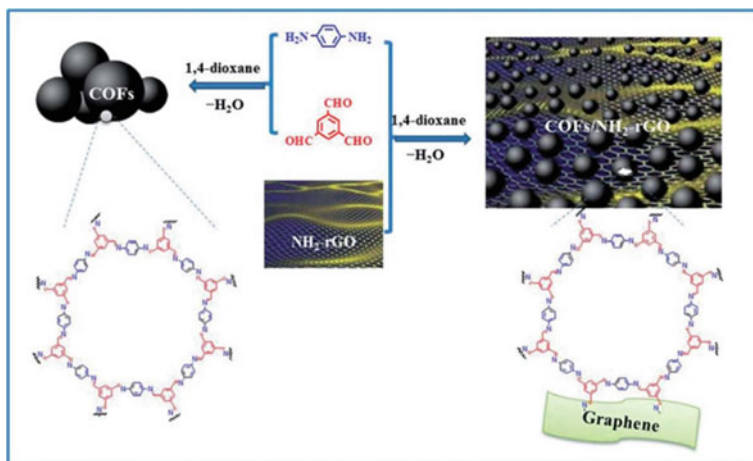
Fig. 5 Schematic of synthesis of graphene-covalent organic framework composite. Adapted with permission from Ref. [38], Copyright 2015, RSC advances, RSC

acid, 1,4-diaminobenzene, and 1,3,5-triformylbenzene, were mixed to the before dispersion consecutively within mild stirring. Furthermore, the dispersion-shifted to an autoclave Teflon-lined. For two days, it was heated at 120 °C. Subsequently, the gained dark green precipitate was secluded by gradual centrifugation, cleaned by the tetrahydrofuran and N,N-dimethylformamide, and dried to obtain novel COFs/NH$_2$–rGO composite. To equivalence the properties of storage of energy of the NH$_2$–rGO-COFs, the COFs were synthesized with the similar procedure for COFs-graphene fabricating without mixing the NH$_2$–rGO into the ambiance of reaction. NH$_2$–rGO–CHO was also synthesized by the reaction of NH$_2$–go with 1,3,5-triformylbenzene in the acetic acid presence to authorize the imine bonds formation between COFs graphene [37] (Fig. 5).

3.3 Synthesis of Porphyrin-Based Polymers in Capacitive Energy Storage

The microporous polymers conjugated based on zinc porphyrin have been conveyed by Gao et al. as stable and functional materials of porous film for supercapacitors use. The Zn (II) 5,10,15,20-tetrakis[(carbazol-9-yl) phenyl] porphyrin (Zn-mTCPP) precursor experiences polymerization electrochemically by the carbazole groups of *N*-substituted work as the direct linker. The fabricated films of CMP hold a 3D network in cross-linking morphology and higher active surface area that proficiently simplifies the transportation of ions. Moreover, the redox-active cores of Zn porphyrin and the carbazole linkages electron conductive condense the polymer based on Zn-mTCPP work as an active material for the promising electrode. Subsequently, the

capacitive energy storage is depicted as higher performance and delineated with the films based on Zn-mTCPP. The electrode film may be worked at a current density of more than 5 A/g, exhibiting a higher source of power and a very higher 142 F/g capacitance. However, the electrode materials based on Porphyrin worked for super-capacitor was fabricated by integrating a redox unit of organic radical of 2,2,6,6-tetramethyl-1-piperidinyloxy (TEMPO) in The COF and is prepared in the formation of nickel 5,10,15,20-tetrakis(4′-tetraphenylamino) porphyrin (NiP) [39]. This cate-gory of crystalline COFs that is porous, along with the functional groups of organic, are immobilized covalently, contributing excellent stability in structure. The porous methodical morphology permits higher-rate transportation of ion and lucid entrees to the positions of redox in between the materials.

3.4 Synthesis of Covalent Organic Polymer-Based Flexible Electrode

Mi et al. has prepared covalent organic polymer over the flexible electrodes for application of supercapacitor. The commercial carbon felt (C.F.) is worked as a flexible substrate, and the C.F. is sized into smaller pieces with the 1.5×1.0 cm size for the further process. After that, the pieces of C.F. are deep under ultrasonication in the solution of ethyl alcohol several times cleaning. The washed pieces of carbon fiber are desiccated at 75°C. The C.F. was drenched with a solution of DMF with COPBTC-Mn liquified at the variational amount. The electrodes of flexible named COPBTC-Mn with C.F. have gained afterward, disappearing the solvent. The Benzene-1,2,4,5-tetracarbonitrile is incorporated like monomers using the process of microwave (for 20 min at 150 °C) for the synthesis of COPBTC-Mn with 1,8-Diazabicyclo (5,4,0) under-7-ene (DBU) use as catalysts. The BTC, DBU and manganese (II) chloride are liquified in ethylene glycol solvent and placed for 20 min in a microwave setup at 150 °C reaction setup [40] (Fig. 6).
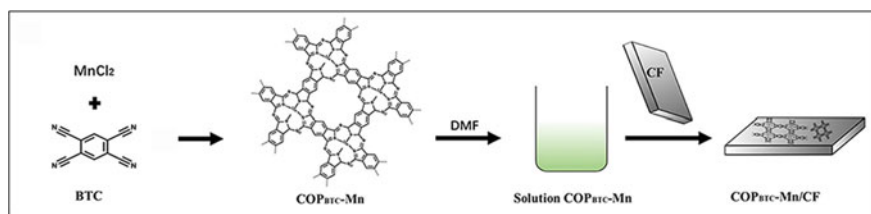
Fig. 6 Schematic of fabrication of flexible electrode based on covalent organic frameworks Figure is adapted with permission from Ref. [41], Copyright The Authors, some rights reserved; exclusive licensee [Frontiers in Materials]. Distributed under a Creative Commons Attribution License 4.0 (CC BY)

3.5   Synthesis of Polymers of Organodisulfides

3.5.1   Synthesis of the Bis(Phenylamino)disulfide (PAD) Monomer

PAD was prepared by the methods described by Su et al. 0.2 mol of aniline and 0.2 mol of triethylamine were liquified in dichloromethane 200 mL. Afterward, in the well-dispersed solution, the sulfur monochloride was mixed in dichloromethane 100 mL and was mixed at a constant rate to maintain the 0–4 °C temperature range. The incorporation is required 2 h approximately, along with the solution kept stirring for 0.5 h. The whole reaction setup is kept within an atmosphere of argon. Furthermore, the amine hydrochloride was extracted from the reaction solvent. The extracted part was cleaned several times by deionized water and dichloromethane.

3.5.2   Preparation of PPAD

Electropolymerization Methods

PPAD was fabricated and fashioned electrochemically at a scan rate of 20 mV/s and gave a smooth superior type cohesive film over the electrode of platinum foil after 50 times cycling in the potential window of 0.20–0.75 V versus Ag/AgCl in solutions of AN consisting monomer 0.1 mol dm^{-3}, with HClO$_4$ 0.5 mol dm^{-3}, and LiClO$_4$ 0.5 mol dm^{-3} for supporting electrolyte. Furthermore, growth film was kept in HClO$_4$ for 2 h at 1.0 mol dm^{-3} to make traces free of monomer and then kept at ambient temperature in a vacuum oven up to 24 h. The undoped powder of PPAD and film was achieved by the prepared powder of blue-green either electrochemically or chemically in an NH4OH solvent for 12 h. The PPAD HCl-doped was also synthesized by placing PPAD undoped in HCl 1.0 mol dm^{-3} solvent aqueous for 12 h. On the other hand, PPAD HCl-doped was somewhat solvable in NMP (N-methyl-2-pyrrolidone); on the other hand, pristine powder of PPAD was fairly solvable in NMP or any other like as dimethyl sulfoxide (DMSO), THF, dimethylformamide (DMF) [42].

3.5.3   Fabrication of PANI

PANi was chemically prepared, as discussed now wise. The solution of 50 mL is prepared to contain Na$_2$S$_2$O$_8$ 16 mmol and was gradually dropwise mixed with vigorous stirring to a solvent of aniline 100 mL of 16 mmol and liquified in aqueous HCl 1.0 mol dm^{-3} for 1 h in 1°–5 °C. The as-synthesized precipitate was extracted, cleaned recurrently with HCl 1.0 mol dm^{-3}, and place in a 24 h constant vacuum. The synthesis of HCl and PANI attained the blue-colored powder with a solution of NH$_4$OH 0.1 mol dm^{-3} to create the solvable base in DMSO and NMP and produce the blue solution. The electropolymerization technique of PANi preparation is analogous to PPAD delineated earlier.

4 Conclusion

We deliver a synopsis of organic materials electrodes, counting their essential information, advancement history, and application perspective. In general, organic materials electrodes' progress has remained in the nascent stage, though 40 years of research later. Fortuitously, they depict huge prospects for ameliorating anxieties on environmental issues and resources, the limitation of the density of energy of cathode inorganic materials, and the electrochemical response discovery of electrodes organic in current ages. Amongst variational categories of organics, it is considered carbonyl compounds conjugated are auspicious in the recent scenario. Simultaneously they possess higher energy density, higher long cycle stability and higher power density value; that's why it's become the proficient one. The materials of organic electrodes are significant for batteries of the solid electrode as they can decrement the device cost, allowing flexibility, and create opportunities for working as multivalent ions, deprived of any complexity classically connected to the inorganic compounds. Numerous matters still happen and need to be addressed before organic electrodes become viable commercially, like low voltage and capacity with less cycling stability. The small molecules functionalization with ionic groups, the redox functionalities integration into organic frameworks and polymers, with the adsorption of the molecules to the graphitic-like surfaces highly conjugated are all auspicious paths to ameliorate the long cycle stability of organic molecules of redox-active and delineated to progress rest of the performance like rate capability. The modification of organic molecules configuration with EDGs or EWGs by the carbon substitution and additional electronegative atoms can deliver an effectual tune to the potential of redox. Those are predictable that the strategy is becoming popular for industry and academia both to configure inexpensive and sustainable devices of energy storage.

References

1. Tarascon, J.M., Armand, M.: Issues and challenges facing rechargeable lithium batteries. Nature **414**, 359–367 (2001)
2. Armand, M., Tarascon, J.-M.: Building better batteries. Nature **451**(7179), 652–657 (2008)
3. Poizot, P., Dolhem, F.: Clean energy new deal for a sustainable world: from non-CO_2 generating energy sources to greener electrochemical storage devices. Energy Environ. Sci. **4**(6), 2003–2019 (2011)
4. Bruce, P.G., Freunberger, S.A., Hardwick, L.J., Tarascon, J.-M.: Li–O_2 and Li–S batteries with high energy storage. Nat. Mater. **11**(1), 19–29 (2012)
5. Liang, Y., Tao, Z., Chen, J.: Organic electrode materials for rechargeable lithium batteries. Adv. Energy Mater. **2**(7), 742–769 (2012)
6. Williams, D.L., Byrne, J.J., Driscoll, J.S.: A high energy density lithium/dichloroisocyanuric acid battery system. J. Electrochem. Soc. **116**(1), 2 (1969)
7. Yoshino, A.: The birth of the lithium-ion battery. Angew. Chem. Int. Ed. **51**(24), 5798–5800 (2012)
8. Salvatierra, R.V., Oliveira, M.M., Zarbin, A.J.G.: One-pot synthesis and processing of transparent, conducting, and freestanding carbon nanotubes/polyaniline composite films. Chem. Mater. **22**(18), 5222–5234 (2010)

9. Cong, H.-P., Ren, X.-C., Wang, P., Yu, S.-H.: Flexible graphene–polyaniline composite paper for high-performance supercapacitor. Energy Environ. Sci. **6**(4), 1185–1191 (2013)
10. Visco, S.J., DeJonghe, L.C.: Ionic conductivity of organosulfur melts for advanced storage electrodes. J. Electrochem. Soc. **135**(12), 2905 (1988)
11. Liu, M., Visco, S.J., De Jonghe, L.C.: Novel solid redox polymerization electrodes: all-solid-state, thin-film, rechargeable lithium batteries. J. Electrochem. Soc. **138**(7), 1891 (1991)
12. Sotomura, T., Uemachi, H., Takeyama, K., Naoi, K., Oyama, N.: New organodisulfide—polyaniline composite cathode for secondary lithium battery. Electrochim. Acta **37**(10), 1851–1854 (1992)
13. Oyama, N.: Development of polymer-based lithium secondary battery. In: Macromol. Symp. **159**(1), 221–228 (2000)
14. Nakahara, K., Oyaizu, K., Nishide, H.: Organic radical battery approaching practical use. Chem. Lett. **40**(3), 222–227 (2011)
15. Song, Z., Zhou, H.: Towards sustainable and versatile energy storage devices: an overview of organic electrode materials. Energy Environ. Sci. **6**(8), 2280–2301 (2013)
16. Shacklette, L.W., Toth, J.E., Murthy, N.S., Baughman, R.H.: Polyacetylene and polyphenylene as anode materials for nonaqueous secondary batteries. J. Electrochem. Soc. **132**(7), 1529 (1985)
17. Zhu, L.M., Lei, A.W., Cao, Y.L., Ai, X.P., Yang, H.X.: An all-organic rechargeable battery using bipolar polyparaphenylene as a redox-active cathode and anode. Chem. Commun. **49**(6), 567–569 (2013)
18. Li, L., Tian, F., Wang, X., Yang, Z., Zhou, M., Wang, X.: Porous polythiophene as a cathode material for lithium batteries with high capacity and good cycling stability. React. Funct. Polym. **72**(1), 45–49 (2012)
19. Huang, Y.-H., Goodenough, J.B.: High-rate LiFePO4 lithium rechargeable battery promoted by electrochemically active polymers. Chem. Mater. **20**(23), 7237–7241 (2008)
20. Yin, Z., Zheng, Q.: Controlled synthesis and energy applications of one-dimensional conducting polymer nanostructures: an overview. Adv. Energy Mater. **2**(2), 179–218 (2012)
21. Song, Z., Xu, T., Gordin, M.L., Jiang, Y.-B., Bae, I.-T., Xiao, Q., Zhan, H., Liu, J., Wang, D.: Polymer–graphene nanocomposites as ultrafast-charge and-discharge cathodes for rechargeable lithium batteries. Nano Lett. **12**(5), 2205–2211 (2012)
22. Wu, Q., Xu, Y., Yao, Z., Liu, A., Shi, G.: Supercapacitors based on flexible graphene/polyaniline nanofiber composite films. ACS Nano **4**(4), 1963–1970 (2010)
23. Liu, M., Visco, S.J., De Jonghe, L.C.: Electrode kinetics of organodisulfide cathodes for storage batteries. J. Electrochem. Soc. **137**(3), 750 (1990)
24. Park, J.E., Kim, S., Mihashi, S., Hatozaki, O., Oyama, N.: Roles of metal nanoparticles on organosulfur-conducting polymer composites for lithium battery with high energy density. In: Macromol. Symp. **186**(1), 35–40 (2002)
25. Zhan, L., Song, Z., Shan, N., Zhang, J., Tang, J., Zhan, H., Zhou, Y., Li, Z., Zhan, C.: Poly (tetrahydrobenzodithiophene): high discharge specific capacity as cathode material for lithium batteries. J. Power Sources **193**(2), 859–863 (2009)
26. Janoschka, T., Hager, M.D., Schubert, U.S.: Powering up the future: radical polymers for battery applications. Adv. Mater. **24**(48), 6397–6409 (2012)
27. Wain, A.J., Wildgoose, G.G., Heald, C.G.R., Jiang, L., Jones, T.G.J., Compton, R.G.: Electrochemical ESR and voltammetric studies of lithium ion pairing with electrogenerated 9,10-anthraquinone radical anions either free in acetonitrile solution or covalently bound to multiwalled carbon nanotubes. J. Phys. Chem. B **109**(9), 3971–3978 (2005)
28. Hanyu, Y., Ganbe, Y., Honma, I.: Application of quinonic cathode compounds for quasi-solid lithium batteries. J. Power Sources **221**, 186–190 (2013)
29. Park, Y., Shin, D.-S., Woo, S.H., Choi, N.S., Shin, K.H., Oh, S.M., Lee, K.T., Hong, S.Y.: Sodium terephthalate as an organic anode material for sodium ion batteries. Adv. Mater. **24**(26), 3562–3567 (2012)
30. Nokami, T., Matsuo, T., Inatomi, Y., Hojo, N., Tsukagoshi, T., Yoshizawa, H., Shimizu, A., et al.: Polymer-bound pyrene-4,5,9,10-tetraone for fast-charge and-discharge lithium-ion batteries with high capacity. J. Am. Chem. Soc. **134**(48), 19694–19700 (2012)

31. Sakaushi, K., Hosono, E., Nickerl, G., Gemming, T., Zhou, H., Kaskel, S., Eckert, J.: Aromatic porous-honeycomb electrodes for a sodium-organic energy storage device. Nat. Commun. **4**(1), 1–7 (2013)
32. Nesvadba, P., Folger, L.B., Maire, P., Novák, P.: Synthesis of a polymeric 2,5-di-t-butyl-1,4-dialkoxybenzene and its evaluation as a novel cathode material. Synth. Met. **161**(3–4), 259–262 (2011)
33. Zhang, H., Zhang, Y., Gu, C., Ma, Y.: Electropolymerized conjugated microporous poly (zinc-porphyrin) films as potential electrode materials in supercapacitors. Adv. Energy Mater. **5**(10), 1402175 (2015)
34. Shin, J.-Y., Yamada, T., Yoshikawa, H., Awaga, K., Shinokubo, H.: An antiaromatic electrode-active material enabling high capacity and stable performance of rechargeable batteries. Angew. Chem. **126**(12), 3160–3165 (2014)
35. Li, B.-Q., Zhang, S.-Y., Kong, L., Peng, H.-J., Zhang, Q.: Porphyrin organic framework hollow spheres and their applications in lithium–sulfur batteries. Adv. Mater. **30**(23), 1707483 (2018)
36. Kazemi, S.H., Hosseinzadeh, B., Kazemi, H., Kiani, M.A., Hajati, S.: Facile synthesis of mixed metal–organic frameworks: electrode materials for supercapacitors with excellent areal capacitance and operational stability. ACS Appl. Mater. Interfaces **10**(27), 23063–23073 (2018)
37. Gao, W., Cheng, J., Yuan, X., Tian, Y.: Covalent organic framework-graphene oxide composite: A superior adsorption material for solid phase microextraction of bisphenol A. Talanta **222**, 121501 (2021)
38. Wang, P., Wu, Q., Han, L., Wang, S., Fang, S., Zhang, Z., Sun, S.: Synthesis of conjugated covalent organic frameworks/graphene composite for supercapacitor electrodes. RSC Adv. **5**(35), 27290–27294 (2015)
39. Zhao-Karger, Z., Gao, P., Ebert, T., Klyatskaya, S., Chen, Z., Ruben, M., Fichtner, M.: New organic electrode materials for ultrafast electrochemical energy storage. Adv. Mater. **31**(26), 1806599 (2019)
40. Liu, M., Zhang, Z., Chen, B., Meng, Q., Zhang, P., Song, J., Han, B.: Synthesis of thioethers, arenes and arylated benzoxazoles by transformation of the C (aryl)–C bond of aryl alcohols. Chem. Sci. **11**(29), 7634–7640 (2020)
41. Mi, C., Peng, P., Xiang, Z.: Soluble covalent organic polymer for the flexible electrode of supercapacitors. Front. Mater. **6**, 242 (2019)
42. Su, Y.-Z., Niu, Y.-P., Xiao, Y.-Z., Xiao, M., Liang, Z.-X., Gong, K.-C.: Novel conducting polymer poly [bis (phenylamino) disulfide]: synthesis, characterization, and properties. J. Polym. Sci. Part A Polym. Chem. **42**(10), 2329–2339 (2004)

Electrochemistry of Organic Electrodes

Jyoti Roy Choudhuri and Jyothi C. Abbar

Abstract Organic electrode materials received significant attention as high electroactive energy materials for storage devices and applications due to their better reactivity towards redox reaction, good specific capacity, and high electrochemical reversibility. The material components include the real more available elements like carbon, oxygen, hydrogen, nitrogen, and sulfur that can be synthesized from suitable precursors in an eco-friendly manner. This book chapter briefly highlights a detailed overview of the charge storage mechanism and its inherent characteristics. It also discusses the electrochemical features of the electrodes that can be modulated by careful adjustment of the functional groups and variation in the molecular structure. The electroactivity of these materials is not limited to the selection of charge carriers but is also capable of storing ions of varying valency. The efficiency of the organic electrodes is evaluated with respect to output performance of battery like power density, energy density, gravimetric density, cycle life and electronic conductivity. Finally, the strategies for the intensification of the electrochemical performance, major challenges, and future perspectives related to the organic electrodes are summarized. In a nutshell, this book chapter will open up new vistas in the field of energy storage devices with organic electrode materials.

Keywords Organic electrodes · Metal-ion battery · Reaction mechanism · Energy storage system · Electrochemistry

1 Introduction

On one side is the exhaustion of fossil fuels and in the contrast, there is a rise of increasing demands for energy. This has led to the global evolution in bringing the new kind of technologies in the field of renewable sources of energy and energy

J. R. Choudhuri · J. C. Abbar (✉)
Department of Chemistry, BMS Institute of Technology and Management, Avalahalli, Bengaluru, Karnataka 560064, India

Visvesvaraya Technological University, Belagavi, Karnataka 590018, India

storage. Energy storage is of vital significance for the amalgamation of fitful renewable sources of power such as solar, tidal and wind, into the grid, which is to be adopted universally in the field of electric vehicles, and also in the ongoing progress in the field of portable electronics, including emerging flexible and wearable applications. Electrochemical energy storage system (EESS) implementation in applications is exceptionally developing from micro-batteries that have a smart card, to large-scale battery packs for electric vehicles, and warehouse-sized reduction–oxidation flow batteries. Even though there is a wide range of improvements and progress in the field of EESS, there is still a gap in fulfilling the need for better performing, much versatile, minute, lighter, and economically viable energy storage solutions [1].

One of the materials that can be used for EESSs is the traditional inorganic metals such as cobalt, lead, iron, nickel, or manganese-related materials for batteries. Inorganic materials depend on the changes of the metal's oxidation state, for storing the charge and are also associated clearly with the counter-balancing of the charged structure with the particular ions. In the case of intercalation compounds for metal-ion batteries, the counter-ion is specific to the inorganic compounds crystal structure due to restriction in the reversibility of the redox reaction, ionic conductivity, and crystal lattice size. This essentially stops the versatility of the inorganic compounds, in which we cannot use the same cathode electrode material for lithium-ion and sodium-ion kind of divergent alkali batteries. The major problems of using inorganic complexes are tedious extraction and synthetic protocols that may harm our nature. Extraction methods involve the discharge of toxic materials that will get cornered underground. On the contrary, the methods that involve synthesis protocols may include a large amount of waste that comes from heavy metals and also they need energy-intensive processing. Additionally, the inherent mechanical properties of these metal oxides make it difficult for them to be used in batteries requiring mechanical flexibility unless nanostructuring is used [2]. In such a case, to realize the extensive and universal usage of EESSs, the above-mentioned challenges are to be overcome.

The other ones are organic materials. Organic materials are expected to bring a great impact on the development of novel EESSs because of their wide abundance, relatively low price, and their synthesis can be designed in such a way that they produce minimal waste and are not energy-intensive [3]. Organic compounds are also different structurally, and they allow us to functionalize them easily with many synthetic protocols. This will allow working on the redox potentials that will help in optimizing the voltages that can be feasible and better for EESSs. The best way is to modify the chemical structure and make the organic material better with better properties like ionic conductivity, rate of electron transfer, capacity retention, and solubility concern resolving to get them utilized for better applications. Also, organic materials are typically not constructed with the selection of counter ions [4]. This means that the same organic material is used for many energy storage devices like lithium-ion, sodium-ion, and multivalent-ion batteries, but up to a certain extent.

Since 1969, organic materials have been studied and literature reports the first organic cathode material as dichloroisocyanuric acid [5] for EESS. After this, a wide variety of small organic molecules were reported by many research groups,

and they were tested primarily as a cathode, after which many other conjugated polymers and derivatives were reported. Later a day arrived when the research using organic electrode materials started to fade in the energy storage field. This is when the inorganic transition metal complexes were started to develop as these complexes can intercalate reversibly the Li-ions at high potential with a high capacity [6]. But, recently again the researchers are focusing on research using organic electrode materials and this has made a huge come back due to increased demand and need for energy storage viz. high performing, inexpensive, and able to accommodate the mechanical property and forms factor needs in emerging devices such as flexible and wearable electronics.

2   Working Principle of Energy Storage Devices

Any EESSs working depends on the potential difference that is in-built and it exists between the two electrodes. This can be termed as an operating voltage. This is defined as the difference in the redox potential of a positive electrode (cathode) and a negative electrode (anode). On making a connection to an external circuit, the potential difference is used to bring the electrochemical reactions at both the electrodes which induces the electron flow from the anode to the cathode. The electron flow leads to oxidation at the anodic site and reduction at the cathodic site during discharging. The charged electrodes are stabilized by the natural accompanying of the flow of counter-ions. In this chapter, we focus on the usage of different kinds of organic electrodes in metal-ion batteries, their working principle, and their reaction mechanism.

2.1   *Metal-Ion Batteries and Their Working Principle*

Metal ion batteries are one type of solid-electrode batteries where energy is stored in solid materials that act as the negative electrode—the anode, and the positive electrode—the cathode. This is in contrast to devices, such as redox flow batteries, that store energy by a potential difference between an anolyte and catholyte where the redox species is dissolved in an electrolytic solution and can diffuse to a current collector for a redox event to occur and charge to flow. These types of batteries are found to operate with unceasing voltage which is nothing but the difference in potential between the anode and the cathode. Due to this, we can observe that, in an experiment of the galvanostatic charging and discharge, as long as the active material completely gets reduced (oxidized), the potential of the electrode or device remains persistent. A sharp redox peak observed in cyclic voltammetry indicates oxidation and reduction happening.

The components of a metal-ion battery include an anode, a cathode, electrolyte, a separator, current collectors, and proper cell casing. Let us see what each one is; Anode is a negative electrode, cathode is a positive electrode, a separator helps in preventing the internal short circuit, the current collectors are needed to collect the charge at each electrode, and finally the casing of the cell is required to keep the components intact all together and helps from getting exposed to the outside environment. Metal ion batteries involve a typical mechanism that involves the reaction between the anodes and cathodes that are charged and balanced by the metal ion. These batteries can be built with just a small amount of electrolyte because the charge balancing ions at an electrode are regularly being restored. Additionally, these batteries can be used with solid-state electrolytes too, hence these metal ion batteries become a suitable and attractive candidate due to the consideration of the mobility of only one ion.

2.2 Metal-Ion Batteries and Their Electrode Materials

Now it is known that in metal ion batteries we can make use of the prominent organic materials as anode or cathode and they can be synthesized in the no-charge state without having the charge balance making ions in the structure. To make the metal-ion batteries operate well, the opposite electrode should have the charge-balancing metal ions as a mandatory feature. As an illustration, if we have a cathode material that does not have any metal ion in its structure, then the anode material must contain metal ion and the same applies in the reverse case. The consequence is that to fulfill this requirement, a counter electrode will be used as a reduced metal like magnesium, sodium, potassium, or lithium, without bothering of whether the organic electrode is going to act as anode or the cathode electrode material.

Researchers are focusing on the usage of organic electrodes as they are of low cost without compromise in their performance. But there is a problem that the organic electrodes operate at relatively low potential when made into a full device, which restricts the total energy and power density. So, on the incorporation of electron-withdrawing groups (EWGs) to cathodes, the potential becomes high where in the organic cathode gains an electron. And on the incorporation of electron-donating groups (EDGs) to anodes, is going to lower the reduction potential, which in turn makes the operating potential high for the device. The device's total operating potential will be increased, but it decreases the C_{theor} since the electron-donating and EWGs unaltering the number of electrons that can be accepted can add weight to the compound. C_{theor} means the maximum amount of the charge that a material can carry with respect to its weight. Another way of tuning the redox potential is by substituting the heteroatoms inside an aromatic moiety and developing the isomers having any impact on the mass: charge ratio of the compound.

Another way of getting rid of this low voltages problem is to make use of those compounds that possess a high mass: charge ratio. These will have a C_{theor} and also high energy densities in a full device but not a high voltage. After looking at these,

the better way is to combine the above-mentioned two strategies i.e., of increasing voltage and also C_{theor}, together. Of course, more work has to be initiated to determine the effective accord between the C_{theor} and voltage. Now coming to the cost-related parameters especially of the organic cathodic materials. Developing materials of less price for various applications that certainly do not demand high energy or power density is important, in addition to the high and better performance of the OEMs. The organic materials in lithium-ion batteries do account for low-cost use along with it the use of electrolytes alternative to lithium can also provide a huge cut down in the price of the device. But lithium is the most expensive one, as it involves the lowest reduction potential and the other one is the highest C_{theor} among other alkali metals. Also, one can expect that cost of lithium will continue to become higher due to the destruction and exhaustion of the resources [3]. Also, note that the pure organic and polymer-based materials can be used as electrode materials for these metal-ion batteries.

3 Reaction Mechanisms in Organic Batteries

We will now study different kinds of mechanisms that the organic electrode materials can undergo.

3.1 Disulfide Reaction

Visco et al. was the one who initiated the use of organosulfur compounds as positive electrode materials in rechargeable batteries [7]. It was studied that the disulfide groups (RS-SR) present in the organosulfur compounds can react reversibly with the Na$^+$ ions and the electrons will generate sodium thiolate (RS–Na$^+$). These organosulfur electrode materials can work from ambient to 150 °C. But, these organosulfur compounds are electrolyte soluble which results in diminished cycle life. Also, thiolates reformation or re-establishment of the disulfide bond gets hindered by a large steric hindrance. To reduce this hindrance effect, a side chain of the anthracene is confined with disulfide groups, which is beneficial for the reconnection of thiolates [8]. The anthracene-based cathode material can reversibly couple with 6 Li$^+$ and 6 e$^-$, which leads to the dissociation as well as the reformation of the disulfide bonds. But it suffers a major drawback regarding solubility and diminished conductivity issues. For overcoming these issues, polymers of organosulfur were synthesized and the polymeric form of the organosulfur was found to have lower solubility issues with organic electrolytes. The disulfide group that is present in the side chain in the polymer is advantageous for the refixing of thiolates [9]. Thus, the polyaniline and polyanthracene derivatives that have the disulfide groups were shown to be the supreme electrode material acting as a cathode in the rechargeable Li batteries [8, 10]. The derivative of polyanthracene has a conjugated chain structure,

that results in better electronic conductivity. The presence of thiolates reduces the steric hindrance of the reformation of the disulfide bond. It showed 300 mAh g^{-1} as high specific capacity with a pair of reversible charging and discharging plateaus at approx. 2.5 V in the 2nd cycle. Solubility issues of the organosulfur polymer and also increasing the organosulfur polymer's reaction kinetics are to be addressed.

In anthra[1′,9′,8′-b,c,d,e][4′,10′,5′-b′,c′,d′,e′]bis-[1,6,6a(6a-SIV)trithia] penta-lene (ABTH), disulfide groups are joined to anthracene, comprising of 3 conjugated benzene rings. The addition of a number of benzene rings to the conjugated structure, high specific capacity, and long cycle life, resulted because of the crystals' strong intermolecular interactions, this plays a vital and key character in good crystal structure maintenance at the time of battery cycling [11]. Along with enlarging the conjugated structure, another way of improving electrochemical performance is by carrying out polymerization. For example, ABTH monomer when polymerized to PABTH polymer, its initial capacity 180–300 mAh g^{-1} was increased due to the high electric conductivity nature of the polymer [8]. Poly[bis(2-aminophenyloxy)disulfide] PAPOD is an organic sulfur. In this structure, there are disulfide groups present as cross-links [10]. The cross-links that are present in the chain of polyaniline in PAPOD, increase the electronic conductivity thereby solving solubility issues in the electrolyte. However, even though the starting capacity is more in comparison to the inorganic electrodes as cathode, still cyclic stability needs to be improved.

3.2   Reaction of an Anion Insertion

Next comes the anion insertion reaction that includes a study on the nitroxide free radicals, amino groups, and heteroatoms. The nitroxide free radicals come under the bipolar organics. Here the nitroxide free radical can gain the Li ions to undergo reduction to a negatively charged state or can gain anions to undergo oxidization to a positively charged state. The mechanism in which the insertion of the anion involves the reaction between a polymeric-free radical and anions. At first, the electrons that are present in the outer shell of the nitroxide radical are moved to a higher reaction potential where in the oxidization to an oxoammonium cation takes place. This can further have bonding with anions like PF_6^-, TFSI$^-$ and ClO^{4-} [12]. The higher electrochemical activity of the free radicals influences faster reaction kinetics between the anions and the nitroxide radical. On contrary, free radical-based polymers may witness higher solubility problems, through which self-discharge occurs. To make the dissolution issue be solved, an attempt was made to attach the nitroxide radical to the backbone of a polymer as it is non-conductive [13]. Another way is to finally anchor the polymeric nitroxide free radical with nanotubes, graphene, and reduced graphene oxide [14]. Such resulted carbon-based free radical composites exhibited an outstanding performance of the battery and the reaction kinetics could be upgraded and also the solubility issue could be solved.

Next is the 2,2,6,6-tetramethylpiperidin-1-oxyl-4-yl (TEMPO) which is one of the most famous nitroxide free radical containing compounds. Organic free-radical polymers usually contain TEMPO in their side chain as an electrochemical active site. A few years ago, Oyaizu et al. made a cross-linkable polynorbornene containing TEMPO, which showed an electrochemical behavior in an electrolyte based on acetonitrile [15]. But they also suffered from dissolution issues showing less capacity, so an attempt was made to use the inorganic insoluble hosts like nanotubes, and graphene or reduced graphene oxide, thereby making the stable organic battery based on TEMPO [16, 17]. Later, poly(2,2,6,6-tetramethylpiperidinyloxy-4-vinylmethacrylate) (PTMA) was studied by Kim et al. in association with carbon nanotubes [12]. Pyrene-functionalized PTMA along with reduced graphene oxide (rGO) was studied by Zhang et al. who stabilized them with a $\pi-\pi$ stacking interaction between rGO and pyrene [18]. In both cases, long cycle life, reversible capacity, fast charging rate were observed. Thus looking at such illustrations we can say that the organic radical polymers with carbon framework are stabilized and can be the best electrode materials for rechargeable batteries.

OEMs with anion insertion reactions can provide a better vista in developing organic cathode materials with high potential. They can help in all such cases where the organic cathodes show low discharge potential like 2–3 V and also such cases where cannot be lithium source. As already seen the anions like PF_6^-, ClO_4^-, $TFSI^-$, are incorporated into organic materials, at high reaction potentials once the out-shell electrons are taken by the functional groups [18–20]. The potential of such a reaction occurs later than 3 V [21, 22]. As lithium-ion for the p-type active material is not required, it can be matched with some other anode materials that can have lithium-ion insertion type, for making a two-ion full cell [23].

3.3 Azo Reaction

In LIBs the azo group (N=N) is observed to be one of the electrochemically active sites [24]. Here what happens is the azo group that has a double bond gets changed to a single bond at the time of the lithiation and vice versa happens at the de-lithiation process. The interesting fact during the lithiation/de-lithiation process is that each of the present nitrogen atoms combines with 1 Li-ion and $1e^-$. Such a reversible process plays a vital role in the electrochemical process of LIBs in the case of azo-based compounds. Here also a high solubility issue is observed in an electrolyte that will lead to capacity fading. The strategy that is done to overcome the solubility issue of azobenzene by the addition of carboxylate group in the azobenzene leads to the generation of a methyl red sodium salt (MRSS) as well as azobenzene 4,4′-dicarboxylic acid lithium salt (ADALS). The ADALS with two carboxylate groups was found to be insoluble in the electrolyte, and also it exhibited extraordinary electrochemical performance in LIBs. It was shown to retain the reversible capacities (126 and 93 mAh g^{-1} for completion of 5000 cycles) and high current density (10C and 20C). This all happened due to the presence of two carboxylate units, which

results in the decrease in solubility of the compound leading to long cycle life. The enhancement in the rate of charge and discharge capability can be explained due to the extended π-conjugation present in the two benzene rings, facilitating the diffusion of an electron as well as lithium-ion. Hence, carboxylated azo compounds are better anode materials in the case of LIBs.

As we saw that aromatic azo compounds' cyclic stability is restricted due to their organic electrolyte dissolution issue. In MRSS, a carboxylate group is present, but the presence of 3° amine group leads to an electrolytic dissolution issue, thereby resulting in low cycle life. For overcoming this issue, two carboxylate groups are included in the aromatic azo compound and prepared ADALS. This may be attributed due to the salt formation of ADALS that increases azo compounds' polar nature. The need for low molecular weight and azo-based conjugated polymers needs to receive better specific capacity and increased electronic conductivity.

3.4 Carbonyl Reaction

Now let us see how the reaction mechanism in carbonyl compounds takes place. This is based on the electrochemical reaction that is reversible in between the Li ions and >C=O groups that are present in the conjugated organic framework. In this case, two or more >C=O groups are needed for reacting with the lithium ions, further including an intramolecular electron transfer within the conjugated organic framework [25]. Two types of carbonyl compounds viz. quinone derivatives and organic anodes of carboxylate derivatives are studied and reported [22, 26]. These >C=O compounds can be employed in the case of rechargeable batteries as electrode materials, even in nonaqueous based various ion (Na^+, Li^+, and K^+) batteries, including batteries involving multivalent ions, and also aqueous batteries. Let us now study (1) anodes of carboxylate; (2) cathodes of quinone; (3) >C=O based electrode materials one by one in this chapter.

Having a high capacity, low reaction potential, and easy modification in the structure are the highlights of employing the organic batteries that have the groups containing carboxylate in the organic anode materials. Here two or more carboxylate groups are found to be electrochemically active and are attached to benzene ring conjugated structure. At the process of lithiation and de-lithiation, the two carbonyls in the carboxylate groups of the di-lithium terephthalate were found to react reversibly with two Li-ions and two e$^-$ leaving with the good capacity of 234 mAh/g even after 50 cycles of charge and discharge. At the same time, the rearrangement of double bonds takes place due to intramolecular transfer within the conjugated structure.

Next is the quinone derivatives where the carbonyl group-based OEMs are used as the organic cathodes. The problem with these is that they don't have the lithium source for the redox reaction. So it needs the lithium source from the anodic site. Of course, there are a few organic cathodes that do have the carbonyl groups, that have lithium sources, but they are sensitive to oxygen and moisture and also electrode fabrication has to be done carefully. But there is one exception which is air-stable as well as a

lithiated cathode material i.e.,1,4-benzenedisulfonate backbone [27]. Two sulfonate groups improvise the reaction potential to approx. 3.25 V, retains reversible capacity 100 mAh g^{-1} at C/20 for 50 cycles. One more exception is the carboxyphenolate-based material that has magnesium substitution that is air-stable and 0.8 V potential increase after halfway replacement of Li$^+$ by Mg^{2+} [28]. The partly replacing Li-ions with Mg ions helps in the electronic effects giving rise in the potential in the redox-active organic skeleton. It has 2 magnesium oxide groups and 2 carboxylate groups acting as cathode and anode centers for reduction and oxidation respectively. Few more carbonyl group-based polymers like polyanthraquinone useful for electric vehicle applications also show charge–discharge capability and high cyclic stability [29]. According to their research polyanthraquinone cathode was known to show a reversible capacity of ~120 mAh/g for 1000 cycles at 1 and 2 C and at a high current density of 20 C it can be charged and discharged, referring to 3 min each charge and discharge. Surface reaction-controlled kinetics is the main reason behind this fast charge and discharge capability of polyanthraquinone and it is because of the amorphous quinone polymer. Likewise in LiBs carbonyl-based OEMs due to their quick reaction kinetics, has opened a pathway for becoming a best cathode materials for even the multivalent metal batteries as they face slow reaction kinetics.

3.5 Imine Reaction

Here we can observe that the nitrogens present in the imine group (C=N) and lithium ions reversibly react. Imine groups are attached to a benzene ring. This involves the intramolecular transfer of electrons in its conjugated system. Let us consider an illustration of π-conjugated quinoxaline-based heteroaromatic molecules (3Q) reported by Peng et al. [30]. The reaction proceeds via a two-step mechanism. In the 1st step, one Li-ion reacts with two –N in the imine groups. The 6 imine groups react with 3 Li-ions such that 2 Ns share a Li-ion and form an N–Li–N structure. In the 2nd step, the Li-ion further reacts with the N–Li–N structure and forms the Li–N structure so that the 2 –N are going to share 2 Li-ions. The 6 imine groups in 3Q could react with 6 Li-ions and 6 e$^-$. Reversible capacity (395 mAh/g), a current density of (400 mA/g), high cycling stability (10,000 cycles) was found for 3Q, which is reported to be the best cyclic performance lives in LIBs. Thus quinoxaline-based imine cathode provides a new light in designing organic batteries with its high energy density, high capacity, and superior longest cycle life.

The organic materials, LC, ALX, 2Q, and 3Q, are found to show quick reaction kinetics (>20 C) and longest cycle life in association with nanotubes and graphene [30, 31]. To prevent dissolution issues and improve the conductivity and cyclic stability, decrease the overall energy density, we need to make use of a more % of conductive carbon additive (>50 wt%) along with them. One more way is to make the polymerization of the organic compounds. [32–34]. Usually, polymers are expected to show specific capacity in comparison to the small organic materials and result in ultra-high capacity which is due to the exfoliated organic nanosheets with

2D structure facilitating the transfer of ion/electron with many sites for oxidation and reduction for the storage of Li.

3.6 Superlithiation Reaction

The kind of mechanism with superlithiation reaction takes place when the conjugated hydrocarbon like polyacetylene (PAc), that has an unsaturated C–C bond and is then converted to a saturated C–C bond during the process of discharging [35]. This happens usually at fewer potentials based on many reported works. The mechanism involves the conversion of unsaturated C–C bonds in the OEMs to saturated C–C bonds. As a result, during the discharge, each carbon atom is capable of binding to a Li-ion and an e^-. In naphthalenetetracarboxylic dianhydride (NTCDA), the C=O combines with Li-ions and e^-. Then, the unsaturated C–C bonds react with Li-ions and e^- at low reaction potentials. The reaction mechanism crosses a massive high capacity of 1000 mAh/g. The anodes involving unsaturated carbon–carbon and carbonyl groups were reported to provide a high specific capacity in LIBs. The detailed reaction involving the reduction of NTCDA by Li ions takes place via two steps [36]. Firstly, 4 Li-ions react with the 4 carbonyl groups 2.61–1.04 V potential window, with the electron transfer in the two benzene rings. Secondly, in a conjugated organic framework, 14 lithium ions are found to react to change C=C to C–C in 1.04 to 0.001 V potential window. A high specific capacity (1800 mAh/g), current density (20 mA/g), 5 times more than commercial graphite anode is obtained throughout the lithiation process of NTCDA. In the case of maleic acid as an example of an anode, an ultrahigh specific capacity (1500 mAh/g), current density (46.2 mA/g) was reported [37]. The theoretical capacity is 116.7 mAh/g but practical capacity was higher than this. This may be due to the adsorption of the Li-ions on the surface. Therefore superlithiation reaction-based anodes are better ones in LIBs.

4 Application of Organic Electrodes Beyond LIBs

So far we got to know that OEMs are extensively employed including the nonaqueous lithium-ion, sodium-ion, potassium-ion, dual or two-ion batteries, multivalent metal batteries, and aqueous batteries. When we start to think beyond lithium batteries, let's start with sodium-ion batteries SIBs. So here, Sodium 4,4′-stilbene-dicarboxylate (SSDC) was used as one of the first fast charging and discharging organic anodes [38]. The fast charging and discharging capability of this compound can be explained due to the extended π-conjugated system, this improvises the charge transport mechanism and also stabilizes the charged and discharged states of SSCD. To get the fast charging and discharging in the organic anode focusing on enlarging the conjugated structure of the organic frameworks is needed. To boost further the capacity of organic anodes in sodium-ion batteries, In organic thiocarboxylate electrodes, Zhao et al. showed in

their work that for replacement of oxygen, sulfur is employed as the redox centers [39]. This is similar to the carboxylate electrodes reaction mechanism, but in this case, thiocarboxylate electrode capacity was able to equate to 567 mAh/g at 50 mA/g which is due to the benzene and sodium ions reaction. By doing the doping sulfur into the carboxylate electrodes, one can improve the battery capacity, electron density as well as conductivity.

Among the various electrode materials that are used for sodium-ion batteries, disodium rhodizonate ($Na_2C_6O_6$) is one such organic cathode that is known to show high energy. Lee et al. in their research showed that $Na_2C_6O_6$ attain a high reversible capacity of 484 mAh/g, energy density of 726 Wh/kg, and energy efficiency greater than 87% and also better cycle retention was shown due to the synergy of the nanostructure and the electrolyte as ether-based [40]. Another quinone-based polymer was reported by Tang et al. i.e., polypentacenetetrone sulfide, with a capacity approx. 290 mAh/g, fast-charge capability approx. 160 mAh/g at 10 A/g and 100 mAh/g at 50 A/g, respectively, and 10,000 ultra-long cycle life [41]. For SIBs, Pyrene functionalized poly(2,2,6,6-tetramethyl piperidiny-1-oxyl-4-yl methacrylate) was studied by Hu et al. that showed high voltage [42]. Like this many organic-based electrodes have been studied and have shown better performance.

OEMs show an exceptional electrochemical performance even in potassium ion batteries KIBs making them universal electrode materials for alkali-ion batteries. This is due to their good structural flexibility and modification ability. In LIBs, SIBs, and KIBs, oxocarbon salts as organic electrodes that can be used [43]. Here, the carbonyl groups play as electroactive centers that react reversibly with Na^+, Li^+, and K^+ in the salts of oxocarbon. The 1.25 M KPF_6-dimethoxyethane electrolyte in KIBs showed ionic conductivity that is higher compared to commonly used PF_6^- electrolytes of LIBs and SIBs. Thus potassium rhodizonate results in fast reaction kinetics (212 mAh/g at 0.2 C and 164 mAh/g at 10 C). This kind of work with efficient electrolytes and OEMs becomes universal electrodes for alkali-ion batteries, and also opens up a new path in developing the advanced OEMs for KIBs as well.

Now let's see what happens in the case of the multivalent metals like Mg, Al batteries. As seen earlier, OEMs having carbonyl groups are the universal electrodes for alkali metals, same can also be used to work with multivalent metals like Mg, Al batteries, which are currently known to make an alternative to LIBs. These are advantageous because of their less price, more abundant, having high volumetric energy density, dendrite free nature [44]. Mg^{2+} and Al^{3+} have strong interaction with the host materials, due to which all cathode materials used for alkali-ion batteries do not suit multivalent metal batteries. So far the chevre phase Mo_6S_8 as a cathode is being fortunate for rechargeable Mg and Al batteries. But it suffered decreased capacity, slow reaction kinetics, and low cycle life. To sort these difficulties, OEMs that are lightweight, available easily, less priced and high sustainability can be the universal cathodes for rechargeable Mg and Al batteries [45].

The various advantages and likely uses of organic electrode materials in different types of rechargeable batteries are portrayed as shown in Fig. 1 [46].
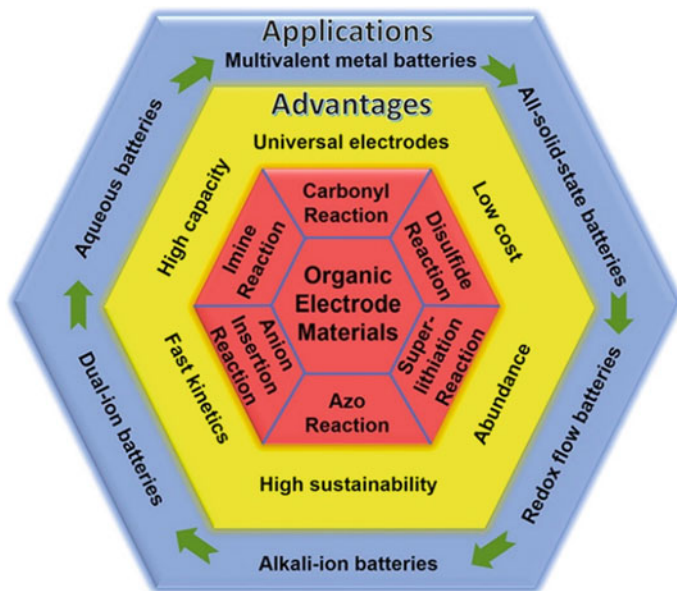
Fig. 1 Organic electrodes with their various advantages and potential applications in rechargeable batteries. Adapted with permission from [46]. Copyright (2020), American Chemical Society

5 Conclusions and Outlook

100s of OEMs are designed and synthesized with reaction mechanisms for rechargeable batteries including the non-aqueous and multivalent metal ion batteries which are proved to show improved electrochemical performance. Wide temperature range (−70 to 150 °C), a wide pH range (1–145), atmosphere (with/without O_2) kind of extreme conditions can be employed for the study using these organic batteries. These OEMs can be employed in rechargeable batteries as the best alternatives for the costly and toxic inorganic counterparts. We found that there are difficulties and concerns to the low electronic conductivity and the dissolution issue in the electrolyte that stops them from undergoing large-scale applications. But we also saw that these issues can be resolved in many possible ways like (1) getting a strong $\pi-\pi$ interaction in between the OEMs and conductive carbon materials like graphene and nanotubes. This will help to solve the dissolution problem in electrolyte and improve the conductivity, and (2) another one is the extension of the π-conjugated system in the OEMs to ease the diffusion of the Li-ion and incorporate carboxylate groups to minimize the solubility concerns; (3) The polarity of the material can be increased and also reduces the solubility by synthesizing new organic salts; (4) organic materials must be polymerized so that they to form long chains and cross-linked insoluble polymers [47]; (5) Liquid electrolyte to be replaced with solid electrolytes which can

provide a solution to the dissolution challenge. By following these above-mentioned strategies one can achieve high rate capability and long cycle life OEMs.

The organic batteries do suffer low energy density that is lower than the inorganic materials-based batteries, it is due to many organic cathodes reaction potential that is less than the inorganic ones. Also, more quantity of the conductive carbon is required in the case of the organic electrodes. However, by looking and considering some of the best features of organic batteries, we can say that they find their suitability for applications in smart grids and wind/solar power plants. Focus has to be made on the potential enhancement of the Li-ion insertion-based organic cathodes by modifying the molecular structure and also by incorporating the electron-withdrawing groups; next is to increase the capacity of the p-type organic materials by instituting many active sites and molecular weight reduction. Alternative to LIBs, multivalent metal batteries are also of importance nowadays. In these, most of the inorganic materials are inactive electrochemically, due to more charge density of Mg^{2+} and Al^{3+}, and trickier intercalation chemistry. Moreover, modification of the molecular structure and OEMs with diverse structural features helps even the multivalent batteries to achieve high capacity. By using anion insertion reactions, by instigating more functional groups in the organic structure, as studied like carbonyl groups, azo groups, imine groups, the theoretical capacity of organic cathodes can be improvised. Thus, high cyclic stability and fast charging and discharge capability in LIBs by using many OEMs are proved so far to be the most promising cathodes and similar strategies can be expected and make them also likely looking to be the best OEMs even in the case of the multivalent metal batteries too.

References

1. Lewis, N.S.: Research opportunities to advance solar utilization. Science **351**, 6271 (2016)
2. Liu, W., Song, M.S., Kong, B., Cui, Y.: Flexible and stretchable energy storage: recent advances and future perspectives. Adv. Mater. **29**(1), 1603436 (2017)
3. Larcher, D., Tarascon, J.-M.: Towards greener and more sustainable batteries for electrical energy storage. Nat. Chem. **7**(1), 19–29 (2015)
4. Hernández-Burgos, K., Rodríguez-Calero, G.G., Zhou, W., Burkhardt, S.E., Abruña, H.D.: Increasing the gravimetric energy density of organic based secondary battery cathodes using small radius cations (Li^+ and Mg^{2+}). J. Am. Chem. Soc. **135**(39), 14532–14535 (2013)
5. Williams, D., Byrne, J.J., Driscoll, J.S.: A high energy density lithium/dichloroisocyanuric acid battery system. J. Electrochem. Soc. **116**(1), 2 (1969)
6. Mizushima, K., Jones, P., Wiseman, P., Goodenough, J.B.: Li_xCoO_2 ($0 < x < -1$): a new cathode material for batteries of high energy density. Mater. Res. Bull. **15**(6), 783–789 (1980)
7. Visco, S.J., Mailhe, C.C., De Jonghe, L.C., Armand, M.B.: A novel class of organosulfur electrodes for energy storage. J. Electrochem. Soc. **136**(3), 661 (1989)

8. Xue, L., Li, J., Hu, S., Zhang, M., Zhou, Y.H., Zhan, C.M.: Anthracene based organodisulfide positive active materials for lithium secondary battery. Electrochem. Commun. **5**(10), 903–906 (2003)

9. Liu, Z., Kong, L., Zhou, Y.H, Zhan, C.M.: Polyanthra [1,9,8-b,c,d,e][4,10,5-b,c,d,e] bis-[1,6,6a(6a-S) trithia] pentalene-active material for cathode of lithium secondary battery with unusually high specific capacity. J. Power Sources **161**(2), 1302–1306 (2006)

10. Su, Y.-Z., Dong, W., Zhang, J.-H., Song, J.-H., Zhang, Y.-H., Gong, K.C.: Poly [bis (2-aminophenyloxy) disulfide]: a polyaniline derivative containing disulfide bonds as a cathode material for lithium battery. Polymer (Guildf) **48**(1), 165–173 (2007)

11. Hu, P., He, X., Ng, M.-F., Ye, J., Zhao, C., Wang, S., Tan, K., Chaturvedi, A., Jiang, H., Kloc, C., Hu, W., Long, Y.: Trisulfide-bond acenes for organic batteries. Angew. Chem. Int. Ed. **131**(38), 13647–13655 (2019)

12. Kim, J.K., Kim, Y., Park, S., Ko, H., Kim, Y.: Encapsulation of organic active materials in carbon nanotubes for application to high-electrochemical-performance sodium batteries. Energy Environ. Sci. **9**(4), 1264–1269 (2016)

13. Hansen, K.-A., Nerkar, J., Thomas, K., Bottle, S.E., O'Mullane, A.P., Talbot, P.C., Blinco, J.P.: New spin on organic radical batteries–an isoindoline nitroxide-based high-voltage cathode material. ACS Appl. Mater. Interfaces **10**(9), 7982–7988 (2018)

14. Choi, W., Ohtani, S., Oyaizu, K., Nishide, H., Geckeler, K.E.: Radical polymer-wrapped SWNTs at a molecular level: high-rate redox mediation through a percolation network for a transparent charge-storage material. Adv. Mater. **23**(38), 4440–4443 (2011)

15. Oyaizu, K., Ando, Y., Konishi, H., Nishide, H.: Nernstian adsorbate-like bulk layer of organic radical polymers for high-density charge storage purposes. J. Am. Chem. Soc. **130**(44), 14459–14461 (2008)

16. Li, Y., Jian, Z., Lang, M., Zhang, C., Huang, X.: Covalently functionalized graphene by radical polymers for graphene-based high-performance cathode materials. ACS Appl. Mater. Interfaces **8**(27), 17352–17359 (2016)

17. Wen, L., Li, F., Cheng, H.M.: Carbon nanotubes and graphene for flexible electrochemical energy storage: from materials to devices. Adv. Mater. **28**(22), 4306–4337 (2016)

18. Zhang, K., Hu, Y., Wang, L., Monteiro, M.J., Jia, Z.: Pyrene-functionalized PTMA by NRC for greater π–π stacking with rGO and enhanced electrochemical properties. ACS Appl. Mater. Interfaces **9**(40), 34900–34908 (2017)

19. Deunf, E., Moreau, P., Quarez, E., Guyomard, D., Dolhem, F., Poizot, P.: Reversible anion intercalation in a layered aromatic amine: a high-voltage host structure for organic batteries. J. Mater. Chem. A **4**(16), 6131–6139 (2016)

20. Rodríguez-Pérez, I.A., Ji, X.: Anion hosting cathodes in dual-ion batteries. ACS Energy Lett. **2**(8), 1762–1770 (2017)

21. Wild, A., Strumpf, M., Häupler, B., Hager, M.D., Schubert, U.S.: All-organic battery composed of thianthrene-and TCAQ-based polymers. Adv. Energy Mater. **7**(5), 1601415 (2017)

22. Kolek, M., Otteny, F., Becking, J., Winter, M., Esser, B., Bieker, P.: Mechanism of charge/discharge of poly (vinylphenothiazine)-based Li–organic batteries. Chem. Mater. **30**(18), 6307–6317 (2018)

23. Speer, M.E., Kolek, M., Jassoy, J.J., Heine, J., Winter, M., Bieker, P.M., Esser, B.: Thianthrene-functionalized polynorbornenes as high-voltage materials for organic cathode-based dual-ion batteries. Chem. Commun. **51**(83), 15261–15264 (2015)

24. Luo, C., Borodin, O., Ji, X., Hou, S., Gaskell, K.J., Fan, X., Chen, J., Deng, T., Wang, R., Jiang, J., Wang, C.: Azo compounds as a family of organic electrode materials for alkali-ion batteries. Proc. Natl. Acad. Sci. U. S. A. **115**(9), 2004–2009 (2018)

25. Wu, Y.L., Horwitz, N.E., Chen, K.S., Gomez-Gualdron, D.A., Luu, N.S., Ma, L., Wang, T.C., Hersam, M.C., Hupp, J.T., Farha, O.K., Snurr, R.Q., Wasielewski, M.R.: G-quadruplex organic frameworks. Nat. Chem. **9**(5), 466–472 (2017)

26. Zhu, H., Yin, J., Zhao, X., Wang, C., Yang, X.: Humic acid as promising organic anodes for lithium/sodium ion batteries. Chem. Commun. **51**(79), 14708–14711 (2015)

27. Lakraychi, A., Deunf, E., Fahsi, K., Jimenez, P., Bonnet, J.-P., Djedaini-Pilard, F., Bécuwe, M., Poizot, P., Dolhem, F.: An air-stable lithiated cathode material based on a 1, 4-benzenedisulfonate backbone for organic Li-ion batteries. J. Mater. Chem. A **6**(39), 19182–19189 (2018)

28. Jouhara, A., Dupré, N., Gaillot, A.-C., Guyomard, D., Dolhem, F., Poizot, P.: Raising the redox potential in carboxyphenolate-based positive organic materials via cation substitution. Nat. Commun. **9**(1), 1–11 (2018)

29. Song, Z., Qian, Y., Gordin, M.L., Tang, D., Xu, T., Otani, M., Zhan, H., Zhou, H., Wang, D.: Polyanthraquinone as a reliable organic electrode for stable and fast lithium storage. Angew. Chem. Int. Ed. **127**(47), 14153–14157 (2015)

30. Peng, C., Ning, G.H., Su, J., Zhong, G., Tang, W., Tian, B., Su, C., Yu, Di., Zu, L., Yang, J., Ng, M.F., Hu, Y.S., Yang, Y., Armand, M., Loh, K.P.: Reversible multi-electron redox chemistry of π-conjugated N-containing heteroaromatic molecule-based organic cathodes, Nat. Energy **2**(7), 1–9 (2017)

31. Hong, J., Lee, M., Lee, B., Seo, D.-H., Park, C.B., Kang, K.: Biologically inspired pteridine redox centres for rechargeable batteries. Nat. Commun. **5**(1), 1–9 (2014)

32. Wang, J., Chen, C.S., Zhang, Y.: Engineering, Hexaazatrinaphthylene-based porous organic polymers as organic cathode materials for lithium-ion batteries. ACS Sustain. Chem. Eng. **6**(2), 1772–1779 (2018)

33. Schon, T.B., Tilley, A.J., Bridges, C.R., Miltenburg, M.B., Seferos, D.S.: Bio-derived polymers for sustainable lithium-ion batteries. Adv. Funct. Mater. **26**(38), 6896–6903 (2016)

34. Lei, Z., Chen, X., Sun, W., Zhang, Y., Wang, Y.: Exfoliated triazine-based covalent organic nanosheets with multielectron redox for high-performance lithium organic batteries. Adv. Energy Mater. **9**(3), 1801010 (2019)

35. Shacklette, L.W., Toth, J.E., Murthy, N.S., Baughman, R.H.: Polyacetylene and polyphenylene as anode materials for nonaqueous secondary batteries. J. Electrochem. Soc. **132**(7), 1529 (1985)

36. Han, X., Qing, G., Sun, J., Sun, T.: How many lithium ions can be inserted onto fused C_6 aromatic ring systems? Angew. Chem. Int. Ed. **124**(21), 5237–5241 (2012)

37. Wang, Y., Deng, Y., Qu, Q., Zheng, X., Zhang, J., Liu, G., Battaglia, V.S., Zheng, H.: Ultrahigh-capacity organic anode with high-rate capability and long cycle life for lithium-ion batteries. ACS Energy Lett. **2**(9), 2140–2148 (2017)

38. Wang, C., Xu, Y., Fang, Y., Zhou, M., Liang, L., Singh, S., Zhao, H., Schober, A., Lei, Y.: Extended π-conjugated system for fast-charge and-discharge sodium-ion batteries. J. Am. Chem. Soc. **137**(8), 3124–3130 (2015)

39. Zhao, H., Wang, J., Zheng, Y., Li, J., Han, X., He, G., Du, Y.: Organic thiocarboxylate electrodes for a room-temperature sodium-ion battery delivering an ultrahigh capacity. Angew. Chem. Int. Ed. **129**(48), 15536–15540 (2017)

40. Liang, Y., Luo, C., Wang, F., Hou, S., Liou, S.C., Qing, T., Li, Q., Zheng, J., Cui, C., Wang, C.: An organic anode for high temperature potassium-ion batteries. Adv. Energy Mater. **9**(2), 1802986 (2019)

41. Tang, M., Zhu, S., Liu, Z., Jiang, C., Wu, Y., Li, H., Wang, B., Wang, E., Ma, J., Wang, C.: Tailoring π-conjugated systems: from π−π stacking to high-rate-performance organic cathodes. J. Mater. Chem. A **4**(11), 2600–2614 (2018)

42. Hu, Y., Zhang, K., Hu, H., Wang, S., Ye, D., Monteiro, M.J., Jia, Z., Wang, L.: Molecular-level anchoring of polymer cathodes on carbon nanotubes towards rapid-rate and long-cycle sodium-ion storage. Mater. Chem. Front. **2**(10), 1805–1810 (2018)

43. Zhao, Q., Wang, J., Lu, Y., Li, Y., Liang, G., Chen, J.: Oxocarbon salts for fast rechargeable batteries. Angew. Chem. Int. Ed. **55**(40), 12528–12532 (2016)

44. Pan, B., Zhou, D., Huang, J., Zhang, L., Burrell, A.K., Vaughey, J.T., Zhang, Z., Liao, C.: 2, 5-dimethoxy-1, 4-benzoquinone (DMBQ) as organic cathode for rechargeable magnesium-ion batteries. J. Electrochem. Soc. **163**(3), A580 (2016)

45. Rodríguez-Pérez, I.A., Yuan, Y., Bommier, C., Wang, X., Ma, L., Leonard, D.P., Lerner, M.M., Carter, R.G., Wu, T., Greaney, P.A., Lu, J., Ji, X.: Mg-ion battery electrode: an organic solid's

herringbone structure squeezed upon Mg-ion insertion. J. Am. Chem. Soc. **139**(37), 13031–13037 (2017)

46. Shea, J., Luo, C.: Organic electrode materials for metal ion batteries. ACS Appl. Mater. Interfaces **12**(5), 5361–5380 (2020)
47. Zhang, K., Hu, Y., Wang, L., Fan, J., Monteiro, M.J., Jia, Z.: The impact of the molecular weight on the electrochemical properties of poly (TEMPO methacrylate). Polym. Chem. **8**(11), 1815–1823 (2017)

Basic and Advanced Considerations of Energy Storage Devices

Antonia Sandoval-González, Erika Bustos, and Carolina Martínez-Sánchez

Abstract The main source of electrical energy consumed by humanity comes from fossil fuel and cannot be stored, it also has low conversion efficiencies and generates environmental pollutants such as CO_2, NO_x, SO_x, as well as lead, and other toxic metals. Another problem for energy management systems is the development of efficient storage techniques. A solution to the second problem requires innovative technologies in the design, manufacture, and characterization of energy storage devices (ESD) to improve efficiency and life while avoiding losses. Immediate attention to electrochemical reactions used in this ESD seeking those having the highest exchange current densities is needed. Additionally, a study of the physical structure of electrodes and the use of minimum molecular weight reagents to be used in the storage systems require scientific study efforts. Significant advances have been ongoing to develop promising organic materials with applications in ESD. However, it is necessary to solve further challenges with storage technology. These include developing electrodes offering high energy density, long life at low cost, and systems that operate at high electrocatalytic activity. This chapter presents the basic and advanced science and engineering aspects of ESD. It includes a basic introduction to their scientific principles, engineering fabrication, and characterization methods needed to understand ESD operation. It also includes information about current advances in ESD technology. Finally, it discusses the importance and the limitations that the use of organic materials has on ESD performance and their role in the environmental impact and utilization of ESD.

Keywords Battery · Capacitor · Charge–discharge · Energy storage · Organic electrode

A. Sandoval-González · E. Bustos · C. Martínez-Sánchez (✉)
CONACYT-Centro de Investigación y Desarrollo Tecnológico en Electroquímica, CIDETEQ, 76703 Pedro Escobedo, Querétaro, Mexico
e-mail: csanchez@cideteq.mx

1 Introduction

We currently live in a world highly dependent on electricity to perform a myriad of life activities as well as for information and communication technologies. In addition to this, the COVID-19 pandemic has made us even more dependent on portable electronic devices to perform basic activities. Some of these include online teaching and learning, communication with family and friends, working in a home office, enjoying leisure activities, and many others. Electric energy can be easily generated, transported, and transformed, even if relatively inefficiently while mostly using fossil fuels. However, until now it has not been possible to store it in practical and inexpensive ways. Humankind needs to look for alternative sources of energy, while quickly developing improved energy storage systems to support these evolving technologies. For this reason, it is important to design energy storage devices (ESD) meeting the criteria shown in Fig. 1.

Electrochemical energy storage (ECES) is a promising energy storage option based on these criteria. ECES incorporates high energy density, contaminant-free operation, high efficiency, long useful life, low maintenance cost, and good operational safety. Over the following sections, we will explore the basic and advanced scientific and engineering aspects of ESD. We will focus on: (1) digitization and the growing demand for electronic devices (need for improved ESD), (2) electrochemical fundamentals of electrochemical energy conversion and storage, (3) the current state of the ESD, (4) advanced manufacturing methods and characterization of ESD, and (5) the environmental impact and sustainability of ESD.
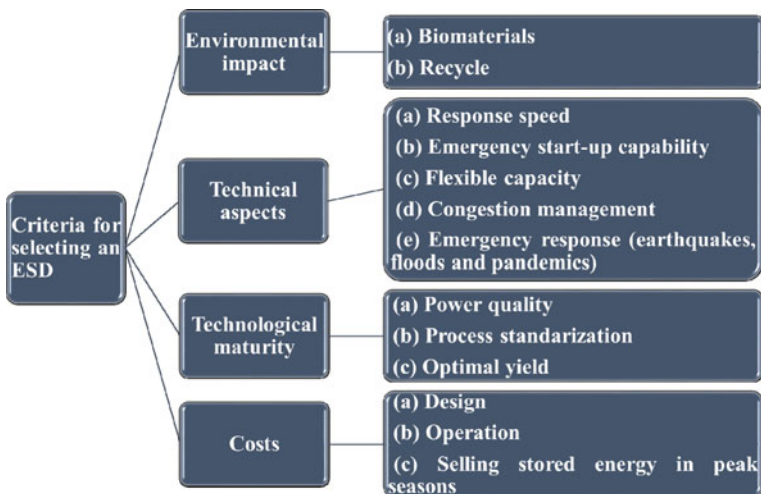
Fig. 1 Criteria for designing an energy storage device

2 Digitization and High Consumption of Electronic Devices

During the twenty-first century, human life has changed abruptly due to the accelerated development in information and communication technologies (ICT). The digitization of electronic devices, mainly for use in industrial processes but increasingly for most life activities has changed everyday life profoundly. Among particular advancements in life quality through digitization is the development of ambulatory medical devices that monitor human health instantly. Likewise, other digital devices have greatly changed society and work, especially in times of the COVID-19 pandemic. The aforementioned devices require massive data communication volume, variety, speed, security, and in some cases miniaturize to provide portability. According to information provided by Morley et al. [1], in 2012, 9% of electricity consumption was used by computers, smartphones, communications networks, data centers, televisions, audiovisual equipment, and broadcasting infrastructure. This value has undoubtedly grown over the next decade. Worldwide, the supply and demand of digital energy are constantly changing, seeking the integration of energy production with technological development and commercialization models [2]. This has brought an increase in the digitization of devices in recent years, which has led to increasing levels of security, efficiency, availability, and durability of energy systems [3]. Considering portable electronic devices, which promise real-time response and can operate as a point energy source using their onboard ESD is another area of interest. These devices often use rechargeable stores (batteries and electrochemical capacitors) for longer life, although currently, all such devices have strict power consumption profiles to achieve battery life they may well become carry along with energy sources with adaptive new designs. Rechargeable batteries are the key to ensuring the stability of the performance of the devices because their performance is sensitive to power consumption. As an example, sales of mobile phones and smartphones have seen exploding year by year. In 2010 less than 300 million units were sold and so far in 2021, over one and a half billion million units have been sold [4]. The continuous increase in the demand for these devices makes it necessary to incessantly search for improved rechargeable energy systems than those currently on the market. One way to increase the energy efficiency of these devices is through the latest generation of innovative technologies, such as the use of polymeric materials. These improved ESD increase smartphone reliability and durability. Current batteries technologies have a limited life. This results from by-products generated during their energy generation reactions and the materials used in making them. Of great interest for an electronic device is for a 'battery' with stable energy production profile and a long service life, while reducing any waste heat generation.

Table 1 shows different brands of laptops and cell phones; data was collected online in the current year (2021). They all use rechargeable lithium batteries for their operation. The capacity of the batteries shown is a function of the number of individual cells that constitute them, usually 4–6. Table 1 also shows that the batteries of the more recent devices have a higher capacity, due to improvements in the development of the electrode materials and the electrolyte used in their manufacture.

Table 1 Devices using lithium rechargeable batteries

Laptop			Cell phones		
Device	Battery capacity (mAh)	Voltage (V)	Device	Battery capacity (mAh)	Voltage (V)
Dell	4800	11.1	Moto G9	6000	3.9
Samsung	4400	11.1	Nokia	1020	3.8
MacBook Pro	6000	10.9	Iphone	3190	3.0
Lenovo	6400	7.4	Phab Lenovo	3550	3.8

Source Author's elaboration

While it is true that technology has advanced, disposable batteries continue to be widely used.

The proceeding review leads us to conclude that the world's population is highly dependent on the consumption of both stationary and portable electrical energy and therefore it is important to develop cheap, lightweight, abundant, and long-life materials that provide better alternatives to the current 'battery' problems resulting from present-day technologies.

3 Electrochemical Fundamentals of Energy Storage Devices Organic Molecules

Mainly, there are two major types of devices for renewable energy storage: lithium-ion batteries and supercapacitors. Both devices consist of a cathode, an anode, and an electrolyte (ionic conductor). The energy storage mechanism is based on a polarization and depolarization process. During the charging process, the cations or anions from the first electrode, or the electrolyte, are transported through the electrolyte and are adsorbed or intercalated in the second electrode, polarizing the system [5]. During the discharge process, ions desorb or deintercalation, from the second electrode and transport back to the first electrode thus depolarizing the system. Figure 2 shows this charging/discharging process of a $LiFePO_4$ battery.

The energy storage mechanism of batteries is based on the rapid intercalation and de-intercalation interleaving of ions (Li^+ for popular 'lithium' batteries, for example). This provides a high energy density, but a lower power level, meaning modest power delivery and limited life cycles. For supercapacitors the charge/discharge cycle is based on the rapid adsorption and desorption of the charged species, leading to high power density and good life cycle stability [6]. Thus, capacitors store energy more efficiently than a traditional battery. In both types of devices, there are redox reactions, when a potential is applied across the pseudo-capacitor, fast reversible redox reactions that occur on the electrode surface, and a charge passes through a double layer.
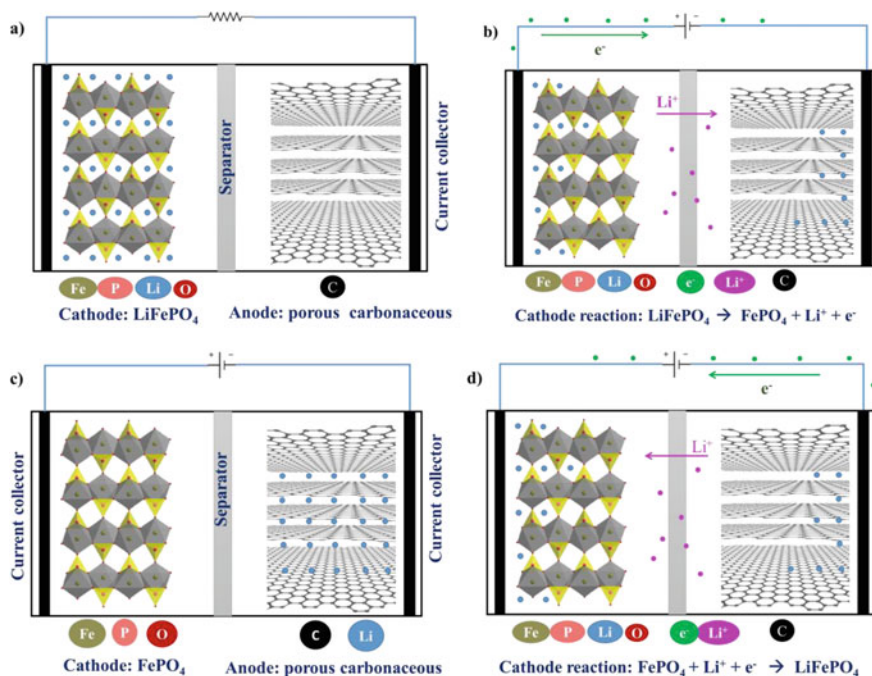
Fig. 2 Charge/discharge cycle of a LiFePO$_4$: (**a**) completely discharged battery, (**b**) battery charging, (**c**) fully charged battery, and (**d**) discharging battery

Electrochemical double-layer capacitors (EDLCs) are supercapacitors that use the reversible adsorption of ions found in the electrolyte on active materials to store energy by accumulating electrostatic charges. In the electrodes used in EDLCs, there are no redox reactions because charge storage occurs through electrostatic forces. The efficiency of these devices depends on the surface contact area between the electrodes and the electrolyte. Pseudo-capacitors offer fast, reversible, faradaic redox reactions, involving multiple electrons transferred into electrode materials. Consequently, they can supply a much higher specific capacitance compared to EDLCs [7].

Electrochemical capacitors store energy directly as surface charge. Batteries, alternatively, store their energy in the chemical reagents that constitute them. Their performance is a function of the kinetics of these reactions and mass transport. Commercial electrochemical capacitors use organic electrolytes (high energy and power density) because they give better results than aqueous electrolytes that operate at low voltage. Electrode materials used in batteries and supercapacitors are of special relevance because the material used, and the size of the particles determines the energy storage mechanism. For this reason, significant effort is ongoing in the development of these materials to improve their performance in ESD.

Generally, ESD uses commercial-grade graphite materials, but they are of limited capacity and offer only moderate performance. In the current literature, one finds

Table 2 Materials used as electrodes in electrochemical capacitors and batteries

Electrode	Charge/discharge cycles	Specific capacitance (F/g)	Specific capacity (mAh/g)	References
Electrochemical capacitors				
NP-C	5000	363	–	[10]
Carbon	10,000	390	–	[11]
PEDOT:PSS	1000	40	–	[12]
$MnCo_2O_4$	4000	2144	–	[13]
$MnCo_2O_4$@PPy	>5000	2933	–	
Batteries				
PQL (Li$^+$)	>100	–	1770	[14]
Fe-MOF/RGO	>200	–	1010	[15]
PDA (Li$^+$)	>580	–	1414	[16]
PVMPT	>1000	–	56	[17]

many reports focusing on inorganic and organic electrodes materials. Considering inorganic materials, most offer low energy and power density, and they are often scarce materials that limit their use and increase their cost. It is safe to say that they cannot satisfy the current demands for the increasing demand for efficient energy storage. On the other hand, the electrodes of organic materials are composed mainly of carbon, oxygen, nitrogen, and hydrogen, allowing them to contain carbonyl, carboxyl, and amine groups. Users obtain them using simple and low-cost synthesis methods. They offer structural diversity, can be molded into various shapes, and offer capacity that can be altered by process demands, all while maintaining environmentally friendliness [8] (Sect. 5). In some cases, organic electrodes require large amounts of additives to ensure conductivity [9]. Table 2 shows different materials used as electrodes in electrochemical capacitors and batteries.

Table 2 shows that the useful life of electrochemical capacitors to store energy is longer than in batteries as measured in charge/discharge cycles, a fact closely related to the electrode material and the electrolyte used. Although electrode development for use in energy storage devices has undergone several decades of research and improvement, there are still problems with them. Sometimes the synthesis method is not adequate, the raw material is not available or is scarce, and some surface functional groups that initially benefit the catalytic activity, but which are unstable, lead to decreased performance over time [18]. Likewise, the carbonaceous materials when used in nano-scale electrochemical capacitors can cause health problems that are not present when they are employed in micron-sized particles. On the other hand, carbon nanotubes can, potentially, cause electrical short circuits, thus damaging the entire electronic device causing total catastrophic failure or, in the least, degraded performance. It is necessary, therefore, to develop materials that have high ionic conductivity, and superior electrochemical performance in redox and catalytic reactions without these potential side effects [19].

4 Characterization of Organic Materials Used as Electrodes in Energy Storage Devices

The properties of an organic-material electrode depend in part on its molecular structure, therefore it is essential to evaluate both the material's structure and its capacity for electronic transfer. In general, these characterizations are divided into both structural and electrochemical issues, see Fig. 3. The combination of both provides complete information about the characteristics of a potential material under study.

4.1 Structural Characterization

4.1.1 Scanning Electron Microscopy (SEM) and Transmission Electron Microscopy (TEM)

By using both SEM and TEM techniques, morphological characteristics of organic materials can be determined at a microscopic level. For example, Co/Zn-metal–organic structures presented translucent nanoscale morphology, which indicates that they are thin, porous, or even hollow materials that can allow the penetration of electrolyte ions [5].

4.1.2 Infra-Red (IR), Raman Spectroscopy and X-Ray Diffraction (XRD)

IR spectroscopy is a commonly used method because it is simple to use and low cost. It offers important information about functional groups present in the chemical structures of organic materials. These, of course, offer specific properties to an organic compound for a given application. Using XRD the crystalline phases that make up the structure of the material are identified. This information can help determine if a
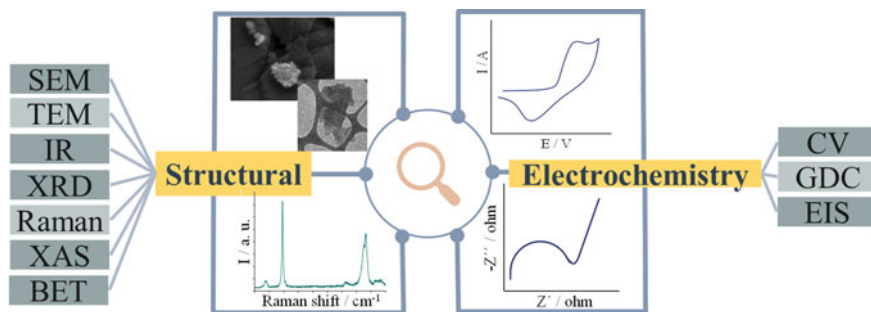
Fig. 3 Commonly used techniques for the characterization of organic electrodes

material can store energy or not. Finally, to monitor and quantify specific molecules in redox states, the Raman spectrographic techniques which provide detailed information about chemical structure, phase and polymorphy, crystallinity, and molecular interactions are used [20].

4.1.3   X-Ray Absorption Spectroscopy (XAS)

XAS is used to monitor and determine the local geometric and/or electronic structure of matter and, thus, is capable of detecting amorphous, disordered, or crystalline species in the material of interest [20].

4.1.4   Brunauer–Emmett–Teller (BET) Analysis

The BET theory explains the physical adsorption of gas molecules, typically nitrogen, on a solid surface and serves as the basis for an analysis technique for the measurement of the specific surface area of materials. BET analysis makes it possible to determine the surface area, diameter, and pore volume of organic materials. Organic materials are generally composed of micropores and mesopores and the surface area is in the order of 10^2 m^2/g. For example, 302.32 m^2/g for porous organic polymers-GO [21] and 429 m^2/g for tetracyanoquimodiethane-metal–organic structures [22] are reported. Based on the greater pore volume, the electrolyte access will be favored while greater surface area provides more active sites, both of which favor materials use in energy storage.

4.2   Electrochemical Characterization

4.2.1   Cyclic Voltammetry (CV)

CV is the electrochemical technique most used to characterize organic electrodes materials. The technique employs the application of a potential sweep over the organic electrode material. Test response is recorded as a current *vs.* potential graph known as a voltamperogram. Oxidation and reduction processes are visible in these voltamperogram graphs as they form small peaks that correspond to the faradaic process at the electrode/electrolyte interface. The oxidation/reduction potential of organic materials can be determined according to the position of these peaks in the voltamperogram curves. This behavior is characteristic of battery-type electrodes [20]. It is common for cyclic voltammerograms to be developed at different scan rates. The increase in peak current with increasing sweep rate suggests that electrolyte ions can quickly enter (or exit) through the pores of the materials in some way. This suggests that speed capacity to charge and discharge the material might be good suggesting a material to be further explored for ESD development. In some

cases, relevant redox peaks are not noticed, but there are shapes similar to a half sheet that indicates the capacitive nature of these materials [6]. A rectangular shape characteristic of double-layer electrochemical capacitors or an almost rectangular shape associated with pseudocapacitors can also be obtained [20]. Finally, there are capacitive materials, for example, the carbon electrode, that show a rectangular shape where the capacitive behavior can be combined with reversible redox waves (due to the electroactive species attached to the carbon electrode).

4.2.2 Galvanostatic Charge–Discharge Curves (GDC)

This analysis technique allows one to explore electronic performance for applicability as electrode material in energy storage devices. GDC is a plot of voltage, as a function of time, (graphing electrical potential *vs* time) at various current densities. In practical applications, where higher maximum current densities are most desirable, it is necessary to investigate the electrochemical properties at different current densities that would occur over any charge/discharge cycle. Based on the shape of the GDC at various current densities, one can deduce expected performance. For example, when observing linear and quasi-symmetric curves the nature of the electrode's charge storage mechanism can be termed pseudo-capacitive. While a fully symmetric shape suggests the kinetics of the fast reaction and high electrochemical reversibility. High material-specific capacitance is attributed to better utilization of the porous structure, and structures that could provide numerous active sites for ion transfer [23].

4.2.3 Electrochemical Impedance Spectroscopy (EIS)

Using EIS the interfacial charge transfer activity and the electrocapacitive characteristics of the materials are studied. This test consists of applying a small potential signal on the electrode and measuring the response in current at different frequencies. Impedance data is commonly represented in the form of an impedance diagram, the so-called Nyquist diagram. The information obtained from the diagram depends on the shape of the spectra. For example, a semicircular shape in the high-frequency zone indicates resistance to charge transfer at the electrode/electrolyte interface. The smaller the semicircle, the lower the resistance to charge transfer. An almost vertical line in the low-frequency region indicates good capacitive behavior and the slope of this line is related to the diffusion resistivity of the electrolyte ions within the pores of the material [21]. By simulating the data to equivalent circuits, it is possible to obtain the resistance to charge transfer values, the capacitance of the double layer between electrolytes and electrodes, as well as other elements that suggest the electrochemical behavior of the materials under study.

5 The Current State of Energy Storage Using Organic Materials as Electrodes

One of the first organic materials used as electrodes, in early lithium batteries, was the carbonyl compound dichloroisocyanuric acid as reported in the 1960s [24]. Subsequently, conductive polymers were explored, which to date are the best option compared to all other organic materials because they offer ionic and electronic conductivity due to their inherent structure. Some of the conductive polymers in use are polypyrrole, polyacetylene, poly(3,4-ethylenedioxythiophene) (PEDOT), and polyaniline. Polymerized nickel complexes with Schiff bases of the salen-type (poli[Ni(Schiff)]) are also reported [25]. Figure 4 shows the trend of reported works in the last decade related to the use of polymeric materials as electrodes for ESD.

From this publication graph, it appears that interest is focused on materials such as polyaniline and polypyrrole. The number of publications has increased considerably over the years for these two polymers. The opposite case is what is observed for polyacetylene where the development of materials based on this polymer is lower compared to other polymers. This may be because it lacks the structural integrity for wider applications. The majority of the investigations focus on polyaniline (PANI), transitions between the reduced, oxidized, and partially reduced/oxidized states that it takes through the electrochemical process reveal the high energy storage capacity of PANI-based devices (32.16×10^6 mAh/g) [26]. According to recent works reported in the literature, some of which are summarized in Table 3, the development of PANI/graphene composites is shown to increase the charge storage performance. The addition of a carbonaceous material acts as a support for PANI, improving its
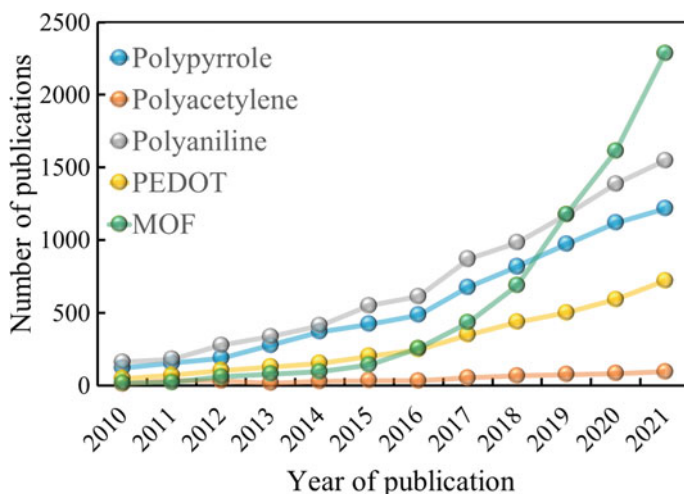
Fig. 4 Articles published in the last 10 years on polymers used as electrodes in energy storage devices. Search *source* https://www.sciencedirect.com/ (Accessed August 23, 2021)

Table 3 Organic materials evaluated as electrodes in energy storage devices

Organic material	Device	Cycles/stability (%)	Current density (A/g)	Specific capacitance (mAh/g)	References
Organic polymers on rGO	Supercapacitor	4000/–	0.2	39.4×10^5	[21]
Poly-TEMPO-methacrylate	Battery	1000/55	0.1	83.0	[25]
Polyaniline/graphene	Supercapacitor	10,000/89	1.0	37.9×10^6	[26]
V_2O_5@polyaniline	Battery	1000/94	5.0	361.0	[28]
Tetracyanoquinodimethane doped copper-organic framework	–	5000/96	2.0	208.8	[22]
Zeolitic imidazolate framework/Fe_2O_3/AC	Supercapacitor	1500/97	6.0	31.1×10^6	[7]
CoS nanobox-MOF/nanoporous carbon	–	10,000/84	10.0	130.0	[33]
Polyimide/metal–organic frameworks	Battery	1800/88	1.0	83.0	[34]
Co-MOF/PANI	Supercapacitor	5000/90	1.0	13.5×10^6	[35]
MOFs-derived porous carbon/polyaniline	Supercapacitor	10,000/94	0.2	17.9×10^6	[36]
MoS_2 nanocrystals in MOF-derived carbon	Battery	150/91	2.0	211.0	[31]

stability without sacrificing conductivity, thus, 89% stability is achieved and a specific capacity of 37.86×10^6 mAh/g for 10,000 cycles [27]. Another option is PANI/V_2O_5 hybrid materials with which 361 mAh/g is reported and excellent stability for 1000 cycles [28]. This suggests that the current approach is to generate a combination of materials that favor conductivity and specific capacity. However, challenges remain to be overcome.

Another novel option is the development of redox polymers that have stable free radical substituents such as nitroxyl radical groups, for example, poly-2,2,6,6-tetramethylpiperidin-1-oxyl-4-yl-methacrylate (PTMA), that have been studied as electrodes in aqueous media. These materials show promise as eco-friendly ESD electrodes [25]. By combining redox polymers (having high capacity) with conductive polymers (to improve electronic conductivity), the best properties of both materials are enhanced. In this sense, the combination of PTAM with polymerized nickel complexes, with salen-type Schiff bases, offers stability for 1000 cycles and a specific capacity of 83 mAh/g.

Metal–organic frameworks (MOF) are a new class of polymeric materials characterized as increased porous materials with a large surface area. They are highly ordered and can be produced with tunable pore size, allowing the incorporation of organic and inorganic components to form a variety of structural topologies with

different porosity levels [5]. These characteristics allow efficient diffusion of electrolyte ions within the electrode. MOF are highly studied as seen in Fig. 4 where the increase in publications in recent years is exponentially exceeding PANI-based studies. The current trend when using MOF is to combine them with other materials to form composite materials and as precursors to synthesize porous carbon [29]. These materials offer improved electrical conductivity and cyclical stability. These metal oxides are generally used to prevent the agglomeration of MOF particles and to promote fast reaction kinetics to achieve high energy and power density. Metal is inherently mono-dispersed in MOF as cations and by controlling annealing conditions MOF-derived metal oxide can be obtained. MOF-derived metal oxide has large, accessible internal surface areas and unique structures that favor electrochemical activity due to large specific surface areas and high numbers of active sites that provide short ion diffusion paths. Some of the metal oxides proposed include RuO_2, MnO_2, $NuCo_2O_4$, Fe_2O_3, $FeOOH$, TiO_2, Mn_2O_3, and Co_3O_4. For example, one bimetallic oxide ($ZnCo_2O_4$) operated as a Co/Zn-MOF electrode offers good electrical conductivity, electrochemical performance (2000 cycles) and specific capacity of 25.9 mAh/g performances improved by more than 300% over Co_3O_4 operated MOF [5].

Another alternative currently being evaluated is the combination of MOF with conductive polymers to promote both electrical conductivity and redox activity [22]. Several conductive polymers have been proposed for these composites such as tetracyanoquinodimethane, polyimide, PANI, polypyrrole, polyvinylpyrrolidone, as seen in Table 3. When using MOF as a precursor to synthesize porous carbons, there are interesting studies on MOF-derived carbon shell-based composite electrodes characterized by a compact and robust interface with pores suitable for lithium-ion penetration and diffusions, the early result indicates a capacity of 3714 mAh/g [30]. In addition, the conductivity of this type of material is improved as has been reported in recent publications [31].

Finally, the literature mentions some novel proposals for ternary nanocomposites made up of conductive polymer/GO/MOFs with high specific capacity for 17.95×10^6 mAh/g and retention of the capacitance of 90% for 1000 cycles so these new materials have good potential for use for example for as electrochemical redox capacitors [32].

Although there have been important advances, it is still necessary to work on the development of stable and high-performing organic materials as electrodes produced using simple synthesis methods that allow for practical scaling.

6 Environmental Impact and Sustainability of Electrochemical Energy Storage Devices

6.1 Environmental Impact

During several United Nations meetings, certain groups have stated that sources of fossil fuels that are available worldwide are being depleted even as new and exciting finds are reported several times a year. Similarly, many of the elements critical to the production of ESD are is rare supply and their extraction is resulting in significant environmental deterioration as well. While developed nations have a significant impact on environmental issues, because they are leaders in technological development, specifically, in manufacturing electronic devices and the source of energy storage for their operation, batteries. The future trend in the consumption of these devices is often the developing nations with primitive systems in place to deal with many of the throw-away products associated with their rapidly growing demand.

Considering ESD specifically, battery electrodes, which are mostly made of rare earth metals that must be extracted by mining in developing nations, by poorly run organizations, can be highly polluting. Finally, of course, it is well known that these so-called rare earth metals are not renewable. Should we carry out a product life analysis of batteries as an ESD, we must consider many issues. First the non-biodegradable metallic and the toxic substances contained therein have a direct detrimental effect on human health and the ecosystem. Finally, most batteries become electronic waste after a single use when they are carelessly thrown away further stressing the environment and human health. Thus, due in part to the scarcity of natural resources and unacceptably high level of energy consumption to manufacture these essentially throw-away devices offering single use or limited reusability suggests continuing the search for alternative ESD. These alternatives must be inherently environmentally friendly, inexpensive, and can store energy over the short, medium, or even long term and be useful for extended life in varying operating conditions. In any technological situation, it is necessary to ensure that the design of a new ESD considers many key points such as (a) reduced greenhouse gas emissions, (b) avoidance of hazardous waste generation, (c) limited modification of the earth during extraction of raw materials, (d) well-defined understanding of, and systems for, recycling of infrastructure and materials, (e) known capacity ranges, (f) known and expected response times, (g) high energy density, (h) high energy/power ratio, (i) good overall cycle efficiency, (j) ability to instantly measure the state of charge or depth of discharge, (k) ability to self-discharge, and (l) ability to extend useful equipment lives.

Considering the above, one way to reduce the environmental impact generated by ESD is to develop renewable, ecological, and high-performance electrodes based on organic compounds. They must have organic structures that are easy to manipulate to obtain the desired properties [37–40]. Another way to reduce environmental deterioration from batteries is to consider 'green chemistry' in their manufacture and to
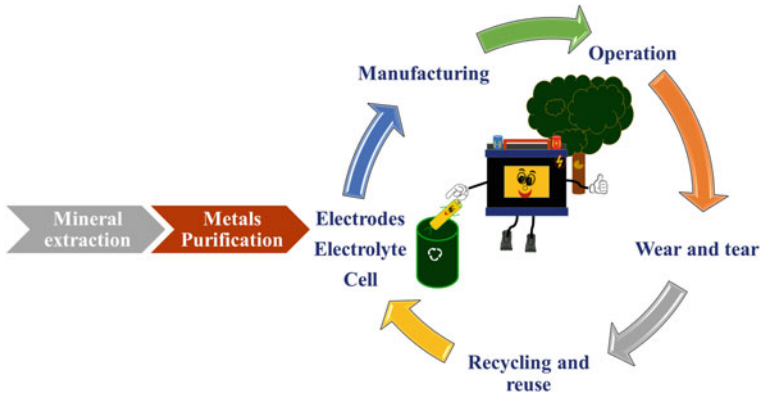
Fig. 5 Life cycle analysis of an energy storage device

improve recovery of the metal components from spent batteries. These reasonably simple steps offer reductions of detrimental environmental impact by about 49% [38]. ISO14040 describes life cycle analysis (LCA) of products and the impacts that these have on resource availability, global climate change, ocean acidification, energy and water usage, toxicity, and ozone layer deterioration, among other issues.

When designing a new ESD, care must be paid to the issues described in the ISO 14000 standards. Devices produced with an eye to this standard should lead to ESD's use because it also indicates sustainable materials and contributes to environmental health during the device's life cycle. Figure 5 presents a schematic representation of the life cycle analysis for an energy storage system.

The life cycle environmental impact assessment of an energy storage device includes: (a) the potential for global climate change, (b) cumulative energy demand, (c) human health, (d) ecosystem quality, and (e) resource indicators. This evaluation depends on the sources and toxicity of the chosen materials making up the device, any environmental damage caused by the extraction of the materials, and the end-of-life issues for the product (including recycling). Typically, the life cycle analysis may also focus only on the energy consumed during the production of a unit of energy storage in the ESD of interest. For example, in Li-ion batteries, 1 kWh of storage capacity is associated with an accumulated energy demand of 328 kWh, emitting 110 kg of $CO_{2\text{-eq}}$ to the atmosphere [41]. Finally, to build environmentally responsible electrochemical ESD, it is necessary to develop devices with shorter charge but longer discharge cycles, especially if the ESD is to be used for vehicles that travel extended distances.

6.2 Sustainability

Essentially, it is wise, in environmental management to live by the axiom: "We do not inherit the earth and its resources for our ancestors we borrow it from our

children." Sustainability considers three important aspects: (a) social, (b) economic, and (c) environmental, which must be adequately addressed during all technological development activities [42].

On a global basis, it has been obvious that economic growth, driven by increasing populations, goes hand in hand with an increase in energy and raw material demand and, unless carefully managed, environmental degradation. It is important to emphasize that the reduction of greenhouse gases production, especially by developing nations where controls are weak, is essential to reducing future environmental impact. But not all is lost. So far this century, sustainable development has been undertaken by many countries around the world. Awareness of and conversion to developing technologies for the generation and storage of clean and/or renewably sourced energy are evolving. Society has begun to take into account the rising energy demands going forward due to accelerating population growth and has begun to embrace both conservation and sustainable technologies to address this growth in demand [43].

Although there are great advances in the generation and use of renewable energy sources the disadvantage that many are intermittent technologies remains. As is said: wind power is available only when the wind blows, tidal power only during changing tides, solar power only when the sun is shining, thus each of these and the other renewable power source based systems need to be coupled to efficient and effective storage technologies to meet the demands of society. In the future human society needs to think of renewable energy sources, and their associated ESD Banks, much as historical society has viewed water reservoirs, for hydroelectric or direct powering of grist, lumber, or other types of mills for millennia [44].

For energy storage systems to be attractive, affordable, and sustainable in the marketplace, they must: (a) provide high performance, (b) keep the cost of materials as reasonable as possible, (c) use abundant rather than limited resources, (d) operate safely in all applications, and (d) respect the environment through life cycle analyses [40]. Additionally, where the appropriate, design of solvent-free batteries [38] is being studied as well. Despite having made significant advances in the development of sustainable ESD, many challenges remain. Some of these include [45]: (a) the need for increased capacity and at elevated energy demand levels, (b) improved electrode/electrolyte interfaces design, (c) introducing higher concentration electrolytes, (d) introducing reduced cost renewable material based electrodes, (f) improving the quality of power available throughout the discharge cycle, (g) improving capacity flexibility, (h) building simulations to evaluate the overall environmental and economic impact of any ESD being designed.

7 Conclusions

Throughout this chapter, evidence was presented that showed that in the industrialized world in which we live, that our lives are increasingly dependent on portable electronic devices. Additionally, because these devices require portable ESD the scientific community has a special interest in the development of sustainable and

high-performance energy storage devices. The most common goal of these studies is to improve ESD electrochemical performance. This performance is directly related to the materials that make up the devices, mainly the electrodes. Carbon-based and organic-based electrodes materials appear to be an excellent choice in part because they are sustainable and abundant and because they can be manufactured in environmentally safe ways. According to current trends, polypyrrole, polyaniline, and metal–organic structures, when used as ESD electrodes, offer high-energy storage capacity and stability for up to 10000 charge/discharge cycles. While offering much promise, these electrode materials still need continuing study to improve electronic conductivity, improve mass density and energy storage capacity, and always lower electrode cost.

Synthesis techniques, performance characterization, and environmental impact are relevant issues when proposing improved electrode materials. While the environmental impact can be mitigated in part by using materials obtained from biomass and/or using green synthesis, sustainable ESD development depends on critical interdisciplinary work linking materials science, engineering, environmental management, and in some cases nanotechnology.

References

1. Morley, J., Widdicks, K., Hazas, M.: Digitalisation, energy and data demand: the impact of Internet traffic on overall and peak electricity consumption. Energy Res. Soc. Sci. **38**, 128–137 (2018)
2. Zhang, Z., Feng, L., Zheng, Z., Wang, G.: Research on energy industry strategy based on intelligent digital upgrading. In: E3S Web of Conferences, vol. 257, 02001 (2021)
3. Borowskii, P.F.: Digitization, digital twins, blockchain, and industry 4.0 as elements of management process in enterprises in the energy sector. Energies **14**, 1885 (2021)
4. O'Dea, S.: Number of smartphones sold to end users worldwide from 2007 to 2021 (2021). https://www.statista.com/statistics/263437/global-smartphone-sales-to-end-users-since-2007/
5. Lim, G.J.H., Liu, X., Guan, C., Wang, J.: Co/Zn bimetallic oxides derived from metal organic frameworks for high performance electrochemical energy storage. Electrochim. Acta **291**, 177–187 (2018)
6. Almeida, M.M., Más, A.A., Silva, T.M., Montemor, M.F.: From manganese oxide to manganese sulphide: synthesis and its effect on electrochemical energy storage performance. Electrochim. Acta **389** 138711 (2021)
7. Chameh, B., Moradi, M., Hessari, F.A.: Decoration of metal organic frameworks with Fe_2O_3 for enhancing electrochemical performance of ZIF-(67 and 8) in energy storage application. Synth. Met. **269**, 116540 (2020)
8. Guo, R., Wang, Y., Heng, S., Zhu, G., Battaglia, V.S., Zheng, H.: Pyromellitic dianhydride: a new organic anode of high electrochemical performances for lithium ion batteries. J. Power Sources **436**, 226848 (2019)

9. Nevers, D.R., Brushett, F.R., Wheeler, D.R.: Engineering radical polymer electrodes for electrochemical energy storage. J. Power Sources **352**, 226–244 (2017)

10. Zhou, M., Pu, F., Wang, Z., Guan, S.: Nitrogen-doped porous carbons through KOH activation with superior performance in supercapacitors. Carbon **68**, 185–194 (2014)

11. Li, Z., Xu, Z., Tan, X., Wang, H., Holt, C.M.B., Stephenson, T., Olsen, B.C., Mitlin, D.: Mesoporous nitrogen-rich carbons derived from protein for ultra-high capacity battery anodes and supercapacitors. Energy Environ. Sci. **6**, 871–878 (2013)

12. Cheng, L., Du, X., Jiang, Y., Vlad, A.: Mechanochemical assembly of 3D mesoporous conducting-polymer aerogels for high performance hybrid electrochemical energy storage. Nano Energy **41**, 193–200 (2017)

13. BoopathiRaja, R., Parthibavarman, M.: Hetero-structure arrays of $MnCo_2O_4$ nanoflakes@nanowires grown on Ni foam: design, fabrication and applications in electrochemical energy storage. J.Alloys Compound. **811**, 152084 (2019)

14. Wu, J., Rui, X., Long, G., Chen, W., Yan, Q., Zhang, Q.: Pushing up lithium storage through nanostructured polyazaacene analogues as anode. Angew. Chem. Int. Ed. **54**, 7354–7358 (2015)

15. Jin, Y., Zhao, C., Sun, Z., Lin, Y., Chen, L., Wang, D., Shen, C.: Facile synthesis of Fe-MOF/RGO and its application as a high performance anode in lithium-ion batteries. RSC Adv. **6**, 30763–30768 (2016)

16. Sun, T., Li, Z.J., Wang, H.G., Bao, D., Meng, F.L., Zhang, X.B.: A biodegradable polydopamine-derived electrode material for high-capacity and long-life lithium-ion and sodium-ion batteries. Angew. Chem. Int. Ed. **55**, 10662–10666 (2016)

17. Kolek, M., Otteny, F., Schmidt, P., Mück-Lichtenfeld, C., Einholz, C., Becking, J., Schleicher, E., Winter, M., Bieker, P., Esser, B.: Ultra-high cycling stability of poly(vinylphenothiazine) as a battery cathode material resulting from π–π interactions. Energy Environ. Sci. **10**, 2334–2341 (2017)

18. Miller, J.R.: Perspective on electrochemical capacitor energy storage. Appl. Surf. Sci. **460**, 3–7 (2018)

19. Jiang, Y., Zhao, H., Yue, L., Liang, J., Li, T., Liu, Q., Luo, Y., Kong, X., Lu, S., Shi, X., Zhou, K., Sun, X.: Recent advances in lithium-based batteries using metal organic frameworks as electrode materials. Electrochem. Commun. **122**, 106881 (2021)

20. Li, S., Lin, J., Xiong, W., Guo, X., Wu, D., Zhang, Q., Zhu, Q.L., Zhang, L.: Design principles and direct applications of cobalt-based metal-organic frameworks for electrochemical energy storage. Coord. Chem. Rev. **438**, 213872 (2021)

21. Xu, L., Liu, R., Wang, F., Ge, X., Zhang, X., Qiao, L., Yang, J.: In-situ synthesis of porous organic polymer on rGO for high-performance capacitive energy storage. J. Energy Storage **25**, 6–11 (2019)

22. Sundriyal, S., Shrivastav, V., Bhardwaj, S.K., Mishra, S., Deep, A.: Tetracyanoquinodimethane doped copper-organic framework electrode with excellent electrochemical performance for energy storage applications. Electrochim. Acta **380**, 138229 (2021)

23. Zhang, M., Zhou, W., Huang, W.: Characterization methods of organic electrode materials. J. Energy Chem. **57**, 291–303 (2021)

24. Lu, Y., Zhang, Q., Li, L., Niu, Z., Chen, J.: Design strategies toward enhancing the performance of organic electrode materials in metal-ion batteries. Chem **4**, 2786–2813 (2018)

25. Vereshchagin, A.A., Vlasov, P.S., Konev, A.S., Yang, P., Grechishnikova, G.A., Levin, O.V.: Novel highly conductive cathode material based on stable-radical organic framework and poly-merized nickel complex for electrochemical energy storage devices. Electrochim. Acta **295**, 1075–1084 (2019)

26. Pal, R., Goyal, S.L., Rawal, I., Gupta, A.K., Ruchi: Efficient energy storage performance of electrochemical supercapacitors based on polyaniline/graphene nanocomposite electrodes. J. Phys. Chem. Solids **154** 110057 (2021)

27. Rauhala, T., Davodi, F., Sainio, J., Sorsa, O., Kallio, T.: On the stability of polyaniline/carbon nanotube composites as binder-free positive electrodes for electrochemical energy storage. Electrochim. Acta **336**, 135735 (2020)

28. Du, Y., Wang, X., Man, J., Sun, J.: A novel organic-inorganic hybrid V_2O_5@polyaniline as high-performance cathode for aqueous zinc-ion batteries. Mater. Lett. **272**, 127813 (2020)

29. Zhang, F., Zhang, J., Ma, J., Zhao, X., Li, Y., Li, R.: Polyvinylpyrrolidone (PVP) assisted in-situ construction of vertical metal-organic frameworks nanoplate arrays with enhanced electrochemical performance for hybrid supercapacitors. J. Colloid Interface Sci. **593**, 32–40 (2021)

30. Gao, R., Tang, J., Yu, X., Tang, S., Ozawa, K., Sasaki, T., Qin, L.C.: In situ synthesis of MOF-derived carbon shells for silicon anode with improved lithium-ion storage. Nano Energy **70**, 104444 (2020)

31. Hu, C., Ma, K., Hu, Y., Chen, A., Saha, P., Jiang, H., Li, C.: Confining MoS_2 nanocrystals in MOF-derived carbon for high performance lithium and potassium storage. Green Energy Environ. **6**, 75–82 (2021)

32. Ajdari, F.B., Kowsari, E., Ehsani, A.: Ternary nanocomposites of conductive polymer/functionalized GO/MOFs: synthesis, characterization and electrochemical performance as effective electrode materials in pseudocapacitors. J. Solid State Chem. **265**, 155–166 (2018)

33. Wei, X., Li, Y., Peng, H., Zhou, M., Ou, Y., Yang, Y., Zhang, Y., Xiao, P.: Metal-organic framework-derived hollow CoS nanobox for high performance electrochemical energy storage. Chem. Eng. J. **341**, 618–627 (2018)

34. Zhou, J., Yu, X., Zhou, J., Lu, B.: Polyimide/metal-organic framework hybrid for high performance Al-organic battery. Energy Storage Mater. **31**, 58–63 (2020)

35. Srinivasan, R., Elaiyappillai, E., Nixon, E.J., Sharmila Lydia, I., Johnson, P.M.: Enhanced electrochemical behaviour of Co-MOF/PANI composite electrode for supercapacitors. Inorg. Chim. Acta **502**, 119393 (2020)

36. Yao, M., Zhao, X., Zhang, Q., Zhang, Y., Wang, Y.: Polyaniline nanowires aligned on MOFs-derived nanoporous carbon as high-performance electrodes for supercapacitor. Electrochim. Acta **390**, 138804 (2021).

37. Escobar, B., Martínez-Casillas, D.C., Pérez-Salcedo, K.Y., Rosas, D., Morales, L., Liao, S.J., Huang, L.L., Shi, X.: Research progress on biomass-derived carbon electrode materials for electrochemical energy storage and conversion technologies. Int. J. Hydrogen Energy **46**, 26053–26073 (2021)

38. Gao, M., Pan, S.Y., Chen, W.C., Chiang, P.C.: A cross-disciplinary overview of naturally derived materials for electrochemical energy storage. Mater. Today Energy **7**, 58–79 (2018)

39. Huang, J., Zhao, B., Liu, T., Mou, J., Jiang, Z., Liu, J., Li, H., Liu, M.: Wood-derived materials for advanced electrochemical energy storage devices. Adv. Func. Mater. **29**, 1–23 (2019)

40. Chen, C., Hu, L.: Nanocellulose toward advanced energy storage devices: structure and electrochemistry. Acc. Chem. Res. **51**, 3154–3165 (2018)

41. Peters, J.F., Baumann, M., Zimmermann, B., Braun, J., Weil, M.: The environmental impact of Li-Ion batteries and the role of key parameters—a review. Renew. Sustain. Energy Rev. **67**, 491–506 (2017)

42. Nowotny, J., Dodson, J., Fiechter, S., Gür, T.M., Kennedy, B., Macyk, W., Bak, T., Sigmund, W., Yamawaki, M., Rahman, K.A.: Towards global sustainability: education on environmentally clean energy technologies. Renew. Sustain. Energy Rev. **81**, 2541–2551 (2018)

43. Luo, J., Hu, B., Hu, M., Zhao, Y., Liu, T.L.: Status and prospects of organic redox flow batteries toward sustainable energy storage. ACS Energy Lett. **4**, 2220–2240 (2019)

44. Chen, L.F., Feng, Y., Liang, H.W., Wu, Z.Y., Yu, S.H.: Macroscopic-scale three-dimensional carbon nanofiber architectures for electrochemical energy storage devices. Adv. Energy Mater. **7**, 1–31 (2017)

45. Acar, C.: A comprehensive evaluation of energy storage options for better sustainability. Int. J. Energy Res. **42**, 3732–3746 (2018)

Basics of Electrochemical Sensors

Cem Erkmen, Didem N. Unal, Sevinc Kurbanoglu, and Bengi Uslu

Abstract A chemical sensor can be defined as an inexpensive, portable, foolproof device that can react with excellent selectivity to a specific target chemical (analyte) to produce a measurable signal output at any analyte concentration. In other words, chemical sensors are systems that are selectively prepared against the component to be analyzed and transform the chemical data obtained by using the target substance concentration in a sample into an analytically useful signal. The analyte interacts with the chemical interface layer. The chemical change that occurs as a result of this interaction is read from the monitor via a signal by using the physical converter. Considering these physical converters, electrochemical sensors are an exciting subject studied by most researchers in many fields, including physical or analytical chemistry, biochemistry, solid-state physics, device manufacturing, electrical engineering, and materials science. Specifically, electrochemical sensors are popular devices due to their low cost, notable detection ability, fast analysis, experimental simplicity, and the ability to perform complex measurements. This chapter introduces the sensor, fundamental principles of electrochemistry, and electrochemical sensors. The most used electroanalytical methods were detailed described to provide an overview of their main applications.

Keywords Electrochemistry · Sensor · Electrochemical sensor · Organic electrodes

1 What is a "Sensor"?

The word sensor comes from the English word to sense, which means to feel. Sensors convert an external stimulus (physical or chemical quantities such as heat, light, humidity, sound, pressure, force, electricity, distance, acceleration, and pH) into electrical signals that can be processed and measured. Sensors are the essential elements

C. Erkmen · D. N. Unal · S. Kurbanoglu · B. Uslu (✉)
Department of Analytical Chemistry, Faculty of Pharmacy, Ankara University, 06560 Ankara, Turkey
e-mail: buslu@pharmacy.ankara.edu.tr

in digital display devices such as cameras and camcorders that detect image information and convert it into electronically processable signals [1–6]. A sensor can be a device, module or subsystem, that converts physical and chemical changes like temperature, pH light, etc., into a measurable signal. The sensors can sense changes in physical quantities like pressure, force, humidity, temperature, current, etc., and these physical and chemical phenomena are converted into electrical signals like the voltage, current, frequency [1–6]. By this flow, one can understand and quantify the changes in the sensor response. There exist two parts in sensors, the transducer and recognition parts. The recognition part captures the changes in the matrix, and the transducer part converts them depending on the recognition type into a measurable signal. According to their sensing mechanism, sensors can be classified as thermal sensors, optical sensors, calorimetric sensors, and electrochemical sensors, etc. [1–6]. The general illustration of the sensor and in daily life, the various traits, and some associated solicitations of the sensors are shown in Fig. 1 [7].

Fig. 1 **a** Parts of an electrochemical sensor. **b** Traits of sensors and their use in the market. Adapted with permission from [7] Copyright (2021) Elsevier

2 Principles of Electrochemistry

Electrochemistry is a 200-year-old discipline that deals with electron transfers on the solution/electrode surface. These transfers take place by reduction or oxidation reactions occurring on the surface. These reactions take place in a structure called an electrochemical cell. This structure is a structure that will allow the exchange between chemical energy and electrical energy. Therefore, electrochemistry is used in many different areas, from chemical analysis to battery technologies, from solar cells to pH sensors [8–14].

If an electron redox reaction is examined in the reduced (r^n) and oxidized forms (o^{n+1}) of an r species seen in Eq. (1),

$$r^n \rightleftharpoons o^{n+1} + e^- \tag{1}$$

When a potential (E) is applied, the reaction equilibrium is disturbed, so the reaction continues in both directions, 'r' is oxidized to 'o', or 'o' is reduced to 'r'. This redox reaction provides an electron flow in the form of a current (i). The formed current is directly proportional to the concentration of the compounds in the electrolyte solution and facilitates quantitative analysis.

In general terms, the current obtained when a target analyte is oxidized or reduced can be described by the following Eq. (2),

$$i = nAFj \tag{2}$$

in this equation, n shows several electrons transferred, A is defined as the working electrode's surface area (cm^2), F is a Faraday constant, and its value is 96,485 C mol^{-1}, and the flux of the target analyte towards the electrode is denoted by j (moles cm^{-2} s^{-1}). The term flux is very critical for a redox reaction to take place. For this flux to occur, the analyte must move from the electrolyte solution to the surface of the working electrode (mass transfer) [8–14]. Therefore, an electron exchange occurs between the surface and the solution by electron transfer. This process is schematized in detail in Fig. 2 [15].

It is a fact that in most electrochemical processes, electron transfer occurs faster than mass transport. When any electroactive species in the sample reaches the working electrode's surface, the reaction is reversed. In this case, mass transfer is also a limiting step. In general, mass transport can occur in three different ways. These three main ways are diffusion, migration, and convection, respectively. The downward movement of an electroactive species in a concentration gradient is recognized by diffusion, while the movement of a charged species under an electric field is a migration phenomenon. Moreover, the changing motion of an electroactive species with mechanical forces or temperature gradients is also defined by convection. So, the Nernst-Planck equation (Eq. 3) is used to describe total flux by one-dimensional mass transfer to an electrode surface [8–14].
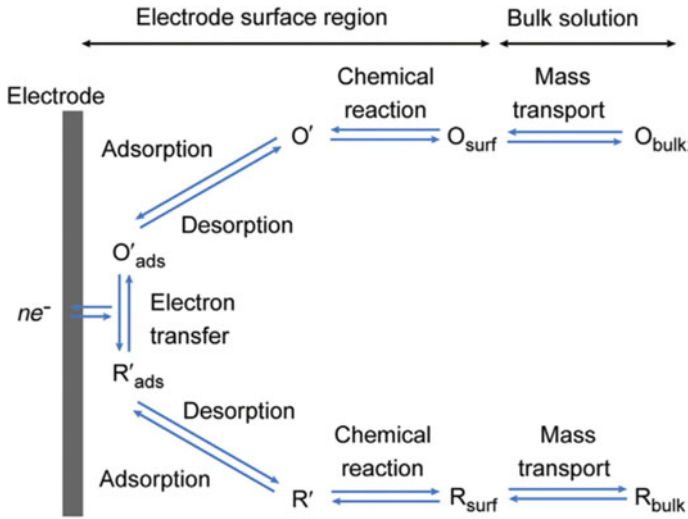
Fig. 2 Schematic representation of the heterogeneous electron transfer occurring in the surface region of the electrode. Adapted with permission from [15]. Copyright (2020) Elsevier

$$j_x = D\frac{\partial C}{\partial x} + \frac{zF}{RT}DC\frac{\partial \varphi}{\partial x} - v_x C^* \tag{3}$$

In this equation, the three different terms are related to diffusion, migration, and convection mass transport, respectively. The diffusion coefficient is represented as D ($cm^2\ s^{-1}$), the concentration is represented as C ($mol\ cm^{-2}$), the charge of the species is represented as z, the molar gas constant is represented as R ($8.314\ J\ K^{-1}\ mol^{-1}$); also, T is the temperature (K), $\delta C/\delta x$ is the concentration gradients at point x, $\delta\varphi/\delta x$ is the potential gradients at point x, and velocity is represented as vx. The flux and the analytical signals can be increased by diffusion, migration, and convection. In addition, migration is preventable when a high concentration of background electrolyte is added. Also, convection can be prevented when the solutions are not mixed and kept at room temperature. In this way, only diffusion is effective for mass transport. Therefore, the analytical equations describing the current and the interpretation of the results obtained become easier [8–14].

3 Introduction to Electrochemical Sensors

As seen in Fig. 3, electrochemical sensors are the most important subclass of chemical sensors [16]. Electrochemical sensors can be referred to as sensors in which an electrochemical device is used as a transducer element to analyze or investigate an electroactive species [17–24].
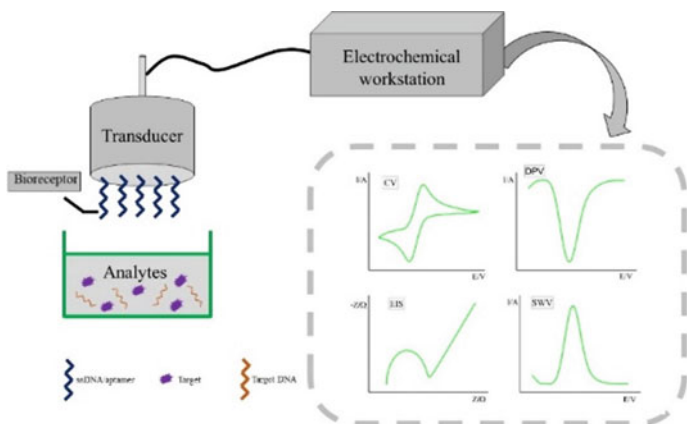
Fig. 3 Schematic diagram of electrochemical sensors. Adapted with permission from [16]. Copyright (2019) MDPI

Historically, the beginning of industrial oxygen monitoring in the 1950s is the cornerstone of electrochemical sensors to be used in many fields in the coming years. Clark, known as the father of the biosensor, proposed the oxygen sensor conception using two electrodes of a cell combined with an oxygen-permeable membrane. This membrane served to separate the electrodes and the electrolyte solution from each other. In this sensor proposed by Clark, oxygen diffused through the membrane and decreased at the indicator electrode. The current obtained by this phenomenon was found to be proportional to the amount of oxygen in the sample. In later times, the Clark oxygen sensor was preferred wide practice application from medicinal chemistry to environmental analysis or industrial monitoring. Despite gaining commercial popularity, Clark oxygen sensors had some drawbacks. The resulting electric current signal was unstable and required pre-calibration processes that often prevented their use. It was also reported that in 1963, during the Cold War, another oxygen sensor was developed and used to analyze water quality in the former Union of Soviet Socialist Republics.

Nowadays, modern electrochemical sensors are frequently used to detect many different physical, chemical, or biological parameters in our daily lives. Electrochemical sensors have been popular in many applications such as environmental monitoring, health and instrumentation sensors, and automobiles, airplanes, mobile phones, and energy or energy storage. In recent years, advances in electronics, engineering, and technology have enabled the production of smaller sensors, mainly more sensitive and more selective, with lower production and maintenance costs [17–20, 25, 26]. Electroanalytical methods based on a transducer element in electrochemical sensors were discussed in detail in successive sections.

4   Overview of Electroanalytical Methods

Electroanalytical methods are used to qualitative or quantitative investigate the analyte by measuring the potential, charge, or current produced by the system in response due to electrical, chemical, or biochemical interaction in an analytical procedure [13, 27]. The electric current electric potential or electric charge produced by the system allows determining the relationship of the species with different parameters such as concentration in the electroanalytical system. Therefore, electroanalytical methods have found a wide range of applications, including medicine, pharmaceutical, industry, energy storage, environmental monitoring, quality control, and analysis [14]. These methods also have many different advantages over traditional analytical methods. These methods provide information about the determination of the oxidation and reduction states of an electroactive species in an electrolyte solution, the mode and transport of electron transfer, and the total concentration of an analyte. Excellent low detection limits can be obtained by electroanalytical methods. These methods contribute to determining the chemical kinetics of the analytes [12].

Moreover, low cost-effectiveness and reproducibility are the essential features that make these methods superior. The electrical signal produced by an electroanalytical method is usually derived in the presence of an analyte. Table 1 presents some basic electroanalytical methods and their classification according to the potential, resistance, and electrical signals they produce.

4.1   *Voltammetric Methods*

Voltammetry is one of the essential classes of electroanalytical methods used commonly for various disciplines such as analytical chemistry, industry, medical or biomedical chemistry, and environmental applications. In this method, the current is produced on the surface of the electrode by the analyte when the potential is applied externally. The potential is applied in different variations during the analysis, either continually or stepwise [28]. Therefore, voltammetry can be defined as a method of measuring the current produced against an applied potential. The obtained curves

Table 1 Classification of electroanalytical methods

Electroanalytical method	Monitored electrical properties	Units
Potentiometry	Potential difference (Volts)	V
Conductometry	Resistance (Ohms)	Ω
Amperometry and voltammetry	Current (Amps) as a function of applied potential	I
Coulometry (Q)	Current as a function of time (Coulombs)	$C = I\,s$
Capacitance (C)	Potential load (Farads)	$F = C\,V^{-1}$

(current (i) vs. potential (E)) as a result of the analysis are called voltammograms [8–14, 18, 28]. Modern voltammetric measurements are usually performed in a cell containing three different electrodes. These electrodes are the working electrode, the reference electrode, and the auxiliary or counter electrode, respectively. The electrode in direct contact with the analyte is the working electrode, and redox events occur on the surface of the electrode during the analysis. Therefore, this electrode behaves like a standard half-cell. Examples of working electrodes frequently used in voltammetry are mercury electrodes, metal electrodes, carbon electrodes, and ultra-microelectrodes. These working electrodes, which have a wide potential range, do not react chemically, are easily produced, and are cost-effective, provide the opportunity to produce sensitive, sensitive electrodes suitable for new technology for electrochemical studies by being modified with various materials today. Improved working electrodes can be obtained by modifying these electrodes with various polymers, metal oxides, nanoparticles, and biological materials [8–14, 18, 28].

Secondly, the reference electrode has a specific reduction potential, and no current flows through it. The main task of the reference electrode is to measure and control the potential of the working electrode. Examples of frequently used reference electrodes are standard hydrogen electrode (SHE), calomel reference electrode (KRE), silver/silver chloride reference electrode (Ag/AgCl), and mercury-mercury (I) sulfate reference electrode [8–14, 18, 28].

The last electrode is called the auxiliary electrode or counter electrode. It acts as a bridge connecting the working electrode and the electrolytic solution. It allows the current produced by the working electrode to pass through the cell without passing through the reference electrode. The schematic representation of general voltammetric cells and electrodes is shown in Fig. 4 [29]. Signals applied to electrochemical cells generate characteristic current responses. Based on these signals, voltammetric methods can be classified. Each method will be described in detail in the following sections.
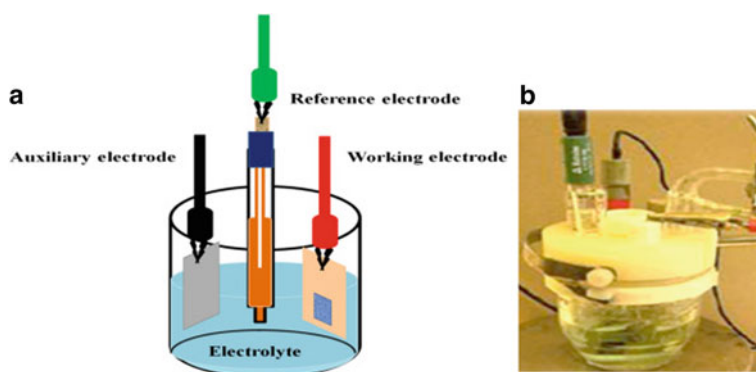
Fig. 4 Three-electrode system consisting of working, reference, and auxiliary electrodes for **a** Schematic representation and **b** Commercially available cell and electrodes. Adapted with permission from [29] Copyright (2022) Elsevier

4.1.1 Cyclic Voltammetry

Cyclic voltammetry is one of the most frequently used electroanalytical methods nowadays. Although it is not used very often in qualitative analysis, it has a wide range of use when examining reduction/oxidation reactions, determining the reactants, and observing the ongoing reactions of the resulting products. In cyclic voltammetry, the current is measured as the potential is shifted in one direction and then the other; hence, the current is measured as a function of voltage in this method. As the current electrode response used in cyclic voltammetry increases and decreases linearly, potential conversion occurs. The application usually starts at the potential where no electrode processes occur, and the voltage is measured at a constant rate until the changing potential is reached [8, 30–33].

The cyclic voltammetry method was developed by Nicholson and Shain in the 1960s and was designed as a simpler analysis method that makes it possible to analyze the shape of the current–voltage curve formed in a voltammetric analysis without having to examine it thoroughly. With the application of this method, it is aimed to determine the rate of heterogeneous electron transfer or homogeneous chemical processes accompanying the charge transfer step by simply measuring the peak voltage and peak current as a function of the rate [8, 30–32]. A general cyclic voltammogram saved for a reversible electrochemical reaction is shown in Fig. 5 [29].

Cyclic voltammetry has had the opportunity to be applied in many fields; these include the analysis of solids in the presence or absence of supporting electrolytes, emulsions or suspensions, polymers, biological systems such as membrane and liquid/liquid systems, enzymes, and bacterial cultures. In addition to being applicable in many different fields, this method also provides important advantages in terms of understanding the thermodynamics of oxidation/reduction processes and understanding the kinetics of heterogeneous electron transfer reactions [8, 30–33].
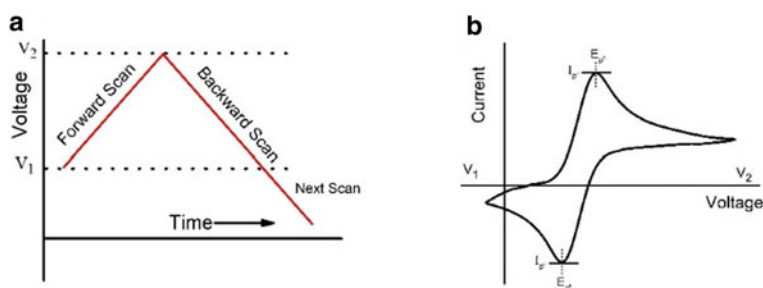
Fig. 5 Cyclic voltammetry response for the redox reaction in an electrochemical cell. **a** Time versus voltage and **b** Voltage versus current graph. Adapted with permission from [29]. Copyright (2022) Elsevier

4.1.2   Linear Sweep Voltammetry

In this method, the electrode potential changes linearly with time (t) and scan rate (v = dE/dt). While applying this method, conventional electrodes generally operate at speeds between 1 mV s^{-1} and 1 V s^{-1}, while scanning speeds of 10^3 or 10^6 V s^{-1} can be increased with ultramicroelectrodes. Scanning is initiated at a potential where there is no electrochemical reaction, and a current begins to increase with the potential at the potential where charge transfer begins. After a maximum value (current peak), this current begins to decrease due to the depletion of the reactants at the interface. Voltammograms obtained as a result of linear scanning voltammetry are sigmoidal curves called "voltammetric waves". There are also peak-shaped voltammetric waves; they can be symmetrical or asymmetrical [8, 9, 12–14, 34].

4.1.3   Pulse Voltammetry

In 1958, a study by Barker and Jenkin introduced pulsed voltammetric methods to the literature. The primary purpose of all voltammetric methods is to reduce the capacitive and residual current and increase the faradaic current. In these methods, the potential unique to each method is applied in the form of pulses. The current is measured at the end of each pulse, where the capacitive current is close to zero. This is one of the best ways to improve the effect of faradaic current and increase the sensitivity of the methods. According to the applied potential form, there are different types of pulse voltammetric methods such as normal pulse voltammetry (NPV), differential pulse voltammetry (DPV), and square-wave voltammetry (SWV) [8, 9, 12–14, 34, 35].

Normal Pulse Voltammetry

In normal pulse voltammetry, a series of pulses with increasing intensity at desired time intervals are applied to the working electrode. The system is based on the principle of increasing the intensity of the pulses linearly and keeping the electrode at a constant voltage that will not cause the analyte reaction between applied pulses. Current values are measured towards the end of the applied pulse, that is when the loading current approaches zero. A sigmoidal voltammogram is obtained when these current values are plotted against the potential [8, 9, 12–14].

Differential Pulse Voltammetry

Differential pulse voltammetry is an electroanalytical method used for the quantification of organic and inorganic substances, especially in very small amounts. In this method, fixed-size pulses are applied to the working electrode at a time interval just before each drop drips. The current is measured twice; the first measurement is

Fig. 6 Potential wave profiles for **a** Differential pulse voltammetry. **b** square-wave voltammetry. Adapted with permission from [36]. Copyright (2017) Elsevier
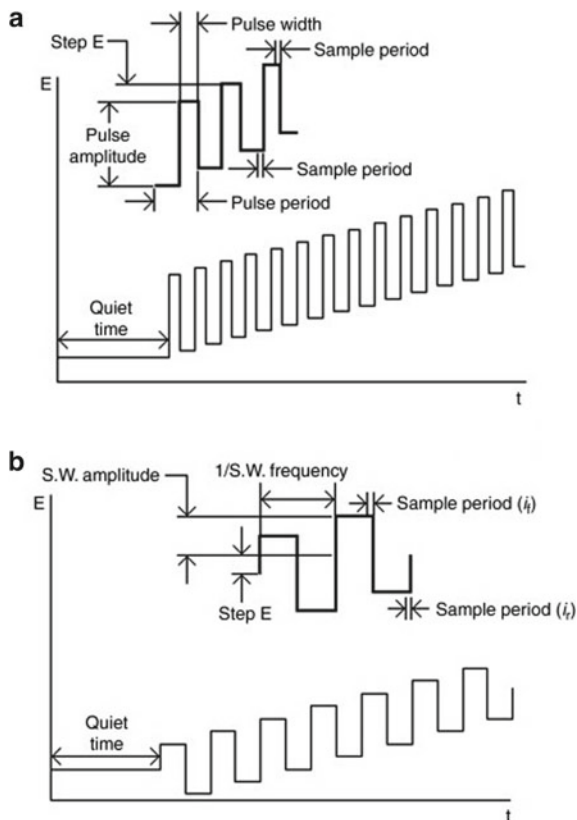
taken just before applying the pulse and the second at the end of the pulse life, at a point where the charging current decreases (Fig. 6a). The first current is subtracted from the second, and the difference is plotted according to the applied potential. The resulting differential pulse voltammogram is a voltammogram consisting of current peaks, the height of which is directly proportionate to the concentration of the analyte being measured. The most important advantage of this method is that it allows measurements at very small concentrations (10^{-8} M). Moreover, it facilitates the quantification of two analytes with similar redox potentials; because when this method is used, there is usually a noticeable difference between the currents from which the peaks of these two species come. A third advantage is that it helps to better eliminate capacitive/background current by taking dual measurements. Thus, it is possible to quantify smaller concentrations [8, 9, 12–14, 36].

Square-Wave Voltammetry

Square-wave voltammetry is another electroanalytical method that uses a very fast voltage scanning rate to complete the entire measurement process in a short time. This method is applied to the voltage working electrode in the form of relatively large rectangular waves [37]. The duration of this rectangular wave cycle (t_{sq}) is equal to the duration of the ladder-shaped voltage steps and is usually between 5 and 10 ms. Two current values are measured in each rectangular pulse cycle, the first at the positive end of the pulse and the second at the negative end of the pulse. A square wave voltammogram is obtained by measuring the difference between these two current values against the potential of the working electrode (Fig. 6b) [36]. In this method, since the measurement is made very fast, reversible processes, they do not give a distinctive current signal; This allows measurements to be taken in oxygenated environments. Thus, rapid measurements can be taken in flow systems where it is difficult to remove oxygen. There is a rate at which a frequency of 1–100 square waves can be achieved in 1 s; this achieves a speed at which a full voltammogram can be obtained in a few seconds, and the analysis time can be drastically reduced. However, these rapid measurements reduce precision; because using shorter pulse intervals will result in a lower i_F/i_C ratio [8, 9, 12–14, 34–37].

4.1.4 Stripping Voltammetry (Anodic and Cathodic)

Stripping analysis is one of the most sensitive electroanalytical methods and is therefore used especially for the quantification of trace metals. The reason for this great sensitivity is the combination of a practical pre-deposition step with advanced measurement processes that create an excellent signal. Because metals are pre-deposited on the electrode, it is possible to reach lower detection limits than solution-phase voltammetric measurements, a lower detection limit of 10^{-10} M [8, 9, 12–14, 34, 35, 38].

Stripping analysis is a two-step technique and is used with mercury electrodes (hanging drop mercury electrode or thin mercury film electrode). The material to be examined is either reduced in mercury and allowed to form amalgams or adsorbed to form an insoluble mercury salt. In the first step of the method, a small part of the metal ions in the solution is deposited on the mercury electrode; Thus, the pre-deposition process of the metal is carried out. This is followed by the stripping phase (measuring phase); at this stage, the electrolysis is terminated, the mixing is stopped, the dissolution (stripping) of the deposition is ensured. According to the feature of the deposition and measurement stages, different stripping analyzes can be applied [8, 9, 12–14, 34, 35, 38].

The pre-deposition process aims to deposit the substance to be analyzed in the solution on the electrode surface with a small surface area. Although pre-deposition allows reaching lower detection limits, the length of the process creates some practical difficulties. The balance between reaching a low limit of detection and analytical practicality can be achieved more effectively with new methods [8, 9, 12–14, 34, 35].

The most commonly used method is anodic stripping voltammetry of all stripping methods. In this method, during the working electrode deposition process, the cathode becomes the anode during the stripping process, and the analyte is oxidized to return to its original form. The pre-deposition process is carried out by cathodic deposition under a controlled time and voltage. The deposition potential is at a more negative potential than the potential at which the most difficult to reduce metal ion can be identified. Metal ions reach the mercury electrode by diffusion or convection, where they are reduced and accumulate as amalgam. Convective convection is achieved by electrode rotation or mixing of the solution. The deposition time is chosen depending on the concentration of metal ions. After the preselected deposition time has elapsed, the convection is stopped, and the potential is measured with anodic, linear, or more precise potential-time (pulse) waveforms. Amalgam-forming metals are reoxidized and stripped from the electrode surface during anodic scanning [8, 9, 12–14, 34, 35].

Cathodic stripping voltammetry is the opposite of anodic stripping voltammetry. In this method, the electrode acts as the anode during the deposition process and as the cathode during the stripping process. This method, which involves the anodic deposition of the analyte, is followed by stripping in a negative potential scan. In other words, the substance to be analyzed first is oxidized on the electrode and forms an insoluble film; Then, this substance is reduced in the negative region, and its measurement is made [8, 9, 12–14].

4.2 Amperometry

Amperometry is one of the most widely used electroanalytical methods, especially for the analysis of biological species. In this method, a constant potential is applied to oxidize or reduce the target analyte, and the resulting current is monitored over time. Since the constant potential is applied from this method, the selection of the most suitable potential is of great importance [39, 40]. Therefore, the chosen potential to oxidize or reduce the selected analyte is determined by voltammetric methods. When voltage begins to be applied, there is an initial charge current. If the charge on the working electrode is considered to be zero, when its potential is suddenly changed, the electrode surface can receive a positive charge. In this case, cations in the region close to the electrode surface will respond to the positive charge by moving away from the electrode; anions will migrate towards the electrode. This migration movement of the ions continues until the positive charges on the surface of the working electrode and the negative charge in the solution become equal. Because this movement of ions is indistinguishable, the resulting current is a small, short-lived, non-faradaic current [8, 9, 12–14, 39, 40].

4.3 Potentiometry

Potentiometry is one of the electroanalytical methods based on the measurement of the electric potential between two electrodes when the cell current is zero. One of these electrodes is typically the reference electrode, while the other is the indicator electrode. Potentiometry is a static interfacial electroanalytical method. The best-known example of potentiometry is the pH meter, which usually relies on glass membrane electrodes to determine the concentration of H^+ ions in solution [8, 9, 12–14]. Basically, it is based on the principle of measuring the concentration of H^+ ions on both sides of the glass membrane, where the interior concentration is known and fixed. A potential difference (V) is obtained in the solutions on either side of the glass membrane, and with this difference, the concentration is meaningfully measured based on the Nernst equation (Eq. 4).

$$ E = E^0 + \frac{RT}{nF} \ln \frac{[RED]}{OXI} \qquad (4) $$

In this equation, cell potential is shown as E; the standard potential of a half-reaction is presented as E^0, the universal gas constant is R, T is temperature; n is the number of electrons involved in the half-reaction (eq. mol^{-1}); F is Faraday's constant; [RED]: activity of reduced species; and [OXI]: activity of oxidized species [8, 9, 12–14].

4.4 Conductometry

Electrical conduction in an electrolyte solution is the migration of positively charged particles to the cathode and negatively charged particles to the anode. "Conductivity" is a measure of current and is directly proportional to the number of charged particles in the solution. The ions all contribute to conductivity; a current carried by any particle depends on the concentration of that particle and its ability to move in the medium [41]. Performing analyses based on direct conductivity measurements is limited due to the properties of the particles. Direct conductivity measurement is not selective in solutions with mixtures of ions since all types of ions in the solution contribute to the total conductivity of a solution. However, since the sensitivity of the method is high, it is very important in some applications. It is mostly used to control the purity of distilled or deionized water. The intrinsic conductivity of pure water is $5 \times 10^{-8} \, \Omega^{-1} \, cm^{-1}$; trace amounts of ionic impurities significantly increase conductivity. Moreover, the most important advantage of the method is that it can be applied to very dilute solutions and systems where the reaction is incomplete. Analysis that cannot be done with the potentiometric or indicator turning point method can be done with this method. However, the accuracy of the method decreases with increasing total electrolyte concentration. The current change that occurs when the titrant is added is masked when the salt concentration in the solution is high [8, 9, 12–14, 41, 42].

4.5 Coulometry

Coulometry is an electroanalytical method that responds to the total charge consumed by the analyte as a result of the redox reaction on the electrode. Calibration is not required as concentration-dependent signals in coulometry can be measured by electric charge, not mass transfer [43, 44].

The Faraday equation shows the total charge passing between the two electrodes during the redox reaction (Eq. 5).

$$Q_t = \int_0^t i(t)dt = zF_n = zF_e v \tag{5}$$

In this equation, electrical charge is shown as 'Q' (Coulombs), 'i' is defined as current (A), 't' shows time (s), the number of electrons exchanged per analyte molecule is shown as 'z', 'F' is Faraday constant (96 487 C mol^{-1}), the number of moles is shown as 'n', 'c' the molar concentration, and 'V' the volume.

Since the electric charge can be measured directly with coulometry, this method increases the accuracy of the analysis and reduces the analysis time. There are basically two types of coulometric analysis options, constant current and constant potential. Although not frequently used in industry, quantification of water in different samples using Karl Fischer titration is the most commonly used approach. This method differs from amperometry and voltammetry as it does not measure concentration-dependent current [8, 9, 12–14, 43, 44].

4.6 Electrochemical Impedance Spectroscopy

Electrochemical impedance spectroscopy (EIS) is an important electroanalytical method used to study mass, charge, and diffusion processes in an electrochemical cell. It can measure the complex electrical resistance of an electrochemical system. Its use has become popular due to the advantages such as being stable compared to other electroanalytical methods, allowing to examine signal changes in a wide application frequency from 1 to 1 MHz, being sensitive, characterization with this technique without damaging the modified surface. This method has often found use in corrosion studies, characterization of film surfaces, batteries, semiconductor electrodes, electrochemical sensors, and biosensors [8, 9, 12–14, 45–48]. EIS measures impedance by frequency change in alternative current (AC) potential. The behavior that occurs in an electrochemical cell can be represented by an equivalent circuit containing resistance (R), inductance (L), and capacitance (C). AC circuit models of faradaic and non-faradaic systems containing these components are shown in Fig. 7a [49].

Fig. 7 a (a) Non-faradaic circuit model, (b) faradaic circuit model. **b** Schematic representation of the EIS circuit and the redox reaction occurring at the working electrode in a conventional electrochemical cell. (i.e., three-electrode system). Adapted with permission from [49, 50]. Copyright (2021) RSC, Copyright (2021) MDPI
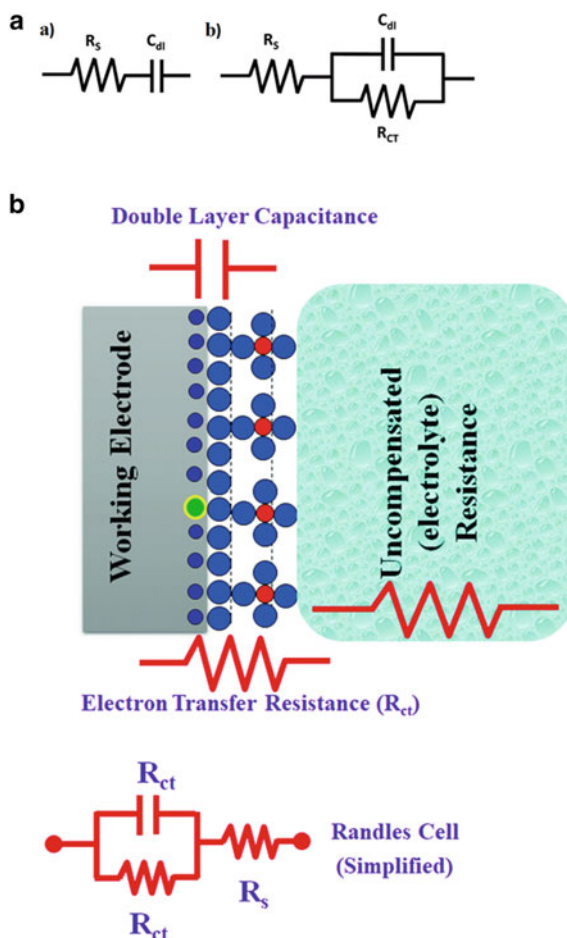
By using these equivalent circuits to interpret the EIS measurements, the values of the test result are obtained and interpreted. With EIS, material properties that can affect properties such as conductivity, resistance or capacitance, and changes in solution-electrode interface electron transfer kinetics can be monitored. The graph of the measured impedance in the virtual plane is called the Nyquist curve. The generated solution resistance (R_s), charge transfer resistance (R_{ct}), and Warburg impedance (W) are summed and displayed in Nyquist plots. A schematic representation of the EIS circuit is shown in Fig. 7b [50].

Parameters used in equivalent circuits to examine the EIS results are as follows:

(i) R_s is electrolyte resistance which relies on the ion concentration, the ion type, as well as the electrode area,

(ii) R_{ct} is charge transfer resistance which is inversely comparable to the electron transfer rate,

(iii) C_{dl} is directly related to double-layer capacitance charge and background current,

(iv)   W is Warburg impedance which results from mass transfer limitations and can be used to evaluate efficient diffusion coefficients.

The EIS method measures the AC passing through the cell by applying a sinusoidal AC potential sent to the system. Although the current generated by the oscillation potential sent to the system is the same, there may be a phase shift. This varies according to the resistance and capacitive properties of the electrochemical system [8, 9, 12–14, 45, 46].

Impedance is the capacity of a circuit element to resist. Unlike the impedance resistor, it contains much more complex circuit elements. For a linear or pseudo-linear system in impedance measurement, the current measured against the sinusoidal potential appears as a sinusoid in shifted phase. The excitation signal is given as a function of time. ε_t is the potential at time t, ε_0 is the amplitude of the signal, and w is the radial frequency shown in Eq. (6).

$$\varepsilon_t = \varepsilon_0 (\sin wt). \tag{6}$$

Impedance plots can be created with two different graphs, Nyquist and Bode. Nyquist charts consist of real (Zreal) and imaginary parts (Zimag). Each point on the Nyquist plot is experimental results corresponding to different frequencies. Zreal and Zimag sum |Z| is the vector impedance. The shape of the semicircle in the Nyquist graph provides information about the electron transfer resistance. Another impedance plot, the Bode plot, provides the same data as Nyquist, but is also a better way to obtain frequency information [8, 9, 12–14, 45, 46].

5   Conclusions and Future Perspectives

Compared to traditional methods, electrochemistry stands out as a method that investigates electron exchange resulting from redox reactions for the investigation of specific analyzes or mechanisms of many different compounds. Nowadays, the progressive development of electrochemical sensor technology has made it possible to reach the limits of more sensitive detection. When sensor technology is used, detection is generally fast, and it is possible to obtain reasonable, simple, and very sensitive results depending on the electroanalytical method and nature of the compound used. The electrochemical sensor design to be chosen should depend on the target compound, the matrix such as serum, urine, or pharmaceutical preparation, the desired sensitivity and selectivity for the target compound, as well as the practical feasibility and cost of the measurement. Therefore, the selection of the electroanalytical method is important in the first step.

The following general points can be considered when choosing electroanalytical methods, (i) cyclic voltammetry is a simple method to carry out analysis and is cost-effective for use; (ii) to obtain more sensitive detection, pulse voltammetry methods such as differential pulse voltammetry or square-wave voltammetry are preferred; (iii) rather than voltammetric methods, amperometry generally presents more selectivity and sensitivity for enzyme-based sensors because fixed oxidation or reduction potential is operated instead of a potential scan, however, less sensitive results are obtained when amperometry used compared to pulse voltammetry methods or impedance spectroscopy; (iv) electrochemical impedance spectroscopy offers many advantages, especially in the high-sensitivity analysis of biological compounds such as proteins, however, impedance is a slower method than other electroanalytical methods, and more complex and expensive potentiostats are needed to use this method.

Considering traditional methods such as chromatographic and optical methods, electrochemical sensors require more simplicity, low-cost instrumentation, and labor power. Electrochemical sensors in general (though there are exceptions) offer superior advantages over these methods in terms of sensitivity, specificity, and selectivity. These advantages depend on the complex matrix of the target compound and sample. One of the most valuable features of electrochemical sensors is that they can be miniaturized for different clinical applications, such as the glucometer, which allows for in situ analysis. Other than the analyte, changes such as the working electrode material, buffer solution pH, or modification can be made in electrochemical methods to avoid non-specific bindings or background signals from solutions and chemicals. However, it is more challenging to avoid background signals with optical methods. To sum up, the use of electrochemical sensor technology can respond to the problems of the era very quickly due to features such as (i) the abundance of the target analyte and matrix, (ii) cost requirements and fast analysis capability, (iii) the amount spent for detection, and (iv) the sensing location (centralized lab vs. in situ measurements) will be able to find solutions and keep up with the developing technology.

References

1. Yonzon, C.R., Stuart, D.A., Zhang, X., McFarland, A.D., Haynes, C.L., Van Duyne, R.P.: Towards advanced chemical and biological nanosensors—an overview. Talanta **67**, 438–448 (2005)
2. Rajendran, M., Ellington, A.D.: Nucleic acids for reagentless biosensors. In: Ligler, F., Taitt, C. (eds.) Optical Biosensors: Present and Future, pp. 369–396. Elsevier (2002)
3. Ronkainen, N.J., Halsall, H.B., Heineman, W.R.: Electrochemical biosensors. Chem. Soc. Rev. **39**, 1747–1763 (2010)
4. Privett, B.J., Shin, J.H., Schoenfisch, M.H.: Electrochemical sensors. Anal. Chem. **82**, 4723–4741 (2010)
5. Fan, Y., Han, C., Zhang, B.: Recent advances in the development and application of nanoelectrodes. Analyst **141**, 5474–5487 (2016)
6. Edwards, G.A., Bergren, A.J., Porter, M.D.: Chemically modified electrodes. In: Zoski, C.G. (ed.) Handbook of Electrochemistry, pp. 295–327. Elsevier, New York (2007)
7. Javaid, M., Haleem, A., Rab, S., Pratap, S.R., Suman, R.: Sensors for daily life: a review. Sens. Int. **2**, 100121 (2021)

8. Compton, R.G., Banks, C.E.: Understanding Voltammetry. World Scientific Publishing (2010)
9. Inesi, A.: Instrumental methods in electrochemistry. Bioelectrochem. Bioenerg. **15**, 531 (1986)
10. Zanello, P.: Inorganic Electrochemistry Theory, Practice and Application. Royal Society of Chemistry, UK (2003)
11. Fry, A.J.: Computational applications in organic electrochemistry. Curr. Opin. Electrochem. **2**(1), 67–75 (2017)
12. Uslu, B., Ozkan, S.A.: Electroanalytical methods for the determination of pharmaceuticals: a review of recent trends and developments. Anal. Lett. **44**, 2644–2702 (2011)
13. Kissinger, P.T., Heineman, W.R., Achterberg, E.P.: Laboratory techniques in electroanalytical chemistry. TrAC Trends Anal. Chem. **15**, 550 (1996)
14. Scholz, F., Stojek, Z., Inzelt, G., Marken, F., Neudeck, A., Bond, A.M., Lovric, M., Retter, U., Lohse, H., Compton, R.G., Fiedler, D.A., Kahlert, H., Komorsky-Lovric, S.: Electroanalytical Methods: Guide to Experiments and Applications, 2nd edn. Springer (2010)
15. Islam, M.N., Channon, R.B.: Electrochemical sensors. In: Bioengineering Innovative Solutions for Cancer, pp. 47–71. Elsevier Ltd. (2019)
16. Wu, Q., Zhang, Y., Yang, Q., Yuan, N., Zhang, W.: Review of electrochemical DNA biosensors for detecting food borne pathogens. Sensors (Switzerland) **19**, 1–32 (2019)
17. Wang, Y., Xu, H., Zhang, J., Li, G.: Electrochemical sensors for clinic analysis. Sensors **8**, 2043–2081 (2008)
18. Bakker, E., Qin, Y.: Electrochemical sensors. Anal. Chem. **78**, 3965–3984 (2006)
19. Goud, K.Y., Satyanarayana, M., Hayat, A., Gobi, K.V., Marty, J.L.: Nanomaterial-based electrochemical sensors in pharmaceutical applications. In: Grumezescu, A.M. (ed.) Nanoparticles in Pharmacotherapy, pp. 195–216. William Andrew Publishing (2019)
20. Palacek, E., Scheller, F., Wang, J.: Electrochemistry of Nucleic Acids and Proteins: Towards Electrochemical Sensors for Genomics and Proteomics. Elsevier Science (2005)
21. Yarman, A., Turner, A.P.F., Scheller, F.W.: Electropolymers for (nano-)imprinted biomimetic biosensors. In: Nanosensors for Chemical and Biological Applications: Sensing with Nanotubes, Nanowires and Nanoparticles, pp. 125–149. Woodhead Publishing (2014)
22. Kriz, D., Ansell, R.J.: Biomimetic electrochemical sensors based on molecular imprinting. In: Techniques and Instrumentation in Analytical Chemistry, pp. 417–440. Elsevier Masson SAS (2001)
23. Oveissi, F., Nguyen, L.H., Giaretta, J.E., Shahrbabaki, Z., Rath, R.J., Apalangya, V.A., Yun, J., Dehghani, F., Naficy, S.: Sensors for food quality and safety. In: Food Engineering Innovations Across the Food Supply Chain, pp. 389–410. Academic Press (2022)
24. Simões, F.R., Xavier, M.G.: Electrochemical sensors. In: Nanoscience and its Applications, pp. 155–178. Elsevier Inc. (2017)
25. Magner, E.: Trends in electrochemical biosensors. Analyst **123**, 1967–1970 (1998)
26. Clark, L.C., Lyons, C.: Electrode systems for continuous monitoring in cardiovascular surgery. Ann. N. Y. Acad. Sci. **102**, 29–45 (1962)
27. Wang, J.: Electroanalytical Techniques in Clinical Chemistry and Laboratory Medicine. VCH, New York (1988)
28. Delahay, P., Mamantov, G.: Voltammetry at Constant Current Review of Theoretical Principles. **12**, 42 (2021)
29. Majeed, S., Naqvi, S.T.R., ul Haq, M.N., Ashiq, M.N.: Electroanalytical techniques in biosciences: conductometry, coulometry, voltammetry, and electrochemical sensors. In: Analytical Techniques in Biosciences, pp. 157–178. INC (2022)
30. Gosser, D.K.: Cyclic Voltammetry Simulation and Analysis of Reaction Mechanisms. VCH (1993)
31. Gosser, D.K.: Cyclic Voltammetry; Simulation and Analysis of Reaction Mechanisms. VCH Publishers, New York (1994)
32. Gileadi, E.: Electrode Kinetics for Chemists, Chemical Engineers and Materials Scientists. VCH Publishers, New York (1993)
33. Elgrishi, N., Rountree, K.J., McCarthy, B.D., Rountree, E.S., Eisenhart, T.T., Dempsey, J.L.: A practical beginner's guide to cyclic voltammetry. J. Chem. Educ. **95**, 197–206 (2018)

34. Laviron, E.: Surface linear potential sweep voltammetry: Equation of the peaks for a reversible reaction when interactions between the adsorbed molecules are taken into account. J. Electroanal. Chem. Interfacial Electrochem. **52**, 395–402 (1974)

35. Mirceski, V., Komorsky-Lovric, S., Lovric, M.: Square Wave Voltammetry Theory an Application Monographs in Electrochemistry. Springer, Berlin, London (2007)

36. Kurbanoglu, S., Uslu, B., Ozkan, S.A.: Carbon-based nanostructures for electrochemical analysis of oral medicines. In: Andronescu, E., Grumezescu, A.M. (eds.) Nanostructures for Oral Medicine A Volume in Micro and Nano Technologies, pp. 885–938. Elsevier (2017)

37. Mirceski, V., Gulaboski, R., Lovric, M., Bogeski, I., Kappl, R., Hoth, M.: Square-wave voltammetry: a review on the recent progress. Electroanalysis **25**, 2411–2422 (2013)

38. Venton, B.J., DiScenza, D.J.: Voltammetry. In: Patel, B.A. (ed.) Electrochemistry for Bioanalysis, pp. 27–50. Elsevier (2020)

39. Amine, A., Mohammadi, H.: Amperometry. Encycl. Anal. Sci. 85–98 (2019)

40. Patel, B.A.: Amperometry and potential step techniques. In: Patel, B.A. (ed.) Electrochemistry for Bioanalysis, pp. 9–26. Elsevier Inc. (2020)

41. Safonova, L.P., Kolker, A.M.: Conductometry of electrolyte solutions. Russ. Chem. Rev. **61**, 959–973 (1992)

42. Clarke, W., Orazio, P.D.: Electrochemistry. In: Clarke, W., Marzinke, M.A. (eds.) Contemporary Practice in Clinical Chemistry, pp. 159–170. Elsevier (2020)

43. Kies, H.L.: Coulometry. J. Electroanal. Chem. **4**, 257–286 (1962)

44. Milner, G.W.C., Phillips, G.: Equipment and technique for constant-current coulometry. In: Phillips, G. (eds.) Coulometry in Analytical Chemistry, Milner GWC, pp. 29–53. Elsevier (1967)

45. Mollarasouli, F., Kurbanoglu, S., Ozkan, S.A.: The role of electrochemical ımmunosensors in clinical analysis. Biosensors **9**, 86 (2019)

46. Bahadır, E.B., Sezgintürk, M.K.: A review on impedimetric biosensors. Artif. Cells Nanomed. Biotechnol. **44**, 248–262 (2016)

47. Bigdeli, I.K., Yeganeh, M., Shoushtari, M.T., Zadeh, M.K.: Electrochemical impedance spectroscopy (EIS) for biosensing. In: Thomas, S., Nguyen, T.A., Ahmadi, M., Yasin, G., Farmani, A. (eds.) Nanosensors for Smart Manufacturing, pp. 533–554. Elsevier Inc. (2021)

48. Grassini, S.: Electrochemical impedance spectroscopy (EIS) for the in-situ analysis of metallic heritage artefacts. In: Dillmann, P., Watkinson, D., Angelini, E., Adriaens, A. (eds.) Corrosion and Conservation of Cultural Heritage Metallic Artefacts, pp. 347–367. Woodhead Publishing Limited, Cambridge, UK (Chapter 16) (2013)

49. Laschuk, N.O., Easton, E.B., Zenkina, O.V.: Reducing the resistance for the use of electrochemical impedance spectroscopy analysis in materials chemistry. RSC Adv. **11**, 27925–27936 (2021)

50. Magar, H.S., Hassan, R.Y.A., Mulchandani, A.: Electrochemical impedance spectroscopy (EIS): principles, construction, and biosensing applications. Sensors **21**, 1–21 (2021)

Conducting Polymer-Based Nanofibers for Advanced Electrochemical Energy Storage Devices

Wenkun Jiang, Yinghui Han, Zhiwen Xue, Yongqi Zhu, and Xin Zhang

Abstract Conducting polymer-based nanofibers possesses not only the electrical and optical properties of metal and non-polar semiconductors but also the flexible mechanical properties and machinability of organic polymers, as well as electrochemical redox activity. Due to the unique characteristics of nanoscale and linear morphology, conducting polymer-based nanofibers are manifested in surface trait, small size effect, quantum size effect, and macroscopic quantum positive tunnel effect, especially in high sensitivity through the doping of metal nanoparticles, which are in line with the development trend of wearable devices with miniaturization, multi-function, flexibility, and intelligence. Therefore, conducting polymer-based nanofibers have potential applications in energy, optoelectronic devices, sensors, molecular conductors, and other fields. This chapter mainly introduces the properties, synthesis methods, and applications of conductive polymer nanofibers for electrochemical energy storage.

Keywords Polymer nanofibers · Conducting polymer · Wearable devices · Flexible supercapacitor · Flexible tactile sensor · Electrochemical energy storage

1 Introduction

With the improvement of the performance requirements of electronic devices, the development trend of electronic devices is gradual to miniaturization, multi-function, and flexible wearable. Due to the advantages of low cost, large-scale preparation, good flexibility, good electrochemical stability, high sensitivity, and large specific surface area, conducting polymer-based nanofibers are been widely used in energy storage equipment and sensor equipment in recent years [1]. The intrinsic conducting

W. Jiang · Y. Han (✉) · X. Zhang
College of Resources and Environment, University of Chinese Academy of Sciences, Beijing 100049, China
e-mail: hanyinghui@ucas.ac.cn

W. Jiang · Z. Xue · Y. Zhu
Department of Mathematics and Physics, North China Electric Power University, Baoding 071003, China

polymer-based nanofiber material has an π conjugated structure to provide the conductive carrier with conductivity, which is one of the most commonly used materials for electronic devices. Filling type conducting polymer nanofiber, by adding a certain amount of conductive filler inside the polymer material, the fillers contact with each other to form a conductive network, providing a path for electron flow, to give polymer nanofiber material good conductivity. The template method is the most extensive efficient method for preparing conducting polymer nanofibers, which are suitable for the mass production of conductive polymer nanofibers. The main characteristic of the template method is that no matter the chemical reaction occurs in the liquid phase or gas phase, the reaction is carried out in an effectively controlled area. No template method by controlling the reaction parameters, the conducting polymer in a certain direction of the preferred growth method, no template removal process, the synthesis process is simple. Electrostatic spinning is used to produce conducting polymer nanofibers by applying an applied electric field in the polymer solution. In this chapter, we will introduce in detail the structure, synthesis methods, and the latest advances in electrochemical energy storage devices for conducting polymer-based nanofibers.

2 Structure and Attributes

2.1 Definitions and Characteristics of Conducting Polymers

Conducting polymers are formed by chemical or electrochemical doping of polymers with conjugated π bonds a class of polymer materials whose conductivity ranges from insulator to conductor. Figure 1 shows the influence of doping on the resistivity of conductive polymerization. Conducting polymer possesses excellent conductivity. According to the different doping degrees, its conductivity can fluctuate in a very
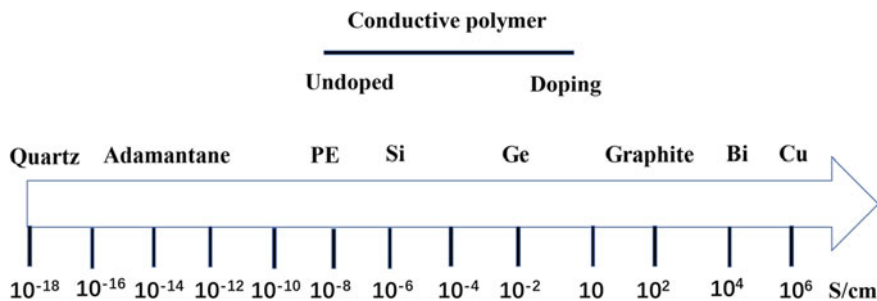
Fig. 1 Influence of doping on the resistivity of conductive polymerization

wide range. Most of the redox reactions and color changes of conducting polymers are reversible. The structure and properties of polymer can be controlled by changing the synthesis methods. It also exhibits a series of excellent optical effects and machinability.

2.2 Classification of Conducting Polymer Nanofibers

2.2.1 Intrinsically Conducting Polymer Nanofiber

Intrinsic type conducting polymer materials refer to themselves with conductive properties of the polymer, also known as structural conducting polymer materials. Its conductivity is realized by providing conductive carriers with π conjugated structure inside the molecular structure. This phenomenon of polyacetylene is shown in Fig. 2. Conjugated polymer, such as polypyridine, polyacetylene, polyaniline, polythiophene, polypyridine, etc., have great application value. However, due to the structure of intrinsic conducting polymer material, they are neither soluble nor fusible and has poor compatibility with other resions. According to the theory of quantum mechanics, delocalization occurs when molecular orbitals in conjugated polymer overlap with each other. In the presence of an external electric field, electrons will break away from the valence band or main chain structure, and an electric current will be formed inside the polymer, thus possessing excellent electrical conductivity. The number of π electrons increases with the increase of the molecular chain length. The lower the activation energy required for π electrons to break out of the band gap, the more likely the electron delocalization phenomenon will occur, and the better the electrical conductivity of polymer materials will be [2]. At present, the most widely studied intrinsic conducting polymer materials are the large delocalized π
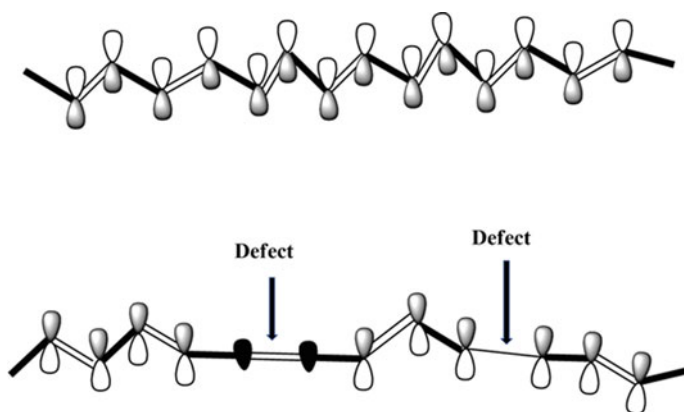
Fig. 2 Diagram of π conjugation in polyacetylene
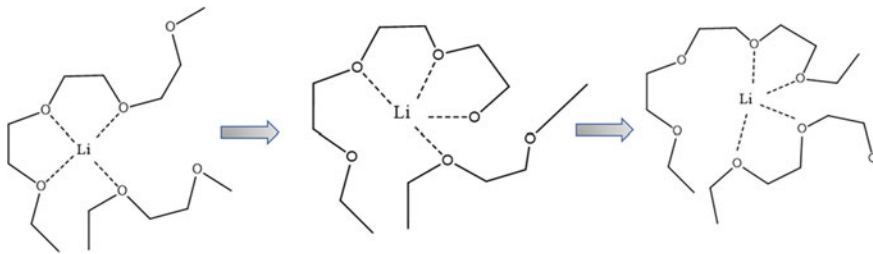
Fig. 3 Migration process of cations in polymers

bond conducting polymer materials and the conjugated structure chemically doped conducting polymer materials, which exhibit certain application potential in solar cells, microelectronic sensors, microwave absorption materials, and other fields [3].

2.2.2 Filled Conducting Polymer Nanofiber

Filled conducting polymer nanofiber material refers to the addition of a certain amount of conducting filler inside the polymer material. When the filler concentration reaches a certain level, the fillers contact each other and then form a conductive network, providing a pathway for electron flow, giving the polymer nanofiber material good conductive performances. The conductivity of filled conducting polymer nanofiber material is dependent on the number of conductive paths in the material, and its conductivity increases after electron acceptor filling, and changes when the content of filler reaches a specific value. Currently, the most commonly used conductive fillers are metal oxide particles, carbon nanomaterials, and new composite particles. This method has the advantages of a simple production process and strong operability [4]. Figure 3 shows the migration of lithium ions in polymer nanofibers.

2.2.3 Nanomaterial-doped Conducting Polymer

Conducting polymer doping falls into two categories: P-doping and N-doping. The full orbital becomes a half-full energy band by doping oxidizing substances into the polymer to capture electrons from the full orbital. Reducing the energy difference between vacant orbitals is called P-doping. Doped with reducing material, electrons are donated to vacant orbit, which lowers the energy of vacant orbit, thus reducing the energy level difference, known as N-doping [5].

3 Synthesis Methods

3.1 Template Methods

In the preparation of conducting polymer nanomaterials, composition, structure, morphology, size, orientation, and arrangement are mainly considered factors. The preparation of conducting polymer nanofibers by the template method has attracted extensive attention in recent years. The template can be designed in advance according to the size and morphology of the synthetic material. Besides the size and morphology, the structure, and the arrangement of synthetic material can also be regulated by the spatial restriction of the template and the regulation of the templating agent [6]. Figure 4 shows the typical preparation of conducting polymer nanofibers by the template method. The benefit of the template method is that no matter the chemical reaction occurs in liquid phase or gas phase, the reaction can carry out in an effectively controlled area, which is the main difference between template methods and ordinary methods.

Compared with direct synthesis, the synthesis of conducting polymer nanofibers using the template method has considerable advantages, including well-controlled morphology and structure, good dispersion stability, and facilitating mass manufacturing [7]. The rigid template-assisted method is a technique to control the structure of conducting polymer nanofibers using anodic alumina templates. The most widely used method is the AAO template-assisted method, which provides nanopores with adjustable pore sizes and shapes for the synthesis of conducting polymer nanofibers. In this way, the conducting polymer nanofibers prepared have a certain size and nanostructure and strong thermal stability [8].

Salgado et al. used silicon nanowire as a template and coated it with poly 3, 4-ethylene dioxythiophene (PEDOT). The nanomaterial can be used as an efficient photocatalyst for solar hydrogen production [9]. Liu et al. used graphene as a template
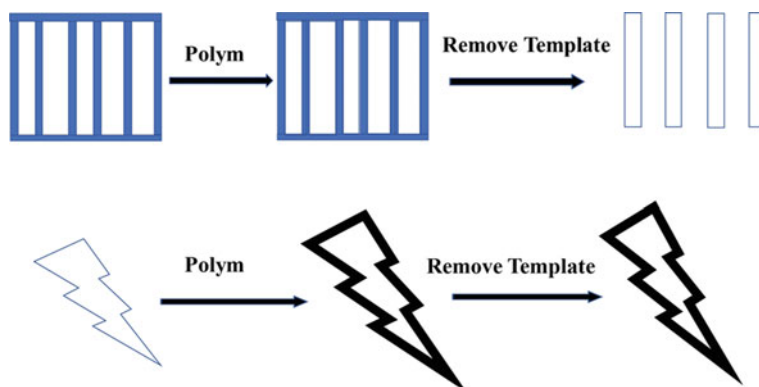
Fig. 4 Schematic diagram of nanofiber preparation by template method

to prepare the PANI micro-nano structure and applied it to supercapacitors [10]. Wu et al. synthesized PANI nanowires with high conductivity and aligned them along pore channels using aluminosilicate molecular sieve McM-41 as a template [11]. Soft templates are usually made of surfactant molecules assembled. It mainly includes a variety of ordered polymers formed by amphiphilic molecules, such as liquid crystals, vesicles, micelles, microemulsions, self-assembly membranes, and self-organizing structures of biomolecules and polymers, etc. This kind of template has a cluster with spatial structure formed by weak intermolecular or intramolecular interaction. Such cluster has obvious structural interfaces, through which the distribution of inorganic materials presents a specific trend [12]. However, the stability of the soft template structure is poor, so the template efficiency is usually not high enough [13].

Pirhady et al. used the soft template method to transform the micro-nano morphology of PANI from nanotubes to nanospheres by changing the surfactant [14]. Anantha-Iyengar et al. used alkyl trimethyl ammonium bromide cations as surfactants and obtained mono-dispersed PPy nanospheres through microemulsion polymerization. The particle size of PPy nanospheres can be well controlled below 5 nm [15].

3.2 Template-free Method

The template-free method is a method in which the conducting polymer grows preferentially in a certain direction by controlling the reaction parameters. This method does not need any template, so there is no need to remove the template, and the synthesis process is simple.

Interfacial polymerization is the most common template-free synthesis method. In this method, the monomer is dissolved in an organic solvent as oil phase, the oxidant is dissolved in doped acid as water phase, and the chemical oxidation polymerization only takes place at the oil/water phase interface. The oil phase can be carbon tetrachloride, chloroform, dichloromethane, and other solvents with higher density than water, benzene, toluene, and other solvents with lower density than water. Interfacial polymerization can effectively inhibit the secondary growth of polymers. With the progress of polymerization reaction, due to hydrophilicity, the primary polymer can quickly disperse in the water phase, which enables continuous polymerization reaction at the interface and effectively avoids the occurrence of agglomeration [16].

Dilute solution polymerization refers to the polymerization method in which the monomer solution containing trace doped acid is carefully injected into the solution containing oxidant without stirring [17]. Subramania et al. used citric acid as dopant and ammonium persulphate (APS) as the oxidant to carry out dilute solution polymerization and synthesized polyaniline nanofibers with a diameter of 20–35 nm and specific capacitance of 298 F/g [18]. Rapidly mixed polymerization refers to the rapid consumption of oxidants in the polymerization of monomers. This method can effectively inhibit secondary growth [19]. Huang et al. used the rapid mixed polymerization method to add oxidant APS drop by drop into the hydrochloric acid solution

containing aniline monomer and synthesized PANI nanofibers with a diameter of 30–35 nm, which was similar to the diameter of polyaniline nanofibers synthesized by interfacial polymerization [20].

3.3 Electrochemical Polymerization

Electrochemical polymerization refers to the method of oxidation polymerization of monomer in the electrolyte on the inert electrode surface by adjusting electrochemical parameters such as voltage, current, and electrolyte concentration under the action of the electric field. Its advantages are that the polymerization rate of conducting polymers can be effectively controlled and in-situ electrical or optical measurement can be directly carried out [21]. Zhou et al. synthesized polyaniline nanofibers by pulse current method (PGM) on the surface of stainless steel. The results showed that the double electric layer capacitance and pseudocapacitance increased with the increase of the surface area of polyaniline. The maximum specific capacitance of polyaniline nanofibers was 609 F/g, the specific energy was 26.8 Wh/kg, and the capacitance attenuation was very small after 1000 cycles [22].

3.4 Electrostatic Square Spinning

Electrostatic spinning is a spinning technology that produces polymer nanofibers by applying an applied electric field in polymer solution (namely, polymer jet electrostatic stretch spinning). It is an important method to produce microfibers. This method is significantly different from the traditional method. Firstly, the polymer solution or melt is charged with several thousand to ten thousand volts of high voltage static electricity. The charged polymer droplets are accelerated at the Taylor cone apex of the capillary under the action of the electric field force. When the electric field force is large enough, the polymer droplets can overcome surface tension and form jet streams. The trickle vaporizes or solidifies during the jet and eventually lands on the receiving device, forming a fibrous blanket similar to nonwovens. The reason why electrostatic spinning can make fibers become nanoscale is that, under the action of the strong electric field, fluid is pushed out of the Taylor cone to form a jet and the diameter becomes smaller [23]. The device is shown in Fig. 5.

Conducting polymer nanofibers are prepared by electrospinning, which can not only improve the specific surface area but also obtain ideal chemical properties. Two main factors are affecting the electrospinning process. One is the properties of the solution, including viscosity, conductivity, surface tension, etc. Spinning equipment parameters, such as hydrostatic pressure in the capillary, capillary tip for solution properties. Some environmental parameters, such as temperature, humidity, and airflow velocity in the spinning chamber, are also affected [24].
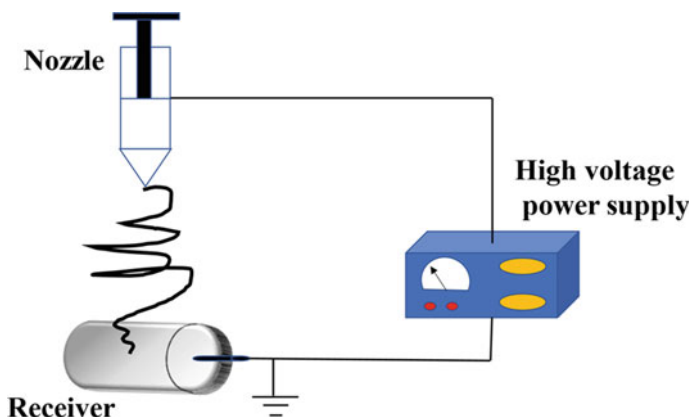
Fig. 5 Schematic diagram of electrospinning

4 Application in Electrochemical Energy Storage Devices

4.1 Lithium Battery

With the rapid development of the electric vehicle industry, lithium-ion battery, as a kind of green new energy battery, has the advantages of high specific energy, fast charging speed, long cycle life, and high safety factor, and has been widely studied and applied. The research and development of novel battery materials with high quality, high reliability, and high safety have become the focus of the development of lithium-ion batteries. The performance of batteries is closely related to electrode materials, electrolytes, and diaphragms. To date, the application of various electro-spinning/electrospraying technologies has promoted the research and development of advanced battery materials [25].

Shun Nakazawa et al. prepared high-performance polyvinylidene fluoride (PVDF) nanofibers based on the crystallization of lithium salts. It was first revealed that the higher β -phase crystallinity of PVDF nanofibers made the composite SPE have higher ionic conductivity and higher number of lithium-ion migration. The PVDF nanofiber composite SPE has good electrochemical stability and mechanical durability through a constant current cycling test. Ass-lib composed of PVDF nanofibers combined with SPEs has excellent rate performance and charge–discharge cycle performance, which will improve the performance of lithium batteries [26]. Min et al. successfully synthesized flower-like $Li_{1.2}Ni_{0.17}Co_{0.17}Mn_{0.5}O_2$ cathode material by using high voltage spinning technology and heat treatment method. Such ordered porous flower-like morphology structure can promote the rapid diffusion of lithium ions, and the cyclic discharge capacity of the assembled lithium battery can be up to 235 mAh/g [27].

Singh et al. prepared PVDF electrospun fiber mat with high porosity, stable thermal size and good compatibility with liquid electrolyte by using electrostatic spinning/thermal crosslinking process, which was used as gel polymer electrolyte (GPE) of lithium battery with ionic conductivity of about 1.48 mS/cm and high discharge capacity [28]. Kong through the electrostatic spinning/thermal crosslinking process such as the preparation of the solid polyimide fluoride (FPI) nanofiber membrane, the membrane has high mechanical strength (31.7 MPa), the smaller the average pore diameter and narrow pore size distribution, to prevent the lithium dendrite growth and penetration aspects show the good performance, can be assembled into safe and reliable lithium-ion battery [29]. Chen made by order electricity spinning technologies such as strong mechanical strength, the tensile strength of 13.96 MPa) and thermal stability of the new sandwich structure between PVDF/poly benzene formyl m-phenylene diamine (PMIA)/PVDF nanofibers battery diaphragm, it has hot obturator function, and the multi-layer assembled battery than commercial polyolefin separator has more stable cycle performance and a better ratio of performance and to design and development of high-performance battery, diaphragm provides a new train of thought [30].

4.2 Fuel Cells

Fuel cells have the advantages of abundant resources, zero emissions, fast start-up, and high efficiency, and are considered as a suitable energy device to solve the problems of greenhouse gases, climate change, and energy shortage. Fuel cells can directly convert chemical energy into electrical energy, mainly divided into two types: proton exchange membrane fuel cells (PEMFCs) and solid oxide fuel cells (SOFCs) [31]. The design and engineering optimization of the battery system plays a crucial role, and it is an indispensable task for the design and advanced manufacturing of battery materials [32].

Rajangam et al. prepared a new type of ultra-low platinum PEMFCs electrode (E-U electrode) by electrostatic spinning and underpotential deposition techniques. Studies have shown that E-U electrode nanofibers structure has the characteristics of high porosity and large specific surface area could reduce the oxygen transfer catalytic layer resistance, which improves the performance of the battery under high current density, after 30,000 times of cyclic voltammograms accelerated stability test, E-U the peak power density of electrode degradation rate is only 4.8%, compared to the conventional electrode showed better durability [33].

Boaretti etc. was prepared by two-step electrostatic spinning and immersion fiber sulfonated poly (ether sPEEK/Aquivion nanocomposite proton exchange membrane, the electrospinning fiber composite membrane compared with not enhanced membrane, it is proton conductivity decreases, but the mechanical properties and dimensional stability has been significantly enhanced, especially containing crosslinking sPEEK composite membrane system showed good mechanical properties and swelling performance but also has lower the electrical conductivity of

the loss, so the mechanical enhanced composite film is suitable for application in PEMFCs [34].

4.3 Solar Cells

Solar energy is a kind of renewable, eco-friendly, sustainable, and abundant clean energy. Solar cells derived from this have been rapidly developed due to the rise of nano-functional materials. The third generation of dye-sensitized solar cells (DSSCs) simulates the principle of natural photosynthesis and converts solar energy into electrical energy under the action of dye-sensitized agents and nano semiconductors to complete energy conversion and storage [35]. As key components of DSSCs, electrolytes, photoanodes, and counter electrodes need to be further achieved with a simple production process, low equipment cost, non-toxic raw materials, and low energy consumption [36].

Dissanayake et al. reported a dye-sensitized solar cell based on electrospinning PAN nanofiber membrane gel electrolyte. DSSCs with a thickness of $9.14\,\mu m$ showed the highest photoelectric conversion efficiency of 5.2%. In addition, the gel electrolyte can be further modified and enhanced by adding an appropriate proportion of inorganic fillers to become composite nanostructures [37]. Sharma by electrostatic spinning technology such as the preparation of the mixed with cobalt sulfide (CoS) nanocomposite membrane PVDF HFP-gel electrolyte (esCPMEs), the study found that evenly dispersed cosine nanoparticles increased the charge transport, and promote the oxidation–reduction to spread in the electrolyte in the system, in which mixed with 1 wt% of cosine esCPMEs DSSCs assembled by the photovoltaic performance of 7.34% [38].

4.4 Supercapacitors

Supercapacitors have fast charged and discharging speed and good cycling performance, which can be better applied in wearable devices. Flexible supercapacitors is now the hot topic of research [39]. Flexible supercapacitors are mainly composed of collector, electrode material, electrolyte, separator, and shell. Flexible supercapacitors can be divided into EDLC and pseudocapacitance supercapacitors according to the different working principles of energy storage. Among them, EDLC mainly uses carbon material as electrode material, which stores and releases energy through the rapid adsorption/desorption process of conducting ions in contact with electrolytes on the surface of electrode material [40]. The charge and discharge process of the pseudocapacitance supercapacitor is completed through a rapid reversible redox reaction on the electrode surface. Due to the redox reaction in the charging and discharging process, the supercapacitor has good energy storage performance and mainly uses metal oxides and conducting polymers as electrode materials.

Zheng et al. developed a method for preparing high quality and independent loads by preparing electrodes PPy through simple vacuum filtration and low-temperature polymerization. The material can be coated on the surface of carbon nanotubes, and closely combined with the carbon nanotubes fiber network, the film surface is smooth, and the carbon nanotubes fiber network can provide a fast electron transmission channel, so it has high conductivity, thus improving the mechanical and electrochemical properties of the material CNT/PPy electrode. The all-solid symmetric supercapacitor assembled from this material has a high energy density, the final capacitance retention rate is greater than 72.2% [41]. Shi et al. prepared PAN nanofibers by electrostatic spinning technology and obtained activated carbon nanofibers (AC-NF) after curing, carbonization and water vapor activation, with a surface area of up to 1230 m^2/g, the specific capacitance of KOH electrolyte is 175 F g^{-1}; Park et al. prepared carbon nanofibers by electrospinning polybenzimidazole (PBI) with a specific surface area of 1220 m^2/g by using electrostatic spinning technology, the specific capacitance is 178 F/g [42].

Using physical activation, Tang et al. obtained granular carbon material with porous structure (aperture 43 nm) by electrospinning PAN solution doped with silica nanoparticles. The specific surface area measured by BET reached 340.9 m^2/g [43]. Chronakis et al. prepared PPy nanofiber film by electrostatic spinning technology, and its conductivity reached 0.5 S/cm, which is much higher than the conductivity of PPy film obtained by the mold forming method and is suitable for use as the electrode material of supercapacitor [44]. Rajesh et al. used 3,4 ethylene dioxythiophene (PEDOT) film prepared by electrostatic spinning as the electrode material of supercapacitor, and the capacitance of the capacitor could reach 30 mAh/g under polymer electrolyte, and it could maintain 90% capacitance after 10,000 cycles [45].

4.5 Flexible Electronics

The emergence of smart devices has changed the way we live and work. But these smart devices have only limited interaction with the environment. Electronic Devices Years of research and development have led to the emergence of flexible, deformable wearable electronic devices that intelligently collect data to enhance the interaction between the device and the environment. The application of conducting polymer nanofibers in new flexible wearable electronic devices with rich human functions may become the main research direction of conducting polymer nanofibers. The development of wearable electronics has led to an increasing convergence of technologies, most importantly integrating electronic functions, mechanical adaptability, and full communication capabilities.

Flexible wearable electronic devices with their unique flexibility, lightweight, portability, flexibility, or stretchability attract the majority of scholars and enthusiasts, with broad application prospects. Flexible conductive materials are indispensable to the fabrication of flexible wearable devices. Flexible conductive materials are mostly composed of flexible substrates and conductive materials, their research and

application promote the development of wearable electronic devices, which can better meet the needs of our human body. It has a wide application prospect in aerospace, medical monitoring, communication and national defense.

4.5.1 Flexible Sensor

Esma Ismailova developed a wearable flexible circuit board and applied it to a wearable keyboard. They made a retractable keyboard with a pattern of electrically conducting polymer circuits on a knitted fabric. The research group uses knitted textile as the flexible substrate of the circuit board, which endows it with stretchability. At the same time, the textile itself has wearable comfort, and the internal flexible circuit diagram is designed as a horseshoe structure, which further improves the performance of the flexible circuit board under tensile conditions. They made electrodes from a mixture of the conducting polymer PEDOT and poly styrene sulfonate (PSS), coated with polydimethylsiloxane (PDMS) as a protective coating, and used capacitive sensors that could sense the touch of a human finger. The flexible wearable keyboard is up to 30% stretchable and can read a volunteer's finger touch. This work is of great significance to the development of the field of flexible electronic devices and provides a new idea for the large-scale manufacturing of lightweight wearable input devices [46].

Liu et al. prepared a pressure sensor with high sensitivity by directly spraying AgNWs on uncured PDMS and compounding with polyethylene dioxythiophene/polystyrene sulfonate. The results show that the polymer sensor with a sandwich structure can obtain a sensitivity of 2.59 kPa^{-1} in the low state, and its strain coefficient is up to 37.8 [47]. Dhand et al., such as insert physical crosslinking of polyvinyl alcohol layer to contain a chemical/trivalent ions formed in the ionic crosslinking polyacrylic acid polymer network (IPN) hydrogels and apply it to the multimodal sensor, found that the preparation of sensors can be independently testing mechanical folding and pressure change, even if heated to a temperature of 90 °C, can still get 3.65 kPa^{-1} Sensitivity [48].

Conducting PPy and polyolefin elastomer (POE) by in situ polymerization preparation into nanometer fiber pulp, recycled template replication preparation of the surface has a unique structure of conducting nanofiber membrane, the monomer mass ratio and film thickness on the influence of the pressure sensor sensitivity, the results showed that when pyrrole (Py) monomer and POE nanofibers ratio of 1:1, the quality of the film thickness of conducting fiber to 48 μm, sensitivity is available up to 39.7 kPa^{-1} The time of stress application and stress removal is only 10 ms and 12 ms respectively [49].

4.5.2 Biomedicine

With the improvement of living standards, people pay increasing attention to physical health, so the medical health monitoring system has been widely concerned, and gradually tends to be used in daily life. At present, the flexible wearable medical and health monitor has been successfully developed, which can adapt to the deformation caused by human activities while maintaining stable performance. Flexible wearable medical health monitors can be used to measure temperature and heat transfer characteristics, record electrophysiological processes and electrical impedance changes, characterize skin hardness, and monitor changes related to quasi-static or dynamic dimensions such as swelling/regression or pulsating blood flow [50].

Joseph Wang used flexible conducting polymers to develop an epidermal electrochemical biosensor that continuously monitors sweat lactate levels and provides a real-time overview of lactic acid sweat dynamics during exercise. In collaboration with Jae-Woong Jeong of the University of Colorado at Boulder and Yonggang Huang of Northwestern University, the team of John A. Rogers of the University of Illinois, USA, developed A flexible health monitor that can be attached to human skin to detect the state of the stomach, heart and other body organs. Their lightweight, low-modulus, skin-compatible architecture enables sensing and measurement of mechanical motion. The structure they designed further promotes the research and development of flexible wearable health monitors and further explores its use in clinical applications to establish pathological functions and conditions, which may be the direction of future research [51–53]. French start-up E-Vone developed a shoe that falls can monitor whether the wearer is referred to as "wrestling shoes" warning system, the shoes with a large number of sensors, the fall will automatically detect the severity of the fall, whether can stand up again, and so on, automatically notifying reservations, it should be great for the sick, the elderly, and avid hikers [54].

As a new generation of synthetic polymers, polymer materials such as PANIs, PPy, and PEDOT not only have good electrical conductivity but also have a simple preparation process and good biocompatibility. Therefore, they can be used as bio-sensitive tissue repair materials, artificial muscles, and pharmaceutical sustained-release materials, etc. D. Mawad by free radical polymerization reaction such as the preparation of PEDOT/polyacrylate hydrogel, the material has a porous three-dimensional framework and showed obvious swelling ratio and excellent mechanical properties, and the electrical activity can under physiological conditions to promote the proliferation and differentiation of myoblast, is a kind of new method for the preparation of conductive biological engineering structure [55]. Kong in acrylic, xylan, and N-isopropyl acrylamide as raw material, under UV irradiation, was prepared by crosslinking copolymerization conducting polymer hydrogel, saying a gel to temperature and pH showed a greater sensitivity, and good biocompatibility, in medicine and intestinal targeted drug delivery has certain potential applications [56].

4.5.3 Flexible Solar Cells

Flexible solar cells can also be called "organic solar cells" (OSCs) or "polymer solar cells" (PSCs) because most of their substrates are organic or polymer. Flexible solar cells have the advantages of low cost, lightweight and flexible layers. Compared with silicon-based solar cells and inorganic semiconductor thin-film solar cells, the flexible active layer is the most significant characteristic of flexible solar cells, making it most suitable for making flexible devices. The photosensitive layer of the flexible solar cell is very thin (about 100–200 nm) and partially transparent. The color of the active layer can be adjusted by adjusting the bandgap of donor and recipient materials, which makes flexible solar cells suitable for the preparation of semi-transparent solar cells. Moreover, with the development of new photovoltaic materials, the power conversion efficiency (PCE) of flexible solar cells has been rapidly improved. The power conversion efficiency of the latest organic solar cells has reached more than 13%. Therefore, the application of flexible organic solar cells in the field of wearable energy and integrated building photovoltaic has attracted great attention in recent years. In addition to flexible organic solar cells, translucent organic solar cells and two transparent electrodes have also attracted widespread attention for aesthetic architectural uses such as foldable solar curtains. In general, the optimized photosensitive layer thickness of organic solar cells is limited to less than approximately 200 nm, and in many cases, such thin organic films are translucent. In addition, the absorption of light in the active layer can be specifically tuned to certain spectral ranges, allowing different colors to appear. The key to fabricating semi-transparent organic solar cells is to select top and bottom electrodes with high transparency, high conductivity and suitable work function. The transparency of the device can be increased simply by reducing the film thickness of the photosensitive layer. However, this results in lower power conversion efficiency because less light is absorbed by the thinner layer. Therefore, it is very important to use effective light capture methods to solve the problems of transmission and absorption. Color perception is also important for future applications of translucent organic solar cells to achieve neutral transparency.

5   Conclusions and Outlook

This chapter classifies conducting polymer nanofibers according to their conductive mechanism. The influence of different types of doping on the conductivity of conducting polymer nanofibers was clarified. The methods of preparing conductive polymer nanofibers are summarized in detail, and the advantages and disadvantages of different methods and application cases are analyzed. Conductive polymer nanofibers are widely used in energy storage devices and sensors. This chapter summarizes the research progress of conductive polymer nanofibers in lithium batteries, fuel cells, supercapacitors, solar cells and flexible devices. Conducting polymer nanofibers are widely used in lithium batteries, fuel cells, supercapacitors

and other energy storage devices, and have broad application prospects in the field of energy storage. Flexible devices made of conductive polymer nanofibers are increasingly used in daily life. Conductive polymer nanofibers have the advantages of low cost, large-scale preparation, good flexibility, good electrochemical stability, high sensitivity and large specific surface area, so they can meet the requirements of flexible wearable devices. Conductive polymer nanofibers will become an irreplaceable material in people's life.

References

1. Yi, F., Wang, J., Wang, X., Niu, S., Li, S., Liao, Q., Xu, Y., You, Z., Zhang, Y., Wang, Z.L.: Stretchable and waterproof self-charging power system for harvesting energy from diverse deformation and powering wearable electronics. ACS Nano **10**, 6519–6525 (2016)
2. Chen, Q., Zheng, J., Yang, Q., Dang, Z., Zhang, L.: Effect of carbon chain structure on the phthalic acid esters (PAEs) adsorption mechanism by mesoporous cellulose biochar. Chem. Eng. J. **362**, 383–391 (2019)
3. Mishra, A.K.: Conducting polymers: concepts and applications. J. At. Mol. Condens. Nano Phys. **5**, 159–193 (2018)
4. Chung, D.D.L.: Materials for electromagnetic interference shielding. Mater. Chem. Phys. **255**, 123587 (2020)
5. Zhang, C., Hsieh, M.-H., Wu, S.-Y., Li, S.-H., Wu, J., Liu, S.-M., Wei, H.-J., Weisel, R.D., Sung, H.-W., Li, R.-K.: A self-doping conductive polymer hydrogel that can restore electrical impulse propagation at myocardial infarct to prevent cardiac arrhythmia and preserve ventricular function. Biomaterials **231**, 119672 (2020)
6. Xie, Y., Kocaefe, D., Chen, C., Kocaefe, Y.: Review of research on template methods in preparation of nanomaterials. J. Nanomater. **2016**, 2302595 (2016)
7. Feng, Y., Li, H.: 9.02—Self-assembly of fullerenes. In: Atwood, J.L. (ed.) Comprehensive Supramolecular Chemistry II, pp. 3–25. Elsevier, Oxford (2017)
8. Wang, Y., Santos, A., Evdokiou, A., Losic, D.: Rational design of ultra-short anodic alumina nanotubes by short-time pulse anodization. Electrochim. Acta **154**, 379–386 (2015)
9. Salgado, R., del Valle, M.A., Duran, B.G., Pardo, M.A., Armijo, F.: Optimization of dopamine determination based on nanowires PEDOT/polydopamine hybrid film modified electrode. J. Appl. Electrochem. **44**, 1289–1294 (2014)
10. Liu, L., Wang, Y., Meng, Q., Cao, B.: A novel hierarchical graphene/polyaniline hollow microsphere as electrode material for supercapacitor applications. J. Mater. Sci. **52**, 7969–7983 (2017)
11. Bhandari, S.: Chapter 2—Polyaniline: structure and properties relationship. In: Visakh, P.M., Pina, C.D., Falletta, E. (eds.) Polyaniline Blends, Composites, and Nanocomposites, pp. 23–60. Elsevier
12. Marcos-Hernández, M., Villagrán, D.: 11—Mesoporous composite nanomaterials for dye removal and other applications. In: Kyzas, G.Z., Mitropoulos, A. (eds.) Micro and Nano Technologies, pp. 265–293. Elsevier (2019)
13. Gong, P., Li, B., Kong, X., Wang, N., Liu, J., Zuo, S.: A new soft template-oriented method for the preparation of hollow analcime microspheres with nanosheets-assembled shells. J. Mater. Sci. **52**, 9377–9390 (2017)

14. Pirhady Tavandashti, N., Ghorbani, M., Shojaei, A.: Controlled growth of hollow polyaniline structures: from nanotubes to microspheres. Polymer (Guildf) **54**, 5586–5594 (2013)
15. Anantha-Iyengar, G., Shanmugasundaram, K., Nallal, M., Lee, K.-P., Whitcombe, M.J., Lakshmi, D., Sai-Anand, G.: Functionalized conjugated polymers for sensing and molecular imprinting applications. Prog. Polym. Sci. **88**, 1–129 (2019)
16. Vauthier, C., Bouchemal, K.: Methods for the preparation and manufacture of polymeric nanoparticles. Pharm. Res. **26**, 1025–1058 (2009)
17. Cheremisinoff, N.P., Rosenfeld, P.: Chapter 1—The petroleum industry. In: Cheremisinoff, N.P., Rosenfeld, P. (eds.) Handbook of Pollution Prevention and Cleaner Production—Best Practices in the Petroleum Industry, pp. 1–97. William Andrew Publishing, Oxford (2009)
18. Mudila, H., Prasher, P., Kumar, M., Kumar, A., Zaidi, M.G.H., Kumar, A.: Critical analysis of polyindole and its composites in supercapacitor application. Mater. Renew. Sustain. Energy **8**, 9 (2019)
19. Han, J., Wang, M., Hu, Y., Zhou, C., Guo, R.: Conducting polymer-noble metal nanoparticle hybrids: synthesis mechanism application. Prog. Polym. Sci. **70**, 52–91 (2017)
20. Huang, J., Kaner, R.B.: Nanofiber formation in the chemical polymerization of aniline: a mechanistic study. Angew. Chem. Int. Ed. **43**, 5817–5821 (2004)
21. Long, Y., Duvail, J., Li, M., Gu, C., Liu, Z., Ringer, S.P.: Electrical conductivity studies on individual conjugated polymer nanowires: two-probe and four-probe results. Nanoscale Res. Lett. **5**, 237 (2009)
22. Hujjatul Islam, M., Paul, M.T.Y., Burheim, O.S., Pollet, B.G.: Recent developments in the sonoelectrochemical synthesis of nanomaterials. Ultrason Sonochem **59**, 104711 (2019)
23. Davoodi, P., Gill, E.L., Wang, W., Shery Huang, Y.Y.: Chapter Two—Advances and innovations in electrospinning technology. In: Kasoju, N., Ye, H. (eds.) Woodhead Publishing Series in Biomaterials, pp. 45–81. Woodhead Publishing (2021)
24. Jose Varghese, R., Sakho, E., Hadji, M., Parani, S., Thomas, S., Oluwafemi, O.S., Wu, J.: Chapter 3—Introduction to nanomaterials: synthesis and applications. In: Thomas, S, Sakho, E.H.M., Kalarikkal, N., Oluwafemi, S.O., Wu, J. (eds.) Nanomaterials for Solar Cell Applications, pp. 75–95. Elsevier (2019)
25. Ding, P., Lin, Z., Guo, X., Wu, L., Wang, Y., Guo, H., Li, L., Yu, H.: Polymer electrolytes and interfaces in solid-state lithium metal batteries. Mater. Today (2021)
26. Amin-Sanayei, R., He, W.: Chapter 10—Application of polyvinylidene fluoride binders in lithium-ion battery. In: Nakajima, T., Groult, H. (eds.) Advanced Fluoride-Based Materials for Energy Conversion, pp. 225–235. Elsevier (2015)
27. Min, J.W., Yim, C.J., Bin, I.W.: Facile synthesis of electrospun $Li_{1.2}Ni_{0.17}Co_{0.17}Mn_{0.5}O_2$ nanofiber and its enhanced high-rate performance for lithium-ion battery applications. ACS Appl. Mater. Interfaces **5**, 7765–7769 (2013)
28. Singh, S.K., Gupta, H., Balo, L., Shalu, S.V.K., Tripathi, A.K., Verma, Y.L., Singh, R.K.: Electrochemical characterization of ionic liquid based gel polymer electrolyte for lithium battery application. Ionics (Kiel) **24**, 1895–1906 (2018)
29. Kong, L., Yan, Y., Qiu, Z., Zhou, Z., Hu, J.: Robust fluorinated polyimide nanofibers membrane for high-performance lithium-ion batteries. J. Memb. Sci. **549**, 321–331 (2018)
30. Chen, Y., Qiu, L., Ma, X., Chu, Z., Zhuang, Z., Dong, L., Du, P., Xiong, J.: Electrospun PMIA and PVDF-HFP composite nanofibrous membranes with two different structures for improved lithium-ion battery separators. Solid State Ionics **347**, 115253 (2020)
31. Weber, A.Z., Balasubramanian, S., Das, P.K.: Chapter 2—Proton exchange membrane fuel cells. In: Sundmacher, K. (ed.) Fuel Cell Engineering, pp. 65–144. Academic, Burlington (2012)
32. Zhang, J., Jiang, S.P.: 9.15—Self-assembly in fuel cells. In: Atwood, J.L. (ed.) Comprehensive Supramolecular Chemistry II, pp. 273–295. Elsevier, Oxford (2017)
33. Rajangam, P., Dharmalingam, S.: Synthesis and characterization of electrospun carbon nanofiber supported Pt catalyst for fuel cells. Electrochim. Acta **112**, 1–13 (2013)
34. Boaretti, C., Pasquini, L., Sood, R., Giancola, S., Donnadio, A., Roso, M., Modesti, M., Cavaliere, S.: Mechanically stable nanofibrous sPEEK/Aquivion® composite membranes for fuel cell applications. J. Memb. Sci. **545**, 66–74 (2018)

35. Piqué, A.: 18—Laser-printed micro- and meso-scale power generating devices. In: Prudenziati, M., Hormadaly, J.B.T.-P.F. (eds.) Woodhead Publishing Series in Electronic and Optical Materials, pp. 526–549. Woodhead Publishing, Cambridge, UK (2012)

36. Zarrintaj, P., Vahabi, H., Saeb, M.R., Mozafari, M.: Chapter 14—Application of polyaniline and its derivatives. In: Mozafari, M., Chauhan, N.P.S. (eds.) Fundamentals and Emerging Applications of Polyaniline, pp. 259–272. Elsevier, The Netherlands (2019)

37. Dissanayake, M.A.K.L., Divarathne, H.K.D.W.M.N.R., Thotawatthage, C.A., Dissanayake, C.B., Senadeera, G.K.R., Bandara, B.M.R.: Dye-sensitized solar cells based on electrospun polyacrylonitrile (PAN) nanofibre membrane gel electrolyte. Electrochim. Acta **130**, 76–81 (2014)

38. Sharma, K., Sharma, V., Sharma, S.S.: Dye-sensitized solar cells: fundamentals and current status. Nanoscale Res. Lett. **13**, 381 (2018)

39. Poonam, S.K., Arora, A., Tripathi, S.K.: Review of supercapacitors: materials and devices. J. Energy Storage **21**, 801–825 (2019)

40. Saha, S., Samanta, P., Murmu, N.C., Kuila, T.: A review on the heterostructure nanomaterials for supercapacitor application. J. Energy Storage **17**, 181–202 (2018)

41. Zheng, T., Wang, X., Liu, Y., Bayaniahangar, R., Li, H., Lu, C., Xu, N., Yao, Z., Qiao, Y., Zhang, D., Pour Shahid Saeed Abadi, P.: Polyaniline-decorated hyaluronic acid-carbon nanotube hybrid microfiber as a flexible supercapacitor electrode material. Carbon N. Y. **159**, 65–73 (2020)

42. Shi, G., Liu, C., Wang, G., Chen, X., Li, L., Jiang, X., Zhang, P., Dong, Y., Jia, S., Tian, H., Liu, Y., Wang, Z., Zhang, Q., Zhang, H.: Preparation and electrochemical performance of electrospun biomass-based activated carbon nanofibers. Ionics (Kiel) **25**, 1805–1812 (2019)

43. Tang, H., Han, D., Zhang, J.: Electrospinning fabrication of polystyrene-silica hybrid fibrous membrane for high-efficiency air filtration. Nano Express **2**, 20017 (2021)

44. Chronakis, I.S., Grapenson, S., Jakob, A.: Conductive polypyrrole nanofibers via electrospinning: electrical and morphological properties. Polymer (Guildf) **47**, 1597–1603 (2006)

45. Rajesh, M., Raj, C.J., Manikandan, R., Kim, B.C., Park, S.Y., Yu, K.H.: A high performance PEDOT/PEDOT symmetric supercapacitor by facile in-situ hydrothermal polymerization of PEDOT nanostructures on flexible carbon fibre cloth electrodes. Mater. Today Energy **6**, 96–104 (2017)

46. Yang, T., Xie, D., Li, Z., Zhu, H.: Recent advances in wearable tactile sensors: materials, sensing mechanisms, and device performance. Mater. Sci. Eng. R Rep. **115**, 1–37 (2017)

47. Liu, H.-S., Pan, B.-C., Liou, G.-S.: Highly transparent AgNW/PDMS stretchable electrodes for elastomeric electrochromic devices. Nanoscale **9**, 2633–2639 (2017)

48. Dhand, A.P., Galarraga, J.H., Burdick, J.A.: Enhancing biopolymer hydrogel functionality through interpenetrating networks. Trends Biotechnol. **39**, 519–538 (2021)

49. Wang, X.-X., Yu, G.-F., Zhang, J., Yu, M., Ramakrishna, S., Long, Y.-Z.: Conductive polymer ultrafine fibers via electrospinning: preparation, physical properties and applications. Prog. Mater. Sci. **115**, 100704 (2021)

50. Lou, Z., Wang, L., Jiang, K., Wei, Z., Shen, G.: Reviews of wearable healthcare systems: materials, devices and system integration. Mater. Sci. Eng. R Rep. **140**, 100523 (2020)

51. Chen, Y., Zhang, Y., Liang, Z., Cao, Y., Han, Z., Feng, X.: Flexible inorganic bioelectronics. npj Flex. Electron. **4**, 2 (2020)

52. Mathew, M., Radhakrishnan, S., Vaidyanathan, A., Chakraborty, B., Rout, C.S.: Flexible and wearable electrochemical biosensors based on two-dimensional materials: recent developments. Anal. Bioanal. Chem. **413**, 727–762 (2021)

53. Manjakkal, L., Dervin, S., Dahiya, R.: Flexible potentiometric pH sensors for wearable systems. RSC Adv. **10**, 8594–8617 (2020)

54. Janson, D., Newman, S.T., Dhokia, V.: Next generation safety footwear. Procedia Manuf. **38**, 1668–1677 (2019)

55. Mawad, D., Artzy-Schnirman, A., Tonkin, J., Ramos, J., Inal, S., Mahat, M.M., Darwish, N., Zwi-Dantsis, L., Malliaras, G.G., Gooding, J.J., Lauto, A., Stevens, M.M.: Electroconductive hydrogel based on functional poly(ethylenedioxy thiophene). Chem. Mater. **28**, 6080–6088 (2016)

56. Kong, W.-Q., Gao, C.-D., Hu, S.-F., Ren, J.-L., Zhao, L.-H., Sun, R.-C.: Xylan-modified-based hydrogels with temperature/pH dual sensitivity and controllable drug delivery behavior (2017)

Conjugated Polymer for Charge Transporting Applications in Solar Cells

Esmaeil Sheibani, Li Yang, and Jinbao Zhang

Abstract Solar cells based on semiconductor heterojunction demonstrate tunable interfaces and high efficiency, showing great potentials in future applications. In heterojunction solar cells, charge transport materials play critical roles in carrier conductivity, recombination kinetics, and charge collection efficiency, which in turn significantly influence the photovoltaic parameters as well as the stability of solar cells. Traditional inorganic and molecular conductors exhibit high promises in optoelectronic properties, however, they are somewhat facing challenges in high material cost, poor device stability, and sophisticated fabricating processes. Alternatively, conducting polymers have been recently recognized as promising charge transport materials due to their advantages of high conductivity, tunable work function, controllable transmittance, and high stability. Careful design and optimization of polymer chemical structures have promoted fast development in tuning their optoelectronic properties and enhancing photovoltaic performance. Therefore, in this chapter, we summarize the recent progress of strategies in designing new conducting polymer materials as a charge transport medium for solar cell application. The current challenges and prospects in the future development of polymer-based charge conductors are discussed.

Keywords Conjugated polymers · Electron-transporting materials · Hole-transporting materials · Perovskite solar cells · Hybrid photovoltaics

E. Sheibani (✉)
Department of Chemistry, University of Isfahan, Hezar Jerib Street, 81746-73441 Isfahan, Isfahan Province, Iran
e-mail: e.sheibani@sci.ui.ac.ir

L. Yang · J. Zhang
College of Materials, Fujian Key Laboratory of Advanced Materials, Xiamen University, Xiamen 361005, Fujian Province, China

Shenzhen Research Institute of Xiamen University, Xiamen, Shenzhen 518000, Fujian Province, China

1 Fundamental Material Requirements for Perovskite Solar Cells

Perovskite solar cells (PSCs) have attracted great research attention over the last few years due to their outstanding photovoltaic performance and cost-effective fabrication processes, becoming one of the most promising photovoltaic technologies for future applications. Although high power conversion efficiencies (PCEs) of over 25% have been achieved for single-junction PSCs, the stability issues of the devices and the high cost of interfacial functional materials greatly limit PSCs' development. Great efforts have been made into optimizing the perovskite composition, develop different device architectures, exploit perovskite fabrication techniques, designing low-cost hole-transporting materials (HTMs) and electron-transporting materials (ETMs).

PSCs employ a typical sandwich structure where perovskite as the light absorber materials is in direct contact with ETMs and HTMs at two sides, which complete the charge separation and collection. Heterojunction structured PSCs have complex interfacial charge transport processes. Upon irradiance, loosely bonded electron and hole pairs with small exciton binding energy are generated, enabling long exciton diffusion length and fast carrier separation at perovskite/HTM and perovskite/ETM interfaces. To obtain high charge collection efficiency, it is favorable for ETMs and HTMs to represent similar charge conductivity to reach balanced charge-transporting capacity. Moreover, ETMs and HTMs, acting as the most critical components in PSCs, have to meet several requirements (depending on device architectures) for obtaining PSCs with high efficiency and stability. Different device architectures have been developed, including planar n-i-p, planar p-i-n, and mesoporous p-i-n structures, as illustrated in Fig. 1. The mesoporous structure is inherited from traditional dye-sensitized solar cells, where the mesoporous TiO_2 layer is used for ETMs. However, the high UV activity of TiO_2 and energy-consuming processes (high temperature of 500 °C) greatly limit the future scalable application. In contrast, planar structures attracted more attention and now are mostly used in PSCs, due to the cost-effective fabrication processes with low temperatures. The charge conductors have distinct roles and influences on charge dynamics, defect passivation, PCEs as well as device stabilities. Therefore, it is highly important to optimize the film morphology, chemical structures, and interfaces for achieving high efficiency and stability PSCs.

Generally, there are some basic requirements for the charge transport layers in different architectures. For the down electrodes which is directly coated on the conducting glass (for example ETM in n-i-p structure or HTM in p-i-n structure), high compactness is needed for blocking back electron transfer and the charge recombination at interfaces. The down electrode needs to be stable in organic solvents (in top layer solution) without dissolution, and should also have satisfied wettability for perovskite solution to promote the formation of perovskite thin film. For the top electrode which is covered on top of perovskite (HTM in conventional structure, and ETM in inverted structure), it acts as a barrier layer that isolate the perovskite film from the surrounding environment. Therefore, its compactness and homogeneity are critical for the protecting effects. Moreover, the top electrode is located between the
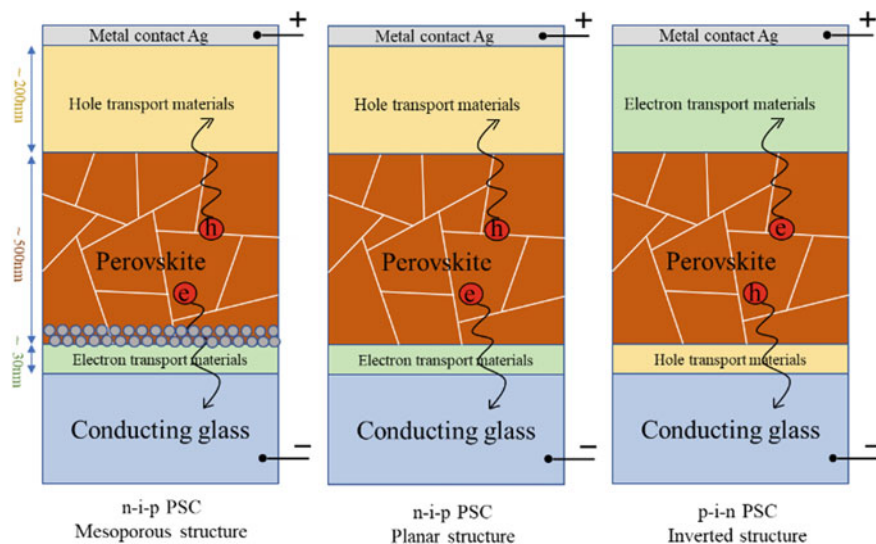
Fig. 1 Different device architectures for PSCs. **a** n-i-p mesoporous structure, **b** n-i-p planar structure and **c** p-i-n inverted structure

metal layer and perovskite, and it should be dense enough to avoid the metal diffusion through it towards the perovskite. For both top and down electrodes, suitable energy levels in relative to perovskite are required for obtaining sufficient interfacial charge transfer, and they need have high transparency if the illumination is from the side where the electrodes are coated.

In a conventional n-i-p structure, the ETM layer is directly coated on the transparent conductive glass (e.g. FTO), followed by the deposition of perovskite and HTM layer. Metal oxides (e.g. TiO_2, SnO_2) are mostly used as ETMs due to their high electron-transporting properties, high transparency, and good energy alignment with perovskite. In addition, perovskite crystallization occurs easily and efficiently on the metal oxide layer owing to their good wetting property on inorganic ETMs. As compared to TiO_2, SnO_2 becomes more attractive because of low temperature (<100 °C) processing, high stability, and little current–voltage hysteresis, presenting the most robust and efficient ETM in n-i-p PSCs. In contrast, there are very few attempts to use organic ETMs in conventional PSCs, because most of the common ETMs are soluble in perovskite solution and the film can be easily destroyed during perovskite formation steps. For the HTMs in n-i-p structure, 2,2′,7,7′-tetrakis(*N*,*N*-di-*p*-methoxyphenylamine)-9,9′-spirobifluorene (spiro-OMeTAD) is the most efficient and popular reference HTM in PSCs, which was first developed and used in solid-state dye-sensitized solar cells. Spiro-OMeTAD is the most representative HTMs in solar cells because it has suitable energy levels, good film quality, high charge transport properties. However, recent work has shown that several drawbacks of spiro-OMeTAD greatly limit its scalable application in PSCs. Firstly, the preparation of spiro-OMeTAD involves tedious and time-consuming processes,

causing a low synthetic yield of 40% as well as a much higher material cost than gold [1]. Thus, a wide range of HTMs based on small organic molecules has recently been explored on PSCs with different core structures such as carbazole [2–4], perylene [5], thiophene [6], spiro [7], helicene [8], phenoxazine [9], triphenylamine [10]. However, for molecular HTMs, their weak interaction with each other significantly limits the charge transport property due to the high energy barrier for hole hopping. This work reveals that conjugated polymers, Fortunately, chemical doping is an effective strategy to enhance the conductivity of molecular HTMs by introducing additional charge carriers during the doping reaction. Lithium bis(trifluoromethanesulfonyl)imide (LiTFSI) and 4-*tert*-butylpyridine (*t*BP) are the most common and efficient additives for molecular HTMs, and several orders of magnitude higher conductivity have been often achieved after molecular doping [11, 12]. However, recent work has demonstrated that these additives have harmful effects on the device's stability [13]. For example, Cheng and coworkers found severe morphological deformation of spiro-OMeTAD film after thermal treatment. Moreover, hygroscopic LiTFSI easily absorbs the moisture in ambient condition and accelerate perovskite degradation [14]. It is also found small lithium ions could migrate and accumulate at interfaces under illumination and/or bias potential, causing fast efficiency decrease in devices.

Lately, inverted configuration captured a surge of interest, due to the cost-effectiveness, feasible fabrication, and suppressed hysteresis. In the inverted PSCs, the HTM layer is deposited on conductive glass, followed by the coating of perovskite and ETM layers, as shown in Fig. 1c. In this configuration, NiO, poly(3,4-ethylenedioxythiophene):poly(styrenesulfonic acid) (PEDOT:PSS), poly(triaryl amine) (PTAA) are the most popular HTMs. NiO has shown promising properties in stability and high PCEs, however, it is observed that high defects and sophisticated fabrication restrict its scalable application [15]. PEDOT:PSS as HTMs is widely used in organic solar cells and perovskite solar cells because of high transparency, high conductivity, and low material cost. However, the acidity of the PSS anion caused ITO electrode corrosion, threatening the long-term stability of PSCs. To date, PTAA, with high film quality and good transporting property, is one of the most efficient and reliable HTMs in n-i-p PSCs. However, it also suffers from the high material cost and poor wettability which influence the perovskite crystallization on top of it. A large number of alternative HTMs for inverted PSCs have been developed and investigated, and more information about material structures and performance can be found in previous reviews [16].

Up to date, three types of ETM comprising fullerene-based, n-type metal oxides and n-type conjugated polymer have been utilized. In general, the n-type conjugated polymer has superior properties compared to their inorganic counterparts, such as tuning bandgap, hydrophobicity, energy level, and chemical stability. Moreover, owing to the molecular chain entanglement in the polymer or self-assembled monolayers, the polymer has a high potential to generate better film quality to alleviate stability issues, thus leading to high photovoltaic performance. Fullerene-based ETL is so far the most popular n-type layer, which can be easily deposited by either solution process or evaporation [17]. But it suffers from inherent features

such as absorbing oxygen and water onto its surface and consequently degrading the perovskite layer, or even reacting with oxygen and water and generating large resistance with metal contact. Moreover, due to its low solubility, it is challenging for PCBM to form a uniform thin film fully covering the perovskite layer. Its deficient adhesion with perovskite may cause PCBM molecular aggregation or various morphological defects. The fairly rough surface of the PCBM causes an imperfect intimate contact with cathode, which influences the charge collection efficiency. It is also found that wide distribution of band tail states in a fullerene-based ETL causes lower Voc and subsequently reduced efficiency [18], even though the charge-transfer rate between the perovskite and the fullerene is much faster than that between the perovskite and TiO_2 in n-i-p structures [19].

Conducting polymers representing promising and robust charge conductors have been widely used in modern and electronics and display technology, such as solar cells, light-emitting diode, thin-film transistor. As charge transport materials in PSCs, conducting polymers need to have high carrier mobility, good film quality, high stability, and low material cost. Although many p-type conducting polymers as HTMs have been designed and investigated, only a few types of n-type polymers have been explored, such as naphthalene diimide (NDI) and perylene diimide (PDI) with two electron-deficient building blocks. Further optimization of polymer chemical structures (side groups, molecular geometry, planarity) is a critical way to tune their optoelectronic properties, such as carrier density, disordering, intra-, and inter-electron transport.

To sum up, charge transport materials in both n-i-p and p-i-n PSCs are essential components for charge separation, transportation, and collection. To date, inorganic and molecular-based materials are widely used as ETMs and HTMs in PSCs, however, they are facing challenges in high materials cost, tedious film fabrication, poor stability, and low conductivity [20, 21].

2 N-type Polymer Semiconductors for Inverted PSCs

As discussed previously, fullerene-based molecules are often used as ETMs and alternative polymer ETMs are limited. It is previously found that poly[(9,9-bis(3′-(*N,N*-dimethylamino)propyl)-2,7-fluorene)-alt-2,7-(9,9-dioctyl-fluorene)] (PFN) exhibits admirable performant and good film-forming properties for small-area PSCs, while it is suffered from low mobility that limited its charge conducting application [22]. Figure 2 demonstrates the recent notable n-type polymer as electron transport layers and interlayers. To generate preferred interfacial dipoles with the cathode electrode for decreasing the work function of the metal cathode, amine-functionalized groups were introduced to the side chains of the fluorine unit to form n-type co-polymer coded as PFN-2TNDI [23]. This polymer exhibited efficient charge collection by accelerating the electron extraction with Ohmic contact and simultaneously passivating the surface traps of perovskite. Results show that the conjugated backbone of the copolymer containing fluorene creates a deep HOMO level with good hole
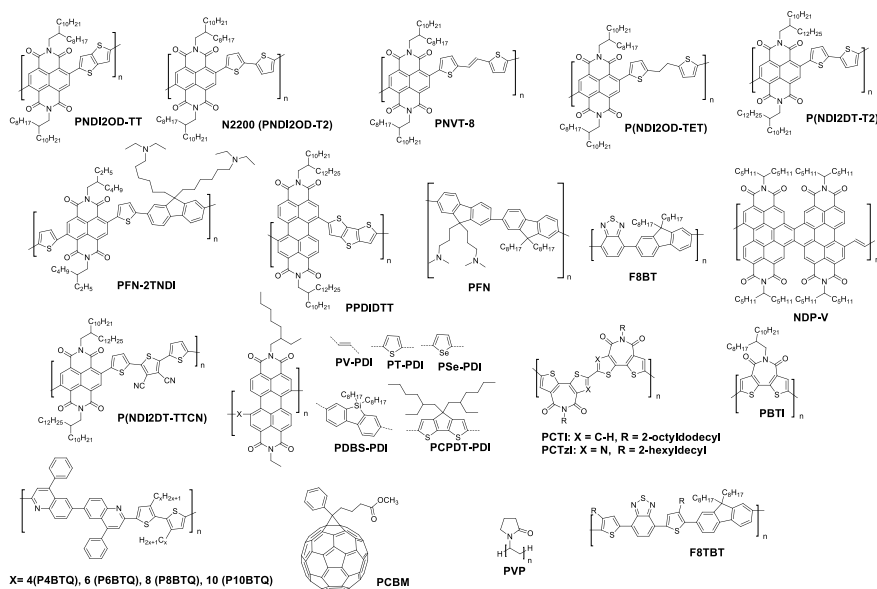
Fig. 2 Chemical structures of polymers used as electron transport layers and interlayers

blocking ability, and thiophene spacers improve polymer packing with better charge transport. The device based on PFN-2TNDI as ETM displayed impressive PCE up to 16.7% whereas control devices based on PCBM ETM merely showed PCE of 12.9%. In contrast, the polymer without amine-functionalization demonstrated a very low PCE of 0.1%. Photoluminescence (PL) and impedance spectroscopy revealed that the alkylamines play critical roles in modulating the electronic properties of the interfacial contacts. Moreover, these polymer ETMs show high efficiency and low hysteresis in the p–i–n PSCs, further demonstrating their feasibility as fullerene alternatives.

Due to high electron affinity and tunable π-skeleton (rigid or planar), perylene diimides (PDI) are considered as practical building blocks for n-type semiconductors. By applying such units in polymers, a good charge transporting and tunable optoelectronic properties through functionalizing PDI or copolymerized PDI can be obtained. PDI based conjugated polymers consisting of different co-polymer units, such as vinylene (V), thiophene (T), selenophene (Se), dibenzosilole (DBS), and cyclopentadithiophene (CPDT), were developed and applied in p-i-n PSCs with a device structure of FTO/PEDOT:PSS/$CH_3NH_3PbI_3$/PX-PDI/Al [24]. Among them, the device with PV-PDI as ETL attains the highest PCE of 10.14%, which was attributed to its superior properties of deeper LUMO energy level, delocalized LUMO in the whole molecule, better planar structure and effective reducing pinholes of perovskite at the interfaces. It is concluded that low dihedral angle between copolymerized units and the PDI is critical for obtaining high electron mobility and efficient PSCs with high short-circuit current (J_{SC}). In contrast, the LUMO of PDBS-PDI and PCPDT-PDI are slightly higher than that of perovskite conduction band, which induced energy-level

mismatch and hindered electron transfers at interfaces, leading to low conversion efficiencies.

Zhan et al. introduced a novel n-type copolymer PPDIDTT containing perylene diimide and dithienothiophene, (Fig. 2) which can effectively extract and transfer electrons and passivate the surface trap states of perovskite [25]. The PPDIDTT modified devices showed PCE of 16.5%, much higher than control devices. Another structure of the large fused polycyclic NDI category shows great potential as ETMs. N-type conjugated polymer naphthodiperylenetetraimidevinylene (NDP-V), delivered PCE 16.54%, while PC61BM attained a maximum PCE of 15.27% when using the device structure of ITO/P3CT-Na/perovskite/NDPV/Rhodamine 101/LiF/Ag (P3CT-Na and Rhodamine 101/LiF as HTM and buffer layer, respectively) [26]. When NDP-V was employed as an interlayer between the perovskite and the ETL C60 for improving the contact property, the device displayed remarkable PCEs of 19.09%, whereas the reference device without NDP-V displayed PCEs of 17.09% with a device architecture of ITO/P3CT-Na/Perovskite/NDP-V/C60/BCP/Ag.

In 2014, Gill and co-workers employed pure poly(9,9-dioctylfluorene-*co*-benzothiadiazole) (F8BT) as the ETL in flexible PSCs, and a PCE of 7.05% was attained [27]. Later, when inserting the thin F8BT layer at the C60/perovskite interfaces, a significant improvement of the PCE from 7.9 to 13.9% was obtained [28].

Some other novel polymers, including poly{[N, N′-bis(2-octyldodecyl)-1,4,5,8-naphthalene diimide-2,6-diyl]-alt-5,5′-(2,2′-bithiophene)} (N2200), poly{[N, N′-bis(alkyl)-1,4,5,8-naphthalene diimide-2,6-diyl-alt-5,5′-di(thiophen-2-yl)-2,2′-(E)-2-(2-(thiophen-2-yl)vinyl)thiophene]} (PNVT-8) and PNDI2OD-TT (Fig. 2) were recently applied as ETM in inverted planar PSCs [29]. The devices containing N2200 as ETM featured a PCE of 8.15% (J_{SC} of 14.70 mA/cm^2, V_{OC} of 0.84 $_V$ and FF of 66%), which is close to 8.51% for the reference device based on PCBM (J_{SC} 14.65 mA/cm^2, VOC 0.83 V, FF 70%). Whereas, the other polymers PNVT-8 and PNDI2OD-TT have been studied with the same device architecture (ITO/PEDOT:PSS/CH$_3$NH$_3$PbI$_{3-x}$Cl$_x$/Polymer/ZnO/Al), and slightly lower efficiencies of 7.47% and 6.47% were obtained, respectively.

Kim et al. functionalized novel n-type polymer with strong electron-withdrawing dicyanothiophene termed as (P(NDI2DT-TTCN)) to possess a deep LUMO level to accompany with a pseudo-planar structure to increase π–π transition, that was confirmed by grazing-incidence wide-angle X-ray scattering (GIWAX) and near-edge X-ray absorption fine structure spectroscopy (NEXAFS) analyses [30]. And the enhanced intramolecular interaction between the thiophene–nitrile groups enable P(NDI2DT-TTCN)) have high electron transfer abilities. It is demonstrated that the devices with P(NDI2DTTTCN) show improved electron extraction ability. P(NDI2DT-TTCN) was further applied in flexible PSCs and exhibited superior mechanical stability compare to the PCBM. The flexible devices exhibited outstanding PCEs over 17.0%, higher than PCBM based devices (14.3%). From AFM measurements, P(NDI2DT-TTCN) film is highly homogeneous and uniform on top of the perovskite layer, completely covering the surfacing and eliminating the

morphological defects or roughness from perovskite. This work demonstrated such building block polymer is promising for ETL applications.

Later, three other naphthalenediimidebithiophene based semiconductor polymers, namely, poly{[N, N′-bis(2-octyldodecyl)-naphthalene-1, 4, 5, 8-bis(dicarboximide)-2, 6-diyl]-alt-5, 5′-(2, 2′-bithiophene)} (P(NDI2OD-T2)), poly{[N, N′-bis(2-dodecyltetradecyl)-naphthalene-1, 4, 5, 8-bis(dicarboximide)-2, 6-diyl]-alt-5, 5′-(2, 2′-bithiophene)} (P(NDI2DT-T2)) and poly{[N, N'-bis(2-octyldodecyl)-1, 4, 5, 8-naphthalenedicarboximide-2, 6-diyl]-alt-5, 5-diyl 2-diyl 2-ethanediyl)bithiophene]} (P(NDI2OD-TET)), were synthesized and employed as ETMs in inverted PSCs [31]. These materials displayed remarkable stabilities by maintaining 87% of the initial PCEs after 270 min, whereas only 3.5% of initial performance was kept for $PC_{60}BM$.

Careful characterization indicated that the polymer structures have great impacts on recombination kinetics. The devices with both polymers P(NDI2OD-T2) and P(NDI2DT-T2) performed similarly to $PC_{60}BM$, but P(NDI2OD-TET) as ETM showed a low PCE of only 0.18%. It was suggested from PL measurements that large PCE variation results from the electron extraction capability of ETMs, rather than the energy offset between polymer (LUMOs) and the perovskite (conduction band).

In 2017, Zhou et al. for the first time incorporated a commercially available non-conjugated polymer poly(vinylpyrrolidone) (PVP) as an interlayer between PCBM and Ag cathode [32]. This interlayer enabled an increase of PCE from 12.55 to 15.9%, due to the formation of a dipole layer that can accelerate the electron transfer from PCBM to Ag cathode and also suppress electron–hole recombination.

To enhance the device stability, Chen and co-workers reported two n-type polymers, namely poly (2,2′-bithiophene-3,3′-dicarboxyimide) (PBTI) and 2,2′-bithiazolothienyl-4,4′,10,10′-tetracarboxydiimide (PDTzTI), which embody bithiophene imide and thienylthiazole imide, respectively [33]. The design strategy is to incorporate sulfur and nitrogen atoms as Lewis base to coordinate with lead cations of perovskite. Devices with the PDTzTI ETM exhibited remarkable PCE of 20.86%, which result from appropriate energy-level alignment (electron-withdrawing of thiazole promotes down-shift the LUMO level), and sufficient trap passivation.

Jenekhe et al. developed a series of soluble n-type conjugated copolymers containing bis(phenylquinoline) and regioregular dialkylbithiophene in the backbone and investigated their electrochemical, photophysical, and electroluminescent properties [34]. Electron deficient heterocyclic conjunction with the emissive electron-donating groups was introduced in these ETMs. The results proved alternation of alkyl chain length from butyl (C4) to dodecyl (C12) in the dialkylbithiophene spacer has a negligible effect on photophysical and electrochemical features. The small variation in electron affinities (LUMO levels), ionization potential (HOMO level), and bandgap of the polymers was attributed to the torsion angle (arise from steric interaction between the alkyl chain) between the thiophene rings in the head-to-tail and head-to-head conformations that is verified by single-crystal X-ray structure of a model compound.

Chen and co-workers investigated the roles of poly(bithiophene imide) (PBTI) ion the passivation of grain boundaries [33]. Due to the reduced ion migration,

the champion device shows a PCE of 20.67% as compared to 18.89% for control devices without PBTI. The device based on PBTI preserved over 70% of the original efficiency after 600 h under 1 sun illumination compared to 56% for the control devices.

In order to reduce the non-radiative recombination occurred at perovskite/PCBM interface, a practical and convenient approach through mixing PCBM with conjugated n-type polymer poly[(9,9-dioctyluorene)-2,7-diylalt-(4,7-bis(3-hexylthien-5-yl)-2,1,3-benzothiadiazole)-2′,2″-diyl] (F8TBT) have been applied to make a homogeneous bulk-mixed (HBM) homogeneous film [17]. The hybrid film shows appropriate energy levels and higher electron mobility, leading to one of the highest PCEs achieved for inverted PSCs. It is seen that polymer composite film was completely covered on the perovskite surface which improves the electron extraction. As a result, the efficiency of the devices with HBM ETL surpasses 20.6% with a high fill factor of 0.82, which is 19% booster than the value without HBM.

In conclusion, inverted PSCs have shown high potentials in scalable applications due to low-temperature fabrication, little hysteresis, and low material cost. Organic charge transport materials are mostly used in inverted PSCs, which are compatible with flexible devices and large-scale roll-to-roll processes. However, the PCEs of inverted PSCs are generally lower than that for n-i-p PSCs, and the fundamental reasons are needed to be explored. Moreover, the stability of inverted PSCs is limited by the top transporting layers, and further optimization of material structure and composition is needed.

3 P-type Polymer Semiconductors for PSCs in Conventional and Inverted Structures

P-type semiconductors as HTMs have received much more research attention compared to n-type materials. A great number of organic HTMs have been designed and studied in PSCs, and more details can be found in previous reviews [35]. As discussed before, different properties are required for HTMs in conventional or inverted PSCs. For example, most small organic molecules cannot be used as HTM which is located beneath the perovskite layer in inverted PSCs, because their films are easily damaged by precursor solutions of perovskite. Therefore, HTMs in p-i-n structure need to be stable without dissolution in organic polar solvents (such as DMF). The HTMs with functional groups can apply dipoles to the conducting substrate and induce work-function alignment, leading to modulation of charge collection efficiencies and interfacial recombination. Furthermore, a high bandgap with high transparency is required for HTMs in inverted PSCs to reduce light losses. Consequently, the HTM exploited in inverted PSCs are predominantly wide band-gap polymers such as PEDOT:PSS, poly(bis(4-phenyl)(2,4,6-trimethylphenyl) amine) (PTAA) and Poly(3-hexylthiophene-2,5-diyl (P3HT). Polymer-based HTM attracted great attention due to its specific properties such as good thermal stress stability, less

corrosive effect on the electrode, tunable optoelectronic, printable flexibility, high mobility, and conductivity.

PEDOT:PSS is a commercialized conductive polymer composed of sodium polystyrene sulfonate and poly(3,4-ethylenedioxythiophene). It has advantages of solution processability, low-temperature annealing process, good electrical properties, and compatibility in flexible, lightweight, and portable electronic devices [17]. However, it is facing severe obstacles for further enhancement of efficiency: (1) due to the acidic nature, it can corrode the indium-doped tin oxide (ITO) electrode and induce migration of indium into PEDOT:PSS; (2) poor electron-blocking ability and incompatible energy levels between its work function (varies from –4.8 to –5.1 eV) and the valence band of $CH_3NH_3PbI_3$ (-5.4 eV); (3) due to the hygroscopic nature of PEDOT:PSS, moisture-induced perovskite degradation is severe in PEDOT based devices, and (4) PEDOT:PSS, especially under low doping states, has somewhat light absorption in visible and near IR regions, which induces light absorption losses in PSCs.

In 2013, Peter Chen et al. applied PEDOT:PSS in inverted planar PSC with moderate PCEs of 4% in $ITO/PEDOT:PSS/CH_3NH_3PbI_3/C60/BCP/Al$ configuration [36]. Later, Snaith et. al., reported PCEs up to 10% and 6% for glass substrate and flexible polymer substrate, respectively [20]. Chun-Guey Wu et al. found a continuous perovskite film can be formed on the PEDOT:PSS surface via a two-step spin-coating method [37]. To further improve the film quality of PEDOT:PSS, Tae-Woo Lee et al. combined PEDOT:PSS with tetrafluoroethylene-perfluoro-3,6-dioxa-4-methyl-7-octene-sulfonic acid copolymer to tune the surface work functions with better energy alignment [38]. In addition, the surface of these films turns into more coarse than pristine PEDOT:PSS, which is valuable for perovskite film formation. Xue et al. introduced conjugated copolymers, termed HSL1 and HSL2, as anode modification layer to justify the anode interface of PEDOT:PSS/perovskite [39]. Figure 3 summarizes the recent development of remarkable p-type polymer as
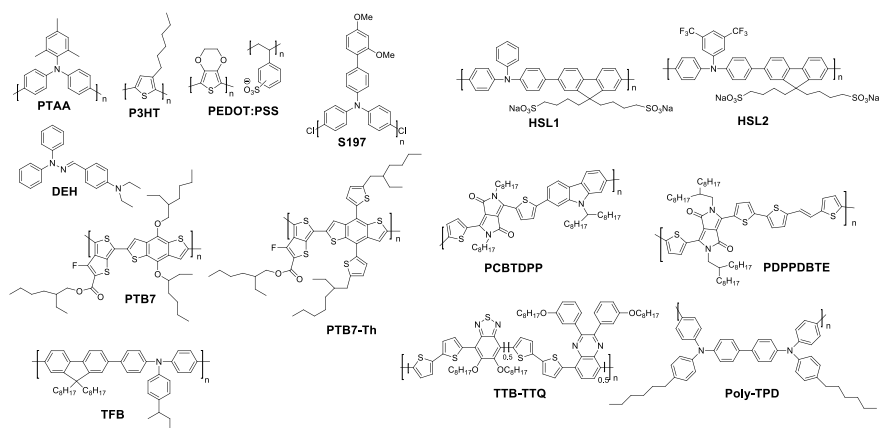
Fig. 3 Chemical structures of polymers used as hole transport layers

hole transport layers. In this tactic polar functional groups are attached to the polymer side chains to enhance the surface energy and hydrophilic nature of the hole selective layers to act effective wetting with the perovskite films (good solvent resilience to the perovskite precursor solution) and cause high-quality film with better treatment and high crystallinity. The LUMO level of HSL1 and HSL2 located at higher energy than the conduction band of the perovskite semiconductors, thus works an electron blocking to hinder electron recombination to the FTO electrode and trap passivation at PEDOT:PSS/perovskite interface, therein longer charger combination lifetime and shorter charge-extraction time acquired.

Recently, side-chain engineering in conjugated polymer backbones is an effective strategy to optimize the optoelectronic properties, molecular packing, and charge transport of polymer materials [40]. Conjugated polymers are composed of two main parts which are the π-conjugated skeleton and peripheral flexible alkyl chains. Side chains are formed in linear and branched ways. Hybrid side chains decorated with different functional groups or insert heteroatom in CH_2 segments are often used to tune the polymer solubility and hydrophilicity. Conjugated polymers containing bulky aromatic units with donor side-groups usually exhibit better conversion efficiencies, even though the main reasons are still under debate. For example, both conjugated polymer PTB7 and PTB7-Th have identical structures except the pendant side chains which are attached to the benzodithiophene units replacing oxygen with thiophene, but the PCEs increased by double for PTB7-Th when blend with P(NDI2OD-T2). The major reason was assigned to the effective charge carriers collection at donor/acceptor interfaces for PTB7-Th [41].

In 2013, p-type polymer poly[N-9-hepta-decanyl-2,7-carbazole-alt-3,6-bis-(thiophen-5-yl)-2,5-dioctyl-2,5-di-hydropyrrolo[3,4-]pyrrole-1,4-dione] (PCBTDPP) (Fig. 3) was studied as a HTM with $CH_3NH_3PbI_3$ as light absorber in device architecture of mp-TiO$_2$/CH$_3$NH$_3$PbI$_3$/PCBTDPP/Au [42]. An encouraging Voc of 1.15 V and PCE of 5.55% associated with good device stability were obtained, which is higher than model p-type polymer P3HT. Detailed characterization has proved that higher hole mobility and suppressed recombination stemming from better interfacial interactions for PCBTDPP are suggested as main factors for achieving high Voc.

Park and co-workers designed donor-π-acceptor type polymer, poly[2,5-bis(2-decyldodecyl)pyrrolo[3,4-c]pyrrole-1,4(2H,5H)-dione-(E)-1,2-di(2,2′-bithiophen-5-yl) ethene] (PDPPDBTE), as HTM in n-i-p PSCs [43]. An impressive PCE of 9.2% was achieved, much higher than the benchmark HTM spiro-MeOTAD (PCE 7.6%). The enhanced performance was benefited from suitable oxidation potential (5.4 eV) and perfect charge carrier mobility of the polymer. In addition, the high hydrophobicity of the PDPPDBTE as an effective barrier prevents the moisture intake to perovskite film, and as a result, the device showed remarkable stability for 1000 h. Kim et al. developed donor–π–acceptor-based conducting polymer TTB–TTQ by combining thiophene and benzothiadiazole in backbones [44]. Owing to the breaking structure symmetry, this polymer has a high solubility in many organic solvents and shows outstanding film quality. The device with doped TTB–TTQ exhibited a PCE of 14.1%, whereas the control device with

spiro-MeOTAD showed inferior efficiency of 11.5%. Another investigation was taken place by designing poly[N,N′-bis(4-butylphenyl)-N,N′-bis(phenyl)benzidine] (poly-TPD) as HTMs in the inverted scheme in which the perovskite film was constructed via sequential deposition method. The optimized device integrated with 40 nm thickness of poly-TPD demonstrated average PCEs of 15.3%.

Seok and co-workers used PTAA as HTMs in conventional structure, and extraordinary efficiency of 12.0% (with J_{SC} = 16.5 mAcm^{-2}, V_{OC} = 0.997 V and FF = 0.727) was achieved [45]. They proposed that the $CH_3NH_3PbI_3$ perovskites somewhat penetrate the TiO_2 film to build a capping layer on top of the TiO_2 layer that shaped a "pillared structure" composed of perovskites/HTMs. Along with EDS mapping and the XPS depth profile, it is verified that PTAA was mainly found near the surface of the pillared structure. Nazeeruddin research group introduced novel oligomer 2,4-dimethoxy-phenyl substituted triarylamine (S197) as HTM in conventional PSCs in the presence of TBP-LiTFSI additives [46]. The cells featured a PCE of 12.0% (Voc of 967 mV, Jsc of 17.6 mA cm^{-2}, FF of 0.55) under 99.6 mW cm^{-2} illumination. The molecular structure is similar to PTAA with additional dimethoxy phenyl and chloride heteroatoms in order to optimize optical and electrochemical properties of PTAA. In the same manner, the champion device with PTAA displayed a PCE of 11.5% (Jsc of 16.2 mA cm^{-2}, Voc of 1025 mV, and FF of 0.69).

To improve the quality of overlying perovskite films, Han et al. fabricated devices by bilayer HTMs with reduced graphene oxide (r-GO) and poly(triarylamine) (PTAA) [47]. This bilayer HTM was applied in both rigid and flexible inverted planar PSCs with the architecture of substrate/ITO/r-GO/PTAA/$CH_3NH_3PbI_3$/PCBM/bathocuproine/Ag. Due to the light absorption of PTAA in the near-UV, the device based on PTAA as HTM revealed poor light-soaking stability. In contrast, when r-GO cover the ITO completely, the unwanted near-UV band became cut-off. Bilayer HTMs with mixing GO and PTAA resulted in high PCEs and long-term stability. High PCEs of 15.7% and 17.2% were obtained in flexible and rigid devices, respectively.

P3HT as one of the most common polymers in solar cell applications has exhibited outstanding properties in charge conducting and material stability. In conventional PSCs, high thickness is needed for the top layer HTM to completely cover the perovskite surface. However, the poor charge collection efficiency due to the thick P3HT layer limits its performance. With the optimized concentration of Li-TFSI/t-BP additives in doped P3HT improved the conductivity and boosted the device efficiency from 6.5 to 13.5%.

To further investigate the effects of HTMs on charge dynamics in PSCs, Haghfeldt and co-worker compared three HTMs, spiro-OMeTAD, P3HT and 4-(Diethylamino)benzaldehyde diphenylhydrazone (DEH) [48]. Photoinduced absorption spectroscopy (PIA) disclosed the hole transfer rate from perovskite to the HTM follows the order spiro-OMeTAD > P3HT > DEH. It was concluded the lower electron lifetime for P3HT and DEH is the main reason of charge recombination and low efficiency with these devices.

To enhance the photovoltaic performance of pristine P3HT, large π-conjugated carbon material, graphdiyne (GD), was blended with P3HT to render effective π−π

stacking interaction between GD particles and P3HT, and meanwhile to perform as a water-resistant dopant and morphological controller of the P3HT [49]. Raman spectroscopy and ultraviolet photoelectron spectroscopy analyses proved the interaction between two materials in the composite HTM.

Snaith et al. designed a composite structure by wrapping single-walled carbon nanotubes (SWNTs) with P3HT to diminish thermal degradation [50]. The composite HTM was fixed in an insulating polymer matrix of poly(methyl methacrylate), and an efficiency of up to 12% was obtained in regular PSCs.

Recently, Li and co-workers studied the stability of different HTMs. They found that both dopant-free P3HT and standard doped spiro-OMeTAD based devices exhibited similar photovoltaic parameters, however, the device containing undoped P3HT showed remarkable stability by maintaining over 95% of initial PCEs after 1300 h. To further enhance PCEs by suppressing the nonradiative recombination, a diphenylamine derivative (poly[(9,9-dioctylfluorenyl-2,7-diyl)-co-(4,4′-(N-(4-s-butylphenyl)diphenylamine)], TFB) (Fig. 3) was applied as buffer ultrathin layer between perovskite and P3HT to compensate the energy-level mismatch, which consequently delivered a record PCE of 15.50% for dopant-free P3HT [51].

4   Outlook

Herein, we have systematically discussed and scrutinized the advancements of efficient conducting polymer-based ETMs and HTM for both conventional (n-i-p) and inverted (p-i-n)-type PSCs. We have investigated model ETMs used in high-performance PSCs with different device configurations. Compared to typical mesoporous PSCs, planar PSCs exhibited many advantages including low-temperature processing, low material cost, and simple fabrication. PSCs with planar architectures received much attention for a future scalable application. Charge transport materials play critical roles in planar PSCs in charge collection, perovskite protection, and interfacial stability, therefore, a large number of alternative ETMs and HTMs are developed to tune their synthetic routes, charge dynamics, stability, and interfacial properties. Conducting polymers with outstanding charge conducting property and high stability received great attention recently.

For inverted planar PSCs, n-type polymer ETMs play the leading roles in controlling the moisture sensitivity, hydrophobicity, dense interlayers with cathode and perovskite contacts. The champion efficiency of inverted PDCs has exceeded 20%, however, it is still far behind the conventional n-i-p PSCs. The fundamental difference in terms of PCEs between inverted and conventional PSCs requires further study. Although many n-type conducting polymers were developed in past years for replacing fullerene HTMs, the performance (including both efficiency and stability) of most polymer HTMs is comparable or even lower than standard fullerene materials. The investigation of polymer ETMs is still under the early stage, and further

development of low-cost and robust polymer ETMs is required for the scalable application of PSCs. Also the techniques for fabrication of large-area polymer ETMs with high quality needs further exploration.

Similarly, HTM has been recognized as a crucial interface modification layer in both conventional (n-i-p) and inverted (p-i-n) PSCs. So far, most HTM-based polymers were designed through the concept of donor–acceptor configuration. Such structures are often associated with a complicated and cost-driving synthesis that limited the large-scale production of such polymers. Moreover, in inverted PSCs, their poor wettability with perovskite precursor solution hindered the growth of high-quality perovskite films. A fundamental understanding of the correlation between polymer structure and its wettability is highly desired. As discussed above, the HTMs with multiple functions are critical to modulate the interfaces and optimize the interfacial charge dynamics. Further exploration of polymer HTMs with functions of passivation and encapsulation presents the future direction of developing new HTMs. Similarly, scalable and robust deposition techniques of polymer HTMs are needed to adapt the large-area fabrication of PSCs.

References

1. Zhang, J., Hua, Y., Xu, B., Yang, L., Liu, P., Johansson, M.B., et al.: The role of 3D molecular structural control in new hole transport materials outperforming spiro-OMeTAD in perovskite solar cells. Adv. Energy Mater. **6**, 1601062 (2016)
2. Wang, L., Sheibani, E., Guo, Y., Zhang, W., Li, Y., Liu, P., et al.: Impact of linking topology on the properties of carbazole-based hole-transport materials and their application in solid-state mesoscopic solar cells. Sol. RRL **3**, 1900196 (2019)
3. Xu, B., Sheibani, E., Liu, P., Zhang, J., Tian, H., Vlachopoulos, N., et al.: Carbazole-based hole-transport materials for efficient solid-state dye-sensitized solar cells and perovskite solar cells. Adv. Mater. **26**, 6629–6634 (2014)
4. Sheibani, E., Heydari, M., Ahangar, H., Mohammadi, H., Fard, H.T., Taghavinia, N., et al.: 3D asymmetric carbozole hole transporting materials for perovskite solar cells. Sol. Energy **189**, 404–411 (2019)
5. Sheibani, E., Amini, M., Heydari, M., Ahangar, H., Keshavarzi, R., Zhang, J., et al.: Hole transport material based on modified N-annulated perylene for efficient and stable perovskite solar cells. Sol. Energy **194**, 279–285 (2019)
6. Li, H., Fu, K., Hagfeldt, A., Grätzel, M., Mhaisalkar, S.G., Grimsdale, A.C.: A simple 3, 4-ethylenedioxythiophene based hole-transporting material for perovskite solar cells. Angew. Chem. **126**, 4169–4172 (2014)
7. Zhu, X.D., Ma, X.J., Wang, Y.K., Li, Y., Gao, C.H., Wang, Z.K., et al.: Hole-transporting materials incorporating carbazole into spiro-core for highly efficient perovskite solar cells. Adv. Funct. Mater. **29**, 1807094 (2019)
8. Lin, Y.-S., Abate, S.Y., Lai, K.-W., Chu, C.-W., Lin, Y.-D., Tao, Y.-T., et al.: New helicene-type hole-transporting molecules for high-performance and durable perovskite solar cells. ACS Appl. Mater. Interfaces **10**, 41439–41449 (2018)
9. Zhang, F., Wang, S., Zhu, H., Liu, X., Liu, H., Li, X., et al.: Impact of peripheral groups on phenothiazine-based hole-transporting materials for perovskite solar cells. ACS Energy Lett. **3**, 1145–1152 (2018)

10. Petrus, M.L., Schutt, K., Sirtl, M.T., Hutter, E.M., Closs, A.C., Ball, J.M., et al.: New generation hole transporting materials for perovskite solar cells: amide-based small-molecules with nonconjugated backbones. Adv. Energy Mater. **8**, 1801605 (2018)

11. Bach, U., Lupo, D., Comte, P., Moser, J.-E., Weissörtel, F., Salbeck, J., et al.: Solid-state dye-sensitized mesoporous TiO$_2$ solar cells with high photon-to-electron conversion efficiencies. Nature **395**, 583–585 (1998)

12. Wang, S., Huang, Z., Wang, X., Li, Y., Günther, M., Valenzuela, S., et al.: Unveiling the role of tBP–LiTFSI complexes in perovskite solar cells. J. Am. Chem. Soc. **140**, 16720–16730 (2018)

13. Liu, J., Wu, Y., Qin, C., Yang, X., Yasuda, T., Islam, A., et al.: A dopant-free hole-transporting material for efficient and stable perovskite solar cells. Energy Environ. Sci. **7**, 2963–2967 (2014)

14. Zhang, J.B., Zhang, T., Jiang, L.C., Bach, U., Cheng, Y.B.: 4-tert-Butylpyridine free hole transport materials for efficient perovskite solar cells: a new strategy to enhance the environmental and thermal stability. Acs Energy Lett. **3**, 1677–1682 (2018)

15. Jeng, J.Y., Chen, K.C., Chiang, T.Y., Lin, P.Y., Tsai, T.D., Chang, Y.C., et al.: Nickel oxide electrode interlayer in CH3NH3PbI3 perovskite/PCBM planar-heterojunction hybrid solar cells. Adv. Mater. **26**, 4107–4113 (2014)

16. Yan, W., Ye, S., Li, Y., Sun, W., Rao, H., Liu, Z., et al.: Hole-transporting materials in inverted planar perovskite solar cells. Adv. Energy Mater. **6**, 1600474 (2016)

17. Yang, D., Zhang, X., Wang, K., Wu, C., Yang, R., Hou, Y., et al.: Stable efficiency exceeding 20.6% for inverted perovskite solar cells through polymer-optimized PCBM electron-transport layers. Nano Lett. **19**, 3313–3320 (2019)

18. Lian, J., Lu, B., Niu, F., Zeng, P., Zhan, X.: Electron-transport materials in perovskite solar cells. Small Methods **2**, 1800082 (2018)

19. Heo, J.H., Han, H.J., Kim, D., Ahn, T.K., Im, S.H.: Hysteresis-less inverted CH$_3$NH$_3$PbI$_3$ planar perovskite hybrid solar cells with 18.1% power conversion efficiency. Energy Environ. Sci. **8**, 1602–1608 (2015)

20. Docampo, P., Ball, J.M., Darwich, M., Eperon, G.E., Snaith, H.J.: Efficient organometal trihalide perovskite planar-heterojunction solar cells on flexible polymer substrates. Nat. Commun. **4**, 1–6 (2013)

21. Zhu, Z., Bai, Y., Zhang, T., Liu, Z., Long, X., Wei, Z., et al.: High-performance hole-extraction layer of sol–gel-processed NiO nanocrystals for inverted planar perovskite solar cells. Angew. Chem. **126**, 12779–12783 (2014)

22. He, Z., Zhong, C., Su, S., Xu, M., Wu, H., Cao, Y.: Enhanced power-conversion efficiency in polymer solar cells using an inverted device structure. Nat. Photonics **6**, 591–595 (2012)

23. Sun, C., Wu, Z., Yip, H.L., Zhang, H., Jiang, X.F., Xue, Q., et al.: Amino-functionalized conjugated polymer as an efficient electron transport layer for high-performance planar-heterojunction perovskite solar cells. Adv. Energy Mater. **6**, 1501534 (2016)

24. Guo, Q., Xu, Y., Xiao, B., Zhang, B., Zhou, E., Wang, F., et al.: Effect of energy alignment, electron mobility, and film morphology of perylene diimide based polymers as electron transport layer on the performance of perovskite solar cells. ACS Appl. Mater. Interfaces **9**, 10983–10991 (2017)

25. Li, H., Liang, C., Liu, Y., Zhang, Y., Tong, J., Zuo, W., et al.: Covalently connecting crystal grains with polyvinylammonium carbochain backbone to suppress grain boundaries for long-term stable perovskite solar cells. ACS Appl. Mater. Interfaces **9**, 6064–6071 (2017)

26. Jiang, K., Wu, F., Zhu, L., Yan, H.: Naphthodiperylenetetraimide-based polymer as electron-transporting material for efficient inverted perovskite solar cells. ACS Appl. Mater. Interfaces **10**, 36549–36555 (2018)

27. Gill, H.S., Kokil, A., Li, L., Mosurkal, R., Kumar, J.: Solution processed flexible planar hybrid perovskite solar cells. Organic Photovoltaics XV: International Society for Optics and Photonics, p. 918418 (2014)

28. Zhao, L., Wang, X., Li, X., Zhang, W., Liu, X., Zhu, Y., et al.: Improving performance and reducing hysteresis in perovskite solar cells by using F8BT as electron transporting layer. Sol. Energy Mater. Sol. Cells **157**, 79–84 (2016)

29. Wang, W., Yuan, J., Shi, G., Zhu, X., Shi, S., Liu, Z., et al.: Inverted planar heterojunction perovskite solar cells employing polymer as the electron conductor. ACS Appl. Mater. Interfaces **7**, 3994–3999 (2015)
30. Kim, H.I., Kim, M.J., Choi, K., Lim, C., Kim, Y.H., Kwon, S.K., et al.: Improving the performance and stability of inverted planar flexible perovskite solar cells employing a novel NDI-based polymer as the electron transport layer. Adv. Energy Mater. **8**, 1702872 (2018)
31. Shao, S., Chen, Z., Fang, H.-H., Ten Brink, G., Bartesaghi, D., Adjokatse, S., et al.: N-type polymers as electron extraction layers in hybrid perovskite solar cells with improved ambient stability. J. Mater. Chem. A **4**, 2419–2426 (2016)
32. Zhou, P., Fang, Z., Zhou, W., Qiao, Q., Wang, M., Chen, T., et al.: Nonconjugated polymer poly (vinylpyrrolidone) as an efficient interlayer promoting electron transport for perovskite solar cells. ACS Appl. Mater. Interfaces **9**, 32957–32964 (2017)
33. Chen, W., Wang, Y., Pang, G., Koh, C.W., Djurišić, A.B., Wu, Y., et al.: Conjugated polymer-assisted grain boundary passivation for efficient inverted planar perovskite solar cells. Adv. Funct. Mater. **29**, 1808855 (2019)
34. Tonzola, C.J., Alam, M.M., Bean, B.A., Jenekhe, S.A.: New soluble n-type conjugated polymers for use as electron transport materials in light-emitting diodes. Macromolecules **37**, 3554–3563 (2004)
35. Sheibani, E., Yang, L., Zhang, J.: Recent advances in organic hole transporting materials for perovskite solar cells. Sol. RRL **4**, 2000461 (2020)
36. Jeng, J.Y., Chiang, Y.F., Lee, M.H., Peng, S.R., Guo, T.F., Chen, P., et al.: $CH_3NH_3PbI_3$ perovskite/fullerene planar-heterojunction hybrid solar cells. Adv. Mater. **25**, 3727–3732 (2013)
37. Wu, C.-G., Chiang, C.-H., Tseng, Z.-L., Nazeeruddin, M.K., Hagfeldt, A., Grätzel, M.: High efficiency stable inverted perovskite solar cells without current hysteresis. Energy Environ. Sci. **8**, 2725–2733 (2015)
38. Lim, K.G., Kim, H.B., Jeong, J., Kim, H., Kim, J.Y., Lee, T.W.: Boosting the power conversion efficiency of perovskite solar cells using self-organized polymeric hole extraction layers with high work function. Adv. Mater. **26**, 6461–6466 (2014)
39. Xue, Q., Chen, G., Liu, M., Xiao, J., Chen, Z., Hu, Z., et al.: Improving film formation and photovoltage of highly efficient inverted-type perovskite solar cells through the incorporation of new polymeric hole selective layers. Adv. Energy Mater. **6**, 1502021 (2016)
40. Jaiswal, M., Menon, R.: Polymer electronic materials: a review of charge transport. Polym. Int. **55**, 1371–1384 (2006)
41. Deshmukh, K.D., Prasad, S.K., Chandrasekaran, N., Liu, A.C., Gann, E., Thomsen, L., et al.: Critical role of pendant group substitution on the performance of efficient all-polymer solar cells. Chem. Mater. **29**, 804–816 (2017)
42. Cai, B., Xing, Y., Yang, Z., Zhang, W.-H., Qiu, J.: High performance hybrid solar cells sensitized by organolead halide perovskites. Energy Environ. Sci. **6**, 1480–1485 (2013)
43. Kwon, Y.S., Lim, J., Yun, H.-J., Kim, Y.-H., Park, T.: A diketopyrrolopyrrole-containing hole transporting conjugated polymer for use in efficient stable organic–inorganic hybrid solar cells based on a perovskite. Energy Environ. Sci. **7**, 1454–1460 (2014)
44. Kim, G.W., Kim, J., Lee, G.Y., Kang, G., Lee, J., Park, T.: A strategy to design a donor–π–acceptor polymeric hole conductor for an efficient perovskite solar cell. Adv. Energy Mater. **5**, 1500471 (2015)
45. Heo, J.H., Im, S.H., Noh, J.H., Mandal, T.N., Lim, C.-S., Chang, J.A., et al.: Efficient inorganic–organic hybrid heterojunction solar cells containing perovskite compound and polymeric hole conductors. Nat. Photonics **7**, 486–491 (2013)
46. Qin, P., Tetreault, N., Dar, M.I., Gao, P., McCall, K.L., Rutter, S.R., et al.: A novel oligomer as a hole transporting material for efficient perovskite solar cells. Adv. Energy Mater. **5**, 1400980 (2015)
47. Zhou, Z., Li, X., Cai, M., Xie, F., Wu, Y., Lan, Z., et al.: Stable inverted planar perovskite solar cells with low-temperature-processed hole-transport bilayer. Adv. Energy Mater. **7**, 1700763 (2017)

48. Bi, D., Yang, L., Boschloo, G., Hagfeldt, A., Johansson, E.M.: Effect of different hole transport materials on recombination in $CH_3NH_3PbI_3$ perovskite-sensitized mesoscopic solar cells. J. Phys. Chem. Lett. **4**, 1532–1536 (2013)
49. Xiao, J., Shi, J., Liu, H., Xu, Y., Lv, S., Luo, Y., et al.: Efficient $CH_3NH_3PbI_3$ perovskite solar cells based on graphdiyne (GD)-modified P3HT hole-transporting material. Adv. Energy Mater. **5**, 1401943 (2015)
50. Habisreutinger, S.N., Leijtens, T., Eperon, G.E., Stranks, S.D., Nicholas, R.J., Snaith, H.J.: Carbon nanotube/polymer composites as a highly stable hole collection layer in perovskite solar cells. Nano Lett. **14**, 5561–5568 (2014)
51. Li, M.H., Liu, S.C., Qiu, F.Z., Zhang, Z.Y., Xue, D.J., Hu, J.S.: High-efficiency CsPbI2Br perovskite solar cells with dopant-free poly(3-hexylthiophene) hole transporting layers. Adv. Energy Mater. **10**, 2000501 (2020)

Conjugated Polymers as Organic Electrodes for Photovoltaics

Bakhytzhan Baptayev, Yerbolat Tashenov, and Mannix P. Balanay

Abstract The use of conjugated polymers as organic electrodes for photovoltaics is very attractive due to their ability to form flexible substrates which can be applied either as an anode or a cathode depending on its configuration. Its properties can easily be tuned via synthetic or post-synthetic treatment processes. In this chapter, an overview of the brief history is given to provide a background on solar cell technology. The conjugated polymers are commonly observed in the third generation solar cells specifically in dye-sensitized, perovskite, and organic solar cells, which mostly utilize them as counter electrodes. First, we briefly discuss the components, criteria, and representative conjugated polymers for dye-sensitized solar cells. Then followed by the composition, mechanism, and utilization of conjugated polymers in perovskite solar cells. Lastly, we introduce the basic configuration of organic solar cells that uses conjugated polymers as both cathode and anode.

Keywords Third-generation solar cell · Dye-sensitized solar cell · Perovskite solar cell · Organic solar cell · Counter-electrode

1 Introduction

The advent of technological advancement and industrialization has led to an increase in energy demand. This hastens the depletion of fossil fuels which supplies 84% of the world's energy. Aside from being a non-renewable energy resource, fossil fuels are also a major contributor to large amounts of greenhouse gases in the air that are

B. Baptayev
National Laboratory of Astana, 53 Kabanbay Batyr Avenue, Nur-Sultan 010000, Kazakhstan

Y. Tashenov · M. P. Balanay (✉)
Department of Chemistry, School of Sciences and Humanities, Nazarbayev University, 53 Kabanbay Batyr Avenue, Nur-Sultan 010000, Kazakhstan
e-mail: mannix.balanay@nu.edu.kz

Y. Tashenov
Department of Chemistry, L.N. Gumilyov Eurasian National University, 2 Satpayev Street, Nur-Sultan 010008, Kazakhstan

137
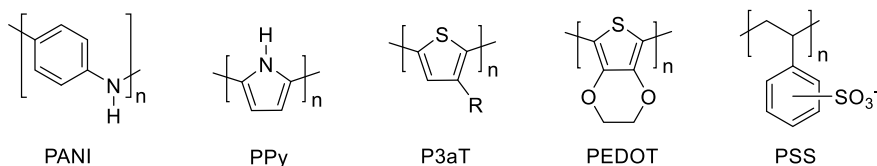
Fig. 1 Structures of the most common conducting polymers used in solar cells

responsible for global warming. A lot of government efforts now focus on investing in the use of renewable energy resources. Among these resources, the energy coming from the sun is the most promising since it can provide the worlds' energy needs that are around 4.5×10^4 TWh by the year 2050. The development of the use of solar cells started with the discovery of the photovoltaic effect when the light was irradiated to metal-coated electrodes which were dipped in an electrolyte in 1839 by Becquerel [1]. In 1883, Charles Fritz conceived the first working solar cell that uses selenium wafers with a thin layer of gold having a power conversion efficiency (PCE) of about 1% [2]. The first practical solar cells having a PCE of ~ 6% were developed by the researchers of Bell Laboratories which uses silicon instead of selenium in 1954 [3]. Since then, various types of materials are utilized to generate electricity from sunlight.

The utilization of conjugated polymers (CPs) in solar cells, since its discovery in 1976 by Shirakawa et al. [4], was mostly applied to three types of third-generation solar cells namely (a) dye-sensitized, (b) perovskite, and (c) organic solar cells. The majority of the CPs utilized in solar cells revolve around specific structures such as polyaniline (PANI), polypyrrole (PPy), poly(3-alkylthiophene) (P3aT), poly(3,4-ethylenedioxythiophene) (PEDOT), and poly(styrene sulfonate) (PSS) (Fig. 1), wherein the latter two usually are used in mixture with each other.

2 Conjugated Polymers in Dye-Sensitized Solar Cells

Dye-sensitized solar cells (DSSCs) originated in 1991 as photoelectrochemical cells mimicking the process of photosynthesis in plants [5]. Since then, DSSCs have been attracting researchers all over the world because of their low cost, ease of fabrication, and remarkable efficiency. Three major components constitute DSSCs: anode, cathode, and electrolyte. The anode is a transparent conducting oxide (TCO) substrate with a thin film of semiconducting nanoparticles such as TiO_2 covered with sensitizing dye molecules. While the cathode is a TCO substrate with a film of an electrocatalyst such as platinum. The third component, a redox electrolyte, is sandwiched between these two electrodes. The schematic representation of the DSSCs is presented in Fig. 2. As electrons of dye become photoexcited upon light absorption, they are injected into the conduction band of the semiconductor and then travel to the cathode via the outer circuit. The redox electrolyte then regenerates
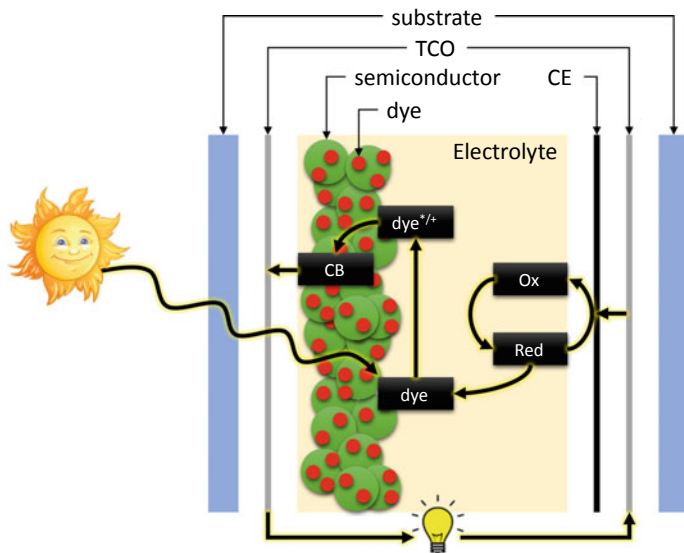
Fig. 2 Schematic representation of the working principle of the dye-sensitized solar cell

oxidized dyes and is subsequently reduced by the electrocatalyst at the cathode. All three components of DSSCs play a significant role in determining device performance; therefore, the design and development of suitable and optimal components is a vital step in constructing a highly efficient DSSCs. The primary criteria in choosing the right component are performance, cost, and processability, in which all of these can be provided by the conductive polymers that make it an attractive material for solar cells. Hence, both anode and cathode can be prepared from transparent and conducting polymers. CPs can replace expensive and scarce platinum electrocatalyst of DSSCs counter electrode (CE) and can also be used as an alternative to the more corrosive liquid redox mediator. In the succeeding sections, we focus on the use of conductive polymers as counter electrodes in DSSCs.

2.1 Conjugated Polymers as Counter Electrodes for Dye-Sensitized Solar Cells

In DSSCs, an anode is an electrode where oxidation occurs, thus collecting electrons. Whereas cathode is the electrode where reduction takes place and hence it collects holes. Mostly, the term 'counter electrode' (CE) is used to define the cathode. The main functions of the CE in DSSCs are two-fold: (i) it reduces the oxidized species of redox couple and (ii) allows the current to flow out and the electrons to go into the device. Therefore, an ideal CE should have an excellent catalytic activity

towards the reduction of the redox mediator and be chemically stable under a corrosive environment of the electrolyte. Other requirements of the CE are large surface area, high conductivity for efficient charge transfer (CT), good optical transparency, and high mechanical flexibility. There are many alternative CEs such as transition metal compounds, carbonaceous materials, metal alloys, and conducting polymers that have outperformed Pt-based CEs. Of the alternatives, CPs are attractive since their properties can be adjusted via synthetic manipulations and post-synthetic treatment methods. Additionally, CPs are abundant, less expensive, have good electrical conductivity, and can be easily synthesized. Common CPs used as DSSC cathode are PANI, P3aT and its derivatives, and PEDOT.

2.1.1 Polyaniline

PANI is one of the conductive polymers which is an extensively studied material as a CE in DSSCs. Among the attractive properties of PANI is that it has three oxidation states with distinct colors. Moreover, it can be fine-tuned via doping with acid or base. A pioneering work of PANI-based cathode for DSSCs was done by Li and colleagues in 2008 [6]. They prepared microporous PANI nanoparticles with a diameter of 100 nm by the aqueous oxidative polymerization reaction with perchloride acid as a dopant in the presence of ammonium persulfate. The porous structure of the polymer benefited its electrocatalytic activity towards reduction of I_3^- which was found higher than the Pt CE. This produced a higher PCE of 7.15% as compared with Pt CE with a PCE of 6.90%. PANI was also used in DSSCs with $Co^{3+/2+}$ electrolytes. Wang et al. reported an oriented PANI nanowire arrays CE which was grown in situ on TCO glass substrate [7]. The 1D structure demonstrated improved electrocatalytic performance compared to random network PANI films and traditional Pt cathode. This resulted in an enhanced short-circuit current density (J_{SC}) and fill factor (FF) in DSSCs with 1D PANI CE which showed a remarkable 8.24% efficiency which is notably higher than in solar cells with random network PANI (5.97%) and Pt CE (6.78%).

The electrocatalytic property, conductivity, and porosity of PANI can be improved through the use of doping. For example, Deng et al. studied the effect of doping PANI with different ions SO_4^{2-}, ClO_4^-, BF_4^-, Cl^-, p-toluenesulfonate (TsO$^-$), and others [8]. Among the ions, it is the sulfate-doped electropolymerized PANI film that demonstrated porous morphology with a higher reduction current compared to Pt CE. It has a low CT resistance (R_{CT}) of 1.3 Ω cm^2, which produces a PCE of 5.6% which is almost comparable to the reference electrode (6.0%).

PANI can also be used to prepare transparent electrodes. Zhao and the company reported on the use of highly uniform transparent PANI counter electrodes prepared by a facile in situ polymerization method [9]. The PANI film exhibited excellent transparency in the visible range 450–750 nm with a maximum of 74% transmittance at 510 nm which made it applicable for bifacial irradiation. Corresponding front and rear side photovoltaic tests of the transparent PANI-based device exhibited 6.54 and

4.26% efficiencies, respectively, which were comparable to Pt-based solar cells with 6.69% PCE.

Methods of preparation of PANI CEs are diverse which include chemical, emulsion-based synthesis, cyclic voltammetric (CV) and potentiostatic polymerization, oxidative polymerization, electropolymerization techniques, etc. Cyclic voltammetric polymerization allows direct deposition of PANI film on the TCO substrate which can be used as a counter electrode. As an example, Zhang et al. reported a CV method-based preparation of PANI CEs with controlled thickness and better adhesion [10]. The electrochemical deposition method can produce PANI with high CT kinetics and good electrical and electrochemical performances [11]. Emulsion polymerization, an economical method of synthesis of CPs, could be useful in preparing hollow structured polymers which is beneficial for increasing surface area and, hence, electrocatalytic activity. Higher photovoltaic performance of emulsion polymerized PANI with hollow spheres compared to a pristine PANI was reported by Ho and colleagues [12]. In addition, the hollow sphered analogs exhibited large surface area and an enhanced electrocatalytic activity towards the reduction of triiodide ions. A novel method based on hexafluoro-isopropanol (HFIP) solution is another cost-efficient method of CPs synthesis. Some reports claim that it may generate a highly concentrated, well dispersed, stable conduction, and more ordered structure of PANI resulting in a remarkable increase of solar cell efficiency [13].

Despite its attractive properties, PANI has several drawbacks as a CE material. Its stability needs to be improved further since it was observed that the self-oxidation of PANI may deteriorate the performance of CEs. Furthermore, PANI's carcinogenic properties may also be a hindrance to its widespread application.

2.1.2 Polypyrrole

Generally, PPy is more of an insulator rather than a conductor but its oxidized form exhibits good conductivity around 2–100 S/cm. The level of conductivity depends on the type of oxidizing agent and oxidation conditions. PPy is thermally stable in the air up to 150 °C. The first application of PPy as DSSC CE was reported by Wu et al. in 2008 [14]. The PPy nanoparticles with a particle size range of 40–60 nm were synthesized following the chemical polymerization method with iodine serving as an initiator. The CE was prepared by soaking the fluorine-doped SnO_2 (FTO) substrate with PPy nanoparticles. The results show that PPy-based CE produced a high electrocatalytic activity with smaller R_{CT} compared to control Pt CE. The PCE of PPy based device outperformed Pt-based DSSC by 11%.

The thickness of PPy film should also be considered for CE fabrication since it was observed that thicker PPy film can negatively affect the performance of the CE due to an increase in R_{CT} [15]. This was observed when ultra-thin PPy nanosheets were synthesized, it exhibited similar morphology as graphene sheets with higher surface area and active sites and a having a 94% transmittance of the CE producing a PCE of 6.8% [16]. As to date, the highest efficiency based on PPy CEs is at 7.73% which is slightly lower than the reference electrode which has a PCE of 8.2% [17].

The main drawbacks of polypyrrole-based cathodes are their high R_{CT} and low conductivity. The performance of PPy counter electrodes is dependent on the synthetic method, morphology, and the type of doping. One way to overcome these issues is by adding PPy to other materials forming composites. This is evident when PPy was mixed to carbon nanotubes (CNT) the R_{CT} and exchange current densities (J_0) of the composite CE was comparable with those of Pt CE which resulted in 6.15% PCE ($\approx$ 97% of Pt CE) [18]. Another research incorporates a multiwalled CNT into PPy that produces a transparent CE which can find an application in bifacial DSSCs. Its R_{CT} was found < 1 Ω cm^2 implying excellent electrocatalytic activity towards reduction of triiodide. Rafique et al. fabricated a CE from copper polypyrrole functionalized multiwall carbon nanotubes (Cu-PPy-FWCNTS) nanocomposite by two-step electrodeposition method on stainless-steel substrate [19]. The hybrid CE exhibited very small R_{CT} (4.31 Ω cm^2) and the efficiency of DSSC with Cu-PPy-FWCNTS outperformed Pt, with PCEs of 7.1% and 6.4%, respectively. The presence of the third composite can further enhance catalytic activity in composites. A recent study showed that the addition of NiS into graphene oxide/PPy composite boosted its J_0 from 5.01 to 7.94 mA/cm^2 and in turn decreased it's R_{CT} [20]. In general, composite CE-based DSSCs outperform their corresponding components due to the synergetic effect. This opens up a way for highly efficient and low-cost DSSCs.

2.1.3   Polythiophene

Polythiophene-based conjugated polymers that were utilized as electrodes in dye-sensitized solar cells normally use an alkyl group to control the solubility of the polymer in solvents which can help improve its chemical stability and compatibility towards electrolytes in DSSCs. An electrochemical deposition method was used to grow a porous poly-3-methyl-thiophene (P3MT) that was used as a CE [21]. The highest reported efficiency was at 2.76% which is 45% lower than the reference electrode. The low in efficiency was mostly attributed to the low J_{SC} (8.88 mA/cm^2 (P3MT) vs. 15.29 mA/cm^2 (Pt)) that was mainly attributed to the low carrier mobility [21]. A group of researchers utilizes poly(3-hexylthiophene) (P3HT) and C$_{61}$-butyric acid methyl ester (PCBM) that were deposited through spin-coating on an FTO plate to be applied as CE in DSSCs [22]. The main problems of using the bare polythiophene utilized as CE are due to the low electrical conductivity and dismal catalytic activity. One way to improve this property is by incorporating graphene or transition metals which are known to show good catalytic activities. This was shown when polythiophene/graphene composites were synthesized via the liquid/liquid interfacial polymerization showed a PCE of 4.8% for the composite (5.1% PCE for Pt), while 3.3% for the bare polythiophene [23]. When a transition metal such as MoS$_2$ was mixed to the bare thiophene, it lowers the R_{CT} by 22% achieving a 38% increase in efficiency compared to the bare polythiophene [24].

2.1.4 Poly(3,4-Ethylenedioxythiophene)

The earliest attempt of using PEDOT as CE for DSSC was reported in 2002 by Saito et al., wherein they applied PEDOT on a conductive glass which demonstrated comparable PCE to the Pt CE in I^-/I_3^- based DSSC [25]. The polymer was synthesized on the TCO substrate while doping it with *p*-toluenesulfonate and poly(styrene sulfonate). TsO-doped PEDOT exhibited almost the same performance as Pt-based cells. The poor performance of PSS-doped PEDOT was due to the reduction of the redox-active site of the conjugated polymer film because of the exposure of PSS preventing the electrolyte to the active site of the PEDOT. The conductivity of PEDOT:PSS can be increased by the means of doping, synthetic conditions, and post-treatment procedures. Ho *et al.* reported that the conductivity of PEDOT:PSS was increased from 2 S/cm to 85, 45, 36, and 20 S/cm after upon treatment with dimethyl sulfoxide (DMSO), *N,N*-dimethyl acetamide (DMAc), *N,N*-dimethyl formamide (DMF), and dichloromethane (DCM), respectively [26]. To further enhance the conductivity a small amount of carbon black (0.02–2 wt.%) was added to the polymeric solution. The electrochemical characterization revealed that DMSO-PEDOT: PSS-based CE exhibited high R_{CT} with a value of 19.4 Ω. The addition of 0.1 wt.% carbon decreased the R_{CT} to 7.2 Ω bringing it to the value like Pt CE. Thus, DMSO-PEDOT:PSS (C: 0.1 wt%) achieved 5.81% efficiency outperforming the reference electrode (5.66% PCE). In another research, bis(trifluoromethanesulfonyl)imide) (TFSI)-doped PEDOT was electrodeposited using cyclic voltammetry over conducting carbon black coated FTO glass producing a PCE of 9.8% [27]. Recently, a group of researchers synthesized PEDOT CE with a conductivity reaching as high as 1021 S/cm which was prepared via iron oxide vapor-phase polymerization [28]. Remarkably, the CE exhibited six times lower R_{CT} than Pt-based cathode guarantying outstanding catalytic activity towards the reduction of I^-/I_3^- redox couple which produces a PCE of 8.4%.

Apart from I^-/I_3^-, the reduction of other redox mediators in DSSCs can also be catalyzed by PEDOT-based counter electrodes. In this regard, PEDOT CEs can replace traditional Pt and Au metal cathodes. An interesting study of DSSC was implemented at indoor conditions using copper$^{2+/1+}$ complexes as a redox shuttle and PEDOT-covered FTO as the counter electrode [29]. The standard indoor light intensity varies between 200 and 2000 lx, in which the cell demonstrated the highest efficiency of 28.9% PCE at 1000 lx and 11.3% at standard AM1.5 conditions. Later in 2018, the group of Professor Grätzel reported a new record efficiency for indoor used DSSC of novel architecture reaching 32% which exceeds the performance of the best Si and GaAs photovoltaics [30]. In the presented architecture, the dye-coated mesoporous TiO_2 anode and the PEDOT cathode are directly contacted without using any spacer allowing attenuation of the resistance of the redox couple, hence, improving the DSSC performance. Using $Cu^{2+/1+}$ based liquid electrolyte, the solar cell demonstrated 13.1% PCE at standard conditions.

Suitable characteristics make conjugated polymers a promising cathode material for dye-sensitized solar cells. Common conjugated polymer materials for DSSC counter electrodes are polypyrrole, polyaniline, polythiophenes, etc. Among them,

Fig. 3 Reported power
conversion efficiencies of
conjugated polymer counter
electrodes based DSSCs
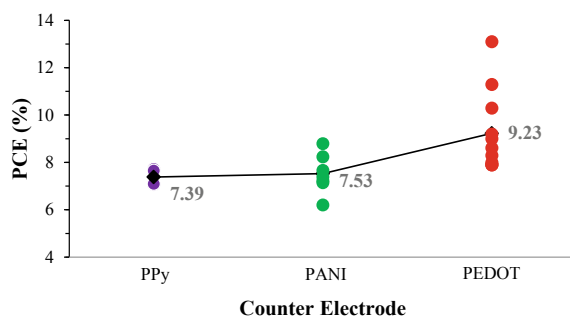
PEDOT-based polymers are the best in terms of conductivity, electrocatalytic activity, and photovoltaic performance. The comparison of the photovoltaic parameters including power conversion efficiency of the recently reported studies reveals that PEDOT exhibits the highest solar cell efficiency (Fig. 3). PPy, on the contrary, has the lowest average efficiency of the reported studies. The overall trend is PEDOT > PANI > PPy.

3   Conjugated Polymers in Perovskite Solar Cells

Perovskite solar cells (PeSC) are considered the 'rising star' of thin-film photovoltaics for a rapid increase of its power conversion efficiency in a short time. PeSC applies a perovskite structured active layer for light harvesting. Generally, perovskite is any material that has the same structure as perovskite mineral $CaTiO_3$ having a generic form ABX_3, where A and B could be any inorganic or organic cations and X are any combination of halides. In PeSCs, the perovskite structured active layer is sandwiched between the electron-transport layer (ETL) and hole-transport layer (HTL) as shown in Fig. 4.

Currently, the power conversion efficiency of PeSC has exceeded 25% making it the champion among emerging technologies and a potential alternative to silicon-based photovoltaics [31]. PeSC uses common *n*-type semiconductors such as TiO_2, SnO_2, ZnO, PCBM and C_{60} as electron-transport layers (ETL) and the *p*-type semiconductors like 2,2′,7,7′-tetrakis[*N*,*N*-di(4-methoxyphenyl)amino]-9,9′-spirobifluorene (Spiro-OMeTAD), poly(triaryl amine) (PTAA), P3HT, PEDOT:PSS, CuI, CuSCN, NiO, etc. as hole-transport layers (HTL). The electrons from photoexcited perovskite layer are injected into ETL and collected at the cathode, whereas holes are traveled via HTL to the anode.
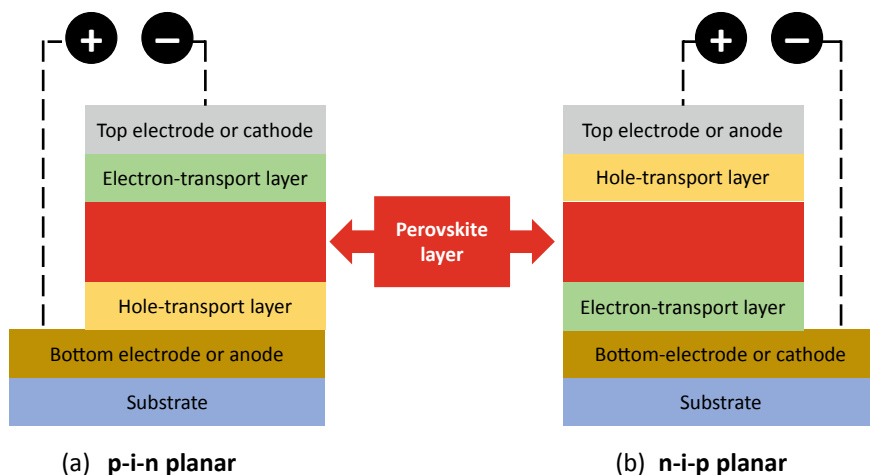
Fig. 4 Schematic diagram of different configurations of perovskite solar cells

3.1 Conjugated Polymer Counter Electrodes for Perovskite Solar Cells

For efficient charge collection and transfer, the CE should have high conductivity and proper work function. Noble metals like Au and Ag are the traditional CEs of the most state-of-the-art PeSCs. The reason is their low sheet resistance (~ 1 Ω/sq) and high light reflectivity. Despite their excellent performance, they have several disadvantages: both Au and Ag can migrate into the device core and react with perovskite halide causing degradation. In addition, their high cost affects the expense of the device. Au CE can take up to 70% of the total device cost [32]. Therefore, there is a need for alternative materials to increase their solar cell lifespan and can be more commercialize.

Conjugated polymers are potential candidates for PeSC counter electrodes. One of the widely used conjugated polymers in PeSC is PEDOT where it can serve both as the bottom and top electrode. In 2014, Jiang et al. first reported the use of PEDOT:PSS as a counter electrode for PeSC [33]. The polymer counter electrode was prepared by transfer lamination technique from its water solution to protect perovskite layer degradation. The final device configuration was glass/FTO/c-TiO_2/m-TiO_2/$CH_3NH_3PbI_3$/Spiro-OMeTAD/PEDOT:PSS and showed a maximum V_{OC} of 1.02 V and PCE of 11.29% under standard AM 1.5 light condition. The fabrication step was done under ambient air conditions.

Stamping transfer is another useful method to fabricate transparent electrodes in perovskite solar cells. Wang et al. fabricated low temperature-based inverted semi-transparent $MAPbI_3$ PeSC where PEDOT served as the top electrode [34]. The device configuration was indium tin oxide (ITO)/PEDOT:PSS/$CH_3NH_3PbI_3$/PCBM/PEDOT:PSS. The work function of

PEDOT electrode was adjusted by treating the polymer solution with PEI (polyethyleneimine) which improved cell efficiency from 0.07 to 4.02%. Park et al. reported improved conductivity and decreased work function of the top electrode after PEI/2-MEA (2-methoxyethanol) modification of PEDOT:PSS [35]. The PEDOT:PSS was dry stamp transferred over PET/ITO/PEDOT:PSS/metal halide perovskite/PCBM to fabricate semi-transparent PeSC. The PCE of the device achieved > 13% at 1 cm^2 area. In 2020, Ma et al. reported on the use of PEDOT:PSS CE in stacking perovskite solar cells with FTO/SnO$_2$/perovskite/Spiro-OMeTAD/PEDOT:PSS device configuration [36]. The physical and chemical properties of the electrode were modified by treating with hexamethylene diammonium diiodide which improved interface contact between photoanode and counter electrode and energy levels were properly matched. The efficiency of the device with 1 cm^2 area reached 15.21%.

Although PEDOT-based top electrodes have shown notable results in perovskite solar cells there are some drawbacks of the polymer which need further investigation. The polymer is usually produced as a water solution and possesses some level of acidity which can cause damage to the cell via degradation. Another issue is the low conductivity of PEDOT-based films compared to metal CEs and ITO that causes sheet resistance to be high. To increase the conductivity certain additives are added to the polymer. Other methods of improving the conductivity need to be studied. The short lifespan of the PEDOT films is another problem that requires attention.

4   Conjugated Polymers in Organic Solar Cells

Organic solar cells (OSCs) have received great attention as a source of green energy because of their considerable advantages associated with low-cost manufacturing, easy fabrication technique, and possibilities to construct lightweight, flexible, and ultrathin devices. Moreover, the implementation of a solution-processing technique for deposition of active layers in OSCs, like roll-to-roll and ink-jet printing technologies, can be transmitted in large area sizes, thereby facilitating the production of OSCs on an industrial scale. Owing to the substantial progress in the synthesis of new materials and device engineering, the PCE of recently developed OSCs has improved significantly and has reached 18.22% in 2020 [37]. However, this PCE indicator is far behind solar cells based on inorganic materials or from perovskite solar cells, which restricts the practical application of OSCs. To overcome this limitation in photon-to-electron conversion efficiency, tremendous research efforts are needed in terms of the introduction of new organic materials, the development of a more effective device structure, and the optimization of solar cell fabrication techniques in OSCs.

To date, among existing devices of OSCs where photoactive layers are represented by single, double (p–n junction bilayer), or bulk-heterojunction (BHJ) structures, the most efficient is based on the latter. The possibility of achieving a relatively high PCE by BHJ configuration is associated with the resolving of two important

internal limitations which are the charge separation from the excited state of the organic semiconductor and the charge transport inside active layers to electrodes surfaces. As illustrated in Fig. 5, the OSC devices with a "normal" and "inverted" structure usually consist of the following layers stacked in parallel: substrate (glass, polymer materials)/bottom or hole-collecting electrode/anode interfacial or hole-transport layer/BHJ active layer/cathode interfacial or electron-transport layer/top or electron-collecting electrode which is an almost similar configuration to PeSCs (Fig. 4). Electrical power generation in OSCs can be summarized as four main steps: (1) incident photons are absorbed by organic polymer active layer resulting in excision generation at the donor–acceptor interface inside BHJ system; (2) separation of generated excision into free charge carriers (electrons and holes); (3) transportation of charge carriers; electrons are transferred through *n*-type organic semiconductor toward cathode surface and holes through *p*-type domains to anode surface; and (4) extraction and collection of charge carriers by electrodes to produce photocurrent.

Maintaining the mobility of charge carriers in one direction and reducing recombination are imperative and depend on the work functions of both electrodes. Mostly, ITO on a glass substrate is generally operated as a transparent hole collecting layer (anode), and metal layer (Al, Ag, Au, etc.) is commonly employed as electron collecting layer (cathode). A high conductivity, transparency, and excellent mechanical stability are the main advantageous properties of ITO, while its rigid structure and high cost are the main highlighted drawbacks. In most cases, the top electrode is a metal layer, the preparation of which requires expensive vacuum deposition facilities, which limits the size and cost of the devices. Therefore, the development
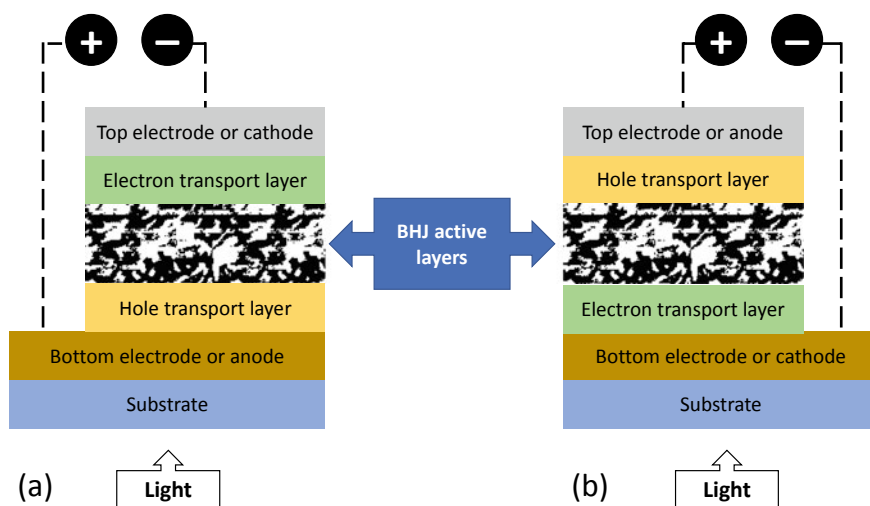
Fig. 5 Device architecture OSCs with **a** conventional and **b** inverted structures

of alternative materials for electrodes has crucial importance. In this aspect, conjugated polymers have become as main alternative materials for both top and bottom electrodes manufacturing.

The most popular CPs used as OSC cathode and anode is PEDOT:PSS. It exhibits a low sheet resistance, a tunable work function (5.0–5.2 eV), a wide range of conductivity (10^{-3}–4 x 10^3 S/cm), remarkably high optical transparency (>90%) in the visible light region, flexibility, and thermal stability. In addition, the application of PEDOT:PSS as electrode materials can be achieved using inexpensive, solution-processed technologies and implemented on a large surface area [38]. Despite the fact, that primary PEDOT:PSS films possess poor conductivity there are several methods to increase it; this can be attained via doping with strong acids, polar organic solvents, various nanomaterials, and pre-and post-treatment methods. For the manufacture of OSC electrodes, PEDOT:PSS aqueous solutions are commercially available under the trade names Clevios PH500, PH510 and PH1000, in which the ratio of PEDOT to PSS is 1:2.5. In addition, aqueous solutions of PEDOT:PSS with a ratio of 1:6 are well known as a commercial product with the market name Clevios PVP AI 4083, which is commonly used as a hole transfer layer in the OSC devices [39].

4.1 PEDOT:PSS as a Bottom Electrode for Organic Solar Cells

The pioneers who utilized PEDOT:PSS deposited on a glass substrate as an anode were Zhang et al. in 2002 [40]. Their result showed for the first time the possibility of using lower-cost and mechanically flexible PEDOT:PSS instead of traditional ITO for the manufacture of rigid OSC electrodes. They achieved an increased conductivity of PEDOT:PSS (10 S/cm) by doping it with glycerol or D-sorbitol. As a result, the OSC device consisting of D-sorbitol-doped PEDOT:PSS anode showed a PCE of 0.36%, while the OSCs with an ITO bottom electrode demonstrated efficiency of 0.46%. This created many research efforts on improving the conductivity of PEDOT:PSS electrodes by doping PEDOT:PSS with various polar solvents such as ethylene glycol, methanol, 2-chloroethanol, and DMSO producing a much higher PCE value than the D-sorbitol-doped PEDOT:PSS. To cite an example, Na et al. firstly reported a high conductive PEDOT:PSS electrodes deposited on rigid (glass) and flexible (PET) substrates [41]. A high conductivity value (550 S/cm) was achieved by doping the CP with 5% DMSO, which led to 3.27% and 2.8% efficiency of the ITO-free OSCs fabricated on glass and plastic substrates, respectively. The exhibited PCE results for PEDOT: PSS-based cells were similar to those of ITO-based devices. Recently, Kim and co-workers compared the performance of the 2-chloroethanol-treated PEDOT:PSS and standard 5% DMSO-doped PEDOT:PSS. According to their study, the 2-chloroethanol-treated CP electrodes showed superior PCE value rather than the DMSO-added films (9.04 vs. 7.63%) due to the electrical conductivity (762 vs. 439 S/cm) [42].

Another effective technique for improving PCE value of OSCs by increasing conductivity is the post-treatment of PEDOT:PSS films with either inorganic or organic acids. For example, Ge and his research group fabricated flexible transparent OSCs with CH_3SO_3H-treated PEDOT:PSS electrode on PET substrate at room temperature (20 °C). Modified PEDOT:PSS film was characterized with excellent electrical and optical parameters: high conductivity (2860 S cm^{-1}), superior optical transparency (90% at 450–900 nm), and smooth surface (RMS = 2.14 nm). Ultimately, the constructed solar cell containing a mixture of poly[(2,6-(4,8-bis(5-(2-ethyl-hexyl)thiophen-2-yl)benzo[1,2-b:4,5-b′]dithiophene)-co-(1,3-di(5-thiophene-2-yl)-5,7-bis(2-ethylhexyl)benzo[1,2-c:4,5-c′]-dithiophene-4,8-dione)] and methyl-substituted 3,9-bis(2-methylene-(3-(1,1-dicyanomethylene)-indanone)-5,5,11,11-tetrakis(4-hexylphenyl)-dithieno[2,3-d:2′,3′-d′]-s-indaceno [1,2-b:5,6-b′]-dithiophene active layer exhibited a high PCE of 10.12% [43]. Regarding the fact that relatively strong acids could be corrosive and harmful to the flexible plastic substrate, Ge's group has recently resolved this issue. They have discovered a high efficiency of 14.17% by folding-flexible OSCs composing of D-sorbitol micro-doped PEDOT:PSS/PET electrode treated with natural acids (citric acid, malic acid, or tartaric acid) [44].

A prominent improvement in the conductivity of PEDOT:PSS films for OSCs can be accomplished by a composite generation with a variety of conductive inorganic materials, including nanocarbon and metallic nanowires (NW). A highly conductive PEDOT:PSS: sulfonated carbon nanotubes (SCNT) composite electrode was prepared by Chen's group. The PEDOT:PSS:SCNT films as a cathode in "inverted" OSCs revealed a high PCE of 9.91% due to great optoelectronic effects (conductivity > 3500 S/cm, transmittance ∼83%) [45]. Recently, Shim et al. have fabricated PEDOT:PSS:CuNW-based transparent composite electrodes for ITO-free OSCs. Based on the PH1000/CuNWs, the optimized flexible OSC with P3HT: indene-C$_{60}$ bisadduct (ICBA) as active layer exhibits the highest PCE of 17.6% under 1000-lx light-emitting diode illumination, with an open-circuit voltage of 713 mV, a short-circuit current of 103 µA/cm^2 and a fill factor of 67.2% [46].

4.2 PEDOT:PSS as a Top Electrode for Organic Solar Cells

Commonly used top electrode materials for OSCs are MoO_3/Ag or LiF/Al. The manufacture of metal electrodes requires expensive and energy-consuming high vacuum equipment. Hence, the replacement of inorganic electrode materials with more profitable ones is a priority task. In this respect, the top electrode based on PEDOT:PSS is an alternative material, which provides tunable conductivity and high transmittance.

One of the effective methods for improving the characteristics of OSC is to minimize the resistance of the PEDOT:PSS electrode, which directly depends on its morphology. Various technologies have been used to make PEDOT:PSS films, including solution-processed, spin coating, screen printing, spray coating, bonding, doctor-blade coating, etc. Lee's group has recently constructed a sequentially printed

PEDOT:PSS/ionic liquid (IL) composite successfully applied as top electrode for OSCs, exhibiting a PCE of 6.32% at an average visible transmittance (AVT) of 35.4% [47]. In 2020, Kim et al. fabricated window-film-type OSCs with PEDOT:PSS as top electrode treated with sulfuric acid. Their OSC device with the following structure PEN/PA/ZnO-NP/PTB7-Th:PC$_{70}$BM/Mo$_x$/H-PEDOT showed excellent performance with PCE of 4.9% along with high transparency (AVT = 42%) [48]. Recently, Ma and co-workers reported a novel composite of phosphomolybdic acid (PMA) and PEDOT:PSS that revealed high affinity with the active layer and printed top Ag nanowires. A spin-coating or doctor-blade coating method were implemented for deposition of constructed buffer layer on a substrate surface (polymer). The use of this composite as top electrodes demonstrated the PCE of 5.01% with an excellent AVT of 50.3% [49]. These research outputs have proved PEDOT:PSS to be an excellent alternative material for both top and bottom electrodes because of their superior optical, electrical, and mechanical properties. Furthermore, the performance of PEDOT:PSS electrodes can be enhanced by the incorporation of miscellaneous doping agents, including carbonaceous nanocompounds, metal grids, and metal nanowires. For future perspective, there are some issues relating to improvement of conductivity, transmittance, and persistence to inner and outer stimuli.

References

1. Becquerel, M.: Mémoire sur les effets électriques produits sous l'influence des rayons solaires. C. R. Hebd Seances Acad. Sci. **9**, 561–567 (1839)
2. Fritts, C.E.: On a new form of selenium cell, and some electrical discoveries made by its use. Am. J. Sci. **s3–26** (156), 465–472 (1883)
3. Chapin, D.M., Fuller, C.S., Pearson, G.L.: A new silicon p-n junction photocell for converting solar radiation into electrical power. J. Appl. Phys. **25**(5), 676–677 (1954)
4. Shirakawa, H., Louis, E.J., MacDiarmid, A.G., Chiang, C.K., Heeger, A.J.: Synthesis of electrically conducting organic polymers: halogen derivatives of polyacetylene, (CH). J. Chem. Soc. Chem. Commun. **16**, 578–580 (1977)
5. O'Regan, B., Grätzel, M.: A low-cost, high-efficiency solar cell based on dye-sensitized colloidal TiO$_2$ films. Nature **353**(6346), 737–740 (1991)
6. Li, Q., Wu, J., Tang, Q., Lan, Z., Li, P., Lin, J., Fan, L.: Application of microporous polyaniline counter electrode for dye-sensitized solar cells. Electrochem. Commun. **10**(9), 1299–1302 (2008)
7. Wang, H., Feng, Q., Gong, F., Li, Y., Zhou, G., Wang, Z.-S.: In situ growth of oriented polyaniline nanowires array for efficient cathode of Co(iii)/Co(ii) mediated dye-sensitized solar cell. J. Mater. Chem. A **1**(1), 97–104 (2013)
8. Li, Z., Ye, B., Hu, X., Ma, X., Zhang, X., Deng, Y.: Facile electropolymerized-PANI as counter electrode for low cost dye-sensitized solar cell. Electrochem. Commun. **11**(9), 1768–1771 (2009)
9. Tai, Q., Chen, B., Guo, F., Xu, S., Hu, H., Sebo, B., Zhao, X.-Z.: In situ prepared transparent polyaniline electrode and its application in bifacial dye-sensitized solar cells. ACS Nano **5**(5), 3795–3799 (2011)
10. Zhang, J., Hreid, T., Li, X., Guo, W., Wang, L., Shi, X., Su, H., Yuan, Z.: Nanostructured polyaniline counter electrode for dye-sensitised solar cells: fabrication and investigation of its electrochemical formation mechanism. Electrochim. Acta **55**(11), 3664–3668 (2010)

11. Tang, Q., Cai, H., Yuan, S., Wang, X.: Counter electrodes from double-layered polyaniline nanostructures for dye-sensitized solar cell applications. J. Mater. Chem. A **1**(2), 317–323 (2013)
12. Huang, K.-C., Hu, C.-W., Tseng, C.-Y., Liu, C.-Y., Yeh, M.-H., Wei, H.-Y., Wang, C.-C., Vittal, R., Chu, C.-W., Ho, K.-C.: A counter electrode based on hollow spherical particles of polyaniline for a dye-sensitized solar cell. J. Mater. Chem. **22**(29), 14727–14733 (2012)
13. Chiang, C.-H., Chen, S.-C., Wu, C.-G.: Preparation of highly concentrated and stable conducting polymer solutions and their application in high-efficiency dye-sensitized solar cell. Org. Electron. **14**(9), 2369–2378 (2013)
14. Wu, J., Li, Q., Fan, L., Lan, Z., Li, P., Lin, J., Hao, S.: High-performance polypyrrole nanoparticles counter electrode for dye-sensitized solar cells. J. Power Sources **181**(1), 172–176 (2008)
15. Makris, T., Dracopoulos, V., Stergiopoulos, T., Lianos, P.: A quasi solid-state dye-sensitized solar cell made of polypyrrole counter electrodes. Electrochim. Acta **56**(5), 2004–2008 (2011)
16. Hwang, D.K., Song, D., Jeon, S.S., Han, T.H., Kang, Y.S., Im, S.S.: Ultrathin polypyrrole nanosheets doped with HCl as counter electrodes in dye-sensitized solar cells. J. Mater. Chem. A **2**(3), 859–865 (2014)
17. Jeon, S.S., Kim, C., Ko, J., Im, S.S.: Spherical polypyrrole nanoparticles as a highly efficient counter electrode for dye-sensitized solar cells. J. Mater. Chem. **21**(22), 8146–8151 (2011)
18. Lee, J.H., Jang, Y.J., Kim, D.W., Cheruku, R., Thogiti, S., Ahn, K.-S., Kim, J.H.: Application of polypyrrole/sodium dodecyl sulfate/carbon nanotube counter electrode for solid-state dye-sensitized solar cells and dye-sensitized solar cells. Chem. Pap. **73**(11), 2749–2755 (2019)
19. Rafique, S., Rashid, I., Sharif, R.: Cost effective dye sensitized solar cell based on novel Cu polypyrrole multiwall carbon nanotubes nanocomposites counter electrode. Sci. Rep. **11**(1), 14830 (2021)
20. Noorani, B., Ghasemi, S., Hosseini, S.R.: Nanostructured nickel sulfide/graphene oxide-polypyrrole as platinum-free counter electrode for dye-sensitized solar cell. J. Photochem. Photobiol. A **405**, 112966 (2021)
21. Torabi, N., Behjat, A., Jafari, F.: Dye-sensitized solar cells based on porous conjugated polymer counter electrodes. Thin Solid Films **573**, 112–116 (2014)
22. Yahia, I.S., Mansour, S.A., Hafez, H.S., Ocakoglu, K., Yakuphanoglu, F.: Photovoltaic properties and negative capacitance spectroscopy of PCBM:P3HT/FTO nanostructured counter electrode for TiO$_2$-based DSSC. J. Inorg. Organomet. Polym. Mater. **22**(6), 1240–1247 (2012)
23. Bora, C., Sarkar, C., Mohan, K.J., Dolui, S.: Polythiophene/graphene composite as a highly efficient platinum-free counter electrode in dye-sensitized solar cells. Electrochim. Acta **157**, 225–231 (2015)
24. Asok, A., Naik, A.A., Arunachalam, S., Govindaraj, R., Haribabu, K.: Microwave assisted synthesis of polythiophene–molybdenum sulfide counter electrode in dye sensitized solar cell. J. Mater. Sci.: Mater. Electron. **30**(14), 13655–13663 (2019)
25. Yasuteru, S., Takayuki, K., Yuji, W., Shozo, Y.: Application of poly(3,4-ethylenedioxythiophene) to counter electrode in dye-sensitized solar cells. Chem. Lett. **31**(10), 1060–1061 (2002)
26. Chen, J.-G., Wei, H.-Y., Ho, K.-C.: Using modified poly(3,4-ethylene dioxythiophene): poly(styrene sulfonate) film as a counter electrode in dye-sensitized solar cells. Sol. Energy Mater. Sol. Cells **91**(15), 1472–1477 (2007)
27. Zhang, J., Long, H., Miralles, S.G., Bisquert, J., Fabregat-Santiago, F., Zhang, M.: The combination of a polymer–carbon composite electrode with a high-absorptivity ruthenium dye achieves an efficient dye-sensitized solar cell based on a thiolate–disulfide redox couple. Phys. Chem. Chem. Phys. **14**(19), 7131–7136 (2012)
28. Kouhnavard, M., Yifan, D., D'Arcy, J.M., Mishra, R., Biswas, P.: Highly conductive PEDOT films with enhanced catalytic activity for dye-sensitized solar cells. Sol. Energy **211**, 258–264 (2020)
29. Freitag, M., Teuscher, J., Saygili, Y., Zhang, X., Giordano, F., Liska, P., Hua, J., Zakeeruddin, S.M., Moser, J.-E., Grätzel, M., Hagfeldt, A.: Dye-sensitized solar cells for efficient power generation under ambient lighting. Nat. Photonics **11**(6), 372–378 (2017)

30. Cao, Y., Liu, Y., Zakeeruddin, S.M., Hagfeldt, A., Grätzel, M.: Direct contact of selective charge extraction layers enables high-efficiency molecular photovoltaics. Joule **2**(6), 1108–1117 (2018)
31. Jeong, J., Kim, M., Seo, J., Lu, H., Ahlawat, P., Mishra, A., Yang, Y., Hope, M.A., Eickemeyer, F.T., Kim, M., Yoon, Y.J., Choi, I.W., Darwich, B.P., Choi, S.J., Jo, Y., Lee, J.H., Walker, B., Zakeeruddin, S.M., Emsley, L., Rothlisberger, U., Hagfeldt, A., Kim, D.S., Grätzel, M., Kim, J.Y.: Pseudo-halide anion engineering for α-FAPbI3 perovskite solar cells. Nature **592**(7854), 381–385 (2021)
32. Chang, N.L., Yi Ho-Baillie, A.W., Basore, P.A., Young, T.L., Evans, R., Egan, R.J.: A manufacturing cost estimation method with uncertainty analysis and its application to perovskite on glass photovoltaic modules. Prog. Photovoltaics Res. Appl. **25**(5), 390–405 (2017)
33. Jiang, F., Liu, T., Zeng, S., Zhao, Q., Min, X., Li, Z., Tong, J., Meng, W., Xiong, S., Zhou, Y.: Metal electrode-free perovskite solar cells with transfer-laminated conducting polymer electrode. Opt. Express **23**(3), A83–A91 (2015)
34. Kim, K.M., Ahn, S., Jang, W., Park, S., Park, O.O., Wang, D.H.: Work function optimization of vacuum free top-electrode by PEDOT:PSS/PEI interaction for efficient semi-transparent perovskite solar cells. Sol. Energy Mater. Sol. Cells **176**, 435–440 (2018)
35. Lee, J.H., Heo, J.H., Im, S.H., Park, O.O.: Reproducible dry stamping transfer of PEDOT:PSS transparent top electrode for flexible semitransparent metal halide perovskite solar cells. ACS Appl. Mater. Interfaces **12**(9), 10527–10534 (2020)
36. Ma, H., Shao, Y., Zhang, C., Lv, Y., Feng, Y., Dong, Q., Shi, Y.: Enhancing the interface contact of stacking perovskite solar cells with hexamethylenediammonium diiodide-modified PEDOT:PSS as an electrode. ACS Appl. Mater. Interfaces **12**(37), 42321–42327 (2020)
37. Liu, Q., Jiang, Y., Jin, K., Qin, J., Xu, J., Li, W., Xiong, J., Liu, J., Xiao, Z., Sun, K., Yang, S., Zhang, X., Ding, L.: 18% Efficiency organic solar cells. Sci. Bull. **65**(4), 272–275 (2020)
38. Fan, X., Nie, W., Tsai, H., Wang, N., Huang, H., Cheng, Y., Wen, R., Ma, L., Yan, F., Xia, Y.: PEDOT:PSS for flexible and stretchable electronics: modifications, strategies, and applications. Adv. Sci. **6**(19), 1900813 (2019)
39. Lövenich, W.: PEDOT-properties and applications. Polym. Sci. Ser. C **56**(1), 135–143 (2014)
40. Zhang, F., Johansson, M., Andersson, M.R., Hummelen, J.C., Inganäs, O.: Polymer photovoltaic cells with conducting polymer anodes. Adv. Mater. **14**(9), 662–665 (2002)
41. Na, S.-I., Kim, S.-S., Jo, J., Kim, D.-Y.: Efficient and flexible ITO-free organic solar cells using highly conductive polymer anodes. Adv. Mater. **20**(21), 4061–4067 (2008)
42. Jang, H., Kim, M.S., Jang, W., Son, H., Wang, D.H., Kim, F.S.: Highly conductive PEDOT:PSS electrode obtained via post-treatment with alcoholic solvent for ITO-free organic solar cells. J. Ind. Eng. Chem. **86**, 205–210 (2020)
43. Song, W., Fan, X., Xu, B., Yan, F., Cui, H., Wei, Q., Peng, R., Hong, L., Huang, J., Ge, Z.: All-solution-processed metal-oxide-free flexible organic solar cells with over 10% efficiency. Adv. Mater. **30**(26), 1800075 (2018)
44. Song, W., Peng, R., Huang, L., Liu, C., Fanady, B., Lei, T., Hong, L., Ge, J., Facchetti, A., Ge, Z.: Over 14% efficiency folding-flexible ITO-free organic solar cells enabled by eco-friendly acid-processed electrodes. iScience **23**(4) (2020)
45. Hu, X., Chen, L., Tan, L., Ji, T., Zhang, Y., Zhang, L., Zhang, D., Chen, Y.: In situ polymerization of ethylenedioxythiophene from sulfonated carbon nanotube templates: toward high efficiency ITO-free solar cells. J. Mater. Chem. A **4**(17), 6645–6652 (2016)
46. Ahsan Saeed, M., Hyeon Kim, S., Baek, K., Hyun, J.K., Youn Lee, S., Won Shim, J.: PEDOT:PSS:CuNW-based transparent composite electrodes for high-performance and flexible organic photovoltaics under indoor lighting. Appl. Surf. Sci. **567**, 150852 (2021)
47. Park, H., Lee, J.-H., Lee, S., Jeong, S.Y., Choi, J.W., Lee, C.-L., Kim, J.-H., Lee, K.: Retarding ion exchange between conducting polymers and ionic liquids for printable top electrodes in semitransparent organic solar cells. ACS Appl. Mater. Interfaces **12**(2), 2276–2284 (2020)
48. Kim, S., Lee, E., Lee, Y., Kim, J., Park, B., Jang, S.-Y., Jeong, S., Oh, J., Lee, M.S., Kang, H., Lee, K.: Interface engineering for fabricating semitransparent and flexible window-film-type organic solar cells. ACS Appl. Mater. Interfaces **12**(23), 26232–26238 (2020)

49. Ji, G., Wang, Y., Luo, Q., Han, K., Xie, M., Zhang, L., Wu, N., Lin, J., Xiao, S., Li, Y.-Q., Luo, L.-Q., Ma, C.-Q.: Fully coated semitransparent organic solar cells with a doctor-blade-coated composite anode buffer layer of phosphomolybdic acid and PEDOT:PSS and a spray-coated silver nanowire top electrode. ACS Appl. Mater. Interfaces **10**(1), 943–954 (2018)

Polymeric Nanofibers as Electrodes for Fuel Cells

Ayesha Kausar

Abstract Fuel cell efficiency has been enhanced using advanced electrode materials. The fuel cell electrodes have been investigated to replace the platinum metal catalysts with polymeric materials. Incidentally, membrane electrode assemblies have been developed. The nanofibrous electrode is unusually applied as a cathode. This chapter discourses the potential of polymeric nanofibers as fuel cell electrodes. In this regard, the electrospun polymeric nanofiber-based catalyzed electrodes have been developed. The thermoplastic and conducting polymers-based nanofibers have been used as fuel cell electrodes. The polymeric nanofiber electrodes may cause enhanced interactions of the catalyst with the reactant gases. The interactions in the nanostructured nanofibers may lead to synergistic effects on the morphology, electrical conductivity, impedance, and fuel cell efficiency. Moreover, the nanofibers may also develop conduction pathways for the proton and electron transport through the membrane electrode assembly. Future perspectives have also been discussed for the development of efficient energy devices.

Keywords Polymer · Nanofiber · Electrode · Catalyst · Fuel cell

1 Introduction

The fuel cells display notable efficiency, high power density, and eco-friendliness to offer clean power sources for use in moveable electronics, electronic automobiles, and power generating devices [1]. Initially, the fuel cells have applied the extremely high price platinum (Pt) catalyst [2]. Later, the studies have focused on the reduction of Pt use in the fuel cell electrodes [3]. The fuel cell electrodes with the low Pt contents, the Pt alloys, and the Pt with non-metal catalysts have been employed. In this regard, polymers have been used in the fuel cell components such as catalysts, electrodes, membranes, etc. [4]. The examinations on the use of polymer-based materials have enhanced the performance of the electrodes, catalysts, or membranes in

A. Kausar (✉)
Nanosciences Division, National Center For Physics, Quaid-i-Azam University Campus, Islamabad 45320, Pakistan

the fuel cells [5]. Nanofibers are one-dimensional materials produced using various precursors such as carbon nanomaterial, polymers, metal oxide, etc. The polymers have been applied as the one-dimensional nanofiber form in the electrodes for the fuel cell assemblies. The polymeric nanofibers have been developed using various fiber formation techniques. However, the nanofibrous electrodes have been mostly formed using the electrospinning technique [6]. The adaptation of polymers into one-dimensional nanofibers has stimulated the improved features of the polymers [7]. The enhanced characteristics of the nanofibers were obtained owing to the nano-size effects and the superior physical and chemical performance [8]. The nanocom-posite nanofibers have also been developed through nanoparticle reinforcement to augment the electrical and fuel cell efficiency properties [9, 10]. The nanofibers can easily develop the conduction pathways in the electrodes to enhance the conduc-tivity and form interactions with the gaseous molecules. Thus, the combination of polymers with platinum catalysts and electrospinning to form the nanofibers have established the synergistic consequence to enhance the electrode performance for the fuel cell. The chapter explains the fundamentals, properties, and significance of one-dimensional polymer-based nanofibers. The nanofibers intended for the fuel cell electrodes have been deliberated. The range of conducting and non-conducting polymers have been used to form the nanofibers. The electrical conductivity, proton conductivity, and solar cell properties have been enhanced through the use of the polymeric and nanocomposite nanofibers.

2   Polymer Nanofibers

The nanofibers are fiber-like structures having a diameter in the nm range, while their length may vary up to several mm. The nanofibers can be produced from diverse polymers. The polymeric nanofibers possess altered physical properties and poten-tial applications. The diameter, properties, and applications of the nanofibers depend on the type of polymer matrix utilized and the method of processing. The polymer nanofibers possess different contours and morphology including solid nanofibers, hollow nanofibers, flat nanofibers, and ribbon-shaped nanofibers. Among all these forms, solid nanofibers have been preferred and frequently prepared and used for various purposes. The polymer nanofiber technology has been developed to form the nanofibers of the conducting and thermoplastic polymers [11]. Thus, the polymer nanofibers are one-dimensional nanomaterials having varying sizes and diameters depending upon the fabrication technique used and the processing parameters. The polymer nanofibers have been prepared using numerous techniques such as electro-spinning, lithography, template method, template-free method, and solution routes [12]. The structure, morphology, electrical conductivity, and physical properties of the polymer nanofibers have been studied and thoroughly analyzed [13]. Moreover, the polymeric nanofibers have been considered to have a large surface area to volume ratio, high porosity, significant power-driven strength, and flexibility properties.

The polymer-based nanofibers have numerous conceivable technical and commercial applications in the coating materials, the membranes, the filtration media, the sensors, the energy devices, tissue engineering, the drug delivery, and the medical diagnosis. Polyaniline (PANI) is a significant kind of the conjugated polymer used to form the nanofibers. The polyaniline nanofibers have considerably high optical properties, electrical conduction, thermal stability, and electrochemical characteristics [14]. Chaudhari et al. [15] prepared the electrospun nanofibers of PANI. The nanofiber has a diameter of 200 nm and a length of $\sim$30 μm. Polyaniline has found practical application in supercapacitors, sensors, electronics, radiation shielding, etc. [16–18]. Electrospinning is a widely used technique for polymeric nanofiber formation [19]. The polymeric nanocomposites have been developed with the nanofillers to form the nanocomposite nanofibers using electrospinning [20]. Among the thermoplastic polymers, the Nafion, poly(acrylic acid) (PAA), polyethylene oxide) (PEO), poly(vinyl alcohol) (PVA), polystyrene, etc. have been electrospun to form the nanofibers. The nanofiber formation by polymers depend upon the molecular weight of the polymers and the polydispersity index values. The choice of polymer for the nanofiber formation depends on the desired end application of the nanofibrous materials.

3   Polymeric Nanocomposite Nanofibers

Electrospinning has been deliberated as a promising technique to develop polymeric and nanocomposite nanofibers [21]. The electrospinning can employ both the solution or melt precursor to form the nanofibers. A simple electrospinning setup is presented in Fig. 1.

The system contains constituents including the needle, syringe, collector, and electric field source. The polymer solution is filled in the syringe. The polymeric nanofibers have been generally industrialized under electrostatic force [22]. The distance between the needle and collector is fixed [23]. The polymer solution droplet arising from the needle forms the jet under the influence of an electric field. The polymer jet travels to the collector. The generated nanofiber is corrected on the collector. The electrospinning parameters can be easily altered to vary the nanofiber size and the morphology. The polymer and the nanocomposite nanofibers of ~ 100–300 nm diameter can be produced [24]. The length of the nanofiber may range up to millimeters [25]. The overall nanofiber properties rely on the polymer solution concentration, nanofiller type, nanofiller content, and electrospinning parameters. Junkasem et al. [26] used the electrospinning method to form the PVA and α-chitin flakes based on nanofibers. The nanofibers had a diameter of 231–969 nm. The thermal stability of the nanocomposite nanofibers was enhanced with the nanofillers loading. Gupta et al. [27] developed the electrospun poly(ethylene glycol) and carbon nanotube-based nanofibers. The poly(ethylene glycol)/carbon nanotube-based nanofiber electrode had a power density of 156 mW/cm^2. Bao et al. [28] produced the poly(vinyl acetate) and graphene-based electrospun nanofibers.
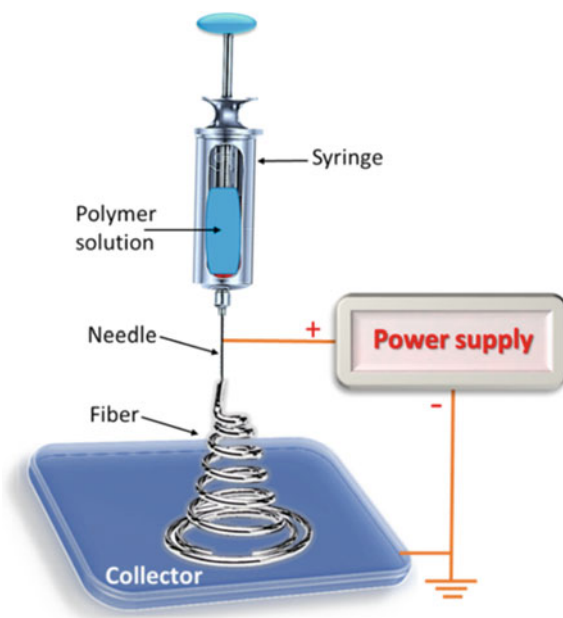
The 0.07 wt.% graphene loading enhanced the optical absorption of the poly(vinyl acetate)/graphene nanocomposite. The nanocomposite has application in ultrafast photonics. Abdah et al. [29] prepared the PVA/graphene oxide nanocomposite nanofibers by the electrospinning method for electrode formation. The nanofiber had a diameter of ~ 117 nm. The PVA/graphene oxide nanofiber-based electrode had a power density of ~ 304.4 W/kg and a capacitance of about 224.3 F/g. Mohamed et al. [30] developed the Ni/Pd supported PVA nanofibers via the electrospinning method. The Ni/Pd supported PVA nanofibers have uniform morphology and homogeneous alignment. The electrocatalyst-based electrode was used for the fuel cell. Hence, electrospinning is the most regularly used technique to generate nanofibers for technical applications, including fuel cell electrodes, due to the forthright setup and the aptitude for large-scale manufacturing of the continuous nanofibers. The ultrathin nanofibers of various polymers have been developed with the manageable diameter, the desired compositions, and the anticipated fiber orientation.

4   Polymeric Nanofiber-Based Nanomaterials as Fuel Cell Electrodes

The polymer and nanocomposite nanofibers have been prepared using various physical or chemical approaches. The polyimide nanofiber synthesis methods may include numerous crucial approaches in addition to the conformist electrospinning method.

These methods include solution blending, melt blending, in-situ polymerization, and frequent post modification processes of the nanostructures. The hot pressing or functionalization methods have been applied for the post-treatment of the polymeric nanofibers. The structure, morphology, and performance of the polymer nanofibers may also be transformed through variable thermal treatments. The freeze-drying method has also been utilized as a post-treatment of the nanocomposite nanofibers. The polymer nanofiber can also be modified through the addition of plasticizers in the polymer nanofibers. The plasticizers have been used to enhance the durability, strength, elasticity, heat resistance, and performance of the nanofiber. In the nanocomposite nanofibers, polymer concentration, nanofiller content, and dispersion, additives, etc. define the structure and morphology of the materials. Both the polymeric and nanocomposite nanofibers have been used to develop the electrodes for the fuel cells. The electrodes have been used as important components in a different types of the fuel cells such as the polymer electrolyte fuel cell, phosphoric acid fuel cell, alkaline fuel cell, molten carbonate fuel cell, and new eco-friendly fuel cells. The up-to-date fuel cell technology may employ environmentally friendly materials with low fuel consumption and less pollution cohort [31]. The polymeric materials have been used to design the fuel cell electrode, electrocatalyst, and electrolyte [32]. The research on the fuel cell electrodes has engrossed the replacement of the platinum metal catalysts from the cathode [33]. In this regard, alloys and composite materials have been used. The membrane electrode assembly (MEA) has been focused to enhance the catalyst interaction with the reactant gases to generate the proton and electron conduction pathways [34]. The morphology of MEA can be altered to affect the performance of the cathode of the polymer electrolyte membrane (PEM). The catalyst type and loading to the MEA are the important factors. The catalyst consumption in the MEA system of the fuel cell electrode must be improved to enhance the PEM cathode performance. The electrode may consist of the catalyst coated MEA, the catalyst coated carbon paper, and the gas diffusion layer. Most importantly, the catalyst coated MEA has been used [35]. The catalyst based on the platinum/carbon (Pt/C) catalysts covered by PEO, PAA, or the catalyst covered with the PVA has also gained attention [36]. Recently, the electrospun fuel cell electrode structures have been designed [37]. These electrodes have lasting life and durability properties. The Nafion, polysulfone or perfluorosulfonic acid have been used to develop the polymer nanofibers for the electrodes. Nafion is a sulfonated tetrafluoroethylene based fluoropolymer. It is a synthetic polymer. Moreover, Nafion has fine ionic properties and often referred as ionomer. Nafion has been frequently used in the fuel cell components. Nafion has low cost, stability, high selectivity and ion exchange properties in the development of the ecological fuel cells [38]. The carrier polymers such as PEO, PAA, or PVA have been applied during the electrospinning process of the nanofibers for the PEM electrodes [39]. The carrier or binding polymers play important role in the nanofiber formation, catalyst loading, and electrode structuration [40]. The cross-linked and non-cross-linked PEO, PAA, or PVA have been used with the catalyst for the fuel cell electrode. The nanofiber electrodes with the PEO, PAA, or PVA binders have revealed high ionic conductivity, power density, high photovoltaic performance, and long working life. These polymers also have a high Pt/C catalyst
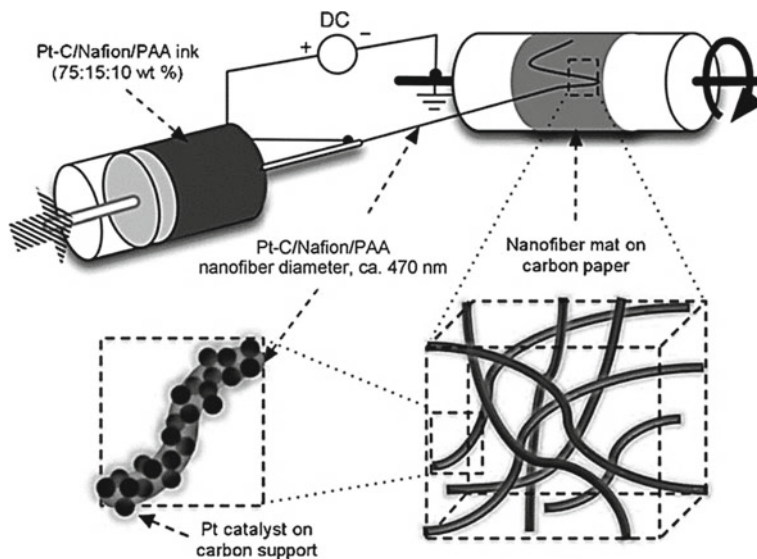
Fig. 2 Experimental design for electrospinning of nanofiber catalyst. Percolating network formation of Pt/C particles in nanofiber by a proton-conducting polymer binder. The nanofibers are collected on a carbon paper/collector drum. Pt/C = platinum/carbon; PAA = poly(acrylic acid). Adapted with permission from [41], Copyright (2011), Wiley

loading capability in the nanofiber form. Zhang et al. [41] prepared the nanofiber electrode through the electrospinning method. The polymer nanocomposite nanofibers were created using the Nafion, the PAA, and the Pt/C catalyst solution. The electrode was used as a cathode in the assembly of the H_2/air fuel cell and the H_2/O_2 fuel cell membranes. Figure 2 shows the electrospinning set up for the formation of nanofiber electrodes. The Nafion and PAA and Pt/C were dissolved in the isopropyl alcohol and water-based solvent. The cathode consists of 75 wt.% of the Pt/C catalyst. The nanofibers were formed under the high potential of 7 kV. The spinneret to collector distance was adjusted as the 9 cm and the flow rate was about 1.5 mL/h. The collector drum was covered with a carbon paper for the nanofibers collection. The nanofibers have the Pt/C particles arranged on the surface. The nanofibers also formed the percolation network in the nanofiber based electrode supporting the electron conduction through the nanofiber. The percolation network was developed with the polymer strands and also the affiliation with the catalyst particles. Wang et al. [42] formed the MEA through the electrospinning/electrospraying (E/E) technique. Table 1 shows the maximum fuel cell power output for E/E cathode. The E/E cathode loaded with the higher Pt (0.052 mg/cm^2) content revealed the higher power density of 1.090 W cm^2 (H_2/O_2). The Pt loading of 0.022 mg/cm^2 was observed at the lower power density of 0.936 W m^2. The cathode also revealed the high electrochemical surface area and inter-connected morphology for the electron conductivity in the fuel cell electrode.

Table 1 Platinum utilization of MEA with E/E cathode

Cathode	Cathode loading, mg/cm^2 Pt	Current density, W m^2
E/E	0.022	0.936
E/E	0.052	1.090

E/E Electrospinning/electrospraying; *MEA* Membrane electrode assemblies. Adapted with permission [42], Copyright (2014), Elsevier

Waldrop et al. [43] formed the electrospun nanofiber electrode using the Pt/C catalyst, Nafion, and PAA. In the Nafion solution, PAA was used as an additive to attain an inter-linked nanofiber structure. The MEA electrode was assembled using the Pt/C catalyst bond using the polymers. The variations in the Pt/C catalyst, Nafion, and PAA compositions of the electrode may enhance the H$_2$/air fuel cell power output. The cathode based on Pt/C catalyst, Nafion, and PAA have connections between the Pt/C catalyst and the Nafion/PAA matrix. Brodt et al. [44] also produced the Nafion and PAA nanofibers with the Pt/C catalyst by the electrospinning method. The cathode was assembled into the MEA. The Pt of 0.10 mg/cm^2 was loaded. The nanofibers had a well-knitted nanostructure and linked Nafion-Pt/C catalyst stricture. The nanofibers possess a high surface area and uniformly dispersed morphology. Shabani et al. [45] developed the electrospun electrode based on the poly(ether sulfone) and the Pt/C catalyst. The electrode had high proton conductivity and oxidative/hydrolytic stability. The nanofibrous electrode was used in the direct methanol fuel cell. The nanofibers had an inter-connected polymer-catalyst structure. The nanofibers have large specific surface area and fine morphology to be utilized as catalyst electrode in fuel cells.

5 Morphology and Properties of Nanocomposite Nanofibers

Electrospinning has been considered an essential method to produce nanostructured electrodes. It is the most authentic technique reported to fabricate polymeric nanofibers for fuel cell electrodes [43]. The electrode material in the PEM fuel cell has developed the percolating network to the electron conduction and the proton conduction phases. The electrospun Nafion-based electrodes have been prepared with a small amount of PEO or PVA matrices. To enhance the electron/proton conduction in the PEM electrodes, PANI has been added to the Nafion. Polyaniline is an important type of conjugated polymer used to form nanofibers. The PANI nanofibers have been processed using the electrospinning method. The PANI solution concentration defines the nanofiber formation through the electrospinning technique. The PANI nanofibers have been applied in the catalysts for the electrodes due to the large surface area, fine applicability, and interactions with the Pt [46]. The PANI nanofibers may form better contacts with the Pt/C catalyst particles. The PANI nanofiber may develop van der Waal interactions with the carbon-based catalyst. The Nafion with conducting

polymer has enhanced conductivity and electrochemical performance [47]. As an important aspect of the PEM electrodes, the morphology of the fuel cell composite has been investigated [48]. The morphology of the nanofiber electrodes has been studied using microscopic techniques such as scanning electron microscopy (SEM), field emission scanning electron microscopy, transmission electron microscopy, atomic force microscopy, scanning probe microscopy, etc. The microscopy techniques have been found more effective to reveal the nanofiber morphology, relative to the X-ray diffraction and the spectroscopic analysis. The microscopic analysis has been used to perceive the nanofiber homogeneity, size, porosity, and alignment features. Mack et al. [49] studied the electrode morphology and performance of PEM fuel cells. The interconnected microstructure of the interface between the catalyst and gas diffusion layer (GDL) of the electrodes was deliberated. The polytetrafluoroethylene (PTFE) was used as an electrode binder. Figure 3 reveals the X-ray microtomography image of the electrode. The GDL and catalyst layers were homogeneously aligned and there was no occurrence of voids between the layers. Figure 4 depicts the start-up behavior of MEA with the sprayed and coated electrodes.

The sprayed electrode revealed a higher cell voltage of 570 mV at a current density of 200 mA/cm^2. Whereas, the coated MEA had a much slower start-up and attained the voltage of 570 mV, 20 h. Simotwo et al. [50] designed the electrospun nanofibers of Nafion/polyaniline for the PEM electrode. The poly(ethylene oxide) was also added during the nanofiber formation. The electrode with the 50/50 wt.% of Nafion/PANI was formed using electrospun material. Figure 5 shows the SEM micrographs of the polyaniline nanofibers. The nanofibers have a uniform morphology and no beads in the structure. The nanofibers had a diameter of ~ 500 nm. Figure 6 reveals the SEM images of the electrospun Nafion/polyaniline-based nanofiber electrode
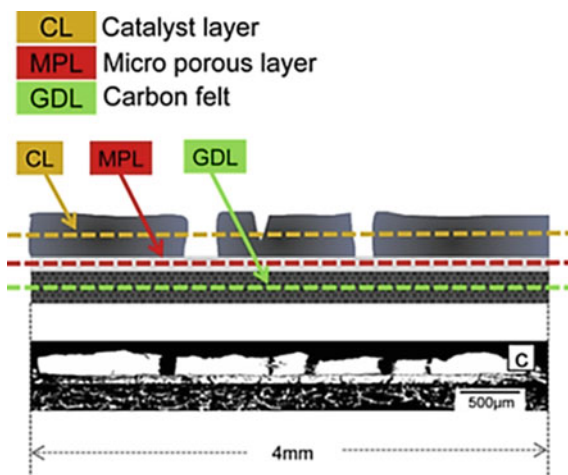
Fig. 3 X-ray micro-tomography image of the electrode. Adapted with permission from [49], Copyright (2014), Elsevier
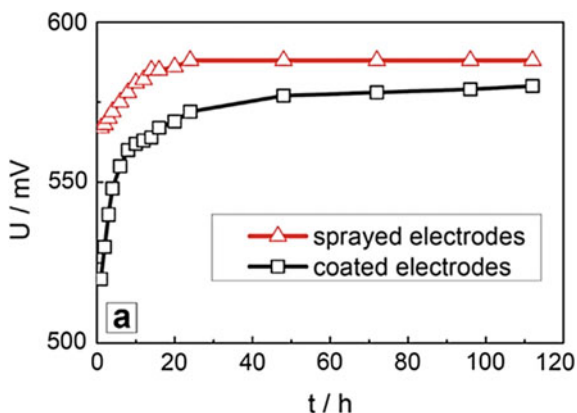
Fig. 4 Start-up behavior of MEA with sprayed and coated electrodes: **a** cell voltage of first 120 h of operation with a current density of 200 mA/cm^2. MEA = membrane electrode assemblies. Adapted with permission from [49], Copyright (2014), Elsevier
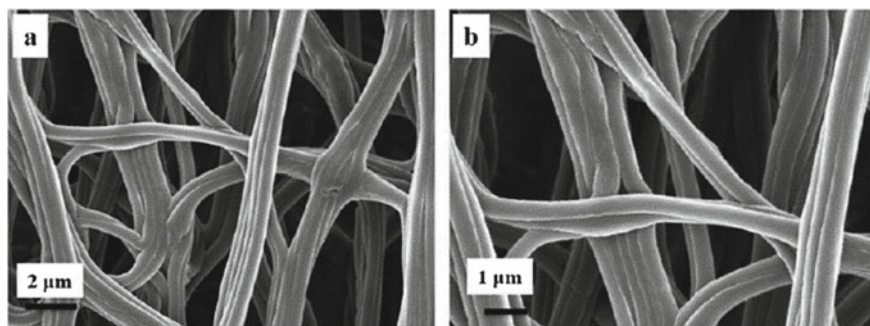
Fig. 5 SEM micrograph of as electrospun PANI. Adapted with permission from [50], Copyright (2016), Elsevier

with the annealing, the compressing, and the acid/water treatments. The nanofibers were annealed at the temperature of 150 °C. The treatments caused the densification of the nanofibers.

Consequently, the inter-fiber distance was decreased and the contact was increased. The void volume of the nanofiber was also decreased after the annealing, compressing, and chemical treatments. The nanofibers were also capable of sustaining the treatment conditions. The impedance values obtained from the Nyquist plot of the electrospun Nafion/polyaniline nanofibers indicated high protonic/electrical conductivity. Thus, the electrospun Nafion/PANI nanofibers revealed the proton conductivity of 0.0078 S/cm and the electron conductivity of 0.0046 S/cm. It was observed that the nanofibers had developed the percolating phases to act as electron/proton-conductors. The transport properties supported the role of the Nafion/PANI nanofibers as catalyst supports for the fuel cells. An important factor
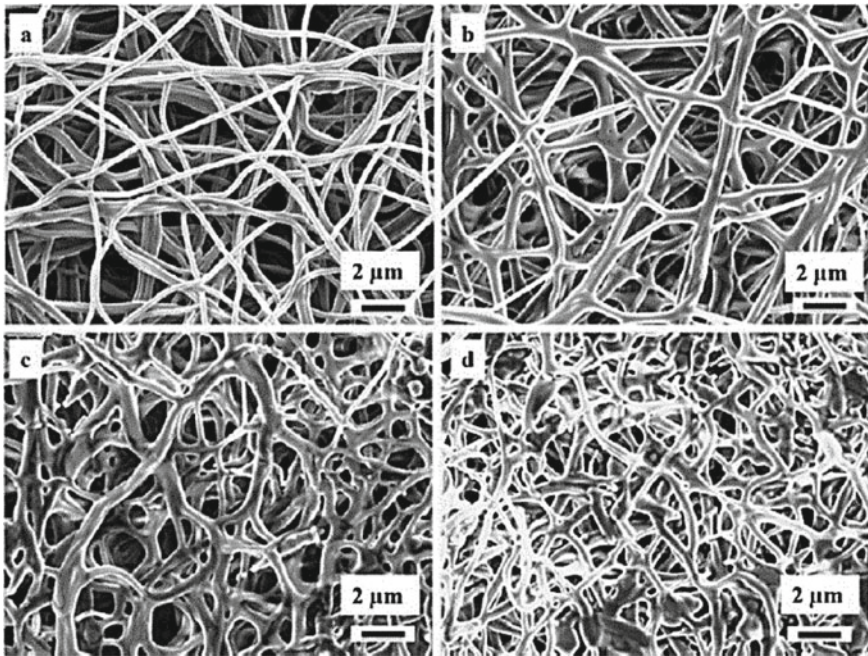
Fig. 6 SEM micrograph of **a** as electrospun Nafion/polayniline; **b** annealed Nafion/polayniline; **c** annealed/compressed Nafion/polayniline; **d** annealed, compressed, and acid/water treated Nafion/polayniline. Adapted with permission from [50], Copright (2016), Elsevier

controlling the morphology of the polymer nanofibers is the optimum high polymer concentration. The very high polymer concentration may have a non-homogeneous, beaded, and un-stable nanofiber structure and microstructure. The diameter of the fiber is also affected by the polymer solution concentration. On the other hand, the use of very low viscosity polymer solution for the polymeric nanofibers may cause nanofiber fragility and weakness. Therefore, the optimal intrinsic viscosity of the polymer solution may develop the robust nanofibers having a smooth surface, robust structure, fine polymer and solvent interactions, and homogeneous morphology of the resulting nanofibers. In this regard, the choice of the suitable solvent is essential to control the polymer solution viscosity, the nanofiber diameter, nanofiber uniformity, crystallinity, morphology, electrical conductivity, durability, and strength properties. Moreover, the polymer solution concentration not only affects the fiber morphology and texture, but also the nanofiber diameter and length. Hence, the influence of the processing factors has been observed on the morphological characteristics of the polymer and nanocomposite nanofibers including the applied voltage and distance between the syringe and the collector in the electrospinning setup. The use of very high applied voltage originates the nanofiller aggregation and bead development in the nanofiber. The bead formation in the nanofibers also brings about the formation of the non-homogeneous microstructure. Consequently, the use of optimum voltage

is desirable for nanofibers with durable, high strength, and homogeneous morphological structures. The morphology of the nanocomposite nanofibers is significantly affected by the nanofiller content. Furthermore, the electrostatic spinning speed may distress the diameter of the polymer nanofibers. The solution flow rate has been known to influence the nanofiber morphology, texture, and diameter. Besides, the optimum low nanofiller content may cause uniform dispersion and alignment in the polymer nanofiber. The uniform dispersion of the nanofillers in the nanocomposite nanofibers may lead to homogeneous morphology. On the other hand, the high nanofillers loading in the nanocomposite nanofibers may form the coarse surface and the beaded nanofibers, and so the inconsistent morphology.

6 Significance and Summary

Present exertions on carbon-supported catalysts rely on the use of polymer nanofibers for the fuel cell electrode. The morphology of the catalyst-based nanofibrous electrode is an important factor for improved fuel cell efficiency. The morphology and microstructure of the polymer nanofibers directly influence the durability and power density of the fuel cell electrodes. The morphology also affects the MEA based fuel cell parameters and the final performance. The catalyst-coated gas diffusion electrode has been formed for the MEA in the PEM fuel cell. The Pt/C catalyst has been frequently researched with polymeric nanofiber-based electrodes. Such materials have been considered as an alternative to replace the expensive Pt catalyst or electrode-based fuel cell electrodes. The nanofibrous electrodes have been usually applied as the cathode in the fuel cell MEA. Electrospinning has been deliberated as the most promising method to develop and form the polymer/catalyst particle interactions via weaving into the nanofiber electrode. The Pt-coated nanofibrous electrodes have been developed using the electrospinning technique. The coating processes such as electrospraying, solution coating, and casting methods, etc. have been used. The polymers such as Nafion, PVA, PAA, etc. have been used as binders or matrices or base material in these polymeric nanofibers. Despite Nafion, PEO, PAA, or PVA, etc. there is a range of polymers that can be used as binders or matrices for the polymeric nanofiber-based electrodes such as polystyrene, polyethylene, polypropylene, poly(methyl methacrylate), epoxy, polycarbonate, and the conducting polymers as polypyrrole, polythiophene, and polythiophene derived polymers. Moreover, the polymer blends may also be used to form the electrospun nanofibers. The cathode developed using electrospun nanofibers of 100–400 nm diameter have been found very efficient in the MEA setup. In the fuel cells, the Pt-based cathode catalyst layer may undergo severe carbon corrosion reactions. A major problem has been observed with the corrosion Pt/C catalysts supports. The corrosion of electrodes may affect the fuel cell start-up or shut-down processes. One of the advantageous use of the polymeric nanofibers-based electrodes has been the lower probability of corrosion in the MEA system. Thus, the research has revealed that the polymeric nanofiber electrodes materials may better survive the harsh motorized operating environments. The

polymeric nanocomposite nanofibers have been usually prepared with the polymer precursor having the nanofiller particles during the nanofiber processing. The dispersion of the nanofiller in the polymer solution has been a significant factor affecting the nanofiber morphology. Accordingly, the electrical, thermal, mechanical, and other essential properties of the nanocomposite nanofibers have been found enhanced relative to the neat polymeric nanofibers. Similarly, the polymeric nanocomposite nanofibers have revealed improved corrosion resistance relative to the neat polymeric nanofibers. However, the challenges remain for the development of the constantly distributed nanofiller in the nanocomposite nanofibers. Thus, focused future attempts are needed to reveal the true potential of nanocomposite nanofibers for fuel cell electrodes. Using the new design combinations and the facile production approaches may yield fine the durability, ultrahigh proton conductivity, electron conductivity, thermal stability, and mechanical properties of the nanofibrous materials.

This chapter is a transitory impression on polymer and nanocomposite nanofibers towards electrode application for fuel cells. Conducting and non-conducting polymeric nanofibers is a rapidly rising research area. The fabrication of the polymer-based nanofibers having sole structural and morphological features has been focused on. The polymer and nanocomposite nanofibers have been synthesized through many fabrication methods. Dissimilar nanofillers have been used with polymeric nanofibers. The microstructures, electrochemical properties, electrical conductivity, mechanical properties, thermal stability, power density, photovoltaic parameters, capacitance, and other physical properties of the polymeric nanofibers have pointed towards the intensified potential of these nanomaterials in the fuel cell electrodes. These nanofibers have unlocked new perspectives for high-performance energy and electronics-related advanced systems. Future development in the field of polymer nanofiber-based electrodes relies on the new design possibilities, the fabrication routes, and the processing parameter-related challenges.

References

1. Dönitz, W.: Fuel cells for mobile applications, status, requirements and future application potential. Int. J. Hydrogen Energy **23**(7), 611–615 (1998)
2. Huang, L., Zaman, S., Tian, X., Wang, Z., Fang, W., Xia, B.Y.: Advanced platinum-based oxygen reduction electrocatalysts for fuel cells. Acc. Chem. Res. **54**(2), 311–322 (2021)
3. Debe, M.K.: Electrocatalyst approaches and challenges for automotive fuel cells. Nature **486**(7401), 43–51 (2012)
4. Winther-Jensen, B., MacFarlane, D.R.: New generation, metal-free electrocatalysts for fuel cells, solar cells and water splitting. Energy Environ. Sci. **4**(8), 2790–2798 (2011)
5. Xie, J., Wang, Z., Xu, Z.J., Zhang, Q.: 'Toward a high-performance all-plastic full battery with a 'single organic polymer as both cathode and anode'. Adv. Energy Mater. **8**(21), 1703509 (2018)
6. Beregoi, M., Evanghelidis, A., Ganea, P., Iovu, H., Matei, E., Enculescu, I.: One side polyaniline coated fibers based actuator. Univ. Politeh. Bucharest Sci. Bull. Ser. B: Chem. Mater. Sci. **79**(4), 119–130 (2017)

7. Fernandes, E.G., Zucolotto, V., De Queiroz, A.A.: Electrospinning of hyperbranched poly-l-lysine/polyaniline nanofibers for application in cardiac tissue engineering. J. Macromol. Sci. Part A Pure Appl. Chem. **47**(12), 1203–1207 (2010)

8. Reynolds, J.R., Thompson, B.C., Skotheim, T.A.: Handbook of conducting polymers, 2-volume set. CRC Press (2019)

9. Su, Z., Ding, J., Wei, G.: Electrospinning: a facile technique for fabricating polymeric nanofibers doped with carbon nanotubes and metallic nanoparticles for sensor applications. RSC Adv. **4**(94), 52598–52610 (2014)

10. Narayanunni, V., Gu, H., Yu, C.: Monte Carlo simulation for investigating influence of junction and nanofiber properties on electrical conductivity of segregated-network nanocomposites. Acta Mater. **59**(11), 4548–4555 (2011)

11. Shinde, S.S., Kher, J.A.: A review on polyaniline and its noble metal composites. Int. J. Innov. Res. Sci. Eng. Technol. **3**, 16570–16576 (2014)

12. Zhu, Y., Li, J., Wan, M., Jiang, L.: Superhydrophobic 3D microstructures assembled from 1D nanofibers of polyaniline. Macromol. Rapid Commun. **29**(3), 239–243 (2008)

13. Kim, B., Koncar, V., Dufour, C.: Polyaniline-coated PET conductive yarns: study of electrical, mechanical, and electro-mechanical properties. J. Appl. Polym. Sci. **101**(3), 1252–1256 (2006)

14. Kausar, A.: Conducting polymer-based nanocomposites: fundamentals and applications. Elsevier (2021)

15. Chaudhari, S., Sharma, Y., Archana, P.S., Jose, R., Ramakrishna, S., Mhaisalkar, S., Srinivasan, M.: Electrospun polyaniline nanofibers web electrodes for supercapacitors. J. Appl. Polym. Sci. **129**(4), 1660–1668 (2013)

16. Neelakandan, R., Madhusoothanan, M.: Electrical resistivity studies on polyaniline coated polyester fabrics. J. Eng. Fibers Fabrics **5**(3), 155892501000500304 (2010)

17. Trivedi, D.C., Dhawan, S.K.: Shielding of electromagnetic interference using polyaniline. Synth. Met. **59**(2), 267–272 (1993)

18. Trivedi, D.C., Dhawan, S.K.: Antistatic applications of conducting polyaniline. Polym. Adv. Technol. **4**(5), 335–340 (1993)

19. Aliheidari, N., Aliahmad, N., Agarwal, M., Dalir, H.: Electrospun nanofibers for label-free sensor applications. Sensors **19**(16), 3587 (2019)

20. Laforgue, A., Robitaille, L.: Fabrication of poly-3-hexylthiophene/polyethylene oxide nanofibers using electrospinning. Synth. Met. **158**(14), 577–584 (2008)

21. Nayak, R., Padhye, R., Kyratzis, I.L., Truong, Y.B., Arnold, L.: Recent advances in nanofibre fabrication techniques. Text. Res. J. **82**(2), 129–147 (2012)

22. Huang, Z.-M., Zhang, Y.-Z., Kotaki, M., Ramakrishna, S.: A review on polymer nanofibers by electrospinning and their applications in nanocomposites. Compos. Sci. Technol. **63**(15), 2223–2253 (2003)

23. Pan, H., Li, L., Hu, L., Cui, X.: Continuous aligned polymer fibers produced by a modified electrospinning method. Polymer **47**(14), 4901–4904 (2006)

24. Long, Y.-Z., Li, M.-M., Gu, C., Wan, M., Duvail, J.-L., Liu, Z., Fan, Z.: Recent advances in synthesis, physical properties and applications of conducting polymer nanotubes and nanofibers. Prog. Polym. Sci. **36**(10), 1415–1442 (2011)

25. Frenot, A., Chronakis, I.S.: Polymer nanofibers assembled by electrospinning. Curr. Opin. Colloid Interface Sci. **8**(1), 64–75 (2003)

26. Junkasem, J., Rujiravanit, R., Supaphol, P.: Fabrication of α-chitin whisker-reinforced poly (vinyl alcohol) nanocomposite nanofibres by electrospinning. Nanotechnology **17**(17), 4519 (2006)

27. Gupta, C., Maheshwari, P.H., Dhakate, S.R.: Development of multiwalled carbon nanotubes platinum nanocomposite as efficient PEM fuel cell catalyst. Mater. Renew. Sustain. Energy **5**(1), 2 (2016)

28. Bao, Q., Zhang, H., Yang, J.x., Wang, S., Tang, D.Y., Jose, R., Ramakrishna, S., Lim, C.T., Loh, K.P.: Graphene–polymer nanofiber membrane for ultrafast photonics. Adv. Funct. Mater. **20**(5), 782–791 (2010)

29. Abdah, M.A.A.M., Zubair, N.A., Azman, N.H.N., Sulaiman, Y.: Fabrication of PEDOT coated PVA-GO nanofiber for supercapacitor. Mater. Chem. Phys. **192**, 161–169 (2017)
30. Mohamed, I.M., Yasin, A.S., Barakat, N.A., Song, S.A., Lee, H.E., Kim, S.S.: Electrocatalytic behavior of a nanocomposite of Ni/Pd supported by carbonized PVA nanofibers towards formic acid, ethanol and urea oxidation: a physicochemical and electro-analysis study. Appl. Surf. Sci. **435**, 122–129 (2018)
31. Hart, D.: Sustainable energy conversion: fuel cells—the competitive option? J. Power Sources **86**(1–2), 23–27 (2000)
32. Kundu, P., Sharma, V., Shul, Y.G.: Composites of proton-conducting polymer electrolyte membrane in direct methanol fuel cells. Crit. Rev. Solid State Mater. Sci. **32**(1–2), 51–66 (2007)
33. Thompson, S.T., Papageorgopoulos, D.: Platinum group metal-free catalysts boost cost competitiveness of fuel cell vehicles. Nat. Catal. **2**(7), 558–561 (2019)
34. Kim, J.R., Premier, G.C., Hawkes, F.R., Dinsdale, R.M., Guwy, A.J.: Development of a tubular microbial fuel cell (MFC) employing a membrane electrode assembly cathode. J. Power Sources **187**(2), 393–399 (2009)
35. Park, S., Popov, B.N.: Effect of a GDL based on carbon paper or carbon cloth on PEM fuel cell performance. Fuel **90**(1), 436–440 (2011)
36. Tan, S., Huang, X., Wu, B.: Some fascinating phenomena in electrospinning processes and applications of electrospun nanofibers. Polym. Int. **56**(11), 1330–1339 (2007)
37. Choi, J., Wycisk, R., Zhang, W., Pintauro, P.N., Lee, K.M., Mather, P.T.: High conductivity perfluorosulfonic acid nanofiber composite fuel-cell membranes. Chemsuschem **3**(11), 1245–1248 (2010)
38. Fumagalli, M., Lyonnard, S., Prajapati, G., Berrod, Q., Porcar, L., Guillermo, A., Gebel, G.: Fast water diffusion and long-term polymer reorganization during Nafion membrane hydration evidenced by time-resolved small-angle neutron scattering. J. Phys. Chem. B **119**(23), 7068–7076 (2015)
39. Chen, H., Snyder, J.D., Elabd, Y.A.: Electrospinning and solution properties of Nafion and poly (acrylic acid). Macromolecules **41**(1), 128–135 (2008)
40. Cho, Y.-H., Jeon, T.-Y., Yoo, S.J., Lee, K.-S., Ahn, M., Kim, O.-H., Cho, Y.-H., Lim, J.W., Jung, N., Yoon, W.-S.: Stability characteristics of Pt1Ni1/C as cathode catalysts in membrane electrode assembly of polymer electrolyte membrane fuel cell. Electrochim. Acta **59**, 264–269 (2012)
41. Zhang, W., Pintauro, P.N.: High-performance nanofiber fuel cell electrodes. Chemsuschem **4**(12), 1753–1757 (2011)
42. Wang, X., Richey, F.W., Wujcik, K.H., Elabd, Y.A.: Ultra-low platinum loadings in polymer electrolyte membrane fuel cell electrodes fabricated via simultaneous electrospinning/electrospraying method. J. Power Sources **264**, 42–48 (2014)
43. Waldrop, K., Wycisk, R., Pintauro, P.N.: Application of electrospinning for the fabrication of proton-exchange membrane fuel cell electrodes. Curr. Opin. Electrochem. **21**, 257–264 (2020)
44. Brodt, M., Han, T., Dale, N., Niangar, E., Wycisk, R., Pintauro, P.: Fabrication, in-situ performance, and durability of nanofiber fuel cell electrodes. J. Electrochem. Soc. **162**(1), F84 (2014)
45. Shabani, I., Hasani-Sadrabadi, M.M., Haddadi-Asl, V., Soleimani, M.: Nanofiber-based polyelectrolytes as novel membranes for fuel cell applications. J. Membr. Sci. **368**(1–2), 233–240 (2011)
46. Ghosh, S., Das, S., Mosquera, M.E.: Conducting polymer-based nanohybrids for fuel cell application. Polymers **12**(12), 2993 (2020)
47. Yusoff, Y.N., Shaari, N.: An overview on the development of nanofiber-based as polymer electrolyte membrane and electrocatalyst in fuel cell application. Int. J. Energy Res. **45**(13), 18441–18472 (2021)
48. Litster, S., Epting, W., Wargo, E., Kalidindi, S., Kumbur, E.: Morphological analyses of polymer electrolyte fuel cell electrodes with nano-scale computed tomography imaging. Fuel Cells **13**(5), 935–945 (2013)

49. Mack, F., Klages, M., Scholta, J., Jörissen, L., Morawietz, T., Hiesgen, R., Kramer, D., Zeis, R.: Morphology studies on high-temperature polymer electrolyte membrane fuel cell electrodes. J. Power Sources **255**, 431–438 (2014)
50. Simotwo, S.K., Kalra, V.: Study of co-electrospun nafion and polyaniline nanofibers as potential catalyst support for fuel cell electrodes. Electrochim. Acta **198**, 156–164 (2016)

Conjugated Polymers as Organic Electrodes for Batteries

Mandira Majumder, Anukul K. Thakur, Archana S. Patole, and Shashikant P. Patole

Abstract Attributed to various causes it is now established that organic matter-based electrodes possess the potential for further improvement in the existing battery technologies while creating novel playgrounds to generate ground-breaking cell configurations. Conjugated polymers (CPs) are characterized as redox-active organic materials exhibiting comparatively high electronic conductivity (as compared to the traditional polymers with insulating properties), superior flexibility, and high electrochemical stability. Credited to these advantages, growing research interest has been recently fixated on the implementation of CPs as potential high-performance organic electrodes for rechargeable batteries. The characteristics of CPs can be tuned through structural modification and incorporation of different functional moieties. With the aid of novel design strategies and core investigations, CPs garner attention as future potential candidates for rechargeable metal-ion batteries as well as for hydronium and proton batteries. To design CPs that can be electrodes for practical applications, it is therefore largely necessary to carry out further extensive investigations on the losses associated with hysteresis as well as the polarization effect of CP nanostructures. This chapter extends a detailed realization of the current state of the organic electrodes for rechargeable batteries. Also, it describes the existing challenges in the field and their possible mitigation strategies. Finally, the chapter highlights some recent remarkable works on the field and ends with a conclusive note about the future possible direction of the research in the field.

Keywords Organic material · Electrodes · Batteries · Conducting polymers · Energy density

1 Introduction

Current progress in electronics with mobility, transportation, and communication systems makes it mandatory to bring up more efficient energy storage modes

M. Majumder · A. K. Thakur · A. S. Patole · S. P. Patole (✉)
Applied Quantum Materials Laboratory (AQML), Department of Physics, Khalifa University of Science and Technology, P. O. Box 127788, Abu Dhabi, United Arab Emirates
e-mail: shashikant.patole@ku.ac.ae

exhibiting large power and energy density. Attributed to the superior characteristics, lithium-ion batteries (LIBs) have gained popularity as commercial energy storage devices [1, 2]. Commercially implemented anodes usually comprise graphite, on the other hand, cathodes comprise lithium metal oxide; electrolytes implemented are a mixture of organic solvents containing lithium salts. Even though currently these materials are used as the most efficient and powerful batteries commercially, they are not yet adequately powerful and exhibit significant drawbacks [3, 4]. The major disadvantage associated with the cathode materials based on intercalation mechanism is prevailing single electron transfer reaction as the only reaction path leading to significant restriction in the maximum attainable charge storage capacity with the commercially possible circumstances around 200 mAh g^{-1}. This limited value of charge storage capacity makes it difficult to fabricate cathode materials having a considerably larger capacity. The manufacture and fabrication of batteries result in the generation of several kinds of hazardous materials and pollutants, including toxic fluoride gases, various carbon and metal dust, together with an excess amount of solid waste, which can result in severe environmental issues including land, air, and water pollution, hazards in the workplace, etc. [3, 5].

In the last few decades, amongst various potential materials researchers have seen the emergence of organic material as a promising candidate that can be implemented as the electrode material in the next generation supercapacitors and batteries [6–8]. Organic materials have various pros as compared to inorganic electrode materials. To discuss a few: (1) Usually, organic materials are cost-effective and available in large quantities in nature; (2) The various electrochemical properties including theoretical charge storage, redox potential, and capacity are easily tunable by altering the structure which is way more difficult in the matter of inorganic materials; (3) The versatility of the organic electrode materials electrochemically active to lithium and other metals including sodium, zinc, magnesium, etc., making it possible to implement the same electrode material in different battery chemistries. Furthermore, a major number of the inorganic electrode materials can carry out reactions involving single electron transfer only, however, organic materials normally are associated with reactions involving multiple electrons [7, 9–11].

Conjugated polymers (CPs) are the materials of prime interest in several applications credited to their unique and striking assets including the large surface area which can result in a larger number of active sites serving as active spots for chemical reactions, an increased number of connected or non-connected channels those may expose the buried active sites to interact with the electrolyte. Amongst the various families of materials conjugated polymers have garnered attention in the past few decades attributed to various unique properties including the presence of π-conjugated skeleton, presence of covalently bonded organic materials [12–14]. Characteristics such as expanded π-conjugated systems, homogeneously distributed micropores, enhanced thermal as well as chemical stability, successful functionalization incorporating various organic moieties, tunable physical properties, and high surface area make them promising. In addition, CPs can be articulated in a spectrum of architecture, including three-dimensional networks, two-dimensional dendrimers, and branched networks [15–17].

2 Fundamentals of Organic Electrode

The development of the organic electrode material started with the implementation of dichloroisocyanuric acid as the cathode material back in the late 1960s in rechargeable lithium batteries. Since its discovery, different kinds of organic materials have been investigated as electrode materials to be implemented as material in energy storage. The initial research phase was concerned with studying the electroactive materials as electrode material and relating the active center's role in improving the electrochemical charge storage properties. Several organic molecules derived materials that possess a similar type of redox-active centers were investigated having similar characteristics as the organic materials [18, 19].

There are different types of organic materials including bipolar, p- or n-type classified according to the charge states during redox reactions. A material with p-type is formed when an electrochemically active polymer structure is extracted with one electron at an initial neutral state, which creates a positive charge in the material. A neutral state is reached by a p-type polymer by oxidation followed by reversible reduction. This indicates that for p-type materials as electrode material the first step should be charging followed by discharging. However, in the case of an n-type material, which can accept an electron to become charged negatively from the initial neutral state accompanied by reversible oxidation resulting in neutralization back, discharge occurs first [20, 21].

The bipolar materials are known to exist in both positive as well as negatively charged states, and so they can get discharged or charged starting from the neutral position creating two distinguishable redox potentials. Organic materials possess a redox potential higher than 2.0 V versus Li/Li^+ which is why organic materials are normally implemented as positive electrodes. Exceptions are a series of terephthalate groups of materials. A cathode is mainly made up of p-type materials in batteries as their redox potentials are normally larger than those of n-type materials. The kinetics of redox reactions are rapid in the case of the p-type materials as compared to those of n-type materials. Nevertheless, one of the drawbacks is the inactiveness of most of the mass and hence their capacity is less [6–10, 22, 23].

3 Conjugated Polymers

CPs are macromolecules comprising of organic composition and are characterized by a backbone of a chain comprising of double and single-bonds in an alternating fashion. The overlapping *p*-orbitals leads to delocalized π-electrons which helps in charge conduction rendering CPs more conducting as compared to the conventional polymers. In the 1980s, CPs were praised to have promising aspects for advanced batteries with eco-friendliness and efficiency. In the case of the CPs, the unique electrical property comes from the overlapping of neighboring π-orbitals creating a band-like structure as possessed by the inorganic semiconductors. Their conductivity

is largely affected by the type of doping, which is caused due to charging and produces anions and cations which become delocalized along the backbone of the polymer [24–26]. Even though the intrinsic conductivity of these CPs are considered to be advantageous, however, attributed to the intrinsic connection between the redox centers and the current collector there exists a major drawback also. The lack of physical and electronic separation between the charged centers and the current collectors results in strong interaction between them causing the influence of the redox potentials of CPs on the doping level and eventually changes with the charging/discharging.

Typically, CPs are synthesized through electrochemical or chemical methods. Conventional chemical synthesis comprises addition and condensation polymerization, providing different effective and accessible paths to prepare a broad range of CPs. Electrochemical synthesis generally is performed in a three-electrode system comprising of a counter (CE), working (WE) and reference electrodes (RE) inserted in a solution consisting of a mixture of monomer, solvent, and electrolyte. CPs get deposited on the surface of the WE along with the passage of the current through the solution. As compared to the conventional chemical synthesis, electrochemical synthesis is preferred as an alternative for the synthesis of CPs in terms of its simplicity and reproducibility together with the production of various novel CPs having complex structures or modified monomers [25, 27, 28].

4 Conjugated Polymers in Batteries as Electrode Materials

Past few decades the redox-active CPs have been used as materials to fabricate electrodes in rechargeable batteries [26]. Han et al. for the first time implemented CP derived from a carbonyl as cathode material in LIBs in 2007 [29]. Significantly, a report by Jiang et al. is considered as the pioneering direct report regarding the direct implementation of CPs in energy storage [30]. In recent times various novel reports regarding CPs' energy storage characteristics especially in various batteries, were introduced. Based on the groups exhibiting redox activeness, CPs can be implemented as an anode as well as cathode material. Similarly, if CPs behave well when implemented as LIBs electrode material, there is a strong likelihood that they will also exhibit good performance in sodium, sulfur, potassium, zinc, magnesium, and other ion batteries, as well. We will emphasize all types of batteries implementing CPs as the electrode material. A major part of research in CP-based electrodes implemented in batteries has focused on the implementation of polyaniline, polypyrrole, polyindole, and polythiophene as the active material [31, 32]. Outline of the stated active materials and their various characteristics are provided in Table 1 [29, 33–47].

Table 1 Overview of conjugated polymers applied as active material in batteries

Material	Battery type	Capacity (mAh/g)	References
Perylene-3,4,9,10 tetracarboxylic dianhydride	Li-ion	120–130	[29]
Anthraquinone-based	Li-ion	130–149	[33]
Poly(3,3′-bithiophene) (as anode)	Li-ion	1215	[34]
cp(S-PMAT) copolymer	Li-sulfur	880	[35]
Sulfur-polypyrrole	Li-sulfur	600–900	[36]
Tubular polypyrrole	Li-sulfur	1151	[37]
Polypyrrole-MnO$_2$	Li-sulfur	1000	[38]
Triazine-trithiophene triacetylenicbenzene	Li-sulfur	1350	[39]
Tetraamino-benzoquinone	SIB	450	[40]
PYT-TABQ/graphene	SIB	245	[41]
Polyimides	SIB	500	[42]
Polypyrrole hollow nanospheres	SIB	320	[43]
Poly(aniline-co aminobenzenesulfonic sodium)	SIB	133	[44]
Poly(pyrene-cobenzothiadiazole)	PIB	428	[45]
KHCF@PPy	PIB	88.9	[46]
Polyimide (PI) and polyquinoneimide (PQI)	PIB	158	[47]

5 Conjugated Polymers Used in Different Batteries

To address the crisis of energy and environmental issues, sustainable and clean energy modes have been investigated, including solar cells, fuel cells, and rechargeable batteries. Presently, LIBs control the mobile electronic market attributed to the large energy density.

5.1 Lithium-Ion Battery

Han et al. for the first time reported CP derived from a carbonyl as a cathode in LIBs in 2007 implemented in energy storage [29]. Perylenetetracarboxylicacid-dianhydride (PTCDA) polymers exhibited promising aspects as organic positive-electrode material delivering both large capacity and long cycle life. As observed from the potential profiles, the PTCDA and the polymers exhibited similar kinds of electrochemical properties during the initial cycle, exhibiting the same discharge charge platforms and charge platforms with capacities of ~ 120–130 mAh/g with efficiencies > 98%. According to these results both the electrode materials act similarly related to the charge/discharge process, and PTCDAs play the role of an active center allowing Li-ion intercalation/de-intercalation. According to the discharge profile of PTCDA it undergoes a two-stage discharge process. In the first stage, for each molecule, two

Li ions were intercalated at the potential range from 2.3 to 2.5 V. However, at the second stage the intercalation of the other two Li-ions takes place in the potential range from 0.9 to 1.3 V.

Molina et al. [33] implemented anthracenedione -based microporous polymers in the presence of carbon nanostructures to be used as electrode material (Fig. 1a). They have reported an effective approach enabling hybrid electrodes with 60 mg/cm^2 of mass-loading containing 20 wt% carbon. So, the designed electrode material could reach high rate capability, 83.7 mAh/g of gravimetric capacity, and large areal capacity i.e. 6.3 mAh/cm^2, together with > 80% of capacity retention. As far as our knowledge, these are the highest values reported so far for similar kinds of organic batteries. In another report, IEP-11-S5R5@S10 electrode based on bucky paper with ~ 15 mg/cm^2 of mass loading delivers 89 mAh/g of capacity at 1C. This result again indicated that higher mass loading leads to higher capacity value, as represented in Fig. 1b and c. It is noteworthy that, the capacity value obtained is sevenfold larger as compared to an alike bucky paper electrode. Electrochemical property determination corresponding to the electrodes implementing polymer synthesized without carbon additives and S5R5@ S10 associated with various mass loads was done implementing
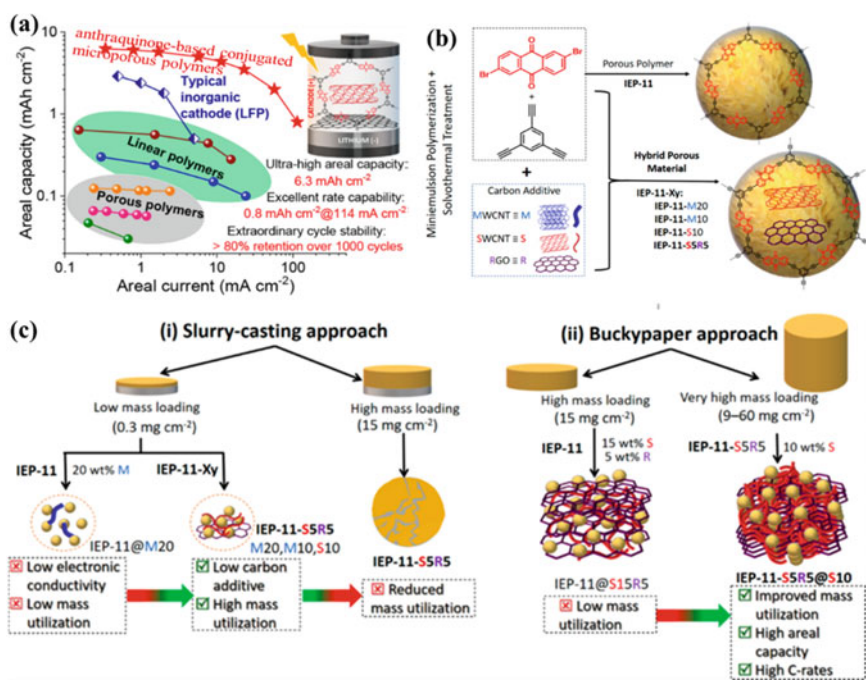
Fig. 1 a Schematic representation of the area capacity versus areal current for various polymer. b Schematic illustration corresponding to the production pathways for IEP-11 and IEP-11-Xy polymer c implemented electrode fabrication methods to result in low and high mass loaded electrodes. Adapted with permission from Ref. [33], Copyright (2020), American Chemical Society

charging-discharging measurements at various C-rates. The areal/gravimetric capacities corresponding to the different active material loading of IEP-11-S5R5@S10 electrodes at C-rate of 0.03C were noted. For electrodes with mass loadings of < 30 mg/cm^2 a theoretical gravimetric capacity of ~ 149 mAh/g could be attained. Additionally, with normalization of the capacity by the electrode area the designing of electrodes was possible having considerably large thickness with a loading of 60 mg/cm^2 and an areal capacity of 6.3 mAh/cm^2. The dependency of the development of areal capacity on the mass loading in the range of 0.2–16.0 mg/cm^2 was almost linear. However, a divergence from the linear nature was observed above the 16.0 mg/cm^2 of mass loading.

Similarly, Zhang et al. [34], demonstrated the synthesis of n-doped poly(thiophene) showing reversible redox characteristics when tested as an anode material in LIB. The poly(3,3′-bithiophene) including a significant number of crosslinked structures provided 696 m^2/g of surface area. The capacity was calculated to be 1215 mAh/g at 45 mA/g, accompanied by remarkable cycling stability and good rate capability corresponding to a capacity retention of 663 mAh/g at 500 mA/g over 1000 cycles.

5.2 Lithium-Sulfur Battery

From the point of view of constrained raw materials and energy resources, energy-storage systems have garnered very wide interest including batteries specifically being the most prominent energy storage mode. The feasibility of a battery-based concept firmly varies following a few issues: (i) device safety, (ii) fair cycling stability, and (iii) large energy density. Lithium and sulfur are amongst the most viable elements that can be implemented for the upcoming advanced batteries due to the large theoretical capacity corresponding to double electron transfer: S + 2e$^-$ → S^{2-} (1672 mAh/g). This energy density shoots an even higher value of 2600 Wh/kg with lithium (2 Li → 2 Li$^+$ + 2e$^-$). According to a report by Zeng et al. [35], copolymerized sulfur in presence of poly(m-aminothiophenol) (PMAT) nanoplates by the means of inverse vulcanization result in significantly crosslinked copolymer (Fig. 2a–c). In the synthesized materials the content of sulfur was ~ 80 wt% which formed chemical bonds with the thiol moieties belonging to the PMAT. A cp(S-PMAT)/C-implemented cathode exhibited 1240 mAh/g of capacity accompanied by rate capacities corresponding to 600 mAh/g at 5C and 880 mAh/g at 1C. 495 mAh/g was the capacity value over 1000 cycles at 2C corresponding to retention of 66.9% with 0.040% per cycle of the decay rate.

Fu et al. [36], designed a composite consisting of sulfur and polypyrrole exhibiting a core–shell geometry with polypyrrole coated spherical sulfur particles. The fundamental sulfur was synthesized by sodium thiosulfate reduction with the help of p-toluenesulfonic acid, as represented in Fig. 2d. Protons on pTSA are provided by sulfonic acid while creating micelles for nucleation of sulfur acting as an anionic surfactant. Figure 2e represents the initial three CV profiles of the cell representing
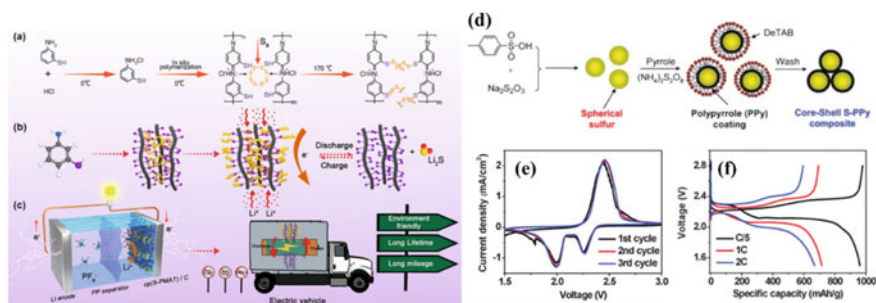
Fig. 2 **a** Schematic representation of the synthesis corresponding to the copolymer. **b** The representation related to the structural evolution for the formation of cp(S-PMAT) and discharge/charge process. **c** Device configuration associated with lithium-sulfur battery implemented with cp(S-PMAT) cathode material. Adapted with permission from Ref. [35], Copyright (2017), Wiley–VCH. **d** Scheme for the synthetic approach related to the core–shell sulfur polypyrrole composites. **e** Initial cyclic voltammograms corresponding to the sulfur polypyrrole composite. **f** Initial discharge/charge voltage vs. discharge profiles. Adapted with permission from Ref. [36], Copyright (2012), Royal Society of Chemistry

two distinct peaks at 2.1 and 2.4 V. Figure 2f represents the initial charge and discharge voltage profiles vs. gravimetric capacities corresponding to the rates of 2C, 1C, and C/5. Both the plateaus in the discharge regions are due to the peaks in the CVs. The initial capacity is 900 mAh/g @C/5 whereas, the capacities at large rates fall to 600 mAh/g.

5.3 Sodium-Ion Battery

Due to the large availability of raw materials, low cost, and better safety of sodium resources, rechargeable sodium-ion batteries (SIBs) have projected themselves as attractive electrochemical energy storage system. Attributed to the similarity of physiochemical properties of lithium and sodium, the selection of electrode materials and the energy storage chemistry for organic SIBs is quite like that of the Li-ion batteries. SIBs are challenged by many disadvantages attributed to the existence of the larger ionic radius of Na^+ as compared to that of Li^+, resulting in more strain along with ion insertion/extraction process, resulting in the breakdown of the inflexible 3D framework comprising of the inorganic electrode materials. As redox reactions are mainly responsible for the charge storage in the organic electrode materials instead of the intercalation mechanism, these materials refrain from any structural damage in case of the large cationic size. Organic electrode materials are characterized by an immense number of redox-active sites and so they are expected to hold a large number of sodium ions. Branched conjugated polymers (BCPs) are observed to possess various rewards including the extended conjugated skeleton, stability in most of the electrolytes, enhanced flexibility, and processability. The branched structures

of BCPs allow easy electrolyte infiltration and ionic transport and result in superior rate performance as compared to the other electrode Fig. 3a. As reported by Xu et al. [40], two conjugated polymers with similar building units (Fig. 3a) were synthesized by rational molecular design. Amongst the polymers, one was a linear conjugated polymer and the other polymer was a BCP. Both of them comprised adequate carbonyl groups and C=N groups. When tested as anodes in SIBs, both the polymers displayed very good Na-storage performance corresponding to capacity of ~ 420 and ~ 450 mAh/g at 0.1 A/g, as shown in Fig. 3b and c. As reported by Chen et al. [41] novel conjugated polymer possessing ladder-like architecture was applied as electrode material for organic SIBs. The polymer/graphene composites could attain a high specific capacity of ~ 245 mAh/g at 0.2 A/g together with an excellent rate performance and cycle stabilities greater than 1400 cycles associated with 98% of capacity retention. In the work, a ladder-like heterocyclic aza-fused poly(quinone) has been synthesized and it has been implemented as electrode material in SIBs. The stability and the rate performance adequately increased as a result of the incorporation of reduced graphene oxide as conductive additives. Organic carbonyl compounds projects themselves as prospective electrode materials as electrode materials for SIBs attributed to their unique positive sides, including redox stability lightweight, earth abundance, and multi-electron reactions. Li et al. [42] implemented two commercial dianhydrides (Fig. 3d) known as naphthalene-1,4,5,8-tetracarboxylic dianhydride (NTCDA) and pyromellitic dianhydride (PMDA) acting as the building units to be polymerized with melamine resulting in dianhydride based
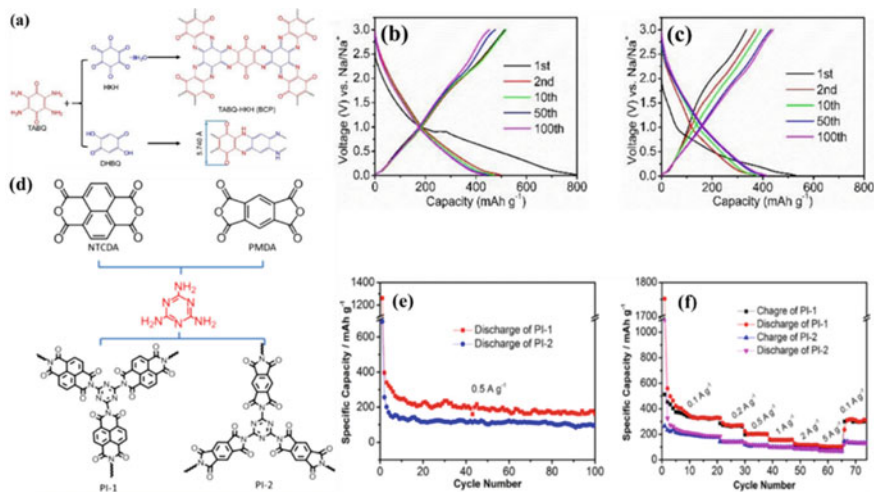
Fig. 3 a The molecular structures and synthesis approach of the fabricated BCP and LCP, and voltage profiled corresponding to the **b** BCP anode and **c** LCP anode. Adapted with permission from Ref. [40], Copyright (2020), Royal Society of Chemistry. **d** Schematic diagram representing the synthesis approach corresponding to the polyimides, **e** Cyclic voltammetry plots at 500 mA/g, **f** rate performance at various current densities. Adapted with permission from Ref. [42], Copyright (2016), Elsevier

polyimides (PIs). It was reported that the cross-linked polymer represents excellent stability and rate capacity corresponding to the capacity of 88.8 mAh/g at 5.0 A/g over 1000 cycles, which renders this material as a promising candidate as electrode material for high-performance SIB (Fig. 3e and f). The capacity of PI-1 was maintained at ~ 176 mAh/g over 100 consecutive voltage cycles at 500 mA/g.

Su et al. [43] reported the synthesis of polypyrrole nanospheres implementing doping using acrylic as templates. The authors reported a large Na storage capacity associated with PPy hollow-nanosphere electrode corresponding to a value 97 mAh/g at 20 mA/g maintaining a capacity of 85 mAh/g over 100 cycles along with stable rate capability.

5.4 Potassium-Ion Battery

Potassium behaves physicochemically and electrochemically in a similar manner to other group elements including lithium and sodium. For instance, electrode potentials *vs.* standard hydrogen electrodes of Li/Li⁺, Na/Na⁺ and K/K⁺ only have very small variations. In comparison with Li, Na and K resources are much more available and are distributed more evenly as compared to Li. As a consequence, SIBs, and potassium-ion batteries (PIBs) have garnered much attention as the most promising alternatives of LIBs. Considering the above-mentioned advantages, research-based on PIBs are gradually emerged and developed in recent years. Table 2 enlists various properties of Li, Na, and K [48].

In addition, the incorporation of PBAs together with different conductive materials has also been implemented to enhance the rate capability and cycle life of the materials in PIBs. Chen et al. [46] investigated polypyrrole incorporated PIB material (KHCF@PPy) integrated through an in-situ polymerization coating approach (Fig. 4a). Several nano cubic structures comprising smooth surfaces were formed in

Table 2 Various assets of the Li, Na, and K

Properties	Li	Na	K
Atomic number	3	11	19
Atomic mass (u)	6.941	22.9898	39.0983
Atomic radius (pm)	145	180	220
Covalent radius (pm)	128	166	203
Melting point (°C)	180.54	97.72	63.38
Crust abundance (mass %)	0.0017	2.3	1.5
Crust abundance (molar %)	0.005	2.1	0.78
Voltage versus S.H.E (V)	−3.04	−2.71	−2.93
Cost of carbonate (US$ t^{-1})	23,000	200	1000
Cost of industrial grade metal (US$ t^{-1})	100,000	3000	13,000
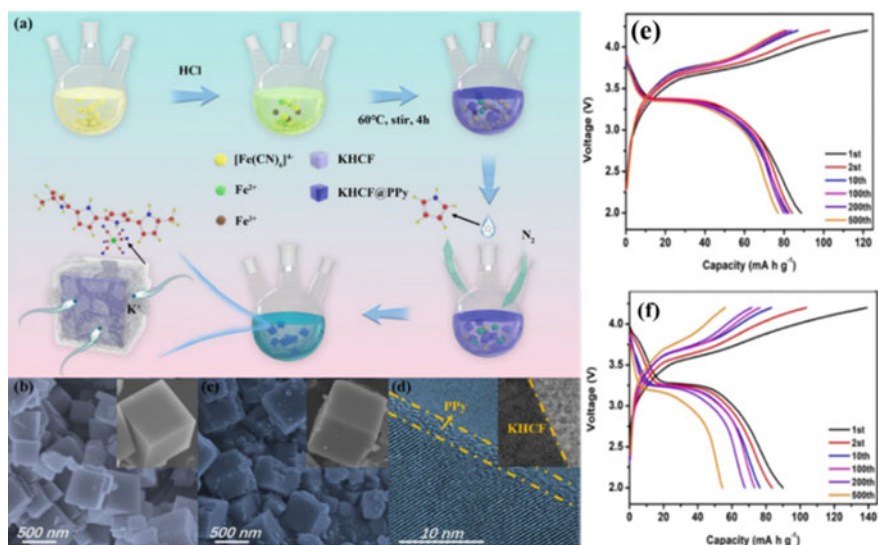
Fig. 4 **a** Illustration of the synthesis approach; **b** SEM of pristine Prussian blue **c** and polypyrrole-modified Prussian blue material **d** TEM micrographs corresponding to polypyrrole-modified Prussian blue and modified Prussian blue (inset of **d**), charge/discharge plots corresponding to **e** KHCF@PPy and **f** KHCF at different cycles. Adapted with permission from Ref. [46], Copyright (2019), American Chemical Society

the pristine KHCF. The size of the edges lies between 500 and 700 nm (Fig. 4b). The polypyrrole-coated KHCF had coarse surfaces as compared to that of pristine KHCF and also showed a small extent of aggregations of PPy on the surfaces (Fig. 4c). The high-resolution TEM micrographs confirmed the existence of a coat of PPy layer on the surface of KHCF. Compared to the pure crystalline KHCF (inset Fig. 4d), Fig. 4d showed that the edges of KHCF@PPy are characterized by a uniform, thin amorphous layer identified as homogeneous PPy coating. PPy was responsible for the improvement in the conductivity and minimized the defect concentration within the composites, reaching a discharge capacity of 88.9 mAh/g at 50 mA/g (Fig. 4e and f) along with an improved cyclability. As the current density increased to 1000 mA/g, initial capacity was maintained at ~ 72 mAh/g which corresponded to almost 85.7% retention over 500 cycles.

Tian et al. [47] reported the synthesis of a family of carbonyl-based organic polymers including two 1D polymers viz., polyquinoneimide (PQI) and polyimide (PI) and a 2D conjugated polymer (PI-CMP). These polymers were implemented as stable organic cathode materials for PIBs. For instance, the immediate relation of electrochemical active organic molecules can enhance the capacity, however, the compressed distribution of potassiated carbonyl moiety could be responsible for fast capacity degradation. Furthermore, the expanded π-conjugation can enhance the cycling stability and the rate capability. These investigations could highlight the

commercial ways to design high-output organic cathode materials and indicate future research direction of the PIBs for large-scale applications.

5.5 Zinc-Ion Battery

In the present day, zinc-ion batteries (ZIBs) have garnered broad attention as a capable alternate mode to the traditional storage modes. The abundantly available Zn metal which is used as the anode material for ZIBs can be extracted with less expense. Also, the anode implemented with Zn exhibits large theoretical capacity, enhanced ability as antioxidant, less redox potential. Furthermore, electrode implemented with Zn is compatible with a wide range of aqueous electrolyte so ZIBs exhibits unique flexibility, safety, and eco-friendliness. Currently, several cathodes including organic compounds and manganese-based composites have been tested for the capacity corresponding to Zn^{2+} storage. Unlike the above electrode materials, CPs are known to possess large conductivity attributed to the extended π–π conjugation chain, which contributes to better storage ability.

Liu et al. [49] reported a successful approach to enhance the electrochemical activity and PANI-based cathode's stability by establishing π-electron conjugation between PEDOT polystyrene sulfonate and PANI on carbon nanotubes. The enhanced properties of the carbon nanotubes-polyaniline-PEDOT polystyrene sulfonate (t-CNTs-PEDOT-PE) post-treated materials were majorly credited to the $–SO_3$-H^+ moieties existing in the polystyrene sulfonate, which acts as an internal proton reservoir and gives enough H^+ for protonation of PANI. This helps in increasing the electrochemical activity of PANI and reversibility. In addition, due to the robust interactions between PEDOT polystyrene sulfonate and PANI resulted in the stretching of π–π conjugation chains enhanced electronic conductivity. The CV and GCD of the electrode material are shown in Fig. 5a and b. A t-CNTs-PA-PE cathode could attain 238 mAh/g of capacity, along with fair rate capability and cyclic stability over 1500 cycles associated with Columbic efficiency of 100% is shown in Fig. 5c–f. By the means of exerting self-standing t-CNTs-PA-PE, a ZIB was successfully fabricated.

5.6 Other Types of Batteries

Apart from the above-discussed types of rechargeable batteries, some other types of batteries implement CP as the electrode material. Based on the Cl^- anion transfer and storage a new type of battery termed Chloride ion battery (CIB) has emerged. CIB shows unique electrochemical properties corresponding to the theoretical volumetric energy densities shooting up to 2500 Wh/L which is more than the value projected by traditional LIB [50]. The CIB comprises a metal chloride/metal electrode together with an ionic liquid electrolyte allowing Cl^- transfer is reported in the proof-of-concept associated with CIB. Zhao reported [51] a chloride ion-doped polypyrrole
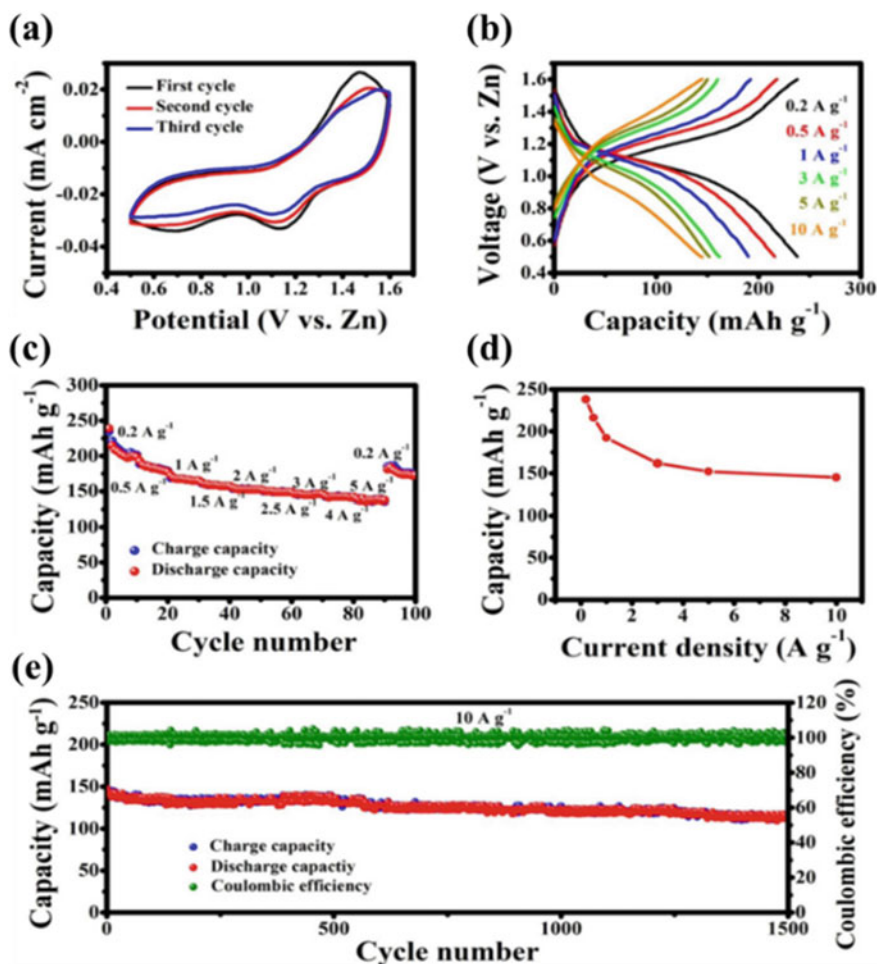
Fig. 5 Electrochemical properties of treated CNTs-PANI-PEDOT: PSS cathode implemented ZIBs, **a**, **b** CV and GCD plots; **c**, **d** rate capability and **e** cyclic life and Coulombic efficiency. Adapted with permission from Ref. [49], Copyright (2019), American Chemical Society

chloride in the size of nanoscale, as a novel cathode material for CIB. The polypyrrole chloride @carbon nanotubes (PPyCl@CNTs) cathode showed a reversible capacity reaching a value of 118 mAh/g along with a long cycle life (Fig. 6a and b).

Zhang demonstrates [52] an ammonium dual-ion battery associated with operating 1.9 V. The battery is comprised of *p*-type radical and *n*-type polyimide polymers as cathode and anode, respectively, and ammonium sulfate solution as the electrolyte. The designed electrode material exhibited a high energy density corresponding to the value of 51.3 Wh kg^{-1} corresponding to a power density of 15.8 kW/kg together with long cyclic life with 86.4% capacity retention over 10,000 cycles at 5 A/g Fig. 6c–f.
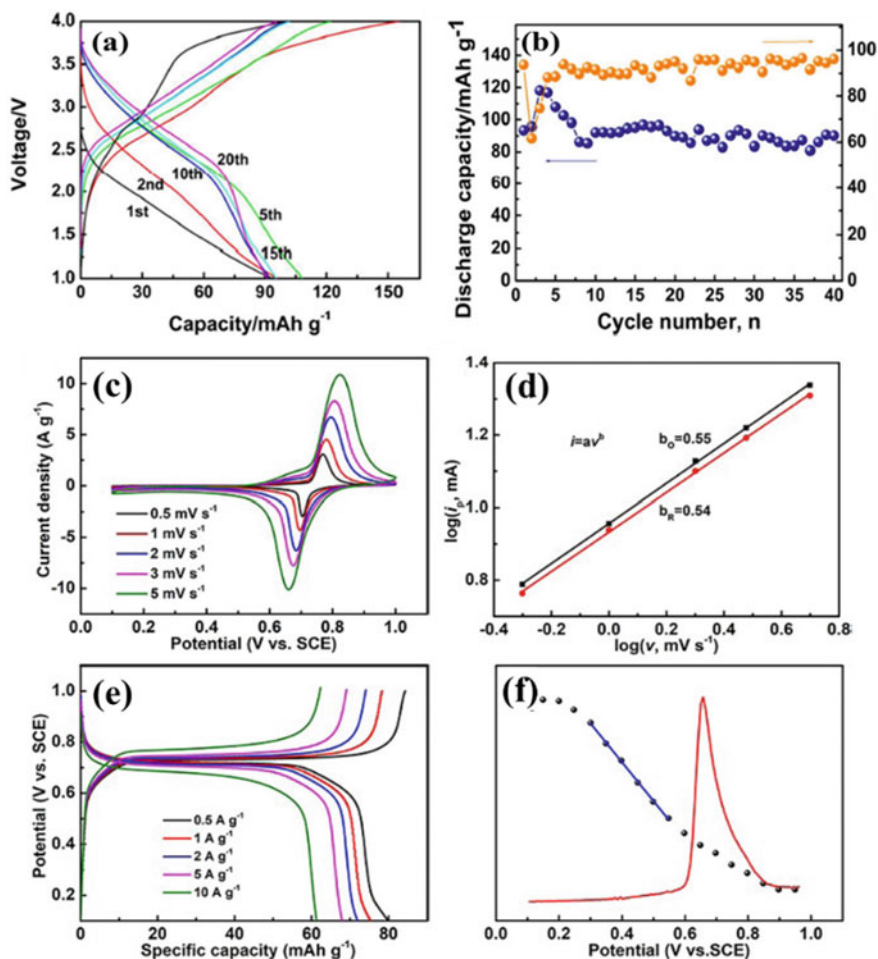
Fig. 6 a Discharge and charge curves, **b** cycle life of PPyCl/Li electrode in 0.5 M PP$_{14}$Cl in PP$_{14}$TFSI at 298 K. Adapted with permission from Ref. [51], Copyright (2017), American Chemical Society. Electrochemical properties of cathode comprising of PTMA. **c** CV profiles at different scan rates, **d** plot of log i_p versus log v, **e** charge–discharge profiles at different current densities, and **f** Model of Mott-Schottky at 1000 Hz. Adapted with permission from Ref. [52], Copyright (2019), Royal Society of Chemistry

Apart from the Li, Na, and Zn rechargeable batteries, magnesium (Mg) batteries (MIBs) also projects themselves as potential energy storage systems for large-scale applications attributed to their high safety without dendrite growth and eco-friendliness. Wang et al. [53] have reported the designing of a MIB implementing organic cathode materials containing π-conjugated aromatic dianhydride-derived polyimides (PIs) and carbon nanotubes (CNTs) composite cathodes. The cathodes

displayed a large performance together with long-term cyclic stability at a large current rate of 20 C for over 8000 cycles.

6 Conclusion and Future Perspectives

In this chapter, we have projected the conjugated conducting polymers as the potential electrode material for implementing them in rechargeable batteries. However, such a system is not free from drawbacks and needs substantial improvement before commercialization. For instance, the scaling up in the aspect of polymer synthesis is a major challenge. Further, more redox activeness of the CPs makes them unstable for repetitive charge–discharge cycles. Hence, the cyclic stability of the rechargeable batteries needs to be improved. Also, the pristine CPs face the problem of agglomeration, which severely limits the exposed active area for redox interaction with the electrolyte. The compositing of CPs with highly porous carbon materials, transition metal oxides, metal sulfides, metal chlorides can improve both the stability of the CP along with improving the charge transfer pathways making it easier for the ions to traverse easily in the electrode material. Also, incorporating them with highly porous carbon material limits the agglomeration and leads to exposure of more surface area for the redox interaction with the electrolyte. So, more focus is given to combining CPs with suitable fillers rather than using the pristine CPs as electrode material in the rechargeable batteries. Furthermore, due to its amorphous nature, it becomes very difficult to establish a structure and property relation which makes proper designing of the electrode material even more challenging. Some works have already started implementing advanced characterizing techniques that would determine the local environment at a nanometer scale and hence for the amorphous materials also a structure and property relation can be established. Nuclear magnetic resonance (NMR) spectroscopy is a popular method that should be implemented more to determine the local environment of the redox-active sites and determine the effect of surrounding atoms in charge storage properties. Altogether, CPs establish themselves as very promising, green, eco-friendly, and sustainable electrode material that can be applied in modern rechargeable batteries.

References

1. Thakur, A.K., Majumder, M., Patole, S.P., Zaghib, K., Reddy, M.V.: Metal-organic framework-based materials: advances, exploits, and challenges in promoting post Li-ion battery technologies. Mater. Adv. **2**(8), 2457–2482 (2021)
2. Majumder, M., Santosh, M.S., Viswanatha, R., Thakur, A.K., Dubal, D., Jayaramulu, K.: Two-dimensional conducting metal-organic frameworks enabled energy storage devices. Energy Storage Mater. (2021)
3. Reddy, M.V., Mauger, A., Julien, C.M., Paolella, A., Zaghib, K.: Brief history of early lithium-battery development. Materials **13**(8), 1884 (2020)

4. Smajic, J., Alazmi, A., Patole, S.P., Costa. P.M.F.J.: Single-walled carbon nanotubes as stabilizing agents in red phosphorus Li-ion battery anodes. RSC Adv. **7**(63), 39997–40004 (2017)

5. Notter, D.A., Gauch, M., Widmer, R., Wager, P., Stamp, A., Zah, R., Althaus, H.-J.: Contribution of Li-ion batteries to the environmental impact of electric vehicles. Environ. Sci. Technol. **44**(17), 6550–6556 (2010)

6. Poizot, P., Gaubicher, J., Renault, S., Dubois, L., Liang, Y., Yao, Y.: Opportunities and challenges for organic electrodes in electrochemical energy storage. Chem. Rev. **120**(14), 6490–6557 (2020)

7. Lu, Y., Chen, J.: Prospects of organic electrode materials for practical lithium batteries. Nat. Rev. Chem. **4**(3), 127–142 (2020)

8. Lee, S., Kwon, G., Ku, K., Yoon, K., Jung, S.-K., Lim, H.-D., Kang, K.: Recent progress in organic electrodes for Li and Na rechargeable batteries. Adv. Mater. **30**(42), 1704682 (2018)

9. Schon, T.B., McAllister, B.T., Li, P.-F., Seferos, D.S.: The rise of organic electrode materials for energy storage. Chem. Soc. Rev. **45**(22), 6345–6404 (2016)

10. Shea, J.J., Luo, C.: Organic electrode materials for metal ion batteries. ACS Appl. Mater. Interfaces **12**(5), 5361–5380 (2020)

11. Yin, X., Sarkar, S., Shi, S., Huang, Q.-A., Zhao, H., Yan, L., Zhao, Y., Zhang, J.: Recent progress in advanced organic electrode materials for sodium-ion batteries: synthesis, mechanisms, challenges and perspectives. Adv. Funct. Mater. **30**(11), 1908445 (2020)

12. Thakur, A.K., Choudhary, R.B.: High-performance supercapacitors based on polymeric binary composites of polythiophene (PTP)–titanium dioxide (TiO_2). Synthetic Metals **220**, 25–33 (2016)

13. Thakur, A.K., Majumder, M., Choudhary, R.B., Singh, S.B.: MoS_2 flakes integrated with boron and nitrogen-doped carbon: striking gravimetric and volumetric capacitive performance for supercapacitor applications. J. Power Sources **402**, 163–173 (2018)

14. Thakur, A.K., Deshmukh, A.B., Choudhary, R.B., Karbhal, I., Majumder, M., Shelke, M.V.: Facile synthesis and electrochemical evaluation of PANI/CNT/MoS_2 ternary composite as an electrode material for high performance supercapacitor. Mater. Sci. Eng.: B **223**, 24–34 (2017)

15. Amin, K., Ashraf, N., Mao, L., Faul, C.F.J., Wei, Z.: Conjugated microporous polymers for energy storage: recent progress and challenges. Nano Energy 105958 (2021)

16. Xu, Y., Jin, S., Xu, H., Nagai, A., Jiang, D.: Conjugated microporous polymers: design, synthesis and application. Chem. Soc. Rev. **42**(20), 8012–8031 (2013)

17. Xie, J., Gu, P., Zhang, Q.: Nanostructured conjugated polymers: toward high-performance organic electrodes for rechargeable batteries. ACS Energy Lett. **2**(9), 1985–1996 (2017)

18. Fuchigami, T., Atobe, M., Inagi, S.: Fundamentals and applications of organic electrochemistry: synthesis, materials, devices. Wiley, Japan (2014)

19. Yu, L., Wang, L.P., Liao, H., Wang, J., Feng, Z., Lev, O., Loo, J.S.C., Sougrati, M.T., Xu, Z.J.: Understanding fundamentals and reaction mechanisms of electrode materials for Na-ion batteries. Small **14**(16), 1703338 (2018)

20. Chen, Y., Wang, C.: Designing high performance organic batteries. Acc. Chem. Res. **53**(11), 2636–2647 (2020)

21. Zhang, L., Wang, H., Zhang, X., Tang, Y.: A review of emerging dual-ion batteries: fundamentals and recent advances. Adv. Funct. Mater. **31**(20), 2010958 (2021)

22. Jouhara, A., Dupré, N., Guyomard, D., Lakraychi, A.E., Dolhem, F., Poizot, P.: Playing with the p-doping mechanism to lower the carbon loading in n-type insertion organic electrodes: first feasibility study with binder-free composite electrodes. J. Electrochem. Soc. **167**(7), 070540 (2020)

23. Huang, J., Dong, X., Guo, Z., Wang, Y.: Progress of organic electrodes in aqueous electrolyte for energy storage and conversion. Angew. Chem. **132**(42), 18478–18489 (2020)

24. Kausar, A.: Review on structure, properties and appliance of essential conjugated polymers. Am. J. Polym. Sci. Eng. **4**(1), 91–102 (2016)

25. Harun, M.H., Saion, E., Kassim, A., Yahya, N., Mahmud, E.: Conjugated conducting polymers: a brief overview. UCSI Acad. J.: J. Adv. Sci. Arts **2**, 63–68 (2007)

26. Novák, P., Müller, K., Santhanam, K.S.V., Haas, O.: Electrochemically active polymers for rechargeable batteries. Chem. Rev. **97**(1), 207–282 (1997)
27. Baeriswyl, D., Campbell, D.K., Mazumdar, S.: An overview of the theory of π-conjugated polymers. Conjug. Conduct. Polym. 7–133 (1992)
28. Mishra, A.K.: Conducting polymers: concepts and applications. J. At. Mol. Condens. Matter Nano Phys. **5**(2), 159–193 (2018)
29. Han, X., Chang, C., Yuan, L., Sun, T., Sun, J.: Aromatic carbonyl derivative polymers as high-performance Li-ion storage materials. Adv. Mater. **19**(12), 1616–1621 (2007)
30. Kou, Y., Xu, Y., Guo, Z., Jiang, D.: Supercapacitive energy storage and electric power supply using an aza-fused π-conjugated microporous framework. Angew. Chem. **123**(37), 8912–8916 (2011)
31. Muench, S., Wild, A., Friebe, C., Häupler, B., Janoschka, T., Schubert, U.S.: Polymer-based organic batteries. Chem. Rev. **116**(16), 9438–9484 (2016)
32. Mike, J.F., Lutkenhaus, J.L.: Recent advances in conjugated polymer energy storage. J. Polym. Sci. Part B: Polym. Phys. **51**(7), 468–480 (2013)
33. Molina, A., Patil, N., Ventosa, E., Liras, M., Palma, J., Marcilla, R.: Electrode engineering of redox-active conjugated microporous polymers for ultra-high areal capacity organic batteries. ACS Energy Lett. **5**(9), 2945–2953 (2020)
34. Zhang, C., He, Y., Mu, P., Wang, X., He, Q., Chen, Y., Zeng, J., Wang, F., Xu, Y., Jiang, J.-X.: Toward high performance thiophene-containing conjugated microporous polymer anodes for lithium-ion batteries through structure design. Adv. Funct. Mater. **28**(4), 1705432 (2018)
35. Zeng, S., Li, L., Xie, L., Zhao, D., Wang, N., Chen, S.: Conducting polymers crosslinked with sulfur as cathode materials for high-rate, ultralong-life lithium-sulfur batteries. Chemsuschem **10**(17), 3378–3386 (2017)
36. Fu, Y., Manthiram, A.: Core-shell structured sulfur-polypyrrole composite cathodes for lithium-sulfur batteries. RSC Adv. **2**(14), 5927–5929 (2012)
37. Liang, X., Liu, Y., Wen, Z., Huang, L., Wang, X., Zhang, H.: A nano-structured and highly ordered polypyrrole-sulfur cathode for lithium–sulfur batteries. J. Power Sources **196**(16), 6951–6955 (2011)
38. Zhang, J., Shi, Y., Ding, Y., Zhang, W., Yu, G.: In situ reactive synthesis of polypyrrole-MnO$_2$ coaxial nanotubes as sulfur hosts for high-performance lithium–sulfur battery. Nano Lett. **16**(11), 7276–7281 (2016)
39. Liu, X., Wang, S., Wang, A., Chen, J., Wang, Z., Zeng, Q., Liu, W., Li, Z., Zhang, L.: A new conjugated porous polymer with covalently linked polysulfide as cathode material for high-rate capacity and high coulombic efficiency lithium-sulfur batteries. J. Phys. Chem. C **123**(35), 21327–21335 (2019)
40. Xu, S., Li, H., Chen, Y., Wu, Y., Jiang, C., Wang, E., Wang, C.: Branched conjugated polymers for fast capacitive storage of sodium ions. J. Mater. Chem. A **8**(45), 23851–23856 (2020)
41. Chen, Y., Li, H., Tang, M., Zhuo, S., Xu, Y., Wang, E., Wang, S., Wang, C., Hu, W.: Capacitive conjugated ladder polymers for fast-charge and discharge sodium-ion batteries and hybrid supercapacitors. J. Mater. Chem. A **7**(36), 20891–20898 (2019)
42. Li, Z., Zhou, J., Xu, R., Liu, S., Wang, Y., Li, P., Wu, W., Wu, M.: Synthesis of three dimensional extended conjugated polyimide and application as sodium-ion battery anode. Chem. Eng. J. **287**, 516–522 (2016)
43. Su, D., Zhang, J., Dou, S., Wang, G.: Polypyrrole hollow nanospheres: stable cathode materials for sodium-ion batteries. Chem. Commun. **51**(89), 16092–16095 (2015)
44. Zhou, M., Li, W., Gu, T., Wang, K., Cheng, S., Jiang, K.: A sulfonated polyaniline with high density and high rate Na-storage performances as a flexible organic cathode for sodium ion batteries. Chem. Commun. **51**(76), 14354–14356 (2015)
45. Zhang, C., Qiao, Y., Xiong, P., Ma, W., Bai, P., Wang, X., Li, Q., Zhao, J., Xu, Y., Chen, Y., Zeng, J.H., Wang, F., Xu, Y., Jiang, J.-X.: Conjugated microporous polymers with tunable electronic structure for high-performance potassium-ion batteries. ACS Nano **13**(1), 745–754 (2019)

46. Xue, Q., Li, L., Huang, Y., Huang, R., Wu, F., Chen, R.: Polypyrrole-modified Prussian blue cathode material for potassium ion batteries via in situ polymerization coating. ACS Appl. Mater. Interfaces **11**(25), 22339–22345 (2019)
47. Tian, B., Zheng, J., Zhao, C., Liu, C., Su, C., Tang, W., Li, X., Ning, G.-H.: Carbonyl-based polyimide and polyquinoneimide for potassium-ion batteries. J. Mater. Chem. A **7**(16), 9997–10003 (2019)
48. Min, X., Xiao, J., Fang, M., Wang, W.A., Zhao, Y., Liu, Y., Abdelkader, A.M., Xi, K., Vasant Kumar, R., Huang, Z.: Potassium-ion batteries: outlook on present and future technologies. Energy Environ. Sci. **14**(4), 2186–2243 (2021)
49. Liu, Y., Xie, L., Zhang, W., Dai, Z., Wei, W., Luo, S., Chen, X., Chen, W., Rao, F., Wang, L., Huang, Y.: Conjugated system of PEDOT:PSS-induced self-doped PANI for flexible zinc-ion batteries with enhanced capacity and cyclability. ACS Appl. Mater. Interfaces **11**(34), 30943–30952 (2019)
50. Chen, C., Yu, T., Yang, M., Zhao, X., Shen, X.: An all-solid-state rechargeable chloride ion battery. Adv. Sci. **6**(6), 1802130 (2019)
51. Zhao, X., Zhao, Z., Yang, M., Xia, H., Yu, T., Shen, X.: Developing polymer cathode material for the chloride ion battery. ACS Appl. Mater. Interfaces **9**(3), 2535–2540 (2017)
52. Zhang, Y., An, Y., Yin, B., Jiang, J., Dong, S., Dou, H., Zhang, X.: A novel aqueous ammonium dual-ion battery based on organic polymers. J. Mater. Chem. A **7**(18), 11314–11320 (2019)
53. Wang, Y., Liu, Z., Wang, C., Hu, Y., Lin, H., Kong, W., Ma, J., Jin, Z.: π-Conjugated polyimide-based organic cathodes with extremely-long cycling life for rechargeable magnesium batteries. Energy Storage Mater. **26**, 494–502 (2020)

Bio-inspired Polymers as Organic Electrodes for Batteries

Hanane Chakhtouna, Brahim El Allaoui, Nadia Zari, Rachid Bouhfid, and Abou el kacem Qaiss

Abstract With the ever-increasing demand for energy sources, worldwide attention has been given to the development of advanced materials for energy storage applications, specifically for batteries. The use of abundant natural resources in such applications seems to be a simple and useful solution since they meet the 3E requirements of (i) excellent performance, (ii) environmental friendliness, and (iii) ease of handling. Indeed, although most academic research demonstrates the superior energy performance of electrode materials proposed in the literature for different types of batteries, they also suffer from early deterioration during charge and discharge cycles, leading to their short lifespan. Bio-inspired polymers such as polysaccharides, natural cellulosic fibers, quinones, flavins, and others represent the most bio-renewable resources suggested for developing and designing highly efficient materials as organic electrodes for batteries. These bio-inspired materials present a great diversity of structures and properties, adapted to the constraints of the environment and the type of electrode envisaged, and even participate in the improvement of their performances for long-term applications. This book chapter aims to provide an overview of recent advances in bio-inspired polymers for energy storage applications, especially as organic electrodes for batteries. Thus, before introducing the different categories of bio-inspired polymers used as electrodes for different types of batteries and the basic principle of their use, it was first found necessary to start with a general state of the art survey on batteries through the presentation of the fundamental principle of their working, their principal components and characteristics.

Keywords Battery · Energy storage · Bio-inspired polymers · Organic electrode · High performances · Long-term applications

H. Chakhtouna · B. El Allaoui · N. Zari (✉) · R. Bouhfid · A. Qaiss
Moroccan Foundation for Advanced Science, Innovation and Research (MAScIR), Composites et Nanocomposites Center (CNC), Rabat Design Center, Rue Mohamed El Jazouli, Madinat El Irfane, 10100 Rabat, Morocco
e-mail: n.zari@mascir.com

H. Chakhtouna · B. El Allaoui
Laboratoire de Chimie Analytique et de Bromatologie, Faculté de Médecine et de Pharmacie, Université Mohamed V, Rabat, Morocco

1 Introduction

Over the past few years, the world's energy consumption has increased significantly, leading to a growing awareness of the need for evolving towards new alternatives more economical to fossil fuels as well as reducing the CO_2 emissions, while meeting the needs of daily consumption [1]. Besides, storage solutions are required to offset the gap between supply and demand. Storage systems can be classified into 5 categories, including, mechanical energy storage (pumped storage), electrical storage (supercapacitors), electrochemical storage (batteries), chemical storage (hydrogen), and thermal storage (sensible and latent heat storage) [2]. The appropriate storage system is chosen based on the application and the required performance. It depends on several parameters, namely technical–economic performance, environmental impact, and social acceptability. Therefore, no storage technology can meet all the criteria imposed. To date, batteries remain the most traditional means of storing electricity in the form of chemical energy because they democratize cost and their advantageous performances [3]. Thus, in terms of energy density, high performance, and low costs, lithium-based batteries are the most promising. Nevertheless, working with liquid electrolytes, which are inflammable and harmful, poses some safety problems, limiting their more widespread and future applications [4]. Thus, the challenge of rechargeable batteries now is to develop battery systems that simultaneously meet both economic and environmental requirements. Therefore, it is to reduce the use of dangerous materials that the bio-inspired polymers as organic electrodes for batteries have been developed [5]. In fact, bio-inspired materials are mainly made of naturally abundant elements such as carbon, oxygen, sulfur, azote, and so on with the real potential to be derived from sustainable and renewable resources. Moreover, most bio-organic electrode materials are compatible with sodium, lithium, nickel, lead, etc. with the possibility of use as an electrode, separator binder per the purposes of the batteries, making them more suitable for a broad range of electrochemical storage arrangements. This book chapter aims to provide an overview of recent studies based on the use of bio-inspired polymers as organic electrodes for batteries, through the presentation of the main categories of these materials, namely, biomass and its derivatives, quinone, and its derivatives and flavin and its derivatives, even the few numbers of available scientific papers relative to this new search field, since these electrodes constitute the novel generation of batteries due to their environmental nature, low-cost, availability and electrochemical performances.

2 Generalities on Batteries

A battery, also known as an accumulator, can be generally defined as an energy storage system capable of converting electrical energy into a reversible chemical process. The functioning of the batteries consists in converting the chemical energy into electrical energy by electrochemical reactions. They are composed of one or

cells connected in series and/or parallel to obtain the desired voltage and capacity. Each cell contains a positive electrode known as cathode, a negative electrode called anode physically separated by a porous membrane and an electrolyte (which can be solid, liquid, or a combination of these two states, such as gelled electrolytes), ensuring the transport of ionic species (anions and cations) from one electrode to the other and the electroneutrality of the system. Batteries are manufactured in several sizes with capacities varying from less than 100 W to several megawatts and in various types with different chemical compositions depending on their application [6, 7]. The positive electrode is a host structure, usually composed of a transition metal oxide with high electrochemical potential, while the negative electrode, which has a lower electrochemical potential, can be an intercalation material. Indeed, the higher the potential difference between the electrodes, the higher the energy density. Besides, batteries can be divided into two main categories: primary and secondary. This section aims to give an overview of batteries by presenting the different types, their fundamental principle, and their characteristics.

2.1 Components of Batteries

All types of batteries are usually made up of four main components, two electrodes (anode and cathode), an electrolyte to move charges between the electrodes, and a separator to prevent shorting as displayed in Fig. 1. The materials used as positive electrodes are chosen for their ability to release electrons. generally, they are metals

Fig. 1 Schematic diagram of battery components. Adapted with permission from [8]
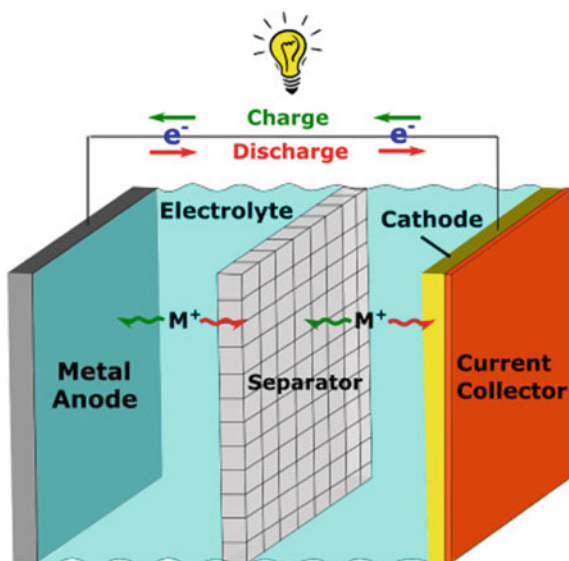
Table 1 Desirable characteristics for battery components

	Characteristics
Cathode	• Strong oxidizing compound • Stable upon contact with the electrolyte • Working voltage is useful • Simple manufacturing process • Low cost
Anode	• Highly effective reducing agent • Excellent coulombic performance • High conductivity • Strong stability • Facility of manufacturing • Low cost
Electrolyte	• Strong ionic conductivity • No electrical conductivity • No reactivity with electrode materials • Resistant to temperature changes • Safety of handling

with high reducing power such as lead, cadmium, lithium, etc. Conversely, the materials of the negative electrode must be strong oxidizers, i.e. capable of fixing the electrons. For this purpose, compounds of oxygen, sulfur, or halogens with other multivalent elements, such as transition elements, are used more frequently. Some batteries use positive electrodes known as insertion electrodes: the material used in this case is a chemical compound whose crystalline structure makes it possible to insert and disinsert charge carriers according to the charge and discharge. It happens that the negative electrode is itself an insertion compound, usually graphite. The electrolyte, which must be a good ionic conductor, is usually composed of a salt dissolved in a solvent that is stable to the electrodes, at least kinetically, and whose properties are chosen to solubilize and ionize this salt. It can be liquid, solid (polymer), or even in a mixed form (gel). Finally, the separator is a membrane made of one or more layers of polymers that separates the active materials. It is through this separation of charge the battery can generate electricity. During the charge or discharge cycle, the ions flow from one electrode to the other through the separator, while electrons migrate from the negative electrode to the positive electrode and through the outside circuit. The main characteristic of the separator is its porosity. Desirable characteristics for the anode, cathode and electrolyte materials are given in Table 1.

2.2 Batteries Fundamental Working Principle

The conversion of chemical energy into electrical energy is carried out through redox or electrochemical reactions, hence the term "electrochemical generators". Each half-reaction of oxidation and reduction takes place on each of the two electrodes, separated by an electrolyte that ensures ionic conductivity and electronic insulation
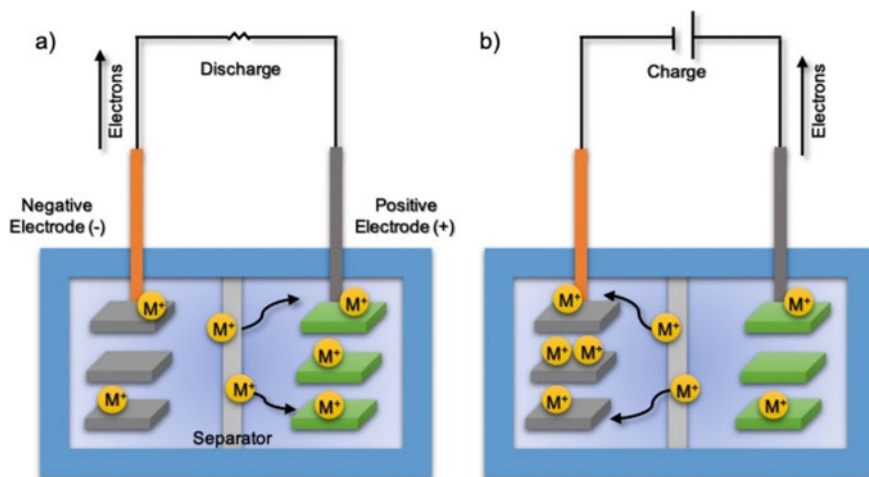
Fig. 2 Example of battery, **a** discharge, **b** recharge. Adapted with permission from [9]

between them. We can also underline here that this conversion is reversible in the case of some batteries (secondary batteries), which distinguishes them from the second type of electrochemical generators, the primary batteries for which the transformation of energy is irreversible. The reversibility of the processes in the case of batteries thus implies two modes of operation. During discharge, the negative electrode is the seat of an oxidation reaction (i.e. a release of electrons) carried by the intermediary of a collector and then the external circuit to the positive electrode, the seat of a reduction reaction or gain of electrons. In charging, the opposite reactions occur: the negative electrode becomes the seat of a reduction reaction, and the positive electrode becomes the seat of an oxidation reaction (Fig. 2).

2.3 Types of Batteries

Depending on the possibility of reuse after one period of use, batteries are classified into two main classes, namely, primary and secondary batteries. Primary batteries may be described as non-rechargeable batteries, in contrast to secondary batteries, which can be reused after discharge [10]. This section aims to highlight the difference between the most used types of batteries for high-energy applications.

2.3.1 Primary Batteries

A primary battery is a type of battery designated for a single use before discarding, meaning that it cannot be recharged with electricity and reused, whereby the inner

reaction happens in only one direction and the lifetime of the battery expires after a single cycle. Indeed, due to their low price, they are particularly appropriate for applications with low energy requirements and simply need a constant voltage. Primary batteries have been around for more than 200 years. The Italian scientist Alessandro Volta built the first practical battery in 1800 [11]. It is composed of a stack of small electrochemical cells each consisting of silver and zinc plates separated by a sheet of cardboard soaked in saltwater. Each cell generated a small amount of electrical energy, and then by connecting all the cells in the stack in series, Volta was able to generate a useful voltage for his experiments. The benefits of this kind of battery are their high energy density, high capacity, ease to use, low-cost, and slow discharge. Carbon-zinc and alkaline batteries are the most popular cell types [12].

2.3.2 Secondary Batteries

Secondary batteries are rechargeable batteries, they can be used during many cycles because the chemical internal reaction can be reversed by applying to it an electric current. Indeed, there are various subcategories of electrochemical storage technologies, which include mainly, lead-based batteries, nickel-based batteries, and lithium-based batteries. Thus, the principle of their work remains the same; the electricity is generated by chemical reactions involving the anode, cathode, and electrolyte, but the difference lies in the chemical composition of electrodes as well as the charge carrier element. Lead acid batteries (LABs), lithium-based, and nickel-based batteries are dominant with a total contribution of 94.8% of the global battery market according to some studies [13]. Table 2 summarizes the characteristics of different types of secondary batteries presented above.

Table 2 Characteristics of different rechargeable batteries available in the market

Features	Pb-acid battery	Ni-Cd battery	Ni-MH battery	Li-ion battery
In use since	Late 1800s	1950	1990	1990
Battery voltage (V)	2.1	1.2	1.2	3.6
Power density (W/kg)	180	140–180	250–1000	1800
Energy density (kW/kg)	30–50	40–60	60–120	150–250
Charging time (h)	8–16	1	1–4	<1
Operating temperature (°C)	Ambient	−40 to +80	Ambient	Ambient
Internal resistance	Low	High	Medium	Low
Cycle life	300–800	1500	1000	500–2000
Memory	No	Yes	No	No
Cost	Medium	Low	High	High
Toxicity	High	High	Low	Low
Maintenance	No	Low	Low	No

3 Bio-inspired Polymers as Organic Electrodes for Batteries

In addition to inorganic materials, a rapidly developing area of research is the use of organic redox materials, especially as positive electrode materials. The materials initially used were p-conjugated polymers, good electronic conductors, such as polyheterocycles, etc. More recently, bio-inspired polymers from biomass and its derivatives, molecules such as quinones and nitroxides have been the subject of many very promising studies [14]. The interest in such materials is related to their natural abundance, their low cost, their very low toxicity, and their intrinsic properties [15]. Indeed, the interest in using bio-inspired electrode materials resides in the many advantages conferred by their structure, their higher specific capacity to inorganic materials, and the possibility of introducing different functional groups for raising or lowering the redox potential, depending on the application. The working principle of batteries based on bio-inspired polymers as organic electrodes is very similar to conventional batteries already mentioned before. The selection of the ideal electrode material, either for the cathode or the anode, is mostly driven by the reversibility of the electrochemical reaction (redox) of the active material. This section provides a comprehensive view of different bio-inspired polymers as organic electrodes for batteries.

3.1 Biomass and Its Derivatives

Since prehistory, biomass has been the first source of energy to be discovered by humans. Biomass resources are very diverse and they are generally classified according to their origins and their physical nature. Lignocellulosic biomass is composed of carbon, hydrogen, oxygen, nitrogen, sulfur in minor proportions, and mineral matters such as Ca, Mg, K, P, Na, Si, etc. It contains also alkaline and alkaline earth minerals as well as metals. Moreover, it is mainly made from three compounds, namely, cellulose, hemicellulose, and lignin (Fig. 3). Cellulose microfibrils, embedded in a complex matrix of hemicellulose, pectin, and proteins, form the external skeleton of plant cells, while lignin is the rigid part of the plant wall and is linked to the hemicelluloses by covalent bonds [16, 17]. Recently, more interest has been shown in the use of biomass wastes for the preparation of different materials for various applications, including energy storage devices due to their low-cost, abundance, non-toxicity, and so on [5]. Biomass wastes can be valorized into cellulose and its derivatives, lignin, or others or might be carbonized through thermal processes with reduced environmental footprint and used in electrodes for batteries (e.g., sodium-ion, lithium-ion, metal–oxygen batteries, etc.) to improve their performances and environmental impacts as well as reduce their costs.
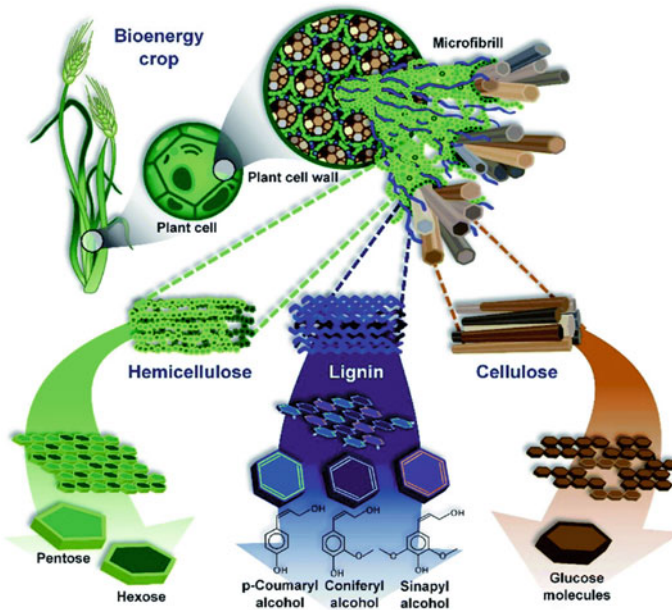
Fig. 3 The structure of the main components of lignocellulosic biomass. Adapted with permission from [18]

(a)   *Cellulose*

Cellulose is known as the most abundant renewable polymer on earth. It is a linear polysaccharide consisting of f β-1,4-linked D-glucose units, comprising macro- and microfibrils to create 3D hierarchical structures. Its amorphous phase possesses a large number of hydroxyl groups susceptible to forming hydrogen bonds with other molecules and is also responsible for its high hydrophilicity. Depending on the dimension and size of the individual cellulose fibrils, there is a variety of cellulosic materials, namely cellulose microfibrils (CMF), cellulose nanofibers (CNF), and cellulose nanocrystals (CNC) [19]. Moreover, due to its outstanding physico-chemical and mechanical properties (the tensile strength and modulus of nanocrystalline cellulose are approximatively equal to 140 and 7.5 GPa), cellulose and its derivatives such as nanocrystalline cellulose has been investigated for the design of bio-inspired polymer as organic electrodes, separators, binders, etc. for batteries [20, 21]. Indeed, cellulose-based batteries are contingent upon the structural, physicochemical, and mechanical properties of the materials of the electrode and the separator nature. The preparation of such batteries involves the immobilization of high conductive materials such as carbon nanotubes, graphite, graphene, metals, onto cellulose fibrils. Thus, cellulose and its derivatives, with abundant functional groups on their surfaces, are capable of forming high strong bonds with other materials through several chemical reactions, resulting therefore in a variety of straightforwardly electrode forms [22]. In this context, Cámer et al. developed a nano-Si/Cellulose composite as anode using

a simple and low-cost technique for improving the deficient features of lithium-ion cells [23]. The resulting composite electrode with high homogeneity, dispersion, and no-agglomeration exhibited outstanding electrochemical performances compared to neat Si electrode, indicating the role of cellulosefibers as green and eco-friendly materials in enhancing the battery features by maintaining interconnectivity between particles, thereby promoting the mobility of charge carriers in the bulk electrode and at the electrode–electrolyte interfaces. Indeed, the electrode with cellulose fibers showed a high specific capacity of about 1400 mAh/g after 50 cycles, versus only 400 mAh/g for the pristine Si electrode. Wang et al. fabricated a novel flexible bio-inspired polymer organic electrode with outstanding electrochemical performances for wearable electronicbased on cellulose, reduced graphene and ternary metal alloy [24]. Cellulose from cotton embedded with reduced graphene was firstly prepared through a dipping-drying method followed by the chemical reduction of amorphous Co–Fe–B alloy at ambient temperature. The structural characterization technique revealed the homogenous distribution of reduced graphene and metal alloy through the cellulose-based electrode. Besides, electrochemical features show that the elaborated electrode displays a high specific capacity of a maximum of 302.6 F/g compared to electrodes without cellulose, which can be attributed according to the authors to the synergistic effect of high conductivity, more accessible electroactive sites, and rapid electron collection efficiency. Thus, the cellulose bio-inspired electrode exhibited also high flexibility without any loss after 3000 charge and discharge cycles or being flexed 300 times, suggesting the excellent electrochemical properties of the elaborated electrode. A novel flexible electrode based on polyaniline and graphene as active material and bacterial cellulose as the material responsible for the flexibility of the electrode have been successfully fabricated using a facile in-situ polymerization followed by vacuum filtration [25]. Indeed, due to the abundance of functional groups on the bacterial cellulose, strong hydrogen bonds, and electrostatic interactions have been trained between the polymer/graphene composite and the cellulose. SEM and TEM images of the resulting electrode show the homogeneity of the prepared electrode over a larger surface and its porous structure, while electrochemical characteristics reveal that the combination of such materials leads to obtaining a highly efficient electrode in terms of specific capacity, areal capacitance, energy density, and conductivity. The electrode displays a high areal capacitance of 4.16 F/cm at a current density of 1 mA/cm, which remains a high value compared to other materials [26]. Li et al. investigated the preparation of cellulose-based cathode for lithium-ion batteries through aqueous slurry mixing and coating processes to improve their electrochemical performances and reduce their environmental risks [27]. In parallel, the authors fabricated a PVDF-based electrode as a reference to compare the performances of both electrodes. Results show that the electrode constituting from carboxymethyl cellulose provided an initial discharging capacity of 255.4 mAh/g at 0.2 C against 266.8 mAh/g in the case of PVDF-based electrodes, indicating the role of cellulose in improving the battery performances (Fig. 4). Recently, Jo et al. prepared cellulose–polyaniline–Al_2O_3 composites as separators for sodium-ion batteries. With the addition of alumina, the cellulose/PAN separator's electrochemical, thermal and mechanical performances have been tremendously upgraded. Compared to other
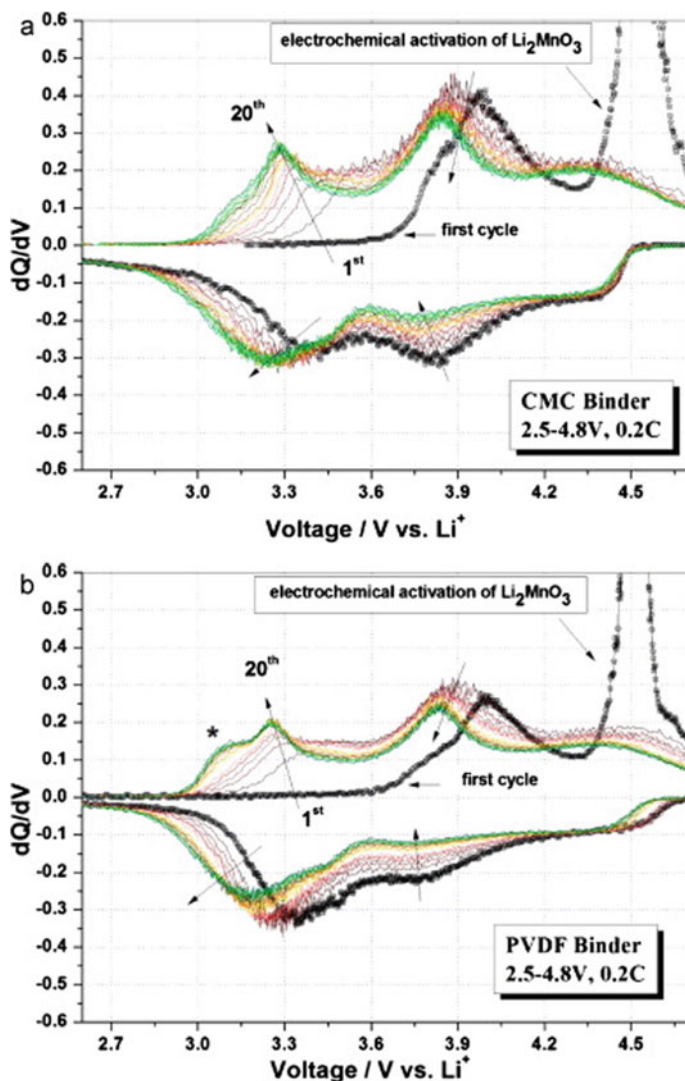
Fig. 4 A derivative plot of the voltage profile for lithium-based battery with CMC (**a**) and PVDF (**b**) binder. Adapted with permission from [27]

separators, the elaborated composite showed high specific capacity with a maximum of 107 mAh/g at a rate of 1 C and high cycling stability of 88% for 300 cycles.

(b)   *Lignin*

Lignin is the second most abundant organic biopolymer in plants after cellulose. This three-dimensional amorphous polymer has been extensively used in many applications, in particular in battery applications as electrodes. Milczarek and his co-author

first reported the possibility of using the quinone group of lignin as a cathode, since then a lot of studies investigated the application of lignin polymer as a green and inexpensive organic electrode for batteries [28]. In this context, Gnedenkov et al. investigated the use of Klason lignin derived from different types of biomass feedstocks, namely, buckwheat, husks of rice, rice straw, and sunflower as an organic electrode for lithium-based batteries [29]. Structural characterization demonstrated that all lignin exhibited amorphous structures whatever the type of biomass. In contrast to the results of the thermal analysis which showed that the thermal stability of the different types of lignin varies with varying the feedstock nature. Moreover, in terms of electrochemical properties, the lignin-derived from buckwheat exhibited a high specific capacity compared with other lignin electrodes, with a maximum of 425 mAh/g. The proposed electrochemical reaction at electrodes upon discharge is given by the following equations:

$$-\underset{|}{C}{=}O + Li^+ + e^- \rightarrow -\underset{|}{C}-O-Li \tag{1}$$

$$2C_6-C_3-OH + 2Li^+ + 2e^- \rightarrow 2C_6-C_3-O-Li + H_2 \tag{2}$$

$$C_6-C_3-O-R^* + 2Li^+ + 2e^- \rightarrow C_6-C_3-O-Li + R^*-Li_2 \tag{3}$$
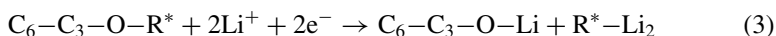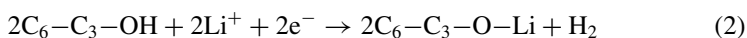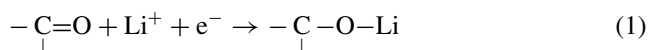
where, $(C_6–C_3)$ is a phenylpropane structural unit of lignin, R^* is $(C_6–C_3)$ or CH_3.

Pyrolysis of lignin has been also investigated to be utilized in electrode batterie. The pyrolysis of lignin involves complex reactions of cyclization, polymerization, condensation, and cracking. The products obtained are CO, CO_2, CH_4, and other gaseous hydrocarbons. Lignin is at the origin of most solid products especially in the case of slow pyrolysis. In this context, Tian et al. fabricated a hierarchical S-doped porous carbon using an easy template approach for high-performance electrode supercapacitors [30]. Indeed, doping heteroatoms such as sulfur into carbon materials is considered an attractive approach for enhancing the intrinsic chemical and electrical features. The resulting carbon layer with an interconnecting open structure and high surface area of 1054 m^2/g exhibited excellent specific capacity (328 F/g), outstanding rate performances, and high cycling stability, with 97% of capacity after 10,000 cycles.

(c) *Biochar*

To enhance the electrochemical features of batteries, especially their conductivity, carbonaceous materials ranging from graphene to carbon with hierarchical porosity and structure have been investigated [31]. Despite having demonstrated reasonable performances, the complex and costly manufacturing process precludes their mass production. Biomass feedstocks such as agricultural and crops wastes, wood, and plant residues are rich in carbon and can be easily burned through thermal conversion and used therefore to produce carbon-based materials such as biochar for energy storage applications. According to the International Biochar Initiative (IBI), biochar

can be described as a porous solid material produced by the thermochemical process of biomass in an environment with limited oxygen [32]. Nowadays, due to its fascinating properties, it is applied to develop new materials in numerous fields including environmental remediation, wastewater treatment, catalysis for fuel cells, and energy storage technologies as an electrode in batteries and supercapacitors [33, 34]. A nitrogen-rich, porous hierarchical carbon from wheat straw has been successfully prepared as anode for Lithium-ion batteries (Fig. 5) [35]. The anode was prepared through an easy and inexpensive technique consisting of treating firstly the raw wheat straw fibers with HCl and KOH to remove impurities and also to improve the surface
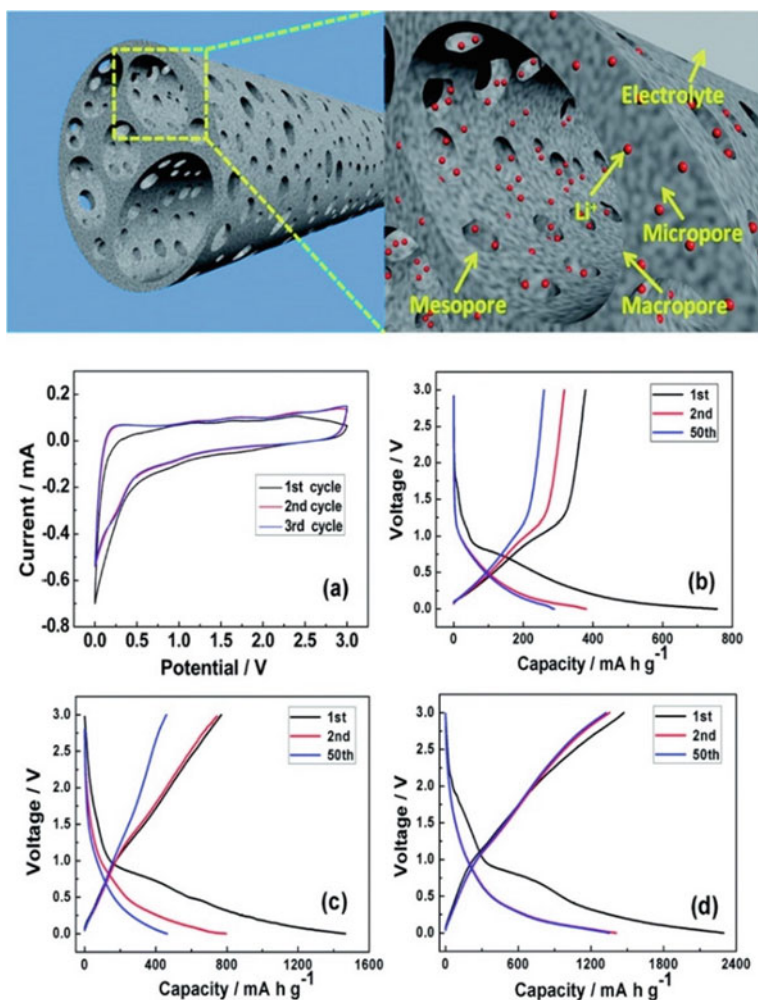
Fig. 5 Hierarchically porous nitrogen-rich carbon morphology and electrochemical performances. Adapted with permission from [35]

properties (porosity and functional groups), and then pyrolyzed under nitrogen flux at high temperature (700 °C) for 1 h. The resulting biochar with a high interconnected structure exhibited a high specific surface area compared to nonactivated wheat straw biochar. The surface area was increased from 24.9 to 916 m^2/g, indicating the role of acid and alkaline treatments in improving the physicochemical features of biochar to be used later as anode for lithium-ion battery. XRD analysis confirmed the amorphous nature of the biochar, which is more beneficial for the intercalation and deintercalation of lithium ions during charge and discharges cycles. Moreover, electrochemical results displayed that the resulting anode exhibits high-rate capability, excellent specific capacity, high current density, and large reversible capacity. In fact, during the first charge–discharge cycle, the anode with activated biochar shows a highly specific capacity of about 1470 mAh/g at a current density of 37 A/g, which is much higher compared to the nonactivated anode. The reversible capacity of the anode is maintained at 1327 mAh/g after 50 cycles, indicating the stability of the elaborated anode. The slight decrease may be attributed to the conversion of the carbon electrode from its virgin form to an active lithium storage host. Li et al. fabricated carbon nanosheets from bacterial cellulose pyrolyzed at high temperature (800 °C) for use as cathode for lithium-sulfur batteries to resolve the problems of Li/S batteries related to the dissolution of polysulfide species, causing their self-discharge and bringing about their rapid capacity depletion [36]. Indeed, cathodes were made by coating Li_2S_6 catholyte on carbon a nanofiber aerogel to obtain a sulfur loading of 2.74 mg/cm^2 and 80% of sulfur across the overall electrode. The resulting cathode exhibited excellent electrochemical performances. The cells demonstrated an initial capacity of 1360 mAh/g at 0.2 C and present outstanding cycle stability in which 76% of the initial specific capacity was maintained after 200 cycles, which might be related to the ultra-strong absorption ability of CNFA for catholyte. Similarly, carbon nanosheets derived also from bacterial cellulose have been prepared to be used as bio-inspired organic anode for sodium-ion batteries [37]. Different carbon nanosheets-based anodes under different pyrolysis temperatures have been prepared to study the role of the temperature of pyrolysis on the electrochemical features of the resulting electrodes. Carbon pyrolyzed at high temperature was found to be the best anode, with a high specific capacity, excellent rate capacity, and cycling stability. The authors attributed this enhancement to its porous structure, an abundance of functional groups, in particular, oxygen functional groups, and excellent surface area. Microporous alkaline activated biochar with high surface area and excellent electronic conductivity was derived from bamboo fibers for use as cathode for Li–S batteries [38]. The electrode with 50 wt% sulfur content exhibits a high initial capacitance of 1295 mAh/g and good capacitance retention of 550 mAh/g after 150 cycles with excellent Coulombic efficiency.

3.2 Quinone/Flavine and Their Derivatives

Quinone and its derivatives are among the most investigated organic electrode materials derived from bio-resources [39]. According to the literature, quinones can be defined as a class of molecules obtained from aromatic substances such as naphthalene, benzene, and so on, through the conversion of –CH= groups into –C(=O)– groups, resulting, therefore, to fully conjugated cyclic diketone structure [40, 41]. They are the main redox-active moieties amongst the natural organic compounds playing a real role in the electron-transport processes. The reversibility of quinone compounds has been known for a few years, in particular through the work of Armand et al. on the reduction of lithium rhodizonate acid which showed a very good capacity of 515 mAh/g in the 1.5–3.5 V potential range [42]. Moreover, the redox characteristics of quinones such as p-benzoquinone or o-benzoquinone have been extensively applied in electrochemical energy storage systems either in the reduced or oxidized state. In this context, Song et al. synthesized a poly (anthraquinone sulfide) with an excellent cyclability, reversibility, and a capacity of 198 mAh/g at the first cycle with a loss of only 7% after 40 cycles. Triptycene-based quinone molecules were used as organic cathode materials in Li-ion batteries to improve their electrochemical features, delivering a specific capacity of 387 mAh/g, an energy density of 1032 Wh/kg 0.1 C rate, and a high capacity stability of 80% after 100 cycles [43]. Notwithstanding the high energy density expected, quinone derivatives are suffering from the dissolution of active materials in conventional organic-based electrolyte systems. Two Cross-conjugated oligomeric quinones have been proposed for use as a bio-inspired organic electrode for lithium-based batteries [44]. Both quinones-based electrodes provided a comparable capacity of over 200 mAh/g with a capacity stability retention of 96% over 250 cycles. The mechanism of the electrochemical reaction at the cathode is given in Fig. 6. Poly(5-amino-1,4-dyhydroxy anthraquinone) were also investigated for use as cathode material of lithium batteries [45]. The cathode was easily prepared through an oxidation approach. At the cutoff voltage of 1.5–3.7 V, the cathode displays an initial discharge capacity of about 101 mAh/g at the current density of 400 mAh/g. Moreover, the elaborated cathode was efficient to prevent the problems related to the dissolution and crystallization of its 5-amino-1,4-dyhydroxy anthraquinone monomer. Besides, the most attractive part of this study, is that the capacity of the cathode increased after 14 cycles reaching a value of 143 mAh/g and then decreased to 129 mAh/g after 50 cycles. Thus, the quinone based electrode shows high-rate capacity even at high current density, indicating the high electrochemical performances of this material. Shimizu et al. were also investigated the impact of introducing of two lithiooxycarbonyl groups into the organiccathode of lithium battery in enhancing their cyclability as well as resolving the problems of the solubility of quinone molecules in electrolyte. Electrochemical results show that the cathode exhibited an initial capacity of 217 mAh/g at 0.2 C rate, which is 73% of the theoretical capacity [46].

The versatility in designing redox flow batteries makes them suitable for efficient low-cost energy storage in large-scale applications. The discovery of inexpensive
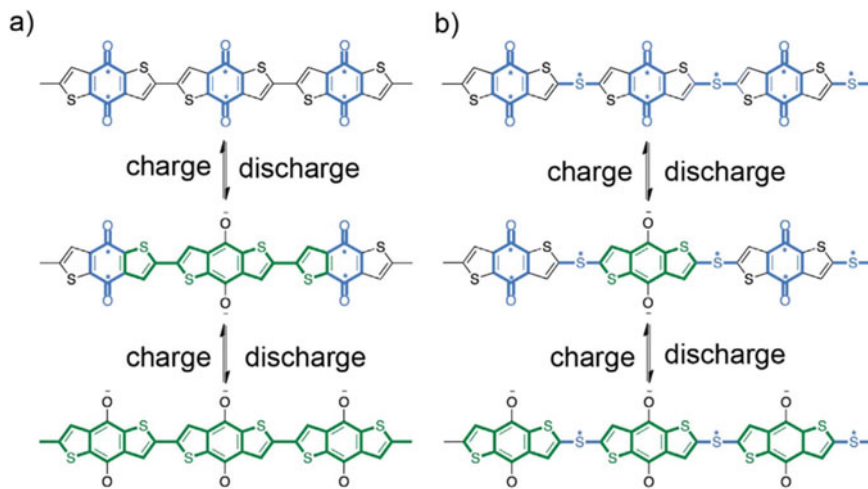
Fig. 6 The electrochemical mechanism of the quinone-based electrode. Adapted with permission from [44]

organic electroactive materials for use in aqueous flow battery electrolytes is therefore a very attractive approach. Flavins are highly versatile electroactive molecules, catalyzing a multitude of redox reactions in biological systems. A redox flow battery using flavin mononucleotide negative and ferrocyanide positive electrolytes in a strong base exhibit stable cycling performance, with a retention capacity greater than 99% over 100 cycles. Sánchez-Díez et al. [47] investigated the role of using flavin redox cycling in mitochondria to lithium rechargeable batteries. The redox reaction of flavin takes place generally during battery function at the diazabutadiene nitrogen atoms in the flavin molecules via two sequential steps namely, single-electron and Li+ transfer steps.

4 Conclusion

In recent years, to overcome the drawbacks of conventional inorganic cathode materials, including their low specific capacity and poor removal system, organic compounds have emerged as promising candidates for use in the next generation of energy storage systems, in particular as electrodes for batteries. Indeed, the present research orientations in this field consist of to

1. use of eco-friendly materials with high electrochemical performance and stability after several cycles.
2. favor less energy-intensive synthesis methods "soft chemistry".
3. develop electrodes based on organic materials (with multiple redox centers) renewable and from biomass and

4. develop new batteries beyond lithium.

In the face of this, biopolymers, such as cellulose or lignin, can be applied in binders, separators, and solid or gel electrolytes, and thus can be used industrially since their production from biogenic precursors is feasible. On the other hand, biopolymers, such as cellulose or lignin, can be applied in binders, separators, and solid or gel electrolytes, and thus can be used industrially since their production from biogenic precursors is feasible. Furthermore, several quinones, mainly explored as cathodic materials, have been obtained from bioresources. Even ionic liquid electrolytes have been synthesized using chemicals purely derived from biomass. Finally, carbonaceous materials are a key component of all types of batteries, not only as host materials for metal ions in the anodes but also, for example, as conductive additives. Using all kinds of biowaste or biogenic chemicals, carbons have been synthesized with the possibility to adjust properties such as porosity or conductivity. As a result, almost all the biomass on Earth could be used in battery applications in the future, either in the form of special biomass-based materials or as precursors for fine chemicals or carbons. While inorganic materials are often preferable when it comes to high voltage or high energy density applications, the disadvantages in terms of sustainability can be completely circumvented by switching to fully bio-derived energy storage devices in the future.

References

1. Owusu, P.A., Asumadu-Sarkodie, S.: A review of renewable energy sources, sustainability issues and climate change mitigation. Cogent Eng. **3**, 1167990 (2016)
2. Guney, M.S., Tepe, Y.: Classification and assessment of energy storage systems. Renew. Sustain. Energy Rev. **75**, 1187–1197 (2017)
3. Behabtu, H.A., Messagie, M., Coosemans, T., Berecibar, M., Fante, K.A., Kebede, A.A., Van Mierlo, J.: A review of energy storage technologies' application potentials in renewable energy sources grid integration. Sustainability **12**, 1–20 (2020)
4. Chen, Y., Kang, Y., Zhao, Y., Wang, L., Liu, J., Li, Y., Liang, Z., He, X., Li, X., Tavajohi, N., Li, B.: A review of lithium-ion battery safety concerns: the issues, strategies, and testing standards. J. Energy Chem. **59**, 83–99 (2021)
5. Liedel, C.: Sustainable battery materials from biomass. Chemsuschem **13**, 2110–2141 (2020)
6. Hadjipaschalis, I., Poullikkas, A., Efthimiou, V.: Overview of current and future energy storage technologies for electric power applications. Renew. Sustain. Energy Rev. **13**, 1513–1522 (2009)
7. May, G.J., Davidson, A., Monahov, B.: Lead batteries for utility energy storage: a review. J. Energy Storage **15**, 145–157 (2018)
8. Borah, R., Hughson, F.R., Johnston, J., Nann, T.: On battery materials and methods. Mater. Today Adv. **6**, 100046 (2020)
9. Martins, V.L., Neves, H.R., Monje, I.E., Leite, M.M., Oliveira, P.F.M.D.E., Antoniassi, R.M., Chauque, S., Morais, W.G., Melo, E.C., Obana, T.T., Souza, B.L.: An overview on the development of electrochemical capacitors and batteries—Part II. **92**, 1–29 (2020)
10. Faria, R., Marques, P., Garcia, R., Moura, P., Freire, F., Delgado, J., De Almeida, A.T.: Primary and secondary use of electric mobility batteries from a life cycle perspective. J. Power Sources **262**, 169–177 (2014)

11. Greene JE (2014) Tracing the 5000-year recorded history of inorganic thin films from ∼3000 BC to the early 1900s AD. Appl. Phys. Rev. **1**, 041302 (2014)
12. Hu, X., Robles, A., Vikström, T., Väänänen, P., Zackrisson, M., Ye, G.: A novel process on the recovery of zinc and manganese from spent alkaline and zinc-carbon batteries. J. Hazard. Mater. **411**, 124928 (2021)
13. Zhao, Y., Pohl, O., Bhatt, A.I., Collis, G.E., Mahon, P.J., Rüther, T., Hollenkamp, A.F.: A review on battery market trends, second-life reuse, and recycling. Sustain. Chem. **2**, 167–205 (2021)
14. Chauhan, N.P.S., Jadoun, S., Rathore, B.S., Barani, M., Zarrintaj, P.: Redox polymers for capacitive energy storage applications. J. Energy Storage **43**, 103218 (2021)
15. B. Esser, F. Dolhem, M. Becuwe, P. Poizot, A. Vlad, D. Brandell, A perspective on organic electrode materials and technologies for next generation batteries. J. Power Sources **482**, 228814 (2021)
16. Wang, F., Ouyang, D., Zhou, Z., Page, S.J., Liu, D., Zhao, X.: Lignocellulosic biomass as sustainable feedstock and materials for power generation and energy storage. J. Energy Chem. **57**, 247–280 (2021)
17. Mateo, S., Peinado, S., Morillas-Gutiérrez, F., La Rubia, M.D., Moya, A.J.: Nanocellulose from agricultural wastes: products and applications—a review. Processes **9**, 1594 (2021)
18. Son, B.T., Long, N.V., Nhat Hang, N.T.: The development of biomass-derived carbon-based photocatalysts for the visible-light-driven photodegradation of pollutants: a comprehensive review. RSC Adv. **11**, 30574–30596 (2021)
19. Chakhtouna, H., Benzeid, H., Zari, N., el Kacem Qaiss, A., Bouhfid, R.: Hybrid materials from cellulose nanocrystals for wastewater treatment. In: Rodrigue, D., el Kacem Qaiss, A., Bouhfid, R.B.T.-C.N.H.N. (eds.) Cellulose Nanocrystal/Nanoparticles Hybrid Nanocomposites: From Preparation to Applications, pp. 115–139. Woodhead Publishing, UK (2021)
20. Zhang, T., Yang, L., Yan, X., Ding, X.: Recent advances of cellulose-based materials and their promising application in sodium-ion batteries and capacitors. Small **14**, 1–20 (2018)
21. Zhu, H., Luo, W., Ciesielski, P.N., Fang, Z., Zhu, J.Y., Henriksson, G., Himmel, M.E., Hu, L.: Wood-derived materials for green electronics, biological devices, and energy applications. Chem. Rev. **116**, 9305–9374 (2016)
22. Wang, Z., Lee, Y.H., Kim, S.W., Seo, J.Y., Lee, S.Y., Nyholm, L.: Why cellulose-based electrochemical energy storage devices? Adv. Mater. **33**, 1–18 (2021)
23. Gómez Cámer, J.L., Morales, J., Sánchez, L.: Nano-Si/cellulose composites as anode materials for lithium-ion batteries. Electrochem. Solid-State Lett. **11**, 101–104 (2008)
24. Wang, W., Li, T., Sun, Y., Liu, L., Wu, J., Yang, G., Liu, B.: Facile and mild method to fabricate a flexible cellulose-based electrode with reduced graphene and amorphous cobalt–iron–boron alloy for wearable electronics. Cellulose **27**, 7079–7092 (2020)
25. Liu, R., Ma, L., Huang, S., Mei, J., Xu, J., Yuan, G.: A flexible polyaniline/graphene/bacterial cellulose supercapacitor electrode. New J. Chem. **41**, 857–864 (2017)
26. Kim, M., Lee, C., Jang, J.: Fabrication of highly flexible, scalable, and high-performance supercapacitors using polyaniline/reduced graphene oxide film with enhanced electrical conductivity and crystallinity. Adv. Funct. Mater. **24**, 2489–2499 (2014)
27. Li, J., Klöpsch, R., Nowak, S., Kunze, M., Winter, M., Passerini, S.: Investigations on cellulose-based high voltage composite cathodes for lithium ion batteries. J. Power Sources **196**, 7687–7691 (2011)
28. Milczarek, G., Inganäs, O.: Renewable cathode materials from biopolymer/conjugated polymer interpenetrating networks. Science **335**, 1468–1471 (2012)
29. Gnedenkov, S.V., Zemnukhova, L.A., Opra, D.P., Sokolov, A.A., Minaev, A.N., Sinebryukhov, S.L.: Prospects of using lignin derivatives as organic electrode materials for lithium batteries, Defect Diffus. Forum **386**, 290–295 (2018)
30. Tian, J., Liu, Z., Li, Z., Wang, W., Zhang, H.: Hierarchical S-doped porous carbon derived from by-product lignin for high-performance supercapacitors. RSC Adv. **7**, 12089–12097 (2017)
31. Chakhtouna, H., Benzeid, H., Zari, N., Bouhfid, R., el kacem Qaiss, A.: Recent progress on Ag/TiO$_2$ photocatalysts: photocatalytic and bactericidal behavior. Environ. Sci. Pollut. Res. **28**, 44638–44666 (2021)

32. Chakhtouna, H., Mekhzoum, M.E.M., Zari, N., Benzeid, H., el kacem Qaiss, A., Bouhfid, R.: Biochar-supported materials for wastewater treatment. In: Inamuddin, T.A.R., Ahamed, M.I., Boddula, R. (eds.) Applied Water Science Volume 1: Fundamentals and Applications, pp. 199–225. Wiley, Hoboken (2021)

33. Conte, P., Bertani, R., Sgarbossa, P., Bambina, P., Schmidt, H.P., Raga, R., Lo Papa, G., Chillura Martino, D.F., Lo Meo, P.: Recent developments in understanding biochar's physical–chemistry. Agronomy **11**, 615 (2021)

34. Chakhtouna, H., Benzeid, H., Zari, N., el kacem Qaiss, A., Bouhfid, R.: Functional $CoFe_2O_4$-modified biochar derived from banana pseudostem as an efficient adsorbent for the removal of amoxicillin from water. Sep. Purif. Technol. **266**, 118–592 (2021)

35. Chen, L., Zhang, Y., Lin, C., Yang, W., Meng, Y., Guo, Y., Li, M., Xiao, D.: Hierarchically porous nitrogen-rich carbon derived from wheat straw as an ultra-high-rate anode for lithium ion batteries. J. Mater. Chem. A **2**, 9684–9690 (2014)

36. Li, S., Warzywoda, J., Wang, S., Ren, G., Fan, Z.: Bacterial cellulose derived carbon nanofiber aerogel with lithium polysulfide catholyte for lithium–sulfur batteries. Carbon N. Y. **124**, 212–218 (2017)

37. Zhang, T., Chen, J., Yang, B., Li, H., Lei, S., Ding, X.: Enhanced capacities of carbon nanosheets derived from functionalized bacterial cellulose as anodes for sodium ion batteries. RSC Adv. **7**, 50336–50342 (2017)

38. Gu, X., Wang, Y., Lai, C., Qiu, J., Li, S., Hou, Y., Martens, W., Mahmood, N., Zhang, S.: Microporous bamboo biochar for lithium-sulfur batteries. Nano Res. **8**, 129–139 (2015)

39. Lee, B., Ko, Y., Kwon, G., Lee, S., Ku, K., Kim, J., Kang, K.: Exploiting biological systems: toward eco-friendly and high-efficiency rechargeable batteries. Joule **2**, 61–75 (2018)

40. Ding, Y., Li, Y., Yu, G.: Exploring bio-inspired quinone-based organic redox flow batteries: a combined experimental and computational study. Chem **1**, 790–801 (2016)

41. Mauger, A., Julien, C., Paolella, A., Armand, M., Zaghib, K.: Recent progress on organic electrodes materials for rechargeable batteries and supercapacitors. Materials (Basel) **12**, 1–57 (2019)

42. Ravet, N., Michot, C., Armand, M.: Novel cathode materials based on organic couples for lithium batteries. MRS Online Proc. Libr. **496**, 263–273 (1997)

43. Kwon, J.E., Hyun, C.S., Ryu, Y.J., Lee, J., Min, D.J., Park, M.J., An, B.K., Park, S.Y.: Triptycene-based quinone molecules showing multi-electron redox reactions for large capacity and high energy organic cathode materials in Li-ion batteries. J. Mater. Chem. A **6**, 3134–3140 (2018)

44. Jing, Y., Liang, Y., Gheytani, S., Yao, Y.: Cross-conjugated oligomeric quinones for high performance organic batteries. Nano Energy **37**, 46–52 (2017)

45. Zhao, L., Wang, W., Wang, A., Yuan, K., Chen, S., Yang, Y.: A novel polyquinone cathode material for rechargeable lithium batteries. J. Power Sources **233**, 23–27 (2013)

46. Shimizu, A., Kuramoto, H., Tsujii, Y., Nokami, T., Inatomi, Y., Hojo, N., Suzuki, H., Yoshida, J.I.: Introduction of two lithiooxycarbonyl groups enhances cyclability of lithium batteries with organic cathode materials. J. Power Sources **260**, 211–217 (2014)

47. Sánchez-Díez, E., Ventosa, E., Guarnieri, M., Trovò, A., Flox, C., Marcilla, R., Soavi, F., Mazur, P., Aranzabe, E., Ferret, R.: Redox flow batteries: status and perspective towards sustainable stationary energy storage. J. Power Sources **481**, 228804 (2021)

Recent Developments in Organic Electrodes for Metal-Air Batteries

Morteza Moradi, Saeed Borhani, and Mehdi Pooriraj

Abstract Recently, the ongoing rapid development of electric transportation technology and stationary applications is the most important reason for the ever-increasing demand for advanced electrochemical energy storage devices. Metal-air batteries (MABs) are viewed as promising energy suppliers thanks to their advantages in terms of high theoretical energy density and safety. The electrode materials are the most important components, determining the performance of batteries and realizing their practical applications. Up to now, various types of air electrodes, such as noble metals and carbon-based materials, have been reported in MAB applications. Besides, on the anode side, coating and alloying strategies using metals and carbon materials have been employed to suppress the main issues like dendrite formation and corrosion of the anode. The attention rate on organic compounds as active materials are rising in energy storage devices due to their electrochemical performance, diversity in the structures, and flexibility. However, despite the many attempts toward using organic materials in MIBs, these materials are barely reported as electrodes for air batteries. In this chapter, a brief explanation of the MAB configuration and the reaction mechanisms at air electrodes is provided. Then, the most recent developments and progress of organic-based electrodes in these batteries are discussed.

Keywords Organic materials · Metal-air batteries · Air cathode electrode

1 Introduction

Owing to the huge energy consumption, and rapidly rising need for sustainable energy supplies, developing robust battery devices have been under development in recent years. MABs are promising candidates as reliable energy storage devices, owing to their safety, environmental friendliness, and high theoretical energy density. For example, lithium-air batteries (LABs) benefit from an outstanding theoretical specific

M. Moradi (✉) · S. Borhani · M. Pooriraj
Department of Semiconductors, Materials and Energy Research Center (MERC), Imam Khomeini Blvd, Meshkin-Dasht, Karaj P.O. Box: 31787-316, Islamic Republic of Iran
e-mail: m.moradialborzi@merc.ac.ir

energy density of 5000–11,000 Wh/kg depending on the nature of the electrolyte and discharged products, which is much advanced compared with other alternative rechargeable batteries and is about comparable to gasoline (13,000 Wh/kg). A comparison concerning the theoretical energy density of different available and under progress energy storage technologies are shown in Fig. 1 [1]. In MABs, the open-cell structure offers significantly larger energy densities than conventional batteries, because they have open-cell structures, allowing the continuous oxygen supply as a reactant from the air as an infinite external source to participate in storing energy at the cathode. Recently, many different chemistries based on (Li, Zn, Al, Mg, and Na)-air cells have been introduced for developing MABs.

In rechargeable MABs, during the operation of the battery, oxygen electrocatalysis reactions occur in alkaline or acidic media. However, as major challenges toward commercialization, most rechargeable MABs suffer from sluggish oxygen reduction reaction (ORR) and oxygen evolution reaction (OER) kinetics, and poor power capability. Self-discharging of the negative electrode, metal anode dendrite formation, charge overpotentials, and degradation of the battery compounds also can be assumed as general issues in MABs [2].

The most essential components that specify the performance of MABs are the air cathodes, and the catalytic activities of the oxygen catalysts. Generally, carbon-based materials, noble metals, metal oxides, and perovskite oxides, as well as organic materials can be employed as cathode catalysts in MABs [3]. To address current challenges regarding the design of air cathode materials, the most important properties to be considered are electrochemical stability, abundant accessibility, low cost, and efficient OER and ORR catalytic activities. For instance, during the oxidation of
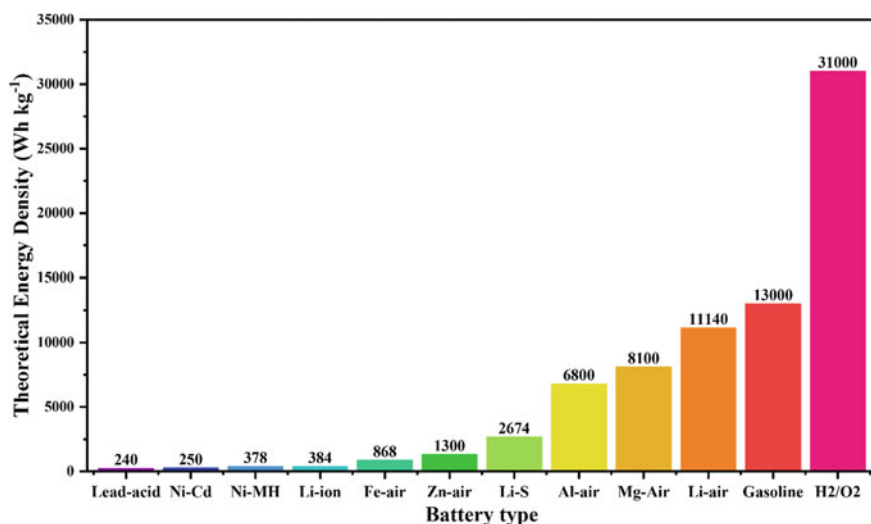
Fig. 1 A comparison of the theoretical energy density of different available and under progress energy storage technologies [1]

Li_2O_2, the decomposition of carbon-based electrodes at the voltages above the 3.5 V, is one of the major obstacles. By replacing carbon-based materials with carbon-free materials, undesired reactions due to carbon decomposition can be avoided. The coating of RuO_2 on the surface of carbon materials, for example, minimizes direct contact between the carbon and Li_2O_2, and improves the battery performance [4].
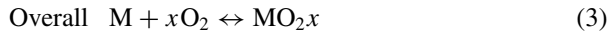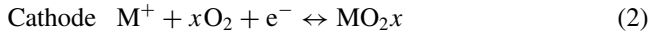
Organic materials including conducting polymers (CPs), metal–organic frameworks (MOFs), covalent organic frameworks (COFs), and organic carbonyl compounds have been barely explored in MABs up to this point, with much of the focus being on inorganic air-cathodes. Organic electrodes due to their easily accessible active sites for the adsorption of oxygen, high electronic conductivity, structural diversity, high surface area, and porosity are promising candidates in MABs [5]. Related to the anodes, mostly, metal plates are utilized in MABs. They benefit from high specific capacity, high reversibility, and low equivalent weight. Compared with MIBs, the solid electrolyte interphase (SEI) film is very complicated in MABs due to the higher amount of C, O, and different types of chemical species. Hence, the SEI film is unstable in MABs and affects negatively their performance. Organic materials and their compositions with other materials are promising candidates to solve the problems caused by unstable SEI films in the anode side of MABs [6]. For instance, Lee and coworkers fabricated a composite protective layer including Al_2O_3 and polyvinylidene fluoridehexafluoro propylene for Li metal anodes [7].

In this chapter, we will outline some of the most recent advancements in the design of organic electrodes for MABs. Firstly, the architecture of MABs will be briefly reviewed, as well as the role of catalytic reactions, occurring on-air electrodes. The most important organic electrodes that have been used in various MABs will then be introduced, along with relevant developments and obstacles.

2 Principle of MAB Configuration

A common MAB is constructed from a pure metal or metal alloy anode, a porous air cathode, a separator, and an ionic conducting electrolyte as shown in Fig. 2. The open cell structure of MABs enables the cathode to receive oxygen continuously from the air as an infinite external source. During discharge, metal ions (M^+) formed by oxidization of metal foils move through the electrolyte to the cathode to react with reduced O_2 molecules, forming metal oxides (MO_{2x}) and depositing on the cathode surface. The active material is adsorbed oxygen, which is reduced by accepting the electrons supplied from the anode with the help of oxygen catalysts, which reduces the amount of free energy required for oxygen reduction and speeds up the process. The positive electrode provides an electron pathway, ion pathway, and gas (O_2) pathway which is introduced in the MAB rather than an intercalation material in metal-ion batteries (MIBs). The reactions are reversed during the charging process, and metal ions move back to the anode, where they will be reduced to metal, on the opposite site O_2 will be produced at the cathode [8]. The reactions can be described as follows:

Fig. 2 Illustration of a typical MAB consisting of pure metal or metal alloy electrode as the anode, a porous air cathode, a separator, and an ionic conducting electrolyte in the discharge process

$$\text{Anode}\quad \text{M(S)} \leftrightarrow \text{M}^+ + \text{e}^- \tag{1}$$

$$\text{Cathode}\quad \text{M}^+ + x\text{O}_2 + \text{e}^- \leftrightarrow \text{MO}_2x \tag{2}$$

$$\text{Overall}\quad \text{M} + x\text{O}_2 \leftrightarrow \text{MO}_2x \tag{3}$$
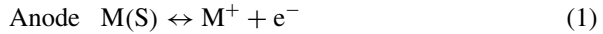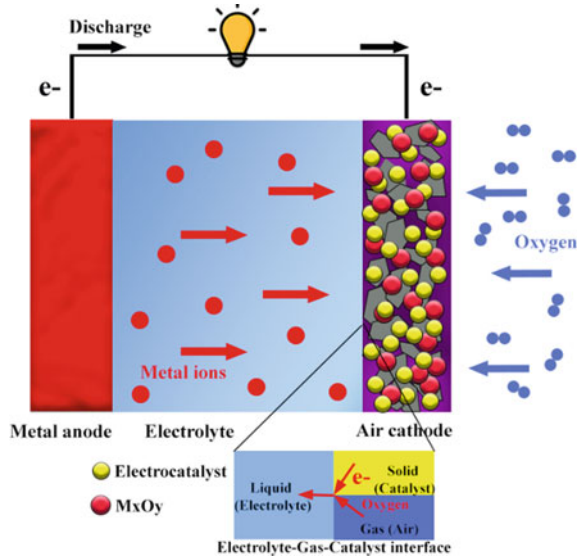
MABs can be classified into two categories: aqueous electrolyte-based devices that are moisture insensitive, such as the Zn-air battery (ZAB), and organic electrolyte-based batteries, such as Li–O$_2$ batteries, that are damaged by moisture because of their metal foils that are sensitive to water. Metal foils made of Zn, Mg, Ca, Al, and Fe are currently employed as anodes in aqueous MABs. Mg-air and Al-air batteries have provided theoretical specific energy densities of 8100 and 6800 Wh/kg, respectively, compared to ZABs, which have shown a theoretical specific energy density of 1300 Wh/kg [9]. However, these batteries suffer from high self-discharging, low coulombic efficiency, and high polarization, which hinder their potential applications. Furthermore, in both of these batteries having a fast and stable recharge process is difficult after discharging. Therefore, among all kinds of batteries, Zn-air and non-aqueous LABs as highly rechargeable MABs are receiving more and more attention for future applications.

The most common electrochemical reactions in rechargeable ZABs with an alkaline electrolyte and LABs with a non-aqueous electrolyte are shown as the following equations. For the ZABs [10]:

The Zn foil can be oxidized in the discharge process at the anode:

$$Zn + 4OH^- \rightarrow Zn(OH)_4^{2-} + 2e^-$$
$$E^0 = -1.250\,\text{V vs. SHE} \tag{4}$$

$$Zn(OH)_4^{2-} \rightarrow ZnO + H_2O + 2OH^- \tag{5}$$
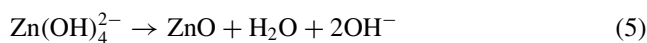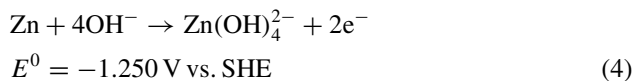
A four-electron reaction pathway at cathode side is:

$$O_2 + H_2O + 4e^- \rightarrow 4OH^-$$
$$E^0 = +0.401\,\text{V vs. SHE} \tag{6}$$

The discharge's overall reaction process is:

$$2Zn + O_2 \rightarrow 2ZnO \tag{7}$$

Through the charging process, ZnO will be reduced to Zn:

$$2ZnO \rightarrow 2Zn + O_2 \tag{8}$$

In LABs, the reactions in anode and cathode parts are [8]:

$$Li_s \leftrightarrow Li^+ + e^- \tag{9}$$

At the cathode, oxygen is reduced in a two-electron:

$$Li^+ + \frac{1}{2}O_2 + e^- \leftrightarrow \frac{1}{2}Li_2O_2 \tag{10}$$
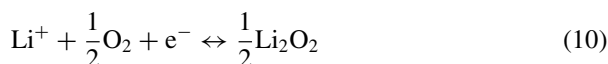
or four-electron reactions:

$$Li^+ + e^- + \frac{1}{4}O_2 \leftrightarrow \frac{1}{2}Li_2O \tag{11}$$
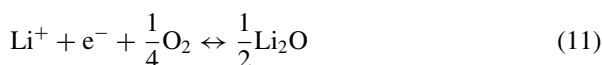
Then, generally, two possible energy-producing reactions in a LAB are:

$$Li^+ + \frac{1}{2}O_2 \leftrightarrow \frac{1}{2}Li_2O_2$$
$$E^0 = +2.959\,\text{V} \tag{12}$$

$$Li^+ + \frac{1}{4}O_2 \leftrightarrow \frac{1}{2}Li_2O$$
$$E^0 = +2.913\,\text{V} \tag{13}$$
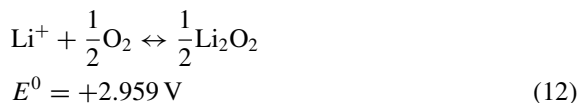
In respect to the developments of air cathodes, two parts should be considered: developing novel porous structures as substrates for oxygen catalysts and configurations of the air cathodes, which is exceedingly similar to the technologies used in fuel cells, and focusing on ORR and OER catalysts with proper oxygen catalytic activities. As a result, the ORR and OER processes are two critical factors that determine the capabilities of MABs.

3 Organic Electrodes for MABs

3.1 Organic-Based Cathode Materials

Generally, organic electrode materials have a great potential to be used in electrochemical applications because of their attractive properties. First, they are inexpensive due to their abundance; also, they can be collected naturally, making them environmentally beneficial. Second, the soft structure of organic materials offers promising potential to design flexible battery systems, including flexible MABs. Furthermore, organic electrode materials, unlike inorganic materials, can be utilized in various MABs since these materials are not limited by choice of counter-ions like MIBs, cathode, or anode materials in MABs can be developed by organic materials such as organosulfides, carbonyl compounds, radical polymers, CPs, MOFs, and COFs [11]. However, such organic materials as electrodes have been reported barely in MAB applications and there are just some reports in using CPs, MOFs, and COFs.

3.1.1 Conducting Polymers (CPs)

Among organic materials, CPs have been attracted much more attention as one of the most promising electrode materials for various electrochemical energy storage systems thanks to their flexibility, excellent electrical conductivity, structural diversity, and ability to participate in redox reactions. CPs are described by a polymer backbone composed of altering single and double bonds. After the discovery of CPs by Shirakawa with synthesizing polyacetylene, the possible use of CPs as electrode materials to store electricity was demonstrated by MacDiarmid [12]. Since then, many kinds of organic electrode materials based on CPs have been reported for rechargeable batteries. The most interesting CPs for battery applications are polyaniline (PANI), poly (3, 4-ethylene dioxythiophene) (PEDOT), and polypyrrole (PPy) [13]. Lu and co-workers for the first time investigated a water-dispersed PANI nanofibers cathode for LAB [14]. The battery with lithium film as the anode, PANI nanofibers, and 1 M LiBF$_4$ electrolyte delivered a high discharge capacity of 3280 mAh/g at the current density of 0.05 mA/cm^2 at the first cycle, and it maintained an approximate 1000 mAh/g at 0.5 mA/cm^2 (Fig. 3a). In addition, as seen in Fig. 3b, after initial degradation during the first three cycles, the battery kept 96% of its
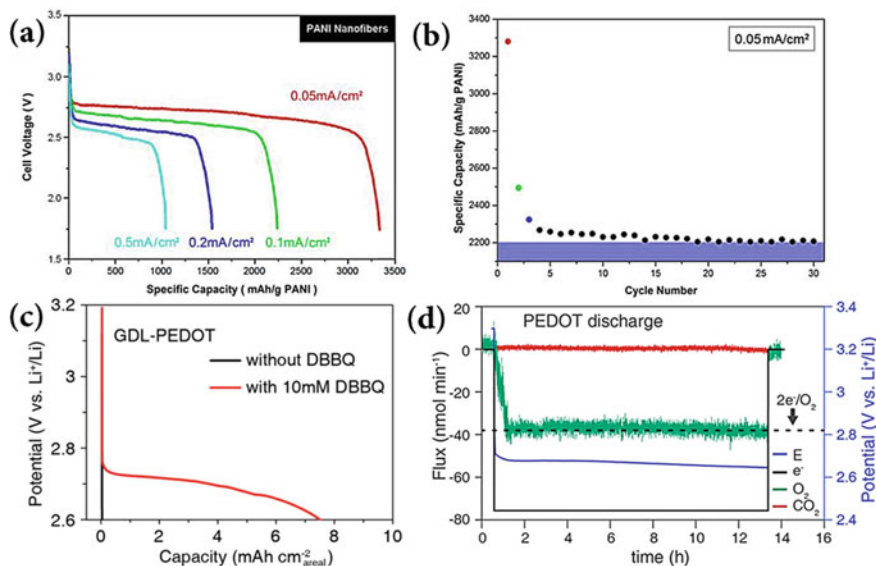
Fig. 3 **a** Discharge curves of PANI nanofibers at different current densities. **b** Discharge curves versus cycle number for Li–O_2 battery based on PANI nanofibers cathode at current density of 0.05 mA/cm^2. Adapted with permission from reference [14], Copyright 2013, American Chemical Society. **c** Discharge profile of PEDOT-, PPY-, and PANI-coated GLD electrodes in 0.5 M LiTFSI-tetraglyme with 10 mM DBBQ and no DBBQ at a current density of 0.2 mA/cm^2 under O_2. **d** In situ DEMS of the first discharge/charge cycle for PEDOT-coated GDL electrode. Adapted with permission from reference [16], Copyright 2020, American Chemical Society

discharge capacity in the next 27 cycles. Cui et al. [15] proposed a self-assembly method to synthesize porous PANI/rGO nanocomposites with different rations of PANI contents (PPGF-30, 30% PANI, PPGF-50, 50% PANI and PPGF-70, 70% PANI). The results show that the PPGF-50 electrode has indicated higher ORR onset potential, lower OER onset potential, as well as larger redox current peaks than that of the other electrodes (PPGF-30 and PPGF-70). These results suggest that the PPGF-50 delivers higher catalytic activity with the reversible generation and decomposition of Li_2O_2 species through the charge/discharge process. In addition, the performance of the optimized PPGF-50 sample was compared with unmixed rGO and PANI, to show the composition effect of PANI and rGO. The pure rGO has a high charge overpotential of 1.29 V, owing to the low catalytic activity of rGO. In contrast, the charge–discharge overpotential for the PPGF-50 is 150 mV, which confirms the beneficial effect of introducing PANI into the cathode. The superior performance for the PPGF-50 electrode, such as the high discharge capacity (36,010 mAh/g at 200 mA/g), low overpotential, and long cyclic life, suggests that the PPGF-50 is an outstanding air cathode for Li–O_2 batteries. These results are ascribed to the synergistic effect of the PANI-rGO composite that improves the electrocatalytic activity as well as the diffusion of oxygen and electrolyte species.

Utilizing CPs as coating layers is an effective approach to designing organic carbon-based cathode materials. In this context, Cao et al. [16] coated PEDOT, PPy, and PANI on a carbon substrate to fabricate three polymer-coated gas diffusion layer (GDL) electrodes. Based on discharge profiles (Fig. 3c), in the presence of a reduction mediator, 2,5-diterbutyl-1,4-benzoquinone (DBBQ) in an electrolyte, the electrode containing PEDOT delivered a higher discharge capacity (7 mAh/cm^2) than other electrodes. The in-situ differential electrochemical mass spectroscopy (DEMS) confirmed the reversible formation and decomposition of Li_2O_2 for the PEDOT cathode, during the charging and discharging processes. Based on Fig. 3d, oxygen consumption was observed without any detection of other gasses. The electron to O_2 (e^-/O_2) ratios for discharge and charge processes were obtained 2.03 and 2.19, respectively, suggesting a good reversible Li_2O_2 decomposition process, which indicates good bifunctional oxygen electrocatalytic performance of the PEDOT-coated carbon cathode. The synergetic effective porosity of CP/carbon cathodes enables these kinds of cathode electrodes to provide high volumetric performance. For instance, PPy@AGCA (activated graphene–carbon aerogel) reported cathode to deliver a high volumetric capacity of 450 mAh/cm^3, which was 1.3–5 times higher than that of other carbonaceous cathodes with the capacity of 90.3–341 mAh/cm^3 [17]. Due to high nitrogen content and ease of synthesizing, PPy and PEDOT enhanced the reaction kinetics and eliminated the side reactions as metal-free electrocatalysts. For example, carbon-free polymer air electrodes based on PEDOT microparticles have been successfully utilized in LABs by Yoon et al. [18]. The electronic conductivity of PEDOT microparticles has been modified by H_2SO_4 treatment. The results showed that H_2SO_4-treated PEDOT delivered the stable initial 3000 mAh/g of capacity.

Furthermore, compared with pure carbon cathode, the H_2SO_4-treated PEDOT microparticles exhibited long cyclic life (263 cycles), and the capacity at a current density of 200 mA/g was set at 1000 mAh/g, without the introduction of redox mediators into the electrolyte. The improved cyclic performance of H_2SO_4-treated PEDOT was because this electrode could suppress side reactions and the accumulation of unwanted reaction products such as CH_3CO_2Li and Li_2CO_3.

Recently, Xie and co-workers developed a polymer cathode for a multimode-switching zinc battery [19]. A well-designed polyaniline-nanorod-array-based "all in one" cathode was able to switch battery mode from Zn-polymer to Zn-air system. The multifunctional battery was developed based on an "all in one" cathode including nanostructured PANI arrays active layers lined up on carbon cloth as a substrate (PANINA/CC), possessing a high oxygen reduction catalytic activity, reversible redox capability, and convenient photothermal sensitivity. The constructed Zn-PANI battery represented a specific capacity as high as 430.0 mAh/g and was able to be a light-sensitive primary ZAB. A rechargeable ZAB also was fabricated, comprising of PANINA/CC cathode and metallic Zn anode in an aqueous solution of $ZnCl_2/NH_4Cl$ as the electrolyte. The battery with a transparent air barrier layer was able to work in three modes, including a rechargeable Zn-polymer, a self-charging Zn-polymer battery, and a primary battery.

3.1.2 MOFs

As a kind of coordination polymers, MOFs are porous crystalline materials with unique characteristics, including high specific surface area, tunable structures, abundant catalytic sites, and redox-active sites, making them attractive materials for gas capture, catalysis, and energy storage [20–22]. MOFs are mostly created by the connection of metal centers or metal clusters with organic ligands to construct extended coordination networks. Owing to the configuration of transition metals, like Ni, Co, Zn, and Fe, and heteroatom-rich organic chemical ligands, MOFs are attractive bifunctional catalysts for MABs. In terms of the composition of catalysts, recent developments of MOF-based materials in MABs are classified into two types: (1) pristine MOFs, (2) MOF-derived materials, including carbon, metal oxides, and sulfides materials. MOFs are often going under thermal pyrolysis and calcination to improve electrochemical performance and increase conductivity. However, the decomposition of MOFs by such methods causes a dramatic decrease in their surface area. This method additionally affects the well-defined MOF structures and transfers a large number of active metal centers into the bulk phase and blocks reactant access to the reactive centers [23]. Hence, improving the conductivity of pristine MOFs based on the fundamental structures and in composition with conductive agents can be considered as alternative approaches. In the following, we will focus on the applications of pristine MOFs as bifunctional electrocatalysts in MABs. For example, Pan and coworkers used a hydrothermal synthesis approach to fabricate a Ru doped conductive 2D MOF $[Ni_6(HHTP)_3(H_2O)_x]_n$ (HHTP = 2,3,6,7,10,11-hexahydroxyltriphenylene) and reported it as air cathode electrocatalyst for a solid-state ZAB [24]. MOFs with porous channels were crystallized in the trigonal space group of P3c1 with ABAB stacked layers. The A layers are formed by a set of 2D extended hexagon $[(NiRu)_3(HHTP)_2(H_2O)_x]_n$ linked by the coordination of HHTP and Ni^{2+}/Ru^{3+}, while the B layers are formed by a set of 0D fragments $[(NiRu)_3(HHTP)(H_2O)_x]$. The characterization results demonstrate that MOFs $[Ni_{5.7}Ru_{0.3}(HHTP)_3(H_2O)_x]_n$ have a higher conductivity (0.05 S/m) than standard MOFs (10^{-8} S/m) because of the modest amount of Ru as a dopant and the unusual 2D structure. ORR activity of 2D MOF $[Ni_{5.7}Ru_{0.3}(HHTP)_3(H_2O)_x]_n$ revealed that the number of transferred electron (n) for $[Ni_{5.7}Ru_{0.3}(HHTP)_3(H_2O)_x]_n$ was around 3.5, indicating approximately $4e^-$ processes toward the ORR. The ORR catalyst $[Ni_{5.7}Ru_{0.3}(HHTP)_3(H2O)_x]_n$ was used to fabricate an all-solid-state ZAB and it provided a high specific capacity of 654 mAh/g at a current density of 5 mA/cm^2 and impressive durability after 200 cycles, suggesting the excellent catalytic activity and promising performance of this catalyst to both ORR and OER in the air electrode of the ZABs.

Adopting bimetallic or multivariate MOFs is another way to design catalysts from MOFs or fabricate active electrode materials for energy storage applications. For example, compared with monometallic MOFs, bimetallic MOFs display better electrocatalytic and electrochemical performance in advanced electrochemical devices. This can be explained by the synergistic effect between different metals and the stronger valence state of metal sites, which plays an important

role in enhancing catalytic performance. Kim's group reported a bimetallic MnCo-MOF-74 material, synthesized by hydrothermal method, as a cathode catalyst in LABs [25]. The cathode electrode was fabricated by slurry consisting of 40 wt% bimetallic MnCo-MOF-74 as the catalyst, 40 wt% ketjen carbon black (K-CB), and 20 wt% PVDF. The cell was assembled in the coin-type Li–O_2 battery with a glass fiber separator, a lithium foil anode, and tetraethylene glycol dimethyl ether electrolyte with 1.0 M bis(trifluoromethane)sulfonamide lithium salt (LITFSI). The bimetallic MnCo-MOF-74 cathodes delivered ultrahigh full discharge capacity of 11,150 mAh/g at the current density of 200 mA/g, and a limited discharge capacity of 1000 mAh/g for 44 cycles, indicating an excellent cyclability, which was significantly longer than monometallic MOFs (Mn-MOF-74, Co-MOF-74). The more high-grade performance of bimetallic MOFs originates from the fact that Mn-MOF-74 promotes the transportation of Li_2O_2 to LiOH products while cannot decompose it sufficiently. In contrast, Co-MOF-74 completely decomposes LiOH to form Li_2O_2 discharge products, but it suffers from low reversibility. The complementary function of Mn and Co metal clusters in MnCo-MOF-74 modifies the reversibility of formation and decomposition of discharge products, which leads to significant improvement in cyclic stability and catalytic durability of Mn-Co-MOF-74.

To boost the electrocatalytic activity of MOFs, these materials can be composited with graphene oxide (GO). Not only GO has good ion conductivity, but also its epoxy and hydroxyl functional groups can be used to fix metal ions in MOFs. For example, Xiao et al. [26] employed a simple in-situ growth of bimetallic ZnCo-zeolite imidazole framework@graphene oxide (ZnCo-ZIF@GO) for an air cathode for ZABs. Due to the synergistic effect of ZIF and GO, the ZnCo-ZIF@GO shows more catalytic active sites and higher ion conductivity than the pure ZnCo-ZIF, leading to excellent improvement in electrocatalytic activities.

3.1.3 COFs

Like MOFs, porous COFs with a high surface area can be widely applied in electrochemical energy storage and conversion devices. Although the chemical reactions occur on the surface of electrodes, the active species also cross from membranes through voids, and therefore, porosity and high surface area play essential roles in developing advanced electrochemical devices. As a subclass of porous polymers, COFs are constructed from organic building blocks linked via covalent bonds, forming an open framework, wherein their backbones are comprised of light elements, like C, N, O, and B. Although Yaghi and coworkers' initial COFs (COF-1 and COF-5) were not even water stable, the exclusive covalent connections may result in COFs with excellent stability under acidic and basic conditions during the continuous development of these materials [27]. In COFs, building blocks and linkage motifs allow building materials with defined chemical structures in the backbones, tuning their pores' size and geometry properties and predicting microstructures and nanochannels for ion diffusion and access to active sites help to modify the chemical and physical properties of the COFs. For example, bipyridines and porphyrins

as nitrogen-containing ligands provide metal incorporation within COFs, offering single-atom metal catalysts for electrocatalysis applications [28]. Introducing redox-active sites in the structures of COFs improves the reversible process in secondary batteries and provides fast kinetics, leading to improvement in capacity. In addition, the extensive conjugation of COFs allows the integration of carbon-based materials such as carbon nanotubes and graphene with COFs through non-covalent interactions, promoting the electrocatalytic performance of COFs/carbon materials compositions. COFs based on the geometric symmetry of their building blocks can be form 2D and 3D structures. 2D COFs, linked by weak van der Waals' force and 2D sheets, form a layered structure by π-π interaction. 2D COFs provide low resistance and also the possibility to control the thicknesses. This feature gives access to few-layer thick nanosheets, which are desirable for battery applications. In 3D COFs, expanded networks in three-dimensional space are formed via building blocks consisting of sp^3 carbon, silane, or boron atoms. There is a remarkable possibility to the structural design of COFs, resulting in considerable attention to use COFs in different battery applications, such as Li-ion batteries (LIBs), zinc-ion batteries (ZIBs), and ZABs. Mainly, COFs are obtained from linking groups, including boroxines, triazines, imines, and hydrazones. For example, COF-based metal-free and/or metal-containing materials, such as polychlorotriphenylmethyl (PTM) radical-based π-conjugated covalent organic radical framework (PTM-CORF), iron-containing bipyridine-COF, porphyrin based 2D covalent organic framework (ZnP-COF), and metalloporphyrin-TTF based COFs can be used as electrocatalysts and active materials for ZABs. Hu et al. [29] reported a COF (HCCP-SA) composed from hexachlorocyclotriphosphazene (HCCP) and dicyanamide (SA) to obtain a set of N, P codoped-carbon nanotubes (CNTs) as metal-free ORR catalysts. Different N, P CNTs named as 700-N, P-CNT, 800-N, PCNT, and 900-N, P-CNT, are fabricated by pyrolysis of HCCP-SA at 350 °C and subsequently calcination at 700, 800, and 900 °C, respectively (Fig. 4a). Using N, P COF coated on carbon nanotubes aids the dispersion of N and P dopants on carbon nanotubes and potentially provides additional catalytic active sites. As seen in Fig. 4b, based on the line scene voltammetry (LSV), 800-N, P-CNT with half-wave potential at −0.162 V shows better electrocatalytic performance. Furthermore, the ZAB containing 800-N, P-CNT as air electrode (Fig. 4c) was assembled and possessed a high voltage range of 1.53 V with good stability at current densities, ranging from 5 to 50 mA/cm^2. Depending on metal species, the electrochemical properties of COFs can be modified and indicate various unique electrocatalytic functions. For example, doping Pt nanoparticles and high conductive Cu or Ag nanoparticles boost the activity and conductivity of COFs toward electrochemical reduction/evolution, respectively [30]. Chen's group prepared a graphydine-like Co-porphyrin COF (Co-PDY) electrocatalyst for oxygen evolution reaction. Co-PDY displayed an excellent catalytic performance for OER with a low overpotential of 270 mV at 10 mA/cm^2 and long-term stability and durability with electrocatalytic current retention of 97.9% after 20 h [31].
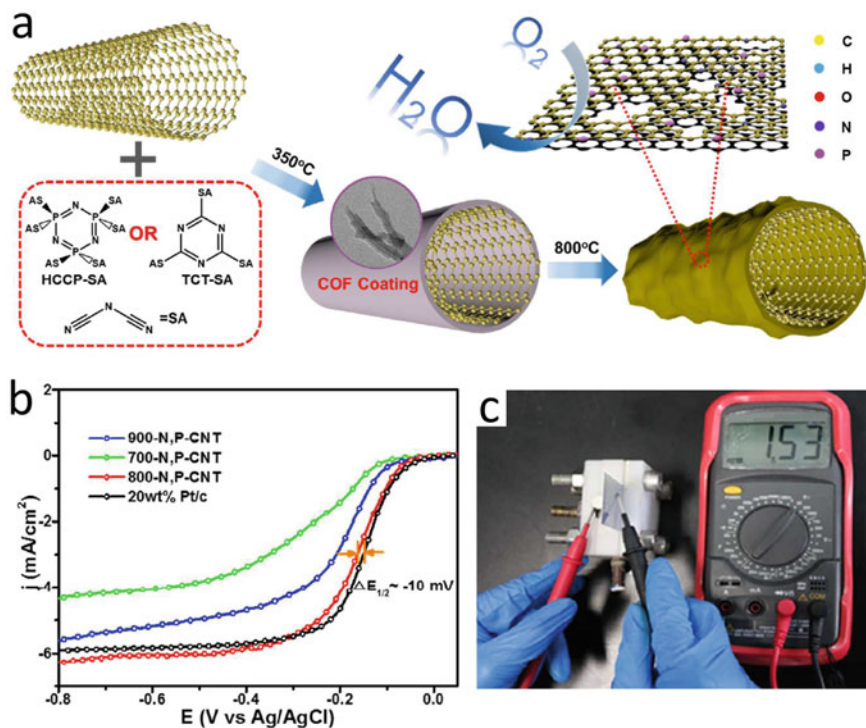
Fig. 4 **a** Schematic illustration of the preparation of 800-N, P-CNT. **b** LSV curves of 700-, 800-, 900-N, P-CNT and Pt/C at a rotation rate of 1600 rpm. **c** Fabricated ZAB and corresponding open-circle potential (OCP). Adapted with permission from reference [29], Copyright 2011, The Royal Society of Chemistry

3.1.4 Bioresource-Derived Polymer Composites

Renewable biomass compounds are favorable abundant precursors to synthesize biopolymers and carbon materials. Biomass precursors from the remains of animal-based, plant-based, and microorganisms have various chemical components [32]. Biomass compounds mainly contain carbohydrates and polysaccharides bioresources, such as cellulose, lignin, chitin, and proteins, which can be extracted as biopolymers for energy storage applications. For example, cellulose with a linear chain of "β-1,4 linked D-glucose" units can be extracted from waste straw or wood. This biopolymer due to its excellent mechanical properties has been used to prepare a gel polymer electrolyte for a LIB by Du et al. [33]. Mostly, biomass materials, which contain biopolymers are bioprecursors have attracted too much attention for preparing carbon materials as an electrode for battery and supercapacitor application since they are rich in carbon compounds and large amounts of H, O, N, and other mineral elements of S, K, Mg, N, and Si. Wang et al. [34] prepared a Cu atom anchored O, N doped porous carbon air electrode for a flexible ZAB by pyrolysis
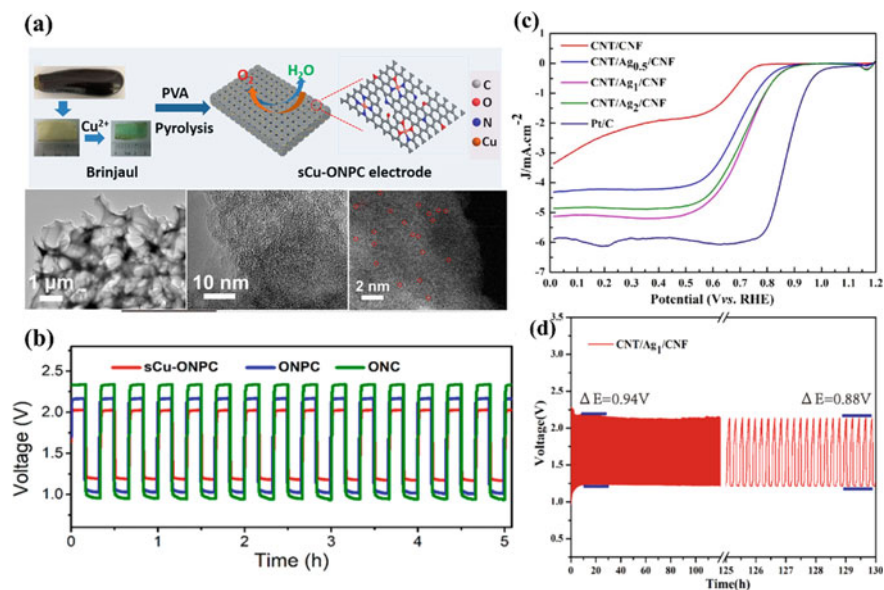
Fig. 5 **a** Synthesis process of sCu-ONPC electrode and the structural images of the electrode based on TEM, HRTEM, and STEM. **b** Charge–discharge cycling performance of constructed ZABs at a current density of 5.0 mA/cm² using sCu-ONPC, ONC, and ONPC air electrodes. Adapted with permission from reference [34], Copyright 2019, American Chemical Society. **c** LSV plots of CNT/CNF, CNT/Agx/CNF, and commercial Pt/C for ORR at a rotation of 1600 rpm. **d** Charge–discharge profiles of the liquid ZAB with CNT/Ag1/CNF air cathode during 130 h. Adapted with permission from reference [35], Copyright 2021, American Chemical Society

treatment of biomass polymer/brinjaul at 800 °C under nitrogen gas (Fig. 5a). The sCu-ONPC electrode exhibited outstanding bifunctional ORR/OER electrocatalytic performance with a half-wave potential value of 0.79 V. A constructed solid-state rechargeable ZAB based on sCu-ONPC air electrode exhibited high stability during 5 h cycling test (Fig. 5b). The unique 3D porous structure with large mesoporous linked voids provides large amounts of active sites for gas-phase O_2 and a high flux of air and electrolytes. Biopolymers can be directly used as support and scaffold for fabrication of electrodes, improving the ORR performance of nanoparticles, and reducing the polarization on the air electrode, because these polymers have excellent adhesion properties, high oxygen densities due to the hydroxyl groups in their structures, and high surface areas. Shengjuan Li and co-workers prepared an Ag nanoparticle-loaded cellulose nanofibers/CNT composite (CNT/Ag/CNF) as a cathode for a flexible ZAB. An optimized amount of silver nanoparticles enhanced the electrical conductivity of CNT/Ag1/CNF (293.2 ± 32.8 S/m) compared to the CNT/CNF electrode (33.0 ± 1.7 S/m). On the other hand, CNF with its high mechanical properties boosted the flexibility of the electrode. As seen in Fig. 5c, the ORR performance of the optimized CNT/Ag1/CNF with a high onset potential of 0.874 V is

also comparable with Pt/C electrocatalyst. CNT/Ag$_1$/CNF air cathode-based-liquid ZAB delivered ultrahigh cyclic stability during 130 h cycles (Fig. 5d) [35].

3.2   Organic Anode Electrodes for MABs

For developing MABs, the vast majority of attention has been paid to air electrode materials, such as noble metals, metal oxides, carbon materials, organic materials, etc. However, there are inevitable issues attributed to the metal anodes in relevant MABs that should be taken into account. The hydrogen evolution corrosion, dendrite formation, and passivation are major challenges that hinder the performance of metal anodes. For example, spontaneous hydrogen evolution reaction between metal and electrolyte courses hydrogen generation and permeation of hydrogen spices in electrode, resulting in electrode corrosion and subsequently reducing the activity of metal anode [36]. Alloying metal anodes with various elements like Mn, C, and Mg can increase the activity of metal anodes and impede the formation of passive layers [37]. Protective conductive layers including carbon materials and polymers protect metal anodes from corrosion and H$_2$ evolution, and simultaneously, these materials improve the conductivity of anode electrodes. Al-air batteries (AABs) have high theoretical specific energies and low cost, however, the formation of Al(OH)$_3$ spices as passive layers trigger the failure during operation and this should be addressed. Deyab's group suggested coating nanocomposites of polyaniline and carbon nanofibers (PANI@XCNF) with different ratios of CNFs on Al anode via electro-deposition method to hinder passive layer and hydrogen gas evolution. Experimental polarization curves of Al and Al/PANI@XCNF in corrosive alkaline solution (4.0 M KOH) indicated that PANI@XCNF protective layers hinder the corrosion reactions [38]. The AAB with a protective layer on the Al anode displayed better performance in terms of stability, capacity, and energy density than that of the battery with intrinsic Al anode. Conductive nanocomposites by forming a physical barrier between the Al electrode and the alkaline electrolyte protect the Al anode from corrosion and decrease the hydrogen evolution. Plus, by providing a conductive pathway, the composition of PANI and CNFs improved the electrical conductivity of the anode. Related to the PANI and CNF nanoparticles, they complement each other since PANI provides a homogenous environment for the unique dispersion of CNFs. On the other hand, CNF nanoparticles inside the PANI texture can heal PANI defects, which act as a diffusion path for the aggressive ions. Buonaiuto and co-workers coated a vinylsilane-substituted on the surface of Li metal by polymerization [39]. Impedance spectroscopy data of electrodes revealed that the stable film of vinyl-substituted silane was formed on Li anode and the cycling tests indicated that the organic layer improved the stability of Li metal, especially in the first 50 cycles in an electrochemical cell.

As shown in Fig. 6a, Lee and co-workers reported a 20 PANI coated on zinc anode to suppress self-discharging, corrosion reactions, and HER in ZAB [40]. The lower corrosion current density of 20PANI-coated Zn than pure Zn anode means that
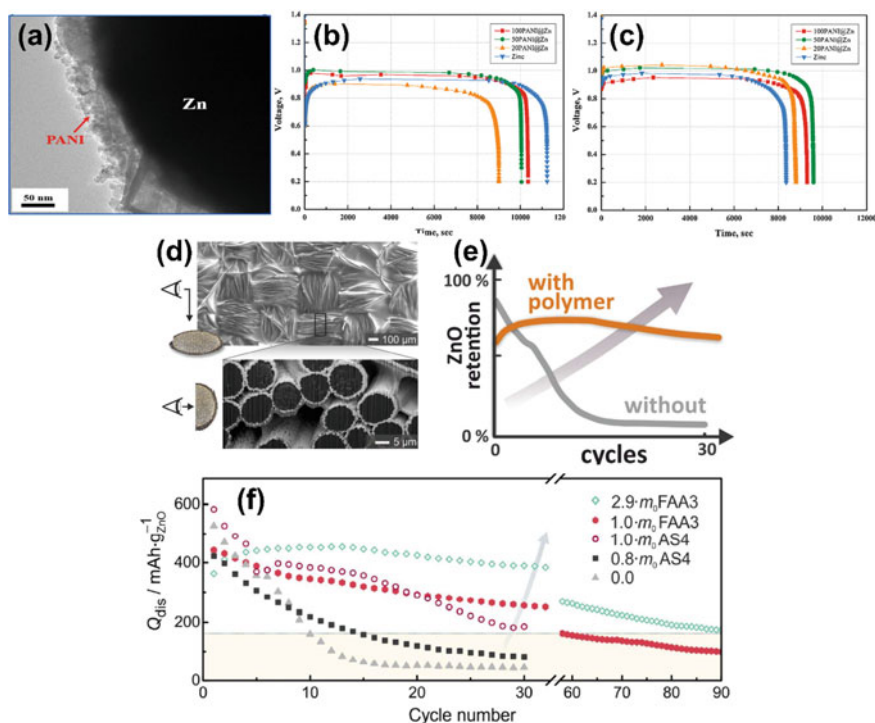
Fig. 6 **a** FE-TEM image of 20PANI@Zn. The electrochemical potential profile of PANI@Zn electrodes and pure Zn electrode, **b** no storage and **c** after storage. Adapted with permission from reference [40], Copyright 2017, Elsevier. **d** The SEM image of IHCP-coated ZnO/C electrode. **e** The stability of uncoated ZnO and IHCP-modified ZnO. **f** Specific discharge capacity of IHCP-modified Zn anodes with different amounts of the IHCPs versus cycle number. Adapted with permission from reference [41], Copyright 2018, American Chemical Society

the PANI layer limits the electrolyte diffusion throughout the zinc particles; then, PANI coating decreases the corrosion of Zn anode in KOH solution. To evaluate self-discharge behavior of ZABs, including PANI-coated Zn anode and uncoated Zn-anode, the measured capacity retention of batteries after 24 h of storage against no-storage conditions at ambient temperature showing that 20PANI@Zn materials had capacity retention of 97.81% which is higher than that of Zn anode (74.40%). However, PANI as a corrosion inhibitor harms the battery performance before storage since the Zn anode can deliver a higher specific discharge capacity than 20PANI@Zn anode (Fig. 6b, c) [40]. Schröder and co-workers fabricated HPC-modified Zn anodes (Fig. 6d, e) to reduce the insulating effect of ZnO layers, leading to high retention and utilization of the active materials [41]. The thickness of the polymer layer has been optimized to reach a proper ion transport and sufficient $[Zn(OH)^4]^{2-}$ confinement to achieve high retention of the active materials during cycling (Fig. 6f). In addition, the average utilization of the anode active materials for IHCP-coated anodes (36.1–50.6%) was calculated, indicating a significant improvement compared with bare Zn

anode (23.3%). According to the mentioned results, it can be concluded that using CPs as protective layers on Zn anodes is a practical approach to enhance the cycling durability of ZABs.

4 Summary

Rechargeable MABs are one of the most important devices to meet the ever-increasing demand for the next generation of energy suppliers, thanks to their ultrahigh-energy densities. However, the commercialization of these batteries is hindered by various technical issues, such as poor intrinsic oxygen catalytic activity, sluggish kinetics, and limited cyclic stability. These issues generate from some challenges toward air cathodes, electrolytes, and metal anodes, such as passivation and pore blockage by insulating discharge products, limited diffusion of reactants to the catalytic active sites, dendrite formation, and high charge overpotentials. Developing catalysts and support materials for air cathode and boosting metal anodes are crucial to obtaining advanced MABs by overcoming the mentioned challenges. Organic electrode materials profit from various advantages, such as lightweight, structural diversity, and comprehensive electrochemical properties, making them highly suitable for sustainable energy storage devices. Due to the boom in electronic devices and electric vehicle technologies during recent years, besides inorganic materials, organic-based electrode materials have been widely studied for MIBs. However, just a few classes of organic materials have been reported in a few types of MABs. In this chapter, we have focused on the applications of organic materials, including CPs, MOFs, and COFs in LABs and ZABs as the most common MABs. After a brief explanation of the basic principle of MABs and reactions' mechanisms, the recent developments toward utilizing organic materials in air cathode electrodes have been discussed. Meanwhile, we also discussed applying organic materials in metal anodes to suppress major issues like dendrite formation, passivation layers, and hydrogen evolution corrosion during battery operation. Although valuable developments have been achieved related to the usage of organic electrode materials in MABs, covering the full potentials of these materials as electrodes in different kinds of MABs should be continued to reach practical applications. Organic materials also suffer from major challenges, such as low electronic conductivity, insufficient ORR/OER catalytic activities, and high solubility in electrolytes, hindering their applications in MABs. In this context, combining with other materials like carbon structures and metal oxides to use synergistic effects, structural engineering, developing all-solid-state electrolytes, and employing electrolyte additives would be effective strategies to address the present issues.

References

1. Zhu, A.L., Wilkinson, D.P., Zhang, X., Xing, Y., Rozhin, A.G., Kulinich, S.A.: Zinc regeneration in rechargeable zinc-air fuel cells—a review. J. Energy Storage **8**, 35–50 (2016)
2. Yi, J., Liu, X., Liang, P., Wu, K., Xu, J., Liu, Y., Zhang, J.: Non-noble iron group (Fe Co, Ni)-based oxide electrocatalysts for aqueous zinc-air batteries: recent progress, challenges, and perspectives. Organometallics **38**, 1186–1199 (2019)
3. Zhu, B., Liang, Z., Xia, D., Zou, R.: Metal-organic frameworks and their derivatives for metal-air batteries. Energy Storage Mater. **23**, 757–771 (2019)
4. Jung, H.-G., Jeong, Y.S., Park, J.-B., Sun, Y.-K., Scrosati, B., Lee, Y.J.: Ruthenium-based electrocatalysts supported on reduced graphene oxide for lithium-air batteries. ACS Nano **7**, 3532–3539 (2013)
5. Schon, T.B., McAllister, B.T., Li, P.-F., Seferos, D.S.: The rise of organic electrode materials for energy storage. Chem. Soc. Rev. **45**, 6345–6404 (2016)
6. Zhang, S., Ren, S., Han, D., Xiao, M., Wang, S., Sun, L., Meng, Y.: A highly immobilized organic anode material for high performance rechargeable lithium batteries. ACS Appl. Mater. Interfaces **12**, 36237–36246 (2020)
7. Lee, D.J., Lee, H., Song, J., Ryou, M.-H., Lee, Y.M., Kim, H.-T., Park, J.-K.: Composite protective layer for Li metal anode in high-performance lithium–oxygen batteries. Electrochem. Commun. **40**, 45–48 (2014)
8. Bruce, P.G., Freunberger, S.A., Hardwick, L.J., Tarascon, J.-M.: Li–O_2 and Li–S batteries with high energy storage. Nat. Mater. **11**, 19–29 (2012)
9. Yu, X., Zhou, T., Ge, J., Wu, C.: Recent advances on the modulation of electrocatalysts based on transition metal nitrides for the rechargeable Zn-Air battery. ACS Mater. Lett. **2**, 1423–1434 (2020)
10. Kundu, A., Mallick, S., Ghora, S., Raj, C.R.: Advanced oxygen electrocatalyst for air-breathing electrode in Zn-Air batteries. ACS Appl. Mater. Interfaces **13**, 40172–40199 (2021)
11. Kang, J.-H., Lee, J., Jung, J.-W., Park, J., Jang, T., Kim, H.-S., Nam, J.-S., Lim, H., Yoon, K.R., Ryu, W.-H., Kim, I.-D., Byon, H.R.: Lithium-air batteries: air-breathing challenges and perspective. ACS Nano **14**, 14549–14578 (2020)
12. Shirakawa, H., Louis, E.J., MacDiarmid, A.G., Chiang, C.K., Heeger, A.J.: Synthesis of electrically conducting organic polymers: halogen derivatives of polyacetylene, (CH). J. Chem. Soc. Chem. Commun. 578–580 (1977)
13. Bi, W., Gao, G., Wu, G., Atif, M., AlSalhi, M.S., Cao, G.: Sodium vanadate/PEDOT nanocables rich with oxygen vacancies for high energy conversion efficiency zinc ion batteries. Energy Storage Mater. **40**, 209–218 (2021)
14. Lu, Q., Zhao, Q., Zhang, H., Li, J., Wang, X., Wang, F.: Water dispersed conducting polyaniline nanofibers for high-capacity rechargeable lithium-oxygen battery. ACS Macro Lett. **2**, 92–95 (2013)
15. Cui, R., Xiao, Y., Li, C., Han, Y., Lv, G., Zhang, Z.: Polyaniline/reduced graphene oxide foams as metal-free cathodes for stable lithium–oxygen batteries. Nanotechnology **31**, 445402 (2020)
16. Cao, D., Shen, X., Wang, Y., Liu, J., Shi, H., Gao, X., Liu, X., Fu, L., Wu, Y., Chen, Y.: Conductive polymer coated cathodes in Li–O_2 batteries. ACS Appl. Energy Mater. **3**, 951–956 (2020)
17. Kim, C.H.J., Varanasi, C.V., Liu, J.: Synergy of polypyrrole and carbon x-aerogel in lithium–oxygen batteries. Nanoscale **10**, 3753–3758 (2018)
18. Yoon, S.H., Kim, J.Y., Park, Y.J.: Carbon-free polymer air electrode based on highly conductive PEDOT micro-particles for Li–O_2 batteries. J. Electrochem. Sci. Technol. **9**, 220–228 (2018)
19. Xie, X., Fang, Z., Yang, M., Zhu, F., Yu, D.: Harvesting air and light energy via "all-in-one" polymer cathodes for high-capacity, self-chargeable, and multimode-switching zinc batteries. Adv. Funct. Mater. **31**, 2007942 (2021)
20. Chameh, B., Moradi, M., Hessari, F.A.: Decoration of metal organic frameworks with Fe_2O_3 for enhancing electrochemical performance of ZIF-(67 and 8) in energy storage application. Synth. Met. **269**, 116540 (2020)

21. Jafari, E.A., Moradi, M., Borhani, S., Bigdeli, H., Hajati, S.: Fabrication of hybrid superca-pacitor based on rod-like HKUST-1@polyaniline as cathode and reduced graphene oxide as anode. Phys. E Low-Dimensional Syst. Nanostruct. **99**, 16–23 (2018)
22. Chameh, B., Moradi, M., Kaveian, S.: Synthesis of hybrid ZIF-derived binary ZnS/CoS composite as high areal-capacitance supercapacitor. Synth. Met. **260**, 116262 (2020). https://doi.org/10.1016/j.synthmet.2019.116262
23. Sanati, S., Abazari, R., Morsali, A., Kirillov, A.M., Junk, P.C., Wang, J.: An asymmetric supercapacitor based on a non-calcined 3D pillared Cobalt(II) metal-organic framework with long cyclic stability. Inorg. Chem. **58**, 16100–16111 (2019)
24. Pan, N., Zhang, H., Yang, B., Qiu, H., Li, L., Song, L., Zhang, M.: Conductive MOFs as bifunctional oxygen electrocatalysts for all-solid-state Zn–air batteries. Chem. Commun. **56**, 13615–13618 (2020)
25. Kim, S.H., Lee, Y.J., Kim, D.H., Lee, Y.J.: Bimetallic metal-organic frameworks as efficient cathode catalysts for Li–O$_2$ batteries. ACS Appl. Mater. Interfaces **10**, 660–667 (2018)
26. Xiao, Y., Guo, B., Zhang, J., Hu, C., Ma, R., Wang, D., Wang, J.: A bimetallic MOF@graphene oxide composite as an efficient bifunctional oxygen electrocatalyst for rechargeable Zn–air batteries. Dalton Trans. **49**, 5730–5735 (2020)
27. Côté, A.P., Benin, A.I., Ockwig, N.W., Keeffe, M., Matzger, A.J., Yaghi, O.M.: Porous, crystalline, covalent organic frameworks. Science **310**, 1166 (2005)
28. Peng, P., Shi, L., Huo, F., Zhang, S., Mi, C., Cheng, Y., Xiang, Z.: In situ charge exfoliated soluble covalent organic framework directly used for Zn–Air flow battery. ACS Nano **13**, 878–884 (2019)
29. Li, Z., Zhao, W., Yin, C., Wei, L., Wu, W., Hu, Z., Wu, M.: Synergistic effects between doped nitrogen and phosphorus in metal-free cathode for zinc-air battery from covalent organic frameworks coated CNT. ACS Appl. Mater. Interfaces **9**, 44519–44528 (2017)
30. Hosokawa, T., Tsuji, M., Tsuchida, K., Iwase, K., Harada, T., Nakanishi, S., Kamiya, K.: Metal-doped bipyridine linked covalent organic framework films as a platform for photoelectrocatalysts. J. Mater. Chem. A **9**, 11073–11080 (2021)
31. Huang, H., Li, F., Zhang, Y., Chen, Y.: Two-dimensional graphdiyne analogue Co-coordinated porphyrin covalent organic framework nanosheets as a stable electrocatalyst for the oxygen evolution reaction. J. Mater. Chem. A **7**, 5575–5582 (2019)
32. Watkins, D., Nuruddin, M., Hosur, M., Tcherbi-Narteh, A., Jeelani, S.: Extraction and characterization of lignin from different biomass resources. J. Market. Res. **4**, 26–32 (2015)
33. Du, Z., Su, Y., Qu, Y., Zhao, L., Jia, X., Mo, Y., Yu, F., Du, J., Chen, Y.: A mechanically robust, biodegradable and high performance cellulose gel membrane as gel polymer electrolyte of lithium-ion battery. Electrochim. Acta **299**, 19–26 (2019)
34. Wang, Y., Jin, M., Zhang, X., Zhao, C., Wang, H., Li, S., Liu, Z.: Direct conversion of biomass into compact air electrode with atomically dispersed oxygen and nitrogen coordinated copper species for flexible zinc-air batteries. ACS Appl. Energy Mater. **2**, 8659–8666 (2019)
35. Li, S., Zhao, W., Zhang, N., Luo, Y., Tang, Y., Du, G., Wang, C., Zhang, X., Li, L.: A tough flexible cellulose nanofiber air cathode for oxygen reduction reaction with silver nanoparticles and carbon nanotubes in rechargeable zinc-air batteries. Energy Fuels **35**, 9017–9028 (2021)
36. Ye, H., Zhang, Y., Yin, Y.-X., Cao, F.-F., Guo, Y.-G.: An outlook on low-volume-change lithium metal anodes for long-life batteries. ACS Cent. Sci. **6**, 661–671 (2020)
37. Ma, J., Wen, J., Gao, J., Li, Q.: Performance of Al–0.5 Mg–0.02 Ga–0.1 Sn–0.5 Mn as anode for Al–air battery in NaCl solutions. J. Power Sources **253**, 419–423 (2014)
38. Deyab, M.A., Essehli, R., El Bali, B.: Performance evaluation of phosphite NaCo(H$_2$PO$_3$)$_3$·H$_2$O as a corrosion inhibitor for aluminum in engine coolant solutions. RSC Adv. **5**, 48868–48874 (2015)
39. Buonaiuto, M., Neuhold, S., Schroeder, D.J., Lopez, C.M., Vaughey, J.T.: Functionalizing the surface of lithium-metal anodes. ChemPlusChem **80**, 363–367 (2015)

40. Jo, Y.N., Kang, S.H., Prasanna, K., Eom, S.W., Lee, C.W.: Shield effect of polyaniline between zinc active material and aqueous electrolyte in zinc-air batteries. Appl. Surf. Sci. **422**, 406–412 (2017)
41. Stock, D., Dongmo, S., Damtew, D., Stumpp, M., Konovalova, A., Henkensmeier, D., Schlettwein, D., Schröder, D.: Design strategy for zinc anodes with enhanced utilization and retention: electrodeposited zinc oxide on carbon mesh protected by ionomeric layers. ACS Appl. Energy Mater. **1**, 5579–5588 (2018)

Conjugated Polymers as Organic Electrodes for Metal-Air Batteries

Anukul K. Thakur, Mandira Majumder, Archana S. Patole, and Shashikant P. Patole

Abstract As compared to the Li-S and Li-ion batteries, the metal-air batteries technology projects itself as a promising candidate for energy storage exhibiting large energy densities. At the cathode of the metal air battery, the reactions are mostly electrochemical processes engaging oxygen reduction and/or oxygen evolution. Oxygen electrocatalyst associated with the cathode plays a major role in determining the characteristics of a metal-air battery from the point of view of power density, rate capacity, the efficiency of capacity retention, and cycling stability. Different materials have been tested and were observed to efficiently improve the oxygen reduction and/or evolution, including conductive polymers, carbonaceous materials noble metals, alloys, nitrides, and oxides. Electrically conductive polymers (CPs), like polypyrrole, polyaniline, polythiophene, poly(3-methyl) thiophene, and poly(3,4-ethylene dioxythiophene), projects themselves as promising electrocatalysts which can effectively replace the noble metals in metal-air batteries. CPs possess both polymer and metal-like characteristics and have garnered large attention as a result of their redox properties, low cost, and improved electric conductivity. Even though the study of the CPs as electrocatalysts has preceded in the initial stages, it is largely restricted as a result of their comparatively smaller conductivity, and inferior efficiency. Vapor phase polymerization is considered as the recent most efficient process of chemical polymerization resulting in the synthesis of CPs with controllable morphology, large conductivity, and improved stability. For providing access to the current improvements in the field of metal-air batteries and realizing advancement in their development, this chapter comprehensively and systematically compares, summarizes, and discusses the state-of-the-art of aqueous and/or nonaqueous metal-air batteries.

Keywords Metal-air batteries · Conjugated polymers · Electrocatalyst · Electrocatalysis · Energy density

A. K. Thakur · M. Majumder · A. S. Patole · S. P. Patole (✉)
Applied Quantum Materials Laboratory (AQML), Department of Physics, Khalifa University of Science and Technology, P. O. Box 127788, Abu Dhabi, United Arab Emirates
e-mail: shashikant.patole@ku.ac.ae

1   Introduction

Metal air batteries (MABs) are of interest as they exhibit a larger theoretical energy density than the Li-ion batteries. The MAB is associated with an external cathode which comprises ambient air, a metal as an anode, and an aprotic or aqueous electrolyte. Unlike the conventional ionic batteries which involve the transfer of metallic ions to the cathode from the anode, MABs comprised of a metal anode referred to as "M" which is oxidized to create metal ions (M^+) that reaches the cathode through the electrolyte to produce metal oxides (MO_{2x}) by reacting with the O_2 [1–3].

The reactions are as follows:

$$\text{Anode}: M(s) \leftrightarrow M^+ + e^-$$
$$\text{Cathode}: M^+ + xO_{2+}e^- \leftrightarrow MO_{2x}$$
$$\text{Overall}: M + xO_2 \leftrightarrow MO_{2x}$$
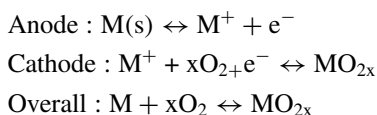
Figure 1a illustrates the primary working principle of the MABs and Fig. 1b, c highlights the theoretical energy densities together with open-circuit voltages corresponding to the various MAB chemistries. In this book chapter, the recent advances of conducting polymers (CPs) as organic electrodes in various MABs has been discussed, including lithium-air (Li-air) batteries, aluminum-air (Al-air) batteries, sodium-air (Na-air) batteries, zinc-air (Zn-air) batteries, magnesium-air (Mg-air) batteries, tin-air (Sn-air) batteries, and iron-air (Fe-air) batteries [4–6].

1.1   *Market Demand & Fundamentals of Metal Air Battery*

Following the perpetual development of the economy worldwide, the energy requirement has significantly increased in the past few decades. Unfortunately, the earth's traditional sources are non-renewable, including oil, coal, and natural gas, whose supply is constrained. This necessitates the emergence of new energy storage modes for developing a bearable society. Advanced supercapacitors, biofuels batteries, and MABs are categorized as the aptest runners to meet the energy storage necessities. Amongst the several energy storage modes prevailing in the market, Li-ion batteries (LIBs) are identified with the best performance. However, attaining a large capacity in LIBs and realizing safe energy storage necessities meant for mobile electronics, remains a challenge. In recent years, MABs have garnered much attention credited to their possible implementation in an open-air atmosphere. MABs can be classified into two classes based on the type of electrolyte used including non-aqueous MABs and aqueous MABs [6–8]. Aqueous aluminum, iron and magnesium-air batteries were designed in the 1960s. Nonaqueous MABs were first designed ~two decades ago, primarily for Li-air, and recently for K-air and Na-air batteries. MABs comprise an air cathode and metal anode. The MAB cathode utilizes oxygen from the surrounding air, which results in major battery weight reduction, having several advantages for many
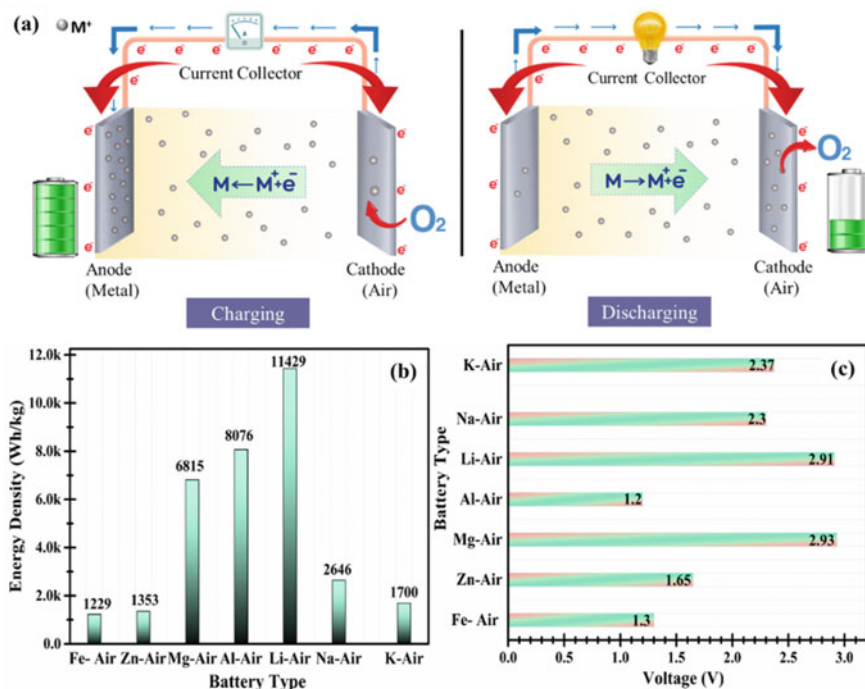
Fig. 1 a Discharging and charging mechanism in a metal-air battery (metal deposits on the electrodes are represented by the grey balls). Adapted with permission from reference [9], Copyright (2021), Royal Society of Chemistry. Bar graph representation corresponding to **b** theoretical energy densities and **c** open-circuit voltages associated with various kinds of metal-air batteries. Adapted with permission from reference [6], Copyright (2019), Elsevier

applications which were impossible to achieve before. As compared to Lithium-ion and other types of batteries currently dominating the market, MABs project themselves as cost-effective, attributed to the availability of the cathode source and the anode can be fabricated using cheap metals, including Al, Zn, Fe, and so on. MABs have garnered attention not only as a result of compact size applicable in portable electric vehicles and electronics but also due to possible implementation in compelling energy transfer stations or energy vehicles as well as to buffer energy from the renewable energy generators such as photovoltaic panel based energy generators, wind turbines, electric grids, and the electric grid end-users [1, 3, 9, 10].

1.2 Configuration of MABs

MABs broadly comprised of four segments: electrolyte, metal anode, air cathode, and separator, as shown in Fig. 1a. The separator is not conducting in nature which

only allows the passage of ions and not electrons. While discharging, oxidation takes place at the metal anode accompanied by metal dissolution in the electrolyte, and reduction of oxygen (ORR) occurs at the cathode. As a result of the open battery configuration implementing air as a reactant, metal-air batteries possess a much large specific capacity. Even though they have a large energy density, there are various challenges associated with these systems which must be eliminated to fabricate them before they can be implemented for practical purposes [1–8]. Figure 1b, c show bar graph representation corresponding to theoretical energy densities and open-circuit voltages associated with various kinds of metal-air battery [6, 8]

2 Conjugated Polymers for Metal-Air Batteries

Oxygen-based electrocatalysts have projected themselves as significant in enhancing the cycling capability, power density, and efficiency of energy conversion associated with the MABs. Large efforts have been put in the designing of electrocatalysts both for primary as well as rechargeable MABs. Furthermore, attributed to the alike principles, the majority of the catalytic materials implemented in fuel cells are also implemented in MABs. Not only the materials but the strategies and techniques incorporated in the fuel cells are effective in enhancing the cathode efficiency in MABs. The electrocatalysts can be broadly categorized into several classes including functional carbon materials, transition metal oxides, metal oxide-nanocarbon, transition metal nitrides, metal-nitrogen complex, noble metals, oxides, alloys, and conjugated polymers [10, 11].

Attributed to the unique semiconductor/metallic properties and their possible utilization in electronics, electrochemistry, and as energy storage material, CPs have garnered huge attention credited to high charge-carrier mobility, good molecular weight, tight p-stacking, decent film-forming properties, and little bandgap. These polymers are of low cost, have large electrical conductivity, unique redox properties, and adequate functionalities [10, 12–16]. Hence, these CPs including Polypyrrole (PPy), Polythiophene (PTh), poly(3,4-ethylene dioxythiophene) (PEDOT), poly(3-methyl)thiophene (PMeT), and polyaniline (PANI) implemented as direct electrocatalysts have lately been observed to show some particular activity as cathode material in the MABs [4, 10, 12].

3 Conjugated Polymers' Use as Metal-Air Battery Materials

3.1 Lithium-Air Battery

Lithium-Air Batteries (LABs) project themselves as promising energy conversion and storage modes attributed to the delivery of high energy density. To elaborate, in

LABs also called Li-O$_2$ batteries, reversible exchange between electric and chemical energies takes place by the means of electrochemical reactions of air (O$_2$) at the cathode and Li at the anode. In the year 1976, Littauer and Tsai put forward the proposal involving Li-air chemistry supported in an aqueous system. Following this, Abraham et al. [17] in the year 1996 reported the pioneering study on a non-aqueous Li-air battery mode implementing an organic polymer electrolyte. Cui et al. [18] synthesized polypyrrole nanotubes implementing a self-sacrificing template and tested it as a cathode material for LABs and studied their performance and compared it with those of granular PPy (GPPy) and acetylene carbon black. At 0.1 mA/cm^2 the discharge potential of electrode based on tubular polypyrrole nanotubes was observed to be higher than GPPy electrode and that of acetylene black electrode. The electrode based on tubular polypyrrole nanotubes exhibited both enhanced rate performance and cyclic life as compared to the carbon black and GPPy electrodes. Zhang et al. [19] reported that PPy could exhibit higher capacity synchronously with enhanced cycling performance as compared to the carbon-based materials credited to its large catalytic activity associated with ORR and also OER. Furthermore, they also showed that dopants incorporated in PPy could significantly improve its electrochemical performance and as proof showed improvement in the electrochemical properties of PPy as a result of Cl-doping.

Synthesis of PEDOT by implementing 3,4 ethylene dioxythiophene monomer through in-situ chemical polymerization with carbon matrix scaffold was reported by Nasybulin et al. [20]. The electrochemical tests revealed that PEDOT could play a major role in reducing the overpotential by 0.7–0.8 V while charging the LAB together with improvement in the discharge capacity. This improvement was mainly credited to the redox activeness of the PEDOT and its role in electron passage at the time of the charge-discharge process. The PANi nanofibrous, designed by the means of a chemical route using a mini emulsion polymerization approach exhibited a discharge capacity of 1380 mAh g catalyst^{-1} at 0.05 mA/cm^2 [21].

Li et al. have synthesized Co$_3$O$_4$-rods forming a mesh with PANi nanotubes followed by their carbonization by a hydrothermal method (Fig. 2a). The fabricated LAB comprising of Co$_3$O$_4$-e-cPANI composite-based cathode showed a capacity of 500 mAh/g after 430 cycles while the capacity was maintained at the value of 1000 mAh/g for the first 226 cycles (Fig. 2b–e) [22]. Furthermore, improvement in the electric conductivity in the cathodes have been tried implementing CPs as binders in non-aqueous Li-air battery. Before this, the implementation of PPy as a functional binder for air cathodes was observed in the work of Cui et al. [23]. Apart from the air cathode, PANi has also been used as a membrane which was reported by Fu et al. [24]. They fabricated the membrane by a proton doping approach which was used as waterproof barriers for LABs. On attachment of the membrane to the air cathode, it improved lithium-ion passage into the electrode along with blocking the entrance for the moisture. This results in less corrosion of the LAB anode. Electrochemical tests indicated that the fabricated lithium-air cells exhibited a specific capacity of 3241 mAh/g [24]. Li et al. reported the synthesis of N-doped graphene through the pyrolysis of polyaniline/graphene oxide composite precursors. The LAB fabricated
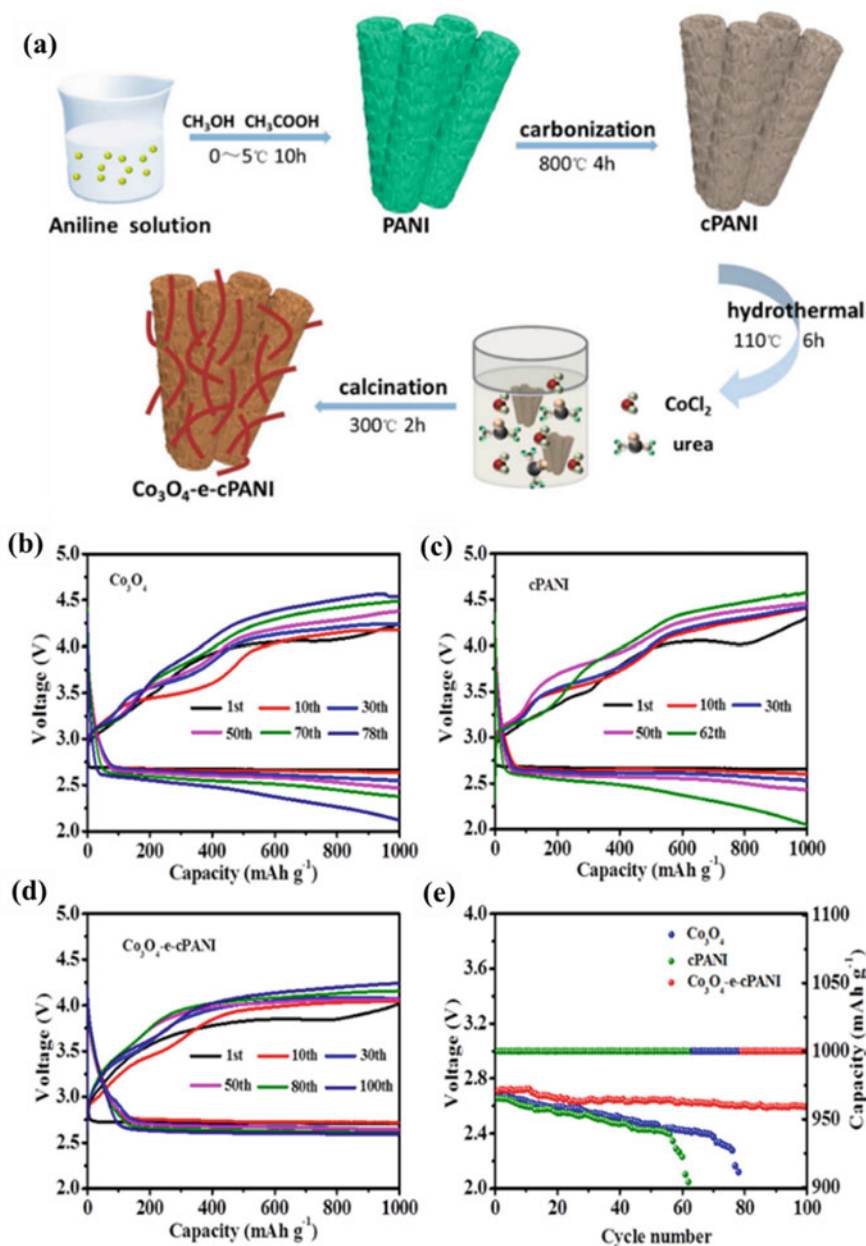
Fig. 2 **a** Schematic illustration for the preparation of Co_3O_4-e-cPANI. Charge/discharge profiles corresponding to **b** Co_3O_4, **c** carbonized polyaniline (cPANI), and **d** the Co_3O_4-e-cPANI composite cathode tested for Li-ion batteries at 100 mA/g exhibiting a capacity corresponding to the value of 1000 mAh/g. **e** The end discharge voltage exhibited by Li-ion batteries implemented with three different cathodes. Adapted with permission from reference [22], Copyright (2019), American Chemical Society

with the N-doped graphene cathode showed a longer cycle life and a larger full-discharge capacity as compared to the LAB comprising of graphene oxide cathode [25]. Recently, a polyethyleneimine (PEI)-scaffolded by anthraquinone (AQ) catalyst has been reported to be implemented as an ORR catalyst for designing a LAB [26]. The incorporation of the anthraquinone-based catalyst enhanced the cycle life of LAB when tested in an electrolyte comprising of traethylene glycol dimethyl ether. Implemented with PEI-AQ polymer, the potential corresponding to the discharge increased to 2.67 V (~70 mV greater than the cells having unmodified PEI polymer/SP or pristine SP). The voltage profiles corresponding to the charging state of both PEI-AQ/SP and pristine SP exhibited a plateau at 4.25 V.

3.2 Aluminum-Air Battery

The Al-air battery (AAB) projects itself as a promising technology satisfying the forecasted future energy demands. AABs project a practical energy density lower than that of LAB (5.20 kWh/kg) corresponding to 4.30 kWh/kg. However, the value of the energy density is much larger as compared to the Zn-air or Mg-air batteries (1.08 kWh/kg). Furthermore, aluminum is much cheaper than the other materials and is abundantly (the second abundant metal after silicon) available as well as environment-friendly, non-toxic, and largely recyclable [27, 28]. CPs have the potential to act as a stable and low-cost alternative to noble metal catalysts. CPs including polyaniline have been implemented as dopants for several years with their first review being published in the year 2005 where the reduction ability was analyzed for the CPs. The possibility of the reduction of the chemisorbed oxygen was reported. Yuan et al. [29] analyzed that the catalytic activity could be improved by doping PANI with C, N, Fe, and Co [30–32]. Several studies have been conducted on polymers analyzing ORR, including polypyrrole [33–35], polythiophene [36], and poly(3,4-ethylene dioxythiophene) [37, 38]. Among the various CPs, PPy has projected itself as most promising attributed to large catalytic activity and a large magnitude of current, lesser than only PANI. Liao et al., [39] developed a composite of PANI and ordered mesoporous carbon (OMC) as the cathode material implemented in an Al-ion battery (AIB) with chloroaluminate ionic liquid (IL) as the electrolyte. During the charging/discharging process, two obvious plateaus appeared at high voltages near to 1.5–1.7 V and 1.1 V. The PANI/OMC cathode showed a specific capacity attaining a value of 140 mAh/g at 100 mA/g, rate capability reaching a value of 118 mAh/g at 2000 mA/g and long cyclic life as shown in Fig. 3a–c. Kuo et al. focused on the fabrication of composite electrode materials for an AAB and enhancing the ORR of the air electrode with the help of matching poly-(3,4-ethylene dioxythiophene) with alpha- and beta manganese dioxide. The catalyst powders of α-MnO_2 and β-MnO_2 are synthesized with the help of the hydrothermal method with the incorporation of several precursors [40]. Recently, the development of polyaniline/graphene oxide composite has been conceptualized through the first principle
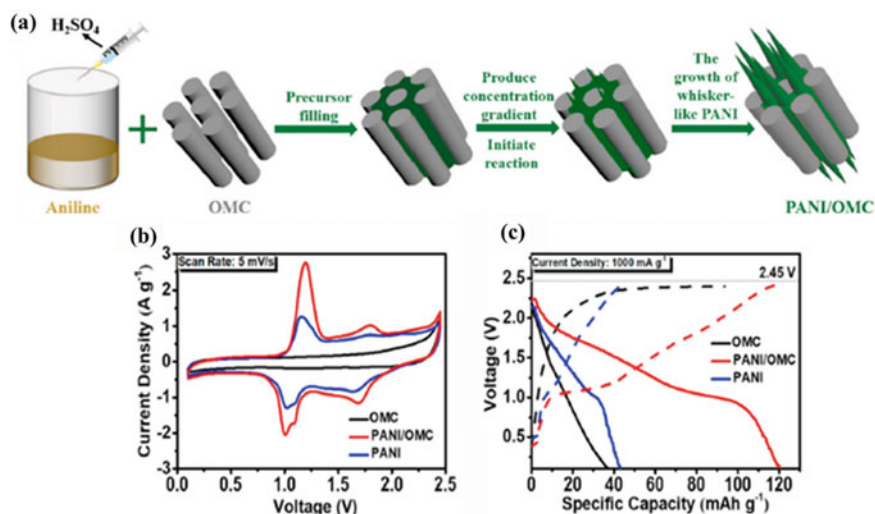
Fig. 3 **a** Schematic illustration representing the synthesis of PANI/OMC, **b** CV plots corresponding to PANI/OMC, OMC, and PANI at 5 mV/s, **c** GCD curves corresponding to PANI/OMC, OMC, and PANI at 1000 mA/g. Adapted with permission from reference [39], Copyright (2019), Elsevier

calculations by Wang et al. [41], exhibiting outstanding performances as a cathode material in AIBs identified with 180 mAh/g of capacity.

3.3 Zinc-Air Battery

Zinc is considered as one of the most broadly implemented electrodes having various advantages, to say a few, it is environmentally friendly, easily available, cost-effective, safe to handle, compatible with an aqueous solution, and exhibits a satisfactory electrochemical performance equivalent to 820 Ah/kg. In addition, Zn is safe to handle as compared to Li and can entirely be recycled. Zinc-air batteries (ZABs) can provide a larger specific energy density when compared to the other energy storage modes attributed to their configuration associated with the MABs. ZABs present a theoretical capacity ~1086 Wh/kg. Zinc-air secondary batteries can be categorized into two classes: mechanically rechargeable systems and electrically rechargeable systems. A ZAB comprises of three parts: an air electrode divided into a catalytic active layer and a gas diffusion layer, Zn metal as an anode, and a separator. Electrically rechargeable ZABs faces several issues including the formation of dendrite at the time of recharging, limited cyclic stability, and the hydrogen evolution reaction (HER), which is attributed to the greater negative reduction potential of Zn as compared to hydrogen [42–44].

Jo et al. [45] reported the use of materials with a coating of PANI as promising anode materials for ZABs. The conductive polymer PANI has been reported to be synthesized implementing various content of HCl followed by its coating onto Zn for refraining from the HER and the corrosion reaction. The rising concentration of APS and aniline in HCl caused a thicker and uniform layer of PANI on zinc particles resulting in its enhanced capacity retention. Furthermore, coating of PANI limited the direct contact between Zn and KOH electrolyte and restricted the reactions leading to the corrosion and HER along with reducing self-discharge (Fig. 4a, b). Polyaniline/Zn-phthalocyanines (PANI@ZnPc) synthesis has been reported by Deyab et al. [46] where PANI@ZnPc has been used to coat the Zn electrode leading to improved electrochemical performance of the ZAB battery. They found that PANI@ZnPc nanocomposite can cause a reduction in the corrosion rate of Zn electrode as compared to that of pristine Zn and PANI-coated Zn. It was claimed that the discharge capacity associated with the Zn-air battery could be enhanced till 713 mAh/g for PANI@ZnPc nanocomposite (Fig. 4c). Furthermore, the incorporation of ZnPc particles led to an enhanced capacity retention of a value up to 98.5%.

Flexible ZABs have also projected themselves as impressive energy storage for flexible and mobile electronics credited to superior eco-friendliness and energy density. The pioneering work by Li et al. [47] reported flexible ZABs implementing novel quaternary ammonium hydroxide-based polymer electrolytes. Tetraethylammonium hydroxide (TEAOH) has been proved effective ionic conductor along with poly(vinyl alcohol) (PVA) in the form of host polymer in the electrolyte comprising of polymer and exhibiting augmented retention capacity of water. The so designed polymer electrolyte could deliver a large ionic conductivity attaining a value of 30 mS/cm even following two weeks. In addition, the as-assembled ZAB comprising of TEAOH-PVA electrolyte showed enhanced performance corresponding to cycling life and discharge characteristics than those comprising of traditionally implemented KOH-PVA electrolyte, without any notable degradation over two weeks. Furthermore, flexible TEAOH-PVA-based ZAB was able to power an LED screen, a light-emitting diode (LED) an electronic watch, and charge a mobile phone (Fig. 4d–i).

Polymer additives including polyethylene glycol, polycarbonate, poly(methyl methacrylate), polypyrrole, polyaniline, and poly (vinyl acetate) limit the dissolution of the products discharged during the charging and discharging processes. Furthermore, along with electrolytes, the incorporation of polymer additives in the anodes leads to improvement in the cycle life of the electrode. Polypyrrole and polyaniline projected themselves as the aptest CPs attributed to a broad range of conductivity, adjustable characteristics, and large stabilities. Conductive polymers can be incorporated into anode to enhance the stability and hence the overall performance of rechargeable batteries. Polyaniline-coated Zn was implemented to restrict the self-discharge properties, limit the corrosion reactions and the HER by refraining from direct contact between KOH electrolyte and Zn [45, 48].

Polyethylenimine aptly limits the dendrite growth in the rechargeable Zn batteries. PEI adsorption onto the Zn surface decelerates the kinetics associated with Zn
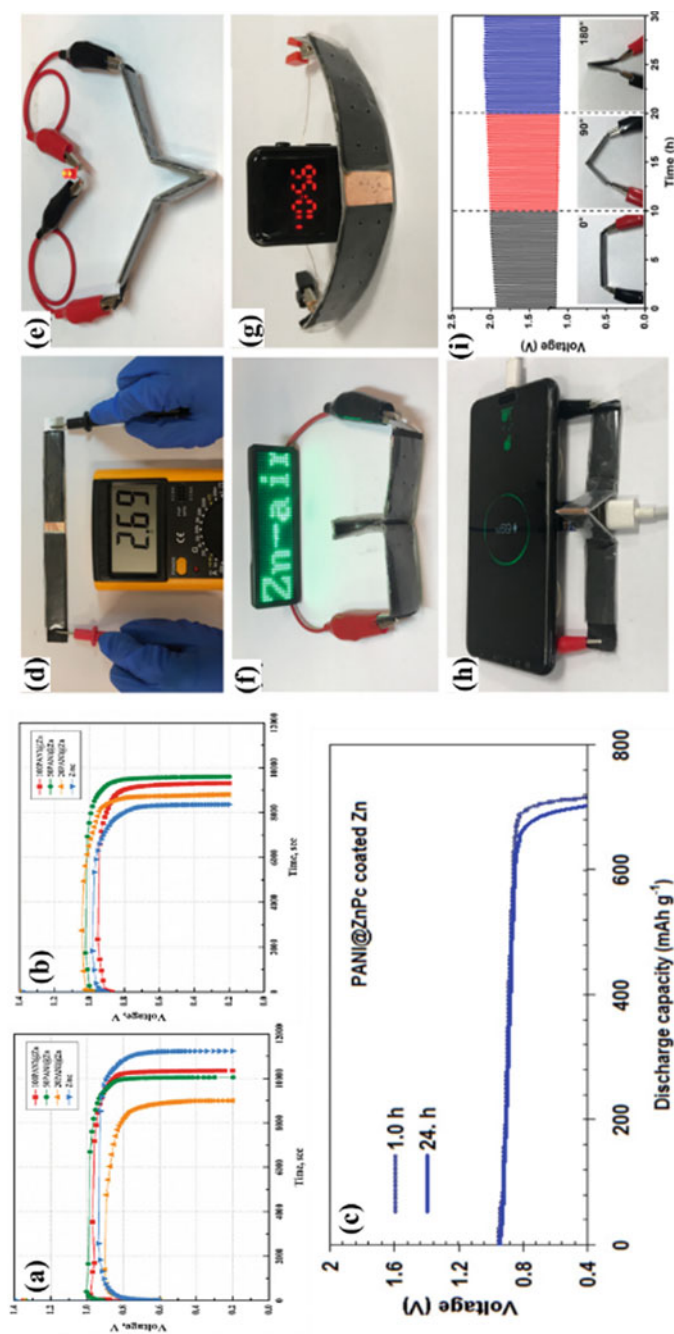
Fig. 4 The electrochemical potential profiles for **a** freshly prepared samples and **b** stored samples at ambient temperature for 24 h. Adapted with permission from reference [45], Copyright (2019), Elsevier. **c** Discharge capacity corresponding to the assembled Zn-air batteries implemented with PANI@ZnPc after the storing for 1.0 h and 24 h at the temperature of 298 K. Adapted with permission from reference [46], Copyright (2019), Elsevier. **d** Digital pictures when two Zn-air batteries were connected in series, **e** an LED light, **f** a screen with LED components, **g** a digital watch, and **h** a cell phone charged by two zinc-air batteries under bending conditions connected in series. **i** Charge–discharge profiles corresponding to the ZABs at several bending angles and their digital pictures. Adapted with permission from reference [47], Copyright (2019), American Chemical Society

electrodeposition limiting the propagation of dendrite tips. Banik et al. studied the implementation of branched polyethyleneimine acting as an additive to restrict the dendrite growth (electrodeposition). They observed that polyethyleneimine concentration corresponding to 50 ppm proved to be very effective (shown in Fig. 5a–d) attributed to adsorption of the additives on the surface of zinc anode serving as a physical barrier to the Zn dendrite growth. [49]

Recently Xiao et al. reported $Fe(CN)_6^{4-}$@PPy precursors comprising of Fe active species dispersion in pre-anchored $Fe(CN)_6^{4-}$ to the polypyrrole matrixes. The formed iron/3S/nitrogen co-doped carbon electrocatalyst showed 20 mV higher onset potential reaching a value of 0.99 V and 50 mV higher than the half-wave potential reaching a value of 0.89 V as compared to the commercial Pt/C catalyst when tested in alkaline medium. When iron/3S/nitrogen co-doped carbon was implemented as the cathode material for ZAB, it exhibited improved cycle life and impressive peak power density as compared to the Pt/C. The synthesis approach for iron/3S/nitrogen co-doped carbon has been illustrated in Fig. 6a. This approach was unlike the traditional template-geometric confinement process involving several steps to obtain M/N-C materials with multiple independent active sites. This work demonstrated the synthesis of iron/3S/nitrogen co-doped carbon electrode material through a simple one-pot synthesis of $Fe(CN)_6^{4-}$@PPy precursor.

To investigate the potential related to the application of Fe/3S/N-C, it was implemented to fabricate a ZAB. To compare, hydrophobic carbon was also coated with Pt/C catalyst serving as a cathode. The ZAB fabricated from Fe/3S/N-C exhibited a larger open-circuit potential (Fig. 6b) corresponding to the value of 1.50 V as
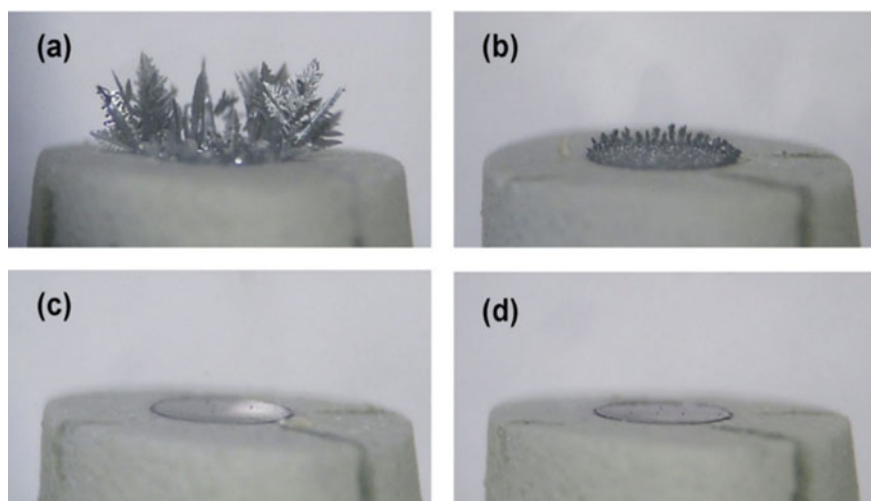
Fig. 5 Elimination of dendritic growth at the time of Zn plating at the various PEI concentration **a** 10 ppm **b** 50 ppm **c** and 100 ppm **d** Zn plating at 50 ppm of PEI concentration or higher. Adapted with permission from reference [49], Copyright (2015), Elsevier
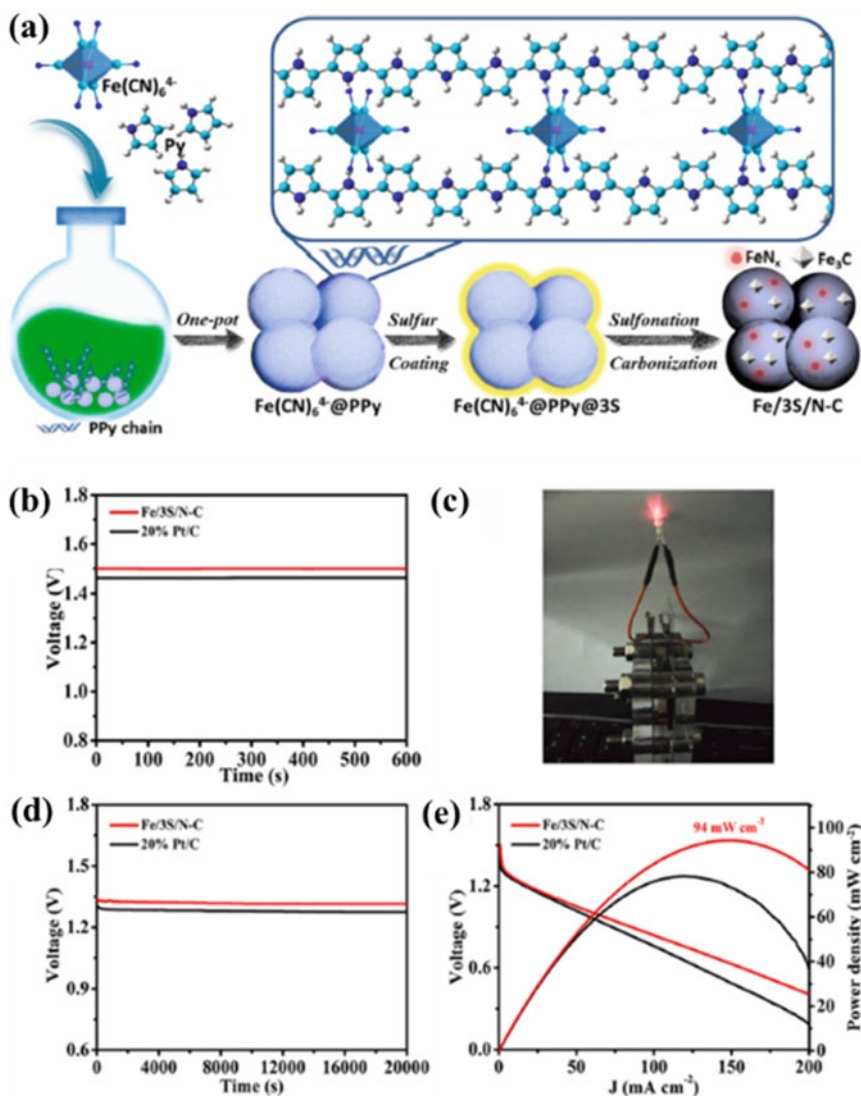
Fig. 6 a Schematic representation of the synthesis of Fe/3S/N-C. Electrochemical performance of the battery, **b** open-circuit potential curves, **c** digital photograph of an assembled air battery powering an LED light implemented with Fe/3S/N-C electrode, **d** galvanostatic discharge potential profile, and e power density and polarization curves. Adapted with permission from reference [50], Copyright (2021), Elsevier

compared to Pt/C corresponding to the value of 1.47 V, which could hence efficiently power a light-emitting diode (LED) as shown in Fig. 6c. ZAB implementing Fe/3S/NC catalyst could attain a larger cell output voltage as compared to Pt/C, as a result of their faster ORR kinetic. However, ZAB implemented with Fe/3S/N-C cathode exhibited a better peak power density corresponding to the value of 94 mW/cm^2.

3.4 Other Air Batteries

Mg-air battery is another kind of MABs that is still left to be explored. Similar to other MABs, the magnesium in the anode is oxidized to Mg^{2+} at the time of discharge producing two electrons. At the air cathode, the oxygen moves through and gets reduced to the OH$^-$ ions corresponding to the reaction with the production of electrons and water. Rechargeable Mg-air batteries project themselves as a promising alternative to the Li-air cells credited to the safety, lesser price as a result of natural abundance on the earth, and large theoretical volumetric density corresponding to a value of 3832 Ah/L associated with Mg anode vs. 2062 Ah/L associated with Li. Despite all these facts, the research on the Mg-air battery is still in its infancy and a limited number of works have been reported related to it. The basic scientific challenges limiting the fast growth of secondary Mg-air battery which is attributed to the deprived thermodynamics and kinetics characteristics precisely owing to the MgO or MgO$_2$ protecting film as the primary discharge product associated with the air-breathing cathode, increasing large polarization and large overpotential. Very recently, the impressive development of rechargeable Mg-air battery focused on coping up with the major limitations corresponding to the organic electrolytes by the means of the combination of the experimental study along with first-principle calculations has been noticed.

Jia et al. [51] reported Mg-air bio-battery which is partly biodegradable comprising of a cathode made of silk fibroin-polypyrrole film along with anode comprising of bioresorbable Mg alloy in a saline electrolyte buffered by phosphate. Polypyrrole has been coated chemically onto silk substrate on one side. The fibroin-polypyrrole film exhibited a conductivity corresponding to a value of ≈1.1 S/cm along with a little catalytic activity for oxygen reduction. The fabricated Mg-air bio-battery showed a discharge capacity corresponding to a value of 3.79 mAh/cm^2 at 10 µA/cm^2 at room temperature, delivering a specific energy density corresponding to a value of about 4.70 mWh/cm^2. To test the electrocatalytic activity associated with the SF-PPy film electrode it was initially reduced by the application of constant potential corresponding to the value of −0.85 V for 600 s. The open-circuit potential was seen to increase immediately after the withdrawal of the applied potential. The Nyquist plots observed implementing the electrochemical impedance spectroscopy (EIS) represented a semicircular region on the real axis followed by a linear region. The impedance property was identified by fitting a model of an equivalent circuit to the Nyquist plot.

Na and K-air batteries are a new development in addition to Li, Zn, Al, Mg air batteries. The replacement of Li by Na has been proven to be a promising solution to limit the Li-air restrictions including high expense, high overpotential, and small Coulombic efficiency. At the time of the typical electrochemical process corresponding to the Na-air battery, the oxidation of the Na-metal occurs, and transfer of Na-ions takes place through the organic-aqueous/organic electrolyte. After the dissolution of the oxygen in the electrolyte in the proximity of the cathode, superoxide species (O_2) evolution occurs, where Na superoxide is created in the form of the discharge product. On the other side, Na-air and K-air based battery research is still in its infancy. However, the lower charging overpotential of these batteries as compared to Li-air batteries are very attractive leading to the possibility of superoxide formation. Nevertheless, these batteries suffer from even more problematic cyclic stability. It remains a puzzle even if their electrochemistry associated with the superoxide has a unique advantage and are promising over Li-air battery.

Hence, this chapter highlights a concise survey related to the major progress in the field of secondary MABs together with a detailed discussion on various reaction mechanisms associated with the MABs. The chapter is mainly concerned with opening up a novel area for utilizing the nanostructures to tune the ideal reaction pathway associated with the cell configuration and to completely understand the future MAB with enhanced cyclic life and energy density [6].

4 Conclusion and Future Perspectives

MABs project themselves as a promising alternative to metal ion or metal sulfur batteries. The MAB cathode utilizes oxygen from ambient air, which leads to significant battery weight reduction, oxygen electrocatalyst associated with the cathode is a major factor determining the performance of a MAB in terms of power density rate capacity, capacity retention efficiency, and cycling stability. CPs are very favorable which can act as cathode material and impart the designed MAB increased power density, improved capacity, lesser weight, and improved lifetime. In this chapter, MABs have been introduced briefly stating their necessity and advantages. Also, the market demand and fundamentals of MABs have been discussed elaborately. Further, the configuration of MABs has been taken into consideration. This is followed by the description of the role of CP as electrode material for MABs. CPs are considered very apt to act as electrode material for the MABs attributed to their compatibility with most of the electrolytes, tunable chemical structure, high surface area, and tunable porosity. The remarkable recent works on Li-air, Al-air, Zn-air, Mg-air, and various other metal-air batteries have been highlighted to describe the state of the art. The existing problems and the scope for improvement have been highlighted as well. It is expected that CPs will act as very apt material for MABs and needs much research to bring out the properties favorable for the MABs. Not only electrodes but advanced characterization techniques are also required to determine precisely the properties of the electrodes that would significantly alter the charge storage properties of the

electrode material. So, with more detailed exploration with advanced tools and techniques, CP implemented MABs could be developed as an efficient energy storage mode with the modern requisite properties.

References

1. Li, L., Chang, Z.W., Zhang, X.B.: Recent progress on the development of metal-air batteries. Adv Sustain. Syst. **1**(10), 1700036 (2017)
2. Li, Y., Lu, J.: Metal-air batteries: will they be the future electrochemical energy storage device of choice? ACS Energy Lett. **2**(6), 1370–1377 (2017)
3. Lee, J.S., Tai Kim, S., Cao, R., Choi, N.S., Liu, M., Lee, K.T., Cho, J.: Metal–air batteries with high energy density: Li–air versus Zn–air. Adv. Energy Mater. **1**(1), 34–50 (2011)
4. Cao, R., Lee, J.S., Liu, M., Cho, J.: Recent progress in non-precious catalysts for metal-air batteries. Adv. Energy Mater. **2**(7), 816–829 (2012)
5. Zhang, X., Wang, X.G., Xie, Z., Zhou, Z.: Recent progress in rechargeable alkali metal-air batteries. Green Energy Environ. **1**(1), 4–17 (2016)
6. Chawla, N.: Recent advances in air-battery chemistries. Mater. Today Chem. **12**, 324–331 (2019)
7. Wang, H.F., Xu, Q.: Materials design for rechargeable metal-air batteries. Matter **1**(3), 565–595 (2019)
8. Wang, C., Yu, Y., Niu, J., Liu, Y., Bridges, D., Liu, X., Pooran, J., Zhang, Y., Hu, A.: Recent progress of metal–air batteries-a mini review. Appl. Sci. **9**(14), 2787 (2019)
9. Thakur, A.K., Majumder, M., Patole, S.P., Zaghib, K., Reddy, M.V.: Metal-organic framework-based materials: advances, exploits, and challenges in promoting post Li-ion battery technologies. Mater. Adv. **2**(8), 2457–2482 (2021)
10. Cheng, F., Chen, J.: Metal–air batteries: from oxygen reduction electrochemistry to cathode catalysts. Chem. Soc. Rev. **41**(6), 2172–2192 (2012)
11. Wang, Z.L., Xu, D., Xu, J.J., Zhang, X.B.: Oxygen electrocatalysts in metal–air batteries: from aqueous to nonaqueous electrolytes. Chem. Soc. Rev. **43**(22), 7746–7786 (2014)
12. He, Y., Han, X., Du, Y., Zhang, B., Xu, P.: Heteroatom-doped carbon nanostructures derived from conjugated polymers for energy applications. Polymers **8**(10), 366 (2016)
13. Thakur, A.K., Choudhary, R.B., Majumder, M., Gupta, G., Shelke, M.V.: Enhanced electrochemical performance of polypyrrole coated MoS2 nanocomposites as electrode material for supercapacitor application. J. Electroanal. Chem. **782**, 278–287 (2016)
14. Thakur, A.K., Choudhary, R.B.: High-performance supercapacitors based on polymeric binary composites of polythiophene (PTP)-titanium dioxide (TiO$_2$). Synth. Met. **220**, 25–33 (2016)
15. Majumder, M., Thakur, A.K., Bhushan, M., Mohapatra, D.: Polyaniline integration and interrogation on carbon nano-onions empowered supercapacitors. Electrochimica Acta **370**, 137659 (2021)
16. Thakur, A.K., Deshmukh, A.B., Choudhary, R.B., Karbhal, I., Majumder, M., Shelke, M.V.: Facile synthesis and electrochemical evaluation of PANI/CNT/MoS ternary composite as an electrode material for high performance supercapacitor. Mater. Sci. Eng. B **223**, 24–34 (2017)
17. Abraham, K.M., Jiang, Z.: A polymer electrolyte-based rechargeable lithium/oxygen battery. J. Electrochem. Soc. **143**(1), 1 (1996)
18. He, W., Wang, X., Ye, L., Pan, Y., Song, Y., Liu, A., Wang, W., Zhang, H., Qi, H., Zhou, M., Wang, Z.: Out-of-Cell oxygen diffusivity evaluation in lithium-air batteries. ChemElectroChem **1**(12), 2052–2057 (2014)
19. Zhang, J., Sun, B., Ahn, H.J., Wang, C., Wang, G.: Conducting polymer-doped polyprrrole as an effective cathode catalyst for Li-O$_2$ batteries. Mater. Res. Bull. **48**(12), 4979–4983 (2013)

20. Nasybulin, E., Xu, W., Engelhard, M.H., Li, X.S., Gu, M., Hu, D., Zhang, J.G.: Electrocatalytic properties of poly (3, 4-ethylenedioxythiophene)(PEDOT) in Li-O2 battery. Electrochem. Commun. **29**, 63–66 (2013)
21. Lu, Q., Zhao, Q., Zhang, H., Li, J., Wang, X., Wang, F.: Water dispersed conducting polyaniline nanofibers for high-capacity rechargeable lithium–oxygen battery. ACS Macro Lett. **2**(2), 92–95 (2013)
22. Li, C., Liu, D., Xiao, Y., Liu, Z., Song, L., Zhang, Z.: Mesoporous Co3O4-Rods-Entangled carbonized polyaniline nanotubes as an efficient cathode material toward stable lithium-air batteries. ACS Appl Energy Mater. **2**(4), 2939–2947 (2019)
23. Cui, Y., Wen, Z., Lu, Y., Wu, M., Liang, X., Jin, J.: Functional binder for high-performance Li–O2 batteries. J. Power Sources **244**, 614–619 (2013)
24. Fu, Z., Wei, Z., Lin, X., Huang, T., Yu, A.: Polyaniline membranes as waterproof barriers for lithium air batteries. Electrochim. Acta **78**, 195–199 (2012)
25. Li, F., Zhu, M., Luo, Z., Guo, L., Bian, Z., Li, Y., Luo, K.: Nitrogen-doped graphene derived from polyaniline/graphene oxide composites with improved capacity and cyclic performance of Li-O 2 battery. J. Solid State Electrochem. **23**(8), 2391–2399 (2019)
26. Huang, K., Li, Y., Xing, Y.: Increasing round trip efficiency of hybrid Li–air battery with bifunctional catalysts. Electrochim. Acta **103**, 44–49 (2013)
27. Ryu, J., Park, M., Cho, J.: Advanced technologies for high-energy aluminum-air batteries. Adv. Mater. **31**(20), 1804784 (2019)
28. Liu, Y., Sun, Q., Li, W., Adair, K.R., Li, J., Sun, X.: A comprehensive review on recent progress in aluminum–air batteries. Green Energy Environ **2**(3), 246–277 (2017)
29. Yuan, Y., Ahmed, J., Kim, S.: Polyaniline/carbon black composite-supported iron phthalocyanine as an oxygen reduction catalyst for microbial fuel cells. J. Power Sources **196**(3), 1103–1106 (2011)
30. Ferrandon, M., Kropf, A.J., Myers, D.J., Artyushkova, K., Kramm, U., Bogdanoff, P., Wu, G., Johnston, C.M., Zelenay, P.: Multitechnique characterization of a polyaniline–iron–carbon oxygen reduction catalyst. J Phys Chemy C **116**(30), 16001–16013 (2012)
31. Gavrilov, N., Pašti, I.A., Mitrić, M., Travas-Sejdić, J., Ćirić-Marjanović, G., Mentus, S.V.: Electrocatalysis of oxygen reduction reaction on polyaniline-derived nitrogen-doped carbon nanoparticle surfaces in alkaline media. J. Power Sources **220**, 306–316 (2012)
32. Trapp, V., Christensen, P., Hamnett, A.: New catalysts for oxygen reduction based on transition-metal sulfides. J. Chem. Soc. Faraday Trans. **92**(21), 4311–4319 (1996)
33. Minisy, I.M., Gavrilov, N., Acharya, U., Morávková, Z., Unterweger, C., Mičušík, M., Filippov, S.K., Kredatusová, J., Pašti, I.A., Breitenbach, S., Ćirić-Marjanović, G.: Tailoring of carbonized polypyrrole nanotubes core by different polypyrrole shells for oxygen reduction reaction selectivity modification. J. Colloid Interface Sci. **551**, 184–194 (2019)
34. Osmieri, L., Zafferoni, C., Wang, L., Monteverde Videla, A.H., Lavacchi, A. Specchia, S.: Polypyrrole-Derived Fe− Co− N− C catalyst for the oxygen reduction reaction: performance in alkaline hydrogen and ethanol fuel cells. ChemElectroChem **5**(14), 1954–1965 (2018)
35. Lin, Z., Waller, G.H., Liu, Y., Liu, M., Wong, C.P.: 3D Nitrogen-doped graphene prepared by pyrolysis of graphene oxide with polypyrrole for electrocatalysis of oxygen reduction reaction. Nano Energy **2**(2), 241–248 (2013)
36. Han, S.J., Jung, H.J., Shim, J.H., Kim, H.C., Sung, S.J., Yoo, B., Lee, D.H., Lee, C., Lee, Y.: Non-platinum oxygen reduction electrocatalysts based on carbon-supported metal–polythiophene composites. J. Electroanal. Chem. **655**(1), 39–44 (2011)
37. Singh, S.K., Crispin, X., Zozoulenko, I.V.: Oxygen reduction reaction in conducting polymer PEDOT: density functional theory study. J Phys Chem C **121**(22), 12270–12277 (2017)
38. Vigil, J.A., Lambert, T.N., Eldred, K.: Electrodeposited MnO x/PEDOT composite thin films for the oxygen reduction reaction. ACS Appl. Mater. Interfaces. **7**(41), 22745–22750 (2015)
39. Liao, Y., Wang, D., Li, X., Tian, S., Hu, H., Kong, D., Cai, T., Dai, P., Ren, H., Hu, H., Li, Y.: High performance aluminum ion battery using polyaniline/ordered mesoporous carbon composite. J. Power Sources **477**, 228702 (2020)

40. Kuo, Y.L., Wu, C.C., Chang, W.S., Yang, C.R., Chou, H.L.: Study of poly (3, 4-ethylenedioxythiophene)/MnO_2 as composite cathode materials for aluminum-air battery. Electrochim. Acta **176**, 1324–1331 (2015)

41. Wang, D., Hu, H., Liao, Y., Kong, D., Cai, T., Gao, X., Hu, H., Wu, M., Xue, Q., Yan, Z., Ren, H.: High-performance aluminum-polyaniline battery based on the interaction between aluminum ion and-NH groups. Sci. China Mater. **64**(2), 318–328 (2021)

42. Luo, M., Sun, W., Xu, B.B., Pan, H., Jiang, Y.: Interface engineering of air electrocatalysts for rechargeable zinc-air batteries. Adv. Energy Mater. **11**(4), 2002762 (2021)

43. Wang, C., Li, J., Zhou, Z., Pan, Y., Yu, Z., Pei, Z., Zhao, S., Wei, L., Chen, Y.: Rechargeable zinc-air batteries with neutral electrolytes: recent advances, challenges, and prospects. Energy Chem. 100055 (2021)

44. Lian, Y., Yang, W., Zhang, C., Sun, H., Deng, Z., Xu, W., Song, L., Ouyang, Z., Wang, Z., Guo, J., Peng, Y.: Unpaired 3d electrons on atomically dispersed cobalt centres in coordination polymers regulate both oxygen reduction reaction (ORR) activity and selectivity for use in zinc-air batteries. Angew. Chem. Int. Ed. **59**(1), 286–294 (2020)

45. Jo, Y.N., Kang, S.H., Prasanna, K., Eom, S.W., Lee, C.W.: Shield effect of polyaniline between zinc active material and aqueous electrolyte in zinc-air batteries. Appl. Surf. Sci. **422**, 406–412 (2017)

46. Deyab, M.A., Mele, G.: Polyaniline/Zn-phthalocyanines nanocomposite for protecting zinc electrode in Zn-air battery. J. Power Sources **443**, 227264 (2019)

47. Li, M., Liu, B., Fan, X., Liu, X., Liu, J., Ding, J., Han, X., Deng, Y., Hu, W., Zhong, C.: Long-shelf-life polymer electrolyte based on tetraethylammonium hydroxide for flexible zinc–air batteries. ACS Appl. Mater. Interfaces. **11**(32), 28909–28917 (2019)

48. Hosseini, S., Soltani, S.M., Li, Y.Y.: Current status and technical challenges of electrolytes in zinc–air batteries: an in-depth review. Chem. Eng. J. **408**, 127241 (2020)

49. Banik, S.J., Akolkar, R.: Suppressing dendritic growth during alkaline zinc electrodeposition using polyethylenimine additive. Electrochim. Acta **179**, 475–481 (2015)

50. Xiao, Z., Wu, Y., Cao, S., Yan, W., Chen, B., Xing, T., Li, Z., Lu, X., Chen, Y., Wang, K. and Jiang, J.: An active site pre-anchoring and post-exposure strategy in Fe (CN) 64-@ PPy derived Fe/S/N-doped carbon electrocatalyst for high performance oxygen reduction reaction and zinc-air batteries. Chem. Eng. J. **413**, 127395 (2021)

51. Jia, X., Wang, C., Zhao, C., Ge, Y., Wallace, G.G.: Toward biodegradable Mg–air bioelectric batteries composed of silk fibroin–polypyrrole film. Adv. Func. Mater. **26**(9), 1454–1462 (2016)

Bio-Inspired Polymers as Organic Electrodes for Metal-Air Batteries

Abhinay Thakur and Ashish Kumar

Abstract Organic materials have gained a lot of interest for their usability as electrodes owing to their abundant structural diversity and high structural tenability, which offer prospects in an environmentally benign manner. The organic electrodes (OEs) have been applied in a large variety of energy storage devices, including metal-air batteries such as lithium-air (Li-air), zinc-air (Zn-air), magnesium-air (Mg-air), and much more. However, complications associated with the metal anodes, catalysts, and electrolytes have hindered the development and implementation of metal-air batteries (MABs), though there are some commercial applications. Tremendous attempts have been made toward their implementation in metal-air batteries, driven by the functionality and expanding awareness of the fundamentals at work in bioinspired polymers with the potential to adjust and increase their electrical and mechanical properties. In the last few decades, innovation in this sector has exploded, resulting in a plethora of bioinspired polymers as organic electrodes that have the potential to propel this cutting-edge subject to new heights. This chapter attempts to deliver a comprehensive understanding of bio-inspired polymers as OEs in the field of metal-air batteries, its recent advancements, synthesizing route, and enhanced performance in various metal-air batteries will be discussed in detail. The main objective of the investigation is to guide and inspire researchers to develop an effective and efficient pathway for obtaining the best and most appropriate bio-inspired polymers as OEs in this new and innovative field.

Keywords Polymers · Organic electrode · Metal-air battery · Li-air · Synthesis · Challenges

1 Introduction

The variable production of wind and solar energy entails the conservation of electrical energy for subsequent utilization. It is not ideal to reduce electricity generation

A. Thakur · A. Kumar (✉)
Department of Chemistry, Faculty of Technology and Science, Lovely Professional University, Phagwara, Punjab 144401, India

throughout situations of high winds or high solar illumination [1, 2]. When integrating sun and wind to fuels, the ability to manage high power from a low energy density and source of energy is vital to accompany the periodic oscillations of wind and light. Several charge and power storage systems are now being developed in response to significant advancements in supercapacitors and batteries for automobiles and portable devices. Electrochemical storage devices for portable electronics must have relatively high energy density; similarly, batteries for electric cars, supercapacitors, and hybrid auto batteries should all have high energy density. Energy density is a minor concern for static electrical energy storage. Metal air batteries have also garnered a lot of interest because of their larger energy capacity, low cost, and ecologically beneficial nature. An electrochemical cell in which air is limited and metal is oxidized is known as a metal-air battery (Fig. 1). Anodes can be made out of metals like potassium, sodium, and lithium, alkaline earth metals including magnesium and calcium, metalloids like Silica and Alumina, and transition elements including zinc and iron. Regardless of the type of anode employed, the electrolyte could be either hydrous/non-hydrous. Separators separate the anode and cathode of other reducing electrodes, which are both made of air.

Metal air batteries are a one-of-a-kind energy storage system because cathodic oxygen delivers an unlimited supply of oxygen from the environment that does
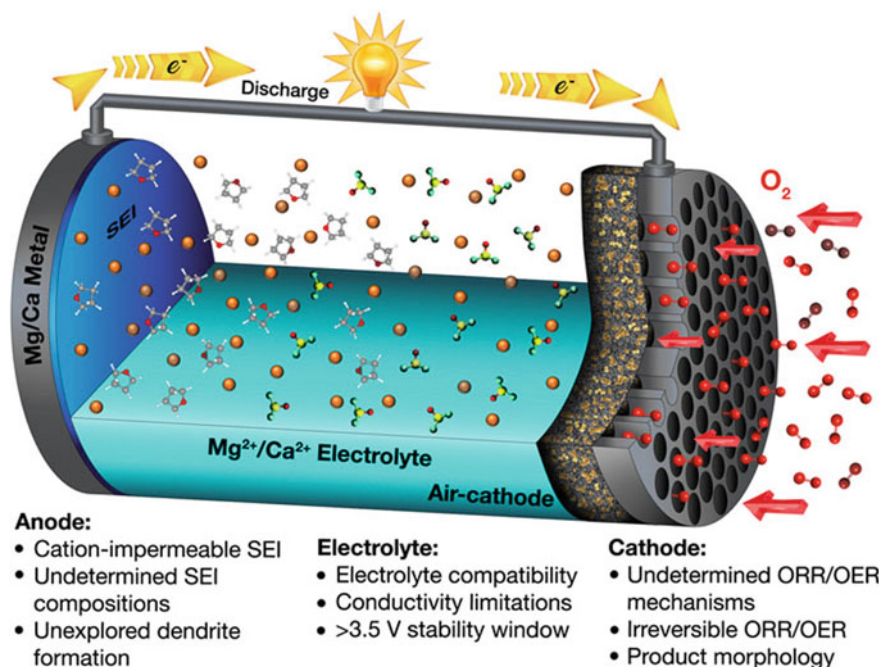
Fig. 1 Schematic illustration of metal-air battery. Adapted with permission [5]. Copyright (2021) The authors, some rights reserved, exclusive licensee Frontiers. Distributed under Creative Commons Attribution License 4.0 (CC BY)

not need to be stored. MABs were initially introduced in the early 1800s, and in 1932, Maiche introduced the firstly non-rechargeable Zn-air battery. Since then, there has been a lot of research and development in the field of MABs. As a result of this experiment, non-protic (non-aqueous) and protic (aqueous) batteries have been developed. Anodic metals including magnesium, aluminum, and iron, as well as an air cathode and aqueous electrolytes, were discovered early on. When the disadvantages of aqueous electrolytes were discovered, non-aqueous electrolyte compositions were developed. As the cathode material (natural O_2) is commonly accessible and the anode could be manufactured with cost-effective metals, such batteries are affordable. Due to their increased power density and heat capacity when compared to typical parallel batteries, MABs appear to be one of the most beneficial and novel options for future demands, particularly for electric vehicles (EVs). Metal air batteries are a type of primary and secondary cell that is among the most advanced. These batteries are often categorized as fuel cells because air circulates throughout the cell between the electrodes. MAB's first research project was an aqueous Zn-air battery, which had been produced using cutting-edge technology and performed similarly to today's batteries. As per the timeline, the inaugural Zn-air battery was invented in 1878 [3, 4]. Metal-air battery technology has advanced greatly in the twenty-first century. Several metals, associated oxygen, and electrolyte interactions, and other catalysts have all been explored in recent years for their enhanced utility, effectiveness, and economic value.

To make a bi-functional catalyst (Co-NC@CoFeS$_2$) for oxygen evolution reaction (OER) and oxygen reduction reaction (ORR), Wang et al. [6] employed a basic in-situ synthesis of cobalt-iron sulfide on Co and N co-doped polyhedral carbon (Co-NC). This usage of Co-NC substrate and cobalt-iron sulfide broadens reaction pathways while also enhancing electron transport efficiency throughout the catalyzed reaction. The merged effects of the Co-NC substrate and the endorsed cobalt-iron sulfide in controlling electrical and chemical interaction, electronic structure, and electrical conductivity were demonstrated, resulting in a voltage gap of 0.646 V among the OER potential at 10 mA/cm^2 and the half-wave potential of the ORR for Co-NC@CoFeS$_2$, implying an improved catalytic potential. An air electrode constructed of Co-NC@CoFeS$_2$ in a rechargeable Zn-air battery has a significant peak power density (174.4 mW/cm^2), high reliability, and a substantial open voltage (1.44 V) over 400 cycles. As a result, this study adds to our understanding of how to develop and manufacture functional electrocatalysts for Zn-air batteries. Figure 2 shows several MABs topologies. A flexible battery's key elements are the cathode, anode, separator, and high conductivity electrolyte. A solid-state electrolyte is a traditional electrolyte for a flexible battery system. To minimize battery weight, a thin metallic plate is utilized as a metal anode.
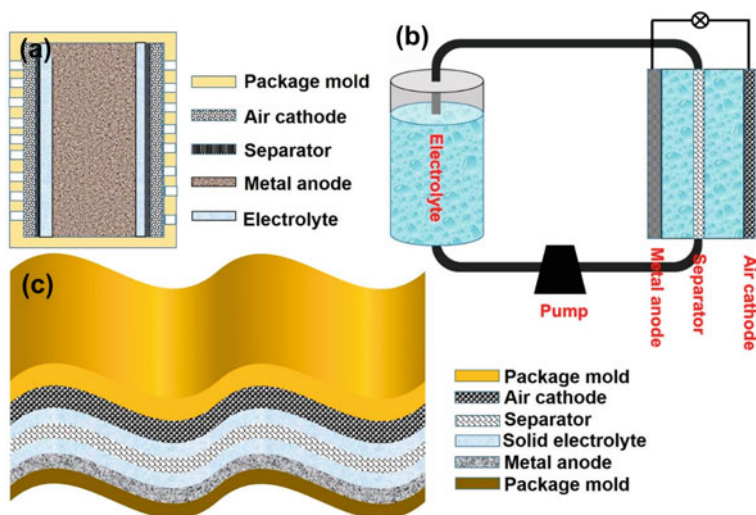
Fig. 2 Several MAB topologies are shown in this diagram: **a** multi-cell static configuration, **b** flow battery, and **c** flexible battery. Adapted with permission [7]. Copyright (2020) The authors, some rights reserved, exclusive licensee MDPI. Distributed under Creative Commons Attribution License 4.0 (CC BY)

2　Bio-inspired Polymers

Polymers derived from the living creature's cells such as shrubs, plants, trees, and microbes are known as natural biopolymers. Such polymers are often built up of a few different kinds of carbon-based repetitive chemical blocks derived from the natural feedstock. The least recognized biopolymers are polysaccharides and proteins, but other biopolymers with complex 3D branched structures, such as lignin, and intricate polymers of long-chain fatty acids, such as cutin, are also included [8, 9]. Polysaccharides, which are made up of carbohydrate monosaccharides bound by o-glycosidic bonds, have a variety of physicochemical characteristics that vary based on the monosaccharide, its activity, and its origin. The most explored materials in the field of battery separator and electrolyte applications are cellulose, chitosan, starch, lignin, carrageenan, agar, alginates, xanthan gum, and guar gum. Each one has its own set of functional features, such as lignin's high oxidative longevity, cellulose acetate's water solubility and thus excellent film-forming capability, and carrageenan's salt compatibility, which makes it appropriate for solid polymer electrolyte (SPE) production.

In considerations of the electrode part, bio-inspired technology could be divided into biomineralization, biotemplating, biomass material, surface modification, and biopolymer material. The size of biotemplating materials determines their classification, and the focus of the discourse is on improving the energy density of the

electrodes. Furthermore, biotemplating is regarded as a cost-effective and environmentally friendly method for simplifying the synthesis of nanomaterials exhibiting intricate mechanisms. These templating techniques also lead to rapid changes in material characteristics, which could increase electrode performance. We cover the utilization of bioinspired polymers as organic electrodes with basic descriptions in the MABs system. Although traditional electrode materials' manufacturing processes are well procured, attempts must be made to improve the imitating procedure to create a biomineralization procedure that facilitates and regulates the use of safe and environmentally friendly starting reagents [10–14].

2.1 Biopolymers—Extraction and Separation

The traditional method of producing paper and pulp involves time-consuming segregation and extraction methods; mechanical, chemical, and thermoelectric methods are used to separate cellulose from hemicellulose and lignin. It takes a lot of energy to extract cellulose for paper manufacture. Burning the dark-brown liquor generated as a waste product throughout the cellulose manufacturing process (containing processed chemicals and lignin derivatives) can offer some processing energy. The preponderance of lignin is used in the manufacturing process to generate heat. Moreover, lignin waste could be utilized as a feedstock for surfactants and dispersion agents, but this only accounts for a small portion of global lignin production[15–18]. As a result of the separation procedure from wood, cellulose is produced as fibers and paper/films.

Chemical procedures that depolymerize biopolymers to monomers would result in the loss of essential polymer properties, highlighting the importance of focusing on extraction methods that preserve at least a few of the lignin polymeric structures. The chemical composition of different sections of plants varies greatly, from leaves and conifers through trunks and heartwood, branches, and roots. As a result, a novel process for isolating lignin from plants must begin with the plant component that contains the most lignin, that is generally the peel or the fruit/nut. Lignin may account for 30–40% of the bark, while the remaining 60–70% exhibit significant chemical diversity. Antibacterial and antifungal polyphenols are common antibacterial and antifungal defense mechanisms found in the bark of several trees. A few of these polyphenols are being utilized for centuries; for instance, tannins derived from bark or acorns are employed for the tanning process to crosslink proteins in animal hides. Even though lignin appears to be the dominant quinone source in bark, researchers should anticipate identifying multiple sources of quinones.

2.1.1 Role as Organic Electrodes

In materials research, it's not uncommon for inorganic materials to set benchmarks, whereas organics offer a cost-effective alternative with adequate efficacy. However, if we study our environment, our gaze is drawn to the structural diversity of life,

which is primarily made up of organics [19–21]. In reality, the perceptual equipment that allows humans to detect that richness is made of organics, demonstrating that the emergent qualities emerging from organic materials' structural organization provide an infinite pool of structure-function correlations.

As a result, organic electrode materials could be created using chemical resources derived from fossil energy reserves. New substances are being created using monomers that can be easily produced from renewable resources. Organic electrode materials have transformed, with contemporary work demonstrating a plethora of novel options. Few organic electroactive compounds can compete with proven inorganic energy storage methods in terms of energy density since they possess a low mass density and frequently necessitate a significant amount of conducting substances in electrode compositions (Wh/kg). The reversibility and low permanence of organic electrode materials are another concern that must be addressed. As the amount of material required for huge electrical energy storage is so huge, precision chemistry employed in the production of organic electrode elements is expected to be prohibitively costly and energy-intensive.

Zhong et al. [22] developed a unique redox donor-acceptor linked microporous polymer with benzene and anthraquinone as intermediates and demonstrated for the unprecedented time that conjugated microporous polymers (CMP) could be used as ultralong-lasting anodes for rechargeable air batteries using C–C linkages. When compared to its linear predecessor, the redox donor-acceptor linked microporous polymer (AQ-CMP) has an interlinked octupole system that provides not only a favorable electrical architecture for improved electron transfer and n-doping activities but also a large volume of the active site for enhancing formula-weight-based redox capabilities. AQ-CMP has a specified potential of 202 mAh/kg (96% of theoretical capacity) at 2 A/g and 100% capacity persistence after 60,000 charge/discharge cycles owing to its highly cross-linked and porous composition. Due to the dissociated electrolyte and cathode configuration, the discharging voltage and voltage efficacy were increased to 1 V and 87.5%, respectively.

3 Organic Electrodes in Metal-Air Batteries

Despite the fact that current battery technologies such as lithium-ion batteries (LIBs) have an uncertain future, MABs have been able to gain interest in the EVs and static power sectors. A timeline of the production of MABs from 1878 to 2019 has been shown in Fig. 3. The first Zn-air battery was proposed in 1878, according to the timeline. Metal-air battery chemistry has made significant advances in the twenty-first century. Several metals, their combinations with oxygen and electrolytes, and other catalysts have all been studied in recent years for their greater utility, efficiency, and economic value. To achieve a driving range of 500 miles, batteries must have a functional specific energy density of 1700 Wh/kg, that is the utilizable specific energy density of gasoline (theoretical specific energy density of the fuel is 13 kWh/kg, but energy conversion potency of the fleet's tank-to-wheel is only 12.6%), as well
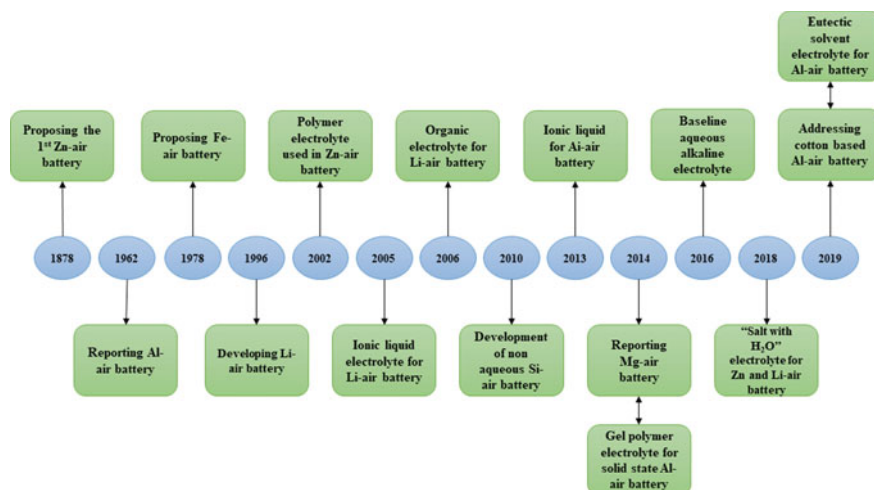
Fig. 3 MABs with an illustrious history. Adapted with permission [26]. Copyright (2021) The authors, some rights reserved, exclusive licensee IOP Science. Distributed under Creative Commons Attribution License 3.0 (CC BY)

as a volumetric energy density of 417 Wh/L. (125 kWh capacity is required for a maximum 300 L battery).

Traditional batteries, like LIBs, rely on electrolyte chemical properties, have a capacity of only 200 Wh/kg, and it's widely expected that future LIB advances will indeed enhance energy densities by up to 30%, with potential densities exceeding 400 Wh/kg [23–25]. As a result, experts are investigating alternate high-energy-density electric vehicle (EV) options that expense less than $100 per kWh. MABs also have much higher theoretical energy densities (1–11 kWh/kg, based on the thermodynamics of active materials except cathode oxygen and related system components) than LIBs, making them a viable alternative for next-generation electrochemical energy storage technologies in Electric vehicles or power system energy storage applications where high consumption is required. Metal anodes (Na, Li, Mg, Zn, Fe, Al, and other metals), atmospheric air open cathodes, and electrolytes, in particular, are used in MABs, that are open electrochemical systems (depending on the type of anode used, aqueous or non-aqueous electrolyte).

MABs, unlike other batteries, can combine standard battery design characteristics with fuel cell design capabilities. MABs also have higher specific energy densities (3–30 times) than LIBs, that only retain the anode's active element (metal) and retrieve the reactant (O_2) from the air cathode via a reduction reaction throughout discharge, implying that the anode metal is the primary weight factor influencing MABs' specific energy density. For example, Li-air batteries' maximum specific energy density, except oxygen cathode or other cell parts, could perhaps attain 11 kWh/kg, which is comparable to gasoline, whereas Zn-air batteries' maximum specific energy density, except oxygen cathode or other cell parts, could even achieve 1.3 kWh/kg, that is

greater than LIBs. Tesla recently filed eight patent claims that cover the use of MAB (Mg, Fe, Zn, Li, Al) batteries as range extenders for LIB batteries. Fluidic Energy (Scottsdale, Arizona), Eos Energy Storage (New York), and Powair (Europe) are among the companies that are putting Zn-air batteries to the test in grid energy storage systems at pilot plants. IBM unveiled the "Battery 500" initiative in 2009, intending to develop Li-air batteries with a 500-mile range (800 km). The usage of magnesium-air batteries in electric vehicles is also being investigated.

3.1 Working Principles of MABs

MABs have a different functioning principle than regular ionic batteries. In traditional ionic batteries, metallic ions are transferred from anode to cathode as shown in Fig. 4. In MABs, metals or alloys form metallic ions at the anode, while O_2 forms hydroxide ions on the cathode. Figure 4 depicts the function of a MAB in an aqueous or non-aqueous electrolyte solution. In an aqueous electrolyte system, O_2 disperses into batteries via the gas diffusion layer and converts to accepting electrons, forming O_2 anions. In a non-aqueous electrolyte solution, O_2 accumulates electrons and becomes an oxygen anion. Metals give up their electrons, forming metallic ions, which dissolve in electrolytes. During the charging operation of a rechargeable MAB, these processes will be reversible.

In electrochemical processes involving MABs, oxygen and metals are involved. The chemical pathway of a primary Zn–air battery comprises ORR at the cathode and Zn oxidation at the anode[27]. Overall, oxygen diffuses into the air electrode and is eventually transformed to hydroxyl ions at the active catalyst film; the hydroxyl ions then transfuses to the anode and mixed with zinc ions to form soluble zinc
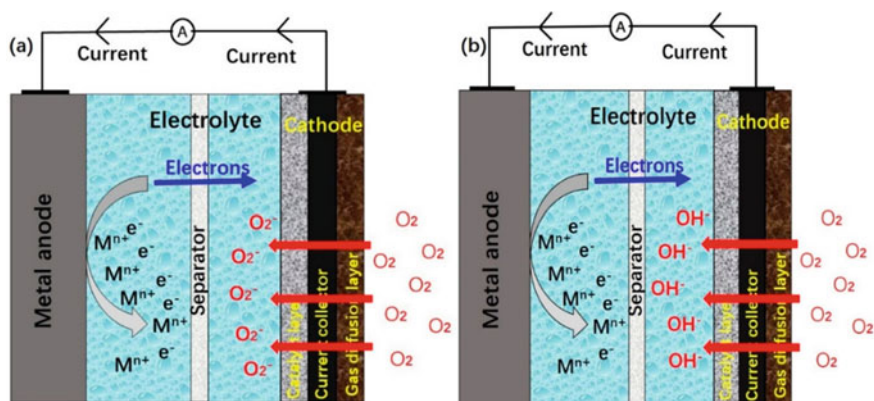
Fig. 4 MAB operating principles illustrations for **a** non-aqueous electrolyte, and **b** aqueous electrolyte. Adapted with permission [7].) Copyright (2020) The authors, some rights reserved, exclusive licensee MDPI. Distributed under Creative Commons Attribution License 4.0 (CC BY

ions ($Zn(OH)_4^{2-}$). $Zn(OH)_4^{2-}$ degrade to ZnO molecule when it achieves saturation concentration. Below are the chemical reaction equations.

$$\textbf{Anode} : Zn \rightarrow Zn^{2+} + 2e^-$$
$$Zn^{2+} + 4OH^- \rightarrow Zn(OH)_4^{2-}$$
$$Zn(OH)_4^{2-} \rightarrow ZnO + H_2O + 2OH^-$$

$$\textbf{Total} : Zn + 2OH^- \rightarrow ZnO + H_2O + 2e^- (E0 = -1.25V).$$

$$\textbf{Cathode} : O_2 + 2H_2O + 4e- \rightarrow 4OH^- (E0 = 0.4V).$$

$$\textbf{Overall reaction} : 2Zn + O_2 \rightarrow 2ZnO (E0 = 1.65V).$$
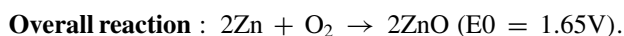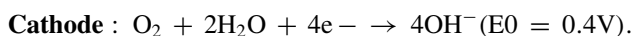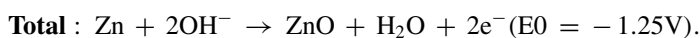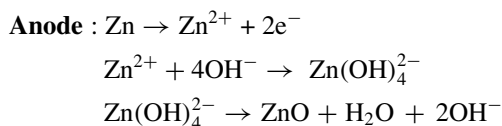
The standard electrode potential in relation to the standard H_2 electrode is denoted by E0. Due to internal battery loss caused by activation, ohmic polarization, and concentration loss, real operating voltages are frequently >1.2 V, substantially lower than the standard potential (1.65 V). MABs are intriguing not only as portable power sources for electronics and electric vehicles, but also as persuasive energy transfer stations or energy storage devices for managing energy flow between renewable energy generators, such as wind turbines and photovoltaic panels, electric grids, and end-users (Fig. 5).

3.1.1 Zn-Air Battery

Small-current applications, like hearing aids, have been served better by zinc-air batteries. In this category, they are the only ones who have been effective and conventional as primary cells. Despite their limited shelf lifespan and recharging capability, zinc-oxygen batteries are the fastest and least reliable way to create a functional secondary metal-air battery. In 1878, the Zn-air battery was the initial MABs battery to be developed. To increase Zn accumulation, multiphase electrolytes were used to create a polymer electrolyte-based Zn-air battery, OER, with a new dendrite-resistant air battery system. Different instruments were utilized to explore various practical and theoretical properties of these batteries, including galvanostatic discharge and electrochemical impedance spectroscopy (EIS), scanning electron microscopy (SEM), and X-ray diffraction (XRD).

The idealized operating principles of an aqueous zinc-air battery with pH-buffered near-neutral electrolytes are shown in Fig. 6. For descriptive reasons, we assume a basic weak acid (HA) as an electrolyte. In the air electrode, dissolved O_2 is transformed to H_2O (reaction i). A change in H^+ concentration causes the weak acid's equilibrium to be interrupted. When H^+ is absorbed locally, the dissociation process,
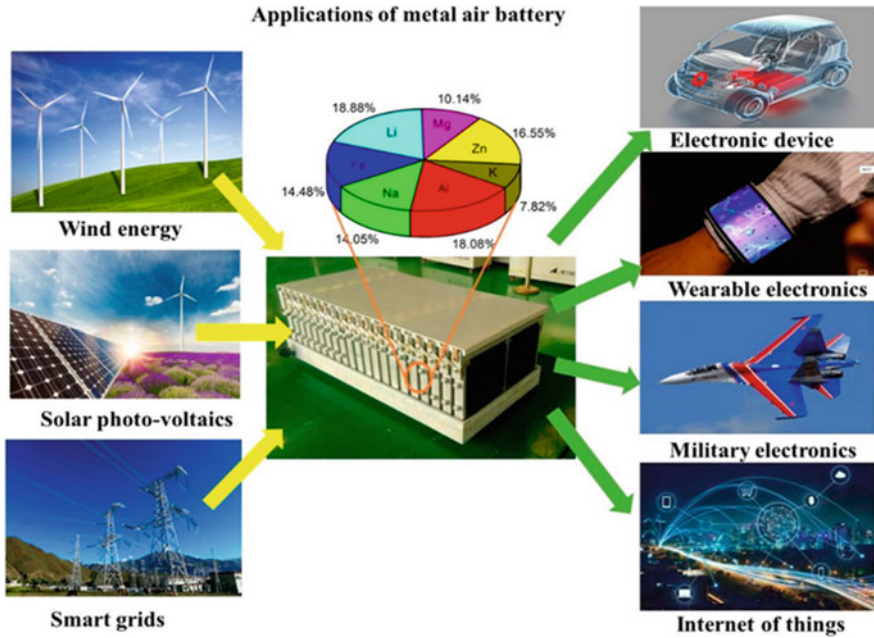
Fig. 5 Applications of metal-air batteries as the source of energy and storage systems. Adapted with permission[7]. Copyright (2020) The authors, some rights reserved, exclusive licensee MDPI. Distributed under Creative Commons Attribution License 4.0 (CC BY)

Fig. 6 Zinc-air battery has pH-buffered near-neutral electrolytes and a generic weak acid, HA, in idealized performance. The direction of discharge is shown by arrows. Adapted with permission [28]. Copyright (2020) The authors, some rights reserved, exclusive licensee Wiley. Distributed under Creative Commons Attribution License 4.0 (CC BY)
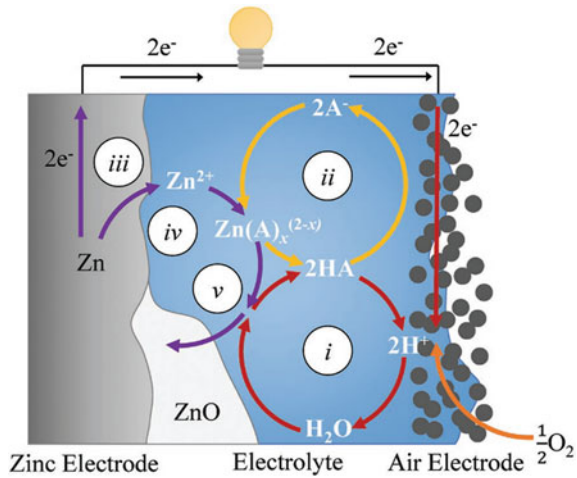
HA $\leftrightarrow$ H$^+$ + A$^-$, moves to the right (reaction ii). At the Zn electrode, the electrochemical oxidation reaction (reaction iii) yields Zn^{2+}, which produces complexes with several electrolyte solutes (reaction iv), least notably with the weak acid's conjugate base, A$^-$. The pH stability of the electrolyte is improved by the formation of complexes between Zn^{2+} and A$^-$. When the solubility limit of zinc is surpassed, zinc gets solidified (reaction v).

3.1.2 Al-Air Battery

Denoted by AAB, the Al-air battery is an excellent energy source for EVs. It has a far higher energy density than LIBs (estimated value of around 8100 Wh/kg). In a new AAB, $(C_4H_9)_4NF$ salt mixed in non-aqueous solvents such as CAN, PC/TEG-DME, and others was reported as a revolutionary organic non-aqueous electrolyte. Other variants of luminium-air battery employ $AlCl_3$ as the electrolyte, Al foil as the gas diffusion electrode, and electrolyte as 1-ethyl-3-methylimidazolium chloride.

3.1.3 Lithium-Air Battery

K. Abraham created the first-ever LAB. A Li$^+$ anode in the type of an electrically conducting membrane and a carbon impregnated air cathode was used. Optimal Li-air batteries might have the maximum energy density of any MABs (theoretical values around 3458 Wh/kg), exceeding Li-ion batteries and making them a viable EES candidate. The oxygen electrode has been the subject of extensive research since its introduction in 1996 to improve its electrochemical reversibility. Since its commercialization in 1996, extensive research has been carried out to improve the oxygen electrode's electrochemical reversibility.

3.1.4 Magnesium-Air Battery

The magnesium serves as an anode, and the cathode is made of air. As a reducing electrode, activated carbon is often utilized. Depending upon the electrode area of the electrolyte substance, catalysts are usually utilized using a light coating of aquaphobic polymer composition and a metallic plate as the conducting element. Supplementary magnesium batteries seem to be primarily in the research and development phase, and one of the most challenging issues has been determining the correct electrolyte combination. SEM, Fourier transform infrared spectroscopy (FTIR), and EIS were used to investigate the electrochemical behavior of a biocompatible ionic liquid including a polymeric electrolyte and Mg-air battery.

3.1.5 Calcium-Air Battery

With comparison to Na and Mg, calcium is abundant in the earth's crust [29, 30]. Calcium is one of the finest, benign, and notable metals in MAB's range, and it has been shown to have numerous applications when used with an aqueous electrolyte. Nirupama U Pujare developed a calcium air battery in 1988 that used a solid electrolyte made up of $CaCl_2$ and Cao molten salts. Calcium can achieve high electrical density at a cheaper cost of production as a metal for metal-air batteries.

Wu et al. [31] created a one-pot iron covalent porphyrin polymers (FePor-CPP) with strategically positioned Fe, N atoms, sodium hypophosphite (NaH_2PO_2) precursors, and a permeable framework, $Co_3[Co(CN)_6]_2$, which were carbonized into N, P-doped carbon nanospheres with the active framework of both bimetallic CoC_x nanoparticles and CoFe phosphides (denoted as CoC_x/CoC). For the oxygen evolution reaction (OER) and oxygen reduction reaction (ORR), better catalytic activity was achieved in an alkaline phase by using $CoC_x/(Co_{0.55}Fe_{1.945})_2P@C$ electrode catalysts, with an overpotential of 0.39 V at 10 mA/cm^2 for OER and $E_{1/2}$ of 0.84 V for ORR, respectively. Furthermore, as an air electrode for a rechargeable Zn-air battery, $CoC_x/(Co_{0.55}Fe_{1.945})_2P@C$ displayed a substantial power density of 131 mW/cm^2 and charge-discharge cycle durability, indicating that $CoC_x/(Co_{0.55}Fe_{1.945})_2P@C$ might be used in energy conversion equipment. The addition of P to the $Co_{0.55}Fe_{1.945}$ alloy caused a shift in the electronic configuration of bimetallic $(Co_{0.55}Fe_{1.945})_2P$, leading to a reduced energy gap between $CoC_x/(Co_{0.55}Fe_{1.945})_2P@C$ and $CoC_x/Co_{0.55}Fe_{1.945}@C$ resulting in excellent electrocatalytic capabilities. Using bio-inspired polymers as OEs, this paper describes a method for producing multifunctional non-precious catalysts for power and energy of electrocatalytic activity.

As illustrated in Fig. 7a [32], a homemade basic Zn-air battery was created using an alkaline electrolyte (6 M KOH + 0.2 M Zn(Ac)$_2$), highly porous carbon polyhedron (FCC@NC) air cathode, and anode as Zn foil. Using the same measurement variables, a comparison study for traditional batteries with Pt/C air cathodes has been examined. The open-circuit potential of the FCC@NC-based primary Zn-air battery was 1.466 V (Fig. 7b), which was much higher than that of commercialized batteries (1.371 V). The FCC@NC battery has a gravimetric energy density of 784.3 Wh/kg$_{Zn}$ and a specific capacity 659.5 mAh/g, quite significantly than the Pt/C battery (694.6 Wh/kg$_{Zn}$ and 614.7 mAh/g; Fig. 7c). The discharge polarization and power density curves also revealed that the FCC@NC cathode had a greater peak power density and current density than typical battery cathodes (Fig. 7d). The maximum power density of the FCC@NC battery was 118.2 mW/cm^2 at 120.0/cm^2, much greater than that of conventional batteries (58.3 mW/cm^2 at 100 mA/cm^2). The FCC@NC-based battery's potential plains in the galvanostatic discharged at differing current densities (around 2–40 mA/cm^2) were also greater than the commercial counterpart (Fig. 7e), suggesting that it is intriguing for both high-power capability and high energy density implementations. Furthermore, by adjoining two FCC@NC-based core Zn-air batteries in a series, a commercialized light-emitting
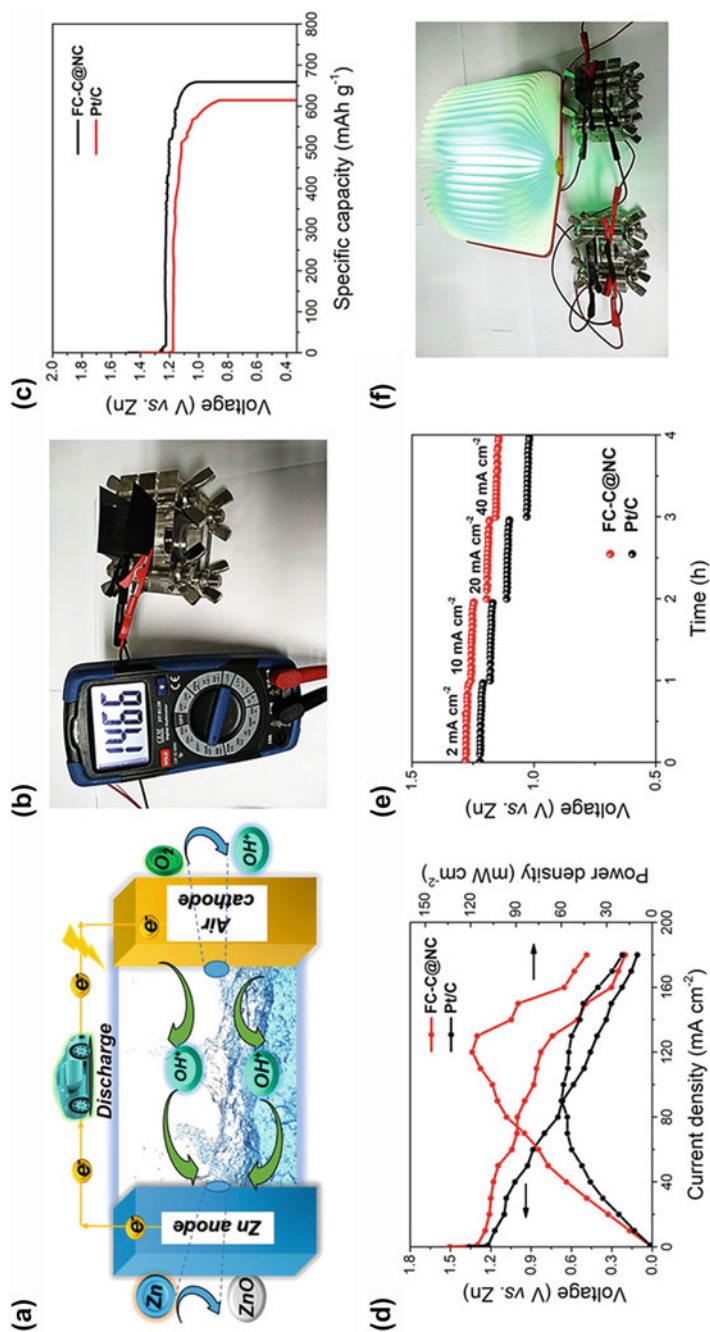
Fig. 7 The efficiency of zinc-air batteries with FCC@NC and Pt/C catalysts as air electrode catalysts, **a** a diagram of the primary zinc-air battery, **b** a photograph of a zinc-air battery with an FCC@NC cathode and a measured open-circuit voltage of 1.466 V, **c** at a current density of 10 mA/cm², discharge curves of FCC@NC and Pt/C-based zinc-air batteries, **d** polarization and power density curves, **e** galvanostatic discharge curves of zinc-air batteries based on FCC@NC and Pt/C air cathodes, respectively, at varied current densities and **f** Photograph of a commercialized LED that is powered by two FCC@NC zinc-air batteries connected in series. Adapted with permission [32]; Copyright (2020) The authors, some rights reserved, exclusive licensee Wiley. Distributed under Creative Commons Attribution License 4.0 (CC BY)

diode (LED) device was efficiently powered for over 2 h without brightness degradation, suggesting high operating stability (Fig. 7f). Finally, the findings showed that the suggested FCC@NC catalyst may be used in real-world zinc-air batteries in ambient conditions.

Zhong et al. [22] found that combining anthraquinone with porous materials and strongly cross-linked improve electrochemical performance significantly. The AQ-CMP anode, as designed, produces near-theoretical potential (202 mAh/g at 2 A/g), exceptional cycling reliability (nearly no disintegration over 60,000 cycles at 20 A/g), and rate potential (58% capacity retention at 20 A/g) that outperforms its regression counterpart (AQ-Lin, 73% retention after 250 cycles) and all other polymer anodes for air batteries. After just replacing the cathode, the CMP-air entire cell had a constant specific capacity of 181 mAh/g at 3 A/g and a maximum recovery rate of nearly 100%. The discharge voltage maximum estimations of all known polymer-air cells were increased considerably more using decoupled cathodes and electrolytes. Ex-situ spectroscopic experiments at 1 V with an 87.5% voltage efficiency revealed the essential importance of CMP's cross-linked porous structure in outstanding stability and efficiency. This study expands the redox CMP family's application possibilities, but it also sheds new light on the architecture of CMP-based electrodes for a variety of energy storage devices.

Oka et al. [9] synthesized poly(2,5-dihydroxy-1,4-benzoquinone-3,6-methylene) (PDBM) by simple addition condensation, which has been evaluated as the anode in an acidic aqueous electrolyte; pH 1. At 0.2 V vs. Ag/AgCl, the polymer exhibited a reverse redox activity, as well as a huge potential (300 mAh/$g_{polymer}$) and excellent cycle stability (500 cycles). A reusable acidic polymer-air battery comprising an air cathode, PDBM anode, and acidic aqueous electrolyte (pH $= 1$) has been constructed for the first time. The active component of the anode produced reversible charging-discharging patterns at an output voltage of 0.5 V, while the active component of the anode had a medium energy density of 172 mWh/g. The development of polymeric anode-active materials for a rechargeable acidic polymer-air battery with a high 1.5 V voltage and higher energy density will be the focus of future research.

Shao et al. [18] created Co-phthalocyanine-based (COPs) by combining phosphonitrilic chloride trimer as linker group and cobalt tetraaminophthalocyanine (CoPc(NH$_2$)$_4$) as an organic core component that also serves as a self-carrier enhanced with P, Co, C, and N to produce Co$_2$P nanoparticles grounded on N, P. The Co$_2$P/NPG demonstrated superior trifunctional electrocatalytic activity forth into the OER, ORR, and HER because to its unique manufacturing and metallic assets, as well as outstanding O$_2$ electrocatalytic activity i.e. overpotential of 0.32 V at a temperature of 10 °C as affirmed by density functional theory (DFT) calculations (89% following 17 h for ORR, 98% following 12 h for OER). After 55 h of usage, rechargeable Zn-air batteries (ZABs) comprising of a cathode made up of Co$_2$P/NPG, electro-catalyst produced a maximum output of around 103.5 mW/cm^2 and had outstanding cycle stability. Furthermore, the ZABs developed might be utilized to run the entire water-splitting process. Finally, the mechanism design of metallophthalocyanine-based COPs allows for additional design flexibility in

multifunctional electrocatalysts, resulting in a more comprehensive green energy infrastructure.

Oka et al. [33] explored the proton-storage abilities and charge of naphthoquinone-substituted poly(allylamine) as an electrode-active material for polymer air secondary batteries. In 0.05 M H_2SO_4 aqueous medium, 1,4-naphthoquinone (NQ) initiates two proton and two-electron redox reactions in a single phase at a potential = 0.05 V (against Ag/AgCl). The rate constants for heterogeneous electron transfer were the same as those for electrochemically reversible redox-active compounds. Finally, NQ was discovered to be a great choice for an electrode-active material in an acidic electrolyte. The NQ-substituted poly(allylamine) (PNQ) had been made by performing a simple nucleophilic substitution between 2 poly(allylamine) and bromo-1,4-naphthoquinone, which allowed the hydrophilic nature of the redox polymer to be modulated depending on the amount of NQ added. A polymer air secondary battery made composed of the Pt/C cathode, PNQ anode, and 0.05 M H_2SO_4 aq. electrolyte demonstrated outstanding cyclability (>100 cycles) and C-rate capability when drained at a low voltage of 0.8 V.

For the LIBs, Lu et al. [34] created a high-performance organic anode substance premised on lignin. As per analytical and empirical observations, chemically pre-lithiation of the lig molecule changed its electron configuration, resolving the organics' fundamental low conductivity. Due to this, the Li-lig-enhanced anode produced a greater preliminary CE, higher density, and superior cycle stability in both full and half cells. According to in-situ FTIR combined of ex-situ x-ray absorption near-edge spectra (XANES) and x-ray photoelectron spectroscopy (XPS) parameters, the excess of electrochemically available and reactive covalently linked C=C group over the Li-lig, as well as the elevated recyclability of Li unbinding/binding on such active regions, is related to certain outstanding Li-ion storage efficiency. The complete cell with the Li-lig/LiFePO₄ electrode showed a strong reversal discharge rate of 135 mAh/g when evaluated at 0.5 C, with outstanding capacity stability of 93.7% over 600 cycles.

4 Limitations

The chemical permanence of organic compounds is determined by the degree of chemical bonding in molecules. The bulk of organic molecules are covalent, and covalent bonds are prone to producing free radicals during charge/discharge operations, as well as interacting with a functional group on the primary chain. Organic electrode materials become inactive due to the presence of side reactions. Furthermore, the substantial volume expansion of organic material causes severe particle pulverization, causing the current collector to break off easily, resulting in poor stability. To enhance the durability of the electrode material, we must optimize both the molecular composition and the shape of the organic material. Inorganic electrolytes, organic compounds, particularly tiny organic molecules, have high intrinsic solubility. Organic electrode materials suffer from quick capacity degradation and

poor cycle stability due to their high solubility. This issue could be solved by using a suitable molecular design or combining organic and inorganic components. Using an aqueous electrolyte could also be a suitable option. As most organic molecules lack free ions or electrons, charge transfer is delayed and electric conductivity is weak. As a result, when producing the electrodes, a substantial amount of carbon is necessary as conductive additives, culminating in a reduction of the overall energy density of MABs. To increase the conductivity of organic electrode materials, molecular engineering, doping, and composition of conductive polymers or inorganic conductive polymers could be employed to improve MAB productivity.

5   Future Outlooks

Future research should take into account the multidimensional features of metal electrodes, particularly those that may have opposing impacts on one another. In secondary MABs, a typical trade-off between energy density and metal electrode cycled efficiency exists. Certain metal electrodes discharge to a wider detail of discharge (DOD) to achieve higher energy densities. The electrodes, on the other hand, find it challenging to revert to their typical morphology during charging, and dendritic development is frequently more extensive. As a result, the cyclic stability of the system must be decreased. Some metal electrodes perform at an extremely shallow DOD to achieve large cyclic frequencies (e.g. 10%). As a result, future rechargeable metal electrode designs should prioritize cycling stability at severe DOD. It's a massive project, but MABs need to do it if they want to compete with LIBs. Sophisticated characterization techniques, especially in situ methods, must be used. Despite various phenomenological research on metal electrodes in MABs, the understanding of battery electrochemistry is still limited. Techniques including FTIR, nuclear magnetic resonance, XRD, and EIS would be critical in increasing our understanding of metal electrodes in situ. These approaches, for example, could be used to identify and monitor intermediate molecules and by-products in a battery, particularly under operating conditions.

6   Conclusion

Following our discussion and investigation of numerous elements of MABs, it may be assumed that MABs have a wide range of applications as energy storage devices for various technology. These air batteries are utilized as energy storage for regulating energy circulation and powerful energy transfer terminals within renewable energy plants, as well as small sources of power for small gadgets and e-mobility. The price of metal-air batteries is greatly decreased, and users may operate the EVs at a cheap cost, because air cathode is of low cost and, in several instances, users could

simply utilize H_2O or salt solution as electrolyte. The battery has outstanding environmental sustainability; less toxic metals could be utilized as anodes, and renewable electrolytes might be utilized to improve the battery's environmental friendliness. All efforts are being made to enhance the cell's efficiency, but the situation is not simple. Because there are so many different tasks to choose from, many of them are incompatible. Improving cyclic life, in particular, could raise the cost of the cell. The current state of battery technology is initially investigated in this chapter. The primary problems are then examined in greater depth. Nonetheless, the area has a lot of room to develop in terms of both the scope of materials examined and the depth of understanding of the qualities that determine/control rate capabilities. Because of their inherent insulating properties, electron transmission in most organic materials is difficult. Augmenting these materials with high amounts of conductive additives can boost the composite's conductivity, but at the expense of inactive mass, lowering the composite's and cell's energy and power density. Poor cycle durability, sluggish electrochemical reactions, ORR/OER overcapacity, performance, low charge/discharge activity, zinc electrode reversibility, and bad rate capability are some of the technological challenges that need to be overcome future commercialization of ZABs. Crystal lattice, surface chemistry, and interlayer properties are all intrinsic structure variations of electrode materials that may be tracked in situ throughout the charge/discharge process using in situ characterization techniques. Furthermore, it is critical to investigate the dynamic evolution of intrinsically modified electrode materials during the charge/discharge process, as this will aid in a better understanding of the reaction mechanism and design considerations for these materials.

References

1. Yi, J., Liang, P., Liu, X., Wu, K., Liu, Y., Wang, Y., Xia, Y., Zhang, J.: Challenges, mitigation strategies and perspectives in development of zinc-electrode materials and fabrication for rechargeable zinc-air batteries. Energy Environ. Sci. **11**, 3075–3095 (2018)
2. Choi, W., Harada, D., Oyaizu, K., Nishide, H.: Aqueous electrochemistry of poly(vinylanthraquinone) for anode-active materials in high-density and rechargeable polymer/air batteries. J. Am. Chem. Soc. **133**, 19839–19843 (2011)
3. Wang, Z.L., Xu, D., Xu, J.J., Zhang, X.B.: Oxygen electrocatalysts in metal-air batteries: from aqueous to nonaqueous electrolytes. Chem. Soc. Rev. **43**, 7746–7786 (2014)
4. Deng, Y.P., Jiang, Y., Luo, D., Fu, J., Liang, R., Cheng, S., Bai, Z., Liu, Y., Lei, W., Yang, L., Zhu, J., Chen, Z.: Hierarchical porous double-shelled electrocatalyst with tailored lattice alkalinity toward bifunctional oxygen reactions for metal-air batteries. ACS Energy Lett. **2**, 2706–2712 (2017)
5. Lu, Y.T., Neale, A.R., Hu, C.C., Hardwick, L.J.: Divalent nonaqueous metal-air batteries. Front. Energy Res. **8**, 1–21 (2021)
6. Wang, Y., Jin, W., Xuan, C., Wang, J., Li, J., Yu, Q., Li, B., Wang, C., Cai, W., Wang, J.: In-situ growth of CoFeS2 on metal-organic frameworks-derived Co-NC polyhedron enables high-performance oxygen electrocatalysis for rechargeable zinc-air batteries, J. Power Sources **512**, 230430 (2021)
7. Wang, C., Yu, Y., Niu, J., Liu, Y., Bridges, D., Liu, X., Pooran, J., Zhang, Y., Hu, A.: Recent progress of metal—air batteries—a mini review. Appl. Sci. **9**, 2787 (2019)

8. Mecerreyes, D., Porcarelli, L., Casado, N.: Innovative polymers for next-generation batteries. Macromol. Chem. Phys. **221**, 1–7 (2020)

9. Oka, K., Furukawa, S., Murao, S., Oka, T., Nishide, H., Oyaizu, K.: Poly(dihydroxybenzoquinone): Its high-density and robust charge storage capability in rechargeable acidic polymer-air batteries. Chem. Commun. **56**, 4055–4058 (2020)

10. Parveen, G., Bashir, S., Thakur, A., Saha, S.K., Banerjee, P., Kumar, A.: Experimental and computational studies of imidazolium based ionic liquid 1-methyl- 3-propylimidazolium iodide on mild steel corrosion in acidic solution experimental and computational studies of imidazolium based ionic liquid 1-methyl-3-propylimidazolium. Mater. Res. Express. **7**, 016510 (2020)

11. Bashir, S., Thakur, A., Lgaz, H., Chung, I.M., Kumar, A.: Corrosion inhibition efficiency of bronopol on aluminium in 0.5 M HCl solution: insights from experimental and quantum chemical studies. Surf Interfaces **20**, 100542 (2020)

12. Bashir, S., Thakur, A., Lgaz, H., Chung, I.-M., Kumar, A.: Computational and experimental studies on phenylephrine as anti-corrosion substance of mild steel in acidic medium. J. Mol. Liq. **293**, 111539 (2019)

13. Bashir, S., Thakur, A., Lgaz, H., Chung, I.-M., Kumar, A.: Corrosion inhibition performance of acarbose on mild steel corrosion in acidic medium: an experimental and computational study. Arab. J. Sci. Eng. **45**, 4773–4783 (2020)

14. Thakur, A., Kumar, A.: Sustainable inhibitors for corrosion mitigation in aggressive corrosive media: a comprehensive study. J. Bio- Tribo-Corrosion **7**, 1–48 (2021)

15. Liu, Y., Chen, F., Ye, W., Zeng, M., Han, N., Zhao, F., Wang, X., Li, Y.: High-performance oxygen reduction electrocatalyst derived from polydopamine and cobalt supported on carbon nanotubes for metal-air batteries. Adv. Funct. Mater. **27**, 1–6 (2017)

16. Marschilok, A.C., Lee, S.H., Milleville, C.C., Chen, P., Takeuchi, E.S., Takeuchi, K.J.: Three-dimensional carbon-conductive polymer-silver composite air electrodes for non-aqueous metal air batteries. J. Compos. Mater. **47**, 33–40 (2013)

17. Park, G.S., Lee, J.S., Kim, S.T., Park, S., Cho, J.: Porous nitrogen doped carbon fiber with churros morphology derived from electrospun bicomponent polymer as highly efficient electrocatalyst for Zn-air batteries. J. Power Sources **243**, 267–273 (2013)

18. Shao, Q., Li, Y., Cui, X., Li, T., Wang, H., Li, Y., Duan, Q., Si, Z.: Metallophthalocyanine-based polymer-derived Co_2 P nanoparticles anchoring on doped graphene as high-efficient trifunctional electrocatalyst for Zn-Air batteries and water splitting. ACS Sustain. Chem. Eng. **8**, 6422–6432 (2020)

19. Fan, X., Liu, J., Song, Z., Han, X., Deng, Y., Zhong, C., Hu, W.: Porous nanocomposite gel polymer electrolyte with high ionic conductivity and superior electrolyte retention capability for long-cycle-life flexible zinc–air batteries. Nano Energy **56**, 454–462 (2019)

20. Liang, Z., Zheng, G., Liu, C., Liu, N., Li, W., Yan, K., Yao, H., Hsu, P.C., Chu, S., Cui, Y.: Polymer nanofiber-guided uniform lithium deposition for battery electrodes. Nano Lett. **15**, 2910–2916 (2015)

21. Zhang, Z., Zuo, C., Liu, Z., Yu, Y., Zuo, Y., Song, Y.: All-solid-state Al-air batteries with polymer alkaline gel electrolyte. J. Power Sources **251**, 470–475 (2014)

22. Zhong, L., Fang, Z., Shu, C., Mo, C., Chen, X., Yu, D.: Redox donor-acceptor conjugated microporous polymers as ultralong-lived organic anodes for rechargeable air batteries. Angew. Chemie Int. Ed. **60**, 10164–10171 (2021)

23. Li, B.Q., Zhang, S.Y., Wang, B., Xia, Z.J., Tang, C., Zhang, Q.: A porphyrin covalent organic framework cathode for flexible Zn-air batteries. Energy Environ. Sci. **11**, 1723–1729 (2018)

24. Zhu, B., Liang, Z., Xia, D., Zou, R.: Metal-organic frameworks and their derivatives for metal-air batteries. Energy Storage Mater. **23**, 757–771 (2019)

25. Xu, G., Nie, P., Dou, H., Ding, B., Li, L., Zhang, X.: Exploring metal organic frameworks for energy storage in batteries and supercapacitors. Mater. Today **20**, 191–209 (2017)

26. Ahuja, D., Kalpna, V., Varshney, P.K.: Metal air battery: A sustainable and low cost material for energy storage. J. Phys. Conf. Ser. **1913**, 012065 (2021)

27. Wang, L., Han, Y., Feng, X., Zhou, J., Qi, P., Wang, B.: Metal-organic frameworks for energy storage: batteries and supercapacitors. Coord. Chem. Rev. **307**, 361–381 (2016)
28. Clark, S., Mainar, A.R., Iruin, E., Colmenares, L.C., Blázquez, J.A., Tolchard, J.R., Jusys, Z., Horstmann, B.: Designing aqueous organic electrolytes for zinc-air batteries: method, simulation, and validation. Adv. Energy Mater. **10**, 1903470 (2020)
29. Wu, Y., Qiu, X., Liang, F., Zhang, Q., Koo, A., Dai, Y., Lei, Y., Sun, X.: A metal-organic framework-derived bifunctional catalyst for hybrid sodium-air batteries. Appl. Catal. B Environ. **241**, 407–414 (2019)
30. Xu, W., Viswanathan, V.V., Wang, D., Towne, S.A., Xiao, J., Nie, Z., Hu, D., Zhang, J.G.: Investigation on the charging process of Li_2O_2-based air electrodes in $Li-O_2$ batteries with organic carbonate electrolytes. J. Power Sources **196**, 3894–3899 (2011)
31. Wu, Y., Xiao, Z., Jin, Z., Li, X., Chen, Y.: The cobalt carbide/bimetallic CoFe phosphide dispersed on carbon nanospheres as advanced bifunctional electrocatalysts for the ORR, OER, and rechargeable Zn–air batteries. J. Colloid Interface Sci. **590**, 321–329 (2021)
32. Zhang, K., Zhang, Y., Zhang, Q., Liang, Z., Gu, L., Guo, W., Zhu, B., Guo, S., Zou, R.: Metal-organic framework-derived Fe/Cu-substituted Co nanoparticles embedded in CNTs-grafted carbon polyhedron for Zn-air batteries. Carbon Energy **2**, 283–293 (2020)
33. Oka, K., Murao, S., Kobayashi, K., Nishide, H., Oyaizu, K.: Charge- and proton-storage capability of naphthoquinone-substituted poly(allylamine) as electrode-active material for polymer—air secondary batteries. ACS Appl. Energy Mater. **3**, 12019–12024 (2020)
34. Lu, G., Zheng, J., Jin, C., Yan, T., Zhang, L., Nai, J., Wang, Y., Liu, Y., Liu, T., Tao, X.: Lithiated aromatic biopolymer as high-performance organic anodes for lithium-ion storage. Chem. Eng. J. **409**, 127454 (2021)

Conjugated Polymers as the Materials for Supercapacitor Electrodes

Md. Mahinur Islam, Md. Sadiqul Islam Sheikh, Md. Abu Bin Hasan Susan, and Md. Mominul Islam

Abstract The advancement of materials and technology has changed our lives and living standards and demand for the future. Smart, portable, thin, and flexible electronic devices such as roll-up displays, touch screens, smart electronics, and wearable sensors have been indispensable components of our modern daily lives, and energy storage has become a burning issue. Supercapacitors are appealing as energy storage devices to simplify this expanding electrical need. In comparison to Li-ion batteries, supercapacitors have a superior power density, a faster charge-discharge cycle, and a higher energy storage capacity. To fabricate flexible supercapacitors conducting polymers based on conjugated polymers are one of the most promising candidates compared to other materials in terms of their flexibility, high redox-active specific capacitance, and essential elastic nature. In this chapter, we discussed conducting polymer-based supercapacitors of different kinds and compared and contrasted various features, and addressed the needs for future research to realize high-performance supercapacitor electrodes.

Keywords Conducting polymers · Supercapacitors · Capacitance · Composites

1 Introduction

Modern civilization faces increasing energy demands for smart appliances that create an upsurge of interest in the fabrication of alternative devices for energy storage which include: capacitors, supercapacitors, and lithium-ion batteries. To address the needs of the future, cutting-edge electronics should essentially have the features of portability and flexibility. The development of a low-cost, light-weight, flexible, and sustainable system associated with high energy and power density has thus, been a prime concern for the next-generation energy storage systems [1, 2]. Supercapacitors, with superior specific capacitance (C_{sp}), high power density, and outstanding stability in applications, emerged as the most promising devices to address the issues.

Md. M. Islam · Md. S. I. Sheikh · Md. A. B. H. Susan · Md. M. Islam (✉)
Department of Chemistry, University of Dhaka, Dhaka 1000, Bangladesh
e-mail: mominul@du.ac.bd

265

A wide variety of materials, such as carbonaceous, oxides, graphene, natural and synthetic polymers and their composites with different morphologies including pores, rods, tubes, dendrimers, networks, self-standing nanostructure assemblies, and so on have been attempted to fabricate supercapacitor electrodes. Pseudocapacitors based on conducting polymers (CPs) are intrinsically highly flexible and show tremendous potential in high-performance portable and flexible supercapacitor applications due to their high conductivity and redox-active capacitance. The family of synthetic polymers with inherent conducting properties have attracted a lot of attention for use as supercapacitor materials as a matrix phase or dispersed phase of composites. In addition, polymers have been widely used as binders for casting active electrode materials of supercapacitors on the conducting solid substrate. As a consequence, there has been renewed interest in the design and development of materials related to CPs or conjugated polymers, which may contribute as credible alternatives to their inorganic counterparts. Since the discovery of polyacetylene in 1977, numerous different conjugated polymers have been developed, including polyaniline (PAni), polypyrrole (PPy), poly(p-phenylenevinylene) (PPV), polythiophene (PT), poly(3,4-ethylene dioxythiophene) (PEDOT) [3]. Many of them have been used in the development of supercapacitor electrodes for practical applications.

This chapter focuses on the development of supercapacitor electrodes based on conjugated polymers and their composites with different carbonaceous materials and metal oxides. Fundamentals associated with conductivity and supercapacitive behaviors of conjugated polymers have been introduced and the fabrication of supercapacitor electrodes with such materials and their performances in applications have been elaborated and summarized in the light of recent literature. The prospects of the polymer family as emerging materials for energy storage devices are also highlighted.

2   Polymer Conductivity

The resistance of the charge/electron flow makes the conventional polymers limited to use. Conjugated polymers with a carbon backbone containing interchangeable single (σ) and double (π) bonds allow the delocalization of electrons, contributing to a variety of electronic, electrical, electrochemical, and optical properties. Polymers that exhibit highly reversible redox behavior and make interconnection with metallic properties are commonly known as conducting polymers [3]. Due to unique electrical conduction and optical properties including the ability to tune the molecular structure, CPs have been receiving considerable interest [3, 4].

The band gap energy (E_g) is the most critical parameter to evaluate electrical conductivity. When two partially filled orbitals of two identical atoms are brought together and interact with each other, they produce two new molecular orbitals, one is bonding orbital with lower energy (valance band) and another one is anti-bonding orbital with higher energy (conduction band) [4]. The E_g is defined as the difference in the magnitude between the lowest unoccupied molecular orbital (LUMO, higher energy) and the highest occupied molecular orbital (HOMO, higher energy).

In other words, the E_g is the minimum energy required to excite an electron up into a conduction band where it can participate in charge transport [7]. In conductor materials, electrons can freely move which increases the possibility of charge transfer as the conduction band overlaps the valance band. When the valance and the conduction bands are separated with a large energy gap to prevent electrons to participate in conduction or cross the gap, then, no electricity is conducted and the material is known as an insulator. The magnitude of metals for conductivity is 10^6 S.cm^{-1}. The large bandgap energy of an insulator makes thermal excitation impossible and the magnitude of conductivity is 10^{-22} S.cm^{-1}[3, 4, 7]. Under certain excitation conditions, semiconductor materials can conduct electricity because of relatively smaller E_g. Usually semiconductors have the E_g of ≤ 1 eV; while the conductivity range is from 10^3 to 10^{-9} S.cm^{-1} [3]. Consequently, several factors have been identified that contribute to the bandgap of conjugated polymers including bond length alternation, resonance energy, planarity of the conjugated structure, donor and acceptor structure, intermolecular interaction, π conjugated length, effects of substituent, etc. [5, 8].

Intensive research has been dedicated to synthesizing novel conjugated polymers with high conductivity by doping. In classical semiconductor materials, the introduction of impurities such as dopants into a crystal lattice to moderate the conductivity is known as doping. The presence of π conjugation makes the concept of doping in CP systems entirely different [3]. In the case of conductive polymers, doping refers to charge transfer by partial reduction (*n*-type) and partial oxidation (*p*-type) [9]. As a result, the movement of the positive or negative charge carriers or electrons along the polymer chain refers to the electrical conductivity. Ions doped aid in the reduction of band gaps between energy levels, hence increasing conductivity (Scheme 1).

The electrical conductivity can be boosted by the incorporation or use of small co-planner monomers, known as dopants. Dopants play an important role by electron-withdrawing or adding the electron to the polymer backbone and transferring the charge. In the doping process, the electrons are extracted from the HOMO of the valence band through oxidation or transfer to the LUMO by reduction as shown in Scheme 1. By this process, charge carriers are produced in the forms of polarons, bipolarons, or solitons and the movement of the charge carriers along the polymer chain is responsible for conduction and its enhancement. Although solitons are produced only in a degenerate system such as polyacetylene [9], polarons, as well as bipolarons, can be formed in systems showing both degeneracy and non-degeneracy [6, 10, 11].

3 History of CPs

Since prehistoric times, polymers are used as wood, skin, bone, and fibers by human beings. However, the most recent generation polymers have in many cases been synonyms to CPs and the term 'polymer' was first introduced by Jacob Berzelius in 1832. PAni was reported only after the two years of this invention. It was considered a plastic material or macromolecular compound due to its solid form rather until
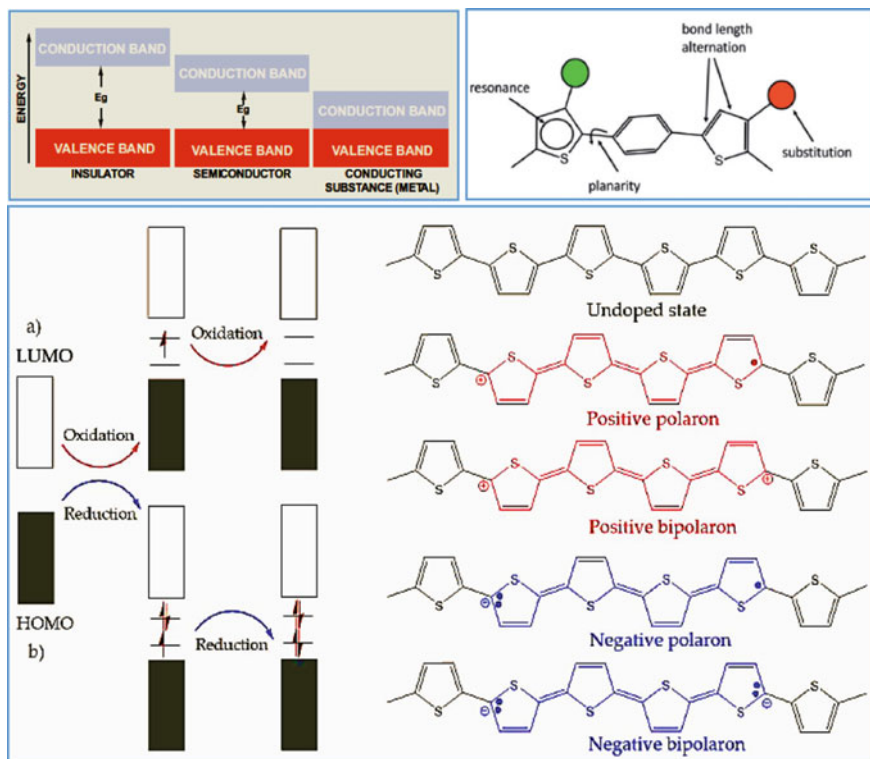
Scheme 1 Upper panel: Visualization of insulator, semiconductor, and conductor through E_g (Left) (Adapted with permission from reference [3], Copyright (2019), Springer) and structural factors contributing to the bandgap energy of the π-conjugated system (Right) (Adapted with permission from reference [5], Copyright (1985), The Royal Society of Chemistry. Lower panel: Chemical structures with an electronic band of PT for **a** p-type and **b** n-type doping (Adapted with permission from reference [6], Copyright (1989), Elsevier)

the 1960s and mechanical properties as a polymeric material have been ignored. Letheby et al. reported chemical polymerization of aniline at the platinum electrode in 1862 [12] and later on the detailed investigation was carried out by Mohilner et al. in 1962 [13]. Furthermore, various chemical oxidative polymerizations of pyrrole were repotted since 1916 and Dallollio et al. reported the electropolymerization of pyrrole in 1968 [14].

In the early 1969's Phillips Chemical Company commercially produced low molecular weight poly(p-phenylene sulfide) only for the thermoplastic applications under the name of Ryton. The early history of many polymers involves polymers in non-conducting forms. But the metallic properties in polymers attracted significant attention since the conductivity may be tuned tuning the molecular structure and they can be developed as per demand and may be easily tailored. The foundation of new CPs was laid by Shirakawa and MacDiarmid as they reported the electrical

conductivity of polyacetylene with the help of doping halogen in 1970 [15]. The CPs such as polyacetylene were developed as potential material with highly promising conductivity and other unique properties and were well-characterized in 1970–1978 [12–15]. Controlling the energy gap through molecular design and attainment of the desired properties have greatly attracted the synthetic chemist in the 1980s. Consequently, the electrochemical doping of CPs created a new scientific direction in the field of polymeric batteries and other electrochemical devices. Furthermore, extensive research has been performed by Heeger et al. in this area for which they were awarded Nobel Prize in 2000.

Since the early nineteenth century, there has been a misconception in understanding the nature of saturated polymers which has drawn less attention in electronic applications. However, the true conjugated polymer has a different electronic configuration such as a conjugated double bond at the backbone. This conjugated double bond contains π electrons in the backbone which move to the conduction band and show similar properties as a metal. But these alterations of the double bond are unstable to form the low (minimum) E_g. As a result, to overcome this problem dopants are introduced as conductive fillers through doping, and alternation of the backbone is stabilized. Conductive polymers thus exhibit specific properties and have been explored in different fields of applications [12–16].

4   Supercapacitors

Electrochemical devices such as supercapacitors are advantageous because of their excellent performance, outstanding stability, and ease of handling for energy storage applications. Supercapacitors fill up the gaps between batteries and conventional capacitors. Although the functions of charge storage are not different from conventional capacitors, a supercapacitor can store a tremendous amount of energy with great discharging capabilities than any other device [1, 16]. Supercapacitors consist of two electrodes that are dipped in an electrolyte and separated by a separator. Upon application of potential, the ions in the electrolyte get separated and form an electrode-electrolyte interface structure. Thus, the charges are stored at these interfaces. However, the charge can be stored through redox reaction or can be achieved by the combination of redox reaction with electrode-electrolyte interface structure. Depending on the charge storage mechanism, supercapacitors can be classified as electric double-layer capacitors (EDLC), pseudocapacitors, and hybrid capacitors.

In EDLCs, the electrolytic ions undergo physisorption at the electrode-electrolyte interface during charging. When polarizable electrodes of EDLCs are immersed in an ion-conducting electrolyte and potential is applied, arrangements or physical absorption of charges are observed at the interface which gives rise to the capacitance. The unique feature of EDLC is the absence of any charge transfer such that no redox reaction is taking place. On the other hand, in pseudocapacitors, the capacitance is the result of a transfer of electrons, i.e., a Faradaic process as shown in Scheme 2 [17]. Pseudocapacitive materials have electrical responses similar to EDLC materials.

(a) Elecrtic double layer capacitor   **(b) Pseudocapacitor**   **(c) Hybrid capacitor**
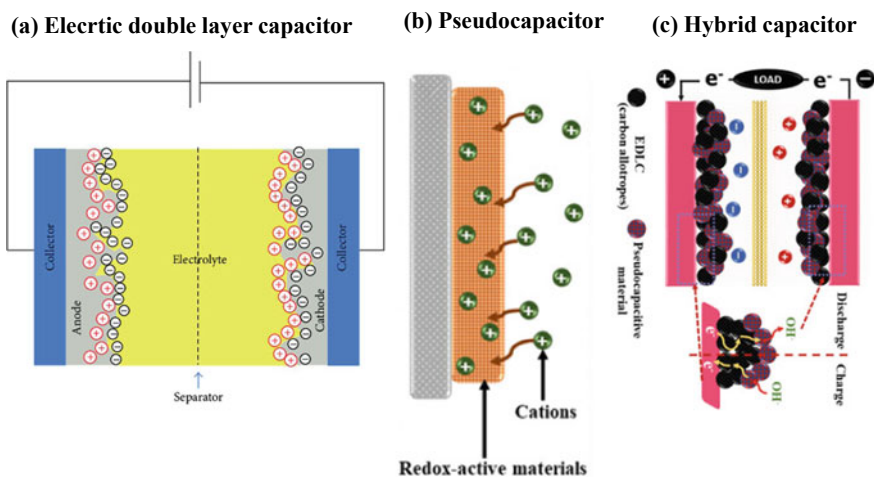
Scheme 2 Charge storage mechanism of **a** electric double layer capacitor, **b** pseudocapacitor, and **c** hybrid capacitor. (Adapted with permission from reference [7, 17], Copyright (2021, 2017), WILEY and Springer, respectively)

However, pseudocapacitors have higher capacitance than EDLCs. As the physisorption of charge is involved in EDLC capacitance, the capacitance depends on the surface area of electrode materials and the thickness of the electrode-electrolyte double layer. Consequently, the capacitance also depends on the accessibility of the ions. The ideal material for the EDLC is thus, carbon allotropes. These materials display high surface area with homogenously distributed pores and high ion conductivity. In contrast, CPs and metal oxides are the ideal materials for pseudocapacitance. As the ions are released and absorbed from the CPs during redox reactions, the π conjugated backbone facilitates charge storage and is responsible for the mechanism of storage for CPs. Hybrid supercapacitors are used to achieve high energy and power density with great stability. As the hybrid supercapacitors consist of both EDLC and redox charge storage mechanisms, they exhibit high C_{sp}. The CPs with carbon-based material or metal oxide provide such type of hybrid capacitance [1, 16, 17].

5   Methods of Fabrication of CPs

Different chemical, electrochemical and physical fabrication methods have been employed for the synthesis of CPs and their composites with tailoring properties. Different sophisticated techniques have been used to characterize the synthesized materials. The techniques involve spectroscopic methods like ultraviolet-visible, Fourier transforms infrared, nuclear magnetic resonance, electron paramagnetic resonance and X-ray photoelectron, thermogravimetric analysis, Brunauer-Emmett-Teller method, microscopic techniques such as field-emission scanning electron

microscopy, transmission electron microscopy, and high-resolution transmission electron microscopy, X-ray diffraction, energy dispersive spectroscopy, etc. The present section will discuss the methods employed for the fabrication of electrode materials.

5.1 CPs in Pristine Form

The structure, morphology, and properties of the materials may be tailored during the synthesis of CP-based electrode materials. The chemical synthesis of CPs in general accounts for various polymerization processes such as step-growth, chain growth, emulsion, in situ oxidative, dispersion, interfacial and precipitation, etc. [19, 20, 38, 39]. Different oxidizing agents such as $FeCl_3$, $Fe(ClO_4)_3$, and $K_2Cr_2O_7$ have been used for the chemical polymerization of monomers. The in situ oxidative polymerization has great importance since it follows a very docile route for the mass production of CPs. Li et al. reported a very easy and inexpensive method for the synthesis of PAni using $NaClO_2$ as an oxidizing agent through oxidative polymerization [18]. Interfacial polymerization is more advantages over the classical step-growth one because of high reaction rates at mild reaction conditions and high final molecular weights. Congenitally uniform and defects-free films can be prepared under controlled conditions.

Other chemical synthesis methods involve counter ion-induced processability, inversion emulsion process, solution blending, dry blending, melt processing, flux methods, electro-deposition, electrospinning, chemical vapor deposition, chemical bath deposition, direct coating, and vacuum filtration techniques. The counter ion-induced processability is a good method to increase the solubility of PAni in a particular solvent. Hence the conductivity of PAni can be enhanced by selecting suitable functionalized protonic acids. Cao et al. investigated the doping of camphor sulfonic acid in PAni, the resulting PAni complex showed better conductivity in meta-cresol compared to virgin PAni [38]. Electrochemical synthesis is relatively straightforward and reproducible. Electrochemical polymerization allows control of the film thickness and polymerization rate. It is increasingly becoming the prime alternative for making CPs. The technique involves dissolving a monomer in a solvent or electrolyte medium with subsequent electro-deposition of a polymer film onto an electrode surface using common electrochemical techniques [39]. The electrochemical polymerization of CPs is advantageous since the reactions can be carried out under ambient conditions, either by varying the potential or current for a particular period. The CPs such as PAni, PPy, PT and PET, etc. can be synthesized using this technique by controlling the thickness of the film. Dubal et al. synthesized of PPy nano bricks following a simple and inexpensive electrodeposition method. Figure 1 depicts the SEM and TEM images, FTIR spectrum, and cyclic voltammograms of PPy thin film. The PPy electrode shows a high C_{sp} value of about 476 F/g within the potential range of -0.4–0.6 V in 0.5 M H_2SO_4 solution and discharge/charge efficiency has been reported as with 89% [20].
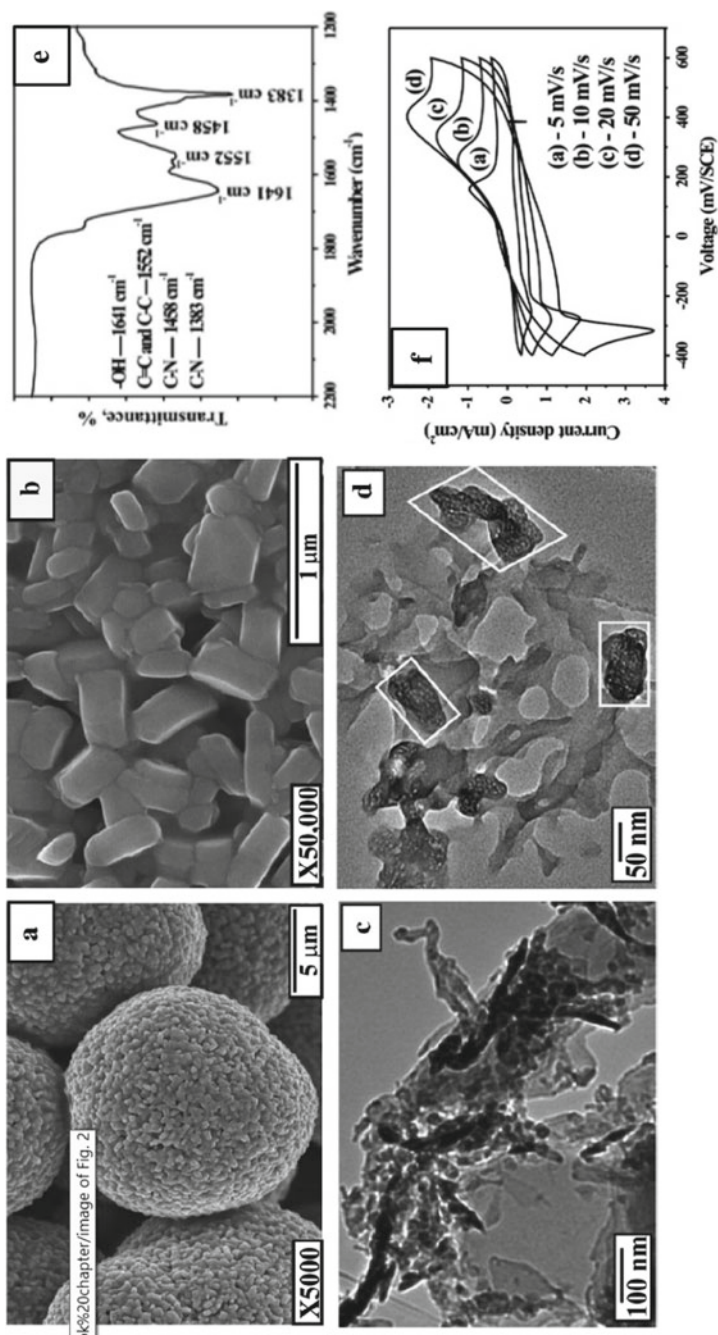
Fig. 1 Scanning electron micrographs at two different magnifications **a** ×5000, **b** ×50,000 and (**c** and **d**) TEM images, **e** FTIR spectrum and **f** cyclic voltammograms of PPy thin film (Adapted with permission from reference [20], Copyright (2019), Elsevier)

5.2 CP Based Binary Composites

To enhance the C_{sp}, the CPs are combined either with carbon materials and transition metals or both. The resultant composite also exhibits much higher power density, energy density, and retention compared to that of individual components. Various methods have been adapted to synthesize the CP-based composites including template synthesis, conventional chemical synthesis, electro-deposition, electrospinning, lithography, etc.

5.2.1 CP/Carbon Binary Composites

Carbon materials, due to their outstanding physicochemical properties such as excellent electronic conductivity, cyclic stability, superior mechanical properties, and significant specific surface area, are combined with CPs to fabricate nanocomposites that display better electrochemical properties compared to their counterparts [20, 26]. Li et al. fabricated PAni nanorods as oriented arrays grown on nanosheets of expanded graphite (EG) by in situ polymerization and the materials prepared showed excellent electrochemical performances as electrodes for supercapacitor applications. The PAni/EG electrode with 10% EG content showed a maximum C_{sp} of 1665 F/g at 1 A/g with significant rate capability associated with good long-term cycling stability [26]. Rajesh et al. prepared PEDOT on a flexible 3D carbon fiber cloth (CFC) following the hydrothermal polymerization method. The composites enhanced the electrode-electrolyte contact area and improved the ion diffusion to give a high C_{sp} of 203 F/g at 5 mV/s. Figure 2 depicts the fabrication, SEM image, and C_{sp} of the PEDOT-CFC electrode [27].

5.2.2 CP/Metal Oxides Composites

The composites of CPs with metal oxide may exhibit better electrochemical performance in supercapacitors because of their promising compatibility. CPs embedded with metal oxide may enhance the conductivity of electrodes significantly by increasing the C_{sp} and rate capability along with cyclic stability. Raj et al. reported the single-step synthesis of cobalt oxide-conducting polyindole (Co_3O_4-PInd) composites by in situ cathodic electro-deposition. The PInd decorated Co_3O_4 showed a C_{sp} of 1805 F/g at a current density of 2 A/g with 82% capacitance retention [30]. Simple thermal and chemical vapor polymerization methods have been used to fabricate PEDOT porous structures enriched with MnO_2 nanoparticles to have a C_{sp} of as high as 321.4 F/g at a 0.5 A/g current density with capacitance retention of 90% after 4000 cycles at a 2.5 A/g [40].
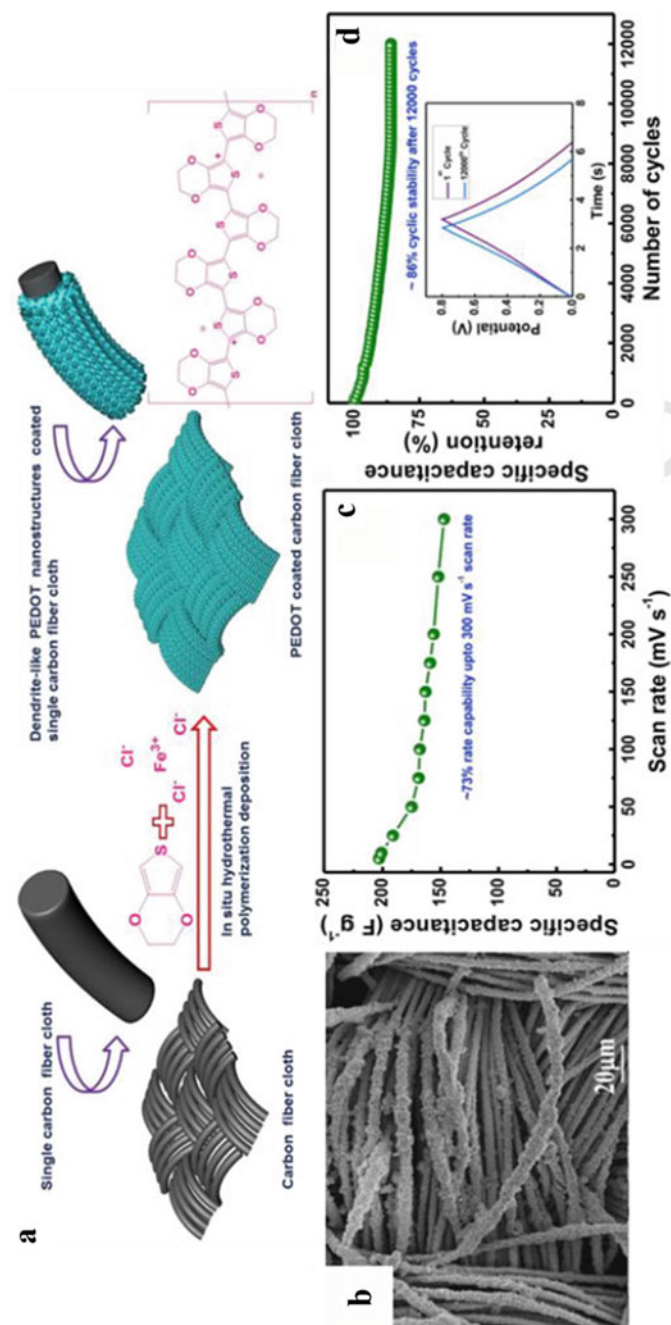
Fig. 2 **a** Fabrication of PEDOT/CFC via in situ hydrothermal polymerization. **b** SEM image of hydrothermally polymerized PEDOT nanostructures coated on CFC. **c** The specific capacitance of symmetrical PEDOT/CFC at different scan rates. **d** Long-term stability of symmetrical PEDOT/CFC over 12,000 cycles at current density 10 A/g. (Adapted with permission from reference [27], Copyright (2019), Elsevier)

5.3   CP Based Ternary Composites

Synthesis of CP-based composites with active materials such as carbon and metal oxides has been an efficient means to enhance the electrochemical performance of supercapacitors via synergistic effects. Zhou et al. synthesized CoO@PPy nanowire array using a simple chemical polymerization method with ammonium persulfate as an oxidizing agent and deposited it onto nickel foam to achieve an impressive C_{sp} of 2223 F/g with retention of 91.5% of the initial capacitance with a cycle up to 20,000 times [35]. Zhu et al. combined in situ polymerization method with a hydrothermal route to synthesize a CuO-PAni-rGO hybrid electrode self-assembled for an electrochemical capacitor. The ternary nanocomposite exhibits a maximum C_{sp} of 634.4 F/g and energy density of 126.8 Wh/kg with a power density of 114.2 kW/kg at a current density of 1.0 A/g with 97.4% specific capacitance retention after 10,000 cycles. The self-assembly procedure, XPS spectra, GCD curves, and C_{sp} of the CuO-PAni-rGO hybrid sample are displayed in Fig. 3 [35]. Raj et al. tuned vertical alignment of PAni on the graphene/zirconium oxide nanocomposite following a novel method involving synthesis of the nanocomposite by in situ hydrothermal methods from their respective precursors. The resulting nanocomposite showed a C_{sp} value of 1360 F/g with an energy density of 104.76 Wh/kg at a power density of 118 W/kg having 90% capacitance retention [41]. The different fabrication methods of CPs and their composites along with their C_{sp} are depicted in Table 1.

6   CPs in Supercapacitor Applications

The C_{sp} of a supercapacitor is highly dependent on the exposed surface area and capability of charge storage through adsorption-desorption or redox reaction. As described earlier, although carbon-based materials give high power density and stability, their applications in high power energy storage devices are limited due to lower C_{sp} values. While metal oxide work at a wide range of charge-discharge potential, their applications are limited due to the high cost, low conductivity, low surface area, poor cycle stability, and toxicity. The CPs conduct electricity through conjugated π electron in the system which is delocalized in the structure/chain and gives rise to metallic characteristics. These systems, however, suffer from the drawback of stability due to the possible alteration of bonds leading to the E_g in the electronic spectrum. As a result, to improve the system and make it stable, dopants need to be introduced. The dopant ions transfer the charge in the form of excess electrons and neutralize the system [36]. The CPs can be doped with p- or n-type dopants as discussed in the preceding section.
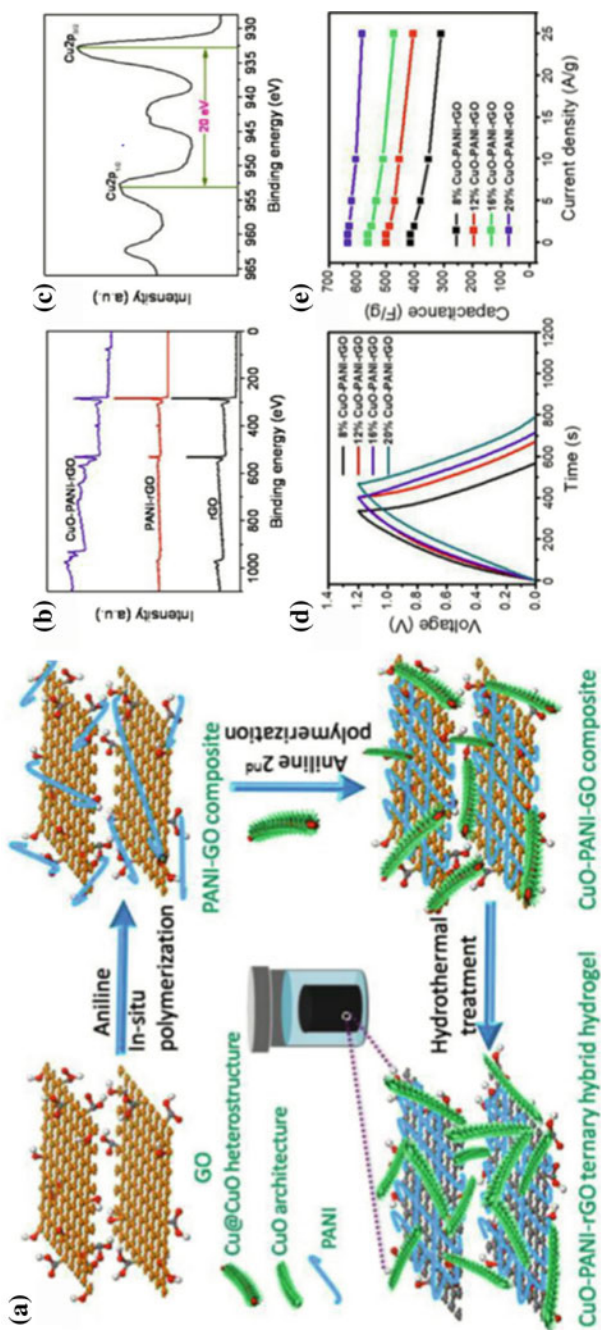
Fig. 3 **a** Self-assembly procedure, **b** XPS survey spectra, **c** high-resolution XPS spectra for Cu 2*p*, **d** GCD curves with different CuO mass loadings from 8.0 to 20.0 wt % at a current density of 1.0 Ag⁻¹, **e** Comparison of the specific capacitances with various CuO contents (8.0–20.0 wt %) and current densities of the typical CuO-PAni-rGO ternary hybrid samples (Adapted with permission from reference [35], Copyright (2016), Elsevier)

Table 1 Synthetic method dependent C_{sp} of different polymers and their composites

Materials	Method of polymerization	C_{sp} (F/g)	References
PAni	In situ oxidative	1062	[18]
	Interfacial polymerization	548	[19]
	Electro-deposition	485	[20]
	Chemical bath deposition	336	[21]
PPy	Oxidative polymerization	427	[22]
	Chemical vapor deposition	115	[23]
PT	Electro-deposition	680	[24]
	Chemical vapor deposition	250	[25]
PAni/EG	In situ polymerization	1665	[26]
PEDOT-CFC	Hydrothermal polymerization	476	[27]
PAni-graphene	Vacuum filtration technique	565	[28]
PPy/CC	Oxidative polymerization	705	[29]
PInd/Co_3O_4	Electro-deposition	1805	[30]
NiO@PPy	In situ polymerization	595	[31]
PAni/GNS/NiO	Oxidative polymerization	1409	[32]
PAni/graphene/ZrO_2	Hydrothermal, oxidative polymerization	1360	[33]
PAni/graphene/$CoFe_2O_4$	Hydrothermal, in situ polymerization	1133	[34]
PAni/rGO/CuO	Hydrothermal, in situ polymerization	634	[33]
CoO@PPy/Ni foam	Oxidative polymerization	2223	[35]
PPy/RGO/Cu_2O-Cu(OH)$_2$	Electro-oxidation	997	[32]
PPy/graphene/SnO_2	One–pot synthesis	616	[36]
PAni/GNS/NiO	Oxidative polymerization	1409	[37]

6.1 PAni Based Supercapacitors

Historically PAni, known as aniline black, is one of the most pioneering CPs which can be synthesized both chemically and electronically. High stability towards the environment, diverse structures, ability to transform from conductive state to resistive one by doping and de-doping, low cost, ease of fabrication make PAni attractive for electrochemical energy storage devices like supercapacitors. Although the electrochemical performance directly depends on the polymer chain and network, doping structure and level and morphology of the structure dictate the diffusion pathway in supercapacitor applications. A good number of chemical methods have so far been employed to synthesize 1D PAni nanostructures such as nanorods, tubes, wires, and fibers. Depending on the level of oxidation, PAni may exist in different

chemical forms: emeraldine base, pernigraniline and leucoemeraldine. The chemical structures control the physical properties including electrical conductivity through doping whether during polymerization or post-polymerization. The doping results in lattice distortion and therefore promotes the electrical conductivity throughout the delocalization of the electron in the polymer matrix [42, 43]. Although, PAni has a high theoretical C_{sp} of 2000 F/g by the combination of electrical double layer and pseudocapacitance. But, in practice, the performance of one single PAni electrode does not match with the theoretical C_{sp}. The maximum C_{sp} of PAni achieved was 950 F/g through large arrays of Pani nanowires vertically aligned on the electrode in 1.0 M HClO$_4$ solution. A low percentage of effective contribution of PAni on capacitance makes the significant difference between the experimental and theoretical C_{sp} and the effectiveness highly relies on diffusion of dopants as well as conductivity of PAni [43]. The outstanding performance of vertically aligned nanowire PAni is due to the advantage of diffusion of ions from the bulk solution to PAni nanowires as illustrated in Fig. 4d. These aligned nanowires of PAni with narrow diameter make the ion diffusion path optimized and reduce the charge transfer resistance which gives the highest C_{sp}. Consequently, the heterogeneous PAni nanofiber harms capacitance. The morphology has a great impact on PAni capacitance and it can be varied
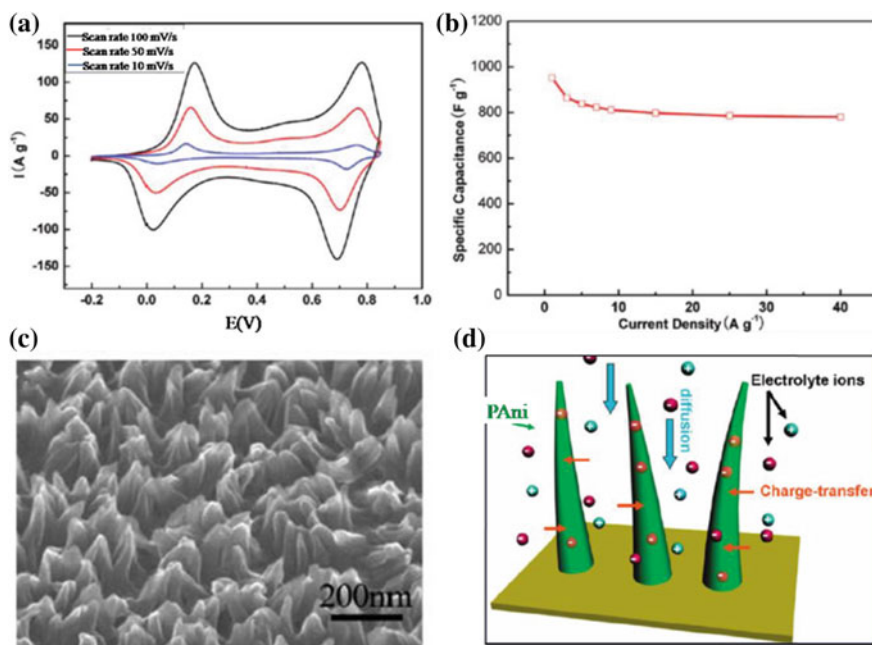
Fig. 4 Electrochemical capacitance behavior of PAni nanowire arrays in HClO$_4$ aqueous solution: **a** Cyclic voltammetry at different scan rates, **b** Specific capacitance in different current densities, **c** Morphologies of PAni nanowire array, **d** Schematic representation of the optimized ion diffusion path in nanowire arrays (Adapted with permission from reference [43], Copyright (2013), WILEY)

from 50 to 950 F/g [23, 25, 44–47]. However, the capacity deviates depending on factors such as synthetic route, methodology, electrode thickness, morphology, and concentration of the electrolyte. Although, PAni has a wide range of capacitance the unstable state during doping and de-doping process with other associated challenges necessitates the development of polymer composites employing PAni as the matrix and carbonaceous or metal oxide as the filler. As the orientations of nanostructure dictate the electrochemical performance of the functional group, hybrid composites have been considered to overcome the challenges where PAni serves the role of high pseudocapacitance [25, 44–51] (see Table 2).

6.2   PPy Based Supercapacitors

PPy has emerged as one of the most promising *p*-type active CP for supercapacitor applications. It has good conductivity and its synthesis is facile and involves low cost. Furthermore, it is stable and associated with high redox pseudocapacitive charge storage [52–54]. The advantages of doped PPy make it fascinating for extensive use in energy storage devices. PPy can be easily prepared through several solvents and water at room temperature with a large quantity. The electrochemical performance of PPy-based electrodes also depends strongly on the methods of preparation of electrodes and effective surface area of the material in resemblance to PAni [36, 42]. PPy with high capacitance has been reported to have a cross-linked structure which allows high ion diffusion and porosity of the active material. However, *n*-doped materials cannot serve as a dopant for PPy, and hence, the application is rather limited to cathode materials of the supercapacitor devices. The dopant with the dense growth of PPy reduces the yield of capacitance per gram [36, 42].

Interestingly, attention has recently been focused on the development of supercapacitor electrodes based on PPy because of their flexibility and conductivity, which are superior to PAni and PT. The highly ordered nanostructure of PPy provides a high surface area and short ion diffusion length to ensure high capacitive performance. A maximum C_{sp} of 566 F/g has been recorded for a large area with a well-defined nanowire array of PPy compared to the other disordered nanowire network and film [52] (Fig. 5). As discussed before morphology and thickness of the film greatly influence the ion transport behavior. Due to a straight diffusion pathway, PPy film should have a higher ion transport rate, but the dense growth makes the ion diffusion difficult and reduces the capacitance. On the other hand, the PPy nanowire array is highly ordered and makes the ion diffusion easy, hence increasing the capacitance per gram. However, the material of this kind is yet to be realized with high performances. A significant development is required to achieve a very high C_{sp} for practical application. Different approaches with various types of composite formation are summarized in Table 2.

Table 2 Summary of the selected high-performance CP-based supercapacitors

Materials	Dopant	Doping method	Morphology	Electrolyte	C_{sp} (F/g)	Stability (cycle number)	Refernces
PAni	–	–	–	–	2000[a]		[23]
PAni	Cl⁻	One step template free method	Aliened array of nanowire	$HClO_4$	950	78% (up to 500)	[43]
rGO-PAni		In situ electro-polymerization	Porous	H_2SO_4	233	No retention (up to 1500)	[25]
PAni	SO_3^-	Template method	Micro-sphere	H_2SO_4	421	55% (up to 1000)	[44]
PAni	Ligno-sulfonate	Chemical polymerization	Micro-tube	HCl	502	53% (up to 10,000)	[45]
PAni	SO_3^-	In situ electro-polymerization	Nano-wire network	H_2SO_4	742	93% (up to 1500)	[46]
PAni-SWCNT	SO_3^-	Electrochemical polymerization	Mesoporous	H_2SO_4	485	93% (up to 1500)	[47]
PAni-Graphite	SO_3^-	In situ polymerization	Needle-like nanowires	H_2SO_4	976	89% (up to 1000)	[48]
PAni-Graphene-MnO_x	Cl⁻	Hydrothermal	Nano-tube	HCl	955	89% (up to 1000)	[49]
PAni-MWCNT- PVDF	SO_3^-	In situ chemical polymerization	Caterpillar	H_2SO_4	1065	92% (up to 1000)	[51]
PAni-Rgo-eCFC		Chemical vapor deposition	Nanowires arrays	H_2SO_4	1145	94% (up to 5000)	[52]

(continued)

Table 2 (continued)

Materials	Dopant	Doping method	Morphology	Electrolyte	C_{sp} (F/g)	Stability (cycle number)	Refernces
PPy	SO_3^-	–	Film	H_2SO_4	378	37% (up to 300)	[53]
PPy	SO_3^-	–	Nanowire	H_2SO_4	414	56% (up to 300)	[53]
PPy	SO_3^-	–	Aligned nanowire	H_2SO_4	566	70% (up to 300)	[53]
CoO@PPy-Ni foam	OH^-	Chemical-polymerization	Aligned nanowire	NaOH	2223	99.8% (up to 2000)	[51]
PPy-rGO-Cu_2O-Cu(OH)$_2$	NO_3^-	Electrochemical	–	$NaNO_3$	997	90% (up to 2000)	[32]
PPy-graphene-SnO_2	–	One–pot synthesis	Film sheet	H_2SO_4	616	98% (up to 1000)	[2]
pTTPA	–	Three fold stille reaction	Porous nanotube	$TBABF_4$	990	–	[54]
PEDOT/MnO_2	–	Chemical vapor deposition	Porous	H_2SO_4	321	90% (up to 4000)	[50]

[a] Theoretical value. rGO: Reduced grapheme oxide; SWCNT: Single-Wall Carbon Nanotube; MWCNT: Multi-Wall Carbon Nanotube; eCFC: Nitrogen-Doped Carbon Fiber Cloth; HQ: Hydroquinone; $TBABF_4$: Tetrabutylammonium Tetrafluoroborate; PSS: Poly(styrene sulfonate); CFC: Carbon Fiber Cloth
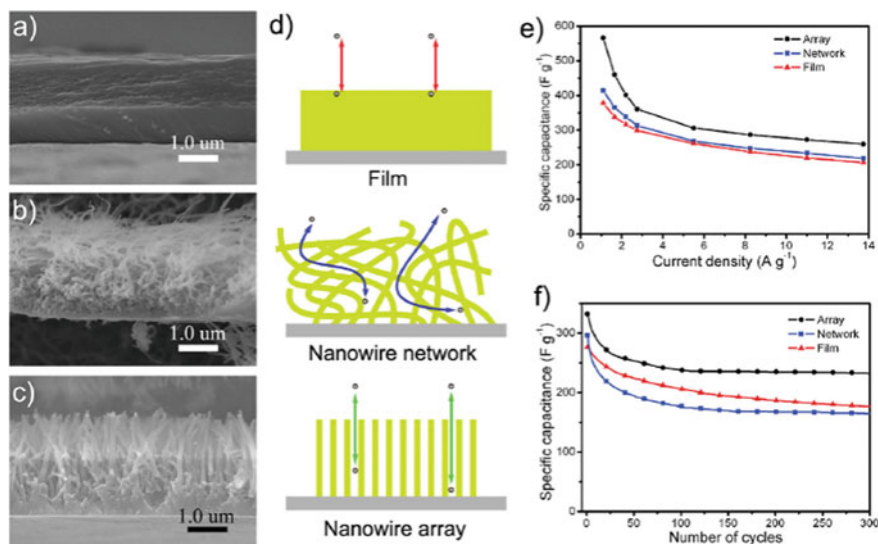
Fig. 5 Conducting PPy nanowire arrays. SEM images of **a** PPy film, **b** PPy nanowire network, and **c** PPy nanowire arrays. **d** Ion transport pathways, **e** Specific capacitances, and **f** Capacitance as a function of the cycle number of PPy with different morphologies. (Adapted with permission from reference [52], Copyright (2010), The Royal Society of Chemistry)

6.3 PT Based Supercapacitor

The PT and its derivative can be doped with both *n*- and *p*-type dopants. The C_{sp} and the stability at air or moisture environment of *n*-doped PT are much lower compared to the *p*-doped polymer, which makes the *n*-doped PT of limited use for supercapacitor applications. However, the high potential window makes the PT derivatives more advantageous than PPy and PAni [36, 42]. PEDOT, poly(3-methyl thiophene) (PMeT)and poly(3-(4-flurophenyl)thiophene) (PFPT) are some of the thiophene-based polymers which can also be successfully used for supercapacitors. Among all thiophene derivatives, PEDOT has been the most attractive and promising pseudocapacitive material for its high electrical conductivity and good environmental stability.

A maximum C_{sp} of 990 F/g has been reported for a new type of thiophene derivative, poly(*tris*(thiophenylphenyl)amine) (pTTPA) in an organic solvent. The formation of porous nanotube enhances the surface area which contributes to the increase of pseudocapacitance [54]. This new class of polymer with excellent electrochemical properties allows the development of such a unique thiophene derivative as summarized in Table 2.

6.4   CP as Matrix Phase in Nanocomposites

To obtain high-performance CP-based supercapacitors, CPs are used as the matrix phase where carbon materials or metal oxides are vertically or horizontally aligned or dispersed through physical or chemical interaction to synthesize the desired nanocomposites. The synthesis of new materials based on tailored multifunctional nanoarchitectures could enhance electronic and ionic conductivities and diffusional and electron transfer processes. The nanocomposites employ electroactive materials in the forms of nanorods, nanowires, nanofibers, nanoflowers, etc. and CPs are used as the matrix phase to improve electrochemical properties. The CP matrix shows pseudocapacitance through doping and de-doping of the polymer backbone through intercalation and de-intercalation of electrolyte ions within the polymer electrode to maintain charge neutrality.

To acquire auspicious interfacial connections and tune desired properties with optimal conditions, homogenous dispersion of carbon nanomaterials or metal oxide nanostructures in the CP matrix is very important. In situ interfacial polymerization seems to be a good method to lower the resistance experienced by the connecting interface of different phases. It also helps to the homogeneous dispersion of the inorganic nanostructures within the polymer matrix and enhances the order of arrangement of polymer chains. Furthermore, to tailor the properties of the materials, the content of inorganic nanostructures and polymer in composites should also be optimized. It is crucial to select appropriate polymer matrix and inorganic nanostructures such as carbon nanomaterials and metal oxides and to optimize the volume fraction of each phase to make the performance of composites; computational modeling helps in this regard and has been gaining increasing popularity.

7   Concluding Remarks and Prospects

The increasing demand for high power and energy devices has promoted research toward the fabrication of high-performance and long-life devices. Supercapacitors show remarkable characteristics in terms of energy storage. The CPs offer promising solutions for supercapacitor materials with high specific capacitance, surface area, porosity, high accessibility of ions, and active site through a redox reaction. Hence the electrochemical performance of CPs highly depends on the architecture as well as the synthetic methods. Therefore, considerable efforts have been made on developing a different architectural structure such as nanowire, nanofiber, and aligned network of CPs which make it excellent electrode material for supercapacitors. The morphology of CPs can be tuned by chemical, electrochemical or photo-doping method and the metallic properties can also be developed by n-type and p-type doping. However, poor cyclic stability, temperature dependence, and insolubility issues restrict CPs for application in high-performance supercapacitors. The aggregation and restating of CPs reduce the surface area as well as diffusion of the electrolyte ion. Hence, the

proper design of CPs can improve capability and help to achieve high-performance-based supercapacitor electrodes. The effective means to improve the performance of CPs with great stability is the fabrication of composites with different carbonaceous materials or with transition metal oxide (TMO) materials. In composite, the CPs serve the major role for high C_{sp} and TMO or carbonaceous materials give support for the growth of high surface with aligned nano-network which makes a well-defined ideal structure for supercapacitor applications.

Finally, the composites are expected to suppress the aggregation and restating and may provide an effective surface area with high ion accessibility. In recent days, the composites of CPs with carbon nanotube, carbon nanofiber, activated carbon, graphene, TMO, etc. are the most promising materials for supercapacitor devices due to ease of synthesis and high flexibility. Despite promises, there are lots of challenges to overcome because of several issues associated with the use of CPs, in other words, CPs for supercapacitor electrodes. With the help of spectroscopy, computer modeling, and simulation methods, extended studies would be able to resolve the issues. A concerted effort is essential to develop a noble pathway for the synthesis of CP-composites with a larger effective surface area and great stability to fulfill the requirements for use as high-performance supercapacitor electrodes.

References

1. Islam, M.M., Mollah, M.Y.A., Susan, M.A.B.H., Islam, M.M.: Frontier performance of *In situ* formed α-MnO_2 dispersed over functionalized multi-walled carbon nanotubes covalently anchored to a graphene oxide nanosheet framework as supercapacitor materials. RSC Adv. **10**(73), 44884–44891 (2020)
2. Shown, I., Ganguly, A., Chen, L.C., Chen, K.H.: Conducting polymer-based flexible supercapacitor. Energy Sci. Eng. **3**(1), 2–26 (2015)
3. Mazumder, M.A.J., Sheardown, H., Al-Ahmed, A.: Functional Polymers. Springer (2019)
4. Rasmussen, S.: Encyclopedia of polymeric nanomaterials. Encycl Polym Nanomater. 1–13 (2020)
5. MacDiarmid, A.G., Mammone, R.J., Kaner, R.B., Porter, L.: The concept of 'doping' of conducting polymers: the role of reduction potentials. Philos. Trans. R Soc. London Ser. A, Math. Phys. Sci. **314**(1528), 3–15 (1985)
6. Krische, B., Zagorska, M.: Over oxidation in conducting polymers. Synth. Met. **28**(1–2), 257–262 (1989)
7. Le, T., Yoon, H.: Fundamentals of conjugated polymer nanostructures. ConjugPolym Nanostruct. Energy Convers. Storage Appl. 1–42 (2021)
8. Scharber, M.C., Sariciftci, N.S.: Low band gap conjugated semiconducting polymers. Adv. Mater. Technol. **6**(4), 2000857 (2021)
9. Heeger, A.J., Kivelson, S., Schrieffer, J.R., Su, W.-P.: Solitons in conducting polymers. Rev. Mod. Phys. **60**(3), 781 (1988)
10. Heeger, A.J.: Semiconducting and metallic polymers: the fourth generation of polymeric materials. Curr. Appl. Phys. **1**(4–5), 247–267 (2001)
11. Rasmussen, S.C.: Revisiting the early history of synthetic polymers: critiques and new insights. Ambix **65**(4), 356–372 (2018)
12. Mohilner, D.M., Adams, R.N., Argersinger, W.J.: Investigation of the kinetics and mechanism of the anodic oxidation of aniline in aqueous sulfuric acid solution at a platinum electrode. J. Am. Chem. Soc. **84**(19), 3618–3622 (1962)

13. Gardini, G.P.: The oxidation of monocyclic pyrroles. Adv. Heterocycl. Chem. **15**(C), 67–98 (1973)
14. Ito, T., Shirakawa, H., Ikeda, S.: Simultaneous polymerization and formation of polyacetylene. J. Polym. Sci. Polym. Chem. Ed. **12**(1974), 11–19 (1974)
15. Shirakawa, H., Ikeda, S.: Infrared spectra of polyacetylene. Polym. J. **2**(2), 231–244 (1971)
16. Jayalakshmi, M., Balasubramanian, K.: Simple capacitors to supercapacitors—an overview. Int. J. Electrochem. Sci. **3**(11), 1196–1217 (2008)
17. Baleg, A.A., et al.: Conducting polymers and composites. In: Jafar Mazumder, M., Sheardown, H., Al-Ahmed, A. (eds.) Functional Polymers: Polymers and Polymeric Composites: A Reference Series. Springer, Cham (2019)
18. Kim, M., Kim, Y.K., Kim, J., Cho, S., Lee, G., Jang, J.: Fabrication of a polyaniline/MoS$_2$ nanocomposite using self-stabilized dispersion polymerization for supercapacitors with high energy density. RSC Adv. **6**(33), 27460–27465 (2016)
19. Abu-Thabit, N.Y.: Chemical oxidative polymerization of polyaniline: a practical approach for preparation of smart conductive textiles. J. Chem. Educ. **93**(9), 1606–1611 (2016)
20. Sharma, K., Arora, A., Tripathi, S.K.: Review of supercapacitors: materials and devices. J. Energy Storage **21**, 801–825 (2019)
21. Parnell, C.M., Chhetri, B.P., Mitchell, T.B., Watanabe, F., Kannarpady, G., Rangu Magar, A.B., Zhou, H., Alghazali, K.M., Biris, A.S., Ghosh, A.: Simultaneous electrochemical deposition of cobalt complex and polypyrrole thin films for supercapacitor electrodes. Sci. Rep. **9**(1), 1–13 (2019)
22. Zhang, Y., Li, M., Yang, L., Yi, K., Li, Z., Yao, J.: Facilely prepared polypyrrole-graphene oxide-sodium dodecylbenzene sulfonate nanocomposites by *in situ* emulsion polymerization for high-performance supercapacitor electrodes. J. Solid State Electrochem. **18**(8), 2139–2147 (2014)
23. Li, H., Wang, J., Chu, Q., Wang, Z., Zhang, F., Wang, S.: Theoretical and experimental specific capacitance of polyaniline in sulfuric acid. J. Power Sources **190**(2), 578–586 (2009)
24. Nejati, S., Minford, T.E., Smolin, Y.Y., Lau, K.K.S.: Enhanced charge storage of ultrathin polythiophene films within porous nanostructures. ACS Nano **8**(6), 5413–5422 (2014)
25. Horng, Y.Y., Lu, Y.C., Hsu, Y.K., Chen, C.C., Chen, L.C., Chen, K.H.: Flexible supercapacitor based on polyaniline nanowires/carbon cloth with both high gravimetric and area-normalized capacitance. J. Power Sources **195**(13), 4418–4422 (2010)
26. Yang, W., Zhao, Y., He, X., Chen, Y., Xu, J., Li, S., Yang, Y., Jiang, Y.: Flexible conducting polymer/reduced graphene oxide films: synthesis, characterization, and electrochemical performance. Nanoscale Res. Lett. **10**(1), 1–7 (2015)
27. Rajesh, M., Raj, C.J., Manikandan, R., Kim, B.C., Park, S.Y., Yu, K.H.: A high performance PEDOT/PEDOT symmetric supercapacitor by facile in-situ hydrothermal polymerization of PEDOT nanostructures on flexible carbon fibre cloth electrodes. Mater. Today Energy **6**, 96–104 (2017)
28. Devi, R., Tapadia, K., Maharana, T.: Casting of carbon cloth enrobed polypyrrole electrode for high electrochemical performances. Heliyon **6**(1), e03122 (2020)
29. Ji, W., Ji, J., Cui, X., Chen, J., Liu, D., Deng, H., Fu, Q.: Polypyrrole encapsulation on flower-like porous NiO for advanced high-performance supercapacitors. Chem. Commun. **51**(36), 7669–7672 (2015)
30. Yang, Y., Yuan, W., Li, S., Yang, X., Xu, J., Jiang, Y.: Manganese dioxide nanoparticle enrichment in porous conducting polymer as high performance supercapacitor electrode materials. Electrochem. Acta **165**, 323–329 (2015)
31. Wu, X., Wang, Q., Zhang, W., Wang, Y., Chen, W.: Nano nickel oxide coated graphene/polyaniline composite film with high electrochemical performance for flexible supercapacitor. Electrochim. Acta **211**, 1066–1075 (2016)
32. Wang, W., Hao, Q., Lei, W., Xia, X., Wang, X.: Graphene/SnO$_2$/polypyrrole ternary nanocomposites as supercapacitor electrode materials. Rsc Adv. **2**(27), 10268–10274 (2012)
33. Giri, S., Ghosh, D., Das, C.K.: Growth of vertically aligned tunable polyaniline on graphene/ZrO$_2$ nanocomposites for supercapacitor energy-storage application. Adv. Funct. Mater. **24**(9), 1312–1324 (2014)

34. Asen, P., Shahrokhian, S.: A high performance supercapacitor based on graphene/polypyrrole/Cu_2O–$Cu(OH)_2$ ternary nanocomposite coated on nickel foam. J. Phys. Chem. C **121**(12), 6508–6519 (2017)
35. Zhu, S., Wu, M., Ge, M.-H., Zhang, H., Li, S.-K., Li, C.-H.: Design and construction of three-dimensional CuO/polyaniline/rGO ternary hierarchical architectures for high performance supercapacitors. J. Power Sources **306**, 593–601 (2016)
36. Kar, K.K.: Springer Series in Materials Science 300 Handbook of Nanocomposite Supercapacitor Materials II (2020)
37. Xiong, P., Huang, H., Wang, X.: Design and synthesis of ternary cobalt ferrite/graphene/polyaniline hierarchical nanocomposites for high-performance supercapacitors. J. Power Sources **245**, 937–946 (2014)
38. Patil, B.H., Patil, S.J., Lokhande, C.D.: Electrochemical characterization of chemically synthesized polythiophene thin films: performance of asymmetric supercapacitor device. Electroanalysis **26**(9), 2023–2032 (2014)
39. Dubal, D.P., Patil, S.V., Kim, W.B., Lokhande, C.D.: Supercapacitors based on electrochemically deposited polypyrrole nanobricks. Mater. Lett. **65**(17–18), 2628–2631 (2011)
40. Zhou, C., Zhang, Y., Li, Y., Liu, J.: Construction of high-capacitance 3D CoO@polypyrrole nanowire array electrode for aqueous asymmetric supercapacitor. Nano Lett. **13**(5), 2078–2085 (2013)
41. Kadam, A.V., Patil, S.B.: Polyaniline globules as a catalyst for WO_3 nanoparticles for supercapacitor application. Mater. Res. Express **5**(8), 85036 (2018)
42. Amarnath, C.A., Kim, J., Kim, K., Choi, J., Sohn, D.: Nanoflakes to nanorods and nanospheres transition of selenious acid doped polyaniline. Polymer (Guildf) **49**(2), 432–437 (2008)
43. Wang, K., Wu, H., Meng, Y., Wei, Z.: Conducting polymer nanowire arrays for high performance supercapacitors. Small **10**(1), 14–31 (2014)
44. Xu, H., Jiang, H., Li, X., Wang, G.: Synthesis and electrochemical capacitance performance of polyaniline doped with lignosulfonate. RSC Adv. **5**(93), 76116–76121 (2015)
45. Gupta, V., Miura, N.: Electrochemically deposited polyaniline nanowire's network a high-performance electrode material for redox supercapacitor. Electrochem. Solid-State Lett. **8**(12), 630–632 (2005)
46. Feng, X., Yan, Z., Chen, N., Zhang, Y., Liu, X., Ma, Y., Yang, X., Hou, W.: Synthesis of a graphene/polyaniline/MCM-41 nanocomposite and its application as a supercapacitor. New J. Chem. **37**(7), 2203–2209 (2013)
47. He, S., Hu, X., Chen, S., Hu, H., Hanif, M., Hou, H.: Needle-like polyaniline nanowires on graphite nanofibers: hierarchical micro/nano-architecture for high performance supercapacitors. J. Mater. Chem. **22**(11), 5114–5120 (2012)
48. Jayakumar, A., Yoon, Y.J., Wang, R., Lee, J.M.: Novel graphene/polyaniline/MnO_x 3D-hydrogels obtained by controlled morphology of MnO_x in the graphene/polyaniline matrix for high performance binder-free supercapacitor electrodes. RSC Adv. **5**(114), 94388–94396 (2015)
49. Shen, J., Yang, C., Li, X., Wang, G.: High-performance asymmetric supercapacitor based on nanoarchitectured polyaniline/graphene/carbon nanotube and activated graphene electrodes. ACS Appl. Mater. Interfaces **5**(17), 8467–8476 (2013)
50. Yang, Y., Hao, Y., Yuan, J., Niu, L., Xia, F.: In situ preparation of caterpillar-like polyaniline/carbon nanotube hybrids with core shell structure for high performance supercapacitors. Carbon N Y **78**, 279–287 (2014)
51. Yu, P., Li, Y., Zhao, X., Wu, L., Zhang, Q.: Graphene-wrapped polyaniline nanowire arrays on nitrogen-doped carbon fabric as novel flexible hybrid electrode materials for high-performance supercapacitor. Langmuir **30**(18), 5306–5313 (2014)
52. Huang, J., Wang, K., Wei, Z.: Conducting polymer nanowire arrays with enhanced electrochemical performance. J. Mater. Chem. **20**(6), 1117–1121 (2010)
53. Zhao, Y., Liu, J., Hu, Y., Cheng, H., Hu, C., Jiang, C., Jiang, L., Cao, A., Qu, L.: Highly compression-tolerant supercapacitor based on polypyrrole-mediated graphene foam electrodes. Adv. Mater. **25**(4), 591–595 (2013)

54. Roberts, M.E., Wheeler, D.R., McKenzie, B.B., Bunker, B.C.: High specific capacitance conducting polymer supercapacitor electrodes based on poly*(tris*(thiophenylphenyl)amine). J. Mater. Chem. **19**(38), 6977–6979 (2009)

Recent and Future Research Related to the Use of Conducting Polymers for Supercapacitors

Quoc Bao Le, Rudolf Kiefer, Tran Trong Dao, Natalia E. Kazantseva, and Petr Saha

Abstract Our subordinate to fossil fuels has caused critical problems like environmental pollution and climate change. Harvesting, processing, and distributing fossil fuels can also create environmental concerns. These reasons determine the need for alternative energy sources to meet the growing demand. Among the alternative energy storage devices, supercapacitor (SC) is a promising one due to superior power density, fast charge/discharge rate, and long cycle life, allowing them to be utilized in many applications. Herein, electrode materials play a vital decisive role in the working performance of SCs. Therefore, the research on electrode materials acquires special attention. Although the performance of capacitors has been significantly improved in recent years, the challenge of developing high-performance materials remains relevant. One of the leading research directions is developing composite electrode materials that should combine the advantages of their components. Conductive polymers (CPs) play an important role in these types of electrodes, as their presence increases the electrical conductivity, and capacitance of SCs. This is due to CP's set of CPs properties: combining the electrical conductivity of metals and semiconductors while maintaining the advantages of polymers such as low cost, lightweight, flexibility, and simple processing. This chapter summarizes recent research and future directions into the use of CPs to develop hybrid electrode materials for SCs.

Keywords Supercapacitors · Conducting polymers · Composites · Electrochemical devices

Q. B. Le (✉) · N. E. Kazantseva · P. Saha
University Institute, Nad Ovčírnou 3685, 760 01 Zlin, Czech Republic
e-mail: lequocbao@tdtu.edu.vn

Q. B. Le · R. Kiefer
Conducting Polymers in Composites and Applications Research Group, Faculty of Applied Sciences, Ton Duc Thang University, Ho Chi Minh City 700000, Vietnam

T. T. Dao
Division of Modeling Evolutionary Algorithms Simulation and Artificial Intelligence, Faculty of Electrical and Electronics Engineering, Ton Duc Thang University, Ho Chi Minh City 700000, Vietnam

© The Author(s), under exclusive license to Springer Nature Switzerland AG 2022
R. K. Gupta (ed.), *Organic Electrodes*, Engineering Materials,
https://doi.org/10.1007/978-3-030-98021-4_16

1   Introduction

Harmful substances released during fuel combustion create severe problems for the environment. Thus, in recent years, the research has focused on alternative materials to solve the problems caused by fossil fuels' overuse. However, renewable energy production also has the peak season and hours that energy storage devices must accommodate. Besides, during the adverse conditions of energy harvesting devices, storage devices are needed. The storage devices should keep a large amount of energy during peak hours and release it when the energy generation process ends [1].

The target aims are to develop promising devices that can be easily fabricated, friendly to the environment and have a long working process. Among energy storage devices, SCs are promising for answering the mentioned requirements. Various kinds of materials can be used for SCs' electrodes fabrication, such as reduced graphene oxide (rGO), carbon black (CB), carbon nanotubes (CNTs), and conducting polymers (CPs) [2]. As for the electrode's materials, conductive polymers can be used as an individual component of a composite electrode or form hybrid composites with other components such as rGO, CB, or CNT. Those composites acquired enhanced functionalities such as higher electrical conductivity, capacitance, or extended stability. The structure and design of CPs on the electrode materials play a vital role in the performance of the SCs [3]. The hybrid materials containing conducting polymers have potential energy storage devices, especially for the SC. This chapter presents the basic principles of energy storage in SCs, the mechanisms of their operation, and analyses of recent research in using CPs-based hybrid composites as electrode materials.

2   Energy Storage Mechanisms of SCs

The increase in the capacitance of SC is achieved by using the electrostatic capacitance of the double layer and the electrochemical pseudo-capacitance. Thus, SC is a high-capacity capacitor in which the capacitance values would be much higher than in conventional capacitors while the voltage limits would be lower. Indeed, compared to the capacitor, the SC can store 10–100 times more energy per unit volume or mass, and it can accept and deliver charge much faster than the batteries. Unlike long-term energy storage devices, supercapacitors can be used where conditions of fast charge/discharge cycles are required, such as cars, buses, trains, and many electronic devices used in recent days.

Electrostatic double-layer capacitors (EDLCs) use carbon-based electrodes or their derivatives with much higher electrostatic double-layer capacitance than electrochemical pseudo-capacitance. The electrical charge is stored at the electrode–electrolyte interface of SC, and the charge separation is a physical process without any faradaic reactions on the electrode surface. Therefore, the surface properties of the electrodes play an essential role in the EDL capacitance. The pore size in porous

EDLCs is recommended to be approximate twice the size of the electrolyte ions to allow full access into the pore walls. In the EDLC, the electrostatic storage of the electrical energy is required by the separation of charge in a Helmholtz double layer [4].

Electrochemical pseudocapacitors use many different electrochemical pseudo-capacitance materials to add to the double-layer capacitance, such as metal oxides or CPs. In redox pseudo-capacitance, the charge is stored through surface or near-surface charge transfer reactions. An intercalation pseudo-capacitance mechanism was recently proposed whereby electron charge transfer between electrolyte and electrode coming from a de-solvated and adsorbed ion. The adsorbed ion does not react with the electrode atoms, which means that only the charge transfer happens without any chemical bond. Thus, faradaic redox reactions with charge transfer obtain the pseudo-capacitance electrochemical storage of the electrical energy [4].

The essential SC device has two working electrodes, as described in Fig. 1. One anode and one cathode of SC are separated by a separator layer and filled with the
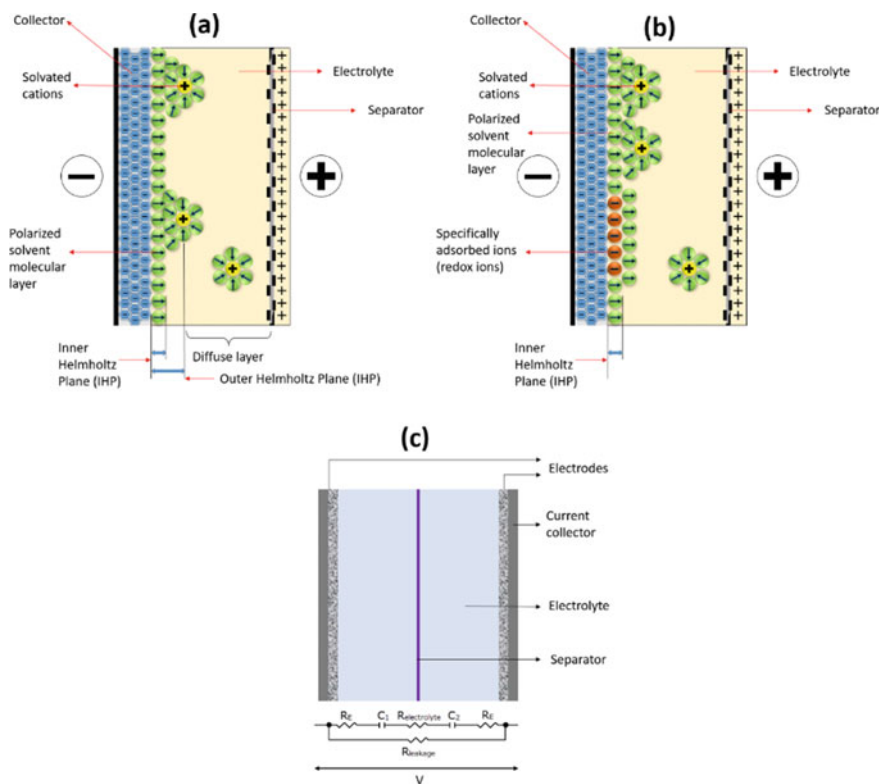
Fig. 1 Simplified view of **a** electrostatic double-layer capacitors, **b** pseudocapacitor with specifically adsorbed ions, and **c** basic configuration of SC cell [4]

electrolytes that enable the movements of the ions. Both electrodes connect to the discrete collectors, which can allow the current flow.

The capacitance C of the SC is expressed as:

$$C = \frac{Q}{V} \tag{1}$$

where Q is the stored charges (in Coulombs), and V is applied potential (in volts). The specific energy (E) is calculated according to Eq. (2), following the total capacitance (C) and the voltage of the cells. The power (P) of the SC can be calculated via the equivalent resistance (R) of the SC and expressed by Eq. (3).

$$E = \frac{1}{2}CV^2 \tag{2}$$

$$P = \frac{V^2}{4R} \tag{3}$$

SC's working performance depends on each chosen material for electrode fabrication.

3 The Role of Conducting Polymers in Supercapacitor Energy Storage Devices

Conducting polymers are vital components of electrode materials for energy storage devices. They have been prepared through various techniques such as electrochemical oxidation/chemical oxidation of the conducting monomer or radical polymerization. The CPs contain overlapping sp2-molecular orbitals and a high degree of π-bond conjugations with irregular single and double bonds along the polymer chains [5]. The CP becomes conductive when a π-bond electron is removed from the conjugated polymer backbone to form a radical cation defect.

CPs exhibit the reversible redox reactions near the surface of the electrodes hence creating the pseudo-capacitance, which can enhance the working performance of SCs. Every material can have pseudo-capacitance and EDLC properties. Modification of the electrode with conductive polymers increases its surface area. Therefore, they build up a Helmholtz layer and eventually contribute to EDLC [5]. Simultaneously, the functional groups of CPs cause the faradaic charge storage reactions, contributing to the total capacitance [6].

High electrical conductivity and electrochemical capacity of CPs are achieved under the high mobility (high kinetic energy) of charge carriers. Furthermore, the CPs should be easily solvated to form the counter ions. The energy storage in SCs modified by CPs mainly depends on the faradic reactions at the electrodes and electrolytes interfaces. It is the charge-transfer process between CPs molecules and the

electrolyte ions. The charge carrier's concentration was changed via the process of n-doping (reduction) when an electron was inserted into the conduction band or p-doping (oxidation) when an electron was removed from the valance band. The simple chemical reactions of charge transfer processes of reduction and oxidation are displayed in Eqs. 4 and 5, respectively:

$$CP + n\text{Red} \rightarrow (C^+)_n CP^{n-} + n\text{Red}^+ \tag{4}$$

$$CP + n\text{Ox} \rightarrow CP^{n+}(A^-)_n + n\text{Ox}^- \tag{5}$$
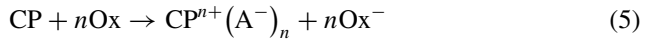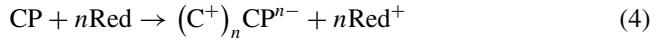
When the reductant (Red) and oxidant (Ox) react with the conducting polymer (CP), they will form the countercations (C^+) and counteranions (A^-) on the CP chains. Hence, it also changes the energy band of CP.

Figure 2 displays the process of PANI doping. It can easily convert between various oxidation states like emeraldine, leucoemeraldine, and pernigraniline via the Faradaic reactions [6]. When PANI is reduced, it accepts electrons from the ambient electrolyte and forms counter anion chains. During the un-doping process, the counter anions release the electrons and convert them back to the lower states of PANI forms [6].

Fig. 2 Schematic chemical representation of the doping and undoing process of PANI [6]

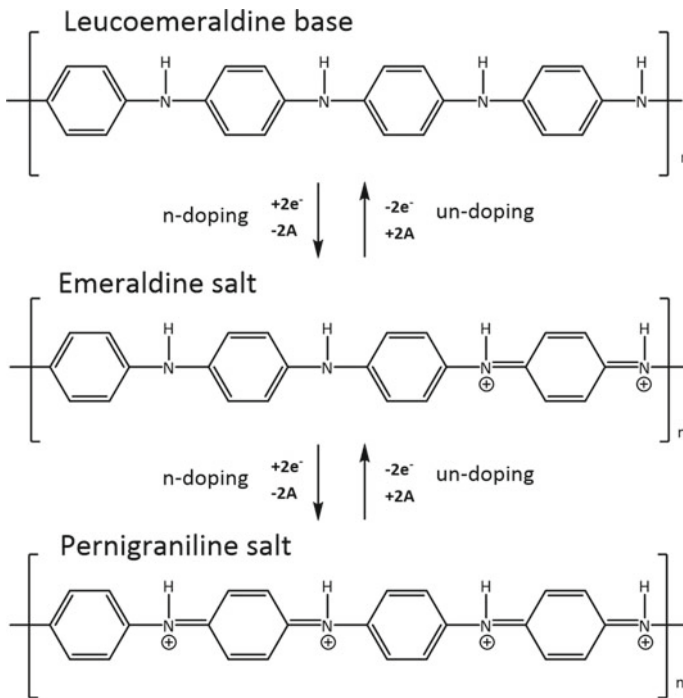The equilibrium geometry of the CP ionized state becomes lower than it is at the ground state, which will shift up a HOMO level and shift down the LUMO level. Those deformation molecules with smaller energy band gaps dispose and charge "islands" across the polymer chain. Those islands' smaller energy band gap allows the electron to transfer from the valance band to the conduction band. Consequently, the more polymer chains are ionized, the more islands will be formed to overlap and distribute across the electrode of SC to enhance polymer electrical conductivity [7].

Various methods have been used for CPs synthesis depending on their desired physicochemical, electrical, and other properties. CPs, upon the application's desires, can contain different mechanical properties and appearance forms. For example, it may be a membrane with good flexibility or high corrosion protection bulk layer [8]. Theoretically, CPs are synthesized via the oxidation of coupling monomers. Firstly, a monomer will be oxidized and form the radical cation. Then, the cation will react with another monomer to form the dimer, and the process will continue to develop the oligomer; hence, the reaction takes the court until it creates the long-chain polymer. There are three vital steps called initiation, propagation, and termination during the reaction process [4]. Those three steps can determine the physicochemical and mechanical properties of the CPs. The initial or oxidation steps can be activated via different methods, including chemical, electrochemical, or photo-included oxidations. Thus, different catalysts and conditions are used to control the polymerization process. Table 1 summarizes the current methods and synthesis conditions of CPs preparation and the results of their applications for SCs.

3.1 Chemical Polymerization

The common method used for CPs synthesis is **chemical polymerization**. This method can involve condensation or addition polymerization if monomers are dissolved in the acidic dopant solution.

In the **addition polymerization** (chain-growth polymerization), the polymer chain is formed by the reaction of the monomer unit at one time through the double or triple bonds in the monomers. Free radicals activate the initiation step, i.e., carbon atoms in the double or triple bonds of the monomers. The radicals will be transferred to another monomer to continue the reaction until they are neutralized [15].

Condensation polymerization (polycondensation) is a step-growth polymerization process where the monomers react to form the macromolecules while releasing condensate by-products such as H_2O or CH_3OH. To operate the polycondensation, the monomers need to have functional groups that can participate in the reactions, i.e., alcohol, amine, or carboxylic acid groups. Those functional groups will react to form the larger molecules when the reaction starts. Via polycondensation, the polymer structure can be controlled using different functional groups in their monomer structures. Because the reaction proceeds step-by-step, the difunctional monomers can react and form the linear polymer. Hence, if tri- or tetra-functional groups containing monomers are used in the reactions, they will make the cross-linked polymers. The

Table 1 Experimental conditions to synthesize the CPs and their SCs applications results

No.	Polymer	Synthesis tragedies	SCs' capacitance	Scanning rate	References
1	PANI	Pre-coated with self-assembled monolayers	809.09 F/g	20 mV/s	[9]
2	PPy	Encapsulated Fe_2O_3 nanotube arrays grown on carbon cloth	237 mF/cm^2	1 mA/cm^2	[10]
3	PVB/PANI/PEDOT:PSS	Hybrid polymer nanocomposite system integrated with polymeric networks and the minimum quantity of GQD loading	352.94 F/g	0.14 A/g	[11]
4	CzT-CMOP	One-pot polycondensation of a rigid building linker with dimethoxymethane at ambient temperature	240 F/g	0.5 A/g	[12]
5	SPANIABF-G	Aniline derivatives and aniline-functional graphene were covalently bonded together and deposited on a carbon nanoparticle substrate	642.6 F/g	1 A/g	[13]
6	PEDOT-MeOH/PEG/WS$_2$	Co-electrodeposition method aqueous solution consisting of monomers, WS$_2$ and PEG	461.5 mF/cm^2	5 mV/s	[14]

CzT-CMOP Covalent organic polymer containing carbazole and Tröger's base; *SPANIABF-G* Self-doped covalently bonded graphene PANI; *PEDOT-MeOH/PEG/WS$_2$* Poly(hydroxymethyl-3,4-ethylenedioxythiophene/poly(ethylene glycol)/tungsten disulfide

example of the reactions is displayed in Fig. 3a. Thus, the polycondensation can be conducted using various monomers to form the specific copolymers, exhibiting a higher performance than the mono-polymers.

Usually, CPs applied on SCs have a linear structure due to their excellent π–π stacking. The linear system can minimize the space within the polymer matrix, increasing the concentration of polymer conjugated on the electrode substrate. The
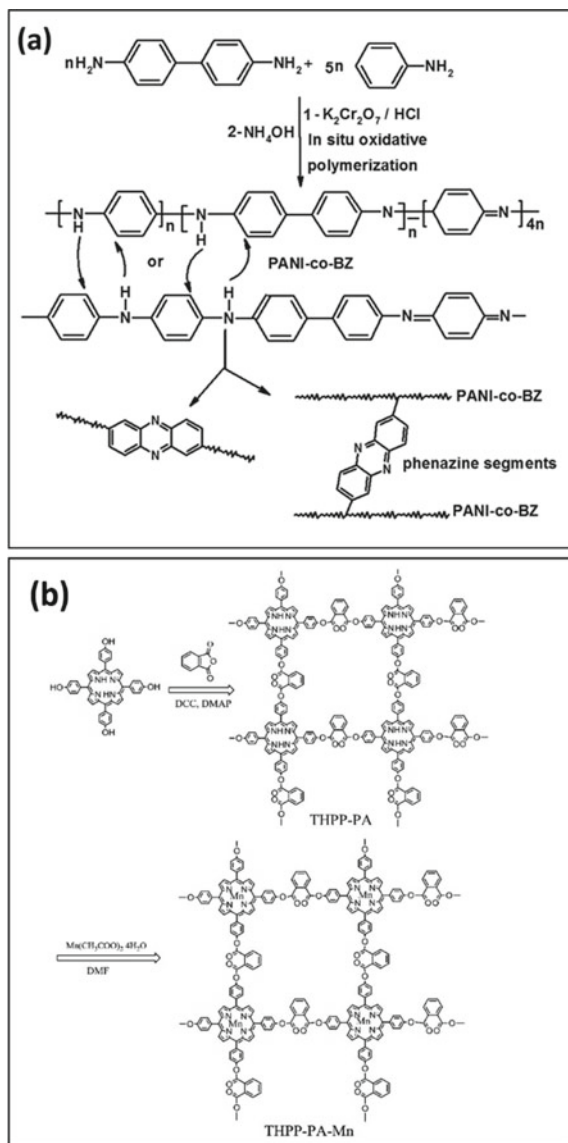
Fig. 3 **a** The tentative structure of the synthesized PANI-co-BZ (PANIBZ1) and formation of phenazine segments (adapted with permission from Ref. [16], Copyright 2021, Springer Nature), **b** synthetic routes for the THPP-PA and THPP-PA-Mn (Adapted with permission from Ref. [17] Copyright 2021, Elsevier)

π−π stacking provides good conductivity in CP due to their electron–hole charge transfer. The longer polymer chain can improve the charge transfer due to the interconnectivity of the ordered polymer structure [18]. However, the linear polymers also hindered the interaction between the electrolyte molecules and the surface of electrode materials because of their small surface areas. Therefore, the double-layer capacitance and the site-specific kinetics of the pseudocapacitive charging process will be limited.

One example of the recent efforts to improve the working mechanism of the copolymer was reported by Cheng et al. The authors used the copolymer made of meso-tetra(p-hydroxyphenyl) porphyrin (THPP) with phthalic anhydride (PA) and then metalizing with manganese acetate via the esterification process. To operate the working performance on the SC, the synthesis polymer was coated on Ni foam and applied as the electrode materials [17]. They developed the idea how to enhance the n-type of ambipolar conductive and electrochemically stable polymers with controllable pore sizes. The synthesized polymer had a cross-linked 3-D structure (Fig. 3b) that could optimize the surface area and facilitate the diffusion rates of solvent and electrolyte molecules' interaction with the electrodes.

3.2   Electrochemical Polymerization

Electrochemical polymerization or electropolymerization is the polymerization process that occurs on solid electrode material's surface. There are two kinds of electropolymerization: the anodic and cathodic electrochemical polymerization processes. The common method applied for CPs synthesis is anodic electropolymerization. The chemical reaction mechanism and the polymer growth kinetics on a conducting surface should be considered for the polymerization processes. However, due to the chemical diversity of the monomers, a common scheme of reaction cannot be provided [19]. Generally, the reaction process is affected by ambient conditions such as solution type, temperature, electrode composition, and current density. At the same time, the main step is the monomer's dimerization reaction, followed by the stepwise chain growth proceeds. The polymer chain forming mechanism should be involved either the coupling between radical cations or the reaction of a radical cation with a neutral monomer [20].

Due to its low reaction yield, cathodic electropolymerization is not common for CPs synthesis. However, this method is usually used for CPs assembly, which is impossible with anodic electropolymerization. Compared to the anodic CPs fabricated films, the coating films via the substrates using cathodic electropolymerization are more stable. Hence, different polymerization processes will lead to the different morphologies of CPs surface. The examples of the mechanism of the anodic and cathodic electropolymerization processes of PANI and PPy are shown in Fig. 4a and b. It should be noted that there may be parallel dimerization reactions that can make the different products of different polymer structures. It should be mentioned
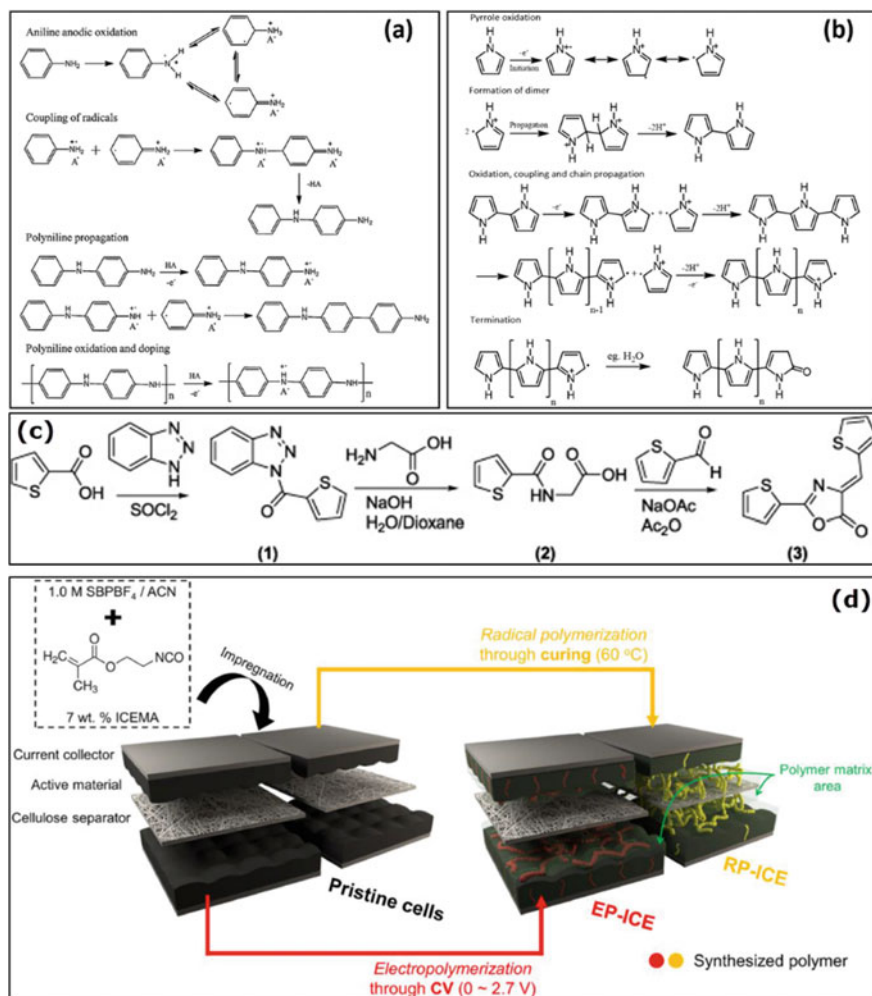
Fig. 4 **a** Mechanism for the anodic electrochemical polymerization of polyaniline (Adapted with permission from Ref. [24], Copyright 2021, Elsevier), and **b** mechanism for the oxidative polymerization of polypyrrole via radical cation formation , **c** preparation of 2-(thiophen-2-yl)-4-(thiophen-2-ylmethylene)oxazol-5(4 H)-one,3 (Adapted with permission from Ref. [22], Copyright 2021, Elsevier), and **d** schematic illustration of the preparation of EP- and RP-ICE cells (Adapted with permission from Ref. [23], Copyright 2021, Elsevier) [25]

that current density, electrolyte type also affects the formation of CPs during the polymerization processes.

The electrochemical behavior of the doped PANI electrodes showed excellent capacitance results. PANI usually showed poor cyclic stability due to its mechanical destruction during the working process [21]. However, via optimizing the dopants on PANI structures, the authors increased its stability to 70% of capacity retention after

2000 cycles and a relatively high specific capacity (722 C/g at 5 mV/s). Moreover, the flexible SCs using those doped-PANI on carbon cloth electrodes showed an excellent energy density of 12.57 Wh/kg at the power density of 283 W/kg with good cycling stability of 73% capacity retention after 3000 cycles.

Being a common material for SCs, PANI is getting great attention from scientists, and their enormous numbers of studies related to it are published annually. However, to increase the efficiency of SCs, it is necessary to create various types of CPs. They can be develop from the common monomer of thiophene such as 2-(thiophen-2-yl)-4-(thiophen-2-ylmethylene)oxazol-5(4H)-one (Fig. 4c) [22]. In addition, polymers can be synthesized for specific purposes such as suppressing the diffusion-controlled self-discharge or maintaining capacitance for SCs, such as 2-isocyanatoethyl methacrylate (ICEMA) (Fig. 4d) [23]. Although the conjugated organic/polymer materials display advantages such as ease of structural modification, facile processability, flexibility, tunable oxidation–reduction, the ions trapping behavior that occurred may limit their electrochemical stability for practical applications. The effect and mechanism for those ions trapping and effects based on CPs still require further studies.

4 Hybrid Composites with CPs for Supercapacitors

Although CPs are promising materials, they still have drawbacks that can restrain their application on SCs. As mentioned, all CPs showed substantial degradation during the doping/undoing process, limiting the stability of SC for long cycles use [5]. Furthermore, during the charge/discharge cycle process, the electronic conductivity of CPs tends to decrease due to the change of their molecular structures. During the working process, the faradaic reactions are conducted on the surface of the CPs. The charges can be stored or released when a CP molecule switches between the highly and poorly conducting states via the electrochemical redox reactions. After a certain number of working cycles, the CPs will be degraded. It leads to decreased electrical current carrying capacity and storage capacitance of SCs [26].

Combining CPs with other materials to form the hybrid composites seems to be a promising solution for those mentioned. The choice of composition will affect the composite properties such as their conductivity, surface areas, chemical endurance, and mechanical resistance of SCs.

4.1 Composites with Carbon-Based Materials

The carbon-based materials (CBMs) showed the tunable properties for SCs applications. They have good electrical conductivity, a large surface area, optimal pore size distribution, and fast electron transfer kinetics [27]. Furthermore, CBMs, which are commonly friendly to environments and low cost, can be classified according to their

Table 2 Recent reports of electrochemical performance of composites made of CPs and CBMs

Composite	Specific capacitance	Current density	Cycles	Retention rate (%)	References
PPy + C_3N_4	810.0 F/g	0.2 A/g	6000	92.0	[29]
3D-FC/GO/CNDS/PANI	2814.5 F/g	0.5 A/g	5000	91.5	[30]
PEDOT:PSS/rGO	214.4 F/g	10 A/g	5000	97.8	[31]
LS-PPy@CFY	245.89 F/cm^3	0.26 A/cm^3	25,000	92.7	[32]
CNT/PANI/HTC	571.0 F/g	1 A/g	1000	73.0	[33]
SDBSDPPy-HC	929.0 F/g	0.5 A/g	2500	90.0	[34]

dimensionality: from zero-dimension (0D) to tree-dimension (3D). This dramatically affects the working performance of SCs characteristics [28].

The composites made from CPs and CBMs may overcome the limitations and drawbacks of every individual component. CBMs usually exhibited excellent EDLC when used as the electrodes for SCs, while CPs showed high pseudo-capacitance [4]. When the composites are made, CPs' agglomeration or mechanical degradation during the working process can be prevented using CBMs. Furthermore, CBMs can facilitate the charge carrier (electron/ion) conduction, increasing the electroactive interfaces.

Some recent research related to the composites made from CPs and CBM is given in Table 2. The main goals of SCs research is their application on the industrial level, and the usage of CBMs is an efficient way to fulfill this purpose. The use of CBM in electrochemical SCs has been thoroughly studied and has shown impressive results. Therefore, the use of hybrid composites makes it possible to over come the shortcomings of SCs in both improving electrical conductivity and achieving cyclic stability.

Recently, the other derivatives of CBMs are being focused on due to their exciting characteristics. One of them is the 2D graphitic carbon nitride (g-C_3N_4), a potential candidate for SCs applications due to its chemical inertness, unrevealed structures, and large surface. There are different ways to compose with CPs, such as the 2D full-organic composite comprised by g-C_3N_4 and polypyrrole (PPy) prepared through a one-step and fast electrochemical co-deposition [29]. An example of CPs composite with C_3N_4 is displayed in Fig. 5a.

Compared to the 2D CBMs, the 3D substrate materials have higher porosity and specific surface area. However, they also have the drawbacks of low conductivity and poor hydrophilic [35]. Due to the sp^2 hybridization within the 2D CBMs structure, they have better electrochemical properties and good electrical conductivity and can be combined with CPs for widespread application in SCs. However, the 2D CBMs can accumulate quickly, such as GO, during synthesis [35]. Furthermore, during the working process in the ambient conditions, the layer made of 2D CBMs can easily peel off from the electrode surfaces.

Therefore, due to the significant advantages of 2D CBM, their application in electroactive devices is of particular interest. One line of research is the combination
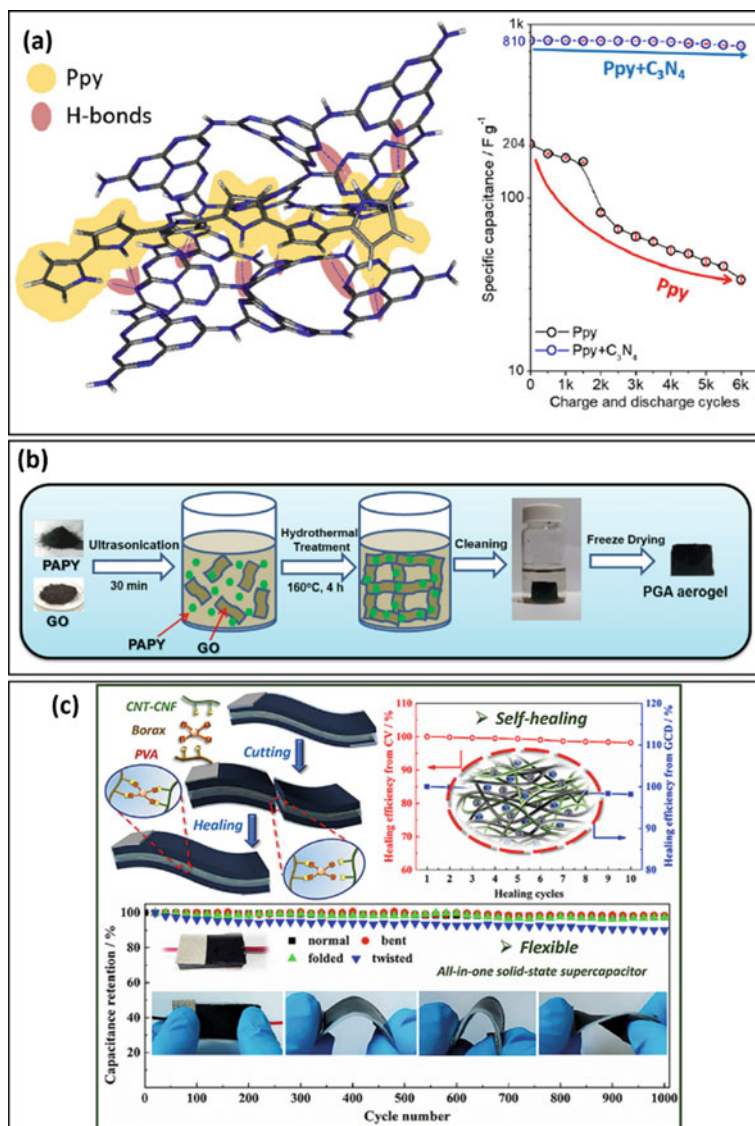
Fig. 5 **a** Optimized structure for C_3N_4/PPy/C_3N_4 interaction and the specific capacitance variation through the cycles (adapted with permission from Ref. [29], Copyright 2021, Elsevier), **b** schematic diagram of the synthetic route of composite made of poly(aniline-co-pyrrole) and rGO hydrogel (Adapted with permission from Ref. [37], Copyright 2021, Elsevier), and **c** schematic illustration of the assembled symmetric supercapacitor and the construction of the solid-state flexible device of CNT-CNF/PVAB composite hydrogels and their self-healing efficiency calculated from CV and G-CD curves. Capacitance retention as a function of cycle number under bending, folding, and twisting deformations at 1.0 A/g (Adapted with permission from Ref. [40] Copyright 2021, Elsevier)

with 3D CBMs such as carbon foam. The study aims to form integrated materials as support matrices for loading electroactive electrodes. The electrical conductivity of the 3D carbon electrodes embedded in the foam can be increased, and the accumulation and deposition of electroactive carrier materials can be prevented [30]. Modifying one-dimensional (CNT) and two-dimensional (rGO) materials with CPs makes it possible to obtain hydrogels with a three-dimensional structure and inherent properties in all components. For example, the π–π interaction of CNTs and GO is exploited to disperse conductively. However, the non-polar CNTs with hydrophobic GO powder can disperse in the high polar solution such as water to form a stable aqueous colloidal solution. Hence, when GO is reduced to rGO and CNTs will be anchored to the rGO sheet, they can form the 3D hierarchical multi-scale structure. The 3D structure can contain the rGO sheets as the "nano-wall" to prevent CNTs from random diffusion. CPs can be conjugated on those 3D structures, which play a role as nano scaffolds, to form the high working performance composite materials of SCs [36].

GO and its derivative reduced graphene oxide (rGO) are well-known CBMs usually used as electrode materials for SCs. Via the hydrothermal treatment, GO can be reduced and obtain the three-dimensional structure of rGO hydrogel, a potential material for SC. However, due to the small size of rGO particles was created, the hydrogel itself can restack during the reaction process. One of the common methods is the hydrogel fabrication via the hydrothermal reaction, transforming GO to rGO (Fig. 5b). CPs can be used as the spacing materials to overcome the restacking matter, therefore improving the working performance of the electrochemical SCs [37].

Besides, CPs can work as spacer components and be conjugated on the substrate via the chemical polymerization process. Thin films of CPs on hydrogel backbone improve the delamination of the rGO sheets, promoting a strong interaction between each composites component [6]. Being an electronic device, the traditional SCs are sensitive to various ambient mechanical deformations. Therefore, one of the recent targets of SCs research is to develop flexible and self-healing wearable SCs from carbon hydrogel [38]. Both the electrode and electrolyte materials are vital factors in developing the new generation of SCs. Hydrogel polymer networks are ideal for those requirements due to their inherent porous structure, high conductivity, and flexibility.

Furthermore, a hydrogel polymer network with high-water content dissolves ions and provides high ion conductivity. They can also maintain the solid shape and size to avoid liquid leakage during various mechanical deformations [39]. Consequently, a carbon-based electrically conductive hydrogel can provide the necessary interface between the electrolyte and the electrodes to enable the high-rate capability of SCs. When CNT-CNF was endowed to form a hydrogel (Fig. 5c), the composite showed high conductivity, flexibility, and stability due to the high uniformly dispersed in the gel matrix of the component [40].

4.2 Composite of Transition Metal Oxides and CBMs Conjugated with CPs

The CBMs, without a doubt, are the adaptive materials for SCs applications. The common CBMs such as graphene, activated carbon, CNTs, or aerogel are usually used for EDLC electrode materials. The carbon-based SCs can have long cyclic stability with good lifetimes. However, their maximum capacitance is limited by the active electrode surface area and the pore size distribution. For instance, the theoretically calculated capacitance of graphene is 550 F/g with a high specific surface area of 2630 m^2/g [41]. Despite introducing CPs into composites, the resulting materials still do not provide the high energy density required in energy storage devices for industrial applications. To solve this problem, transition metal oxides (TMOs) and their derivatives are being investigated as the components materials to enhance the working performance of composite electrode materials (Fig. 6a).

Tremendous research efforts are being made to find decent electrode materials to improve the electrochemical characteristics of SCs [35]. The combination of CPs, CBMs, and TMOx can enhance the electrode materials' electrochemical properties and electrical conductivity. Moreover, the hybrid composites' faradaic behavior can increase the specific capacitance and specific energy of the SCs, while the EDLC behavior can enhance the cyclic stability and high specific power.

However, the TMOs are not the perfect materials for SCs, either. They still have several disadvantages: high price and toxicity to the environment, as well as poor electrical conductivity. To improve the performance of SCs, bimetallic oxides have been investigated in which the synergistic effect of the elements characterizes the presence of two different metal ions. The bimetallic oxides have more active reaction sites and higher electrical conductivity than the single or binary metal oxides. For example, some common bimetallic oxides such as $ZnMn_2O_4$ or $NiCo_2O_4$ exhibited excellent working performance when used as composite materials for SCs electrodes [42]. Bimetallic metal oxides are considered as one of the most potential electrode materials for SCs, due to their properties like crystalline electronic structures, defects, spins, and synergetic effects. Furthermore, they also showed working performance increase when forming the composite with CBMs and CPs.

Developed from TMOs, transition metal sulfides (TMSs) have attracted tremendous attention. Transition metal sulfides such as MoS, CoS, NiS, MnS, FeS represent potential materials for energy storage applications due to the excellent electrochemical characteristics that are better than TMOs due to the presence of sulfur atoms. Besides, sulfur's lower electronegativity compared to oxygen can facilitate electron transfer in the TMS structure easier than in TMO [42]. The bimetallic sulfide showed superior electrochemical characteristics and higher electrical conductivity than their oxide counterparts, increasing the redox reaction process. Most of the TMSs' research is focused on their combination with CBMs. However, the combination of TMS and CP is a promising path for the future. For instance, the electrode for SC based on MoS_2 composed with PPy and rGO (MP-rGO) (Fig. 6b) had shown 1942 F/g at 1 A/g and 80.2% of capacitance retention. The formed 3D network architecture of
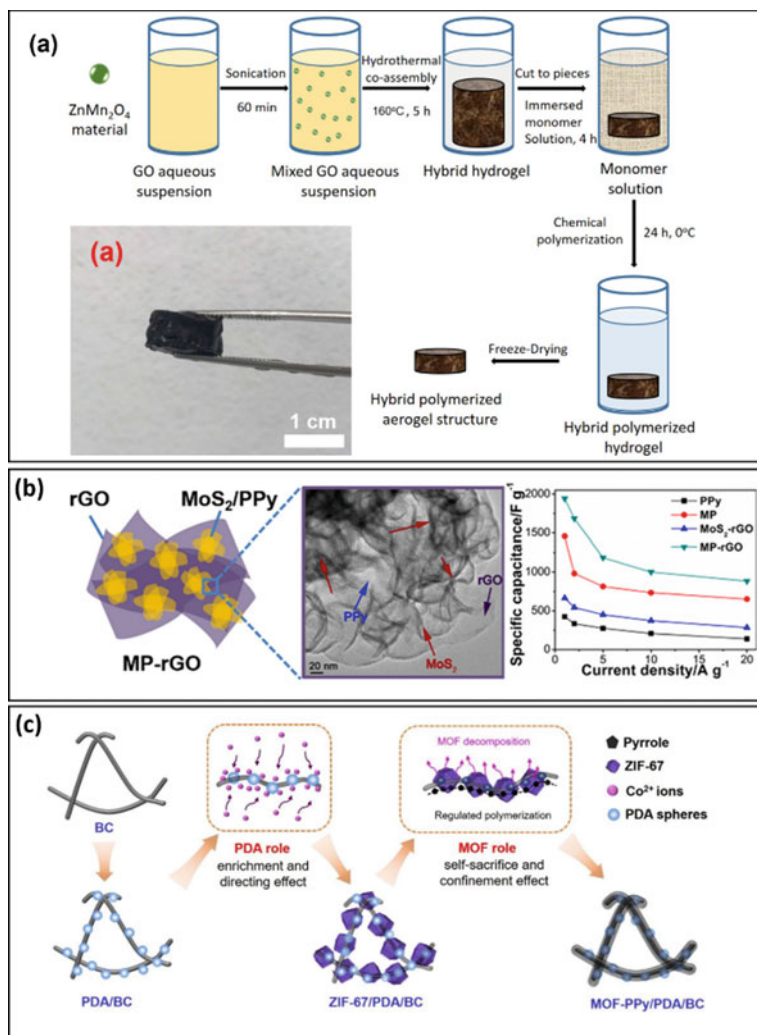
Fig. 6 a Schematic representation of the preparation process of hybrid aerogel based on rGO, $ZnMn_2O_4$ and conducting polymers (PANI, PPy) and the synthesized hybrid hydrogel (Adapted with permission from Ref. [42], Copyright 2021, Springer Nature), **b** MP-rGO (MoS_2 composited with PPy and rGO) structure with its TEM image and the specific capacitance of PPy, MP, MoS2-rGO (Adapted with permission from Ref. [43], Copyright 2021, American Chemical Society), and **c** MP-rGO versus various current densities, and the proposed of the template-engaged polymerization process of ZIF-67 polyhedrons on bacterial cellulose membrane modified by polydopamine (PDA) (Adapted with permission from Ref. [44], Copyright 2021, Elsevier)

the composite composed of overlapped nanoflakes helps shorten the ion diffusion path inside the structure. Hence the synergistic effect between the amorphous PPy layers and MoS_2 nanosheets in the composite also provides more active sites and surface and interior heterogeneity [43].

Metal–organic frameworks (MOFs) created by organic linkers and metal ions have also been considered as coordination polymers that showed good application for electrochemical devices [45]. MOFs are distinguished by various structure choices based on metal ions and organic linkers (Fig. 6c) [44]. The MOFs can enhance electrolyte ions' adsorption/desorption behavior during EDLC charging/discharging of SCs and give potential opportunities in turning their electronic and electrochemical properties [46]. The changes in organic linkers may lead to a shift in their crystalline structures and electrochemical properties. MOFs have shown good electrical properties, high stability, and large potential window. However, their electrodes' energy densities are still limited [5]. Hence the composite with CPs to increase the working performance was used as the solution.

The CPs can promote any carbonaceous material's electrochemical properties due to the high doping/dedoping rate during the charge/discharge process. During oxidation, ions are transferred to the polymer backbone, while ions are returned to the electrolyte during reduction. Consequently, the charge in the CPs occurs in the entire volume of the composites, rather than only on the surface of CMBs. This led to the higher capacitance of the composites compared to single materials only [47].

Moreover, CPs can serve as an intercalated spacer to further enhance the host surface area of the materials. In contrast, MOF powders can serve as a stable and underlying conductive network with high electrical conductivity and improved cycling stability. Such composite materials can help prepare the next generation of electrochemical energy harvesting and storage devices with long cycle life [48]. In 2021, our group published a paper related to zinc-MOF (Zn-MOFs) composites with rGO and PANI applied for SCs [6]. Those composites exhibited excellent working performance, i.e., the specific capacitance of about 372 F/g with retentions higher than 84% after the 5000 cycles.

5 Future Perspective

The CPs, with excellent specific capacities and capacitance, show good electrochemical performance relative to the energy storage devices. Their flexibility, high conductivity, easy processability can bring future potential applications. However, CPs also have some disadvantages that may restrain their use as components of SCs in industrial production. Those drawbacks are unavoidable and related to the CPs organic structure degradation mechanisms. During the long working process, the charge exchange processes cause an effect on the organic polymer chains, leading to the destruction of the polymer structure. The primary strategy for improving the working performance of CPs and their cycle-life in SCs application is making the composite with other materials such as CBMs and metal derivatives.

Changing the fabrication methods of the devices will lead to a change in their storage capacitance and energy density. Hence, the morphology of materials will affect the composite working performance too. Recently, the research trend has been to focus on the nanometer-scale of the materials morphologies, thus enhancing the specific surface area of the particles. It will facilitate the interaction between ions and the molecules on the surface of the electrode. The larger the particular area of the surface, the easier the exchange can happen. Variety of composite forming from the combination of CPs and the discussed alternative materials such as CBMs, TMOs, TMSs, MOFs have shown the potential in applications of CPs based composites in SCs electrode materials.

The study of self-healed flexible SCs is also an important direction that can have many open opportunities for researchers in the future. Thus, composites based on CBMs texture have shown high working performance and flexible, tensile properties.

Although there are many investigations related to the applications of CPs on SCs, they are still one of the most promising materials for their use in hybrid composites. CPs can provide comparable specific capacitance at significantly lower cost, high conductivity, and good mechanical properties. Consequently, CPs deserve further study to create electrodes and devices with a high specific capacity.

References

1. Xu, J., Wu, H., Lu, L., Leung, S.-F., Chen, D., Chen, X., Fan, Z., Shen, G., Li, D.: Integrated photo-supercapacitor based on bi-polar TiO_2 nanotube arrays with selective one-side plasma-assisted hydrogenation. Adv. Funct. Mater. **24**, 1840–1846 (2014)
2. Patil, S.H., Gaikwad, A.P., Sathaye, S.D., Patil, K.R.: To form layer by layer composite film in view of its application as supercapacitor electrode by exploiting the techniques of thin films formation just around the corner. Electrochim. Acta **265**, 556–568 (2018)
3. Kopecká, J., Kopecký, D., Vrňata, M., Fitl, P., Stejskal, J., Trchová, M., Bober, P., Morávková, Z., Prokeš, J., Sapurina, I.: Polypyrrole nanotubes: mechanism of formation. RSC Adv. **4**, 1551–1558 (2014)
4. Basnayaka, P.A., Ram, M.K.: A review of supercapacitor energy storage using nanohybrid conducting polymers and carbon electrode materials. In: Conducting Polymer Hybrids, pp. 165–192 (2017)
5. González, A., Goikolea, E., Barrena, J.A., Mysyk, R.: Review on supercapacitors: Technologies and materials. Renew. Sustain. Energy Rev. **58**, 1189–1206 (2016)
6. L. Quoc Bao, T.-H. Nguyen, H. Fei, I. Sapurina, F.A. Ngwabebhoh, C. Bubulinca, L. Munster, E.D. Bergerová, A. Lengalova, H. Jiang, T. Trong Dao, N. Bugarova, M. Omastova, N.E. Kazantseva, P. Saha, Electrochemical performance of composites made of rGO with Zn-MOF and PANI as electrodes for supercapacitors, Electrochim. Acta. 367 (2021) 137563.
7. T.O. Magu, A.U. Agobi, L. HITLER, P.M. Dass, A Review on Conducting Polymers-Based Composites for Energy Storage Application, J. Chem. Rev. 1 (2019) 19–34.

8. Hall, P.J., Mirzaeian, M., Fletcher, S.I., Sillars, F.B., Rennie, A.J.R., Shitta-Bey, G.O., Wilson, G., Cruden, A., Carter, R.: Energy storage in electrochemical capacitors: designing functional materials to improve performance. Energy Environ. Sci. **3**, 1238 (2010)

9. D. Kiymaz, A. Kiymaz, H. Dincalp, C. Zafer, Enhanced performance of ultra-thin polyaniline supercapacitor via aniline blue-WS SAMs with rich nucleation site, J. Phys. D. Appl. Phys. 54 (2021) 315501.

10. Y. Wang, Z. Du, J. Xiao, W. Cen, S. Yuan, Polypyrrole-encapsulated Fe2O3 nanotube arrays on a carbon cloth support: Achieving synergistic effect for enhanced supercapacitor performance, Electrochim. Acta. 386 (2021) 138486.

11. D. Arthisree, W. Madhuri, N. Saravanan, B. Dinesh, S. Saikrithika, A.S. Kumar, A ternary polymer nanocomposite film composed of green-synthesized graphene quantum dots, polyaniline, polyvinyl butyral and poly(3,4-ethylenedioxythiophene) polystyrene sulfonate for supercapacitor application, J. Energy Storage. 35 (2021) 102333.

12. A.F.M. El-Mahdy, J. Lüder, M.G. Kotp, S.W. Kuo, A tröger's base-derived covalent organic polymer containing carbazole units as a high-performance supercapacitor, Polymers (Basel). 13 (2021).

13. C.Y. Kung, T.L. Wang, H.Y. Lin, C.H. Yang, A high-performance covalently bonded self-doped polyaniline–graphene assembly film with superior stability for supercapacitors, J. Power Sources. 490 (2021) 229538.

14. Liang, A., Cai, Y., Wang, J., Xu, L., Zhou, W., Xue, Z., He, Y., Xu, J., Duan, X.: Co-electrodeposited porous poplar flower-like poly(hydroxymethyl-3,4-ethylenedioxythiophene)/PEG/WS2 hybrid material for high-performance supercapacitor. J. Electroanal. Chem. **891**, 115261 (2021)

15. McKeen, L.W.: Introduction to plastics and polymers, permeability. Permeability Properties of Plastics and Elastomers, pp. 21–40 (2017). https://doi.org/10.1016/b978-0-323-50859-9.00002-6

16. Al-Hussaini, A.S.: New crystalline poly(aniline-co-benzidine)/bentonite microcomposites: synthesis and characterization. Polym. Bull. **76**, 323–337 (2019)

17. Cheng, Z., Qiu, Y., Tan, G., Chang, X., Luo, Q., Cui, L.: Synthesis of a novel Mn(II)-porphyrins polycondensation polymer and its application as pseudo-capacitor electrode material. J. Organomet. Chem. **900**, 120940 (2019)

18. Pace, G., Bargigia, I., Noh, Y.Y., Silva, C., Caironi, M.: Intrinsically distinct hole and electron transport in conjugated polymers controlled by intra and intermolecular interactions. Nat. Commun. **10** (2019)

19. G. Inzelt, Chemical and Electrochemical Syntheses of Conducting Polymers, in: Conduct. Polym., Springer Berlin Heidelberg, Berlin, Heidelberg, 2012: pp. 149–171.

20. Fomo, G., Waryo, T., Feleni, U., Baker, P., Iwuoha, E.: Electrochemical polymerization. In: Chem. Bull./Huaxue Tongbao, pp. 1–28 (2021)

21. Li, L., Raji, A.R.O., Fei, H., Yang, Y., Samuel, E.L.G., Tour, J.M.: Nanocomposite of polyaniline nanorods grown on graphene nanoribbons for highly capacitive pseudocapacitors. ACS Appl. Mater. Interfaces **5**, 6622–6627 (2013)

22. Hür, E., Arslan, A., Hür, D.: Synthesis and electrochemical polymerization of a novel 2-(thiophen-2-yl)-4-(thiophen-2-ylmethylene)oxazol-5(4H)-one monomer for supercapacitor applications. React. Funct. Polym. **99**, 35–41 (2016)

23. Chung, J., Park, H., Jung, C.: Electropolymerizable isocyanate-based electrolytic additive to mitigate diffusion-controlled self-discharge for highly stable and capacitive activated carbon supercapacitors. Electrochim. Acta **369**, 137698 (2021)

24. Naveen, M.H., Gurudatt, N.G., Shim, Y.-B.: Applications of conducting polymer composites to electrochemical sensors: a review. Appl. Mater. Today. **9**, 419–433 (2017)

25. Gvozdenovic, M., Jugovic, B., Stevanovic, J., Grgur, B.: Electrochemical synthesis of electroconducting polymers. Hem. Ind. **68**, 673–684 (2014)

26. Xu, Y., Lu, W., Xu, G., Chou, T.W.: Structural supercapacitor composites: a review. Compos. Sci. Technol. **204**, 108636 (2021)

27. Rudolf, H.: Composites and copolymers containing redox-active molecules and intrinsically conducting polymers as active masses for supercapacitor electrodes—an introduction. Polymers (Basel) **12** (2020)

28. Kumar, S., Saeed, G., Zhu, L., Hui, K.N., Kim, N.H., Lee, J.H.: 0D to 3D carbon-based networks combined with pseudocapacitive electrode material for high energy density supercapacitor: a review. Chem. Eng. J. **403**, 126352 (2021)

29. Gonçalves, R., Paiva, R.S., Lima, T.M., Paixão, M.W., Pereira, E.C.: Carbon nitride/polypyrrole composite supercapacitor: boosting performance and stability. Electrochim. Acta **368** (2021)

30. Guo, Y., Su, J., Yang, H., Gu, F., Song, Y., Zhu, Y.: Flexible foam carbon/graphene oxide/Schiff base polymer-derived carbon/polyaniline for high-performance supercapacitor. Ionics (Kiel) **27**, 2639–2647 (2021)

31. Wang, Y., Liu, G., Liu, Y., Yang, J., Liu, P., Jiang, Q., Jiang, F., Liu, C., Ding, W., Xu, J.: Heterostructural conductive polymer with multi-dimensional carbon materials for capacitive energy storage. Appl. Surf. Sci. **558**, 149910 (2021)

32. Liu, X., Zang, L., Liang, C., Liu, Q., Deng, Y., Yang, C., Qiu, J.: Design and fabrication of high performance flexible supercapacitor with polypyrrole@carbon fiber yarn electrode and redox active dopants. Synth. Met. **271**, 116654 (2021)

33. Stott, A., Tas, M.O., Matsubara, E.Y., Masteghin, M.G., Rosolen, J.M., Sporea, R.A., Silva, S.R.P.: Exceptional rate capability from carbon-encapsulated polyaniline supercapacitor electrodes. Energy Environ. Mater. **3**, 389–397 (2020)

34. Bhardwaj, P., Singh, S., Kharangarh, P.R., Grace, A.N.: Surfactant decorated polypyrrole-carbon materials composites electrodes for supercapacitor. Diam. Relat. Mater. **108**, 107989 (2020)

35. Borenstein, A., Hanna, O., Attias, R., Luski, S., Brousse, T., Aurbach, D.: Carbon-based composite materials for supercapacitor electrodes: a review. J. Mater. Chem. A **5**, 12653–12672 (2017)

36. Tang, C., Long, G., Hu, X., Wong, K.W., Lau, W.M., Fan, M., Mei, J., Xu, T., Wang, B., Hui, D.: Conductive polymer nanocomposites with hierarchical multi-scale structures via self-assembly of carbon-nanotubes on graphene on polymer-microspheres. Nanoscale **6**, 7877–7888 (2014)

37. Tran, V.C., Sahoo, S., Hwang, J., Nguyen, V.Q., Shim, J.-J.: Poly(aniline-co-pyrrole)-spaced graphene aerogel for advanced supercapacitor electrodes. J. Electroanal. Chem. **810**, 154–160 (2018)

38. Guo, Y., Zhou, X., Tang, Q., Bao, H., Wang, G., Saha, P.: A self-healable and easily recyclable supramolecular hydrogel electrolyte for flexible supercapacitors. J. Mater. Chem. A. **4**, 8769–8776 (2016)

39. Han, J., Lei, T., Wu, Q.: High-water-content mouldable polyvinyl alcohol-borax hydrogels reinforced by well-dispersed cellulose nanoparticles: dynamic rheological properties and hydrogel formation mechanism. Carbohydr. Polym. **102**, 306–316 (2014)

40. Han, J., Wang, H., Yue, Y., Mei, C., Chen, J., Huang, C., Wu, Q., Xu, X.: A self-healable and highly flexible supercapacitor integrated by dynamically cross-linked electro-conductive hydrogels based on nanocellulose-templated carbon nanotubes embedded in a viscoelastic polymer network. Carbon N. Y. **149**, 1–18 (2019)

41. Balaji, T.E., Tanaya Das, H., Maiyalagan, T.: Recent trends in bimetallic oxides and their composites as electrode materials for supercapacitor applications. ChemElectroChem **8**, 1723–1746 (2021)

42. Le, Q.B., Vargun, E., Fei, H., Cheng, Q., Bubulinca, C., Moučka, R., Sapurina, I., Tran, T.D., Kazantseva, N.E., Saha, P.: Effect of PANI and PPy on electrochemical performance of rGO/ZnMn$_2$O$_4$ aerogels as electrodes for supercapacitors. J. Electron. Mater. **49**, 4697–4706 (2020)

43. Hao, J., Liu, H., Han, S., Lian, J.: MoS2 nanosheet-polypyrrole composites deposited on reduced graphene oxide for supercapacitor applications. ACS Appl. Nano Mater. **4**, 1330–1339 (2021)

44. Zhou, J., Yuan, Y., Tang, J., Tang, W.: Metal-organic frameworks governed well-aligned conducting polymer/bacterial cellulose membranes with high areal capacitance. Energy Storage Mater. **23**, 594–601 (2019)

45. Xu, M., Wang, W., Liu, Y., Zhong, Y., Xu, X., Sun, Y., Wang, J., Zhou, W., Shao, Z.: An intrinsically conductive phosphorus-doped perovskite oxide as a new cathode for high-performance dye-sensitized solar cells by providing internal conducting pathways. Sol. RRL **3**, 1–11 (2019)
46. Baumann, A.E., Burns, D.A., Liu, B., Thoi, V.S.: Metal-organic framework functionalization and design strategies for advanced electrochemical energy storage devices. Commun. Chem. **2**, 1–14 (2019)
47. Ma, J., Su, D.Y., Liu, Z.G., Jiang, L., Hao, J., Zhang, Z.J., Meng, X.K.: Conducting polymers based composite electrode materials in supercapacitor application. IOP Conf. Ser. Earth Environ. Sci. **267** (2019)
48. Zhu, L.N., Zhang, L.Z., Wang, W.Z., Liao, D.Z., Cheng, P., Jiang, Z.H., Yan, S.P.: [Zn(BDC)(H2O)2]n: a novel blue luminescent coordination polymer constructed from BDC-bridged 1-D chains via interchain hydrogen bonds (BDC = 1,4-benzenedicarboxylate). Inorg. Chem. Commun. **5**, 1017–1021 (2002)

Polymeric Nanofibers as Electrodes for Supercapacitor

Check for updates

Rinki Malik, Payal Tyagi, Suman Lata, and Rajender Singh Malik

Abstract Globally increasing amenities of living for achieving a convenient route towards life that solely depends on the energy miniatures upsurge the essentiality of energy storage devices. So, there is a need for sustainable energy sources that have high energy density and power density and do not create any harm to the atmosphere; with this approach, supercapacitors find a more appropriate place among similar energy appliances. In today's epoch, one-dimensional polymeric nanofibers are one of the most intriguing materials for supercapacitors' device fabrication. Polymeric nanofibers have unique characteristics such as their controllable porous nature, high surface area, high electrical conductivity with stress and strain tolerance potential, and, with these properties, they have an excellent bending ability i.e., intrinsic flexibility of polymer shackles, self-healable tendency also that make them better material for the wearable electronic devices in electronic watches, toys, electric guitar, grill, electric pressure cooker, etc. In this chapter, different techniques for synthesizing polymeric nanofibers along with their advantages and a few disadvantages are given and various polymers used for the synthesis of polymeric nanofibers are also studied. These nanofibers' hybrids/composites in supercapacitor application are deliberately examined with their brief explanations. Indubitably, a supercapacitor can make a remarkable place in the world of electronic devices through polymeric nanofibers, at the same time, despite the noteworthy progress in the development of flexible polymeric nanofibers based supercapacitors, their power and energy densities still need to further be enhanced for practical appliances with effective cost so come into range of a common person.

Keywords Nanofibers · Polymeric nanofibers · Synthesis techniques · Electrode material · Supercapacitors

R. Malik · P. Tyagi · S. Lata · R. S. Malik (✉)
Deenbandhu Chhotu Ram University of Science and Technology, Murthal, Haryana 131039, India
e-mail: rsmalik.chem@dcrustm.org

R. Malik
Pt. Neki Ram Sharma Government College, Rohtak, Haryana 124001, India

1   Introduction

Hydrocarbons like petroleum; diesel, Compressed Natural Gas (CNG), Liquefied Petroleum Gas (LPG), coal, etc. are the reservoirs of fossil fuel for accomplishing the energy demands globally. All the above-mentioned sources are nonrenewable with limited stock and are being exploited vigorously while the worldwide energy consumption accelerated at a startling pace [1]. So, the necessity of some sustainable and renewable energy sources with a green impact on the environment has been a concern of present-day researchers. Now a day's, the ongoing research is being majorly focused on green and renewable sources like wind, solar, hydro energy, but more or less, these energies are mainly controlled or captured by our natural climatic conditions. In this way, with the regular variations in climate, rapid reduction in hydrocarbon fossil fuels stock, and the ever-increasing energy demand all over the world, there is a dire need for environmentally clean, renewable, high power and energy density electrochemical energy storage devices [2, 3].

From the last few decades and in the ongoing scenario, mobile, laptops, electronic watches, toys, electric guitars, grills, electric pressure cookers, robotic vacuum cleaners, hybrid electric vehicles, etc. have brought expediency in life [4]. These minuscule appliances require energy storage devices that contain high power and energy density with small size and should be more flexible so that they may be modified according to the usage. Batteries, as electrochemical energy storage maneuvers are the frequently used devices in most of the appliances due to their high energy density, simultaneously have little power density and life cycle with environmentally hostile nature; thus, this tendency forces the researchers to look forward towards other energy storage devices (ESD) that improve power and energy density parameters with environmentally approachable characteristics [5, 6].

Supercapacitors (SCs), among the parallel developed/developing electrochemical appliances like batteries, fuel cells, are the ESDs that address most of the problems concomitant to fossil fuel depletion, renewable energy sources, and also meet the current demand of energy globally. SRs also called electrochemical capacitors or ultracapacitors, have an ample amount of power as well as energy density, a long life cycle that is a prominent factor for efficient ESDs. All these characteristics make them promising candidates in the form of electrochemical ESD and conveniently replace batteries in many appliances. SC devices comprise of two electrodes separated by a separator and the space between electrodes and the separator is filled with an electrolyte [7]. When the potential is applied, the ions in the electrolytic solution travel towards the electrode surface carrying opposite charges. It depends on the surface area of the electrode material that how much ions can hoard on the electrode. When the discharge of the device occurs then all the ions leave the electrode and locomote towards the solution. In this way, charging-discharging is transpired.

Generally, the charge hoarding up the tendency of an electrode depends on the porosity, size, chemical nature, structure, and surface area of the material of the indicator electrode. Thus, one should know, how these properties of the electrode material are précised for the accomplishment of high specific capacitance. Mainly three types

of materials are used for the SC's electrodes (1) Carbon materials like:- graphene oxide (GO), multi-walled carbon nanotubes (MWCNTs), activated carbon (AC) [8] (2) Metal oxides such as MnO_2, NiO_2, etc. (3) Conducting polymers (CPs) like polyaniline, polypyrrole, polythiophene, etc. Among the three, the CPs are considered as reassuring electrode material for SCs. CPs have a long pi backbone for the transfer of electrons/charge, easy synthesis, nice intrinsic electrical conductivity, lightweight, high resistance to heat, effortless hybrid synthesis with carbon material or using metal oxides, and flexible nature. It is a prime need for the boosting of the surface area of the electrode and the attainment of convincing specific capacitance [9].

Fibers are the materials that provide a better approach to scientists in energy research owing to bending, twisting, and stretching characteristics. Nanoparticles agglomerate and make clusters straightforwardly while nanofibers form mesh and do not undergo agglomeration. Macromolecular systems like polymers orient in fibers through different techniques and increase the interactive options, in a similar way, processing techniques of polymers offer controllable diameter of polymeric fibers. In comparison to bulk and 2-D materials like paper sheets, films, 1-D polymeric fibers with diameter < 1 μm offer high electrical conductivity, good stress tolerance tendency, well ordered and controllable pore size that assist in enlargement of the surface area and flexibility in tiny volumes. The surface area that is in contact with electrolyte hoards more ions in the material for the double-layer formation, oriented pores offer high rate capability via electrodynamics, and stress tolerance/flexibility cooperate for the exterior distortion without degradation of device performance. These characteristics make the fibers a more appropriate material to act as a catalyst in electrochemical reactions, in tissue engineering, in drug delivery, and now potentially used as energy storage materials in supercapacitor devices. There is many different techniques for fibers' synthesis like wet spinning, solution drying, electrospinning, self-assembly, template method, drawing, and phase separation with a wide application range such as tissue engineering, thermos plastic foams, protective clothing, and energy storage material as shown in Fig. 1 [10, 11].

In this chapter our focused points will be different processing techniques, parameters associated with fibers, polymer-based formulations utilized to get polymeric nanofibers' synthesis, and how all these are interrelated to enhance SRs device performance. We will also contribute towards future prospective for upcoming research pursuits.

2 Polymeric Nanofibers

Polymeric nanofibers are one dimensional component in nano diameter scale. Size, morphology, orientation, aspect ratio, and conductivity of polymeric fibers are controlled via processing techniques, different environmental parameters, and polymer properties. It has been observed from various literature that more than 50
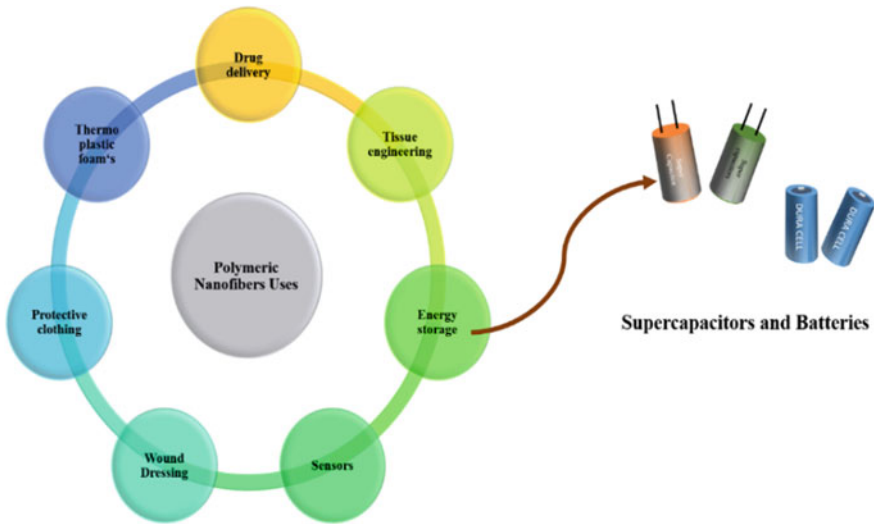
Fig. 1 Applications of polymeric nanofibers

polymers are spun in too long elastic fibers up to 10 m length consisting nano measure diameter [12].

2.1 History

Polymeric fibers from cellulose synthesis were discovered in the eighteenth century where Count Hilaire de Chardonnet restored cellulose after the hydrolysis of cellulose nitrate and patented in 1885. It came into commercial production in 1891 and now fabrication of synthetic fibers is in billions of kilograms per year. The progress of these fibers depends upon new advances, utilization in today's era, and findings in synthesis techniques, new spinning methods, and, in some cases, new polymer solvents. Carothers and co-workers of Du Pont Co. prepared first such fibers in the early 1930s by condensation polymers. They first developed polyesters then turned to the thermally stable aliphatic polyamides. Nylon 66 was promotionally produced in 1938. In the mid of 1934–1944, Anton Formhals first time synthesized the nanofibers and after that he patented them. Since then, many synthetic polymers or fibers formations have been examined in nanofiber synthesis. In 1953 poly (ethylene terephthalate) fibers were introduced by Whinfield and Dickson. Ziegler, Natta, and others investigated isotactic polypropylene and fibers in the 1950s. Nylons, polyesters, polyacrylics, and polyolefins comprise the present major classes of synthetic fibers. Many represent innovations of polymer- and fiber-making technology. Examples are Spandex elastic fibers, heat- and flame-resistant fibers from polyfluorocarbons, polybenzimidazole, and aramids, and high-strength, high-modulus fibers from graphite

and aramids [13, 14]. In 1966, Harold Simons fabricated a device that could produce thin and light-weighted diverse nanofibers.

3 Morphology and Characteristics of Polymeric Nanofibers

The structure and characteristics of nanofibers determine their charge storage potential. Different techniques are used to determine the morphology of the polymeric nanofibers.

3.1 Morphology

The morphology of polymeric nanofibers is determined through scanning electron microscopy (SEM), transmission electron microscopy (TEM), and atomic force microscopy (AFM). All these characterizations narrate the orientation of fibers, roughness, size, diameter range, hollow nature in the internal part of polymeric fibers. All these properties are related to the storage and surface area of the material and are also connected to the specific capacitance in SRs.

3.2 Properties of Nanofibers for Supercapacitors

Polymeric nanofibers are very interesting for electronic devices like SCs because of their higher charge mobility in order of magnitude than thin films. Nanofibers undergo molecular assembly, π mounding of polymeric fibers on longitudinal axis with the alignment of polymer backbones. These factors enhanced surface area via decreasing diameter in nanoscale. The exceptionally large space created through nano fibrillation attributes to dramatically different behavior including crystal nucleation, enhanced ductility, and increased strength and stiffness. Additionally, the flexibility of the nanofibers results in the formation of a dense, entwined fibril network even at a low concentration that ultimately causes changes in the electrical conductivity and viscoelastic response of the composite.

Flexible SCs are the need of society where polymeric nanofibers as electrode material full fill the requirements of the stretchable, flexible, and bendable devices. Strain and tensile strength modulus, bending, stretching mechanically properties of nanofibers reduced the internal defect formation in polymeric nanofibers [15].

4 Techniques for Synthesis of Polymeric Nanofibers

Physical, chemical, mechanical, thermal practices are used for the fabrication of nanofibers. There are many techniques for the synthesis of polymeric nanofibers such as drawing, electrospinning, phase separation, self-assembly, template synthesis as depicted in Fig. 2. All of these are described sequentially [16, 17]. Table 1 shows that there is a change in diameter with the alteration of techniques and different types of polymer used for spinning.

4.1 Drawing

Drawing is a basic technique for nanofibers fabrication. In this, a viscoelastic fluid droplet is applied on a surface and a sharp tip micropipette is drawn from the droplet for the synthesis of liquid fibers. Subsequently, liquid has been faded from the liquid fibers and the solidification of the fibers has been done. This is a simple technique that mainly depends upon the viscoelastic solution of polymer, drawing speed of micropipette and rate of evaporation of the solvent. It is limited only to the lab-scale and only small productivity can take place via this procedure.
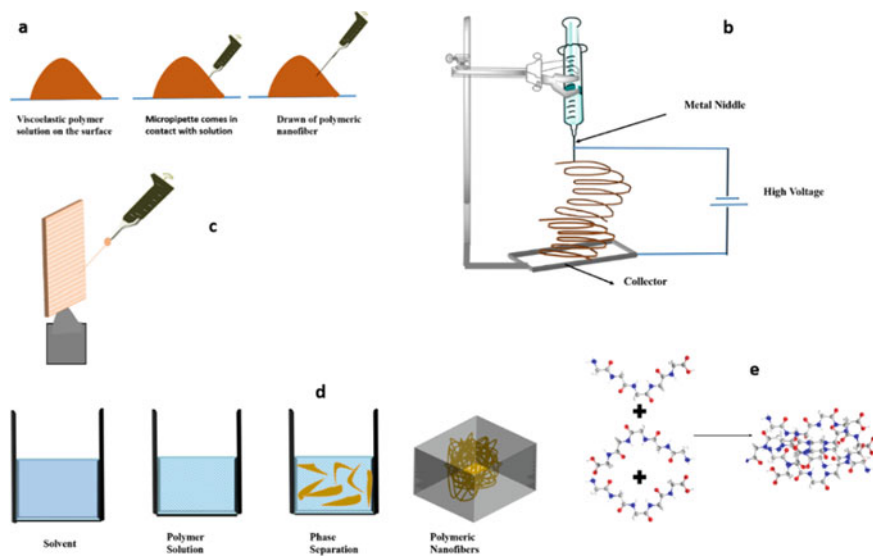
Fig. 2 Techniques for the synthesis of polymeric nanofibers **a** Drawing **b** Electrospinning **c** STEP **d** Phase separation **e** Self-assembly

Table 1 Different methods for polymeric nanofiber synthesis with a range of diameter (Adapted with permission from reference [10], Copyright (2020), Elsevier

Preparation method	Material	Solvent	Diameter control	Fiber diameter (nm)
Electrospinning	PEO	Water	Initial jet diameter, L-R curvature, transition slope	~ 140
	PEO	Dichloromethane	–	278
	6F-PI	DMAc	–	50
	PI (BPDAPPA)	DMAc	–	~ 300
	PLA	Chloroform/acetone	–	159
	PLA	TFE	Injection rate	90
	PLA (PLA/PANI)	HFP		130
	PLA (PLLA/PDLA)	DCM/pyridine	Solution concentration, blend ratio, rotational speed	346
	PAN	DMF	Voltage, flow rate	344
	PAN	DMF	Voltage, solution concentration	270
	PAN	DMF	Voltage, solution concentration	~ 100
	PMMA	DMF	LiCl salt concentration	~ 900
	PMMA	Chloroform	Injection rate	1000
	PS	Toluene		200
	PVDF-TeFE	Methylethylketone/DMF	Solution concentration	380
	PCL	Chloroform/methanol	–	511
	PCL	Dichloromethane	–	98
	PA6	–	Solution concentration	60
	PA6(O-MMT added)	Formic acid	Solution concentration, organic additive	95

Table 1 (continued)

Preparation method	Material	Solvent	Diameter control	Fiber diameter (nm)
	PA6(3)T	Acetone, DMF/chloroform	DMF concentration	250
Gel-electrospinning	Polyethylene	*p*-xylene	Solvent type	570
Solution blow spinning	PS	Toluene	Injection rate, gas pressure	220
	PLA	TFE		80
	PLA	Chloroform/acetone	–	289
	PLA/PANI	HFP		140
	PDLLA	Chloroform/methanol	–	125
	PMMA	Chloroform		1000
	HMWFG	Acetic acid	Solution concentration, air pressure, feed rate	39.2
	PVDF-TeFE	Methylethylketone/DMF	Solution concentration	530
	PS	Dimethyl-formamide	–	1949
	pDTEc	Dioxane		677
	PCL	Chloroform		231
	PCL	Dichloromethane		317
	PEO	Dichloromethane	–	267
Melt blowing	PP (MFI:1550)	–	Die geometry (AGR die)	780
	PP (metallocene, MFI:1800)	–	Die geometry, polymer throughput	300
	PP (MFI:1200)	–	Drum rotation velocity, air flow rate	600
	PP (MFI:300)	–	Polymer viscosity, fluid injection	438
	PP (MFI:1500)	–	Processing temperature	300
	PP	–	DCD, air flow rate	260
	PS			380

Table 1 (continued)

Preparation method	Material	Solvent	Diameter control	Fiber diameter (nm)
	PS	–	Polymer viscosity, air flow rate	620
	PBT	–	Processing temperature	440
Melt electrospinning	PCL	–	Collector speed	~ 1000
	PCL		Voltage, working distance, temperature	850
	PLA		Gas injection	180
	PLA		Laser output, DCD	< 1000
	PLA		Working distance, voltage	3000
	PGLA		Composition	530
In situ nanofibrillation	PECTFE (matrix: PBT)	–	Blend component	70
	PBT (matrix: SP)	–	Blend composition, matrix polymer	86
	PBT (matrix: SP)		Blend composition, matrix polymer	82
	PVDF (matrix: SP)		Blend composition, matrix polymer	36
	PA6 (matrix: PLA)		Blend composition	200
	PET (matrix: PP)		Draw ratio	~ 220
	PTFE (matrix: PP)		Blend composition	~ 200
	PTFE (matrix: PP)		Blend composition	~ 200
	PA6 (matrix: PP, coupling agent: PP-g-MA)		Coupling agent content	1100

Table 1 (continued)

Preparation method	Material	Solvent	Diameter control	Fiber diameter (nm)
	PBT (matrix: HDPE, coupling agent: EVA9-Bu$_2$SnO)		Coupling agent content, draw ratio	1130

4.2 STEP Technique

Spinneret-based tuneable engineering parameters (STEP) is a technique where 3-dimensional nanofibers formation takes place. In this method, the micropipette work as a spinneret, and the rotating device is mounted on a position where it can undergo rotational and translational motion. The polymer solution extrusion has been done via micropipette and extended on the movable device in a parallelogram filament structure continuously. The diameter of the fibers depends upon several factors like polymer solution, concentration, speed of movable substrate, solvent properties. This technique faces the deposition of fragile fibers at a submicron distance.

4.3 Template Synthesis

In this method, a template generally a metal oxide membrane is used for the synthesis of nanofibers. In this procedure, the polymer solution restrains on the nanoporous membrane and feels the pressure of water from the other side so the extrusion of the polymer solution takes place in filament arrangement. The long fibers have not been fabricated in this method and the diameter of these rely on the porous structure of the membrane.

4.4 Phase Separation

This is also a 3-dimensional nanoscale technology for the construction of polymeric scaffolds in nanofibers. This technique consists mainly of three steps (1) dissolution of polymer in a particular solvent (2) gelation (3) extraction of solvent from the gel subsequently freeze-drying in a vacuum. In this, gelation temperature is the crucial step where the liquid–liquid or liquid–solid phase separation has been done. Polymer solution concentration is also a key factor to determine the porous nature of the nanofibers.

4.5 Self-Assembly

It is also a nanofibrous scaffold bottom-up fabricating technique where the pivotal role is played through intermolecular interactions in the small units. In this method, small molecules come together through the non-covalent bond i.e., hydrogen bonding, Vander walls, π-π, and electrostatic interaction. These interactions are weak however when they work together actually determine the structure of macro-molecular nanofibers and their stability. This technique fabricates thinner diameter nanofibers conversely this is a very complicated and elaborated method.

4.6 Electrospinning

Electrospinning is a procedure where electrostatic phenomena are used to generate nanofibers fibers. A classic electrospinning arrangement contains (1) a high voltage source (2) spinneret, it may be a micropipette, syringe, or needle (3) collecting unit for the fibers. First, an electric field generates between one of the electrodes and a positively charged spinneret filled with a polymer solution. As the electrostatic charge is higher than the surface tension of the solution, there is the formation of an electrically charged jet of polymer solution at the metal needle tip. When polymer solution overcomes the surface tension by electrostatic forces then there is the formation of Taylor cone after increasing the voltage charge strands come out from the Taylor cone. Subsequently, the charge jet strands move through the spinneret towards the counter electrode and evaporate the solvent, which leads to the formation of continuous polymer fibers having diameters in the range of tens of nanometers to a few micrometers (depending on electrospinning parameters) that gather on the collecting unit. The electrospinning method can effectively be a spin solution for nanofibers fabrication devoid of using surfactants and other solvents that are poisonous and prohibited for medical and other applications.

Many factors affect the synthesis of nanofibers. They are broadly classified into three considerations (1) process parameters that contain high voltage, the distance between the needle and collector, and flow rate of the solution. The increased electric voltage and the short distance between the needle and collector induce the formation of beading in the nanofibers. In the same way, the flow rate of the solution should be in constant way otherwise non-uniform nanofibers with large diameter or lower diameter are fabricated after the high or low flow rate of solution respectively. (2) Contexture parameters that include humidity and temperature. Humidity affects the morphology of fibers. There is the formation of circular pores and large diameters in polymeric nanofibers with a surge in humidity. The viscosity of the polymer solution decreases as temperature increases thus it allows the polymer solution to spin under room temperature resulting in a smaller fiber diameter. (3) Polymer solution parameters such as surface tension of the solution, viscosity, conductivity, and polymer molecular weight. The low viscosity of solution results in the formation of beading

morphology of the fibers while high viscosity is liable for the large diameter of the fibers. High conductivity and molecular weight polymers are responsible for the smooth long fibers with high mechanical strength. Thus above-mentioned factors regulate the diameter, length, and porous nature of polymeric nanofibers.

5   Different Polymers for Nanofibers Synthesis

Different synthetic and natural polymers are utilized for the fabrication of polymeric nanofibers depending on their mechanical strength, conducting properties, elastic, bent, and stress and strain potential with spinnability. Synthetic polymers like polyaniline, polypyrrole, poly (3,4-ethylenedioxythiophene), polyvinyl alcohol, polyglycolic acid, polyglycerol, etc. have high mechanical strength, processing, and easy modification while they lack biocompatibility and are environmentally benign. On the other side natural polymers such as collagen, cellulose, lignocellulose, gelatin, chitosan, fibrinogen, etc. are biochemical activity compounds with no safety issues for nature but lack of processing and modification capacity.

So to overcome the hitches of synthetic and natural polymers, they are united via different processing methods and fabricate hybrid arrangements.

6   History, Mechanism, and Applications of Polymeric Nanofibers in Supercapacitors

Formerly with the growth of technology for electronic materials from the last 50 years, the era of supercapacitor technology has come. In 1957, the first supercapacitor having porous carbon electrodes based on an electronic double layer mechanism was invented by H. Becker. Electric double-layer capacitors (EDLC) were officially documented in 1966 by the Standard oil company, Cleveland (SOHIO). In the last 10 years, SCs are exemplified by high power density than batteries so that these can store/deliver a huge amount of energy in a short time. Furthermore, a long life cycle without material degradation in comparison to batteries makes supercapacitors attractive for many long-lasting appliances.

6.1   Mechanism of Charge Storage

Supercapacitor stores energy like a capacitor but it differs from capacitors mainly in two ways (1) Its electrode plates have a bigger area than capacitor (2) It contains separator which decreases the distance between the electrode plates.

Similar to a capacitor, SCs have electrodes but are effectively large and spongy than capacitors which accumulate more charge. Both the electrodes are immersed in the electrolyte and separated by a very thin insulating material. These are mainly of two types depending on the charge storage mechanism [18].

The electric double layer (EDL) capacitor does not involve any type of reaction. Capacitance is generated through the separation of the charges across the electrolyte so that EDL capacitors have high charge/discharge cycles. The not only capacitance associated with EDL but capacitance correlated with the surface reactions where electron charge transfer takes place between electrode and electrolyte is also important [19]. This capacitance is known as pseudocapacitance. EDL capacitor and pseudocapacitance are shown in Fig. 3. Different equations are used for the calculation of specific capacitance which are as follows

$$C_v = \int IdV / \upsilon m V \tag{1}$$

where C_v is specific capacitance (F/g) computed from CV curves, [20] I is current density (A/cm^2), V is the potential window (volts), m is the active mass of material (g), and υ is scan rate (V/s)

$$C_s = I \times \Delta t / m \times \Delta \upsilon \tag{2}$$

where C_s (F/g) is specific capacitance from GCD curves [21], I (A) is currently applied, m (g) is the active mass, $\Delta \upsilon$ is the potential window and t (s) is the discharge time.
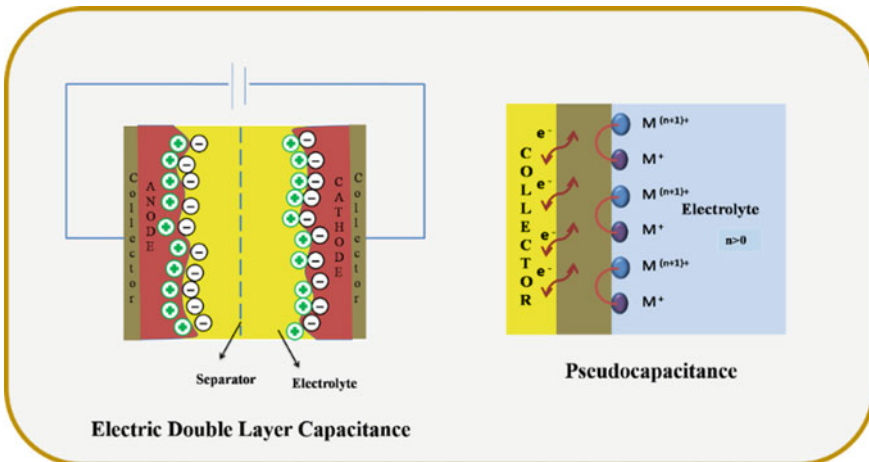

Fig. 3 Mechanism of charge storage in supercapacitors

$$E = \frac{1}{2 \times 3.6} \times C \Delta V^2 \qquad (3)$$

where E is energy density (Wh/kg), C is the specific capacitance (F/g), ΔV (volt) voltage window.

$$P = 3600 \times \frac{E}{t} \qquad (4)$$

Here, P is power density (W/kg) and t is discharge time in GCD.

6.2   Polymeric Nanofibers for Supercapacitors

Polymers are unique in respect of their electrical conductivity (CPs i.e. π-π bond associated polymers) through charge transport, mechanical stability, elasticity, and flexibility. Nanofibers synthesized through polymers are the considerable motifs for the charge storage in one-dimensional structures [11]. 1-D polymeric nanofibers orienting in a comprehensive arrangement and containing charge carrying ability in a proper fashion assist in the storage of charge in SCs. Polymers transform their volume during charging-discharging which causes a reduction in cyclic stability of the electrode material in SCs. So, to enhance the cyclic stability, energy density, and maintain power density, researchers focus on the synthesis of hybrid materials in an oriented manner. Today, along with the synthesis of 2-D nanostructures like films, sheets, papers, etc. for supercapacitor, there is fabrication of 1-D scaffolds which provide stretchability, bending ability, and high charge stowing tendency that makes them promising components for supercapacitor device application. Zhuanpei Wang and his coworkers developed internal tandem stretchable fiber-shaped SCs (T-SFSS) to circumvent the problem of mechanical stability and high electrochemical performance. They synthesized fibers from the PEDOT: PSS via a wet spinning method. They developed a T-SFSS assembly that consists of eight serially connected cells having voltage output of 12.8 V with an energy density of 41.1 μWh/cm^2 and power density 3520 μW/cm^2, with stretching ability of 400% without capacitance degradation [22]. Ji Eon Yang et al. synthesized material of activated carbon nanofibers (ACNF) via the carbonization of electrospun polyacrylonitrile and after that aniline was coated on ACNF through the mean of cyclic voltammetry. ACNF-PANI provided a specific capacitance of 832 F/g at a current density of 1 A/g. It maintains specific capacitance up to 92% even after 1000 cycles [23]. A simple, but effective approach for polymerizing CPs on flexible substrates is vapor deposition polymerization. Carbon nanofibers (CNF) with polymers proceed with the synergistic effect of the components in the material. So, CNF and polyaniline (PANI) both are added to fabricate a material that possesses high electrical conductivity, tunable mechanical constancy, improved environment benign, etc. PANI-CNF coated materials having thickness 20 nm are

synthesized using one step vapor deposition method that improved electrochemical performance of supercapacitor providing 264 F/g value of specific capacitance [24]. Poly (styrene-b-butadiene-b-styrene) (SBS) polymeric nanofibers were fabricated using electrospinning followed by a coating of single-walled carbon nanotubes (SWCNTs). The electrode material assembled in a two-electrode system using 1-ethyl-3-methylimidazolium bis(trifluoromethylsulfonyl)imide (EMIM][NTf2]) as electrolyte offers a stretchable SCs consisting of the volumetric capacitance of 15.2 F cm^{-3} at 0.021 A cm^{-3} and swallow strain up to 40% [25]. As the morphology and doping of the material are also allied with the electrochemical performance. So, porous hollow nitrogen-doped carbon nanofibers can be used for SCs because nitrogen doping mounts the electrical conductivity and wettability of the surface for the absorption and adsorption of the electrolyte ions. Porous hollow carbon nanofibers are synthesized using high nitrogen contents (13.4%) through co-axial electrospinning and consequent phase separation process by utilizing poly (styrene-co-acrylonitrile) (SAN) and polyacrylonitrile (PAN)/polyvinylpyrrolidone (PVP) mixture as a core and a shell respectively. The designed structure accomplishes an energy density of 4.12 Wh/kg on power density of 15 kW/kg, and also maintains 92.33% retention rate in 10,000 charge/discharge cycles [26]. Electrospinning is an effective approach for the fabrication of polymeric nanofibers and synthesis of hollow composited material. Polyacrylonitrile (PAN) and polymethyl methacrylate (PMMA) composite polymeric nanofibers electrospun via electrospinning and consequently went for carbonization. The electrochemically measurement of these nano fiber materials was done in the two-electrode method and specific capacitance of 140.8 F/g at a current density of 10 A/g was observed for porous carbon nanofiber mats set of PAN/PMMA = 7:3. The specific capacitance decreased by 4.6% after 10,000 charge/discharge cycles of the porous carbon nanofiber mats prepared at PAN/PMMA = 7:3 [27]. Allotropes of carbon such as graphite attain much greater attention than transition metal oxide. Polyaniline (PANI) when syndicate with the polyvinyl alcohol (PVA) then the resulting polymer attributes qualities of both the polymer. However, when graphite inclusion occurs with the PANI-PVA polymeric solution, subsequently formation of polymeric nanofibers take place through electrospinning. Aleena Rose and his colleagues made the PANI-PVA-GO composite and observed specific capacitance of 438.8 F/g that was much larger than PANI-PVA (143.3 F/g) [28]. Hexachlorocyclotriphosphazene (HCCP) and 4,4-sulfonyldiphenol (BPS) were used for the synthesis of organic–inorganic hybrid polymeric nanofibers (PNFs) via the in-situ template method henceforth they undergo carbonization and the formation of heteroatom-doped mesoporous carbon nanofibers (HMCNFs) take place. HMCNFs under a three-electrode system delivered the specific capacitance of 214.9 F/g in 6 M KOH electrolyte in a current density of 0.1 A/g [29]. Electrospinning technique was used for the fabrication of carbon nanofibers via the blending of polyacrylonitrile (PAN) and high decomposition temperature polymer polysulphone (PSF) which also acts as activating agent. The stabilized PAN-PSF polymers are processed for carbonization and synthesized porous carbon nanofibers (CNFs) because introduce PSF polymer enhanced mesoporous structure of CNFs and graphitization. The CNFs offered a specific capacitance of 289 F/g with a scan rate of

10 mV/s. The device maintains 100% retention of capacitance even after 6000 cycles with an energy density of 36 Wh/kg [30]. Kun Zhou and his associates synthesized a new class of material by gelation where PANI hydrogels were arranged with the PANI nanofibers in presence of $V_2O_5 \cdot nH_2O$ nanowires. Here, $V_2O_5 \cdot nH_2O$ not only acts as an oxidant but also works as a template for the 3-D motifs fabrications. However, $V_2O_5 \cdot nH_2O$ were come out from the composite with the formation of salts. Thus, pure PANI nanofibers formation had been taken place. Ultrathin PANI nanofiber as a supercapacitor electrode exhibits a high specific capacitance of 636 F/g, the rate capability, and good cycling stability ~ 83% capacitance holding after 10,000 cycles [31]. Yifan Diao et al. developed rust-based vapor-phase polymer (RVPP) from poly(3,4-ethylenedioxythiophene) (PEDOT) nanofibers consuming a rust layer of steel which assist in oxidation of monomer unit via vapor phase deposition technique with control of polymer nano fibrillar pattering on the 2-D surface as appealing in Fig. 4. After that peeling of PEDOT polymeric nanofibers had been done independently. They measured the electrochemical performance of the PEDOT nanofibers in two-electrode materials via cyclic voltammetrically and galvanostatic charge–discharge method as represented in Fig. 4. They observed a specific capacitance of 181 F/g in a current density of 3.5 A/g for a device assembly. Even after 38,000 cycles, retention of 80% assessment is a highly recommendable value for the device [32].

J. Cárdenas-Martínez with his colleagues made a flexible solid-state supercapacitor where PEDOT: PSS acted as both electrode material and collector whereas PVA/H_3PO_4 gel acted as electrolyte. They synthesized PEDOT: PSS nanofibers using electrospinning technique consuming polyethylene oxide as a binder and dimethylformamide (DMF) as a solvent. The electrode material in device assembly attained areal capacitance equal to 1.8 mF/cm^2 and a gravimetric capacitance of 3.6 F/g at a discharging current of 5 µA/cm^2. It also maintained 92% retention after 1000 cycles at a discharge current of 5 µA/cm^2 [33].

Stretchable and dynamic deformation with temperature-resistant materials is the prime importance for the fabrication of polymeric nanofibers. Given this, F. M. Guo with his co-workers arranged wet polypyrrole (PPy)/CNTs nanofibers (Fig. 5) with diamond wire-drawing dies with reducing diameter up to 100 µm where the shrinking effect of dies molded the films into fibers. In electrochemical measurements, cyclic voltammetry represented a rectangular shape with a specific capacitance of 302 F/g in 1 M H_2SO_4. Two electrode method was also done for the measurement of material of solid-state flexible supercapacitor in H_3PO4/PVA gel electrolyte which was called flexible fiber shaped supercapacitor (FSSCs) and delivered value of 69 F/g specific capacitance with high power density and an energy density of 3.8 kW/kg and 3.6 Wh/kg respectively [34].

Stress–strain and bending ability, temperature dependency were also monitored in these polymeric nanofibers. Muhammad Amirul Aizat Mohd Abdah et al. synthesized ternary hybrid composite of functionalized carbon nanofiber/polypyrrole/manganese oxide and offered specific capacitance of 409.88 F/g that was much higher than f-CNF/MnO_2 and f-CNF/PPy composites. It had remarkable cycling ability during charging-discharging i.e., 86.30% capacitance retention above 3000 cycles [35].

A brief of polymeric nanofibers synthesis technique and their electrochemical performance for supercapacitor is represented in Table 2.
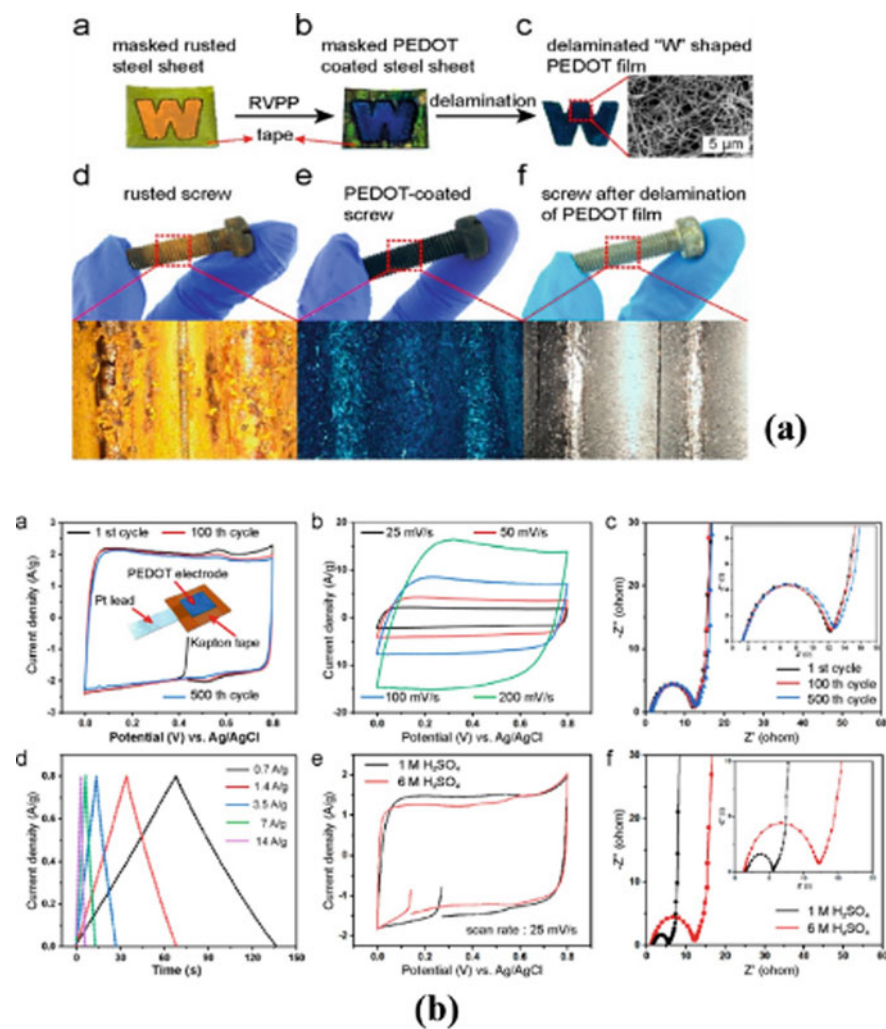
Fig. 4 **a** PEDOT coating on the three-dimensional rusted surface **b** Three electrode system electrochemical characterization of RVPP—PEDOT **c** Two electrode system electrochemical characterization of RVPP—PEDOT (Adapted with permission from reference [32], Copyright (2019), ACS
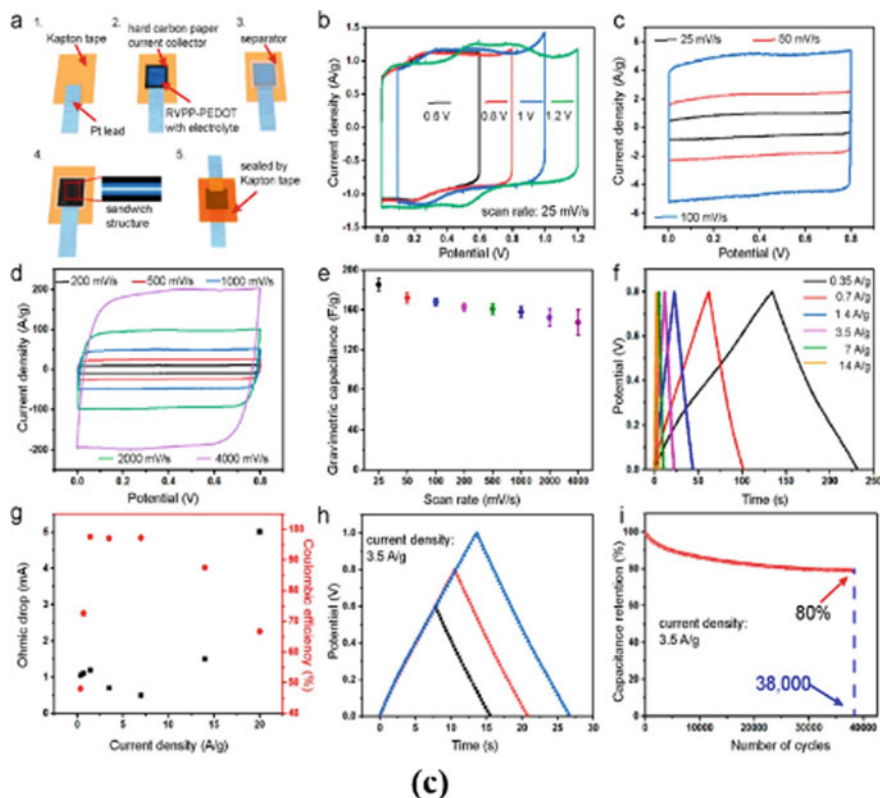
Fig. 4 (continued)

7   Conclusion and Future Aspects of Polymeric Nanofibers

In this chapter, we have swotted the contemporary progress in polymeric nanofibers-based flexible supercapacitor electrodes that have one-dimensional nature. Fabrication of polymeric nanofibers has been exercised by different techniques and each technique develops unique characteristics based upon the morphology and conductivity of the nanofibers. They show structural variations during the charging-discharging process of electrochemical measurements. It is observed that portable electronic supercapacitor devices with small, thin, stretchable, wearable, and dynamic deformation can be developed through the utilization of polymeric nanofibers. The hybrids of polymeric nanofibers with carbon-containing structures or blending with other polymers to reduce the snags of polymeric fibers are more frequently used. Enhancement of specific capacitance can also occur when polymeric nanofibers are fabricated as composites with transition metal oxide/s. where pseudo-capacitance of them is also used. The dynamic supramolecular contact in the polymer network even allowed for the building of self-healing behavior because, during the charging-discharging,

the material shrinks or deforms from its original morphology, specifically in high-performance SCs. Despite the noteworthy progress in the development of flexible polymeric nanofibers-based SRs, their power and energy densities still need to be enhanced further for the outstanding practical appliances of the area. Mostly, the electrospinning technique is used for the synthesis of fibers but it comprises many shortcomings like mechanical strength and crystallinity with the special requirement of voltage, conducting targets, etc. So, to overcome this, there is a need of furthering some other amalgamated methods of fiber fabrications with in situ polymerization techniques such as heat treatment, chemical grafting, and control fiber assembly to enhance the physicochemical and morphological properties of nanofibers. Also, the porosity is the key factor for the storage of electrolyte ions, there is also scope for improvement in this section as well. There should be an oriented selection of appropriate materials to introduce porosity in fibers with the possibility to obtain a high voltage window for SCs. However, one more aspect for the storage devices is the consideration towards cost efficiency, so there should be adaptable techniques and materials for utilizing the polymeric nanofibers synthesis to fabricate supercapacitor
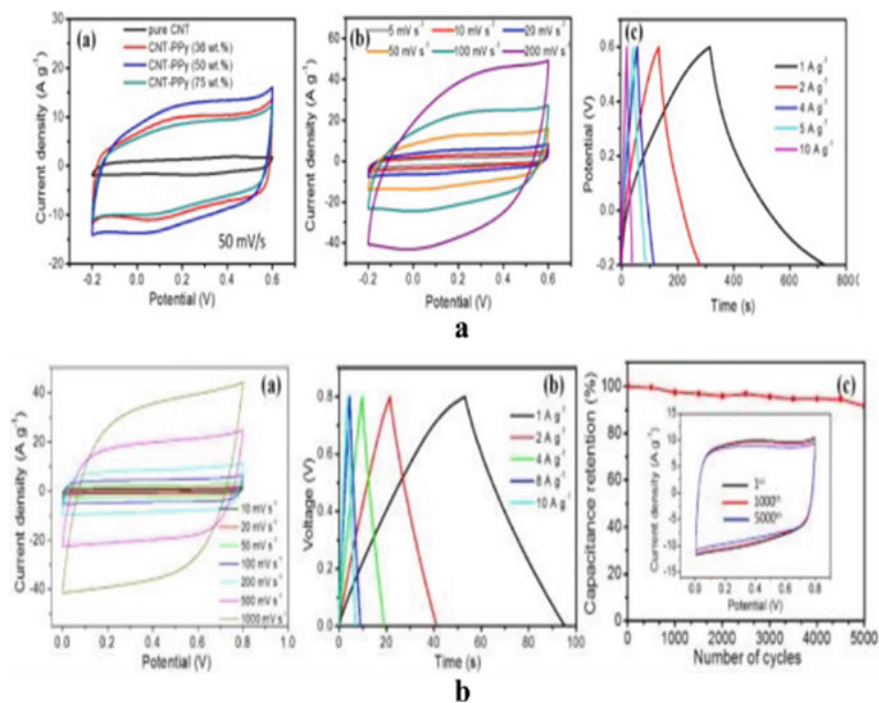
Fig. 5 **a** Electrochemical characterization of CNT-PPy electrode **b** Capacitive performances of a FSSC with PPy content **c** Static capacitive, mechanical and electrical properties of the CNT-PPy FSSCs under deformation of 50 wt.% (Adapted with permission from Ref. [34], Copyright (2016), RSC
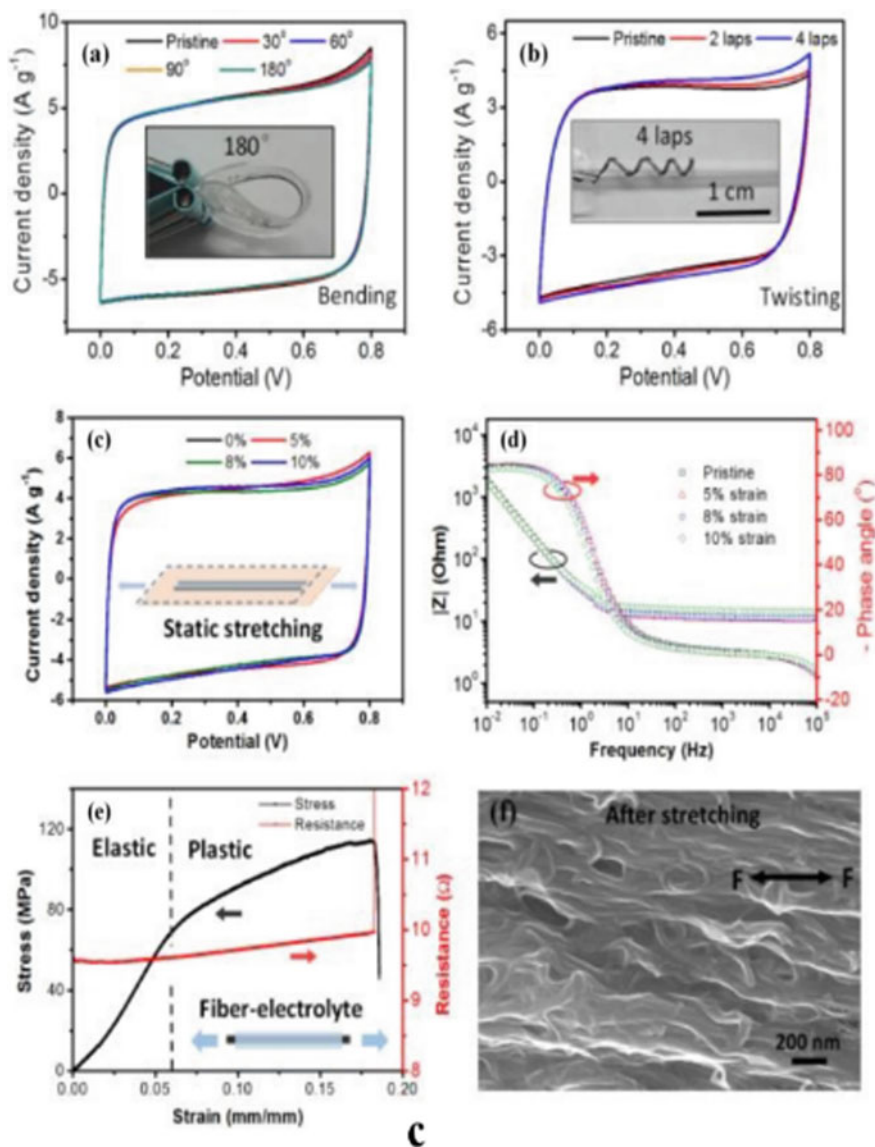
Fig. 5 (continued)

devices and thus can be customized accordingly in the markets. Supercapacitor technology is an exciting realization technique that could be explored to efficient output or improved steadily.

Table 2 Brief description of polymeric nanofibers for the supercapacitor applications

Material	Technique	Electrolyte	Specific capacitance	Cyclic stability	Electrode	References
Nanocarbons/manganese dioxide/PEDOT: PSS fibres	Wet Spinning	0.01 mol dm^{-3} PBS solution and 0.1–0.5 mol dm^{-3} KCl solution	351 F/g	84.2% after 1000 cycles	Three electrode	[36]
PVA-GO/PEDOT	Electrospinning and electrodeposition	1 M KCl	224.27 F/g at 50 mV scan rate	82.41% after 2000 CV cycles	Three electrode	[37]
PANI/HCFs Omnidirectional	Electrospinning and scrolling on template	PVA/H$_3$PO$_4$ gel	339.3 F/g (85.1 mF cm_1)	74.2% after 3000 cycles at 0.5 A/g	Two electrode	[38]
PANI nanofibers/GO	APS polymerization	1 M H$_2$SO$_4$	780 F/g at 0.5 A/g	91.21% after 1000 cycles	Three electrode	[39]
NiCo$_2$O$_4$@NWAs	Hydrothermal and polymerization	3 M KOH	2244 F/g	89.2% retention after 5000 cycles	Three electrode	[40]
G/Ppy fibers	Wet spinning	H$_2$SO$_4$/PVA	(65–72 F/g)	100% retention after 1000 cycles	Two electrode	[41]
HCF (Hollow RGO/conducting polymers	Soft template	PVA/H$_3$PO$_4$	63.1 F/g	96% retention after 10,000 cycles	Two electrode	[42]
MnAc$_2$-PEDOT-Ppy	Wet spinning, electrodeposition, conducting polymer coating	PVA/H$_3$PO$_4$	549 F/g	89% after 1000 cycles	Three electrode	[43]

(continued)

Table 2 (continued)

Material	Technique	Electrolyte	Specific capacitance	Cyclic stability	Electrode	References
Pen ink/Plastic fibers	Dip coating method	1 M Na_2SO_4	11.9–19.5 mF/cm^2	Robust remains after 15,000 cycles	Two electrode	[44]
MnO2/PEDOT: PSS/CNT fiber and OMC/CNT fiber	Dipping, Annealing	cellulose sodium (CMC)/Na_2 SO_4 gel	21.7 F/g at 0.085 A/cm^3	85% after 10,000 cycles	Two electrode	[45]

References

1. Lokhande, C.D., Dubal, D.P., Joo, O.S.: Metal oxide thin film based supercapacitors. Curr. Appl. Phys. **11**, 255–270 (2011)
2. Kim, S., Chou, P.H.: Energy harvesting with supercapacitor-based energy storage (2015)
3. Delille, G., François, B.: A review of some technical and economic features of energy storage technologies for distribution system integration, Int. Conf. Electr. Mach. Power Syst. 67–72 (2008). http://l2ep.univ-lille1.fr/pagesperso/francois/EEEP09.pdf
4. Zhang, Y., Feng, H., Wu, X., Wang, L., Zhang, A., Xia, T., Dong, H., Li, X., Zhang, L.: A facilely prepared polypyrrole–reduced graphene oxide composite with a crumpled surface for high performance supercapacitor electrodes.pdf. Int. J. Hydrogen Energy. **34**, 4889–4899 (2009)
5. Sharma, P., Bhatti, T.S.: A review on electrochemical double-layer capacitors. Energy Convers. Manag. **51**, 2901–2912 (2010)
6. Mohd Abdah, M.A.A., Azman, N.H.N., Kulandaivalu, S., Sulaiman, Y.: Review of the use of transition-metal-oxide and conducting polymer-based fibres for high-performance supercapacitors, Mater. Des. **186**, 108199 (2020)
7. Malik, R., Lata, S., Soni, U., Rani, P., Malik, R.S.: Carbon quantum dots intercalated in polypyrrole (PPy) thin electrodes for accelerated energy storage. Electrochim. Acta. **364**, 137281 (2020)
8. Malik, R., Lata, S., Singh, R.: Study of super capacitive pursuance of polypyrrole/sulphonated poly (ether ether ketone)/multi walled carbon nanotubes composites for energy storage. J. Energy Storage. **27**, 101162 (2020)
9. Malik, R., Lata, S., Malik, R.S.: Electrochemical behavior of composite electrode based on sulphonated polymeric surfactant (SPEEK/PSS) incorporated polypyrrole for supercapacitor. J. Electroanal. Chem. **835**, 48–59 (2019)
10. Anstey, A., Chang, E., Kim, E.S., Rizvi, A. Kakroodi, A.R., Park, C.B., Lee, P.C.: Nanofibrillated polymer systems: Design, application, and current state of the art. Prog. Polym. Sci. **113**, 101346 (2021)
11. Liao, M., Ye, L., Zhang, Y., Chen, T., Peng, H.: The recent advance in fiber-shaped energy storage devices. Adv. Electron. Mater. **5**, 1–14 (2019)
12. Ramalingam, M., Tiwari, A.: Polymeric nanofibers and their applications in sensors. Intell. Nanomater. Process. Prop. Appl. 801–826 (2012)
13. Morgan, P.W.: Brief history of fibers from synthetic polymers. J. Macromol. Sci. Part A Chem. **15**, 1113–1131 (1981)
14. Large, M.C.J., Poladian, L., Barton, G.W., van Eijkelenborg, M.A.: History and applications of polymer fibres and microstructured fibres. Microstruct. Polym. Opt. Fibres. 1–20 (2008)
15. Yang, H.: Recent advances of flexible electrospun nanofibers-based electrodes for electrochemical supercapacitors: A minireview. Int. J. Electrochem. Sci. **14**, 7811–7831 (2019)
16. Nemati, S., Kim, S., Shin, Y.M., Shin, H.: Current progress in application of polymeric nanofibers to tissue engineering. Nano Converg. (2019)
17. Patel, G.C., Yadav, B.K.: Chapter 4. Polymeric nanofibers for controlled drug delivery applications. Elsevier Inc. (2018)
18. Zhang, L.L., Lei, Z., Zhang, J., Tian, X., Zhao, X.S.: Supercapacitors: Electrode materials aspects. Encycl. Inorg. Bioinorg. Chem. (2011)
19. Yan, J., Wang, Q., Wei, T., Fan, Z.: Recent advances in design and fabrication of electrochemical supercapacitors with high energy densities. Adv. Energy Mater. 4 (2014)
20. Zhang, J., Jiang, J., Zhao, X.S.: Synthesis and capacitive properties of manganese oxide nanosheets dispersed on functionalized graphene sheets. J. Phys. Chem. C. **115**, 6448–6454 (2011)
21. Liu, W., Yan, X., Lang, J., Peng, C., Xue, Q.: Flexible and conductive nanocomposite electrode based on graphene sheets and cotton cloth for supercapacitor (2012)

22. Wang, Z., Cheng, J., Guan, Q., Huang, H., Li, Y., Zhou, J., Ni, W., Wang, B., He, S., Peng, H.: All-in-one fiber for stretchable fiber-shaped tandem supercapacitors. Nano Energy **45**, 210–219 (2018)

23. Yang, J.E., Jang, I., Kim, M., Baeck, S.H., Hwang, S., Shim, S.E.: Electrochemically polymerized vine-like nanostructured polyaniline on activated carbon nanofibers for supercapacitor. Electrochim. Acta. **111**, 136–143 (2013)

24. Jang, J., Bae, J., Choi, M., Yoon, S.H.: Fabrication and characterization of polyaniline coated carbon nanofiber for supercapacitor. Carbon N. Y. **43**, 2730–2736 (2005)

25. Yoon, J., Lee, J., Hur, J.: Stretchable supercapacitors based on carbon nanotubes-deposited rubber polymer nanofibers electrodes with high tolerance against strain. Nanomaterials (Basel, Switzerland) 8 (2018)

26. Kim, J.G., Kim, H.C., Kim, N.D., Khil, M.S.: N-doped hierarchical porous hollow carbon nanofibers based on PAN/PVP@SAN structure for high performance supercapacitor. Compos. Part B Eng. **186**, 107825 (2020)

27. He, G., Song, Y., Chen, S., Wang, L.: Porous carbon nanofiber mats from electrospun polyacrylonitrile/polymethylmethacrylate composite nanofibers for supercapacitor electrode materials. J. Mater. Sci. **53**, 9721–9730 (2018)

28. Rose, A., Guru Prasad, K., Sakthivel, T., Gunasekaran, V., Maiyalagan, T., Vijayakumar, T.: Electrochemical analysis of graphene oxide/polyaniline/polyvinyl alcohol composite nanofibers for supercapacitor applications. Appl. Surf. Sci. **449**, 551–557 (2018)

29. Chen, K., Huang, X., Wan, C., Liu, H.: Heteroatom-doped mesoporous carbon nanofibers based on highly cross-linked hybrid polymeric nanofibers: Facile synthesis and application in an electrochemical supercapacitor. Mater. Chem. Phys. **164**, 85–90 (2015)

30. Wang, H., Wang, W., Wang, H., Jin, X., Niu, H., Wang, H., Zhou, H., Lin, T.: High performance supercapacitor electrode materials from electrospun carbon nanofibers in situ activated by high decomposition temperature polymer. ACS Appl. Energy Mater. **1**, 431–439 (2018)

31. Zhou, K., He, Y., Xu, Q., Zhang, Q., Zhou, A., Lu, Z., Yang, L.K., Jiang, Y., Ge, D., Liu, X.Y., Bai, H.: A hydrogel of ultrathin pure polyaniline nanofibers: oxidant-templating preparation and supercapacitor application. ACS Nano **12**, 5888–5894 (2018)

32. Diao, Y., Chen, H., Lu, Y., Santino, L.M., Wang, H., D'Arcy, J.M., D'Arcy, J.M.: Converting rust to PEDOT nanofibers for supercapacitors. ACS Appl. Energy Mater. **2**, 3435–3444 (2019)

33. Cárdenas-Martínez, J., España-Sánchez, B.L., Esparza, R., Ávila-Niño, J.A.: Flexible and transparent supercapacitors using electrospun PEDOT: PSS electrodes. Synth. Met. **267**,116436 (2020)

34. Guo, F.M., Xu, R.Q., Cui, X., Zhang, L., Wang, K.L., Yao, Y.W., Wei, J.Q.: High performance of stretchable carbon nanotube-polypyrrole fiber supercapacitors under dynamic deformation and temperature variation. J. Mater. Chem. A. **4**, 9311–9318 (2016)

35. Mohd Abdah, M.A.A., Abdul Rahman, N., Sulaiman, Y.: Ternary functionalised carbon nanofibers/polypyrrole/manganese oxide as high specific energy electrode for supercapacitor. Ceram. Int. **45**, 8433–8439 (2019)

36. Garcia-Torres, J., Crean, C.: Ternary composite solid-state flexible supercapacitor based on nanocarbons/manganese dioxide/PEDOT: PSS fibres. Mater. Des. **155**, 194–202 (2018)

37. Mohd Abdah, M.A.A., Zubair, N.A., Azman, N.H.N., Sulaiman, Y.: Fabrication of PEDOT coated PVA-GO nanofiber for supercapacitor. Mater. Chem. Phys. **192**, 161–169 (2017)

38. Yang, D., Ni, W., Cheng, J., Wang, Z., Li, C., Zhang, Y., Wang, B.: Omnidirectional porous fiber scrolls of polyaniline nanopillars array-N-doped carbon nanofibers for fiber-shaped supercapacitors. Mater. Today Energy **5**, 196–204 (2017)

39. Zhou, Q., Wei, T., Yue, J., Sheng, L., Fan, Z.: Polyaniline nanofibers confined into graphene oxide architecture for high-performance supercapacitors. Electrochim. Acta. **291**, 234–241 (2018)

40. Kong, D., Ren, W., Cheng, C., Wang, Y., Huang, Z., Yang, H.Y.: Three-dimensional NiCo$_2$O$_4$@polypyrrole coaxial nanowire arrays on carbon textiles for high-performance flexible asymmetric solid-state supercapacitor. ACS Appl. Mater. Interfaces. **7**, 21334–21346 (2015)

41. Ding, X., Zhao, Y., Hu, C., Hu, Y., Dong, Z., Chen, N., Zhang, Z., Qu, L.: Spinning fabrication of graphene/polypyrrole composite fibers for all-solid-state, flexible fibriform supercapacitors. J. Mater. Chem. A. **2**, 12355–12360 (2014)
42. Qu, G., Cheng, J., Li, X., Yuan, D., Chen, P., Chen, X., Wang, B., Peng, H.: A fiber supercapacitor with high energy density based on hollow graphene/conducting polymer fiber electrode. Adv. Mater. **28**, 3646–3652 (2016)
43. Garcia-Torres, J., Crean, C., Garcia-Torres, J., Crean, C.: Multilayered flexible fibers with high performance for wearable supercapacitor applications. Adv. Sustain. Syst. **2** (2018)
44. Fu, Y., Cai, X., Wu, H., Lv, Z., Hou, S., Peng, M., Yu, X., Zou, D.: Fiber supercapacitors utilizing pen ink for flexible/wearable energy storage. Adv. Mater. **24**, 5713–5718 (2012)
45. Cheng, X., Zhang, J., Ren, J., Liu, N., Chen, P., Zhang, Y., Deng, J., Wang, Y., Peng, H.: Design of a hierarchical ternary hybrid for a fiber-shaped asymmetric supercapacitor with high volumetric energy density. J. Phys. Chem. C. **120**, 9685–9691 (2016)

Conjugated Polymers as Organic Electrodes for Flexible Supercapacitors

Wei Lyu, Zhujun Chen, Hongyu Zuo, Likuan Teng, Jian Chen, and Yaozu Liao

Abstract Flexible supercapacitors (FSCs), as a class of flexible energy storage devices, have attracted considerable interest in recent years. Conjugated polymers are a class of promising organic electrodes for FSCs since they demonstrate high flexibility and excellent electrochemical performance. In this chapter, we will introduce the working mechanism of supercapacitors including electrical double-layer capacitor (EDLC) and pseudocapacitors firstly, as well as the electrode structures in FSCs. Chemical structures and energy storage mechanism of conjugated polymers including typical conducting polymers (CPs), emerging conjugated microporous polymers (CMPs), covalent organic frameworks (COFs), and conjugated polymers-based composites will be summarized secondly. Conjugated polymers-based FSCs with multidimensional architectures including one dimensional (1D) fiber-shaped structures, two dimensional (2D) planar structures, and three dimensional (3D) hydrogel will be reviewed. The typical fabrication process and electrochemical performance of these FSCs will be analyzed. The major challenge of conjugated polymers-based electrodes such as poor cyclic stability, relatively low device efficiency, and effective strategies for solving those problems will be finally proposed.

Keywords Conjugated polymers · Organic electrodes · Flexible supercapacitors · Mechanism · Electrochemical performance

W. Lyu (✉) · Z. Chen · H. Zuo · L. Teng · J. Chen · Y. Liao (✉)
State Key Laboratory for Modification of Chemical Fibers and Polymer Materials, College of Materials Science and Engineering, Donghua University, No. 2999 Renmin North Road, Songjiang District, Shanghai 201620, China
e-mail: wlyu@dhu.edu.cn

Y. Liao
e-mail: yzliao@dhu.edu.cn

1 Introduction

Along with growing demands for flexible devices, flexible energy storage devices with merits including small size, lightweight, high flexibility, and deformation tolerance are highly desired [1]. Among energy storage devices, supercapacitors are commonly used owing to their low-cost fabrication, high power, and energy density. However, supercapacitors generally show an inflexible and bulky configuration consisting of inorganic material, such as metal oxides, metal alloys, and carbon materials. Fortunately, due to the rapid progress in the development of polymer materials including gel polymer electrolytes and conjugated polymer electrodes, various prototypes of new flexible supercapacitors (FSCs) have been achieved. Although inorganic materials exhibit higher energy storage performance, conjugated polymer electrodes materials show higher flexibility owing to their spontaneously changeable chains' conformations by internal rotations among single bonds [2]. The mechanical properties such as Poisson's ratio, elastic modulus, toughness, and thermal expansion coefficient of conjugated polymers make them promising as flexible electrode materials [3]. In the following sections, we will concentrate on recent processes in the usage of conjugated polymers as organic electrodes materials.

2 Flexible Supercapacitors (FSCs)

Supercapacitors are promising alternatives to traditional capacitors and batteries for energy storage. Supercapacitors have attracted considerable interest because of their fast storage capability, superior power density, high charge, discharge efficiency, and ultralong cycle life [4]. A supercapacitor is usually consisting of an electrode, separator, electrolyte, and current collector (Fig. 1a).

2.1 Working Mechanism

Based on the charging mechanism or materials used in the electrodes, supercapacitors can be categorized as electrical double-layer capacitors (EDLCs) and pseudocapacitors (Fig. 1a). EDLCs store energy through adsorbing anions and cations to establish double layers on electrode–electrolyte interfaces [6]. In the nineteenth century, Helmholtz first proposed and shaped the concept of EDLC where charges of opposite polarities are layered at the electrode–electrolyte interface (Fig. 1b). Later, Gouy and Chapman refined this simple model and introduced a diffuse layer model, which, however, overestimated EDLC capacitance as the capacitance decreases with the increased separation distance (Fig. 1b). A combination of the Helmholtz model and Couy-Chapman model was then proposed by Stern, in which Stern layer composing of adsorbed ions and counter-ions was introduced (Fig. 1b). In this way, both the
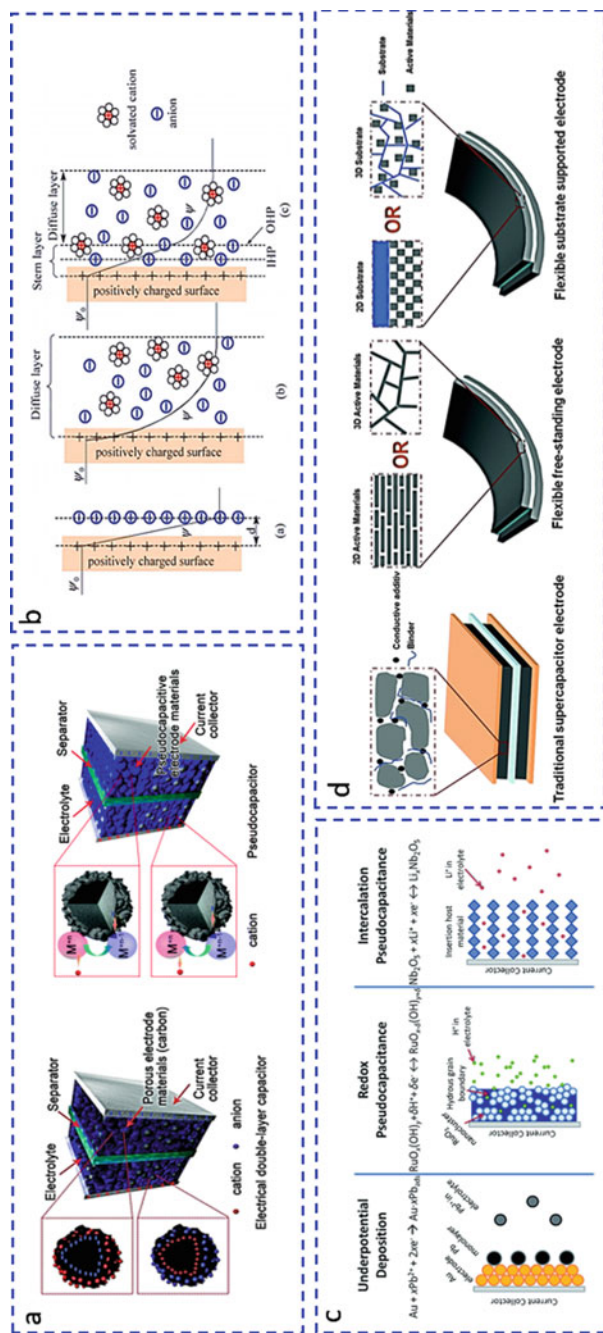
Fig. 1 **a** Schematic diagram of supercapacitors. Adapted with permission from reference [5], Copyright (2015), Royal Society of Chemistry; **b** Three models of an electric double layer. Adapted with permission from reference [6], Copyright (2016), Elsevier; **c** Different types of reversible redox mechanisms. Adapted with permission from reference [7], Copyright (2014), Royal Society of Chemistry; **d** Schematic showing the conventional and flexible electrodes. Adapted with permission from reference [8], Copyright (2015), Royal Society of Chemistry

inner Stern layer and diffusive layer contribute to particle distribution, avoiding the rapid rise of capacitance when the point charges move closer to the electrode–electrolyte interface. EDLC behavior is highly related to the porosity of electrode material according to its energy storage mechanism. Studies have shown that the optimal pore size is ~ 0.7 nm for aqueous electrolytes, while this value becomes 0.8 nm for organic electrolytes [9]. Monte Carlo simulation results indicated that the inverse correlation between capacitance and pore size may be due to the exponential screening effect, which is formed by electrostatic interactions between ions inside the pore and image-charge attraction of ions to the pore surface [10].

Compared with EDLCs, pseudocapacitors provide much higher energy densities due to the faradaic charge-transfer process by the oxidation or reduction of chemicals. However, pseudocapacitors exhibit lower power densities than EDLCs since the shrinking and swelling process during the faradaic charge-transfer process can cause short cycle life and poor mechanical stability. Several faradic mechanisms (underpotential deposition, redox pseudocapacitance, and intercalation pseudocapacitance) resulting in capacitive electrochemical features were identified by Conway (Fig. 1c) [7]. Generally, conjugated polymers exhibit redox pseudocapacitance, in which faradaic charge transfer occurs on the electrode's surface or near-surface (Fig. 1c).

2.2 Electrode Structures in FSCs

A FSC device is generally composed of flexible electrodes, a solid-state electrolyte, and a flexible packaging material. Different from the electrodes in commercial supercapacitors which are generally fabricated with a slurry casting method, the flexible electrodes in FSCs are expected to be fabricated without binder and conductive additives since these additives could make electrodes easily crack or peel off the current collector (Fig. 1d) [8].

3 Conjugated Polymers

Conjugated polymers are materials exhibiting a backbone of alternating single and multiple bonds and a band structure resulting from π-conjugation by the overlap of the π-orbitals [11]. Conjugated polymers have the potential to achieve electrical properties upon doping comparable with those of noncrystalline inorganic semiconductors, making them promising for many applications including supercapacitors. In the past decades, traditional conducting polymers (CPs) are the commonly studied conjugated polymers in supercapacitors because of their low-cost, environmental-friendly, simple synthesis, and conducting in a doped state. Recently, conjugated microporous polymers (CMPs) and covalent organic frameworks (COFs), as the emerging conjugated polymers, have attracted considerable attention for electrode

materials of supercapacitor because they have the advantages of inherent porosity, high specific surface area, and strong molecular design, which are conducive to electron transport and enhance reversible redox reactions.

3.1 Traditional CPs

CPs exhibit the combination properties of conventional polymers and semiconductors. CPs have shown great potential in energy storage. The polymer nature makes CPs promising candidates for flexible devices. The first investigated CP, polyacetylene (PA), was found in 1977 [12]. Since then, many CPs including polyaniline (PANI), polypyrrole (PPy), polythiophene (PT), poly(3,4-ethylenedioxythiophene) (PEDOT) were discovered. Figure 2a shows the chemical structures of these traditional CPs. Due to their unique reversibly doping/dedoping redox electrochemical process, CPs can store energy through the faradaic charge-transfer process and endow the supercapacitor with high specific pseudocapacitance. Take PANI as an example for the doping/dedoping mechanism, PANI is oxidized and doped through two redox reactions involving the transformation from its leucoemeraldine base state (insulator) to emeraldine base state (semiconductor) and from emeraldine base state (semiconductor) to emeraldine salt (metal) state, accompanying with the structural
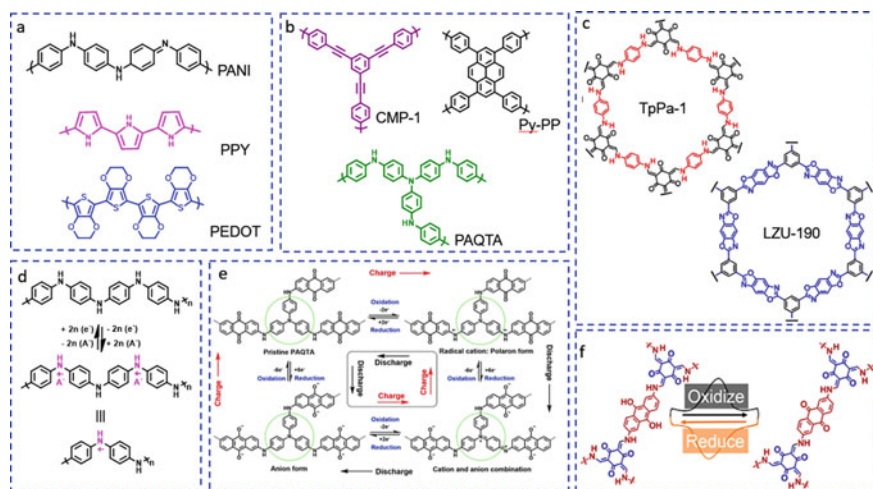
Fig. 2 Chemical structures of **a** three typical traditional CPs: PANI, PPy, and PEDOT; **b** three typical CMPs: CMP-1, Py-PP, and PAQTA; **c** two typical COFs: Tapa-1 and LZU-190. Adapted with permission from reference [22], Copyright (2019), American Chemical Society; the working mechanism of **d** PANI. Adapted with permission from reference [13], Copyright (2001), American Chemical Society; **e** PTQTA; Adapted with permission from reference [20], Copyright (2018), Wiley and **f** DAAQ-TFP COF in supercapacitor. Adapted with permission from reference [24], Copyright (2013), American Chemical Society

change in the unpaired spin per repeat unit with a positive charge (Fig. 2d) [13]. The specific capacitance of PANI nanostructures-based electrodes has been reported up to 1284 F g^{-1} [14], which is highly related to the synthetic methods. Comparably, PEDOT demonstrates a relatively lower specific capacitance than PANI due to its high molecular weight but shows a relatively better cyclic stability because PEDOT presents the minimum side reactions. Moreover, PEDOT-based electrode material shows an advantage for assembling asymmetric supercapacitors with relatively wider potential windows, high power, and energy density. Unfortunately, all pure CPs electrodes showed poor processability resulting from their conjugated structures and short cycling life resulting from the occurrence of swelling and shrinkage of chains upon doping-dedoping processes. Preparation of micro/nanostructured pure CPs materials and CPs-based composite materials are two effective methods to solve the above problems [15, 16].

3.2 Emerging CMPs and COFs

CMPs, as an emerging class of conjugated polymers, exhibit 3D macromolecular networks with permanent micropores (*i.e.*, < 2 nm), which are built by the covalent connection of rigid and π-conjugated building blocks with multi functionalities [17, 18]. High surface areas and plenty of porosity from CMPs allow the charge to get access to active sites from the electrolyte to be stored on the surface to obtain EDLC capacitance, while the ease in tunability of CMPs allows numerous heteroatom-containing active redox sites to be integrated to offer the excellent pseudocapacitive performance. Therefore, both contributions make CMPs as emerging promising electrode materials for supercapacitors in recent years. CMPs, such as CMP-1 and Py-PP shown in Fig. 2b, are normally prepared by C–C coupling reactions [19]. However, the electronic conductivity and redox activity of such CMP materials is poor and cannot enow the electrode material with a satisfying capacitance. Introduction of specially designed redox-active moiety into CMP backbond is an effective strategy to endow CMPs with excellent electrochemical performance [20, 21]. For example, Liao et al. synthesized conjugated microporous polyaminpanthraquinone (PAQ) networks via Buchwald-Hartwig coupling allowing for the formation of redox-active C-N bond (Fig. 2b) [20]. The obtained PAQs showed a high energy density. Mechanism study results indicated that the redox reaction for PTQTA was based on the combination of a strong electron donor (triphenlyamine, TA) and acceptor (anthraquinone, AQ), where AQ involved a two-electron reduction leading to a dianion and PAQTA formed as a PANI-like leucoemeraldine base bearing a TA which can be oxidized into a radical cation and then delocalized to a bipolaron via obtaining two electrons (Fig. 2e).

COFs are a new emerging class of conjugated polymers exhibiting crystalline porous structures linked via covalent bondings (Fig. 2c) [22]. They show the merits of high porosity, low density, high chemical stability, and sufficient building blocks, making them promising in various applications. Similar to CMPs, COFs-based electrodes can exhibit both EDLC and pseudocapacitive energy storage ability. However,

the relatively poor conductivity and fewer redox sites are the main drawbacks limiting their further application in supercapacitors. Fortunately, progress has been made to address these two serious problems recently, including enlarging π-conjugation, growing thin films on electrodes, and combining with carbon nanomaterials to improve the conductivity, as well as incorporating redox-active monomers into backbone to endow COFs with pseudocapacitive performance [23]. For example, Dichtel et al. described a 2D DAQQ-TFP COF with a reversible electrochemical process and stable capacitance over at least 5000 charge–discharge cycles (Fig. 2f) [24]. The well-defined and rapid redox process was attributed to the 2D layered architecture of DAQQ-TFP COF and the increased capacitance was related to both its electroactive monomer and anthraquinone subunits.

3.3 Conjugated Polymers Composites

As mentioned above, pure conjugated polymers suffer from poor cycling stability, incorporation conjugated polymer with other materials can offer an effective solution to overcome this problem. Different types of conjugated polymers-based composites materials, including carbon materials, pseudocapacitive materials of transition metal oxides/hydroxides, and 2D nanomaterials were prepared [25]. Carbon materials are promising conducting substrates for conjugated polymers to enhance the electrochemical performance of electrodes owing to the synergistic effect of EDLC from carbon materials and pseudocapacitance from conjugated polymers. Moreover, carbon materials can serve as frameworks to stabilize conjugated polymers and therefore limit the swelling and shrinking of polymer chains during the cycles. Comparably, pseudocapacitive materials of transition metal oxides/hydroxides exhibited lower rate capability due to the low electrical conductivity but showed higher capacitance than carbon materials. Conjugated polymers can effectively improve the electrical conductivity, facilitate electron transport and protect transition metal oxides/hydroxides in the composites to keep the integrity, therefore endowing the composites with high specific capacitance, high rate capability, and excellent cycling stability. Because of the facile charge transfer between conjugated polymers and 2D nanomaterials, the formed composites can inherit the properties with a synergistic effect of each component. To further increase the electrochemical performance of conjugated polymers, ternary composites that are mainly in the form of CNT/graphene/conjugated polymers or carbon materials/metal oxide/conjugated polymers have been fabricated [25].

4 Conjugated Polymers-Based Electrodes for FSCs

Typically, the configurations of FSCs involved conjugated polymers organic electrodes including 1D fibers, 2D parallel architectures, and 3D hydrogels have been

widely studied in the last decades. The different configurations using various fabrication techniques endow FSCs with different mechanical and electrochemical characteristics. Here, we will present the recent studies of conjugated polymers-based electrodes with various configurations and properties for FSCs.

4.1 Conjugated Polymers-Based 1D Fiber Electrodes for FSCs

Different from the traditional 2D planar FSCs, 1D fiber-shaped FSCs exhibit the advantages of good compatibility with clothes, exceptional mechanical flexibility and miniaturization potential, and the possibility for integration with other multi-functional or self-powered systems [26, 27]. So far, fiber-shaped FSCs with parallel, twisted and coaxial structures have been developed (Fig. 3a). Similar to planar FSCs, two parallel fiber electrodes are arranged and separated by the polymer gel electrolyte for the parallel fiber FSCs [25]. The twisted-fiber structure which is achieved by twisting two fiber electrodes and separated by polymer gel electrolyte has the merits of increased interfaces for enhanced capacitance. The coaxial structure is generally achieved by assembling the current collector, core electrode, electrolyte, outer electrode, and current electrode layer by layer, in which the contact area is increased and internal resistance is decreased. Therefore, fiber-shaped FSCs with the coaxial structure shows an improved performance than those with twisted structure.

The production of 1D fiber-shaped FSCs mainly depends on the fabrication of fiber-shaped flexible electrodes. So far, plastic wires, metal wires, and carbon wires have been studied for the fiber-shaped flexible electrodes. The first used fibers were the plastic wires whose insulating nature limited the electrochemical performance of FSCs. Although metal fibers exhibit high conductivity, the heavyweight nature limits the gravimetric energy and power density of FSCs. Comparably, carbon-based wires with the nature of conductive, lightweight, and flexible are promising for fiber electrodes, which can serve as the current collector for devices and active material for energy storage at the same time. Moreover, conjugated polymers are generally insoluble powders due to their conjugated chains, which are difficult to be processed into flexible fibers using traditional methods. Combined conjugated polymers with carbon-based wires is therefore an effective strategy for constructing conjugated polymers-based high-performance fiber-shaped FSCs. Here, we will concentrate on the fabrication of conjugated polymers-based 1D fiber electrodes and discuss their relative merits and drawbacks.
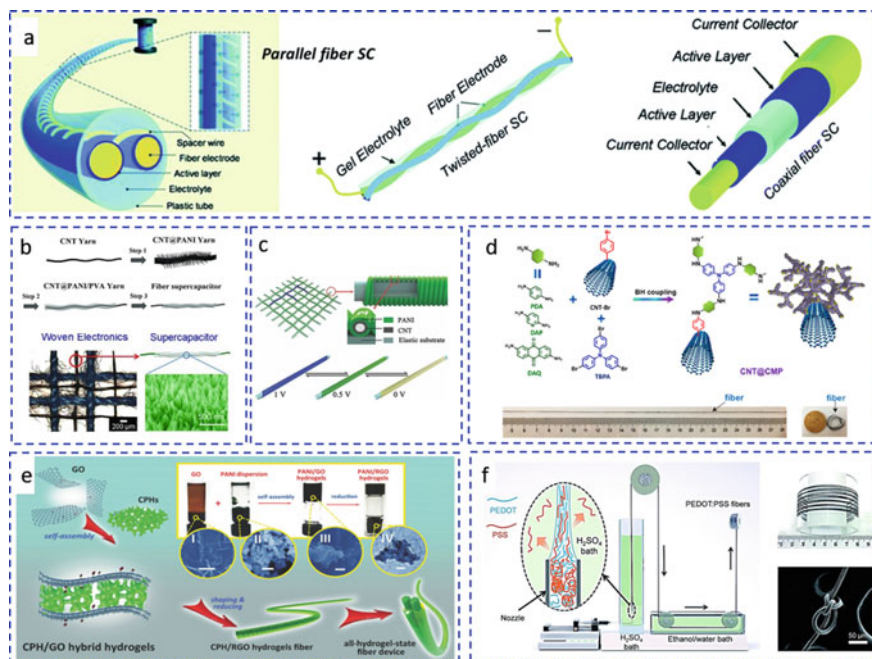
Fig. 3 **a** Schematic showing fiber-shaped FSCs with parallel, twisted and coaxial structures. Adapted with permission from reference [25], Copyright (2020), Royal Society of Chemistry; **b** Schematic showing CNT@PANI two-ply yarn supercapacitors. Adapted with permission from reference [28], Copyright (2018), Wiley; **c** Schematic showing electrochromic FSC. Adapted with permission from reference [29], Copyright (2014), Wiley; **d** Synthetic route and typical image of CNT@CMPs fibers. Adapted with permission from reference [27], Copyright (2020), American Chemical Society; **e** Schematic showing PANI/GO hydrogels fiber-based FSC. Adapted with permission from reference [30], Copyright (2018), Wiley; **f** Schematic showing set-up for the wet-spinning of PEDOT:PSS fibers and photo and SEM image of PEDOT:PSS fiber. Adapted with permission from reference [32], Copyright (2019), Royal Society of Chemistry

4.1.1 Depositing Method

Depositing conjugated polymers on carbon-based wires by *in-situ* polymerization or electrochemical polymerization is extensively adopted for the fabrication of conjugated polymers-carbon composites fiber electrodes due to its ease of preparation process. Wei et al. reported twisted FSCs using CNT@PANI@PVA yarns, which were prepared by *in-situ* polymerizing PANI nanowire arrays on the CNT yarn. As-prepared FSCs can be woven or knitted into wearable electronic devices due to their high flexibility (Fig. 3b) [28]. Peng et al. reported an electrochromic fiber-shaped FSCs by electro-depositing PANI onto a CNT sheet wounded on an elastic rubber fiber. The obtained aligned CNT/PANI fiber-shaped FSCs were flexible and stretchable, and showed chromatic transitions upon the charge–discharge process resulting from the deposited PANI active material, making the FSCs become an intelligent

smart electronic product sensing changes in the level of stored energy (Fig. 3c) [29]. Although the deposition method is simple, it could not provide stable and tightly bonded coatings, making the redox-active conjugated polymers easily peel off the current collectors and endowing the FSCs with unsatisfied mechanical stability.

4.1.2 Grafting Method

Grafting conjugated polymers onto current collectors by tight bonds has been demonstrated to be an effective strategy to enhance the mechanical stability and energy storage performance of FSCs. For example, Liao et al. adopted Buchwald-Hartwig coupling to *in-situ* graft polytriphenylamine (PTPA)-based CMP network onto the bromo-functionalized CNT fibers and obtained flexible CNF@PTPA fibers (Fig. 3d) [27]. As-prepared CNF@PTPA fiber electrodes present a high three-electrode areal specific capacitance. Remarkably, the assembled twisted symmetric two-electrode FSCs exhibit a high specific capacitance and deliver a high energy density, with excellent flexibility and mechanical stability retaining 84.5% of the initial capacitance after 10,000 bending cycles.

4.1.3 Self-Assembly Method

Fabrication of conjugated polymers-carbon hybrid materials via the self-assembly method is another effective way to endow composite fiber with improved mechanical properties because of their molecular interaction. Yu et al. reported interconnected, self-standing 3D nanostructured conductive polymer/graphene hydrogels by the self-assembly of GO and phytic acid doped CP (PANI, PPy) via π-π stacking, hydrogen bond, and electrostatic interaction and shaped the hybrid hydrogels into fibers which were finally reduced to the final CP/RGO fiber electrode (Fig. 3e) [30]. The assembled parallel symmetric fibrous device with PVA/H_2SO_4 gel as electrolyte exhibited arbitrary flexibility and a considerable volumetric energy density.

4.1.4 Wet-Spinning Method

A wet-spinning method is a simple one-step process for continuous fabrication of fibers in fundamentally unlimited length, which is suitable for the scale-up fabrication for the fiber electrodes. Qu et al. developed graphene/PPy (G/PPy) fibers by a simple and direct wet-spinning method in which $FeCl_3$ solution was coagulation bath and the mixture of GO and Py was the extrusion fluid [31]. Electrochemical study results indicated that a diameter of 25 μm endowed the G/PPy fiber with the best capacitance owing to the limitation of ion transport distance through the fibers and the effective amounts of graphene within the fibers.

Except for wet-spinning of conjugated polymers-based composite fibers, highly conductive PEDOT:PSS fibers could also be fabricated by the wet-spinning method by extruding PEDOT:PSS dispersion into a concentrated H_2SO_4 bath to remove the insulating PSS component and form the fiber. Razal et al. adopted the wet-spinning method to fabricate a highly conductive PEDOT fiber (3828 S/cm) by using concentrated H_2SO_4 as the coagulation bath (Fig. 3f) [32]. A long fiber-shaped FSC with a length up to 12 cm was fabricated by paralleling two fibers on the supporting substrate. The reported PEDOT:PSS fibers are promising in achieving long fiber-shaped FSCs without compromising their length capacitance.

Although fiber-shaped FSCs demonstrated promising mechanical and electrochemical performance for highly efficient wearable supercapacitors, the low energy density is the limitation for fiber-shaped FSCs' practical applications compared with micro-batteries or conventional supercapacitors. Further increasing the high specific capacitance and cell voltage are effective approaches for achieving the highly efficient energy density of fiber-shaped FSCs.

## 4.2 Conjugated Polymers-Based 2D Planar Electrodes for FSCs

Two widely studied 2D architectures for FSCs, *i.e.*, sandwiched stacked structure and interdigitated planar structure are shown in Fig. 4. The bulky sandwiched structure is incompatible with the planar geometry of the miniaturized microelectronics and unsuitable for electronic circuitry. Comparably, the emerging planar interdigitated microelectrodes exhibit the advantages of space-saving, shorter ion transport paths, better penetration of electrolyte ions, facile interconnection and integration within the electronic systems, less areal energy. However, the micro-patterning step used in the fabrication of interdigitated microelectrodes limits their scale-up for commercial applications.

4.2.1   2D FSCs with Sandwiched Stacked Structure

Paper/Film-Based FSCs

A suitable flexible substrate or free-standing electrode film is needed for manufacturing 2D planar FSCs devices. Owing to the excellent mechanical and flexibility properties of the paper/film, paper/film-based FSCs including functional-conductive-cellulose and carbon nanomaterials-film-based FSCs are typically studied. Cellulose nanofiber (CNF)-based paper exhibits the merits of low-cost, biodegradability, high aspect ratio, porous structures, and large surface roughness. Combined conjugated polymers with CNFs could enhance the electrochemical performance of CNFs and the mechanical property of conjugated polymers, making the composites promising
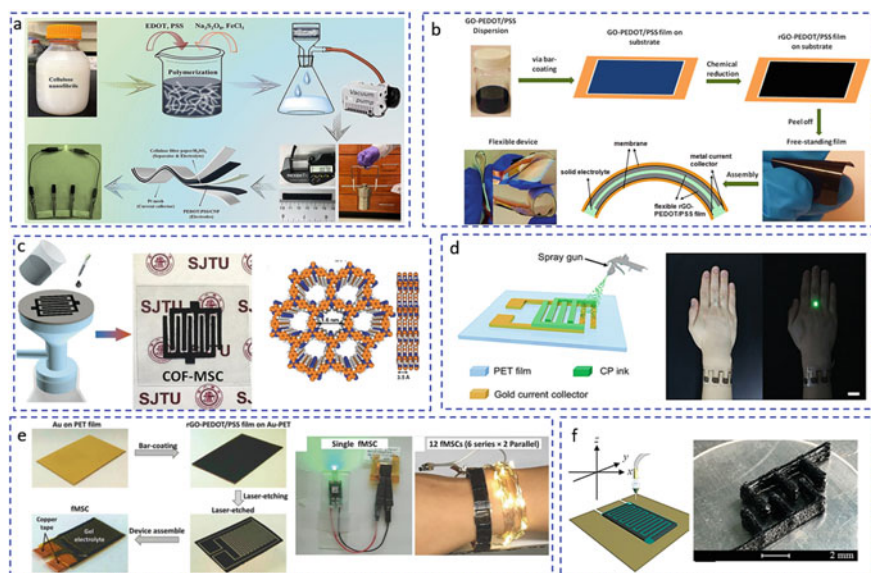
Fig. 4 **a** Schematic showing the preparation and property of PEDOT:PSS/CNP FSC. Adapted with permission from reference [33], Copyright (2022), Elsevier; **b** Schematic showing the preparation of rGO-PEDOT/PSS films and a photo of assembled FCS. Adapted with permission from reference [34], Copyright The Authors, some rights reserved; exclusive licensee Nature. Distributed under a Creative Commons Attribution License 4.0 (CC BY); **c** Schematic showing the fabrication of COF-MSC and its optical photo and view of eclipsed AA-stacking model of g-C$_{34}$N$_6$-COF. Adapted with permission from reference [37], Copyright (2019), Wiley; **d** Schematic showing the preparation of printed MSCs and photo of a green LED bulb powered by an integrated circuit of MSCs wristband. Adapted with permission from reference [39], Copyright (2019), Wiley; **e** Schematic showing the preparation of rGO-PEDOT/PSS-based MSCs and optical images of powered LEDs. Adapted with permission from reference [40], Copyright (2021), Royal Society of Chemistry; **f** Schematic showing 3D printing process and photos of the printed interdigital electrodes. Adapted with permission from reference [41], Copyright (2018), American Chemical Society

for the flexible electrodes of FSCs. For example, Si et al. fabricated a flexible and conductive PEDOT:PSS/CNF nanopaper by vacuum filtration and DMSO post-treatment (Fig. 4a) [33]. The prepared paper electrode showed excellent flexibility, high tensile strength, and high electrical conductivity.

Free-standing carbon nanomaterials-film has attracted considerable attention owing to their ultrathin, lightweight, excellent conductivity, and mechanical properties, which can be assembled through vacuum filtration-induced self-assembly or bar-coating from stable dispersion or direct CVD growth. Moreover, the porous structure of the carbon nanomaterials-film makes it an ideal substrate for supporting conjugated polymers and the formed free-standing composite film is an attractive electrode for FSCs. For example, Liu et al. prepared a large-area free-standing rGO-PEDOT/PSS film via a simple bar-coating method where PEDOT/PSS served as the conductive matrix to prevent re-stacking of the rGO layer and enhance the energy

storage performance of the free-standing electrode film (Fig. 4b) [34]. The assembled FSC device almost kept the original capacitance upon bending at a different angle 1000 times.

Other 2D materials like MXenes are also promising substrate materials that could be incorporated with conjugated polymers to form the flexible film electrode. Zhi et al. reported a free-standing and conductive hybrid film by intercalating PPy into layered I-Ti$_3$C$_2$ to enhance PPy's capacitance and cycling stability because of the formed strong bonds between PPy backbones and I-Ti$_3$C$_2$'s surface [35]. The assembled ultra-thin FSCs exhibited a stable energy storage performance upon any bending states for 10,000 charging/discharging cycles.

Fabric/Textile-Based FSCs

Since the development direction of FSCs in wearable devices has tended toward electronic devices with comfortable and breathable properties in recent years, 2D fabric/textile-based FSCs with the characteristics of lightweight and mechanical flexibility have attracted considerable interest. Except for the above-mentioned fiber-shaped FSCs which can be weaved into 2D fabric/textile-based FSCs, coating CPs onto the surface of the textile substrate is a typical construction method. For example, Wang et al. prepared PEDOT/MXene decorated cotton fabrics by a facile vapor phase polymerization and spray-coating strategy [36]. The assembled fabric FSCs exhibited a superior specific capacitance.

4.2.2 2D FSCs with Interdigitated Planar Structure, i.e., Micro-Supercapacitors (MSCs)

To meet the demands of microelectronic devices, micro-supercapacitors (MSCs) consisting of an array of indigitated electrodes with micron-scale sizes have been fabricated. Typically, three strategies (bottom-up, up-down, and 3D printing) are used to fabricate MSCs. The following parts will focus on these strategies.

Bottom-Up Strategy

For the bottom-up strategy, electrode materials are deposited on the specified position in a flexible substrate via different ways like vacuum filtration, electrodeposition, spray coating, and mechanical pressing. For example, Zhang et al. reported an effective synthetic strategy to obtain a fully conjugated g-C$_{34}$N$_6$-COF by Knoevenagel condensation. The as-synthesized new conjugated polymer showed enhanced electrochemical performance and a flexible paper electrode for MSCs can be easily gained by assembling with CNT by vacuum filtration with an interdigital mask (Fig. 4c) [37]. The obtained g-C$_{34}$N$_6$-COF-based MSC exhibited a moderate areal capacitance for COF-based electrode materials.

However, the mass fabrication of MSCs by bottom-up strategy is a challenge, developing cheap and stable conjugated polymers-based electrode inks is one of the effective approaches. Chen et al. adopted a simple assemble-disperse strategy to obtain a low-cost and air-stable CP ink by forming PANI/citric acid (CA) nanosheets hydrogel through the supramolecular interactions (Fig. 4d) [38]. The printed MSCs prepared by mask-assisted spray coating delivered a high areal capacitance, outperforming most state-of-the-art CP-based FSCs.

Up-Down Strategy

For the up-down strategy, an active materials-based film is performed firstly and followed by the etching process to remove unwanted materials achieving interdigital electrodes. Dry etching including plasma, laser, or mechanical scribing and wet etching techniques have been widely used in the up-down approach. For instance, Chen et al. reported rGO-PEDOT/PSS-based MSCs by combining bar-coating and laser-etching technology (Fig. 4e) [39]. The As-prepared MSC device showed an areal capacitance of 84.7 mF/cm^2 and high cycling stability.

3D Printing

Although MSCs have the merits of the unique planar interdigital architecture for wearable electronic devices and integrated circuits, MSCs demonstrate a limited mechanical property for wearable FSCs which requires a flexible capability to stretch to ~ 30% strain for adapting body movements' tension and maintaining the functionaries at the same time [40]. Recently, 3D printing technique has been introduced to fabricate high-performance MSCs owing to its unique merits of manufacturing different patterns and geometries in a simple, high speed, and scalable way. Developing 3D printable conjugated polymers-based inks with specific rheological properties is crucial for the preparation of MSCs. Bai et al. employed GO as a thixotropic agent to tune the rheology of PANI and prepared the 3D printable PANI/GO gel inks (Fig. 4f) [41]. After reduction of GO, an MSC with high performance using PANI/RGO interdigital electrodes was constructed.

4.3 Conjugated Polymers-Based 3D Hydrogel Electrodes for FSCs

Hydrogels are a class of 3D cross-linked networks of hydrophilic polymers with flexible and excellent mechanical properties, which contain a certain amount of water. The inherit soft and wet properties of hydrogels can give a superior interface between the ionic and the electronic transporting phase, making them promising for FSCs.

As shown in Fig. 5a, for the traditional FSCs with sandwich structure, gel polymer electrolytes can only be touched by the surface of the solid electrode, leading to poor electrochemical performance. Comparably, all electrode active materials can contact electrolyte ions and the assembled FSCs are expected to show enhanced capacitance and rate performance [42]. Combined conjugated polymer with hydrogels can endow the materials with the excellent electrochemical properties of conjugated polymer and superior mechanical properties of hydrogels. Therefore, conjugated polymer hydrogels including pristine and hybrid hydrogel have been recently widely explored for FSCs' electrode materials, as well as conjugated polymer-based all-in-one hydrogel FSCs.
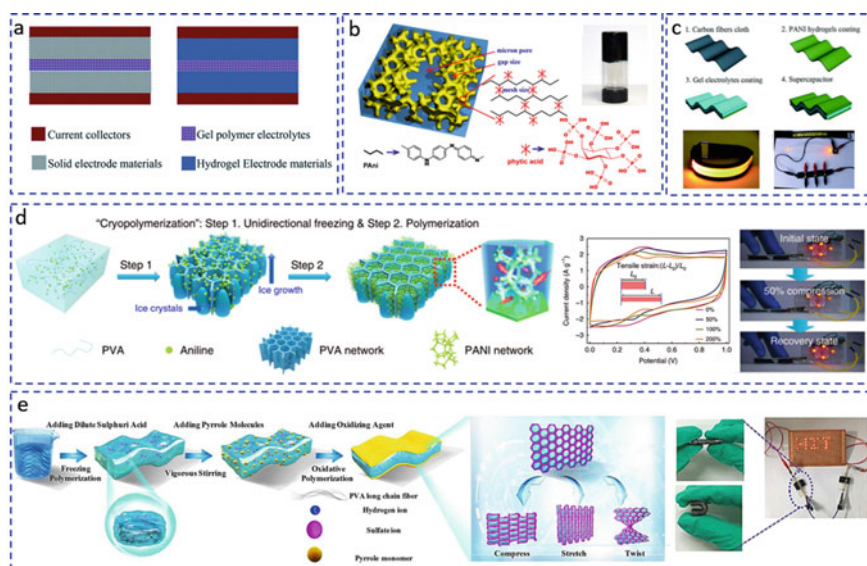
Fig. 5 a The configuration of traditional and hydrogel FSCs. Adapted with permission from reference [42], Copyright (2014), Royal Society of Chemistry; **b** Schematic illustrations and photograph of 3D hierarchical microstructure of phytic acid gelated and doped PANI hydrogel. Adapted with permission from reference [43], Copyright (2018), American Chemical Society; **c** Schematic illustrations and photos of PANI-hydrogel-based FSCs. Adapted with permission from reference [42], Copyright (2014), Royal Society of Chemistry; **d** Schematic showing the preparation process of APPH, CV curves of the assembled APPH-FSCs and photos of 4 powered LEDs under different states. Adapted with permission from reference [47], Copyright The Authors, some rights reserved; exclusive licensee Nature. Distributed under a Creative Commons Attribution License 4.0 (CC BY); **e** Schematic showing the fabrication of PHP device and the photographs showing the practical application. Adapted with permission from reference [49], Copyright (2019), Elsevier

4.3.1   Pristine Conjugated Polymer Hydrogel Electrodes

Generally, small molecules with multifunctional groups including phytic acid, tannic acid, and CuPcTs were used to crosslink conjugated polymer chains to form pristine hydrogel [43–45]. These small molecules play the role of dopants and cross-linkers during the polymerization process. For example, Bao et al. used phytic acid with an excess of phosphorous groups to obtain PANI hydrogel by pronating the amine and imine groups and rending PANI hydrogel with hydrophilic property (Fig. 5b) [43]. As-prepared PANI hydrogel electrode showed an efficient electrochemical performance. The above-mentioned preparation method for pristine conjugated polymer hydrogels is simple and the obtained hydrogels without other insulating polymer components show higher conductivity. Moreover, the microstructure, mechanical and electrochemical properties of pristine conjugated polymer hydrogel can be regulated by changing the synthesis conditions. However, the skeleton used to be very rigid and the prepared hydrogels are easy to break and degrade, and a flexible substrate is needed for the fabrication of FSCs. Ma et al. further used carbon fiber cloth to support as-prepared PANI hydrogel and fabricate the flexible electrode without any binder (Fig. 5c) [42]. The assembled symmetric FSC devices possessed excellent flexibility without sacrificing their electrochemical performance.

4.3.2   Conjugated Polymer-Based Hybrid Hydrogel Electrodes

Various conjugated polymer-based hybrid hydrogels have been fabricated to enhance pristine conjugated polymer hydrogels' mechanical properties. However, nonconducting hydrogel matrix and polymers always decrease the electrical properties of the hybrid hydrogel, which is a big challenge for the application of conjugated polymer-based hybrid hydrogel electrodes. So far, several strategies including supramolecular self-assembly and crypolymerization have been proposed to design the hybrid hydrogel with efficient electrochemical and mechanical properties. Ma et al. adopted boronic acid to crosslink polyvinyl alcohol (PVA) and PANI by supramolecular assembly [46]. The assembled FSC device demonstrated a high gravimetric capacitance and energy density. Liu et al. presented a crypolymerization strategy to obtain an anisotropic PVA/PANI hydrogel (Fig. 5d) [47]. Due to the formed rigid PANI nanofibrous scaffold and microcrystalline regions of PVA, as-prepared PVA/PANI hydrogel exhibited a high mechanical strength. The assembled FSCs exhibited an excellent electrochemical property owing to the formed anisotropic porous structures and bi-continuous ionic conductive/electrochemically active phases.

4.3.3   Conjugated Polymer-Based All-in-One Hydrogel FSCs

To improve FSC devices' stability under large deformation, all-in-one hydrogel-based FSCs integrating electrodes and electrolytes have been developed recently. Depositing or *in-situ* growing conjugated polymer hydrogels on the upper and lower

side of hydrogel electrolyte is the common way to fabricate all-in-one hydrogel FSCs [48, 49]. For example, Wang et al. prepared PPy-PVA/dilute sulphuric acid hydrogel electrolyte firstly, and then *in-situ* polymerized conductive PPy (Fig. 5e) [49]. As-prepared all-in-one hydrogel FSC maintained 90% of areal capacitance when the tensile strain of the device reached 110% and showed a high energy and power density. On the other hand, all-in-one hydrogel FSCs with multifunctional characteristics such as self-healing, fatigue-resistant, and self-recovering originating from the hydrogel electrolytes can be easily designed and developed [50]. However, they generally showed low energy and power density, which limits their practical application in energy storage.

5   Conclusion and Perspectives

In the last decades, conjugated polymers have been widely developed as organic electrodes for FSC devices because of their high flexibility and excellent electro-chemical properties. Herein, we have presented the recent progress in the design and preparation of different conjugated polymers including traditional CPs, emerging CMPs, and COFs and their composites materials as electrodes with different dimensional architectures for FSCs. The effect of the fabrication methods and the electrode configurations on the mechanical and electrochemical performance of FSCs have been specifically summarized.

Conjugated polymers electrodes show the drawbacks of relatively short cycle life and poor rate capability performance, while forming conjugated polymers-based composites especially with carbon nanomaterials can effectively improve the mechanical flexibility, conductivity, and cyclic stability of FSCs. Although 1D fiber-shaped FSCs demonstrate high compatibility with textiles, exceptional mechanical flexibility, and miniaturization potential for wearable FSCs than those with 2D planar structures, designing highly stretchable conjugated polymers-based 1D fiber-shaped electrodes and assembled FSCs exhibiting stable mechanical properties and excellent energy storage performance is still one of the big challenges for its practical applications. For 2D planar FSCs, MSCs show more promising in wearable FSCs than 2D FSCs with bulky sandwiched structures due to their merits of space-saving, shorter ion transport paths, better penetration of electrolyte ions, facile interconnection, and integration within the electronic systems. However, it is still desirable to establish an inexpensive technology for the mass manufacturing of MSCs for its practical application. Conjugated polymers-based 3D hydrogel electrodes are found to exhibit enhanced mechanical properties, capacitance, and rate performance than traditional FSCs, but the low energy density limits their practical application in energy storage. Therefore, developing an uncomplicated, low-cost, and environmental-friendly strategy for achieving high-performance conjugated polymer-based FSCs is still a challenge.

References

1. Shi, Q., Sun, J., Hou, C., Li, Y., Zhang, Q., Wang, H.: Advanced functional fiber and smart textile. Adv. Fiber Mater. **1**, 3–31 (2019)
2. Nelson, M.R., Borkman, R.F.: Internal rotation barriers: ab initio calculations on substituted ethyl benzoates and benzoic acids as models for polyester flexibility. J. Mol. Struct. Theochem. **432**, 247–255 (1998)
3. Jiang, L., Yuan, L., Wang, W., Zhang, Q.: Soft materials for wearable supercapacitors. Soft. Sci. **1**, 5 (2021)
4. Raza, W., Ali, F., Raza, N., Luo, Y., Kim, K.-H., Yang, J., Kumar, S., Mehmood, A., Kwon, E.E.: Recent advancements in supercapacitor technology. Nano Energy **52**, 441–473 (2018)
5. Zhong, C., Deng, Y., Hu, W., Qiao, J., Zhang, L., Zhang, J.: A review of electrolyte materials and compositions for electrochemical supercapacitors. Chem. Soc. Rev. **44**, 7484–7539 (2015)
6. Gonzalez, A., Goikolea, E., Barrena, J.A., Mysyk, R.: Review on supercapacitors: Technologies and materials. Renew. Sust. Energ Rev. **58**, 1189–1206 (2016)
7. Augustyn, V., Simon, P., Dunn, B.: Pseudocapacitive oxide materials for high-rate electrochemical energy storage. Energy Environ. Sci. **7**, 1597–1614 (2014)
8. Shao, Y., El-Kady, M.F., Wang, L.J., Zhang, Q., Li, Y., Wang, H., Mousavi, M.F., Kaner, R.B.: Graphene-based materials for flexible supercapacitors. Chem. Soc. Rev. **44**, 3639–3665 (2015)
9. Kondrat, S., Georgi, N., Fedorov, M.V., Kornyshev, A.A.: A superionic state in nano-porous double-layer capacitors: insights from Monte Carlo simulations. Phys. Chem. Chem. Phys. **13**, 11359–11366 (2011)
10. Raymundo-Piñero, E., Kierzek, K., Machnikowski, J., Béguin, F.: Relationship between the nanoporous texture of activated carbons and their capacitance properties in different electrolytes. Carbon **44**, 2498–2507 (2006)
11. Stott, T.L., Wolf, M.O.: Electronic interactions in metallated polythiophenes: what can be learned from model complexes. Coord. Chem. Rev. **246**, 89–101 (2003)
12. Shirakawa, H., Louis, E.J., MacDiarmid, A.G., Chiang, C., Heeger, A.J.: Synthesis of electrically conducting organic polymers halogen derivatives of polyacetylene. Chem. Commun. 578–580 (1977)
13. Heeger, A.J.: Semiconducting and metallic polymers: The fourth generation of polymeric materials. J. Phys. Chem. B **105**, 8475–8491 (2001)
14. Peng, C., Hu, D., Chen, G.Z.: Theoretical specific capacitance based on charge storage mechanisms of conducting polymers: Comment on 'Vertically oriented arrays of polyaniline nanorods and their super electrochemical properties.' Chem. Commun. **47**, 4105–4107 (2011)
15. Wang, Z., Zhu, M., Pei, Z., Xue, Q., Li, H., Huang, Y., Zhi, C.: Polymers for supercapacitors: Boosting the development of the flexible and wearable energy storage. Mater. Sci. Eng. R-Rep. **139**, 35 (2020)
16. Lyu, W., Yu, M., Feng, J., Yan, W.: Facile synthesis of coral-like hierarchical polyaniline micro/nanostructures with enhanced supercapacitance and adsorption performance. Polymer **162**, 130–138 (2019)

17. Liao, Y., Weber, J., Faul, C.F.J.: Conjugated microporous polytriphenylamine networks. Chem. Commun. **50**, 8002–8005 (2014)

18. Liao, Y., Weber, J., Mills, B.M., Ren, Z., Faul, C.F.J.: Highly efficient and reversible iodine capture in hexaphenylbene-based conjugated microporous polymers. Macromolecules **49**, 6322–6333 (2016)

19. Lee, J.S.M., Cooper, A.I.: Advances in conjugated microporous polymers. Chem. Rev. **120**, 2171–2214 (2020)

20. Liao, Y., Wang, H., Zhu, M., Thoma, A.: Efficient supercapacitor energy storage using conjugated microporous polymer networks synthesized from Buchwald-Hartwig coupling. Adv. Mater. **30**(12), 1705710 (2018)

21. Li, H., Lyu, W., Liao, Y.: Engineering redox activity in conjugated microporous polytriphenylamine networks using pyridyl building blocks toward efficient supercapacitors. Macromol. Rapid. Commun. **40**, 1900455 (2019)

22. Kandambeth, S., Dey, K., Banerjee, R.: Covalent organic frameworks: Chemistry beyond the structure. J. Am. Chem. Soc. **141**, 1807–1822 (2019)

23. Sajjad, M., Lu, W.: Covalent organic frameworks based nanomaterials: Design, synthesis, and current status for supercapacitor applications: A review. J. Energy Storage **39**, 102618 (2021)

24. Deblase, C.R., Silberstein, K.E., Truong, T.-T., Abruña, H.D., Dichtel, W.R.: β-Ketoenamine-linked covalent organic frameworks capable of pseudocapacitive energy storage. J. Am. Chem. Soc. **135**, 16821–16824 (2013)

25. Zhao, C., Jia, X., Shu, K., Yu, C., Wallace, G.G., Wang, C.: Conducting polymer composites for unconventional solid-state supercapacitors. J. Mater. Chem. A **8**, 4677–4699 (2020)

26. Chen, M., Wang, Z., Li, K., Wang, X., Wei, L.: Elastic and stretchable functional fibers: A review of materials, fabrication methods, and applications. Adv. Fiber Mater. **3**, 1–13 (2021)

27. Lyu, W., Zhang, W., Liu, H., Liu, Y., Zuo, H., Yan, C., Faul, C.F.J., Thomas, A., Zhu, M., Liao, Y.: Conjugated microporous polymer network grafted carbon nanotube fibers with tunable redox activity for efficient flexible wearable energy storage. Chem. Mater. **32**, 8276–8285 (2020)

28. Wang, K., Meng, Q., Zhang, Y., Wei, Z., Miao, M.: High-performance two-ply yarn supercapacitors based on carbon nanotubes and polyaniline nanowire arrays. Adv. Mater. **25**, 1494–1498 (2013)

29. Chen, X., Lin, H., Deng, J., Zhang, Y., Sun, X., Chen, P., Zhang, Z., Guan, G., Peng, H.: Electrochromic fiber-shaped supercapacitors. Adv. Mater. **26**, 8126–8132 (2014)

30. Li, P., Jin, Z., Peng, L., Zhao, F., Xiao, D., Jin, Y., Yu, G.: Stretchable all-gel-state fiber-shaped supercapacitors enabled by macromolecularly interconnected 3D graphene/nanostructured conductive polymer hydrogels. Adv. Mater. **30**(18), 1800124 (2018)

31. Ding, X., Zhao, Y., Hu, C., Hu, Y., Dong, Z., Chen, N., Zhang, Z., Qu, L.: Spinning fabrication of graphene/polypyrrole composite fibers for all-solid-state, flexible fibriform supercapacitors. J. Mater. Chem. A **2**, 12355–12360 (2014)

32. Zhang, J., Seyedin, S., Qin, S., Lynch, P.A., Wang, Z., Yang, W., Wang, X., Razal, J.M.: Fast and scalable wet-spinning of highly conductive PEDOT:PSS fibers enables versatile applications. J. Mater. Chem. A **7**, 6401–6410 (2019)

33. Du, H., Zhang, M., Liu, K., Parit, M., Jiang, Z., Zhang, X., Li, B., Si, C.: Conductive PEDOT:PSS/cellulose nanofibril paper electrodes for flexible supercapacitors with superior areal capacitance and cycling stability. Chem. Eng. J. **428**, 131994 (2022)

34. Liu, Y., Weng, B., Razal, J.M., Xu, Q., Zhao, C., Hou, Y., Seyedin, S., Jalili, R., Wallace, G.G., Chen, J.: High-performance flexible all-solid-state supercapacitor from large free-standing graphene-PEDOT/PSS films. Sci. Rep. **5**, 17045 (2015)

35. Zhu, M., Huang, Y., Deng, Q., Zhou, J., Pei, Z., Xue, Q., Huang, Y., Wang, Z., Li, H., Huang, Q., Zhi, C.: Highly flexible, freestanding supercapacitor electrode with enhanced performance obtained by hybridizing polypyrrole chains with mxene. Adv. Energy Mater. **6**(21), 1600969 (2016)

36. Zheng, X., Shen, J., Hu, Q., Nie, W., Wang, Z., Zou, L., Li, C.: Vapor phase polymerized conducting polymer/MXene textiles for wearable electronics. Nanoscale **13**, 1832–1841 (2021)

37. Xu, J., He, Y., Bi, S., Wang, M., Yang, P., Wu, D., Wang, J., Zhang, F.: An olefin-linked covalent organic framework as a flexible thin-film electrode for a high-performance micro-supercapacitor. Angew. Chem. Int. Edit **58**, 12065–12069 (2019)
38. Chu, X., Chen, G., Xiao, X., Wang, Z., Yang, T., Xu, Z., Huang, H., Wang, Y., Yan, C., Chen, N., Zhang, H., Yang, W., Chen, J.: Air-stable conductive polymer ink for printed wearable micro-supercapacitors. Small **17**(25), 2100956 (2021)
39. Liu, Y., Weng, B., Xu, Q., Hou, Y., Zhao, C., Beirne, S., Shu, K., Jalili, R., Wallace, G.G., Razal, J.M., Chen, J.: Facile fabrication of flexible microsupercapacitor with high energy density. Adv. Mater. Technol. **1**(9), 1600166 (2016)
40. Zhang, X., Jiang, C., Liang, J., Wu, W.: Electrode materials and device architecture strategies for flexible supercapacitors in wearable energy storage. J. Mater. Chem. A **9**, 8099–8128 (2021)
41. Wang, Z., Zhang, Q., Long, S., Luo, Y., Yu, P., Tan, Z., Bai, J., Qu, B., Yang, Y.: Three-dimensional printing of polyaniline/reduced graphene oxide composite for high-performance planar supercapacitor. ACS Appl. Mater. Interfaces **10**, 10437–10444 (2018)
42. Wang, K., Zhang, X., Li, C., Zhang, H., Sun, X., Xu, N., Ma, Y.: Flexible solid-state supercapacitors based on a conducting polymer hydrogel with enhanced electrochemical performance. J. Mater. Chem. A **2**, 19726–19732 (2014)
43. Pan, L., Yu, G., Zhai, D., Lee, H.R., Zhao, W., Liu, N., Wan, H., Tee, B.C.K., Shi, Y., Cui, Y., Bao, Z.: Hierarchical nanostructured conducting polymer hydrogel with high electrochemical activity. Proc. Natl. Acad. Sci. USA **109**, 9287–9292 (2012)
44. Zhou, L., Fan, L., Yi, X., Zhou, Z., Liu, C., Fu, R., Dai, C., Wang, Z., Chen, X., Yu, P., Chen, D., Tan, G., Wang, Q., Ning, C.: Soft conducting polymer hydrogels cross-linked and doped by tannic acid for spinal cord injury repair. ACS Nano **12**, 10957–10967 (2018)
45. Wang, Y., Shi, Y., Pan, L., Ding, Y., Zhao, Y., Li, Y., Shi, Y., Yu, G.: Dopant-enabled supramolecular approach for controlled synthesis of nanostructured conductive polymer hydrogels. Nano. Lett **15**, 7736–7741 (2015)
46. Li, W., Gao, F., Wang, X., Zhang, N., Ma, M.: Strong and robust polyaniline-based supramolecular hydrogels for flexible supercapacitors. Angew. Chem. Int. Edit. **55**, 9196–9201 (2016)
47. Li, L., Zhang, Y., Lu, H., Wang, Y., Xu, J., Zhu, J., Zhang, C., Liu, T.: Cryopolymerization enables anisotropic polyaniline hybrid hydrogels with superelasticity and highly deformation-tolerant electrochemical energy storage. Nat. Commun. **11**, 62 (2020)
48. Wang, K., Zhang, X., Li, C., Sun, X., Meng, Q., Ma, Y., Wei, Z.: Chemically crosslinked hydrogel film leads to integrated flexible supercapacitors with superior performance. Adv. Mater. **27**, 7451–7457 (2015)
49. Yin, B.-S., Zhang, S.-W., Ke, K., Wang, Z.-B.: Advanced deformable all-in-one hydrogel supercapacitor based on conducting polymer: Toward integrated mechanical and capacitive performance. J. Alloy. Compd. **805**, 1044–1051 (2019)
50. Guo, Y., Zheng, K., Wan, P.: A flexible stretchable hydrogel electrolyte for healable all-in-one configured supercapacitors. Small **14**(14), 1704497 (2018)

Organic Electrodes for Flexible Energy Storage Devices

Kwadwo Mensah-Darkwa, Daniel N. Ampong, Daniel Yeboah, Emmanuel A. Tsiwah, and Ram K. Gupta

Abstract Modern society is witnessing a presumed fourth industrial insurgency characterized by a boom of intelligent and digital electronic devices as the globe progresses toward electromobility and, with it, decarbonization of its electrical supply is urgently needed. As a result, battery and supercapacitor demand has skyrocketed, as the need for the ores, metals, and materials used to manufacture them. This chapter intends to demonstrate that there is room to develop organic-based electrodes for electrochemical energy storage devices. Organic electrode materials are an alternative to the traditional inorganic electrode materials, which require intercalation and are promising candidates for advancing next-generation multifaceted and sustainable energy storage systems. We present a comprehensive overview of the fundamental understanding, history of development, types, synthesis methods, and specific applications of organic electrodes by starting with robust structural analysis. The use of organic electrodes in flexible supercapacitors and flexible batteries and their electrochemical and mechanical properties are addressed.

Keywords Organic electrodes · Flexible supercapacitors · Batteries · Electrochemical energy storage · Carbon nanofiber

K. Mensah-Darkwa (✉) · D. N. Ampong
Department of Materials Engineering, College of Engineering, Kwame Nkrumah University of Science and Technology, Kumasi, Ghana

D. Yeboah
Department of Materials and Manufacturing, Institute of Industrial Research—Council for Scientific and Industrial Research, Accra, Ghana

E. A. Tsiwah
Department of Materials Science and Engineering, School of Chemistry and Materials Science, University of Science and Technology of China, Hefei, China

R. K. Gupta
Department of Chemistry, Kansas Polymer Research Center, Pittsburg State University, Pittsburg, KS 66762, USA

1   Introduction

Environmental and energy issues have been one of the significant confronting challenges humans face in the twenty-first century. These two challenges have been well captured in the United Nations' sustainable development goals for effective implementation. The goal regarding energy development is to achieve "affordable and clean energy" for all. Since the inception of this goal, scientists have, over the past decade, aspired to achieve sustainable, efficient, eco-friendly, and affordable energy systems to meet man's industrialization and technological drive. This could be realized by replacing the high carbon-footprint conventional energy sources with renewable energy. The proliferation of consumer portable electronics such as sensors, smartwatches, communication systems, electronic skins, etc., has necessitated the need for flexible materials. The units of these flexible devices include current collectors, gel electrolytes, separators, and flexible working electrodes. Electrodes are the most important components of storage devices. The conventional inorganic electrode materials have been successful in most applications due to their excellent electrochemical performance. Nonetheless, inorganic electrode materials are too rigid and cannot withstand mechanical bending, twisting, and flexing. Researchers and scientists over the past decade have directed attention to the use of organic materials for different substrates, electrodes, electrolytes, etc., to rival the inorganic materials for improved performance.

The quest for revolutionary electrochemical energy storage (EES) systems is now widely acknowledged by experts in the field and regular people who want to use various mobile, portable, and intelligent electronic devices that make their lives safer, easier, and more fun. Batteries and supercapacitors are examples of EES devices. Organic material-based electrodes can improve existing EES systems while also opening up new avenues for the development of innovative device topologies for a variety of applications. Organic electrodes and compounds have excellent performance parameters such as large potential windows, specific energy, mechanical stability, and ease of manufacture. Organic electrode materials are exciting alternatives for large-scale electrochemical energy storage devices due to their outstanding performance and inexpensive cost. Currently, the problem of developing an efficient storage system that simultaneously transcends all the performance metrics remains a significant challenge to researchers. Understanding electrochemical storage mechanisms are likely to improve with organic materials in solid-state EES systems. The flexibility of organic materials' molecular structure allows for a wide range of properties. The ease of fabrication also helps minimize the costs imposed by the intricate functionalization induced by tuning.

It is unnecessary to use redox-active organics as the major functional electrode components to achieve fast charge kinetics at the electrolyte/electrode interface. Regardless of the approach, the electrical properties of solid organic electrode materials are essential. In particular, thick electrodes are in high demand because they can boost specific energy densities while cutting costs. Deficiency in electrical conduction is responsible for power losses in thick electrodes. Electronic conductivity of

the device is challenging to design since it relies on unstable and challenging mechanism to disperse carbonaceous materials. Loss of interparticle connections is also a major cause of carbon electrode aging due to active material volume changes. Designing thin and flexible carbon electrodes is critical for EES device performance. Carbonyl groups, conductive polymers, organodisulfides, and conjugated carbonyl compounds are some organic materials employed as EES electrodes.

Because flexible EES devices made from organic electrodes are unquestionably required to combat the troubling global warming, this chapter summarizes the perspective of flexible EES devices made from organic electrodes.

2 Methods for the Synthesis of Organic Materials for Energy Storage Devices

2.1 Pyrolysis

Pyrolysis involves changing the composition of material via its decomposition due to high temperatures. It takes place in an inert (argon and nitrogen) environment. It can be solely employed or combined with other methods [1]. Boron-doped reduced graphene for flexible asymmetric supercapacitor electrodes can be prepared by pyrolysis, at 1000 °C, following a hydrothermal route. A slurry of pyrolyzed material, binder, and solvent are coated onto bendable substrates such as carbon cloth and graphite sheet. To ensure adhesion to the substrate, day-long drying is done at about 85 °C. Material synthesis via pyrolysis is less time and energy-consuming [1]. For that reason, it is well adapted for biochar from spent coffee grounds for use in novel tandem photocatalytic fuel cell-supercapacitor devices. The procedure involves grounded spent coffee which is weighed and heated at 850 °C for an hour in the presence of 0.2 oxygen needed for complete combustion. The resulting char is mixed with electroactive additives and a binder to form a slurry; then coated onto cloth substrates and annealed at 300 °C to be used as a supercapacitor electrode [2]. In pyrolysis, chitin is heated from room temperature to a moderate temperature to produce biochar.

2.2 Hydrothermal and Solvothermal Synthesis

The solvothermal method provides good interaction between nanocomposite structures for energy devices. Generally, the process involves mixing precursors in a soluble organic solvent and heating in an autoclave for hours. Upon cooling to room temperature, the products are centrifuged and washed with deionized water, ethanol, or both to remove organic solvents, after which drying is performed. n-TiO_2/n-Gr composite was prepared through a solvothermal process: as-synthesized

GO is dispersed in isopropanol and ammonia solution. After that, titanium (IV) butoxide is added. The mixture is heated in an autoclave for 12 h at 150 °C followed by centrifugation in ethanol and drying at 50 °C [3]. Compared to the conventional template method of making composites, the solvothermal process is more straight-forward since it can be carried out as a one-step process. Also, the morphology of products can be controlled due to differences in polarity and dispersibility of the system. Moreover, electrodes made by the hydrothermal method, a similar process to solvothermal, employing water as a solvent, have also been explored.

2.3 Microwave Method

Microwave synthesis is a green method used for organic and inorganic material synthesis. It is based on polar molecular interactions influenced by an alternating electromagnetic field. As a result, faster synthesis is achieved compared to other methods of synthesis, which require hours or days. The technique allows for manip-ulating electronic states on the surface of synthesized materials. The process involves mixing precursors to form a uniform colloidal suspension which is transferred into a microwave tube to be reacted for a specified time and temperature. The product is obtained by centrifugation and washing with an organic solvent (ethanol, DMF) and subsequent drying [4]. A tung oil-based ultraviolet curable oligomer was synthesized via a microwave-assisted method. TO and CA were used as precursors. The material showed good strength and heat-resistant properties desired in coating applications [5].

2.4 Mechanochemical Synthesis

This method relies on mechanical energy from a ball mill to drive chemical synthesis between starting materials. It is low-cost, simple, and can be used for large-scale synthesis. Precursors are placed into an agate jar with agate balls. The mixture is milled at constant rotational speed for ~12 h at room temperature. Products are sintered at ~700 °C under inert gas flow [6]. The mechanochemical method has been used to prepare advanced materials for batteries and supercapacitors. Via direct ILAG mechanochemical synthesis, anode ZIF-8/C for LiS batteries showed a 50% increase in the initial charge–discharge process [7]. A one-pot mechanochemical method has been used to form a 3D PEDOT:PSS aerogel for electrodes [8].

2.5 Sonochemical Method

This is a wet chemical method that uses ultrasonic irradiation to drive synthesis reactions between precursors through a process of sound cavitation, bubble growth, and implosion in the liquid phase. A specialized sonicator is used. The method offers homogeneous particles with reduced aggregation, increased purity, and dispersity [9]. It has been used for carbon, metal oxides, and metal phosphate nanocomposites. It is cost-effective and less time-consuming compared to other wet methods. After sonochemical syntheses such as hydrothermal [10] and calcination, additional procedures can be carried out. Calcination, if performed, is to remove volatile molecules and adsorbed water to improve nanoparticle crystallinity.

3 Types of Energy Devices and Charge Storage Mechanism

3.1 Chemical Energy Storage Technologies

For chemical energy storage technologies, chemical species are used to generate secondary energy forms, e.g., electricity and heat, through latent or immediate chemical transformations. These species can be in the form of gases such as hydrogen, natural gas, and biogas or liquids such as methanol, diesel, and kerosene, or solids such as propylene, biomass, and coal. Hydrogen can be produced and stored as a chemical energy form or employed as fuel for conversion to electrical energy, like in fuel cells.

3.1.1 Hydrogen and Fuel Cell

Hydrogen is a highly efficient fuel with energy yields 2.75 times higher than hydrocarbons [11]. Generating hydrogen via water electrolysis, methanol-reforming, and ammonia decomposition is possible. Water electrolysis is considered the most promising and environmentally friendly means. A fuel cell continuously converts chemical energy into fuel, commonly hydrogen, into electrical energy. It makes use of both the fuel and an oxidant during its process. It operates with high efficiency of 60% compared to combustion technologies, has low emissions, and does not emit noise. Fuel cells consist of the anode, electrolyte, and cathode placed in adjacent order. At the anode, hydrogen undergoes an oxidation reaction which generates cations ($H_2 \rightarrow 2H^+ + 2e^-$) that migrate to the cathode via the electrolyte and free electrons that flow through the external circuit. Conversely, oxygen reduces to water at the cathode by the cations and electrons [12].

3.2 Electromagnetic and Electrostatic Energy Storage Technologies

An electric field or a magnetic field produced by a current-carrying coil can be used to store energy in the form of electromagnetic energy. Devices that store energy in this form include electrical double-layer capacitors (EDLC) and superconducting magnetic energy storage (SMES). These two technologies' working principles are well-known and documented. Typically, the EDLC stores electrostatic energy between two electrodes separated by an insulating material impregnated with an electrolyte. The electrode material has a significant impact on the performance of the energy storage capacity of the supercapacitor. Carbon-based materials, transition metal oxides, and conducting polymers make up the majority of capacitor electrode materials. All of these materials offer mechanical flexibility in their applications.

3.2.1 Electrical Double-Layer Capacitors

An EDLC has two electrodes and a porous separator with an electrolyte. The separator is often an insulating membrane between the two electrodes. Its primary function is to retain the electrolyte and facilitate ion conduction between the two electrodes. The primary energy storage mechanism of EDLCs is the fast adsorption/desorption of conductive ions in the presence of an electrolyte. Efficient energy storage depends on the electrode material's surface area, ion conductivity, and chemical structure. EDLCs have a higher power density but a lower energy density.

Flexible energy storage devices must perform under a variety of bending or folding conditions due to their operating conditions. The device must have superior mechanical performance under repetitive bending without significant performance loss to be applied in flexible energy storage—EDLCs store charges in electric double layers forming near the electrode/electrolyte interfaces. Thus, the process is highly reversible, and the cycle life is essentially infinite.

3.3 Electrochemical Energy Storage Technologies

Electrochemical energy storage technologies deal with all types of secondary batteries. Batteries transform chemical energy into electrical energy via an oxidation–reduction electrochemical mechanism. The main difference between this technology and fuel cells is that these batteries are charged upon completing a discharge half of their cycle to an external load. After that, an external source of electrical energy is stored in the battery during the charging half. For fuel cells, on the other hand, reactants (i.e., hydrogen and oxygen) supplying the energy are not stored in the cell. Instead, they are continuously supplied to cell electrodes from an external source [13].

3.3.1 Batteries

Batteries such as lead-acid, Ni–Cd, Ag–Zn, Ni–H$_2$, Br$_2$–Zn, and Na–S, have been developed for various applications. Batteries are known to have cycle lives of about 1200 cycles. Lithium-ion batteries (LIBs) have become of interest because they have high energy densities, making them durable even in small volumes. In certain works, organic materials that have electroactivity are incorporated into fabricated electrodes for Li-ion batteries [14]. When added, they provide alternative ions e.g., Na$^+$, K$^+$, Mg^{2+}, and Ca^{2+} that substitute Li ions to improve the performance of LIBs. For example, potassium ion inserted organic batteries have improved performance in previous works [15]. Graphene and other carbon compounds have also been used for batteries. Their interconnected networks, broad surfaces, and pore diameters help store energy via electrochemical species intercalation. As a result, they improve Li-ion-graphene hybrid energy storage performance. [16].

## 4 Organic Materials for Flexible Supercapacitors

The demand for high-quality energy storage devices for portable gadgets has grown over the last decade. Supercapacitors (SCs) fabricated from organic components present such great features to be used for advanced applications. The utilization of carbon nanotubes, nanofibers, carbon aerogels, graphene, and graphene oxides, among others, has increased SC performance. This section discusses various organic applications, their substrates, electrolytes, and electrodes.

4.1 Substrate

4.1.1 Carbon Nanofiber

Carbon nanofibers are porous, flexible, and mechanically strong with a large surface area. Because CNFs are hydrophobic, they must be modified to increase specific energy and capacitance. The adjustment will improve electrolytic ion transport and interaction between electrolyte and electrode. One of the recent ways to modify CNFs is by using plasma to treat them. Ghanashyam and Kyung [17] investigated CNF treated with ambient plasma for flexible SC devices using nickel foam electrodes and gel electrolytes. This increased the CNF's active surface area by a factor of three, reducing the resistance of the electrochemical charge transfer. The treated CNF also showed higher flexibility and higher capacitance retention after 10,000 cycles making it suitable for SC applications. Porous CNFs can be synthesized by electrospinning followed by carbonization. Chen and co-workers [18] recently adopted this feasible method by blending acetylated sugarcane bagasse and polyacrylonitrile using electrospinning, and they later carbonized the samples (Fig. 1a). The synthe-
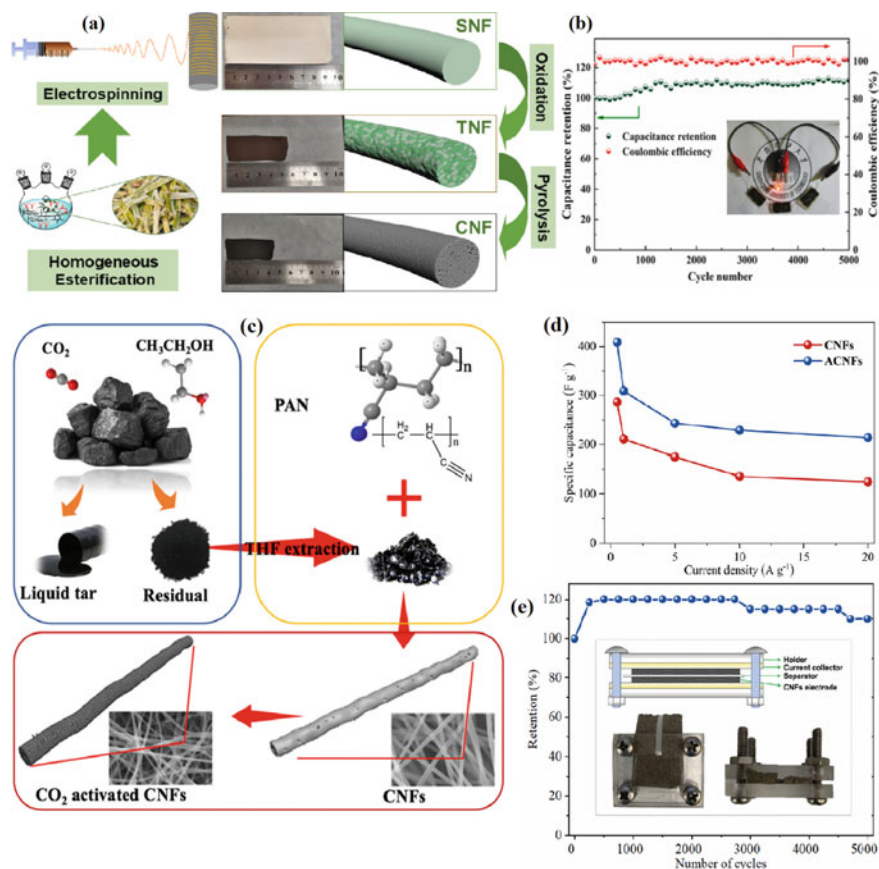
Fig. 1 **a** Schematic process, (b) cycling performance, and charge and discharge efficiency of synthesized CNF electrode. Adapted with permission from [18]. Copyright (2021) Elsevier. **c** Schematic process for preparing CNFs and ACNFs, **d** gravimetric capacitances against current densities of CNFs and ACNFs, **e** galvanostatic charge/discharge curves (current density of 1 A/g) of ACNFs in a two-electrode system. Adapted with permission from [19]. Copyright (2020) Elsevier

sized samples showed higher flexibility and recorded a specific capacitance of 289.5 F/g, and demonstrated outstanding capacitance retention of 111.8% after 5000 cycles, as shown in Fig. 1b. Binder-free and free-standing activated CNFs (ACNFs) were produced in a CO_2 environment by Wang and colleagues [19] using carbonization and activation process as shown in Fig. 1c. The device was used for SC electrode and recorded a specific capacitance of 409 F/g (Fig. 1d) with superior capacitance retention, as shown in Fig. 1e.

4.1.2 Carbon-Based Textile

High conductivity, mechanical strength, flexibility, and surface area make carbon-based textiles ideal materials for SC devices. The wide diameter of each carbon fiber unit makes the ion diffusion channel long, increasing ionic diffusion resistance. In SC, a shorter diffusion length increases ionic diffusion. Simple synthesis methods such as treating cotton fabrics with ammonia can be used to obtain activated carbon cloth (ACC) with a highly porous structure and large surface area [20]. The ACC obtained a high specific capacitance of 215.9 F/g at a current density of 1 A/g when used as an SC device, maintaining 98% of its original capacitance after 20,000 cycles. This performance can be attributed to the nitrogen doping effect of the activated carbon cloth. Recently, a novel approach has been adopted to develop PANI@carbon@textile using carbonization techniques assisted with H_2SO_4 (Fig. 2a) for wearable electrodes [21]. The device showed high conductivity, good flexibility, and uniform capacitive distribution due to the unique H_2SO_4 carbonization degree, which enhanced the fabric support. The device, when used for SCs maintained stable capacitance with a high degree of mechanical stability under bending conditions, as shown in Fig. 2b. Textile SCs were also fabricated from conductive cotton-fabric and graphene electrodes and their electrochemical performance was reported by Flores-Larrea et al. [22]. To improve upon the energy density and capacitance of the device, the researchers introduced a cubic phase of NiO:Yb microparticles. The existence of oxygen vacancy
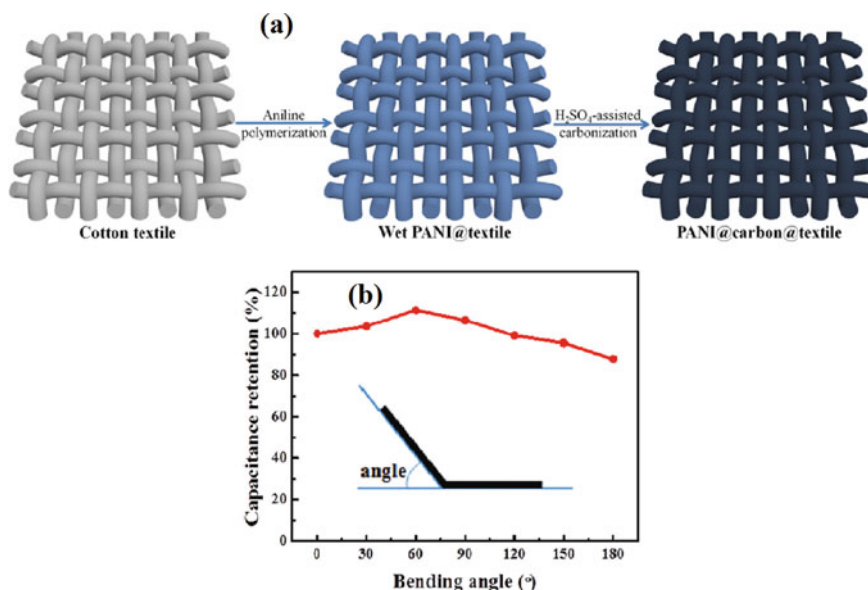
Fig. 2 **a** Fabrication process for PANI@carbon@textile electrode. **b** Capacitance retention of the constructed all-solid-state SC device. Adapted with permission from [21]. Copyright (2021) Elsevier

defects, among other properties induced by the processing, accounted for the charge storage due to rapid ionic diffusion in the SC electrode.

4.2 Electrolyte

Electrolytes, a critical component of SCs, affect the device's electrochemical characteristics, rate capabilities, voltage window, and cycling stability. The mechanical degradation of these devices caused by frequent bending, compressing, and stretching is a critical challenge. Hydrogel electrolytes with self-healing properties can control such damage while maintaining good electrical contact between the electrode and electrolyte. The self-healing ability of hydrogel electrolytes and good electrochemical performance and safety when used in solid-state SCs can be attributed to the fluidity of the chain molecules and the availability of hydrogen bonds in their structure. Organic liquid electrolytes used in conventional SCs are flammable and may explode at high operating temperatures. To avert this problem, organic gel polymeric electrolytes, which are fire-retardant, can be adopted. The organic gel electrolyte does not only inhibit fire but also warrants enhanced ionic conductivity, excellent flexibility, and good electrochemical performance in SC applications [23]. The potential window of SCs is critical to its performance, which is influenced by the electrolyte. Metallic organic framework made from hollow shell core of $NiCo_2O_4$ provides an excellent potential window with high capacitance when used in battery-like SCs due to the structure of $NiCo_2O_4$. It helps to increase the device's life cycle and provides maximum safety of the electrolyte [24].

4.3 Electrode Materials

Electrode materials are essential to determine the performance of SCs. Organic electrodes consist of various carbon-based materials such as carbon nanotubes (CNTs), graphene, graphene oxide (GO), activated carbon (AC), carbon nanofibers (CNFs).

4.3.1 Activated Carbon Flexible Supercapacitors

Activated carbon used in commercial SCs is primarily obtained from coconut shells, wood, and coal polymers due to the raw materials' abundance and stable electrochemical properties. Despite the merits possessed by AC, its pore structure is underutilized, and it has low conductivity. To overcome these issues, AC is frequently mixed with binders and conductive additives, which impact the electrode's flexibility and energy density during fabrication. Li et al. [25] designed flexible and self-standing film of activated carbon/carbon nanotube/reduced graphene oxide (AC/CNT/RGO) (Fig. 3a) and studied the electrochemical performance in flexible SCs. The device recorded
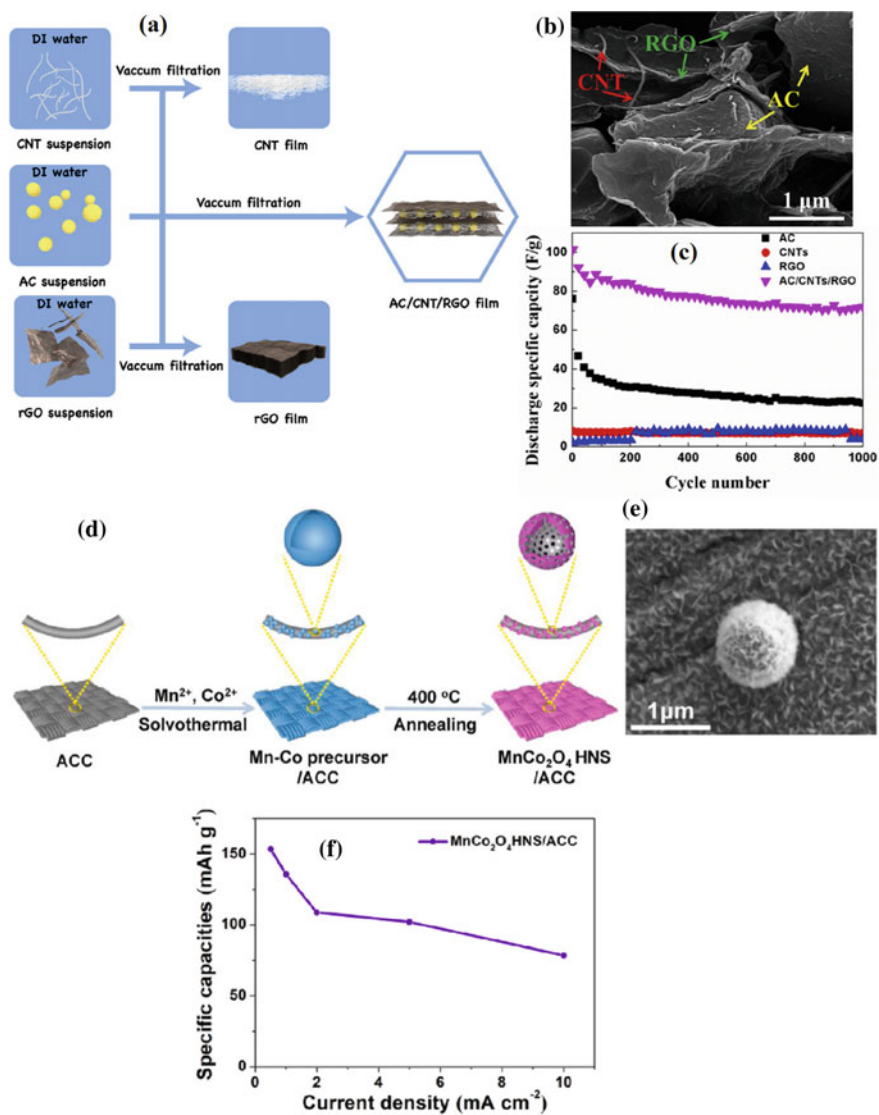
Fig. 3 a Preparation process of the fabricated AC/CNT/RGO film, b SEM image of the cross-section of AC/CNT/RGO film, (c) Cycling performances of the electrode devices. Adapted with permission from [25]. Copyright (2018) Elsevier. d Schematic fabrication process, e SEM image, and f specific capacities at various current densities of $MnCo_2O_4$ HNS/ACC. Adapted with permission from [27]. Copyright (2021) Elsevier

suitable specific capacitance of 101 F/g at 0.2 A/g current density, as shown in Fig. 3c. The networks of CNT (Fig. 3b) enhanced the electrode's electrical conductivity, which accounted for the observed performance. Irradiations from microwaves can be used to prepare carbon cloth-based composite electrode materials for highly efficient SCs with enhanced electrochemical properties and resistance to harsh mechanical conditions. The pores at the surface of the carbon fibers are effectively activated by microwave irradiation, improving the device's performance [26]. It is believed that the hollow structures in electrode materials create enormous open networks which shorten ion diffusion paths and enhance ionic transport. Zhu et al. [27] synthesized $MnCo_2O_4$ hollow nano-spheres on activated carbon cloth ($MnCo_2O_4$ HNS/ACC) using a simple technique as shown in Fig. 3d. When used as a flexible asymmetric SC electrode, a high specific capacitance (Fig. 3f) and improved mechanical stability were recorded due to the open networks (Fig. 3e).

4.3.2 Carbon Nanotubes Flexible Supercapacitors

CNTs exhibit an open network of tubes and are mainly studied for SC applications due to their unique electrical properties and mechanical stability. When combined with various electrode materials, the electrochemical and mechanical performance of the device improves. For example, the poor electrical conductivity of most conducting polymers limits its real-life application in energy storage and conversion systems despite their abundant functional groups. CNTs can be composited with polymers with conjugated micropores to improve their electrical conductivity, flexibility, and capacitance in SCs due to the synergistic effect between the two materials. A scale-up and straightforward composite electrode can be synthesized for highly flexible, tough, and tear resistance SC by using CNTs, PEDOT:PSS, and Tyvek coated with Ag. This composite electrode material features high conductivity and mechanical stability. A specific mass capacitance of up to 138.7 F/g can be obtained at a scan rate of 50 mV/s due to the improved crystallinity of the various active materials [28]. Another way to overcome the poor conductivity, flexibility, and low electron delivery of electrode materials such as MXene and porous carbon in high capacity solid-state SCs is to introduce CNT with a 1D structure into the material. This helps to tighten the porous carbon on MXene flakes and relieve the phenomenon of self-stacking of MXene-based electrode films [29].

4.3.3 Graphene-Based Flexible Supercapacitors

Graphene has been studied over the years for SC applications. It is a 2-dimensional carbon sheet monolayer with conjugated sp^2 configuration and excellent conductivity, which can be employed in SCs without polymeric binders. It also features good thermal and chemical stability, a wide potential window, and high flexibility. One major problem during its application is the restacking of graphene sheets which accounts for the loss of electrochemical performance. Researchers over the years

have dedicated attention to solving the restacking problem. The addition of surfactants and carbonaceous materials into graphene sheets can prevent the restacking effect. To overcome the possibility of graphene restacking, Hamra et al. [30] utilized the microwave irradiation (MW) technique to simultaneously exfoliate and reduce nanoplatelets of graphene (GNPs) and GO and studied their electrochemical performance for SCs. Micrograph images showed success in the exfoliation process, revealing a porous structure in GO and GNPs with loose stacked layers as shown in Fig. 4a, b. The composite material (mixture of MW-GNPs, MW-GO, and polypyrrole (PPy)) showed good electrochemical performance, with the single device exhibiting promising capacitance retention as compared to the stacked device even after 1000 bending cycles when used as SC electrode (Fig. 4c). The volume of vacuum filtration of rGO/tannin (rGO/TA) slurry mixture can be controlled to achieve high-performance flexible SCs with tunable electrochemical performance. This procedure is done to prevent aggregation of graphene sheets and create more redox-active sites in the device, thanks to the TA coating [31]. Carbon black on the micro-scale can be
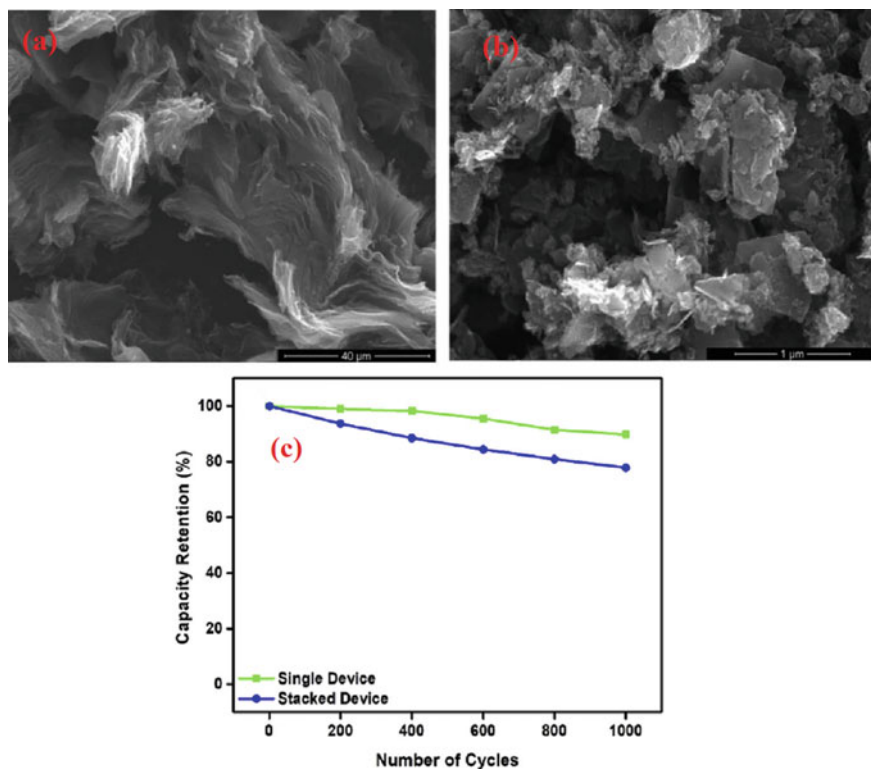
Fig. 4 FESEM images of **a** porous MW-GO and **b** loose stacked MW-GNPs layers. **c** Cycling stability performances of MW-G. mix-PPy SC device at 1 A/g. Adapted with permission from [30]. Copyright (2020) Elsevier

used as spacers and carbon powder on the nanoscale to produce a graphene-based fiber with a porous structure for portable electronics. The wet spinning technique is used to synthesis the all-carbon composite material with a large surface area and high mechanical and electrochemical performance. The all-carbon electrode material also helps to prevent the stacking of graphene sheets [32].

5 Organic Materials for Flexible Batteries

5.1 Polymer Electrolytes

The composite polymer electrolytes consisting of inorganic ceramic powders and polymer matrix demonstrate advantages of both polymer and ceramic electrolytes: high ionic conductivity at room temperature, wide electrochemical window, and good mechanical performance. Guo et al. found out that coating tantalum doped lithium lanthanum zirconate garnet (LLZTO) nanoparticles with polydopamine (PDA) and further grafting it with PEGDE will form poly (ethylene glycol) (PEG) brush which will enhance the interfacial compatibility between polyethylene oxide (PEO) matrix and LLZTO nanoparticles as shown in Fig. 5a, b. This resulted in excellent cyclic stability of 152.3 mAh/g [33]. Ye et al. also prepared a thin and flexible blended gel polymer electrolyte (GPE) for dendrite-free solid-state lithium metal batteries (SSLMBs). The as-prepared GPE had a strong strain at 529.94 $\pm$ 10% (Fig. 5d), and also delivered a cell capacity of 150 mAh/g at 0.3C (Fig. 5c) [34]. Pandurangan reported the preparation of polymer-garnet composite electrolyte (PGCE) membranes consisting of PEO polymer, tantalum doped LLZTO filler, lithium perchlorate salt, and as-synthesized comb-like structured polymer exhibiting a current density of 0.09 mA/cm^2 [35].

5.2 Graphene-Based Materials

Flexible cathode materials are pivotal for the performance of flexible lithium-ion (LiS) batteries. The flexible electrode should overcome the typical issues of LiS batteries, for instance, low conductivity, the collapse of cathode electrode structure due to sulfur volume expansion, and the shuttle effect. Yang et al. reported a facile template-free way to fabricate holey reduced graphene oxide free-standing paper (HGP) as sulfur host of flexible LiS battery. The cross-linked holey network structures of HGP offered abundant active sites for polysulfides adsorption and conversion. The flexible LiS battery based on HGP/S electrodes exhibited an initial capacity of 1073.2 mAh/g and retained discharge capacity of 681 mAh/g after 200 cycles at 0.1C under continuous bending, Fig. 6a [36]. Hao et al. then introduced a three-dimensional nitrogen-doped porous graphitized carbon (MS-NPC) designed by employing maize
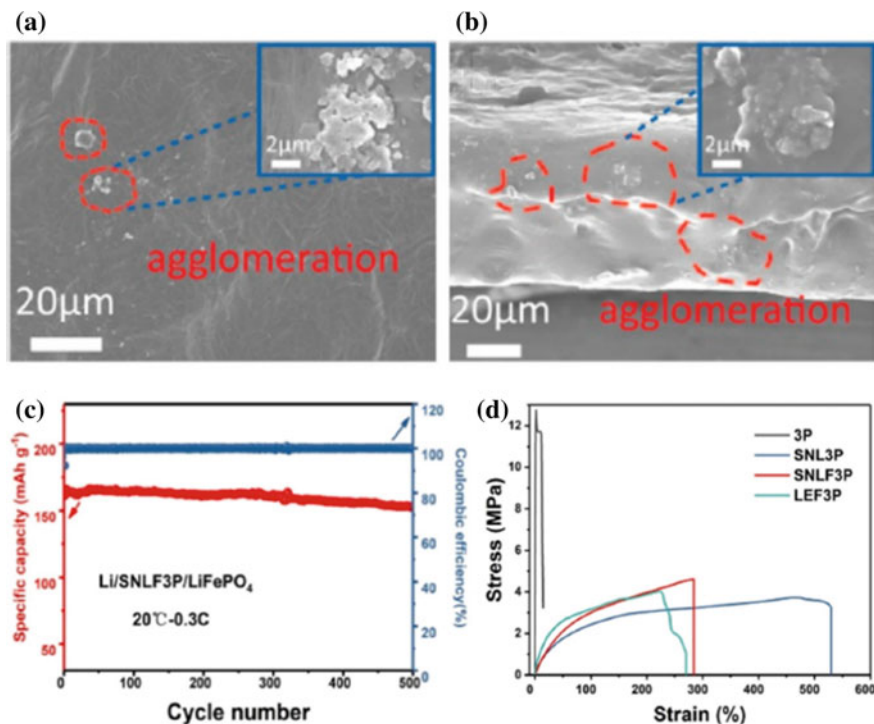
Fig. 5 **a** Surface and **b** cross-sections SEM images of as-prepared 2 wt% LLZTO/PEO. Adapted with permission from [33]. Copyright (2021) Elsevier. **c** Cycling performances of the solid-state lithium metal batteries at 0.3C. **d** Stress–strain curves of as-prepared GPE. Adapted with permission from [34]. Copyright (2021) Elsevier

straw as carbon precursors. The polarization curve of ZAB using MS-NPC presented a small voltage gap, indicating its satisfying discharge ability, with the peak power density of 127.9 mW/cm^2 which is even better than 20% Pt/C (118.6 mW/cm^2) as shown in Fig. 6b [37]. Medina Lopez then reported the electrochemical performance of flexible batteries whose graphene anodes were decorated with magnetic alloy microparticles of NiMnIn, NiMnGa, and NiMnSn. These oxides enhanced the graphene batteries' capacity, energy density, and discharge times. The highest energy density (343.5 Wh/kg) and capacity (621.7 mAh/g) were obtained for the GB that contained NiMnGa microparticles (Fig. 6c) [38].
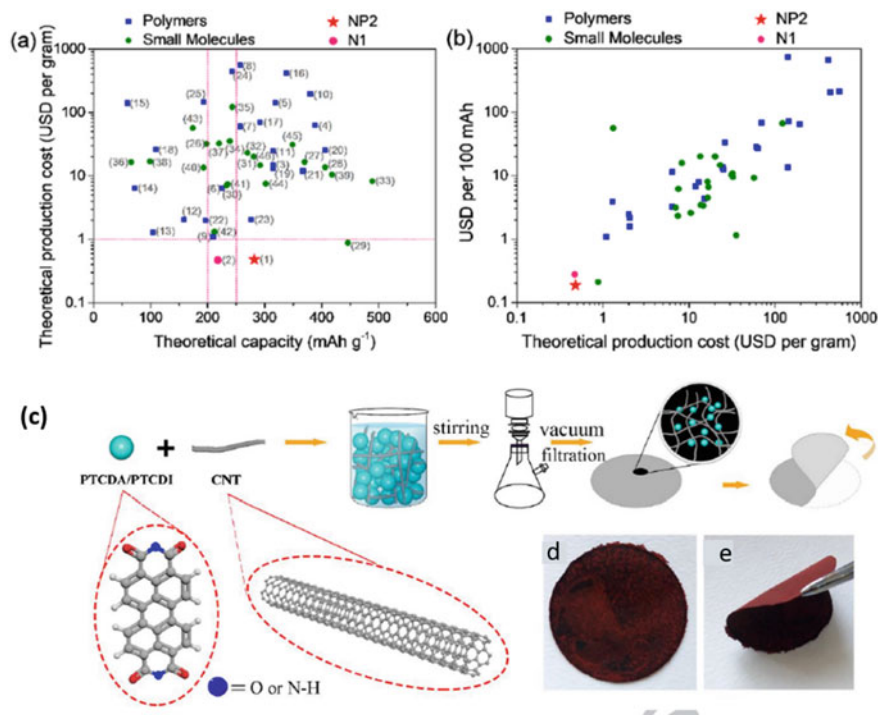
5.3 Carbonyl Compounds

Carbonyl polymers, such as poly (anthraquinonyl sulfide) and poly (benzoquinonyl sulfide), are typically selected as cathode materials for lithium-organic batteries
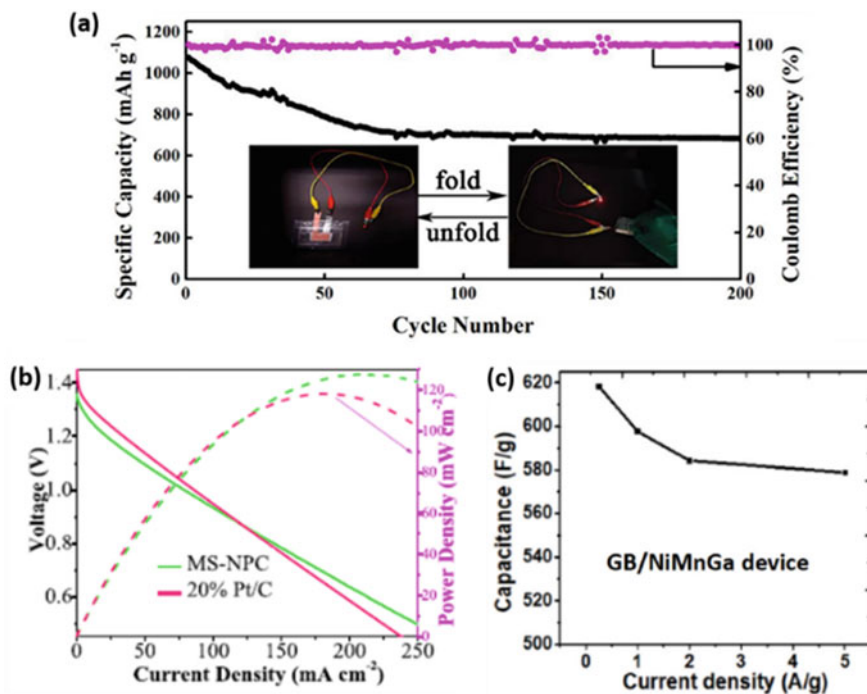
Fig. 6 **a** Cycling performance and Coulombic efficiencies of HGP/S based soft-packed LiS batteries at 0.1C under continuous bending operations. Adapted with permission from [36]. Copyright (2020) Elsevier. **b** polarization and power density curves of ZAB using MS-NPC and 20% Pt/C catalysts. Adapted with permission from [37]. Copyright (2021) Elsevier. **c** The curve of capacitance vs. current density for the GB/NiMnGa device. Adapted with permission from [38]. Copyright (2020) Elsevier

(LOBs) because of their inherent high theoretical capacity and low solubility in the electrolyte. However, their commercialization is hindered by their relatively complex synthesis routes, low yields, and high cost. Li et al. obtained a carbonyl polymer poly (piperazine-alt-benzoquinone) (NP2) from the polymerization of vanillin and piperazine with oxidative amination at the theoretical production cost of US $0.48 per gram, which exhibits a high reversible capacity of 257 mAh/g, leading to a cost performance of US $0.19 per 100 mAh (Fig. 7a, b) which is superior to the reported carbonyl polymers [39]. Fang et al. prepared sulfur-linked carbonyl polymers which have direct high-temperature sulfurization treatment of perylene-3,4,9,10-tetracarboxylic dianhydride (PTCDA) with sulfur powder and applied it in rechargeable aluminum batteries. The as-prepared PTCDA sulfide polymer (PTCDA-SP) delivers a reversible capacity of 110 mAh/g at a current density of 100 mA/g [40]. Yuan et al. then developed a free-standing and flexible film based on aromatic carbonyl compound/CNTs composite by a vacuum filtration strategy for the first time (Fig. 7c–e). The flexible organic cathode showed excellent lithium and sodium storage properties, including high reversible capacity [41].

Fig. 7 Comparison plots for reported carbonyl compounds, NP2, and N1 **a** theoretical production cost versus theoretical capacity, **b** US dollar per 100 mAh versus theoretical production cost. Adapted with permission from [39]. Copyright (2021) Elsevier. **c** Schematic illustration of the fabrication process for the PCFCs. **d** and **e** Digital photographs of the free-standing and flexible PCFCs electrode. Adapted with permission from [41]. Copyright (2018) Elsevier

5.4 Activated Carbon

Activated carbon cloth is a promising material for energy storage devices due to its flexibility, conductivity, and surface area. However, the non-optimized pore structures limit their application as electrode material in batteries with organic electrolytes, providing high energy density and power density due to the high applied cell voltage. Dai et al. synthesized a nitrogen-doped activated carbon cloth with hollow tubular fiber units, high surface area, controllable hierarchical porous structure, and beneficial surface functional groups via a simple ammonia treatment of commercial cotton fabrics. Based on this hierarchical porous hollow carbon cloth, the resulting organic-electrolyte exhibited a high specific capacitance (up to 215.9 F/g at 1 A/g) [20]. Sun et al. presented a simple strategy of using Ketjen black coated on one side of polypropylene separator as an ultralight barrier against the shuttle effect of quinone cathode in OLBs. The separator realized a high energy density of 782 Wh/kg and good capacity retention of up to 60% at 0.5C over 500 cycles [42].
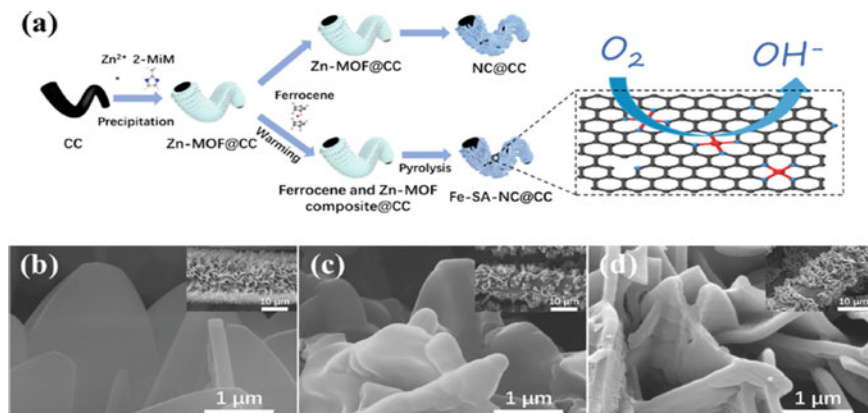
Fig. 8 a Scheme for preparing Fe-SA-NC@CC and NC@CC. SEM images of **b** Zn-MOF@CC, **c** NC@CC, and **d** Fe-SA-NC@CC. Adapted with permission from [43]. Copyright (2021) Elsevier

5.5 *Carbon Nanotubes and Nanofibers*

With the advent of flexible electronics comes an increased demand for low-cost, high-durability energy storage solutions. Flexible metal-air batteries have been explored as future power source candidates. However, the oxygen reduction reaction performance at the air cathode is often restricted by inherent electrocatalytic activity and electrode configuration. To solve these problems, Huang et al. developed a novel approach utilizing the gas diffusion and subsequent pyrolysis process based on ferrocene and zinc-based metal–organic framework (Zn-MOF) as shown in Fig. 8 below. This Zn-MOF was used to prepare nitrogen-doped carbon flakes which were modified with iron single atoms (Fe-SA) on carbon cloth (CC) as a self-supporting electrode (Fe-SA-NC@CC) for the aluminum-air battery. The aluminum-air battery showed a stable discharge voltage of ~1.5 V at 1 mA/cm^2 [43]. Wei et al. proposed and prepared a novel flexible ordered carbon nanofiber membranes including cellulose nanocrystal and MnS nanoparticles which were prepared through the microfluidic spinning technology and carbonization process. The lithium/lithium iron phosphate batteries were then assembled with the flexible device, which displayed a superior electrochemical performance [44].

6 Conclusion

Organic electrode materials are still in their infancy. Concerns about resource depletion, environmental issues, prices, and the energy density constraint of inorganic electrode materials, as well as recent electrochemical performance breakthroughs, have drawn researchers to organic electrodes. Flexible batteries and supercapacitors

are also required to support the increased demand for portable and sophisticated electronic devices. Aspects such as electrolytes, electrode materials, substrates, and device architecture have a significant impact. In addition to their established production process, organic materials have strong electrical conductivity and stable chemical and physical properties. Hybrid electrodes using carbon materials and transition metal oxides or conductive polymers have been investigated to achieve high electrochemical performance. Designing electrode materials with enhanced mechanical properties to adapt to flexing, bending, twisting, and novel nanostructures with superb electronic conductivity to facilitate charge transport requires extra care.

Furthermore, the device architecture is crucial in determining the energy density within a given mass of storage material. To achieve flexible energy devices with optimum performance, the type of electrolytes and packaging materials must also be addressed. This fundamental knowledge and peculiar applications of the various types of energy storage devices, particularly flexible supercapacitors and batteries, have been addressed in this chapter. In addition, synthesis and fabrication techniques employed in the production of carbon electrodes have been highlighted. This chapter also discussed various techniques for improving integrated storage systems with many functionalities and great flexibility to meet the demand for portable, smart, and wearable electronic and monitoring equipment.

References

1. Pandian, P. M., Pandurangan, A.: Flexible asymmetric solid-state supercapacitor of boron doped reduced graphene for high energy density and power density in energy storage device. Diam. Relat. Mater. **118**,108495 (2021)
2. Andrade, T.S., Vakros, J., Mantzavinos, D., Lianos, P.: Biochar obtained by carbonization of spent coffee grounds and its application in the construction of an energy storage device. Chem. Eng. J. Adv. **4**, 100061 (2020)
3. Maity, C.K., Hatui, G., Tiwari, S.K., Udayabhanu, G., Pathak, D.D., Chandra Nayak, G., Verma, K.: One pot solvothermal synthesis of novel solid state N-Doped TiO_2/n-Gr for efficient energy storage devices. Vacuum **164**, 88–97 (2019)
4. Wu, W., Xu, J., Tang, X., Xie, P., Liu, X., Xu, J., Zhou, H., Zhang, D., Fan, T.: Two-dimensional nanosheets by rapid and efficient microwave exfoliation of layered materials. Chem. Mater. **30**, 5932–5940 (2018)
5. Zhang, J., Shang, Q., Hu, Y., Zhang, F., Huang, J., Lu, J., Cheng, J., Liu, C., Hu, L., Miao, H., Chen, Y., Huang, T., Zhou, Y. (2020). High-biobased-content UV-curable oligomers derived from tung oil and citric acid: Microwave-assisted synthesis and properties. Eur. Polym. J. **140**, 109997
6. Zhang, B., Wang, H., Liu, C., Li, D., Kim, H.K., Harris, C., Lao, C.Y., Abdelkader, A., Xi, K.: Facile mechanochemical synthesis of non-stoichiometric silica-carbon composite for enhanced lithium storage properties. J. Alloys Compd. **801**, 658–665 (2019)
7. Souza, B.L., Chauque, S., de Oliveira, P.F.M., Emmerling, F.F., Torresi, R.M.: Mechanochemical optimization of ZIF-8/Carbon/S8 composites for lithium-sulfur batteries positive electrodes. J. Electroanal. Chem. **896**,115459 (2021)
8. Cheng, L., Du, X., Jiang, Y., Vlad, A.: Mechanochemical assembly of 3D mesoporous conducting-polymer aerogels for high performance hybrid electrochemical energy storage. Nano Energy **41**, 193–200 (2017)

9. Acharya, J., Raj, B.G.S., Ko, T.H., Khil, M.S., Kim, H.Y., Kim, B.S.: Facile one pot sonochemical synthesis of CoFe2O4/MWCNTs hybrids with well-dispersed MWCNTs for asymmetric hybrid supercapacitor applications. Int. J. Hydrogen Energy **45**, 3073–3085 (2020)

10. Iqbal, M.Z., Khan, J., Siddique, S., Afzal, A.M., Aftab, S.: Optimizing electrochemical performance of sonochemically and hydrothermally synthesized cobalt phosphate for supercapattery devices. Int. J. Hydrogen Energy **46**, 15807–15819 (2021)

11. Demirbaş, A.: Hydrogen and boron as recent alternative motor fuels. Energy Sources **27**, 741–748 (2005)

12. Ralph, T.R., Hards, G.A., Keating, J.E., Campbell, S.A., Wilkinson, D.P., Davis, M., St-Pierre, J., Johnson, M.C.: Low cost electrodes for proton exchange membrane fuel cells: performance in single cells and ballard stacks. J. Electrochem. Soc. **144**, 3845–3857 (1997)

13. Buckley, D.N., O'Dwyer, C., Quill, N., Lynch, R.P.: Electrochemical Energy Storage. In: Energy storage options and their environmental impact, pp. 115–149. The Royal Society of Chemistry (2019)

14. Esser, B., Dolhem, F., Becuwe, M., Poizot, P., Vlad, A., Brandell, D.: A perspective on organic electrode materials and technologies for next generation batteries. J. Power Sources **482**, 228814 (2021)

15. Gannett, C.N., Melecio-Zambrano, L., Theibault, M.J., Peterson, B.M., Fors, B.P., Abruña, H.D.: Organic electrode materials for fast-rate, high-power battery applications. Mater Rep. Energy **1**, 100008 (2021)

16. Ahmad, Y., Colin, M., Gervillie-Mouravieff, C., Dubois, M., Guérin, K.: Carbon in lithium-ion and post-lithium-ion batteries: recent features. Synth. Met. **280**, 0–2 (2021)

17. Ghanashyam, G., Kyung, H.: Plasma treated carbon nanofiber for flexible supercapacitors. J. Energy Storage **40**, 102806 (2021)

18. Chen, W., Wang, H., Lan, W., Li, D., Zhang, A., Liu, C.: Industrial crops & products construction of sugarcane bagasse-derived porous and flexible carbon nanofibers by electrospinning for supercapacitors. Ind. Crop. Prod. **170**, 113700 (2021)

19. Wang, T., He, X., Gong, W, Sun, K., Lu, W., Yao, Y., Chen, Z.: Flexible carbon nano fi bers for high-performance free-standing supercapacitor electrodes derived from Powder River Basin coal. Fuel **278**, 117985 (2020)

20. Dai, P., Zhang, S., Liu, H., Yan, L., Gu, X., Li, L., Liu, D., Zhao, X.: Electrochimica acta cotton fabrics-derived flexible nitrogen-dope d activate d carbon cloth for high-performance supercapacitors in organic electrolyte. Electrochim Acta **354**,136717 (2020)

21. Song, P, He, X., Tao, J., Shen, X., Yan, Z., Ji, Z., Yuan, A., Zhu, G., Kong, L.: H$_2$SO$_4$-assisted tandem carbonization synthesis of PANI @ carbon @ textile flexible electrode for high-performance wearable energy storage. Appl. Surf. Sci. **535**, 147755 (2021)

22. Flores-Larrea, L., Rivera-Mayorga, J.A., Kshetri, Y.K., Rodriguez-Gonzalez, V., Garcia, C.R., Lee, S.W., Oliva, J.: Highly efficient textile supercapacitors fabricated with graphene/NiO:Yb electrodes printed on cotton fabric. J. Alloys Compd. **886**, 161219 (2021)

23. Na, R., Lu, N., Zhang, S., Huo, G., Yang, Y., Zhang, C., Mu, Y., Luo, Y., Wang, G.: Facile synthesis of a high-performance, fire-retardant organic gel polymer electrolyte for fl exible solid-state supercapacitors. Electrochim Acta **290**, 262–272 (2018)

24. Ensafi, A.A., Heydari-Soureshjani, E., Taghipour-Jahromi, A.R., Rezaei, B.: Bimetallic metal organic framework-derived for both battery-like supercapacitor (electrolyte study) and hydrogen evolution reaction. Electrochim Acta **395**, 139192 (2021)

25. Li, X., Tang, Y., Song, J., Yang, W., Wang, M., Zhu, C., Zhao, W., Zheng, J., Lin, Y.: Self-supporting activated carbon/carbon nanotube/reduced graphene oxide fl exible electrode for high performance supercapacitor. Carbon N Y **129**, 236–244 (2018)

26. Jeon, H., Jeong, J.-M., Hong, S.B., Yang, M., Park, J., Kim, D.H., Hwang, S.Y., Choi, B.G.: Facile and fast microwave-assisted fabrication of activated and porous carbon cloth composites with graphene and MnO2 for flexible asymmetric supercapacitors. Electrochim Acta **280**, 9–16 (2018)

27. Zhu, Z., Zhang, Z., Zhuang, Q., Gao, F., Liu, Q., Zhu, X., Fu, M.: Growth of MnCo2O4 hollow nano-spheres on activated carbon cloth for flexible asymmetric supercapacitors. J. Power Sources **492**, 229669 (2021)

28. Liu, T., Li, C., Liu, H., Zhang, S., Yang, J., Zhou, J, Yu, J., Ji, M., Zhu, C., Xu, J.: Tear resistant Tyvek/Ag/poly (3,4-ethylenedioxythiophene): Polystyrene sulfonate (PEDOT:PSS)/carbon nanotubes electrodes for flexible high-performance supercapacitors. Chem. Eng. J. **420**, 127665 (2021)

29. Yang, K., Luo, M., Zhang, D., Liu, C., Li, Z, Wang, L., Chen, W., Zhou, X.: Ti3C2Tx/carbon nanotube/porous carbon film for flexible supercapacitor. Chem. Eng. J. **427**, 132002 (2022)

30. Hamra, A.A.B., Lim, H.N., Huang, N.M., Gowthaman, N.S.K., Nakajima, H., Rahman, M.M.: Microwave exfoliated graphene-based materials for flexible solid-state supercapacitor. J. Mol. Struct. **1220**, 128710 (2020)

31. Yang, C., Yang, J., Liang, C., Zang, L., Zhao, Z., Li, H., Bai, L.: Flexible supercapacitors with tunable capacitance based on reduced graphene oxide/tannin composite for wearable electronics. J. Electroanal. Chem. **894**, 115354 (2021)

32. Liu, P., Niu, J., Wang, D. (2021). Honeycomb-like mesoporous all-carbon graphene-based fiber for flexible supercapacitor application: effect of spacers. Colloids Surf. A Physicochem. Eng. Asp. **616**, 126291

33. Guo, Q, Xu, F., Shen, L., Wang, Z., Wang, J., He, H., Yao, X.: Poly(ethylene glycol) brush on Li6.4La3Zr1.4Ta0.6O12 towards intimate interfacial compatibility in composite polymer electrolyte for flexible all-solid-state lithium metal batteries. J. Power Sources **498**, 229934 (2021)

34. Ye, X., Xiong, W., Huang, T., Li, X., Lei, Y., Li, Y., Ren, X., Liang, J., Ouyang, X., Zhang, Q., Liu, J.: A blended gel polymer electrolyte for dendrite-free lithium metal batteries. Appl. Surf. Sci. **569**, 150899 (2021)

35. Pandurangan, S., Kaliyappan, K., Ramaswamy, A. P., Ramaswamy, M.: Polymer-garnet composite electrolyte based on comb-like structured polymer for lithium-metal batteries. Mater. Today Energy **21**, 100836 (2021)

36. Yang, J., Shan, X., Guo, Z, Duan, L., Zhang, X., Lü, W.: A facile synthetic strategy of free-standing holey graphene paper as sulfur host for high-performance flexible lithium sulfur batteries. J. Electroanal. Chem. **876**, 114728 (2020)

37. Hao, X., Chen, W., Jiang, Z., Tian, X., Hao, X., Maiyalagan, T., Jiang, Z. J.: Conversion of maize straw into nitrogen-doped porous graphitized carbon with ultra-high surface area as excellent oxygen reduction electrocatalyst for flexible zinc–air batteries. Electrochim Acta **362**, 137143 (2020)

38. Lopez-medina, M., Hernandez-navarro, F., Mtz-enriquez, A.I., Oliva, A.I.: Enhancing the capacity and discharge times of flexible graphene batteries by decorating their anodes with magnetic alloys NiMnM x (M x = Ga , In , Sn). **256** (2020)

39. Li, C., Liu, X., He, Z., Tao, W., Zhang, Y., Zhang, Y., Jia, Y., Yu, H., Zeng, Q., Wang, D., Xin, J.H., Duan, C., Huang, F.: Low-cost carbonyl polymer design for high-performance lithium-organic battery cathodes. J. Power Sources **511**, 230464 (2021)

40. Fang, L., Zhou, L., Cui, L., Jiao, P., An, Q., Zhang, K.: Sulfur-linked carbonyl polymer as a robust organic cathode for rapid and durable aluminum batteries. J. Energy Chem. (2021)

41. Yuan, C., Wu, Q., Shao, Q., Li, Q., Gao, B., Duan, Q.: Free-standing and flexible organic cathode based on aromatic carbonyl compound/carbon nanotube composite for lithium and sodium organic batteries. J. Colloid Interface Sci. (2018)

42. Sun, Y., Wang, X., Yang, A., Huang, Y., Jia, W., Jia, D.: Functional separator with a lightweight carbon-coating for stable, high-capacity organic lithium batteries. **418**, 1–9 (2021)

43. Huang, L., Zang, W., Ma, Y., Zhu, C., Cai, D., Chen, H., Zhang, J., Yu, H., Zou, Q., Wu, L., Guan, C.: In-situ formation of isolated iron sites coordinated on nitrogen-doped carbon coated carbon cloth as self-supporting electrode for flexible aluminum-air battery. Chem. Eng. J. **421**, 129973

44. Wei, L., Deng, N., Wang, X., Zhao, H., Yan, J., Yang, Q., Kang, W., Cheng, B.: Flexible ordered MnS@CNC/carbon nanofibers membrane based on microfluidic spinning technique as interlayer for stable lithium-metal battery. J. Memb. Sci. **637**, 119615 (2021)

Electrochemically Generated Organic Polymeric Electrodes for Application in Electronics and Optoelectronics

Miguel A. Gervaldo, Yone M. Renfige Rodriguez, Raúl A. Rubio, Lorena P. Macor, Claudia A. Solis, Javier E. Durantini, and Luis A. Otero

Abstract In this chapter some practical applications of electrochemically generated polymers are described. This chapter is focused on the utilization of electrochemically generated organic polymeric electrodes in electronic and optoelectronic devices. Electropolymerization is a very versatile procedure that can be used to construct organic films over metallic contacts or transparent conducting oxides. By selecting the correct polymerization group and the correct desired functionality, a significant number of monomers can be designed and synthesized to generate polymers. Some examples of devices based on electrogenerated organic polymers are solar cells, supercapacitors, and electrochromic devices. Solar cells convert sunlight into electric energy. Light absorption by the photoactive material produces electron–hole pairs, which are later separated, and they travel to the electronic contacts generating an electric work. Supercapacitors can store the energy generated by other energy sources with the ability to transform it into electric energy for its utilization when it is necessary. Electrochromic devices can modulate the light intensity and spectral distribution that go through them by modifications in their optical properties when their redox properties are changed.

Keywords Electropolymerization · Perovskite · Supercapacitors · Electrochromics · Organic polymers

1 Electropolymerization

Electropolymerization or electrochemical polymerization has emerged as a powerful tool to produce organic or organometallic polymeric films over a large number of solid electrode materials [1]. The methodology involved in electropolymerization

M. A. Gervaldo (✉) · Y. M. R. Rodriguez · R. A. Rubio · L. P. Macor · C. A. Solis · J. E. Durantini · L. A. Otero
Departamento de Química, Instituto de Investigaciones en Tecnologías Energéticas y Materiales Avanzados (IITEMA), Universidad Nacional de Río Cuarto-CONICET Agencia Postal Nro. 3, X5804BYA Río Cuarto, Córdoba, Argentina
e-mail: mgervaldo@exa.unrc.edu.ar

is very simple and reproducible, and it has several advantages over chemical polymerization and other deposition methods. Depending on the electrochemical technique used, film thicknesses can be easily controlled by changing the experimental conditions such as scan rate, deposition time, monomer concentration, and potential window, for example. In the same way, the morphology of the obtained films can be modified by varying experimental conditions and electrochemical parameters. Electrogenerated films commonly present better adherence to the substrates than covalent adsorbed molecules are rarely dissolved by organic compounds. Compared to chemical synthesis, electropolymerization is carried out in just one single step and the obtained polymers do not require a posterior purification because only the monomer is present in the solution. Also, it does not produce several amounts of waste. Moreover, depending on the required polymer application, several monomers can be designed by just choosing the correct electropolymerizable and functional groups.

2 Electrochemical Techniques Used for Electropolymerization

Electrochemical polymerization is commonly carried out using potentiostatic (constant potential), potentiodynamic (cyclic voltammetry (CV) or pulsed potential), galvanostatic (constant current) or galvanodynamic (pulsed current) techniques [1].

Potentiodynamic polymerization requires the use of the CV technique. In a typical potentiodynamic polymerization, the applied potential is linearly increased from an initial to a final or inversion potential value, switched back to the initial potential and then the cycle is repeated. During this cycling, the monomer can be oxidized and then reduced again, and by the application of several cycles, polymerization film deposition occurs. Besides, increases in the oxidation–reduction peak currents are observed on successive cycles and commonly new redox systems related to oxidation–reduction of the polymer appear.

Potentiostatic polymerization consists of the application of a constant potential value close to the oxidation (or reduction) potential of the monomer for a determinate time. By changing the applied potential time, the thickness and polymer length are controlled. To know the applied potential needed to produce the polymerization process, a previous electrochemical characterization is recommended. By using CV, the monomer oxidation/reduction potential values are determined and posteriorly used in the potentiostatic polymerization. These redox values are necessary to obtain the potential window where the polymerization process may happen and to avoid side reactions or monomer overoxidation.

Galvanostatic polymerization consists of the application of constant current for a determinate time. Generally, when the current starts flowing, the monomer is oxidized forming radical cations that couple one to each other enlarging the polymeric chain. In a galvanodynamic polymerization, current pulses are applied to the monomer

solution, when the current passes through the solution, oxidation of the monomer occurs and film growing is observed. On the contrary, when the current is removed no further polymerization is observed.

Electrochemical polymerization commonly proceeds by a mechanism that involves oxidation or reduction of the monomer, although oxidative polymerization is commonly seen. Electrochemical oxidation of the monomers produces radical cations which react with other radical cations or with a neutral monomer generating dimers. These dimers precipitate over the electrode surface and can be later oxidized again generating new dimeric radical cations that couple with other radical cations, (or dimers) extending the polymeric chain. This polymerization mechanism is commonly accepted for polyaniline (PANI), polycarbazole (PCBZ), and Poly(3,4-ethylenedioxythiophene) (PEDOT), being the resulting polymers lineal (Fig. 1a). Another way to obtain linear polymers is by the use of monomers containing a target functionality or a central core substituted with two electropolymerizable groups, where one of the two reactive positions are blocked, leading to a polymer with the cores connected by dimmers (Fig. 1a). This approach is commonly used for example, in donor–acceptor polymers. Tridimensional or branched polymers can be obtained using monomers with star-shaped or dendritic structures containing electropolymerizable groups (Fig. 1a).

3 Equipment and Experimental Setup Used for Electropolymerization

Nowadays several commercially available electrochemical workstations have all the above-mentioned technique capabilities, known as potentiostat–galvanostat. These have different specifications, such as DC-potential range, compliance voltage, maximum current, acquisition rate, applied dc-potential resolution, applied potential accuracy, current ranges, current accuracy, and so on.

In most of the electrochemical techniques used for electropolymerization, a conventional three-electrode cell is used (Fig. 1b). These electrodes are named working, reference and counter, and they are immersed in the solvent-electrolyte system where the monomer is dissolved. The working electrode (where the redox reactions occur) can be Pt, Au, glassy carbon, pyrolytic graphite, and a conductive transparent glass such as Indium Tin Oxide (ITO). The reference electrode measures the potential at the working electrode and it can be an Ag–AgCl reference electrode, which consists of an Ag wire coated with a silver chloride layer immersed in saturated KCl solution (used in aqueous electrolyte-solution), or a silver wire (pseudoreference) is used with organic solvents. The counter electrode is commonly made of a large area of inert metal such as Pt.

Polymers generated by electrochemical techniques present several advantages over other deposition and synthetic methods. The electropolymers are very functional
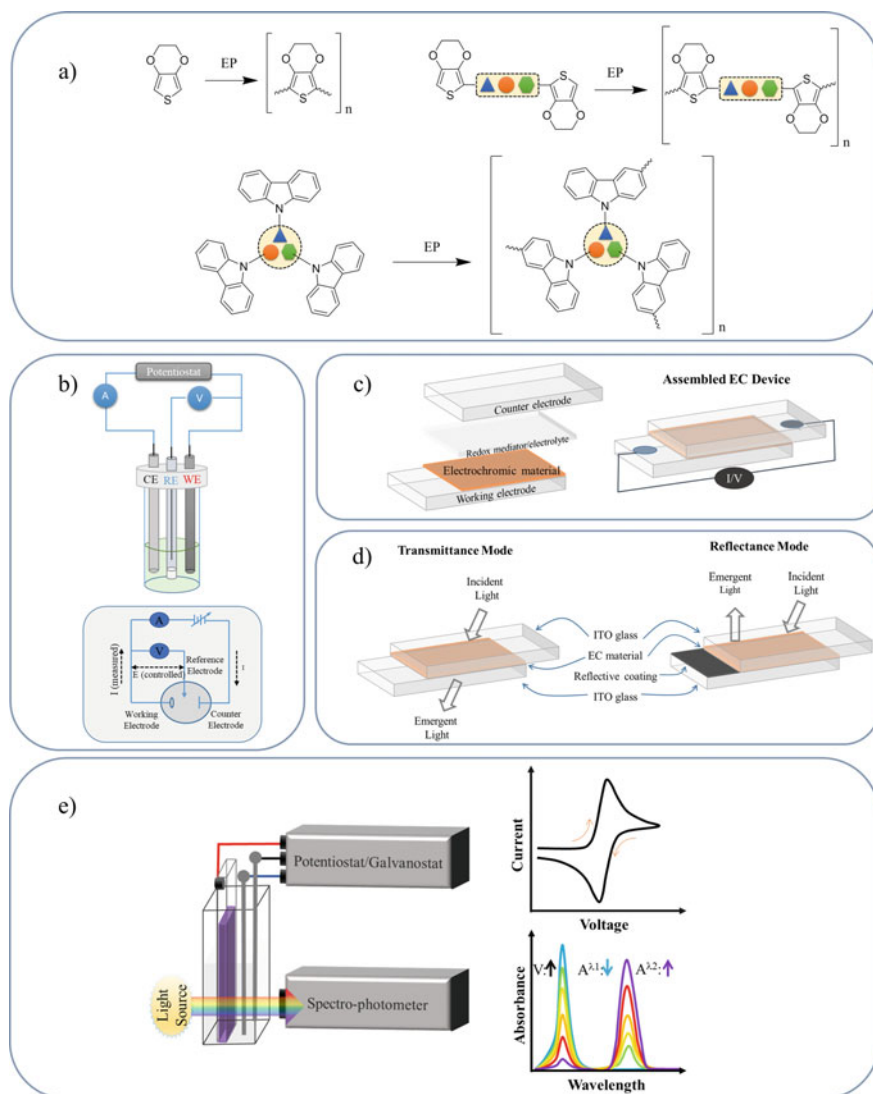
Fig. 1 **a** Different types of polymers. **b** Three electrode cell configuration. **c** Schematic representation of an EC device. **d** EC device operation modes. **e** Schematic representation of a spectroelectrochemical cell

materials with numerous applications in electronic and optoelectronic devices. In the following section, some of these applications will be described.

4 Applications of Electropolymers in Electronic and Optoelectronic Devices

4.1 Electrochromics

Originally suggested by J. R. Platt in 1961 [2], electrochromism is defined as a reversible change in the optical properties of a material when an external potential is applied to it. The changes in the optical properties of the materials are related to modifications in their redox processes. When the electrochromic (EC) material is oxidized or reduced, it changes its redox state and its electronic structure, and as a result, the absorption spectra in the different redox states are different, leading to several colorations. The first studies on electrochromism were focused on the obtention of materials with changes in the visible region for their uses principally in smart windows [3]. Later their applications were extended to IR smart windows [4], military camouflage [5], thermal control, and optical communication [6]. The simplest architecture of an EC device needs a working electrode where the active material suffers optical changes, a counter electrode, and an electrolyte for ionic transport between the electrodes (Fig. 1c). The EC material is deposited by different techniques over the working electrode (spin coating, spray coating, electrochemical polymerization, etc.). Commonly, the two electrodes (working and counter) are sandwiched containing a liquid or a gel electrolyte between them. EC devices present two operation modes: by transmission or reflectance (Fig. 1d). In the transmission mode, the two electrodes must be transparent to allow light passage through the devices. In the reflectance mode, one of the electrodes is transparent while the other one is coated with a reflective layer like gold, silver, or aluminum.
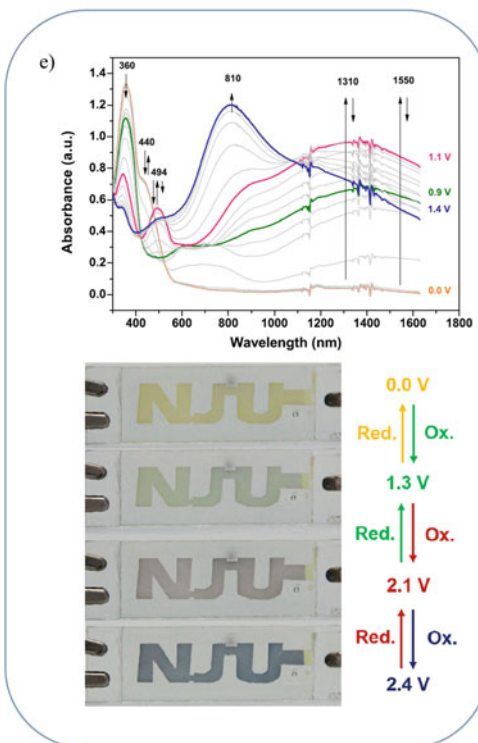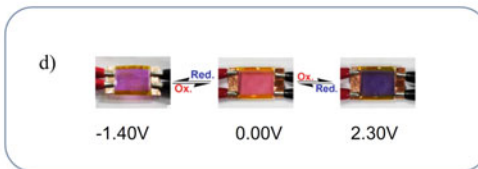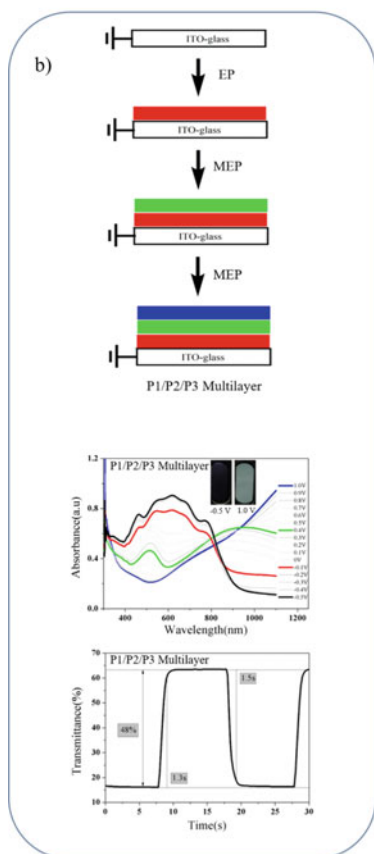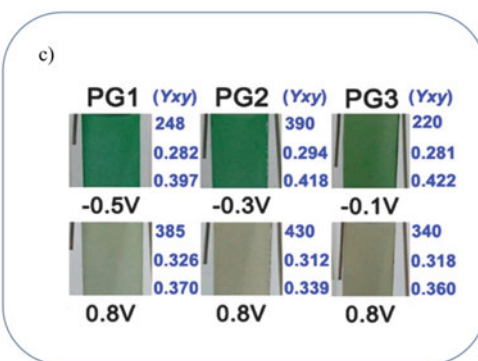
In the development of a new EC material, the initial characterization is commonly carried out by CV, where the material has previously been deposited over an electrode or is dissolved in the electrolyte solution. This characterization is performed in a three-electrode cell configuration. By analysis of CV, the redox processes that suffer the material can be identified. The spectral changes that occur during oxidation or reduction of the EC material are studied by spectroelectrochemistry. In this technique, the spectroscopic properties of the material are monitored as a function of the applied potential (Fig. 1e). The performance of an EC material is made by comparison of standard parameters such as optical contrast (ΔT, ΔA, and ΔOD), which is defined as the maximum transmittance, absorbance, and optical density change between two different states, for example, bleached and colored. The response time (for colored or bleached state) is defined as the time required to reach a change of 95% of the maximum transmittance or absorbance at a defined applied potential. The coloration efficiency (CE) is the change in optical density ΔOD for the charge consumed per unit of electrode area (cm^2/C). Cyclic stability is the capacity of a material to maintain its initial EC properties under repetitive cycling [7]. By a combination of electrochemical and spectroelectrochemical studies, the above-mentioned parameters can be obtained.

Until now, several organic and inorganic compounds have been studied as EC materials. The most investigated inorganic materials include tungsten trioxide (WO_3), vanadium pentoxide (V_2O_5), nickel oxide (NiO), and other transition metal oxides [8]. The organic EC materials can be divided into two classes: small molecules and conducting polymers. Conducting polymers have several advantages; they form good quality films, easy processing, and by chemical modification of monomer structure EC polymers with different colorations can be obtained. Typical examples of EC polymers include PEDOT, poly(pyrrole) (PPy), poly(thiophene) (PTh), PANI, and their derivatives [9]. These polymers can be deposited over metallic and transparent (ITO) electrodes by electrochemical polymerization. Apart from these, several related polymers can be created by using monomers containing the desired functionality unit substituted with electropolymerizable groups, obtaining polymers with linear, branched, or dendritic structures. Some examples of these kinds of polymers electrochemically synthesized, and strategies to achieve the wanted color are mentioned in the following paragraphs.

Black to transmissive EC materials presents several applications in energy-saving windows, electronic paper, and switchable displays. To obtain films with a black coloration the material must have absorption in the whole visible range, although this is difficult to find in a unique polymer. A strategy to obtain a black color is by the combination of two or more polymers with absorptions in different regions, covering all the visible wavelengths. For example, by changing the monomer feed ratios (EDBT to MTTP (Fig. 2a)) in the electrochemical copolymerization of two donor–acceptor monomers with green and blue colors in their neutral states, copolymers with different spectral characteristics were obtained (Fig. 2a) [10]. The EDBT:MTTP = 1:1 ratio was conducted to the obtention of a black copolymer (called PEM-11) in the neutral state. PEM-11 showed a good cyclability, retaining 94% of its electroactivity after 2000 cycles, a ΔT of 35% at 590 nm and a 64% in the NIR region (1500 nm), and switching times of 0.6 and 0.8 s between the neutral and oxidized states.

In a similar approach, a black-to-transmissive EC material was designed using three EDOT based polymers (named as P1, P2, and P3) [11]. By sequential electropolymerization of the corresponding monomers in a layered structure (Fig. 2b), films with black coloration were obtained by additive primary colors red (P1), green (P2), and blue (P3). The multilayered films (P1/P2/P3, P2/P1/P3, and P3/P2/P1) presented a wide absorption band in the 350 to 850 nm region covering the visible spectrum. P1/P2/P3 multilayer had a CE of 151.6 cm^2/C, a ΔT of 48%, and switching times of 1.3 s and 1.5 for the colored and bleached state respectively.

EC polymers with changes between green and brown, and also with absorptions in the IR regions can be used for military camouflage. Polymers with these characteristics were obtained by electropolymerization of donor–acceptor monomers containing two EDOT units covalently connected to quinoxaline benzene disubstituted [5]. In the neutral state the so-called PG1, PG2, and PG3 polymers showed a green coloration, while in the oxidized state they presented a sand-brown coloration and the presence of bands in the NIR and IR regions (Fig. 2c). PG3 was used as EC material in a sandwich-like EDC.

a)

H3CO   OCH3

PMTTP

COPOLYMERIZATION

PEM-11

PEDBT

b)

ITO-glass

EP

ITO-glass

MEP

ITO-glass

MEP

ITO-glass

P1/P2/P3 Multilayer

P1/P2/P3 Multilayer

-0.5 V   1.0 V

Absorbance(a.u)

Wavelength(nm)

P1/P2/P3 Multilayer

1.3s

48%

1.3s

Transmittance(%)

Time(s)

c)

PG1 (Yxy)   PG2 (Yxy)   PG3 (Yxy)

248	390	220
0.282	0.294	0.281
0.397	0.418	0.422

-0.5V   -0.3V   -0.1V

385	430	340
0.326	0.312	0.318
0.370	0.339	0.360

0.8V   0.8V   0.8V

d)

Red.   Ox.
Ox.   Red.

-1.40V   0.00V   2.30V

e)

360

440

494

810   1310   1550

1.1 V

0.9 V
1.4 V

0.0 V

Absorbance (a.u.)

Wavelength (nm)

0.0 V
Red.   Ox.
1.3 V
Red.   Ox.
2.1 V
Red.   Ox.
2.4 V

◄**Fig. 2** **a** Chemical structure and coloration of the polymers used in the copolymerization processes, and color of the resulting copolymer (PEM-11). Adapted with permission from Ref. [10], Copyright 2020, Elsevier Ltd. **b** Scheme of the multilayer electrochemical polymerization for P1/P2/P3 multilayer, the absorption spectrum of P1/P2/P3, and transmittance change between the redox states. Reprinted with permission from Ref. [11], Copyright 2021, Elsevier Ltd. **c** Photographs and corresponding (Y; x; y) values of PG1, PG2 and PG3 film on an ITO-coated glass slide in the fully neutral and oxidized states. **d** Photos of sandwich-type ITO-coated glass EC devices using the TPAPTPI film as an active layer. Adapted with permission from Ref. [12], Copyright 2017, Elsevier Ltd. **e** Absorption spectra of PDTP-Ph-TPA on ITO at various applied potentials and photographs showing the color change of EC devices at different applied potentials. Adapted with permission from Ref. [13], Copyright 2014, Elsevier Ltd. **c** Adapted with permission from Ref. [5]. Copyright Yu, H., Shao, S., Yan, L., Meng, H., He, Y., Yao, C., Xu, P., Zhang, X., Hu, W., Huang, W., some rights reserved; exclusive licensee Royal Society of Chemistry. Distributed under a Creative Commons Attribution License 3.0 (CC BY) https://creativecommons.org/licenses/by/3.0/

Another color needed to create RGB (red, green, blue) devices is the red one. A red-colored polymer was synthesized using an ambipolar monomer formed by a perylene diimide core connected to two triphenylamine (TPA) units (TPA-PTDI) [12]. In the neutral form, the polymer (TPA-PTPI) exhibited an Indian red color, while in the fully oxidized state the color changed to deep blue. In the first reduced state of TPA-PTPI, almost no change in its color was seen while at more negative potentials a violet color was observed. TPA-PTPI showed a ΔT of 73%, a switching time of 6.1 s at 715 nm, and a loss of 10% in T after 100 step cycles between the neutral and oxidized states. The authors fabricated a sandwich-type EC device (Fig. 2d) with red coloration in the neutral state, a blue-purple color at 2.3 V, and a violet color at -1.40 V.

EC materials that work in both the UV–Vis and near-IR region are very attractive because it is possible to follow the near-IR EC process with the naked eye. To do this, a monomer (called DTP-Ph-TPA) containing both 3,4-dithienylpyrrole (DTP) and TPA was electropolymerized [13]. PDTP-Ph-TPA polymer showed a yellow color in the neutral state and in the first oxidized state the color turned green with two absorption bands in the 1000 to 1650 nm range. In the second and fully oxidized states, pink and blue colors were observed respectively. PDTP-Ph-TPA had a ΔT of about 70% at 1550 and 1310 nm, with responses times of 2.8 and 1.4 s and a CE of 125 cm^2/C at 1550 nm. The sandwich-like device exhibited several colors in the potential range between 0 and 2.4 V (Fig. 2e).

4.2 Solar Cells

Solar energy is a clean, abundant, and free available source of energy that could be a solution to the increasing energy demand. In this frame, photovoltaic solar cells are devices that convert solar energy into electrical work. There are several photovoltaic solar cell types such as silicon, CIGS (copper indium gallium diselenide), cadmium

telluride (CdTe), quantum dots, dye-sensitized, organic and perovskite (PS) based solar cells among others.

Perovskite solar cells (PSSCs) have significantly attracted the interest of the research community due to their low cost, easy manufacturing, and high power conversion efficiency (PCE). PCEs have increased from the 3.8% in 2009 to around 25% to the present [14]. Organic–inorganic and all inorganic PS have a general ABX_3 structure (Fig. 3a), where A is a monovalent cation (Cs^+, Rb^+, methylammonium (MA^+), or formamidinium (FA^+)), B is a divalent metal cation (Pb^{2+} or Sn^{2+}), and X is a halide anion (I^-, Br^-, Cl^-, or their combinations). Typically, PSSCs are formed by five layers; a transparent conductive oxide, an electron selective contact and transporting layer (ETL), a light-absorbing PS material, a hole selective contact and transporting layer (HTL), and a metal electrode. PSSCs can be classified into two major configurations; regular and inverted (Fig. 3b). In both cases, the working principle is the same. After light absorption by the PS layer, electron–hole pairs are created, then the holes and electrons travel to the corresponding selective transport layers and finally to the contacts (Fig. 3c).

Comparison of the PSSCs performance is made by PCE = (P_{max}/E_{tot} A) $_\times$ 100, where P_{max} (I_m x V_m) is the max power of the cell, A is the cell area, and E_{tot} is the total incident irradiance (under incident light irradiation of AM1.5G at 100 mW cm^{-2}). From the I-V curves (current–voltage) I_m (max short-circuit current), V_m (max open circuit voltage), I_{sc} (short-circuit current) and V_{oc} (open circuit voltage) can be obtained (Fig. 3d). Fill factor (FF) is defined as FF = ($I_m \times V_m$)/($I_{sc} \times V_{oc}$) [15]. One more important parameter is the incident photon-to-current efficiency (IPCE), IPCE = (J_{sc} 1240/P_{inc} λ) where J_{sc} (A cm^{-2}) is the short circuit current density, P_{inc} (W cm^{-2}) is the power of the incident light at the measured wavelength, and λ is the wavelength (nm). In an IPCE graph, IPCE is plotted versus λ, and commonly this graph is compared with the absorption spectrum of the photoactive material (Fig. 3e). A match between both graphs is indicative that the photoactive material is responsible for the observed photocurrents. The setups used on the obtention of I–V curves and IPCE are depicted in Fig. 3f, g.

One of the most relevant aspects to further improve the performance and stability of the PSSC is the material engineering for the interfaces between the PS and the HTL and between the PS and the ETL. Numerous HTLs and ETLs have been used in PSSCs including small molecules [16], organic polymers [17], and p-type (HTL) and n-type (ETL) inorganic semiconductors [18]. Organic polymers present several advantages such as solution processing at low temperatures, mechanical flexibility, decent hole mobility and they can avoid thermal-induced diffusion and segregation in the interfaces under working conditions [19–22]. Most of these polymeric transport materials are deposited by spin coating, a method that produces large amounts of waste. The HTLs and ETLs deposited by this method, not only need to be soluble in the appropriate solvent but also, can be partially removed from the substrate by the solvent used in the posterior PS layer deposition step. Electrochemical polymerization allows the obtention of HTL and ETL materials directly generated over contact collector electrodes.
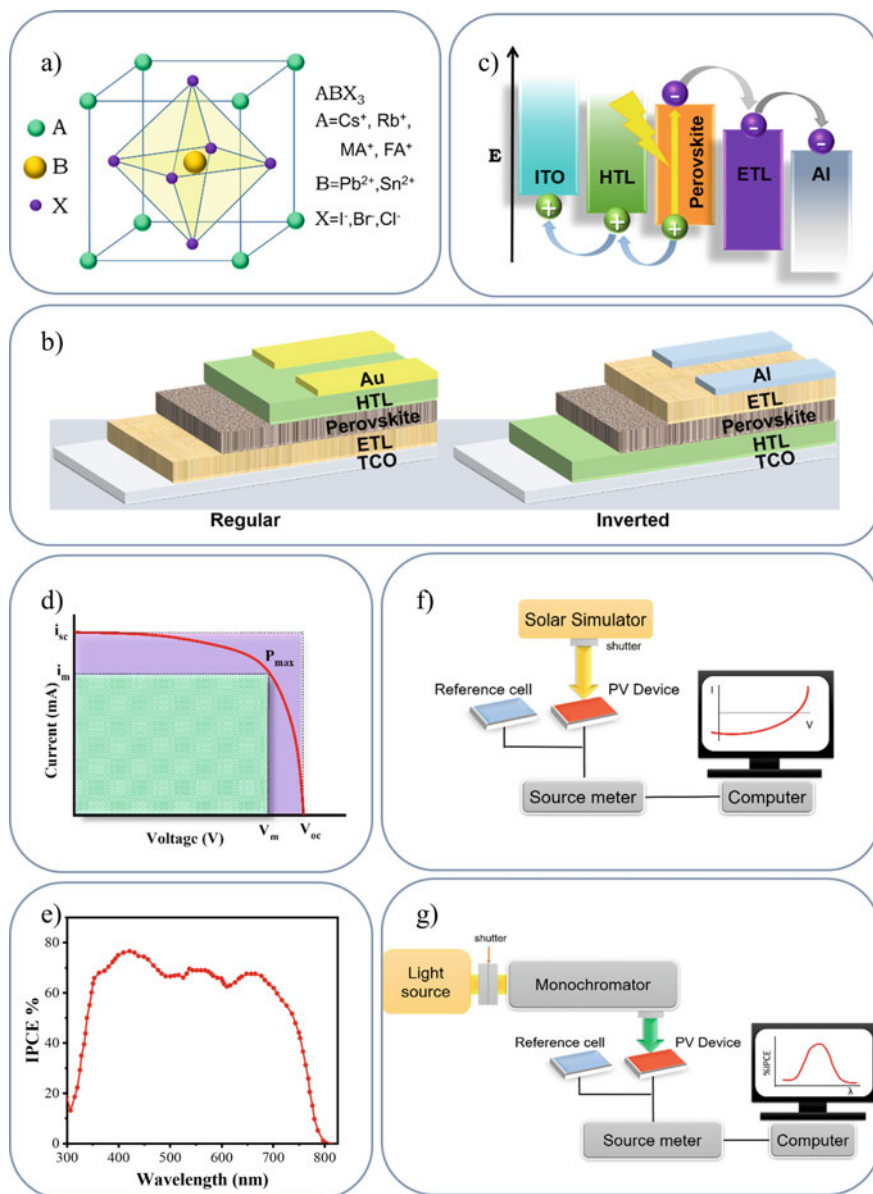
Fig. 3 **a** General structure of PS. **b** Different PSSC configurations. **c** PSSCs working mechanism. **d** I–V curve. **e** IPCE plot. **f** Setup for obtention of I-V curves. **g** Setup for obtention of IPCE

In this sense, PANI was one of the first electropolymers used as HTL in PSSC[23]. It was deposited over FTO electrodes using a two-step CV methodology. A sandwich-like configuration was fabricated using a double TiO_2 (blocking and mesoporous) layer deposited over FTO (photoanode) and the FTO/PANI electrode (cathode). The PS layer was formed by injecting a $CH_3NH_3PbI_3$/g-butyrolactone solution in the gap between the two electrodes. The polymer presented correct HOMO and LUMO values to allow a good electron and hole transport with the PS layer (Fig. 4a). The PSSC with PANI as HTL showed a PCE of 7.3% and it decreased to 6.7% after 1000 h of operation indicating good stability. Posteriorly the same authors used electropolymerized PEDOT instead of PANI as HTL [24]. The PSSC with PEDOT had a much better performance than PANI, with front and rear PCEs of 12.33% and 11.78% respectively.

The effect of the HTL HOMO level on the performance of PSSCs was studied using different polymers prepared by electrochemical polymerization (Fig. 4b) [25]. After optimization of the HTLs thicknesses, ITO/HTM/$CH_3NH_3PbI_3$/C_{60}/BCP/Ag inverted solar cells were fabricated using the different electropolymers. It was found that the V_{oc} of the devices constructed with the different HTLs increased with the work function of the HTL closer to the HOMO level of the PS. Finally, the best-optimized device showed a PCE of 16.5%, a FF of 0.75, a V_{oc} of 1.03 $_V$, and a J_{sc} of 21.6 mA/cm^2.

Carbazole-based polymers are also worth mentioning. A carbazole monomer was electropolymerized by CV over ITO electrodes and the film (called PAF-86) was used as HTL in an inverted PSSC [26]. Freshly prepared PSSC presented a PCE of 5.04%, J_{sc} of 13.1 mA/cm^2, V_{oc} of 0.98 V, and a FF of 0.39. After 5 days without encapsulation, there was an improvement in the PCE (9.48%) (Fig. 4c), which was attributed to better surface contact between PS and PAF-86 film. The IPCE% spectrum showed values of around 70% in the 390 to 760 nm range, matching the absorption spectrum of the PS layer (Fig. 4c).

In the above-mentioned examples, the HTLs were electropolymerized over the FTO electrode and then the PS layer was deposited over the HTL. An interesting aspect in the formation of the PSSC is the deposition of the HTL over the PS layer. Samu et al. [27] demonstrated for the first time the electrodeposition of a PEDOT layer directly over a PS film and its application in a regular configuration solar cell (Fig. 4d). They found that using EDOT as a monomer the PS layer degraded during the deposition because of the high oxidation potential of EDOT. To resolve this, bisEDOT, which has a lower oxidation potential, was used as a monomer. The PEDOT layer was successfully deposited over the PS layer and the complete assembled solar cell showed a decent PEC of 5.9%.

To avoid the use of TiO_2 as ETL in PSSC with a regular configuration, Suarez et al. [28] reported the electropolymerization of an EDOT monomer holding a fullerene unit (EDOT-C_{60}), and the resulting polymer (poly-EDOT-C_{60}) was used as an ETL in solar cell devices (Fig. 4e). By changing the number of polymerization cycles, films with different thicknesses and absorbances were prepared. The XRD diffractograms of PS deposited over FTO and Poly-EDOT-C_{60} showed similar peaks, which corroborated that the electropolymer did not affect the PS crystallization process. The
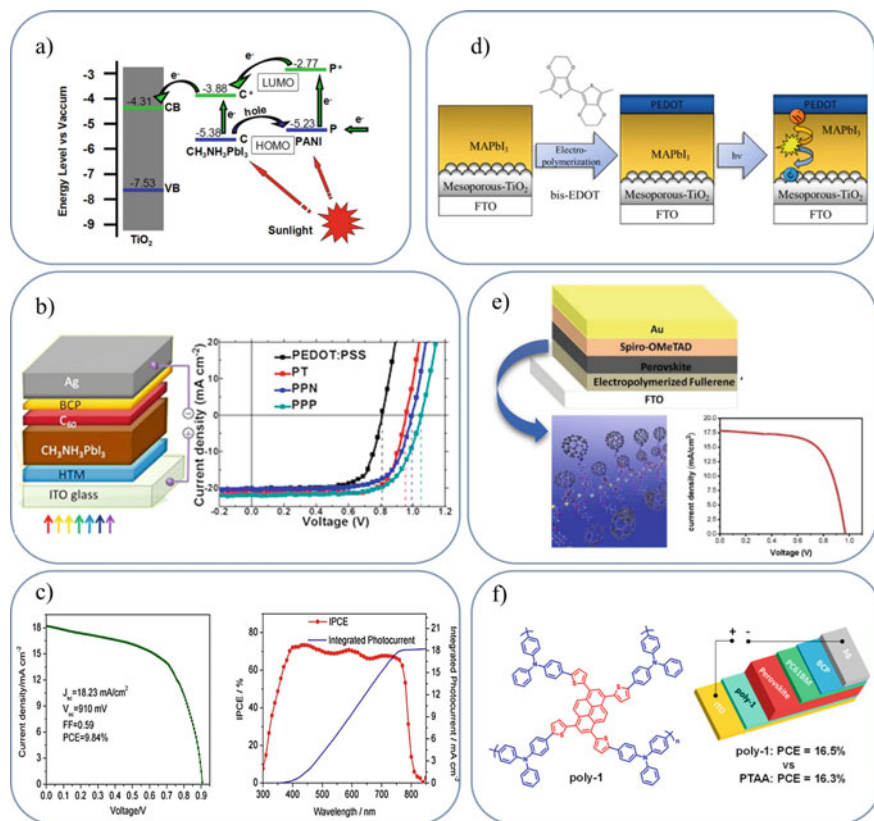
Fig. 4 **a** Schematic energy levels of the TiO_2, $CH_3NH_3PbI_3$, and PANI. Reprinted with permission from Ref. [23], Copyright 2014, Elsevier Ltd. **b** Schematic representation of the inverted PSSC and current density–voltage (J-V) curves of solar cell devices with different HTMs under simulated AM1.5 sun light of 100 mW cm^{-2} irradiance. Adapted with permission from Ref. [25], Copyright 2015, Elsevier Ltd. **c** J − V curve (right) and IPCE spectra and integral photocurrent (left) of the PAF film based PSSC. Adapted with permission from Ref. [26], Copyright 2017, American Chemical Society. **d** Schematic illustration of the Assembly and Operation of the PSSC with PEDOT Hole-Transporter. Reprinted with permission from Ref. [27], Copyright 2018, American Chemical Society. **e** Schematic representation of the PSSC, three-dimensional structure of poly-EDOT-C_{60}, and representative J-V curve under illumination. Adapted with permission from Ref. [28], Copyright 2018, Elsevier Ltd. **f** Chemical structure of the used polymer and schematic illustration of the PSSC device structure with poly-1. Reprinted with permission from Ref. [29], Copyright 2020, American Chemical Society

best cell with a Poly-EDOT-C_{60} had a PCE of around 11%, while the cell without electropolymer a PCE of only 3%.

Also, a pyrene-based electropolymer (poly-1) was used as HTL in inverted PSS (Fig. 4f) [29]. By using UPS (ultraviolet photoelectron spectrometry) measurements, a HOMO of -5.4 eV was measured for poly-1, indicating that the polymer

is suitable for hole transport and extraction. Poly-1 demonstrated a good wettability by DMF solvent and PS deposited over poly-1 had large grain sizes, reduced grain boundary, and a smooth surface. Poly-1 with different thicknesses (obtained by changing the polymerization cycles) were tested in a configuration ITO/poly-1/PS/PC$_{61}$BM/BCP/Ag solar cell. The best performance was obtained with a poly-1 film of 50 nm, which presented a PCE of 16.5%. The cell retained 91% of the initial PCE after 1000 h without encapsulation.

4.3 Supercapacitors

As energy store systems, several devices such as batteries, fuel cells, and electrochemical capacitors (supercapacitors) can be mentioned [30]. Compared to batteries, supercapacitors hold fast storage capability, better cyclic stability, and higher density power, although they cannot store a lot of charge like in batteries. Therefore, supercapacitors are appropriate for applications where large amounts of charge must be quickly provided. Supercapacitors are formed by two electrodes containing the active material, an electrolyte, and a separator. Supercapacitors store energy by non-Faraday or Faradaic processes known as electrical double-layer capacitors (EDLCs) and pseudocapacitors or redox capacitors (PSCs) (Fig. 5a) [31]. EDLCs store charge by electrostatic interactions in the interface between the electrode and the electrolyte (like a Helmholtz double-layer capacitor) [31]. During charging the electrons move from one electrode to the other across the external circuit, and ions present in the electrolyte concentration in the electrode with the opposite charge: cations on the negative and anions on the positive electrode. Therefore, a double layer capacitance is produced on each electrode. In PSCs charge is stored by fast and reversible Faradaic redox reactions between the electrode and the electrolyte (electron transfer by oxidation or reduction). During charge–discharge processes, redox reactions occur and ions are inserted-released from the material. PSCs exhibit higher specific capacitances than EDLCs because the redox reaction happens in both the bulk and on the electrode material surface, while in EDLC the store mechanism is a surface process. Therefore, materials with a high surface area are used in EDLCs. The most used material for EDLCs is carbon, it presents a low cost, high availability and it can be obtained in many different forms like nanotubes, fibers, and sponges. Carbon-based materials such as single-walled carbon nanotubes, graphene, graphene oxide, and reduced graphene have been vastly used for EDLCs [32].

The electrochemical performances of the different electrode materials are characterized by CV, galvanostatic charge–discharge (GCD), and electrochemical impedance spectroscopy (EIS). The parameters that are generally reported by the researchers are specific capacitance [CE (F/g)], capacitance retention (R%), cycling stability, energy [ED (Wh/kg)], and power density [PD (kW/kg)] [33]. CE can be calculated from either CV or GCD curves. From CV CE = $Q/(Vm)$, where m(g) is the mass of the active materials, Q(C) is the average charge during the charging and discharging process, and V (V) is the potential window (Fig. 5b). From GCD
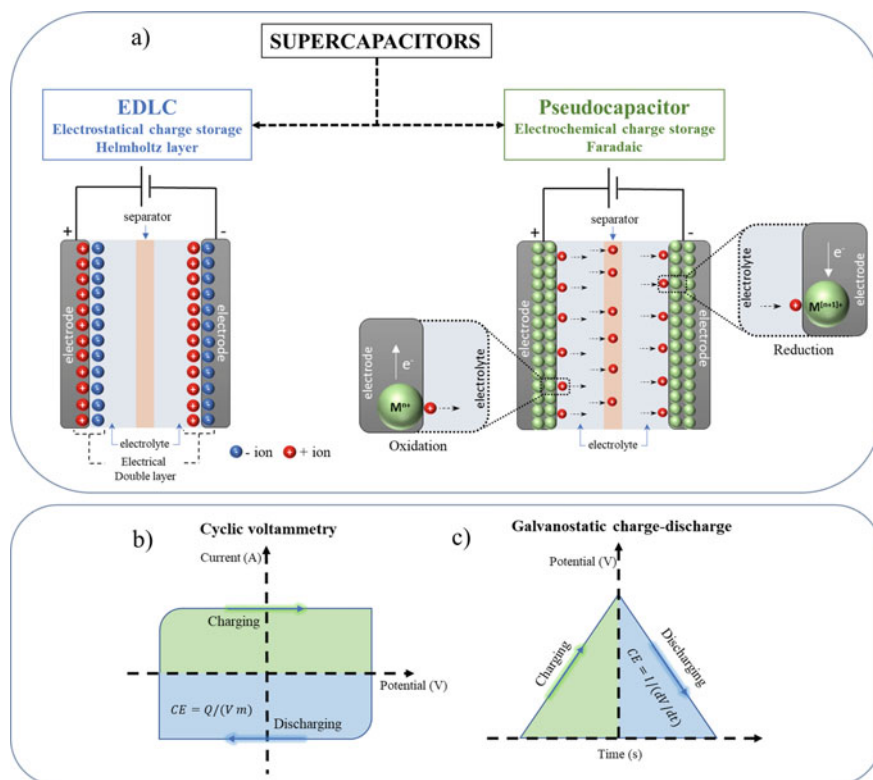
Fig. 5 **a** Supercapacitor charge storage mechanisms. **b** Representative CV showing the charging-discharging processes. **c** Representative GCD curve showing the charging-discharging processes

curves $CE = I/(dV/dt)$, where I is the discharging current per mass unit applied to the electrode, and dV/dt is the slope during the voltage drop in the GCD curves (Fig. 5c). Capacitance retention is the ratio between the CE after "n" number of cycles and the initial capacitance (CE final/CE initial) $\times$ 100). Initial characterization of the capacitive or pseudocapacitive material is commonly carried out in a three-electrode cell configuration because in this form the obtained information comes exclusively from the target electrode without interference from the other electrode. The two-electrode setup is generally used in supercapacitive device prototypes or final products.

Until now, several metal oxides like RuO_2, IrO_2 MnO_2, V_2O_5, NiO, Co_3O_4 have been used as pseudocapacitive materials [34]. Although promising results have been obtained with these oxides, some of them are expensive (IrO_2 and RuO_2), are not flexible, and have low conductivities. Besides metallic oxides, conducting polymers have also been used as pseudocapacitive materials. They present low fabrication costs, high specific energy and power, decent conductivities, low weight and are flexible. PPy, PANI, PTh, and several related conducting polymers have been studied as pseudocapacitive materials [33]. Because the performance of the PSC is influenced

by the polymerization methodology, different techniques such as in-situ polymerization, interfacial polymerization, emulsion polymerization, and electrochemical polymerization have been used. Of particular interest in this chapter are PSC materials obtained by electrochemical polymerization.

As an example, PEDOT was electrodeposited over tantalum electrodes by a galvanostatic method using cetyltrimethylammonium bromide (CTAB) as surfactant and supporting electrolyte[35]. By changing the CTAB concentration films formed by micro/nanorods, nanoparticles and blocks were obtained (Fig. 6a). Different polymerization mechanisms were proposed to explain the diverse morphologies. CV shapes of PEDOT micro/nanorods, particles, and blocks were all rectangular and GCD curves were symmetrical for the three films. Both response shapes are indicative of an adequate charge storage and release mechanism. The materials presented specific capacitances of 86.80, 29.44, and 15.22 F/g, respectively. The cycling stability of PEDOT micro/nanorods was better than the obtained for particles and blocks. PEDOT micro/nanorods retained around 90% of the initial capacitance after 1000 cycles, while for PEDOT particles and blocks the capacitance decreased 32% and 54%, respectively.

Using other common polymers, electrodeposited PANI and PPy nanowires (NW) were covered with a carbonaceous shell, by a simple hydrothermal reaction using glucose, to overcome the structural instability caused by volumetric swelling and shrinking in charge/discharge processes [36]. PANI and PPy films showed capacitance retention of only 25% after 10,000 cycles, while PANI and PPy NW with the carbonaceous shell attained capacitance retention of 95% and 85% after the same number of cycles (Fig. 6b). SEM images of PANI and PPy NW before and after cycling showed that most of the PANI and PPy disappeared. Contrarily PANI and PPy with the coated shells presented almost no change in the structural changes after 10,000 cycles.

Materials with three-dimensional network structures were obtained by using indole-containing monomers, and the capacitive properties of the electrogenerated films were studied [37]. All polymers (called 5-PICA, 6-PICA, and 7-PICA) showed a sponge-like morphology formed by connected NW (Fig. 6c). GCD curves of 5-PICA, 6-PICA, and 7-PICA NW had the typical shapes of PSCs with symmetric anodic and cathodic charge values, with specific capacitances of 355, 383, and 430 F/g at a current density of 2.5 A/g (Fig. 6c), and capacitance retention of 94.5%, 95.1%, and 96%, after 1000 cycles.

PPy films were synthesized by chemical (c-PPy) and electrochemical polymerization (e-PPy) and the performance of the two pseudocapacitive materials were compared (Fig. 6d) [38]. e-PPy showed rectangular CVs and triangular GCD curves and high specific capacitances, and c-PPy presented deformed CVs and GCD. e-PPy retained 80% of the initial capacitance after 130,000 charging/discharging cycles, while c-PPy quickly degraded after 95,000 cycles with capacitance retention of only 20%. SEM images indicated no changes in the morphology of e-PPy but c-PPy structure collapsed after the GCD cycles. A flexible capacitor using e-PPy was constructed (Fig. 6d). CVs and GCD curves were almost identical under different deformations confirming the bending properties of the device.
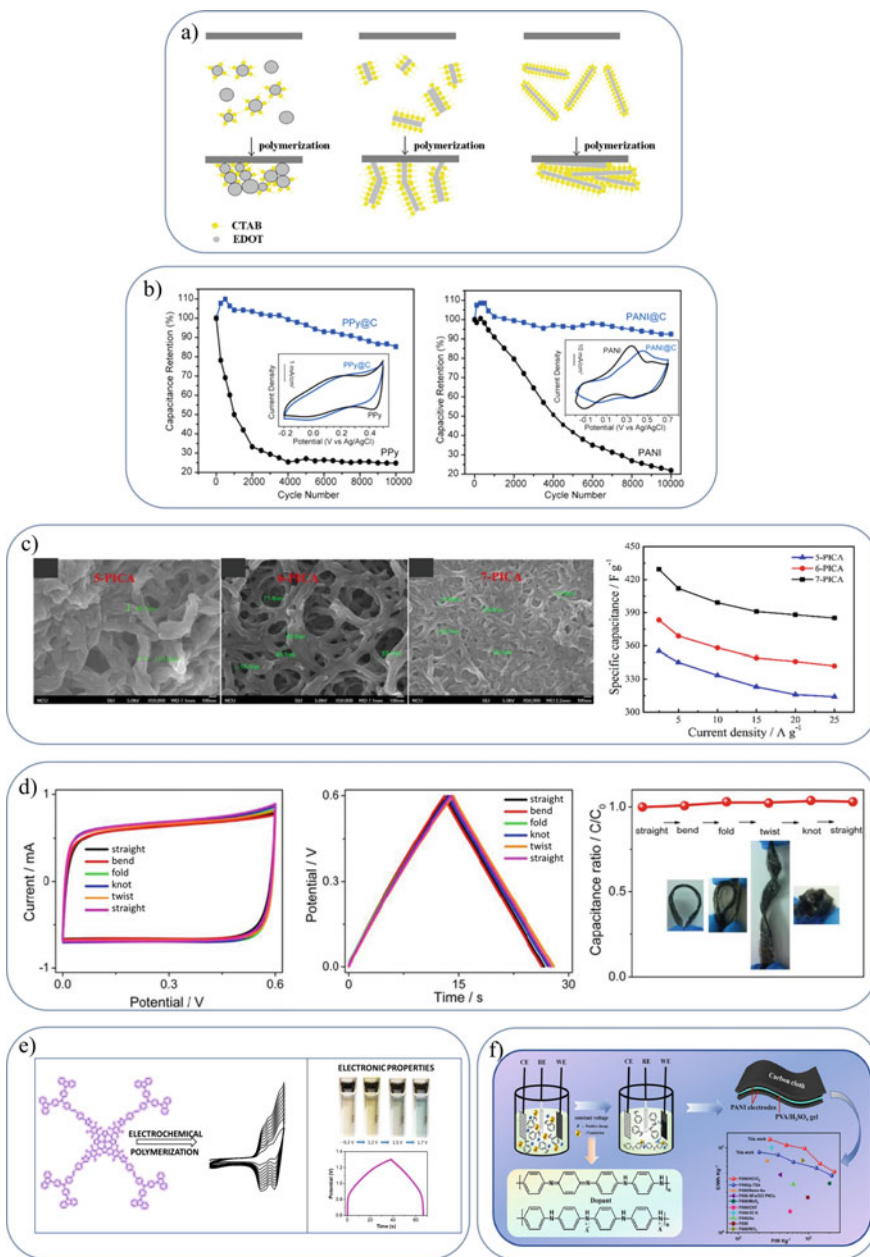
◄**Fig. 6** **a** PEDOT mechanism formation of particles, rod-like, and blocks. Reprinted with permission from Ref. [35], Copyright 2009, Elsevier Ltd. **b** Capacitance retention of PANI and PPy with and without the core shells. Adapted with permission from Ref. [36], Copyright 2014, American Chemical Society. **c** SEM images and specific capacitances of 5-PICA, 6-PICA and 7-PICA prepared on the ITO electrodes. Adapted with permission from Ref. [37], Copyright 2015, Elsevier Ltd. **d** Flexibility tests of supercapacitors made of e-PPy: CVs, GCDs, and capacitance ratio under various deformations. Adapted with permission from Ref. [38], Copyright 2016, American Chemical Society. **e** Chemical structure of the porphyrin monomers used, color changes during oxidation, and GCD curve of the porphyrin polymer. Reprinted with permission from Ref. [39]. Copyright 2020 Royal Society of Chemistry **f** PANI electrodeposition setup, schematic illustration of flexible PANI symmetric devices, and Ragone plots of PANI-based device solid-state devices. Reprinted with permission from Ref. [40]. Copyright 2021 Elsevier Ltd.

A carbazole functionalized porphyrin monomer with a dendronized structure was used to create by electropolymerization a microporous polymer (Fig. 6e) [39]. The film morphology was characterized by particles forming a network with a sponge-like tridimensional structure, providing channels for ion diffusion. GCD curves showed a triangular shape with a specific capacitance of 277 F/g at a current density of 4.5 A/g and capacitance retention of about 80% after 3000 cycles. Also, because of the EC properties of the film, the charge–discharge process can be followed by the change in the coloration of the film (Fig. 6e).

PANI films were electrochemically polymerized by constant current over flexible electrodes using different supporting electrolytes and the impact on the electrochemical properties was studied (Fig. 6f) [40]. PANI films were electropolymerized under constant current. Depending on the used dopant, films with different morphologies and coverage, from the smooth surface and formicary-like porous interior to unevenly covered cauliflower-like morphology were obtained. GCD curves for the different PANI samples were triangular and symmetrical shapes. All-solid-state symmetric supercapacitors were constructed using PANI/$HClO_4$ and PANI/p-toluenesulfonic acid as pseudocapacitive materials. PANI/$HClO_4$ device showed an energy density of 12.57 Wh/kg at the PD of 283 W/kg, while PANI/p-TSA device had an energy density of 8.86 Wh/kg at the PD of 199 W/kg (Fig. 6f).

References

1. Fomo, G., Waryo, T., Feleni, U., Baker, P., Iwuoha, E.: Electrochemical polymerization. In: Jafar Mazumder, M., Sheardown, H., Al-Ahmed, A. (eds.) Functional Polymers. Polymers and Polymeric Composites: A Reference Series, pp. 105–131. Springer, Cham (2019)
2. Platt, J.R.: Electrochromism, a possible change of color producible in dyes by an electric field. J. Chem. Phys. **34**, 862 (1961)
3. Dyer, A.L., Bulloch, R.H., Zhou, Y., Kippelen, B., Reynolds, J.R., Zhang, F.: A vertically integrated solar-powered electrochromic window for energy efficient buildings. Adv. Mater. **26**, 4895–4900 (2014)
4. Granqvist, C.G., Arvizu, M.A., Bayrak Pehlivan, I., Qu, H.Y., Wen, R.T., Niklasson, G.A.: Electrochromic materials and devices for energy efficiency and human comfort in buildings: a critical review. Electrochim. Acta **259**, 1170–1182 (2018)

5. Yu, H., Shao, S., Yan, L., Meng, H., He, Y., Yao, C., Xu, P., Zhang, X., Hu, W., Huang, W.: Side-chain engineering of green color electrochromic polymer materials: toward adaptive camouflage application. J. Mater. Chem. C **4**, 2269–2273 (2016)

6. Brooke, R., Mitraka, E., Sardar, S., Sandberg, M., Sawatdee, A., Berggren, M., Crispin, X., Jonsson, M.: Infrared electrochromic conducting polymer devices. J. Mater. Chem. C **5**, 5824–5830 (2017)

7. Ming, S., Zhen, S., Lin, K., Zhao Li, Xu.J., Lu, B.: Thiadiazolo[3,4-c] pyridine as an acceptor toward fast-switching green donor−acceptor-type electrochromic polymer with low bandgap. ACS Appl. Mater. Interfaces **7**, 11089–11098 (2015)

8. Wu, W., Wang, M., Ma, J., Cao, Y., Deng, Y.: Electrochromic metal oxides: recent progress and prospect. Adv. Electron. Mater. **4**, 1800185 (2018)

9. Kim, J., Rémond, M., Kim, D., Jang, H., Kim, E.: Electrochromic conjugated polymers for multifunctional smart windows with integrative functionalities. Adv. Mater. Technol. **5**, 1900890 (2020)

10. Xu, Z., Yue, H., Wang, B., Zhao, J., Wang, M., Zhang, Y., Xie, Y.: Color tuning for black-to-transmissive conjugated copolymer with excellent electrochromic properties via electrochemical copolymerization of two donor-acceptor type monomers. Mater. Des. **194**, 108903 (2020)

11. Yan, S., Fu, H., Zhang, L., Dong, Y., Li, W., Ouyang, M., Zhang, C.: Conjugated polymer multilayer by in situ electrochemical polymerization for black-to-transmissive eletrochromism. Chem. Eng. J. **406**, 126819 (2021)

12. Hsiao, S.H., Chen, Y.Z.: Electrochemical synthesis of stable ambipolar electrochromic polyimide film from a bis(triphenylamine) perylene diimide. J. Electroanal. Chem. **799**, 417–423 (2017)

13. Lai, J.C., Lu, X.R., Qu, B.T., Liu, F., Li, C.H., You, X.Z.: A new multicolored and near-infrared electrochromic material based on triphenylamine-containing poly(3,4-dithienylpyrrole). Org. Electron. **15**, 3735–3745 (2014)

14. Jeong, J., Kim, M., Seo, J., Lu, H., Ahlawat, P., Mishra, A., Yang, Y., Hope, M.A., Eickemeyer, F.T., Kim, M., Yoon, Y.J., Choi, I.W., Darwich, B.P., Choi, S.J., Jo, Y., Lee, J.H., Walker, B., Zakeeruddin, S.M., Emsley, L., Rothlisberger, U., Hagfeldt, A., Kim, D.S., Grätzel, M., Kim, J.Y.: Pseudo-halide anion engineering for α-FAPbI3 perovskite solar cells. Nature **592**, 381–385 (2021)

15. Zhang, Y., Ye, L., Hou, J.: Precise characterization of performance metrics of organic solar cells. Small Methods **1**, 1700159 (2017)

16. Rodríguez-Seco, C., Cabau, L., Vidal-Ferran, A., Palomares, E.: Advances in the synthesis of small molecules as hole transport materials for lead halide perovskite solar cells. Acc. Chem. Res. **51**, 869–880 (2018)

17. Wang, L., Zhang, F., Liu, T., Zhang, W., Li, Y., Cai, B., He, L., Guo, Y., Yang, X., Xu, B., Gardner, J.M., Kloo, L., Sun, L.: A crosslinked polymer as dopant-free hole-transport material for efficient n-i-p type perovskite solar cells. J. Energy Chem. **55**, 211–218 (2021)

18. Singh, R., Singh, P.K., Bhattacharya, B., Rhee, H.W.: Review of current progress in inorganic hole-transport materials for perovskite solar cells. Appl. Mater. Today **14**, 175–200 (2019)

19. Nia, N.Y., Matteocci, F., Cina, L., Di Carlo, A.: High-efficiency perovskite solar cell based on poly(3-hexylthiophene): influence of molecular weight and mesoscopic scaffold layer. Chemsuschem **10**, 3854–3860 (2017)

20. Huang, X., Wang, K., Yi, C., Meng, T., Gong, X.: Efficient perovskite hybrid solar cells by highly electrical conductive PEDOT:PSS hole transport layer. Adv. Energy Mater. **6**, 1501773 (2016)

21. Bi, D., Yi, C., Luo, J., Décoppet, J.D., Zhang, F., Zakeeruddin, S.M., Li, X., Hagfeldt, A., Grätzel, M.: Polymer-templated nucleation and crystal growth of perovskite films for solar cells with efficiency greater than 21%. Nat. Energy **1**, 16142 (2016)

22. Zhou, Z., Zhao, Y., Zhang, C., Zou, D., Chen, Y., Lin, Z., Zhen, H., Ling, Q.: A facile one-pot synthesis of hyper-branched carbazole-based polymer as a hole-transporting material for perovskite solar cells. J. Mater. Chem. A **5**, 6613–6621 (2017)

23. Xiao, Y., Han, G., Chang, Y., Zhou, H., Li, M., Li, Y.: An all-solid-state perovskite-sensitized solar cell based on the dual function polyaniline as the sensitizer and p-type hole-transporting material. J. Power Sources **267**, 1–8 (2014)
24. Xiao, Y., Han, G., Wu, J., Lin, J.-Y.: Efficient bifacial perovskite solar cell based on a highly transparent poly(3,4-ethylenedioxythiophene) as the p-type hole-transporting material. J. Power Sources **306**, 171–177 (2016)
25. Yan, W., Li, Y., Li, Y., Ye, S., Liu, Z., Wang, S., Bian, Z., Huang, C.: High-performance hybrid perovskite solar cells with open circuit voltage dependence on hole-transporting materials. Nano Energy **16**, 428–437 (2015)
26. Wang, Y., Zhang, S., Wu, J., Liu, K., Li, D., Meng, Q., Zhu, G.: Electropolymerization porous aromatic framework film as a hole-transport layer for inverted perovskite solar cells with superior stability. ACS Appl. Mater. Interfaces **9**, 43688–43695 (2017)
27. Samu, G.F., Scheidt, R.A., Zaiats, G., Kamat, P.V., Janáky, C.: Electrodeposition of hole-transport layer on methylammonium lead iodide film: A strategy to assemble perovskite solar cells. Chem. Mater. **30**, 4202–4206 (2018)
28. Suárez, M.B., Aranda, C., Macor, L., Durantini, E., Heredia, D.A., Durantini, E.N., Otero, L., Guerrero, A., Gervaldo, M.: Perovskite solar cells with versatile electropolymerized fullerene as electron extraction layer. Electrochim. Acta **292**, 697–706 (2018)
29. Shao, J.-Y., Yu, B., Wang, Y.-D., Lan, Z.-R., Li, D., Meng, Q., Zhong, Y.-W.: In-situ electropolymerized polyamines as dopant-free hole-transporting materials for efficient and stable inverted perovskite solar cells. ACS Appl. Energy Mater. **3**, 5058–5066 (2020)
30. Olabi, A.G., Onumaegbu, C., Wilberforce, T., Ramadan, M., Abdelkareem, M.A., Al-Alami, A.H.: Critical review of energy storage systems. Energy **214**, 118987 (2021)
31. Conway, B.: Electrochemical supercapacitors: scientific fundamentals and technological applications. Springer Science and Business Media, Berlin (1999)
32. Wang, Y., Zhang, L., Hou, H., Xu, W., Duan, G., He, S., Liu, K., Jiang, S.: Recent progress in carbon-based materials for supercapacitor electrodes: a review. J. Mater. Sci. **56**, 173–200 (2021)
33. Zhang, X., Xiao, Z., Liu, X., Mei, P., Yang, Y.: Redox-active polymers as organic electrode materials for sustainable supercapacitors. Renew. Sustain. Energy Rev. **147**, 111247 (2021)
34. An, C., Zhang, Y., Guo, H., Wang, Y.: Metal oxide-based supercapacitors: progress and prospectives. Nanoscale Adv. **1**, 4644–4658 (2019)
35. Li, Y., Wang, B., Chen, H., Feng, W.: Improvement of the electrochemical properties via poly(3,4-ethylenedioxythiophene) oriented micro/nanorods. J. Power Sources **195**, 3025–3030 (2010)
36. Liu, T., Finn, L., Yu, M., Wang, H., Zhai, T., Lu, X., Tong, Y., Li, Y.: Polyaniline and polypyrrole pseudocapacitor electrodes with excellent cycling stability. Nano Lett. **14**, 2522 (2014)
37. Ma, X., Zhou, W., Mo, D., Hou, J., Xu, J.: Effect of substituent position on electrodeposition, morphology, and capacitance performance of polyindole bearing a carboxylic group. Electrochim. Acta **176**, 1302–1312 (2015)
38. Huang, Y., Zhu, M., Pei, Z., Huang, Y., Geng, H., Zhi, C.: Extremely stable polypyrrole achieved via molecular ordering for highly flexible supercapacitors. ACS Appl. Mater. Interfaces **8**, 2435–2440 (2016)
39. Durantini, J., Rubio, R., Solis, C., Macor, L., Morales, G.M., Mangione, M.I., Heredia, D.A., Durantini, E.N., Otero, L., Gervaldo, M.: E lectrosynthesis of a hyperbranched dendrimeric porphyrin polymer: optical and electronic characterization as a material for bifunctional electrochromic supercapacitors. Sustain. Energy Fuels **4**, 6125–6140 (2020)
40. Zhang, M., Nautiyal, A., Du, H., Wei, Z., Zhang, X., Wang, R.: Electropolymerization of polyaniline as high-performance binder free electrodes for flexible supercapacitor. Electrochim. Acta **376**, 138037 (2021)

Polymeric Nanofibers as Electrodes for Sensors

Sultana Rahman, Ozge Selcuk, Faiza Jan Iftikhar, Sevinc Kurbanoglu, Afzal Shah, Mohammad Siddiq, and Bengi Uslu

Abstract The chapter is meant to examine the performance of electrodes blended with nanofibers. This study concerns the synthesis, characterization, and applications of electrodes and polymeric nanofibers. Electrospinning is a basic, simple, and adaptable strategy for creating submicron and nano size filaments. Owing to their enormous surface territory and permeable design, electrospun nanofibers can be utilized widely in biomedical, ecological, defensive attire, and sensors applications. Nano filaments of micron measurement and various compound organizations were prepared. Sensors are set up instruments of synthetic investigation utilized in both electrochemical and optical detecting modes. They permit understanding into ion concentrations in different examples, offering reliable performance. One of the methods of improving this class of sensors is to investigate the advantages of nanoscale receptor layers. In this regard, nanofibers appear to be a profoundly attractive alternative because of novel properties identified with the geometry of this class of nanomaterials. Cyclic voltammetry was applied to examine the changes of behavior of electrodes with various diameters. The result displayed that diameter of nanofibers diminished with decreasing polymer concentration focus and applied voltage and expanding tip-to-collector distance while feeding rate of rate did not have a critical impact on nanofiber diameter. This chapter gives a brief outline of a few electrospun nanofibers applications, focusing on biosensor or nanosensor applications. Here, polymeric nanofibers as an electrode for sensors properties of affectability, selectivity, and identification are fundamentally assessed. Current challenges in this area and prospective future work are likewise discussed.

S. Rahman · F. J. Iftikhar · A. Shah · M. Siddiq
Department of Chemistry, Quaid-i-Azam University, Islamabad 44000, Pakistan

S. Rahman · O. Selcuk · S. Kurbanoglu · B. Uslu (✉)
Department of Analytical Chemistry, Faculty of Pharmacy, Ankara University, Ankara 06560, Turkey
e-mail: buslu@pharmacy.ankara.edu.tr

F. J. Iftikhar
NUTECH School of Applied Sciences and Humanities, National University of Technology, Islamabad, Pakistan

1 Introduction

Nanotechnology has been hailed as the revolutionary science to synthesize materials with enhanced properties than their bulk counterparts. The emerging field of nanotechnology relies on nanoscale dimensions of the material that renders sensitivity and selectivity due to its extremely small size and high surface area (SA), which offers to make device miniaturization viable. This allows manipulation of the material at the atomic and molecular level to adopt them for different applications such as medicine, environmental analysis, optics, and materials [1, 2]. The nanomaterials are defined as having one dimension, at least less than 100 nm constituting a single or multiple phases. Nanomaterials can be of different dimensions, i.e., 0, 1, 2, and 3-D materials [3]. Among these, 1-D nanofibers have been of particular interest due to their highly porous nature and large surface area, ease of production and morphological control, affordability, flexibility, and the possibility to modify with other materials to obtain synergism [2, 4]. The different applications of NFs are tissue and bone engineering as biodegradable scaffolds, biofriendly and biodegradable membranes [5, 6], drug delivery applications by nanofibrous mats with a low amount of medication loading and reduced toxicity [7, 8], as antibacterial membranes [9], as electrochemical energy storage [10] and efficient electrochemical sensors doped with CNTs and MNPs as novel sensing devices for small molecules [11, 12].

A polymeric solution is used to fabricate a 1D nanostructure such as nanotubes, nanofibers, nanowires, nanoflowers, and even some non-conventional nanostructures at a nanometric scale. Additionally, these NFs can be prepared by different methods. There are 5 distinct methods to fabricate NFs. One method known as the gas-assisted spinning method utilizes gases to draw the polymer to the desired thickness [13]. A centrifugal spinning method, as the name implies, uses centrifugal force to fabricate NFs. The method includes the rotary jet and force spinning method [14, 15]. Another method comprises the traditional spinning method by employing different polymers with spinnerets having different geometries. Another method uses an electric field for the fabrication of NFs and is classed as an electrospinning method that uses a melt or precursor solution with a single or multiple nozzles. However, when no [16, 17] nozzle is used, it is called a needleless electrospinning method [18] that improves NF's productivity rate, as developed by Elmarco® company. These are standard electrospinning techniques. Similarly, electrospinning may produce coaxial NFs by using two different polymers that form a core-shell structure, while the co-electrospinning technique obtains single and bilayer nanostructure [19]. Moreover, a method exists that combines centrifugal spinning with an electric field to draw an NF of properties of choice. In addition, self-assembly, phase separation, flash spinning [20, 21], etc., are still being used at laboratory scale; however, they have not been commercialized. Among them all, electrospinning has been hailed as the
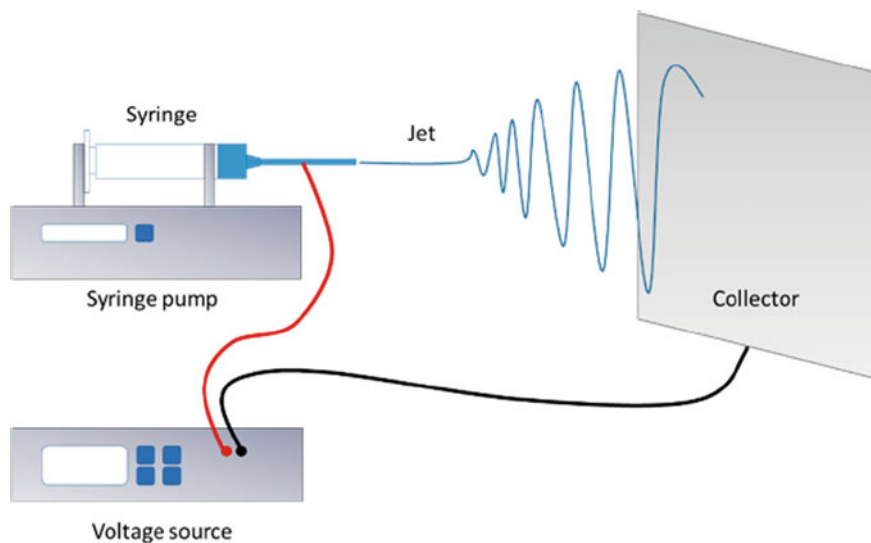
Fig. 1 A scheme showing the setup for the electrospinning technique. Adapted with permission from [22] Copyright (2019) MDPI

most effective, economical, scalable, and easy-to-use technique and hence a widely used method for the production of versatile, tunable nanomaterials. However, its popularity has been contingent on the success of nanotechnology.

A schematic diagram of the electrospinning procedure is displayed in Fig. 1. The Electrospinning technique was first patented in 1938 by Anton. It contains three parts: a power supply with high voltage, a spinneret that constitutes a needle with a small diameter, and a metal collector. The technique uses a high electric field of 1–3 kV/cm applied between the needle tip and the grounded conductor to synthesize highly porous, layered nanofibrous structures with diameters as thin as ~5–20 nm that jets towards the collector, which if other methods are used, may pose difficulty in production. The process of electrospinning has come a long way by improving the process parameters to produce nanoscale polymers. The polymer is introduced as a precursor solution that triggers the spherical droplet to be drawn into a conical shape towards the grounded collector when the surface tension is overcome by the application of an electric field [22].

2 Current Research Methods for Producing Polymer Nanofibers

Different polymers natural as well as synthetic polymers such as polyaniline [23], polyethylene terephthalate [24], polyacrylonitrile [25], polyvinyl alcohol [26],

polyethylene oxide [27], polyamide [28], and polyvinylchloride [29], etc., have been prevalently employed to fabricate different nanofibers with different pore size and shape. The different parameters that can decidedly affect the properties of the NFs obtained are the molecular weight of the polymer, solution parameters such as humidity, temperature, surface tension, viscosity, the concentration of the solution, and electrospinning setup itself polymers require different ambient and solution conditions [30]. The viscosity is a key parameter in making one select optimum conditions for preparing electrospun NFs, as is the molecular weight, which has a substantial effect on the viscosity of the polymer that in turn affects the morphology of the as-fabricated fibers such as a change from a beaded to a porous fiber is observed [31]. By overseeing the size and morphology of electrospun NFs, different functionalities for a wide array of application can be addressed.

The NFs synthesized by electrospinning methods render them with highly long length, tiny pores and diameters, and large SA/unit mass. Different morphologies for different applications have so far been developed by modulation of electrospinning parameters such as a uniaxial and biaxial aligned mesh of NFs, porous NFs, necklace, or web, ribbon-like NFs, and multichannel tubular NFs [32] as shown in Fig. 2.

The need for fast and selective detection of different analytes by developing analytical tools has led to developing sensing platforms using nanotechnology to allow the sensing devices to be more specific, robust, and faster with better performance and parameters. In this regard, nanofibers seem to fit the bill snugly. Thus, nano-based electrospinning techniques leverage manipulation and control of the functionalities and responses of the different NF-based sensors. The chapter focuses on polymeric NFs as electrochemical sensors and is assessed because of their affectability, selectivity, and identification of the analyte of interest. Thus, modified Electrospun NFs have been extensively used to detect various biomedical relevant molecules and drugs such as neurotransmitters, enzymes, hormones, and antibiotics using different polymeric NF-based matrices [33, 34]. Similarly, metal ion detection such as Hg^{2+}, Cd^{2+}, Pb^{2+}, As^{3+} by either functionalizing the NF with compounds such as quantum dots, nanoparticles, or caron nanomaterials, nitrogen-doped carbon NFs introduced into the polymeric solutions. It spun to the designed NF, or modification of the surface of the already electrospun NF has been carried out [35, 36].

3 Applications of Polymer Nanofibers as Sensors

Polymer nanofiber sensors are used in many different areas such as wound healing, determination of gases, humidity, metal ions, and food.

Relative humidity (RH) is one of the environmental factors that have a significant impact on various industries such as food, agriculture, medicine, biology, and textiles. To measure and monitor humidity accurately, RH sensors have gained great popularity among all chemical sensors. Although they are mainly used to monitor humidity, they can also be used to monitor breath because our exhaled breath is saturated with water. This breath monitoring system is a kind of personal health
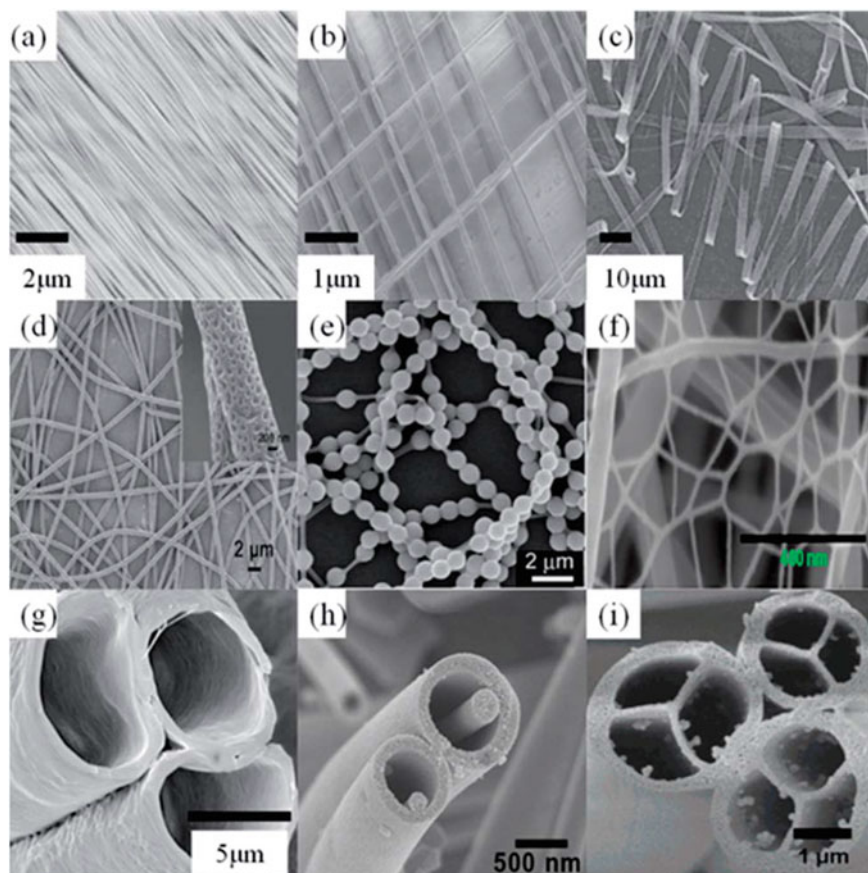
Fig. 2 Electrospun NFs with various morphologies aligned **a** uniaxially, or **b** biaxially, **c** ribbon-shaped, **d** porous NFs, **e** necklace-shaped, **f** web-like, **g** hollow shaped, **h** microtubular and, **i** multichannel tubular. Adapted with permission from [32]. Copyright (2019) MPDI

monitoring device that can be used for routine monitoring of breathing activities with a simple technique for early diagnosis of some serious health problems such as apnea, asthma, and chronic obstructive pulmonary disease. For these reasons, there is a need to develop a portable and flexible device that can be used to monitor RH and respiration on any surface. Polymer-based sensors offer high sensitivity, flexibility, and low-cost applications.

Many studies have shown that polymers for a variety of industrial applications can respond to any humidity change down to the micron diameter of industrial applications. In recent times, polymer-based humidity sensors have been reported to exhibit unique sensing properties by adjusting electrical properties, including capacitance, at different humidity and conductivity points depending on the humidity content of the polymer. The active layer of PEO is a suitable candidate for humidity sensors

since the ionic conductivity changes as RH changes. PEO has fascinated attention for advances in humidity sensing due to its nontoxicity, water-solubility, biodegradability, and biocompatibility. Therefore, searching for a unique sensing material and methods to fabricate high-performance sensors is extremely desirable. As shown in Fig. 3, Ahmad et al. fabricated humidity sensors from multi-walled carbon nanotubes (MWCNT), copper oxide (CuO), and PEO by electrospinning and obtained affordable, efficient, flexible, and stable composite nanofibers. The morphology and structure of the composite was investigated by SEM, Fourier transform infrared spectroscopy and X-ray diffraction analysis. The performance of PEO/CuO/MWCNT nanofibers was studied using LCR meter and % RH at different frequencies. The results showed that composite nanofibers containing 1 and 3% MWCNT combined with CuO in the PEO matrix exhibited strong resistive and capacitive response with high sensitivity to humidity at 25 °C in the range of 30–90% RH. Among the nanocomposites, 1% MWCNT showed resistive fast response time and prolonged recovery time of 22 s within 3 s. The fabricated sensor showed a high capacitive response to humidity, high sensitivity, good linearity, and fast recovery and response times. Due to these remarkable features, the sensors can be used in many fields, such as health and medical monitoring and industrial measurements [37].

Lung pressure is one of the most important conditions for biotics. It gives information about lung pressure, inhalation, exhalation capacity, swelling, and other respiratory problems. Manikandan et al. reported a piezoelectric sensor based on polyvinylidene fluoride (PVF)/fullerene(F) for measuring pulmonary pressure under distension conditions. This functional mechanism of the device monitors the level of air pressure coming out of the lungs during exhalation. Though each person has a unique lung capacity, it is classified by age, gender, height, and airway capacity. When air is
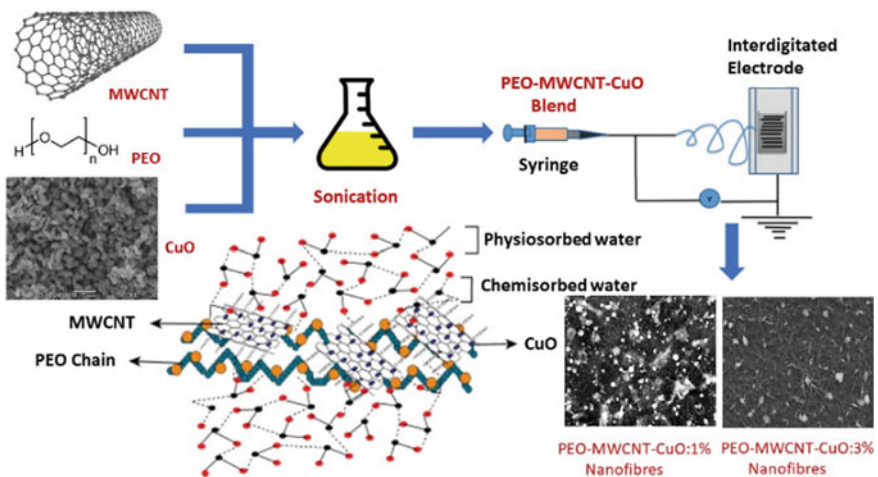
Fig. 3 Schematic representation of PEO/CuO/MWCNT sensor fabrication and characterization. Adapted with permission from [37]. Copyright (2021) MDPI

blown from the mouth into the sensor due to a change in pressure, the piezoelectric film generates an electrical signal in response to the periodic deformation. The developed PVF/F film sensor (Fig. 4) with high sensitivity to pressure variations was used here. To achieve this breakthrough, the sensor was completely encapsulated by the insulating layer, and the noise was suppressed. To confirm the physicochemical properties, the PVF/F nanofiber sensors were thoroughly characterized using SEM, X-ray diffraction and Fourier transform infrared spectroscopy. Nowadays, various types of blowers are used in clinics and hospitals, but these modules are manually operated, and the accuracy is also poor. This sensor is more accurate than the commercially available ones. It has been tested with a commercially available pressure sensor and is based on optimizing the sensor function to measure lung pressure. Therefore, it respects lung pressure and allows accurate monitoring of the current state of lung capacity with a promising detection device for monitoring lung pressure in-home care [38].

In 2020, Wen et al. fabricated a polymer nanofiber sensor in the form of a tennis racket with high humidity sensitivity. In this way, a method was developed to use bionic muscle nanofibers to produce a mechanical contraction. It is a unique method to fabricate a fiber optic humidity sensor in the form of a high sensitivity tennis racket consisting of a U-shaped probe and electrospun nanofibers. An innovative conductive poly(3,4-ethylenedioxythiophene): polystyrene sulfonate (PEDOT:PSS) polymer with PVA doping was fabricated using a low-cost electrospinning technology to achieve better humidity sensitivity. The functional nanofibers of the racket consist of two types of polymer molecules that were positively conjugated with electrospun polymers at an electric current of about 1.7 kV/cm. The interlocking polymer network that was electrospun was used to stretch PEDOT:PSS@PVA polymers. The interlocking traffic/H_2O interaction will play an important role in improving the
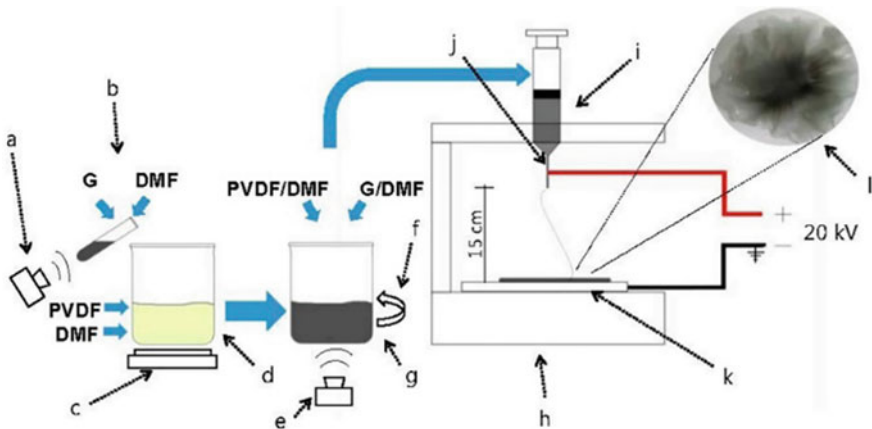

Fig. 4 The fabrication process of PVF/F sensor. Adapted with permission from [38]. Copyright (2021) Elsevier

humidity-related polymers. The sensitivity of the sensor was found to be $-0.990/\%$ RH [39].

Polymer nanofibers are developed and used for drug analysis, medical diagnostics and diagnostic devices. 17α-ethinylestradiol is a female synthetic hormone, which can possibly disrupt the human endocrine system of organisms and cause serious health problems, so its detection even at the lowest levels helps to prevent health problems. In 2018, Pavinatto et al. developed a one-step highly sensitive electrochemical biosensor based on Laccase-functionalized polyvinylpyrrolidone(PVP)/chitosan(CHIT)/reduced graphene oxide(rGOx) electrospun nanofibers for the determination of 17α-ethinylestradiol. The production process of FTO(PVP/CHIT/rGOx)Laccase is shown in Fig. 5. For the PVP nanofibers, the polymeric solution used to electrospun the nanofibers was prepared by dissolving PVP in ethanol and CHIT in acetic acid: water solution. The nanofibers were electrospun on FTO electrodes connected to the metallic collector with a settling time of 2.5 h. The hybrid nanofibers deposited on the FTO electrode have good electrochemical properties with a synergistic effect between PVP, CHIT and rGOx and are suitable to combine the enzyme laccase. The FTO/(PVP/CHIT/rGOx)/Laccase sensor achieved a very low detection limit of 0.15 p mol L^{-1} by the amperometric method. The platform was successfully used for the detection of 17α-ethinylestradiol in synthetic and human urine and exhibited a very low detection limit and good repeatability [40].

According to the state of the art, the physical condition of the human body can be easily monitored by analyzing biomarker gasses from the breath. Koo et al. synthesized porous WO_3 nanotubes by simple layer-by-layer self-assembly and calcinated on polymeric nanofiber templates. Poly(methyl methacrylate) was prepared by electrospinning as a template. Ionic polymers were then deposited on poly(methyl methacrylate) to change the surface charge of poly(methyl methacrylate) nanofibers. The performance of the gas detectors was investigated in a high humidity atmosphere
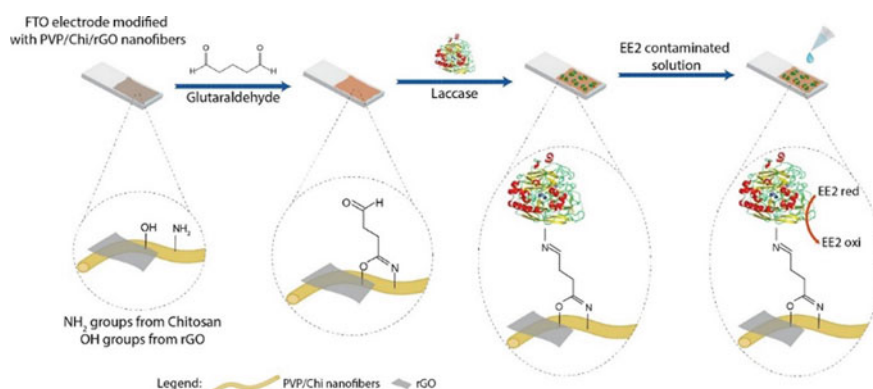

Fig. 5 Schematic representation of FTO/(PVP/CHIT/rGOx)/Laccase electrochemical biosensor for 17α-ethinylestradiol determination. Adapted with permission from [40]. Copyright (2018) Elsevier

using the original WO_3. The results show that layer-by-layer synthesis is a promising method to prepare functionalized hollow semiconductor metal oxides with different catalysts, leading to a potential application in the analysis of exhaled air for the diagnosis of asthma and lung cancer [41].

The key element of the breath sensor for respiratory detection, which right determines the stability and reliability of respiration monitoring, is the sensitivity of the material to humidity. Polymeric materials, which are gaining increasing attention due to their versatile nature, controllable and adjustable performance, and low cost, have the disadvantage of low sensitivity and long response/recovery time for humidity sensors over the entire humidity range, which is insufficient for respiratory humidity monitoring applications. Composites, morphology modification, and molecular structure modification (crosslinking or incorporation of polar groups such as NR_3^+Cl, SO_3H, $COOH$, etc.) have been used to make polymers more suitable for fast-response humidity sensors. Many common methods have been reported to improve the performance of polymers in the development of polymer humidity sensors.

Nanofibers are more favorable for transferring water molecules than thin films and may indirectly progress the performance of polymer nanofiber-based sensors. Li et al. fabricated a humidity sensor based on electrospun sulfonated polyether ketone(SPEK) @poly(viny butyral)(PVB) composite nanofibers for monitoring of non-contact respiration. The porous structure of the composite nanofibers with an appropriate PVB ratio gives the sensor high sensitivity, a wide operating range in relative humidity, and a short response/recovery time. Thus, this sensor enables real-time recording and monitoring of respiration and non-contact determination of skin humidity. Moreover, the mechanism of humidity measurement and equivalent circuits were systematically studied by matching the complex impedance. A fast and stable polymeric humidity sensor based on SPEK@PVB composite nanofibers is demonstrated and applied to respiration monitoring and non-contact measurement for the first time. For the fabrication sensor, firstly, a thin-film sensor was fabricated from SPEK by drop-casting or electrospinning with a nanofiber sensor. The nanofiber humidity sensor was found to have low hysteresis and fast response/recovery time. To improve the sensor performance, different proportions of PVB were added to the electrospinning solution to fabricate SPEK@PVB composite nanofiber sensors. The composite nanofiber humidity sensor with a ratio of SPEK to PVB of 1:3 features high sensitivity, a wide operating range of relative humidity, low hysteresis, <1 s response time, 5 s recovery time, and stable detection performance. The non-contact breath monitoring detection performance of the SPEK@PVB sensor were also investigated, showing that the SPEK@PVB sensor is suitable as a sensor for real-time monitoring [42].

Wearable and stretchable electronics are characterized by their lightness, high flexibility, and ease of integration into functional devices or textiles. In general, there are two main applications for stretchable electronics: epidermal electronics and biosensors for local monitoring of human physiological activities. As was reported by Gao et al., fabricated a composite of carbon nanotubes (CNT) and polyurethane (Fig. 6), which is characterized by electrical conductivity, extreme stretchability, and high
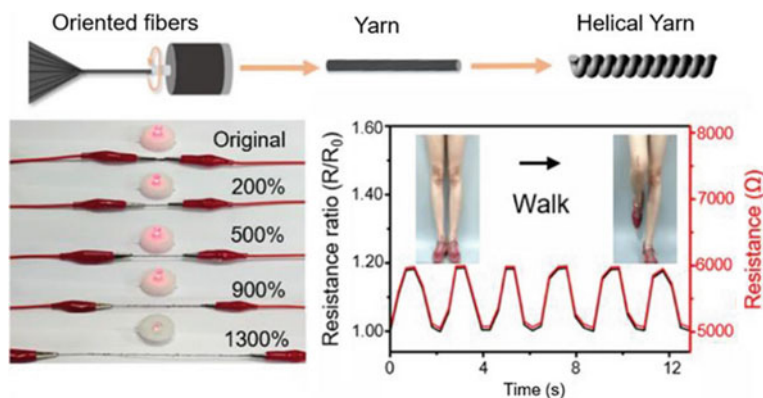
Fig. 6 Application of CNTs/polyurethane as strain sensor. Adapted with permission from [43]. Copyright (2020) American Chemical Society

bending. The synergy of elastic polyurethane molecules provided excellent stretchability of the spiral yarn, while the CNT was stably wrapped into the yarn with a simple twisting strategy and provided good conductivity. With simple electrospinning and spray coating procedure, Gao et al. have created a versatile method for producing ultra-high tensile, CNT and polyurethane nanofiber helical yarn. CNT/polyurethane helical yarn can remove the constraint of intrinsic solid characteristics on the material's stretchability, thanks to the synergetic impact of a soft polymer chain and nanofibrous helical coil structure. A densely coiled CNT network created a strong physical link between CNTs and polyurethane, resulting in a more stable conducting net. The yarn obtained steady conductivity and recovery capabilities within 900% deformation and kept conductivity after stretching up to 1700%. Furthermore, it can monitor human motion as a responsive strain sensor by simply adjusting the content of CNT. These low-cost CNT/ polyurethane helical yarns have ultra-high stretch and are ideal for smart wearable textiles, huge tension sensors, soft robotics, and smart actuators. This comprehensive and cost-effective strategy is promising for ultra-elastic wearable electronics [43].

Conductive polymer-based nanofibers are limited for the fabrication of smart textiles because they can be adapted to different fabric architectures. The fabrication of conductive polymer-based nanofiber by the electrospinning technique is of great interest to combine the exceptional processability of textiles with the excellent electrochemical properties of individual nanofibers. The creation of a continuously aligned array could allow the extraordinary electrical performance of specific nanofibers to be realized in macroscale devices. In 2017, Wu et al. reported a new processing method to efficiently fabricate uniaxially aligned coaxial nanofiber yarns based on conductive polymers. They have fabricated self-enveloping PANI@PAN nanofibers, a single polymer-based conductive yarn, by combining a new electrospinning process and in situ solution polymerization for ammonia (NH_3) sensor. To prepare the PANI@PAN uniaxially aligned coaxial nanofiber yarn sensor, PAN was

first thoroughly dissolved in N,N-dimethylformamide as an electrospinning solution. A new electrospinning device developed by Wu et al. was used to continuously prepare PAN uniaxially oriented nanofiber yarns. The PANI layers were then electrospun via a chemical oxidative polymerization process in situ onto the surface of the PAN nanofibers from PAN uniaxially oriented nanofiber yarns, and core hair PANI@PAN nanofibers were produced. Lastly, the dark green single strands of the PANI@PAN were washed and dried overnight in a vacuum at 25 °C. The results showed that the nanofiber structure in PANI@PAN provides a large surface area for the free diffusion of NH_3 and that the highly aligned nanofiber assembly of PANI@PAN uniaxially aligned coaxial nanofiber yarns facilitates excellent sensitivity of the yarn sensor and fast response/recovery upon exposure to 10–2000 ppm NH_3 at 25 °C. In addition, the yarn-based sensor provides excellent repeatability and stability in NH_3 detection. More significantly, the PANI@PAN sensor exhibited flexible and robust mechanical strength that could be fabricated into defined electronic textiles using various textile forming processes, namely knitting, warp knitting, and embroidery. To support potential gas detection applications, the electrical responses of PANI@PAN to NH_3 at 25 °C were measured. In addition, the ability of PANI@PAN to fabricate various textile architectures using different textile forming techniques was investigated to demonstrate the versatility and feasibility of PANI@PAN nanofiber as a material for smart textile applications [44].

The rational design of flexible pressure sensors that can operate with high precision over a wide linear range is attracting considerable attention due to their potential applications in wearable electronics. Liu et al. report an easy-to-fabricate textile-based pressure sensor with ultra-high sensitivity and high linearity based on a top bridge of PANI-wrapped nonwoven fabric and screen-printed interdigitated textile electrodes. PANI was synthesized in-situ on the surface of the fibers, and the silver electrodes were screen printed. Both fabrication processes are simple and inexpensive and are suitable for future large-area and large-volume production. The fabrication process of the PANI-based pressure sensor and the digital photo of the fabricated sensor is shown in Fig. 7. For the flexible textile pressure sensors, PANI-modified
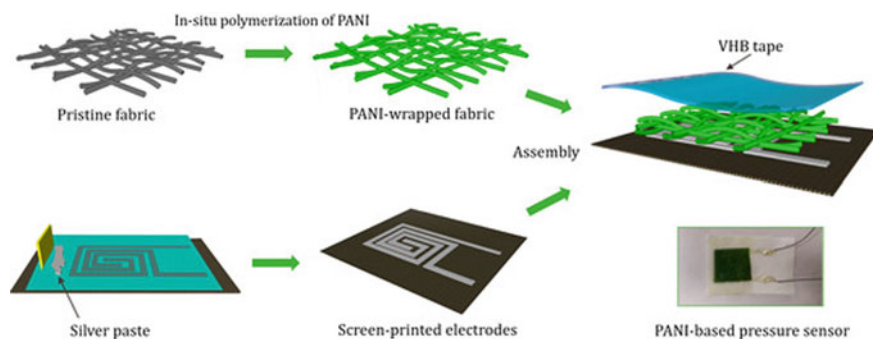
Fig. 7 The fabrication process of the PANI sensor. Adapted with permission from [45]. Copyright (2019) MDPI

nonwoven fabric was used as the piezoresistive layer, which was covered with screen-printed interdigital electrodes on the bottom side. Thin VHB tape was also used to attach the two layers. Liu et al. used nonwoven fabrics wrapped with polyaniline nanofibers as the active material to construct high-performance flexible pressure sensors from all fabrics with textile electrodes interleaved on the bottom surface. Because of the unique layer-by-layer structures, the large surface roughness of the PANI-coated fabric, and the good conductivity of the interconnected textile electrodes, the resulting pressure sensor is superior. It exhibits very high sensitivity with a wide linear range, fast response/relaxation time, and a low detection limit (0.46 Pa) [45].

4   Conclusions, Challenges, and Future Perspectives

Co-electrospinning of NF mats with healing properties is being hotly pursued, and to this end, innovative interactive dressing by employing poly(caprolactone)/poly(vinyl alcohol)/Collagen modified with biological active bitter gourd extract is reported. This dressing has been found to interact with the wound and bring about healing by altering the environment of the wound [46]. Graphene sheets have been used in nanocomposite sensing devices for increasing the SA and catalytic properties; however, the π-π stacking in graphene sheets results in irreversible aggregation[47]. For electrospun polymeric solutions decorated with nanoparticles, the large specific surface energy of the solution tends to make the nanoparticles aggregate, with them being inhomogeneously distributed in the polymer matrix, causing loss of functionality. This issue of aggregation can be overcome by using graphene-wrapped nanomaterials for sensing applications [48].

Furthermore, a new class of smart materials such as shape memory polymers (SMPs) has gained widespread attention due to their property of memorizing their original shape before they are exposed to a trigger and reforming back to the original shape after the trigger with widespread applications in robotics, smart devices etc. It is found that the electrospinning technique renders fibrous SMPs with micro or nano characteristics that result in improved performance in biomedical applications [49]. Still, some limitations need to be overcome to regulate cell behaviors, scaffolds, and bone repairs by improving the rate of shape memory of biomimetic SMPs that becomes unmanageable in response to a trigger by optimizing the paraments that control the dynamical change for cell behaviors. Moreover, these studies have been conducted only in vitro for bone repair and skin regeneration as it is still a challenge to evaluate the damage and degradation process in vivo for bone and skin tissue. Similarly, technologies to synthesize SMPs should focus on combination techniques involving electrospinning and 3D printing that will simplify the production of complex fibrous structures. In conclusion, polymer nanofiber sensors have created significant attention due to their use in a wide variability of industrial applications such as chemical and biological sensing applications. Polymer nanofibers

will be indispensable for next-generation sensors by using different methods such as composite, surface modification, and molecular structure modification.

References

1. Iftikhar, F.J., Shah, A., Akhter, M.S., Kurbanoglu, S., Ozkan, S.A.: Introduction to nanosensors. In: New Developments in Nanosensors for Pharmaceutical Analysis, pp 1–46 (2019)
2. Mane, P.P., Ambekar, R.S., Kandasubramanian, B.: Electrospun nanofiber-based cancer sensors: A review. Int. J. Pharm. **583**, 119364 (2020)
3. Pokropivny, V.V., Skorokhod, V.V.: Classification of nanostructures by dimensionality and concept of surface forms engineering in nanomaterial science. Mater. Sci. Eng. C **27**, 990–993 (2007)
4. Greiner, A., Wendorff, J.H.: Electrospinning: a fascinating method for the preparation of ultrathin fibers. Angew. Chemie. Int. Ed. **46**, 5670–5703 (2007)
5. Qi, S., Zhao, B., Tang, H., Jiang, X.: Determination of ascorbic acid, dopamine, and uric acid by a novel electrochemical sensor based on pristine graphene. Electrochim Acta **161**, 395–402 (2015)
6. Xue, J., Xie, J., Liu, W., Xia, Y.: Electrospun nanofibers: new concepts, materials, and applications. Acc Chem. Res. **50**, 1976–1987 (2017)
7. Thakkar, S., Misra, M.: Electrospun polymeric nanofibers: New horizons in drug delivery. Eur. J. Pharm. Sci. **107**, 148–167 (2017)
8. Thenmozhi, S., Dharmaraj, N., Kadirvelu, K., Kim, H.Y.: Electrospun nanofibers: new generation materials for advanced applications. Mater. Sci. Eng. B **217**, 36–48 (2017)
9. Xu, J., Liu, C., Hsu, P.-C., Liu, K., Zhang, R., Liu, Y., Cui, Y.: Roll-to-Roll transfer of electrospun nanofiber film for high-efficiency transparent air filter. Nano. Lett. **16**, 1270–1275 (2016)
10. Wu, J., Qin, X., Miao, C., He, Y.-B., Liang, G., Zhou, D., Liu, M., Han, C., Li, B., Kang, F.: A honeycomb-cobweb inspired hierarchical core–shell structure design for electrospun silicon/carbon fibers as lithium-ion battery anodes. Carbon. N Y **98**, 582–591 (2016)
11. Supraja, P., Tripathy, S., Krishna Vanjari, S.R., Singh, V., Singh, S.G.: Label free, electrochemical detection of atrazine using electrospun Mn2O3 nanofibers: towards ultrasensitive small molecule detection. Sens. Actuators B Chem. **285**, 317–325 (2019)
12. Zhang, P., Zhao, X., Ji, Y., Ouyang, Z., Wen, X., Li, J., Su, Z., Wei, G.: Electrospinning graphene quantum dots into a nanofibrous membrane for dual-purpose fluorescent and electrochemical biosensors. J. Mater. Chem. B **3**, 2487–2496 (2015)
13. Li, H., Huang, H., Meng, X., Zeng, Y.: Fabrication of helical microfibers from melt blown polymer blends. J. Polym. Sci. Part B Polym. Phys. **56**, 970–977 (2018)
14. Agubra, V.A., De La Garza, D., Gallegos, L., Alcoutlabi, M.: Force Spinning of polyacrylonitrile for mass production of lithium-ion battery separators. J. Appl. Polym. Sci. **133**(42847), 1–8 (2016)
15. Sun, J., Zhang, Z., Lu, B., Mei, S., Xu, Q., Liu, F.: Research on parametric model for polycaprolactone nanofiber produced by centrifugal spinning. J Brazilian Soc. Mech. Sci. Eng. **40**, 186 (2018)
16. Huang, Z.-M., Zhang, Y.-Z., Kotaki, M., Ramakrishna, S.: A review on polymer nanofibers by electrospinning and their applications in nanocomposites. Compos. Sci. Technol. **63**, 2223–2253 (2003)
17. Su, Z., Ding, J., Wei, G.: Electrospinning: a facile technique for fabricating polymeric nanofibers doped with carbon nanotubes and metallic nanoparticles for sensor applications. RSC Adv. **4**, 52598–52610 (2014)
18. Wang, X., Niu, H., Lin, T., Wang, X.: Needleless electrospinning of nanofibers with a conical wire coil. Polym. Eng. Sci. **49**, 1582–1586 (2009)

19. Kenry, L.C.T.: Nanofiber technology: current status and emerging developments. Prog. Polym. Sci. **70**, 1–17 (2017)
20. Whitesides, G.M., Grzybowski, B.: Self-Assembly at all scales. Science **80-**(295), 2418–2421 (2002)
21. Xia, L., Xi, P., Cheng, B.: High efficiency fabrication of ultrahigh molecular weight polyethylene submicron filaments/sheets by flash-spinning. J. Polym. Eng. **36**, 97–102 (2016)
22. Thomas, M.S., Pillai P.K., Farrow, S.C., Pothan, L.A., Thomas, S.L.: Electrospinning as an important tool for fabrication of nanofibers for advanced applications—a brief review. Gen. Chem. **7**, 200022–200022 (2021)
23. Li, M., Guo, Y., Wei, Y., MacDiarmid, A.G., Lelkes, P.I.: Electrospinning polyaniline-contained gelatin nanofibers for tissue engineering applications. Biomaterials **27**, 2705–2715 (2006)
24. Ma, Z., Kotaki, M., Yong, T., He, W., Ramakrishna, S.: Surface engineering of electrospun polyethylene terephthalate (PET) nanofibers towards development of a new material for blood vessel engineering. Biomaterials **26**, 2527–2536 (2005)
25. Hou, H., Ge, J.J., Zeng, J., Li, Q., Reneker, D.H., Greiner, A., Cheng, S.Z.D.: Electrospun polyacrylonitrile nanofibers containing a high concentration of well-aligned multiwall carbon nanotubes. Chem. Mater. **17**, 967–973 (2005)
26. Yang, E., Qin, X., Wang, S.: Electrospun crosslinked polyvinyl alcohol membrane. Mater. Lett. **62**, 3555–3557 (2008)
27. Deitzel, J.M., Kleinmeyer, J.D., Hirvonen, J.K., Beck Tan, N.C.: Controlled deposition of electrospun poly(ethylene oxide) fibers. Polym. (Guildf) **42**, 8163–8170 (2001)
28. Heikkilä, P., Harlin, A.: Parameter study of electrospinning of polyamide-6. Eur. Polym. J. **44**, 3067–3079 (2008)
29. Zhu, H., Qiu, S., Jiang, W., Wu, D., Zhang, C.: Evaluation of electrospun polyvinyl chloride/polystyrene fibers as sorbent materials for oil spill cleanup. Environ. Sci. Technol. **45**, 4527–4531 (2011)
30. Haider, A., Haider, S., Kang, I.-K.: A comprehensive review summarizing the effect of electrospinning parameters and potential applications of nanofibers in biomedical and biotechnology. Arab. J. Chem. **11**, 1165–1188 (2018)
31. Ramakrishna, S., Fujihara, K., Teo, W.-E., Lim, T.-C., Ma, Z.: An introduction to electrospinning and nanofibers. In: An Introduction to Electrospinning and Nanofibers. World Scientific Publications, pp. 1–382 (2005)
32. Chen, K., Chou, W., Liu, L., Cui, Y., Xue, P., Jia, M.: Electrochemical sensors fabricated by electrospinning technology: an overview. Sensors (Switzerland) **19**, 3676 (1–19) (2019)
33. Bahrami, G., Ehzari, H., Mirzabeigy, S., Mohammadi, B., Arkan, E.: Fabrication of a sensitive electrochemical sensor based on electrospun magnetic nanofibers for morphine analysis in biological samples. Mater. Sci. Eng. C **106**, 110183 (2020)
34. Samie, H.A., Arvand, M.: Label-free electrochemical aptasensor for progesterone detection in biological fluids. Bioelectrochemistry **133**, 107489 (2020)
35. Tang, Q., Zhu, G., Ge, Y., Yang, J., Huang, M., Liu, J.: AuNPs-polyaniline nanosheet array on carbon nanofiber for the determination of As(III). J. Electroanal Chem. **873**, 114381 (2020)
36. Liu, S., Zhang, X.: Preparation of nitrogen doped carbon nanofibers for electrochemical determination of Cd(II) and Pb(II) Ions. Int. J. Electrochem Sci. 9838–9848 (2020)
37. Ahmad, W., Jabbar, B., Ahmad, I., Jan, B.M., Stylianakis, M.M., Kenanakis, G., Ikram, R.: Highly sensitive humidity sensors based on polyethylene oxide/CuO/multi walled carbon nanotubes composite nanofibers. Mater. (Basel) **14**, 1–19 (2021)
38. Manikandan, N., Valleti, K., Karupasamy, K., Divagar, M., Subramaniam, S.: The monolithic α, β crystal structural design of piezoelectric poly (vinylidene fluoride) (PVDF) polymer/fullerene based sensor array for the measurement of lung pressure. Sens. Bio-Sensing Res. **32**, 100418 (2021)
39. Wen, H.-Y., Liu, Y.-C., Chiang, C.-C.: The use of doped conductive bionic muscle nanofibers in a tennis racket–shaped optical fiber humidity sensor. Sens. Actuators B Chem. **320**, 128340 (2020)

40. Pavinatto, A., Mercante, L.A., Facure, M.H.M., Pena, R.B., Sanfelice, R.C., Mattoso, L.H.C., Correa, D.S.: Ultrasensitive biosensor based on polyvinylpyrrolidone/chitosan/reduced graphene oxide electrospun nanofibers for 17α—Ethinylestradiol electrochemical detection. Appl Surf Sci **458**, 431–437 (2018)
41. Koo, W.T., Choi, S.J., Kim, N.H., Jang, J.S., Kim, I.D.: Catalyst-decorated hollow WO3 nanotubes using layer-by-layer self-assembly on polymeric nanofiber templates and their application in exhaled breath sensor. Sens. Actuators B Chem **223**, 301–310 (2016)
42. Li, X., Zhuang, Z., Qi, D., Zhao, C.: High sensitive and fast response humidity sensor based on polymer composite nanofibers for breath monitoring and non-contact sensing. Sens. Actuators B Chem. **330**, 129239 (2021)
43. Gao, Y., Guo, F., Cao, P., Liu, J., Li, D., Wu, J., Wang, N., Su, Y., Zhao, Y.: Winding-Locked carbon nanotubes/polymer nanofibers helical yarn for ultrastretchable conductor and strain sensor. ACS Nano **14**, 3442–3450 (2020)
44. Wu, S., Liu, P., Zhang, Y., Zhang, H., Qin, X.: Flexible and conductive nanofiber-structured single yarn sensor for smart wearable devices. Sens. Actuators B Chem. **252**, 697–705 (2017)
45. Liu, K., Zhou, Z., Yan, X., Meng, X., Tang, H., Qu, K., Gao, Y., Li, Y., Yu, J., Li, L.: Polyaniline nanofiber wrapped fabric for high performance flexible pressure sensors. Polymers (Basel) **11**, 1120 (2019)
46. Salami, M.S., Bahrami, G., Arkan, E., Izadi, Z., Miraghaee, S., Samadian, H.: Co-electrospun nanofibrous mats loaded with bitter gourd (Momordica charantia) extract as the wound dressing materials: in vitro and in vivo study. BMC Complement Med. Ther. **21**, 111 (2021)
47. Georgakilas, V., Tiwari, J.N., Kemp, K.C., Perman, J.A., Bourlinos, A.B., Kim, K.S., Zboril, R.: Noncovalent functionalization of graphene and graphene oxide for energy materials, biosensing, catalytic, and biomedical applications. Chem. Rev. **116**, 5464–5519 (2016)
48. Tsiamis, A., Diaz Sanchez, F., Hartikainen, N., Chung, M., Mitra, S., Lim, Y.C., Tan, H.L., Radacsi, N.: Graphene wrapping of electrospun nanofibers for enhanced electrochemical sensing. ACS Omega **6**, 10568–10577 (2021)
49. Chen, H.-M., Wang, L., Zhou, S.-B.: Recent progress in shape memory polymers for biomedical applications. Chinese J. Polym. Sci. **36**, 905–917 (2018)

Quinones and Organic Dyes Based Redox-Active Organic Molecular Compounds Immobilized Surfaces for Electrocatalysis and Bioelectrocatalysis Applications

Sairaman Saikrithika, Yesudas K. Yashly, and Annamalai Senthil Kumar

Abstract Owing to the facile electron-transfer behavior, molecular redox-compound-based electrochemical oxidation and reduction reactions have been referred to as superior systems for a variety of electrocatalytic and electroanalytical applications. In general, redox-active organic molecules based on quinones and organic dyes like methylene blue, meldola's blue, neutral red, methylene green, and thionine-based species have been referred widely for electrocatalytic and bioelectrocatalytic oxidation/reduction reactions. Indeed, the preparation of stable and highly redox-active mediator surface-confined electrochemical systems is a challenging task. In the literature, covalently immobilized organic moiety-modified electrodes have been often encountered for serious surface fouling problems. On the other hand, carbon nanomaterial coupled organic redox mediator prepared by multiple π-π immobilization interactions between the aromatic conjugated e^- and sp^2 carbon of graphitic site have shown superior stability and in turn enhanced electron-transfer functional activity. The selectivity and efficiency towards the target analyte are dependent on the choice of materials and methods for modifying electrodes. In this book chapter, we review the preparation and characterization of various quinone and organic dyes based redox-mediator immobilized carbon nanomaterial modified electrodes for electrocatalytic and bioelectroctalytic applications.

Keywords Organic redox molecules · Quinones · Organic dyes · Surface-confined redox systems · Electrocatalysis · Bioelectrocatalysis

S. Saikrithika · A. Senthil Kumar (✉)
Nano and Bioelectrochemistry Research Laboratory, Carbon Dioxide and Green Technology Research Centre, Vellore 632014, Tamil Nadu, India

S. Saikrithika · Y. K. Yashly · A. Senthil Kumar
Department of Chemistry, School of Advanced Sciences, Vellore Institute of Technology, Vellore 632014, Tamil Nadu, India

1 Introduction

Design and development of nanomaterial surface-confined molecular electrodes (heterogeneous) are paramount of interest in molecular catalysis, photoelectrochemical, electronics, electrochemical sensor, energy systems, etc. [1]. For the case of heterogeneous electrocatalyst systems, the molecules present in the diffusion layer which is closest to the electrode surface are highly-active for electron-transfer reactions. Such a heterogeneous electrocatalyst requires only a minimum amount of molecular active-species and provides high turn-over frequency over the homogeneous electrocatalytic systems. The beauty of electrochemistry is to custom-made chemically modified electrode (CME)-architecture and apply it for tunable electron-transfer applications [2]. The working–CME acts as a tunable system to pump (reduction) or withdraw (oxidation) electrons from the test-analyte by adjusting the potential and current directions suitably. Electrocatalytic property is one of the unique features of the CME that has been used for electrochemical synthesis, electrochemical sensor and bioelectrochemical sensor, fuel cell, and biofuel cell applications. In general, electrocatalytic reactions are associated with a reduction in the over-potential ($\eta = E_{observed} - E_{ideal}$/V) of electrochemical reaction. This article covers organic redox mediators quinones and organic dye molecule-based CMEs for electrocatalytic and bioelectrochemical applications.

Originated from the natural processes, wherein, plastoquinone (PQ) involves in the electron-shuttling process between the photosystem and cytochrome c and with several energy centers, quinones based on 1,2-dihydroxy benzene (catechol, CA) and 1,4-dihydroxy benzene (Hydroquinone, HQ) have been referred to as benchmarking organic redox molecules in electrochemistry. Similarly, organic dyes such as methylene blue (MB), meldola's blue (MLB), nile blue (NB), and thionine (Th) showed the wonderful electron-transfer property and served as a co-factor for the bioelectrocatalytic oxidation/reduction reactions [3]. For instance, MB and Th-based dye coupled Horseradish peroxidase (HRP) enzyme for bioelectrocatalytic reduction of H_2O_2 and associated application in electrochemical immunosensor, etc. [4].

These organic molecules provide a well-defined proton-coupled electron-transfer system for a variety of mediated oxidation/reduction reactions both in aqueous and non-aqueous solutions. What inspired us to prepare this article is the active site (either inorganic or organic moiety) which stabilized the protein structure of the natural enzyme and its selective catalytic/biocatalytic function to the target molecule. For example, flavin active *glucose oxidase enzyme* (GOD) for selective glucose oxidation (Scheme 1) and non-heme mixed valent di Fe(μ-OH) active site stabilized *nitric oxide reductase enzyme* for NO reduction reactions, etc. [5, 6]. Biomimicking study of the natural system is not simple, a large number of hurdles to be overcome even to biomimic single function of the enzymatic activity. Note that enzyme active sites are unstable outside the protein matrix. In this article, we covered the biomimicking model concept, to develop target selective electrocatalytic systems by chemically modifying electroactive mediator (P/Q) within a polymer or inorganic or carbon matrix structure, similar to an active site stabilized protein structure of the enzyme and
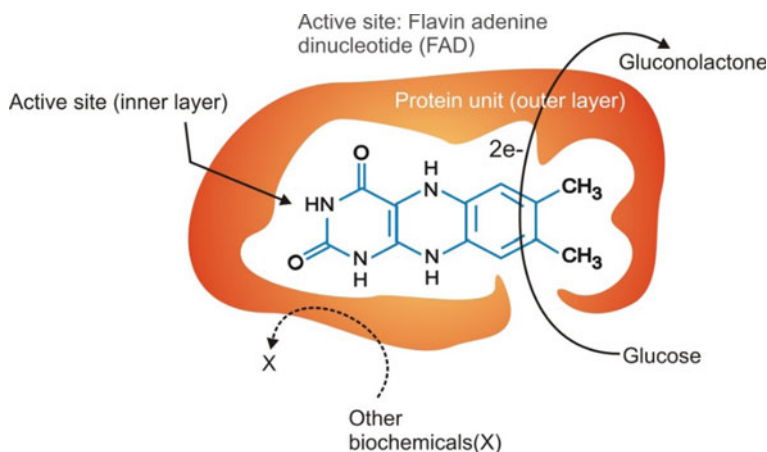
Scheme 1 Cartoon for the *glucose oxidase enzyme* (GOD) and its selective glucose oxidation reaction

further to electrocatalytic oxidation or reduction reaction suitable for amperometric electrochemical sensor applications (Scheme 1).

In general, for redox mediator impregnated CME preparation, the following methodologies have been adopted: (i) covalent immobilization, (ii) self-assembled monolayer (SAM), (iii) electro-polymerization and (iv) ion-exchange method. This article covers various methods of preparation and electrocatalytic/ bioelectrocatalytic applications of the organic redox mediators, quinones, and organic dyes-based CMEs.

1.1 Benzo-quinone Based Modified Electrodes for Electrocatalysis

Generation of surface functional groups such as carboxylic, carbonyl, and amino on the working electrode is one of the prim routes for the impregnation of redox-active organic molecules. Table 1 summarizes the different benzoquinone (BQ, an oxidized form of HQ) (Scheme 2) based modified electrodes fabricated for electroanalytical applications that have been collected from the Scopus® index search using the keywords "Quinone, redox mediators, electroanalytical application". In 1991, Hoogvliet et al. developed methyl viologen (MV) derivative and p-benzoquinone (p-BQ) immobilized glassy carbon electrodes (GCE) by chemical modification method and used for bioelectrocatalytic reduction of H_2O_2 in couple with HRP enzyme. In a typical procedure, the GCE surface was activated by exposing it with a 5% dilute solution of dichromate (15 min) or hypochlorite (16 h) in pH 7 phosphate buffer solution (PBS). In addition, electrochemical anodization by oxidizing GCE up to 1.6 V in a pH 7 buffer was explored. A significant amount of carboxylic functional group

Table 1 Benzoquinone-based chemically modified electrodes for electroanalysis

	CME	Analyte	Tech	E° / E_{app} (V)	pH	LOD/ Linear range (μM)	References
1	GCE*@p-BQ	H_2O_2	FIA	0.0	7.0[b]	0.1 ng	[7]
2	GCE/PEO+PHD	Glu NADH	CA	0.0	7.0[a]	0–10,000	[8]
3	EGCE/p-BQ	NADH	CV, Amp i-t	0.25	7.0[b]	10–90	[9]
4	GCRDE@AAQ	Oxygen	RDE	−0.55		8.3 ppm	[10]
5	SAM-Au/o-QP	Thiols	CV	0.3	3.0[a]	0.25–1%	[11]
6	SAM-Au/NQF	L-Tyr	CV	−0.5	7.0[b]	5000	[12]

AAQ Aminoanthraquinone diazonium cations; *EGCE* epoxy–graphite composite electrode; *GCE* Glassy carbon electrode; *GCRDE* Glassy carbon rotating disk electrode; *Glu* Glucose; *NQF* naphthoquinone-functionalized; *o-QP* o-quinone-capped phenylene ethynylene; *p-BQ* p-benzoquinone; *PEO* poly(ethylene oxide); *PHD* Phenanthroline-5,6-diones; *SAM-Au* self assembled monolayer on gold electrode; *Tyr* tyrosine
*Anodized
[a]Ag/AgCl
[b]SCE
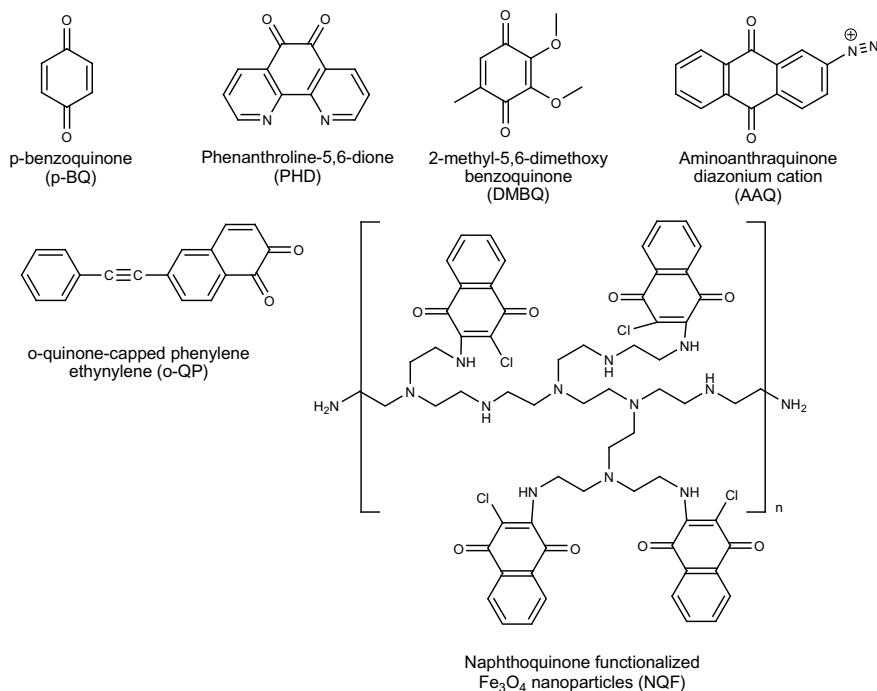
Scheme 2 Structures of various quinones and their derivatives that are covered in this chapter

was generated and further involved in coupling with amino functional group of MV derivatives and ethylene diamine linker and subsequently for BQ immobilization via C-N and C-C bond formations. Such modified electrodes showed well-defined redox peaks at about 0 V and −0.7 V vs SCE for surface-confined BQ and MV redox sites. Utilizing these redox features as a cofactor, bioelectrocatalytic reduction and flow injection analysis (FIA) of H_2O_2 sensing was demonstrated by adsorbing HRP on the electrode surface or taking hydrogenase enzyme in the solution phase condition. Although such methodology provides an efficient route for the bioelectrocatalytic application, the stability of the electrode was not up to the mark. About 20% of surface fouling was noticed after the electrodes are being used continuously for 3–4 h. [7]. In 1996, Geng et al. reported the utilization of heterocyclic quinone and poly(ethylene oxide) (PEO) modified GCE and plasma-treated carbon strip electrodes for detecting NADH and glucose, respectively. The electrode surface was modified by drop-casting a mixture of 5% PEO and the mediator on polished GCE and the strip electrodes. Considering their low redox potential (0.2 V vs Ag/AgCl) and efficient oxidation of NADH, Phenanthroline-5,6-dione-redox mediator (PHD) was chosen as a model for the heterocyclic quinone system. For the case of glucose biosensor application, two units of glucose dehydrogenase (GDH) enzyme dissolved pH 7 PBS were used [8].

In 2004, Simon et al. reported the comparison of six different redox mediators viz, potassium hexacyanoferrate, MLB, dichlorophenolindophenol (DCPIP), p-BQ, o-phenylenediamine (o-PD), and 3,4-dihydroxybenzaldehyde (3,4-DHB) as surface-confined redox systems for the electrocatalytic oxidation of NADH in pH 7 PBS. A graphite composite electrode, prepared using graphite powder and epoxy resin, was used as a working electrode. This electrode was used for the immobilization of the redox mediators via three methods, viz, epoxy-graphite composite electrode, adsorption, and electropolymerization processes. The leakage of the redox mediator and low sensitivity and reproducibility are the major drawbacks with the composite and adsorption-based CMEs. On the other hand, no such complications were noticed with the electropolymerized systems. Among the redox mediators used, o-PD and DCPIP have exhibited high sensitivity and selective response towards the electrocatalytic oxidation and amperometric sensing of NADH [9]. In 2009, Kullapere et al. reported an electrochemical reduction of dissolved oxygen using rotating disk GCE (GCRDE) that has been covalently modified with in-situ synthesized anthraquinone diazonium cations from 1-aminoanthraquinone or 2-aminoanthraquinone (AAQ) as the precursor. It has been found that the nature of the electrolyte, such as acetonitrile and an acidic solution did not influence the in-situ generation of the diazonium cation process [10]. In 2011, Wendland et al. reported an in-situ self-assembled thiolated quinone on a gold electrode (SAM-Au/o-QP) as an electrocatalyst for oxidation of ethanethiol in pH 3 acetate buffer solution. At first, two numbers of thiolated o-quinone capped phenylene-ethynylene (o-QP) electrocatalysts were synthesized and subsequently dissolved in a drop of concentrated sulfuric acid mixed dichloromethane (DCM) and methanol (MeOH) mixture (1:1) solvent, wherein, the thiol group was in-situ generated via acetate hydrolysis. The as-prepared electrodes were found to exhibit good reproducibility with no surface fouling effect

[11]. In 2018, Hou et al. reported an interesting work on the conversion of L-phenylalanine or L-tyrosine to dopachrome via L-DOPA formation using CuFe-Prussian blue like nanoparticles or naphthoquinone derivative/Fe_3O_4 nanoparticles (NQF) modified gold electrode (SAM-Au/NQF) as electrocatalyst in presence of L-ascorbic acid/H_2O_2 in pH 7 PBS [12]. From the collective information, it can be summarized that the quinone-based redox systems can be immobilized by composite, in-situ polymerization, diazonium coupling, simple adsorption, and SAM systems (Fig. 1). Each one has its own merits and demerits in terms of redox activity and stability.
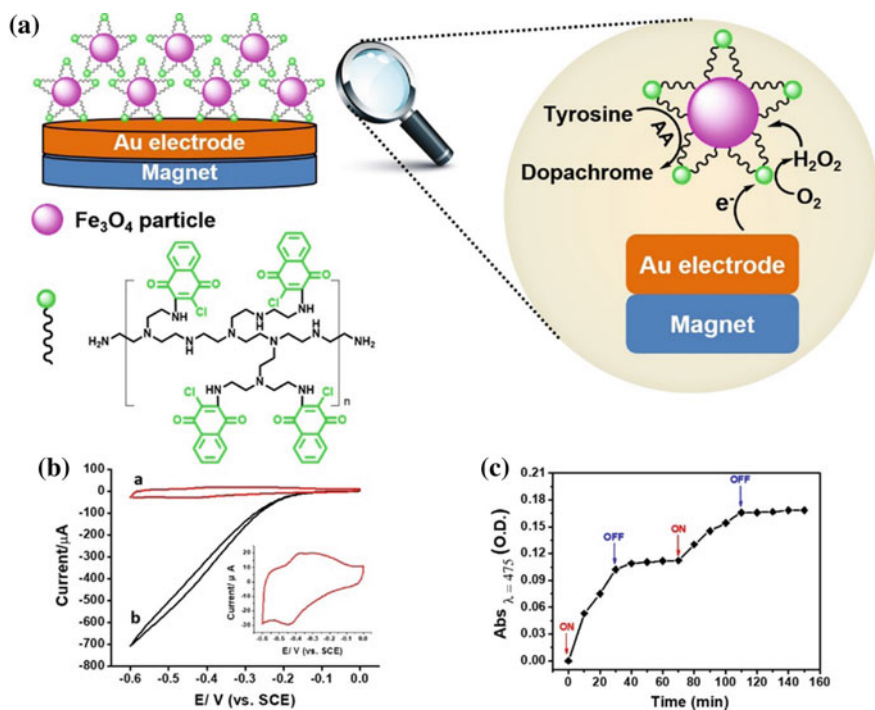
Fig. 1 **a** Schematic illustration for the conversion of L-Tyr to dopachrome on a naphthoquinone functionalized iron oxide nanoparticles; **b** Cyclic voltammetric responses of the modified electrode towards the conversion of O_2 to H_2O_2 in N_2 atmosphere (curve a) and O_2 atmosphere (curve b); **c** Aerobic oxidation of L-Tyr to dopachrome using switchable electrocatalysis. Adapted with permission from reference [12], Copyright (2018), American Chemical Society

1.2 Hydroquinone Based Modified Electrodes for Electrocatalysis

Owing to the high water solubility, immobilization of hydroquinone (HQ) on the electrode surface is a challenging task. Table 2 summarizes the literature collection obtained from Scopus® using the keywords "Hydroquinones, redox mediators, electroanalytical application". Following are some of the representative methodologies summarized for the HQ immobilization on various carbon-based electrodes (Table 2). The structures of different HQ and their derivatives discussed in this chapter are given in Scheme 3. A mixture of HQ + GOD along with graphite and mineral oil as paste electrodes (CPE + HQ + GOD) were used for glucose biosensing application. The only disadvantage of this glucose sensor is the surface passivation of the electrode by glucose adsorption upon prolonged potential cycling [13]. Alternatively, in-situ synthesized poly-HQ (PHQ) by soybean peroxidase enzyme assisted partial hydrolyzation of arbutin (hydroquinone-β-D-glucopyranoside) (HQG) was found to be a better choice for the above case [14]. In another case, a glucose sensor based on PHQ@GOD enzyme-modified carbon rod electrode (CRE/HQG + GPQQ), wherein, PHQ was first prepared by laccase-enzyme assisted deglycosylation of arbutin and in next, GOD enzyme mixed composite system was reported. The PHQ formation was found to be independent of the degree of enzyme hydrolysis of arbutin. The sensor exhibits a long linear range of glucose detection (0–2.5 mM) [15].

Table 2 Hydroquinone-based chemically modified electrodes electroanalysis

	CME	Analyte	Tech	E°/E$_{app}$ (V)	pH	LOD/Linear range (µM)	References
1	CPE + HQ + GOD	Glu	FIA	0.15	7.4[a]	0–60,000	[13]
2	GCE/PHQ + GP@GOD	Glu	CV, Amp i-t	0.4	7.0[b]	1–30,000	[14]
3	CRE/HQG + GPQQ	Glu	CV	0.2	7.0[a]	0–2500	[15]
4	BPGE/PHQ	DNA	CV	0.0	7.0[a]	–	[16]
5	SAM-Au@HQTS		CV	0.6	7.0[a]	–	[17]
6	GCE@DHQS	Hyd	CV	0.25	7.5[a]	1.6	[18]
7	Au/PPy@HQ	HQ	CV		7.0	5	[19]

BPGE basal pyrolytic graphite electrode; *CPE* Carbon paste electrode; *CRE* Carbon Rod electrode; *DHQS N*, *N*-bis(dihydroxybenzylidene)-1,2-diaminobenzene; *Glu* Glucose; *GOD* Glucose oxidase; *GP* Graphite powder; *GPQQ* Pyrroloquinoline quinone dependent glucose dehydrogenase; *HQG* Hydroquinone-β-D-Glucopyranoside (Arbutin); *HQ* Hydroquinone; *HQTS* hydroquinonethiosulfate; *Hyd* Hydrazine; *PHQ* poly (hydroquinone); *PPy* Polypyrrole; *SAM Au* self-assembled monolayer gold electrode
[a]Ag/AgCl
[b]SCE

Hydroquinone
(HQ)

Poly (hydroquinone)
(PHQ)

Hydroquinone-thiosulfate
(HQTS)

Hydroquinone-β-D-Glucopyranoside
(Arbutin) (HQG)

N,N-bis(dihydroxybenzylidene)-1,2-diaminobenzene (DHQS)
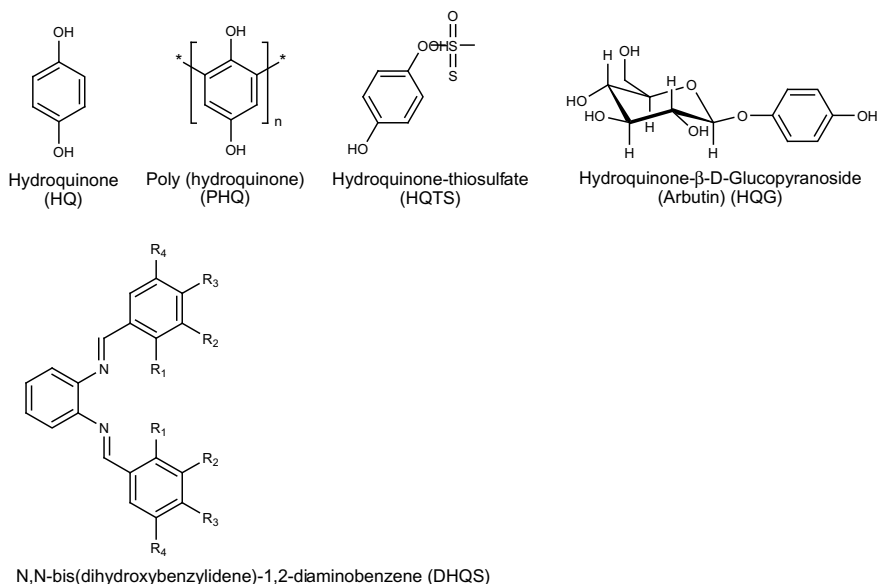
Scheme 3 Structures of hydroquinone and its derivatives that are discussed in this chapter

A label-free DNA biosensor was reported based on DNA hybridization on an in-situ synthesized PHQ by deglycosylation of poly(arbutin) using peroxidase enzyme over a pyrolytic graphite electrode as the base matrix [16]. First, the pyrolytic graphite electrode was modified with the synthesized PHQ, followed by immobilizing a single-stranded DNA probe. This electrode was used for the detection of DNA, wherein the target single-strand DNA hybridizes with the probe on the electrode, wherein HQ behaves as an intercalator and electrochemical redox signaling system. The authors stated that this technique can be used for label-free detection of DNA [16]. In another report, selective anodic pulse deposition of HQ-thiosulfate (HQTS) and naphthoquinone-thiosulfate on gold disk electrode surface as a SAM (SAM-Au) was reported, where an irreversible conversion of thiosulfate to thiol-radical was observed at 0.6 V vs Ag/AgCl with HQTS. The SAM preparation was completed in just 40 s owing to an increase in the mass transport of thiosulfate to the electrode. Utilizing the kinetically hindered self-adsorption, the micropatterning of molecular SAM was also achieved [17]. In continuation, HQ salophen derivatives (by combining o-phenylenediamine and dihydroxybenzaldehyde) (DHQS) modified GCE was fabricated via simple adsorption and electrochemical deposition, followed by application to electrochemical oxidative detection of hydrazine was reported. The electrochemical behavior of the modified electrode surface showed a linear dependence on increasing pH [18]. Meanwhile, the cytotoxicity of HQ towards V79 cells was studied by an in-situ release method. In prior, HQ doped polypyrrole (Ppy) film was fabricated on the bare gold electrode by electropolymerization of pyrrole in HQ containing electrolyte. It has been found that the adsorbed HQ was released

Change of electrode potential
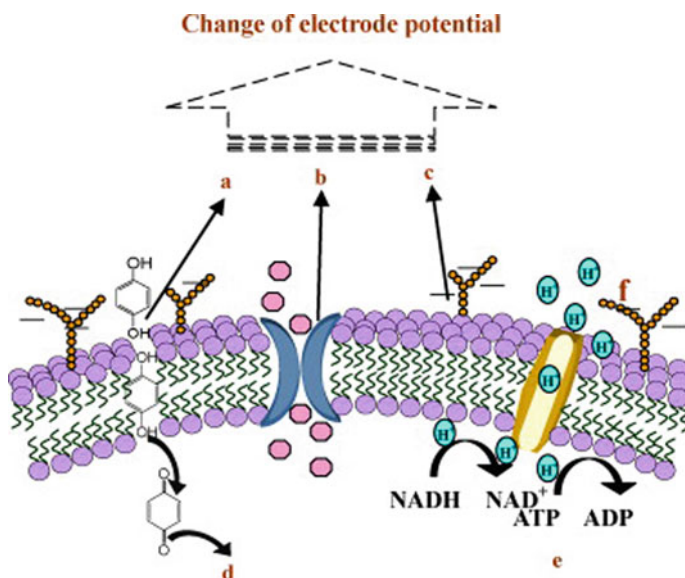
Fig. 2 Schematic illustration for the fabrication of the biosensor and the potentiometric changes happening due to HQ exposure; Changes of **a** cellular metabolism, **b** ion transport, **c** cell morphology and growth, **d** cellular redox state, **e** redox reaction and **f** negative glycoprotein array. Adapted with permission from reference [19], Copyright (2010), Elsevier

in-situ under applied potential and V79 cells grew over them. A potentiometric HQ sensing method was used for the bioanalytical study. It has been concluded that HQ is non-toxic up to 30 µM concentration of HQ (Fig. 2) [19].

1.3 Organic Dye-Based Chemically Modified Electrode for Electroanalytical Applications

Various organic dyes, viz., MLB, polymerized MLB (PMLB), poly nile blue (PNB), poly(brilliant cresyl blue) (PBCB), poly (neutral red) (PNR), poly(methylene green) (PMG) (Scheme 4) based CMEs were covered in this section for the electrocatalysis of different analytes. In this work, highlights on the preparation of the surface-confined redox dyes and its electrochemical features were summarized in Table 3, 4, 5 and 6. The literature data were collected from Scopus® source using the keywords "Organic dyes, redox mediators, electroanalytical applications".

Meldola's blue (MLB)

Nile blue (NB)

Neutral red (NR)

Brilliant cresyl blue (BCB)
Poly (brilliant cresyl blue) (PBCB)

Methylene green (MG)
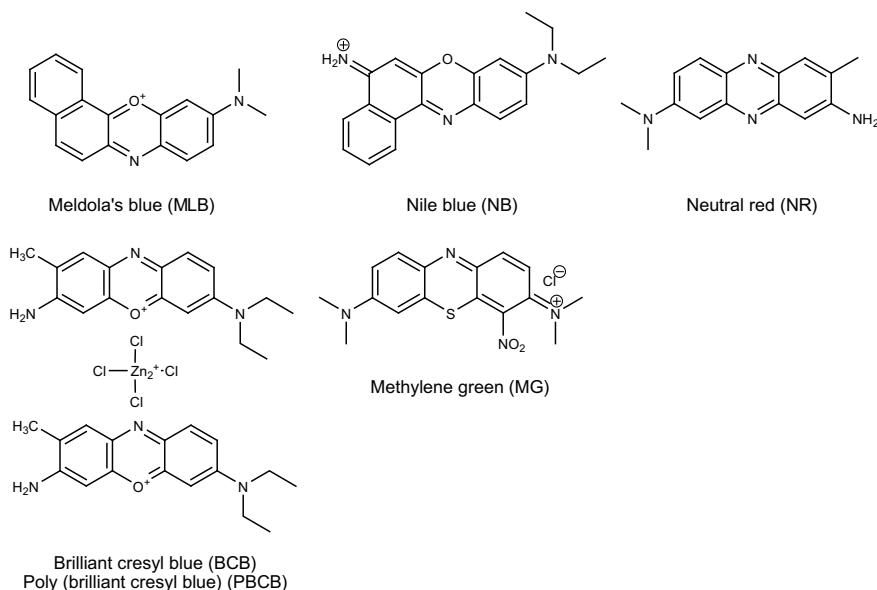
Scheme 4 Structures of the organic dyes that are discussed in this chapter

1.3.1 Meldola's Blue

There are thirteen articles reported for NADH detection using MLB-modified electrodes (Table 3). In general, MLB modified electrode was fabricated via synthesis of carbon-based nanocomposite for the detection of NADH. In 1996, Kubota et al. modified MLB on titanium phosphate grafted silica gel (STP) was described. The carbon paste electrode (CPE) technique was adopted to prepare the CME suitable for NADH sensing at 0 V versus SCE in a neutral pH condition [20]. In 2007, Zhu et al. reported MLB adsorbed carbon nanotube (CNT) modified GCE by surface modification technique, wherein, the CNT modified electrode was immersed in a dilute MLB solution for 10 min [21]. It is likely that a strong π-π interaction between the sp^2 carbon of CNT and aromatic πe^{-s} of MLB involved for the stabilization of the redox mediator. The modified electrode showed an electrocatalytic NADH oxidation signal at −0.1 V vs SCE tested using chronoamperometry technique. Observed electrocatalytic behavior is superior to that of the conventional graphite powder modified electrode. In another method, MLB modified screen printed electrodes (SPE) were prepared using electropolymerization (by applying constant potential) and Nafion-composite formation (by mixing polysulfone (PS), MLB and graphite) methods for the detection of NADH [22]. The authors integrated their electrodes with glutamate dehydrogenase-enzyme, for ammonium ion sensing application (in couple with NADH-cofactor). Although both the electrodes exhibited good electrocatalytic activity towards NADH, the nanocomposite showed higher reproducibility with an absence of any surface-fouling complication. In another case, bulk modified

SPE was prepared by printing a mixture of zirconium phosphate (ZrP), MLB, and graphite (GP) ink over a polyester film-substrate followed by a constant potential electrochemical deposition of Reinecke salt (RS) ($NH_4[Cr(NCS)_4(NH_3)_2] \cdot H_2O$) that helps for precipitation of MLB as an ammonium salt on the surface, was reported for electrochemical sensing of NADH [23]. Further, to this electrode, glutaraldehyde and a mixture of glycerol dehydrogenase +Nafion (Nf) were coated for its application as a glycerol sensor in association with NADH as a cofactor. Similarly, a titanium oxide-cellulose acetate (TCA) mixture incorporated with MLB and graphite powder-based CPE was prepared [24]. For the preparation of TCA, titanium

Table 3 Meldola's blue-based chemically modified electrodes for NADH detection

S. No.	CME	Analyte	Tech	E°/E_{app} (V)	pH	LOD /linear range (μM)	References
1	CPE + STP + MLB	NADH	CV, amp i-t	0.0	7.4[b]	10–50	[20]
2	GCE/CNT/MLB	NADH	CA	−0.1	6.8[b]	0.048	[21]
3	SPE/PS + MLB + GP	NADH	Amp i-t	− 0.1	6.5[b]	20–500	[22]
4	SPE/GP + ZrP + MLB/RS	NADH	FIA	0.05	8.5[a]	10–100	[23]
5	CPE + TCA + MLB	NADH	CV, CA	0.02	7.0[b]	100	[24]
6	SPE/SG + MLB + SWCNT	NADH	CV, Amp i-t	−0.05	7.5[a]	6	[25]
	SPE/SG + MLB + SWCNT/LDH	D-lactate	CV, Amp i-t	−0.05	7.5[a]	16	
7	GCE/SWCNT + MLB	NADH	CV, Amp i-t	−0.05	7.4[a]	0.4	[26]
	GCE/SWCNT + MLB/MDH + Nf	L- Malic acid	Amp i-t	−0.05	7.4[a]	0 − 2500	
8	STGSb/MLB	NADH	CV	−0.14	7.5[b]	3	[27]
9	SiSnSbC/MLB	NADH	CA	−0.05	7.3[b]	0.15	[28]
10	GCE@PEDOT@AgNP/MLB	NADH	CV, Amp i-t	−0.05	7.0[b]	0.1	[29]
11	PGE/MLB	NADH	CV, CA	−0.15	7.0[b]	1000 - 10,000	[30]
12	SPE/CNF/MLB + rGO	NADH	Amp i-t	+ 0.05	7.4[b]	0.5	[31]
		Benzaldehyde	CA	+0.05	9.5[a]	17	

(continued)

Table 3 (continued)

S. No.	CME	Analyte	Tech	E°/E$_{app}$ (V)	pH	LOD /linear range (μM)	References
13	SPE/CNF/NiAm + MLB	NADH	FIA, Amp i-t	0.05	7.4[a]	0.5	[32]

AgNP silver nanoparticles; *CNF* carbon nanofiber; *CNT* Carbon nanotube; *CPE* Carbon paste electrode; *GCE* glassy carbon electrode; *GP* Graphite; *LDH- d* lactate dehydrogenases; *MDH-L* malate dehydrogenase; *MLB* Meldola's Blue; *MWCNT* Multi-walled carbon nanotube; *Nf* Nafion; *NiAm* nickel hexamine complex; *PEDOT* Poly(3,4-ethylenedioxythiophene); *PGE* pencil-drawn graphite electrode; *PS* Polysulfone; *rGO* reduced graphene oxide; *RS* Reinecke salt; *SG* Sol-Gel; *SiSnSbC* Sb(V) immobilized on SiO$_2$/SnO$_2$/graphite compressed disk electrode; *SPE* Screen-printed electrode; *STGSb* Sb(V) immobilized on SiO$_2$/TiO$_2$/graphite compressed disk electrode; *STP* silica gel surface coated with titanium (IV) oxide; *SWCNT* single-walled carbon nanotube; *TCA* TiO$_2$ immobilized on the cellulose acetate; *ZrP* Zirconium Phosphate

[a]Ag/AgCl
[b]SCE

butoxide was added to cellulose acetate + acetic anhydride syrup under constant stirring followed by the addition of double-distilled water. The electrochemical sensor showed current linearity in a window, 0.1–2 mM with a detection limit, 0.1 μM for the NADH. In another report, a novel MLB/sol-gel-based nanocomposite was fabricated for NADH detection [25]. In the preparation of sol-gel, tetramethoxysilane and methyltrimethoxysilane mixture was dissolved in a dilute HCl (as a catalyst) to form a transparent sol followed by the addition of MLB and SWCNT on it. This sol-gel was coated on SPE for the electrochemical detections of NADH and D-lactate, wherein for the latter one D-lactate dehydrogenase (LDH) enzyme was immobilized on the electrode. In the next year, part of the team members have developed an NADH sensor based on MLB and SWCNT and further extended it to L-mallic acid detection in couples with L-malate dehydrogenase (MDH) enzyme on the modified electrode surface [26].

In 2010, a Sb-O-Ti ceramic material (STGSb) was formed by sol-gel processing technique using SbCl$_2$, SiO$_2$, TiO$_2$, and graphite as precursors, followed by pressing the material into a disk electrode with copper wire (electrical contact) for electrochemical sensing of NADH application [27]. MLB was adsorbed by immersing the electrode in 0.1 mM of MLB solution for an hour. Similarly, an ionic SiO$_2$/SnO$_2$/Sb$_2$O$_5$ based ceramic electrode was prepared by sol-gel methodology followed MLB modification via surface-ion exchange method [28]. A disk electrode was prepared by mixing this nanocomposite with graphite powder and used for NADH detection in biological samples. In 2010, Balamurugan et al. have reported poly(3,4-ethylene dioxythiophene) (PEDOT)-sodium dodecyl sulfate (SDS)/Silver nanoparticle (AgNP) modified GCE prepared by potential cycling of the precursor electrode with 1 mM AgNO$_3$ dissolved NaNO$_3$ solution. The MLB was immobilized by exposing the precursor electrode with a dilute solution of MLB at room

Table 4 Meldola's blue-based chemically modified electrodes for electroanalysis

S. No.	CME	Analyte	Tech	E^o/E_{app} (V)	pH	LOD/linear range (μM)	References
1	SPE/MLB/NADH/HSDH	Androstenone	CA, DPV	+0.05	7.0[a]	0.3 ppm	[33]
2	CPE + STP + MLB + FDH	Fructose	CV	0.02	4.5[b]	0–5000	[34]
3	GCE@PMLB/HRP/GOD/Nf	H_2O_2	CV, Amp i-t	−0.30	7.0[a]	500	[35]
4	CPE + MWCNT + MLB + ADH	EtOH	Amp i-t	0.0	7.5[b]	5	[36]
	SPE/GP + ZrP + MLB/RS/GLYDH + Nf	Glycerol	FIA	0.1	8.5[a]	2.8	

ADH Alcohol dehydrogenase; *CPE* Carbon paste electrode; *FDH* Fructose-5-Dehydrogenase; *GCE* Glassy carbon electrode; *GLYDH* Glycerol dehydrogenase; *GOD*-Glucose oxidase; *GP* Graphite; *HRP*- horseradish peroxidase; *HSDH* 3α-hydroxysteroid dehydrogenase; *MLB* Meldola's Blue; *MWCNT* Multi-walled carbon nanotube; *Nf* Nafion; *PMLB* Polymerized Meldola's Blue; *RS* Reinecke salt; *SPE* Screen-printed electrode; *STP* silica gel surface coated with titanium (IV) oxide; *ZrP* Zirconium Phosphate
[a] Ag/AgCl
[b] SCE

Table 5 Nile blue-based chemically modified electrodes for electroanalysis

S. No	CME	Analyte	Tech	E°/E$_{app}$ (V)	pH	LOD/linear range (μM)	References
1	GCE/SWCNT@PNB/ADH	EtOH	CV	+ 0.1	8.3[b]	~50	[37]
2	GCE/SWCNT@PNB/GDH	Glu	CV, Amp i-t	−0.03	8.5[b]	5	[38]
3	GCE@AP/GOD/IONP/CHIt/NB	Glu	Amp i-t	−0.60	7.0[a]	19	[39]
4	CPE/rGO + NB@NiO	Glu	CV, Amp i-t	−0.04	4.0[a]	2.2	[40]
5	GCE@NB	H$_2$O$_2$	CV, Amp i-t	−0.15	7.0[a]	0.17	[41]
	GCE@NB/GOD	Glu		−0.45		0.44	
6	CFME/Au/BA + NB	H$_2$O$_2$	DPV, CV	0.3	7.4[a]	0.02	[42]
7	GCE/IONP + CHIt@PNR	H$_2$O$_2$	CA, Amp i-t	−0.4	7.0[a]	4.3	[43]
	GCE/IONP + CHIt@PMG					5.6	
	GCE/IONP + CHIt@PNB					4.4	
8	GCE@PNB	Oxygen	CV	−0.5	5.3[b]	0.78	[44]
9	GCE/GN + PNB	Oxygen	LSV	−0.5	7.0[b]	8.3 ppm	[45]
	GCE/GN + PNB/GOD	Glu	CV			2.1	
10	GCE@PNB	Nitrite	CV, DPV	0.8	7.1[b]	0.1	[46]
11	GCE/MWCNT@PNB	AA	CV	0.1	5.3[b]	10.8	[47]
			Amp i-t	0.0		2.4	

(continued)

Table 5 (continued)

S. No	CME	Analyte	Tech	E°/E$_{app}$ (V)	pH	LOD/linear range (μM)	References
12	QC/GPE/NMPA/dsDNA/NB	DNA	LSV	−0.47	7.45 [a]	–	[48]
13	GCE/NB + rGO@AuNP	DA	CV, SWV	0.15	7.0[b]	0.001	[49]
14	SPE/NSPC + pTTBA /NB	Hemoglobin	CV	−0.5	7.4[a]	0.8	[50]
15	GCE/ CeO$_2$ + NB	Hyd	CV, CA, DPV	+0.9	7.0[a]	0.057	[51]
16	PIGE/ PAMAM/PNB	Many biological analytes	CV		7.0[b]	0.13–1667	[52]

AA Ascorbic acid; *ADH* alcohol dehydrogenase; *AuNP* gold nano particles; *Au-QC* gold quartz crystal; *BA* 5-((1,2-dithiolan-3-yl)-N-(4-(4,4,5,5-tetramethyl-1,3,2-dioxaborolan-2-yl)phenyl)pentanamide; *CeO$_2$* cerium oxide; *CHlt* Chitosan; *CPE* Carbon paste electrode; *GCE* Glassy carbon electrode; *GDH* Glucose dehydrogenase; *Glu* Glucose; *GN* Graphene Nanosheets; *GOD* Glucose oxidase; *IONP* Iron oxide nanoparticles; *MWCNT* Multi-walled carbon nanotube; *NB* Nile blue; *NiO* nickel oxide; *NMPA* NH$_2$ modified oligonucleotides immobilized on EDC activated mercaptopropionic acid (MPA); *NSPC* N,S-doped porous carbon; *PAMAM* poly(amido amine) dendrimer; *PIGE* Paraffin impregnated graphite electrode; *PMG* poly (methylene green); *PNB* Poly Nile Blue; *PNR* poly (neutral red); *pTTBA* poly(2,2′:5′,5″-terthiophene-3′-p-benzoic acid; *rGO* reduced graphine oxide; *SPE* Screen-printed electrode; *SWCNT* Single-walled carbon nanotube
[a] Ag/AgCl
[b] SCE

Table 6 Poly(brilliant cresyl blue)-based chemically modified electrodes for electroanalysis

S. No.	CME	Analyte	Tech	$E°/E_{app}$ (V)	pH	LOD/linear range (μM)	References
1	GCE@PBCB/AuNP/HRP	H_2O_2	CV, Amp i-t	-0.07	7.0^a	0.5 μM	[53]
2	GCE@PBCB/ IONP + CHIt	Epinephrine	DPV	$+ 0.2$	7.0^a	0.310 ± 0.06 μM	[54]

AuNP gold nano particles; *CHIt* Chitosan; *GCE* Glassy carbon electrode; *HRP* horseradish peroxidase; *IONP* Iron oxide nanoparticles; *PBCB*-Poly(brilliant cresyl blue)
^{a} Ag/AgCl

temperature. The sensor systems showed a calibration plot in a window, 10–500 μM with a detection limit value, 0.1 μM [29]. In 2017, a pencil-drawn graphite electrode (PGE), fabricated using 4B pencil, was reported for the electrocatalytic oxidation of NADH [30]. The working electrode was drawn on a wax treated conventional office paper with silver and gold as reference and counter electrodes, over which MLB was allowed to immobilize (for 15 min) by drop-casting and sued for NADH detection (Fig. 3).

The commercially available carbon nanomaterial (SWCNT, mesoporous carbon, carbon nanofiber (CNF)) coated SPE modified with MLB were used for the NADH detection. The best result was obtained for MLB adsorbed over CNF modified SPE [31]. Further to this electrode, NAD^+/NADH-cofactor-dependent aldehyde dehydrogenase-enzyme was immobilized for electrochemical detection of benzaldehyde. In 2020, the same group of researchers reported a similar kind of work, with a slight modification of combining MLB with nickel hexamine chloride complex (NiAm) for the detection of NADH. The modified electrode was extended to FIA of benzaldehyde in couple with aldehyde dehydrogenase-enzyme on the electrode [32].

Apart from the detection of NADH, MLB based CMEs were effectively used as a cofactor for the detection of androstenone (a steroidal hormone present in the
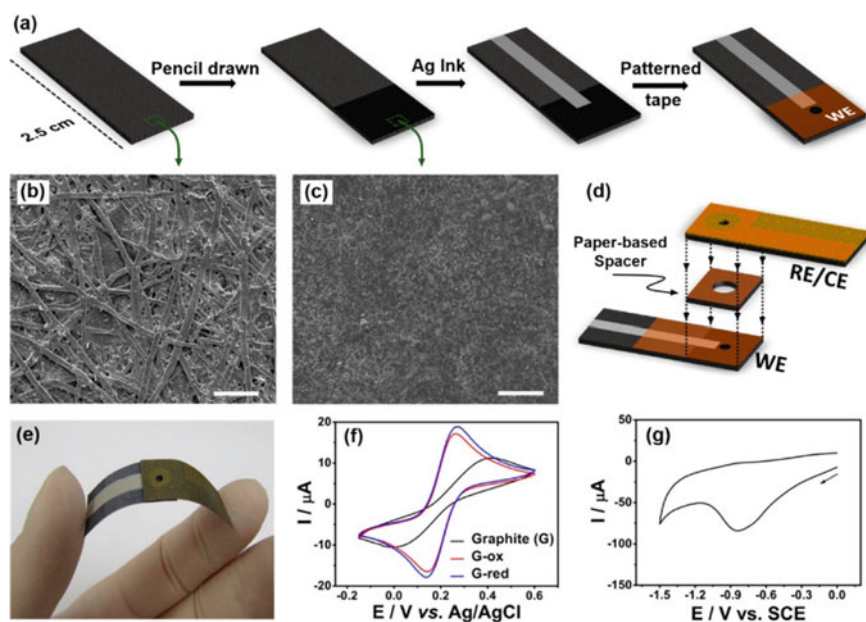

Fig. 3 Schematic illustration for the fabrication of the SPE (**a**), SEM images of the wax paper before and after pencil drawing (**b**, **c**), illustration for assembling of the electrode (**d**), an image of the finally assembled electrode (**e**), cyclic voltammetric responses in $[Fe(CN)_6]^{3-}$ at a scan rate of 30 mV/s (F) and $H_2PO_4^-/HPO_4^{2-}$ at a scan rate of 50 mV/s (G). Adapted with permission from reference [30], Copyright (2017), American Chemical Society

testes of boars) in couple with 3α-hydroxysteroid dehydrogenase enzyme (HSDH) [33], fructose in couple with fructose dehydrogenase (FDH) enzyme [34], H_2O_2 by a couple with HRP enzyme and further to glucose and choline in association with their respective enzymes [35], and ethanol by incorporating alcohol dehydrogenase (ADH) [36] on the modified electrode surfaces (Table 4).
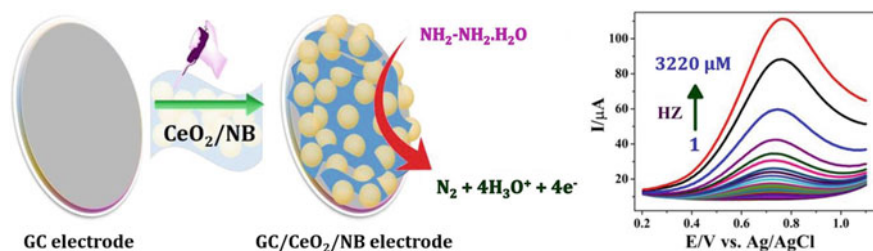
1.3.2 Nile Blue

NB, structurally similar to MLB, is a widely used organic dye for electrocatalytic oxidation/reduction reactions. NB is either adsorbed as such or electrochemically polymerized to form poly-NB (PNB) over the electrode surface. In the literature, the NB based sensors and biosensors have been reported for the detection of various analytes such as glucose (in couple with GOD or GDH), NADH, oxygen, H_2O_2, DNA (hybridization), AA, DA, hemoglobin, nitrite, vanillin, and hydrazine [Table 5]. In 2007 and 2008, Du et al. reported PNB immobilized SWCNT modified GCE for electrocatalytic oxidation of NADH and further to ethanol and glucose biosensor application in couple with ADH and GDH respectively [37, 38]. In another work, a layer-by-layer assembly of iron oxide nanoparticles (IONP), chitosan (CHIt), GOD and NB cast over an aminophenyl (AP) modified GCE was used as a sensor platform for glucose biosensing application [39]. A linear calibration in a window, 19 μM– 8.6 mM has been demonstrated. In another case, an enzymeless sensor for glucose was fabricated using nickel oxide(NiO)/Pd that has been modified on NB decorated reduced graphene oxide (rGO) was deposited in alkaline condition. An ampero- metric technique has been demonstrated with a detection limit value 2.2 μM [40]. In continuation, NB immobilized GCE via diazonium chemistry has been used for electrochemical detection of H_2O_2 and further to glucose (after being coupled with GOD enzyme) [41]. Selective detection of glucose in a human plasma sample was demonstrated as a proof of concept.

A radiometric electrochemical detection of H_2O_2 and other reactive oxygen species (ROS) in a single-drop whole blood sample relating to oxidative stress was reported recently [42]. Herein, gold cones coated carbon fiber microelectrode (CFME/Au) modified with 5-(1,2-dithiolan-3-yl)-N-(4-(4,4,5,5-tetramethyl-1,3,2- dioxaborolan-2-yl)phenyl)pentanamide (electrochemical probe) (BA) and NB (as an internal reference) was prepared. The developed sensor has shown remarkable selectivity against potential interferences in whole blood samples especially for AA, UA, and DA (Fig. 4). In the next report, NB and its derivatives (methylene green, MG and neutral red, NR) were electrochemically polymerized in a eutectic solvent, ethaline to PNB, poly-MG (PMG), and poly-NR (PNR) individually over IONP modified GCEs [43]. After immobilizing the catalase enzyme over them, these electrodes were used as biosensors for H_2O_2 detection. Similarly, PNB modified GCE and GCE/Graphene oxide that has been prepared by electrochemical oxida- tive and reductive polymerization methods were used as electrocatalysts for the dissolved oxygen reduction and sensing applications in pH 5.3 [44] and neutral pH [45] respectively. In the latter case, the modified electrode was extended to glucose
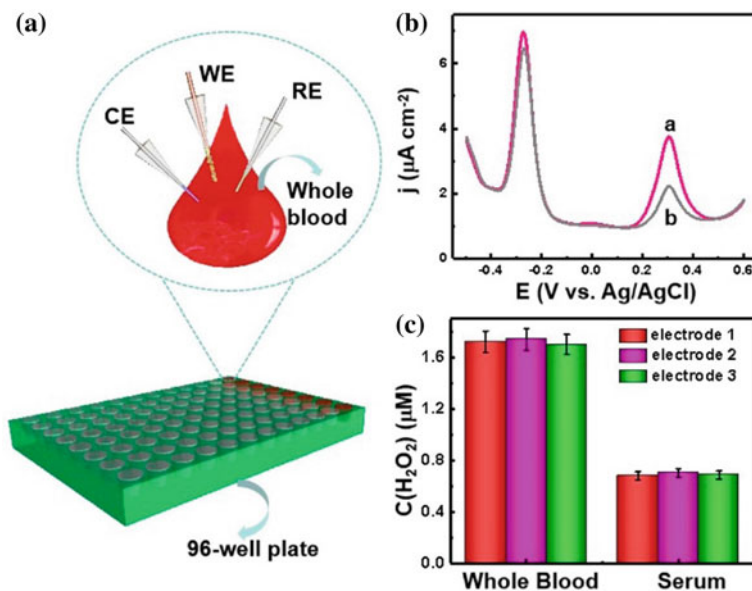
Fig. 4 **a** The detection of H_2O_2 in a drop of blood using the prepared 96 well plates; (B) DPV responses of the three electrodes in whole blood (curve a) and serum (curve b); (C) Corresponding comparison of the H_2O_2 levels in whole blood and serum obtained from the three electrodes. Adapted with permission from reference [42], Copyright (2020), Elsevier

detection by immobilizing the GOD on it. Similar to the former report, electrochemical oxidative polymerization of NB over a pre-anodized GCE was carried out for the detection of nitrite in food samples [46]. In continuation, potential cycling assisted polymerization of NB was performed over functionalized MWCNT modified GCE for the sensitive and selective detection of ascorbic acid [47]. Apart from the above, NB based chemically modified biosensors have been fabricated for the detection of biological samples, viz., (a) targeted single-stranded DNA, via intercalation of NB on respective probe single-stranded DNA modified gold quartz crystal electrode (Au-QC) [48], (b) thiol-terminated dopamine using rGO/NB/Au-nanoparticle(AuNP)/GCE matrix by electrochemical impedance analysis in pH 7 PBS mixed with 0.1 M KCl. [49], (c) hemoglobin (Hb) and glycated Hb fraction using NB immobilized poly(2,2':5',5″-terthiophene-3'-p-benzoic acid)/N,S-doped porous carbon (pTTBA/NSPC) nanocomposite-CME. A mediated electrochemical reduction signals were noticed in the above cases. Amongst various organic dyes investigated, NB, toluidine blue (TBO) and NR, NB-modified electrode showed the best result [50], (d) carcinogenic hydrazine using NB/cerium oxide (CeO_2) nanohybrid modified GCE [51] (Fig. 5), and (e) series of analytes like L-dopa, gallic acid, AA, L-tryptophan, riboflavin, DA, paracetamol, butyl hydroxyanisole, uric acid, and vanillin independently using dendrimer/PNB modified electrode [52].

Fig. 5 An organic-inorganic nileblue—CeO$_2$ (CeO$_2$/NB) nanohybrid chemically modified electrode for determination of the environmental pollutant, carcinogenic hydrazine (HZ) in environmental water samples. Adapted with permission from reference [51], Copyright (2020), Elsevier

1.3.3 Poly(Brilliant Cresyl Blue)

Apart from these dyes, poly(brilliant cresyl blue) (PBCB), a derivative of MB-based molecular compound, was also used for the detection of H$_2$O$_2$ [53] and epinephrine [54]. In both works, electrochemical polymerization was carried out for the preparation of PBCB over the GCE in the presence of AuNP and iron oxide nanoparticles (IONP) + chitosan (CHIt) mixture respectively. For the detection of H$_2$O$_2$, HRP enzyme was immobilized on the surface, but no enzyme was used for the detection of epinephrine (Table 6).

2 Conclusions and Future Prospects

The collective literature survey denotes, quinone and organic dyes-based molecular species are excellent choices for the preparation of surface-confined electron-transfer systems and application to various electrochemical works. It has been observed that benzoquinone, hydroquinone, and organic dyes have an apparent standard electrode potential near to 0 V versus Ag/AgCl in a neutral pH condition, wherein, there is a minimal effect for the interference by other common electroactive species. Thus, small molecules such as NADH, dissolved oxygen, thiols, H$_2$O$_2$, hydrazine, uric acid, etc. were selectively oxidized/reduced on the quinone and organic dye-surface-confined electrodes at a suitable experimental condition. These organic-redox mediators are good candidates as a cofactor for the NADH coupled bioelectrochemical oxidations of glucose, D-lactate, glycerol, ethanol, fructose etc. The followings are some of the workable topics to be explored much in the future: (i) biofuel cells and electrochemical immunosensors and bioelectro-organic synthesis. Although there are few reports available in the literature, in consideration of the effective electrochemical feature, many more reports are yet to come. (ii) Since, the organic-redox mediator modified electrodes have proton-coupled electron-transfer nature, electrochemical pH sensors are a plausible extension of the present work. (iii) Molecular

wiring of biomolecules (enzymes) and applications towards direct electron-transfer (DET) functions. Plausibly, the amino-functional groups of the organic dyes are the key linking agents for enzymes and further to DET studies. (iv) Orientation and dynamics of the organic redox-active molecules on the carbon nano-substrates is an important topic yet to be studied in the literature to understand the selective electrocatalytic activity of the surface-confined system. (v) Electrocatalytic oxidation of the surface-confined molecular systems in organic media should be explored. Overall, several new avenues are yet to be studied in detail with these present organic molecules.

References

1. Murray, R.W., Higuchi, T. (eds.): Techniques of chemistry: molecular design of electrode surfaces, Vol. XXII. Wiley, Michigan (1992). ISSN 0082-2531
2. Zen, J.-M., Kumar, A.S., Tsai, D.-M.: Recent updates of chemically modified electrodes in analytical chemistry. Electroanalysis **15**, 1073–1087 (2003)
3. Dalkiran, B., Brett, C.M.A.: Polyphenazine and polytriphenylmethane redox polymer/nanomaterial–based electrochemical sensors and biosensors: a review. Microchim Acta **188**, 178 (2021)
4. Gayathri, C.H., Mayuri, P., Sankaran, K., Kumar, A.S.: An electrochemical immunosensor for efficient detection of uropathogenic E. coli based on thionine dye immobilized chitosan/functionalized-MWCNT modified electrode. Biosens. Bioelectron. **82**, 71–77 (2016)
5. Krzyczmonik, P., Socha, E., Skrzypek, S.: Electrochemical detection of glucose in beverage samples using poly(3,4-ethylenedioxythiophene)-modified electrodes with immobilized glucose oxidase. Electrocatalysis **9**, 380–387 (2018)
6. Kumar, A.S., Tanase, T., Iida, M.: In situ nanostructure formation of (μ-hydroxo)bis(μ-carboxylato) diruthenium units in nafion membrane and its utilization for selective reduction of nitrosonium ion in aqueous medium. Langmuir **23**, 391–394 (2007)
7. Hoogvliet, J.C., Van, O.S.P.J.H.J., Mark, E.J.V., van Bennekom, W.P.: Modification of glassy carbon electrode surfaces with mediators and bridge molecules. Biosens. Bioelectron. **6**, 413–423 (1991)
8. Geng, L., Boguslavsky, L.I., Kovalev, I.P., Sahni, S.K., Kalash, H., Skotheim, T.A.: Amperometric biosensors based on dehydrogenase/NAD and heterocyclic quinones. Biosens. Bioelectron. **11**, 1267–1275 (1996)
9. Simón, B.P., Fàbregas, E.: Comparative study of electron mediators used in the electrochemical oxidation of NADH. Biosens. Bioelectron. **19**, 1131–1138 (2004)
10. Kullapere, M., Seinberg, J.M., Maeorg, U., Maia, G., Schiffrin, D.J., Tammeveski, K.: Electroreduction of oxygen on glassy carbon electrodes modified with in situ generated anthraquinone diazonium cations. Electrochim Acta **54**, 1961–1969 (2009)
11. Wendland, T.R., Muntean, B.S., Kaur, J., Mukherjee, J., Chen, J., Tan, X., Attygalle, D., Collins, R.W., Kirchhoff, J.R., Tillekeratne, L.M.V.: In situ self-assembly of thiolated ortho-quinone capped electrocatalysts for bioanalytical applications. Electroanalysis **23**, 2275–2279 (2011)
12. Hou, J., González, M.V., Fadeev, M., Liu, X., Lavi, R., Willner, I.: Catalyzed and electrocatalyzed oxidation of L-tyrosine and L-phenylalanine to dopachrome by nanozymes. Nano. Lett. **18**, 4015–4022 (2018)

13. Motta, N., Guadalupe, A.R.: Activated carbon paste electrodes for biosensors. Anal. Chem. **66**, 566–571 (1994)
14. Wang, P., Amarasinghe, S., Leddy, J., Arnold, M., Dordick, J.S.: Enzymatically prepared poly(hydroquinone) as a mediator for amperometric glucose sensors. Polymer **39**, 123–127 (1998)
15. Laurinavicius, V., Kurtinaitiene, B., Liauksminas, V., Jankauskaite, A., Simkus, R., Meskys, R., Boguslavsky, L., Skotheim, T., Tanenbaum, S.: Reagentless biosensor based on PQQ-depended glucose dehydrogenase and partially hydrolyzed polyarbutin. Talanta **52**, 485–493 (2000)
16. Nakano, K., Hirayama, G., Toguchi, M., Nakamura, K., Iwamoto, K., Soh, N., Imato, T.: Poly(hydroquinone)-coated electrode for immobilizing of 5'-amine functioned capture probe DNA and electrochemical response to DNA hybridization. Sci. Technol. Adv. Mater **7**, 718–725 (2006)
17. Nann, T., Urban, G.A.: Deposition of hydroquinone-thiosulfate on gold by means of anodic oxidation. J. Electroanal Chem. **505**, 125–132 (2001)
18. Parra, M.R., Lorenzo, E., Pariente, F.: Synthesis and electrocatalytic activity towards oxidation of hydrazine of a new family of hydroquinone salophen derivatives: application to the construction of hydrazine sensors. Sens. Actuators B **107**, 678–687 (2005)
19. Wang, Y., Chen, Q., Zeng, X.: Potentiometric biosensor for studying hydroquinone cytotoxicity in vitro. Biosens. Bioelectron **25**, 1356–1362 (2010)
20. Kubota, L.T., Gouvea, F., Andrade, A.N., Milagres, B.G., Neto, G.D.O.: Electrochemical sensor for NADH based on meldola's blue immobilized on silica gel modified with titanium phosphate. Electrochim Acta **41**, 1465–1496 (1996)
21. Zhu, L., Zhai, J., Yang, R., Tian, C., Guo, L.: Electrocatalytic oxidation of NADH with meldola's blue functionalized carbon nanotubes electrodes. Biosens. Bioelectron. **22**, 2768–2773 (2007)
22. Simon, B.P., Macanas, J., Munoz, M., Fabregas, E.: Evaluation of different mediator-modified screen-printed electrodes used in a flow system as amperometric sensors for NADH. Talanta **7**, 2102–2107 (2007)
23. Radoi, A., Compagnone, D., Batič, M., Klinčar, J., Gorton, L., Palleschi, G.: NADH screen-printed electrodes modified with zirconium phosphate, meldola blue, and Reinecke salt. Application to the detection of glycerol by FIA. Anal. Bioanal. Chem. **387**, 1049–1058 (2007)
24. Hoffmann, A.A., Dias, S.L.P., Benvenutti, E.V., Lima, E.C., Pavan, F.A., Rodrigues, J.R., Scotti, R., Ribeiro, E.S., Gushikem, Y.: Cationic dyes immobilized on cellulose acetate surface modified with titanium dioxide: Factorial design and an application as sensor for NADH. J. Braz Chem. Soc. **18**, 1462–1472 (2007)
25. Arvinte, A., Sesay, A.M., Virtanen, V., Bala, C.: Evaluation of meldola blue-carbon nanotube-sol-gel composite for electrochemical NADH sensors and their application for lactate dehydrogenase-based biosensors. Electroanalysis **20**, 2355–2362 (2008)
26. Arvinte, A., Rotariu, L., Bala, C., Gurban, A.M.: Synergistic effect of mediator–carbon nanotube composites for dehydrogenases and peroxidases based biosensors. Bioelectrochemistry **76**, 107–114 (2009)
27. Maroneze, C.M., Luz, R.C.S., Landers, R., Gushikem, Y.: $SiO_2/TiO_2/Sb_2O_5$/graphite carbon ceramic conducting material: preparation, characterization, and its use as an electrochemical sensor. J. Solid. State Electrochem **14**, 115–121 (2010)
28. Canevari, T.C., Vinhas, R.C.G., Landers, R., Gushikem, Y.: $SiO_2/SnO_2/Sb_2O_5$ microporous ceramic material for immobilization of meldola's blue: application as an electrochemical sensor for NADH. Biosens. Bioelectron. **26**, 2402–2406 (2011)
29. Balamurugan, A., Ho, K.C., Chen, S.M., Huang, T.-Y.: Electrochemical sensing of NADH based on meldola blue immobilized silver nanoparticle-conducting polymer electrode. Coll Surf A: Physicochem Eng. Aspects **362**, 1–7 (2010)
30. Santhiago, M., Strauss, M., Pereira, M.P., Chagas, A.S., Bufon, C.C.B.: Direct drawing method of graphite onto paper for high performance flexible electrochemical sensors. ACS Appl. Mater Interfaces **9**, 11959–11966 (2017)
31. Titoiu, A.M., Lapauw, M., Petrareanu, G.N., Purcarea, C., Bolado, P.F., Marty, J.-L., Vasilescu(s), A.: Carbon nanofiber and meldola Blue based electrochemical sensor for NADH: Application to the detection of benzaldehyde. Electroanalysis **30**, 1–14 (2018)

32. Titoiu, A.M., Petrareanu, G.N., Visinescu, D., Dinca, V., Bonciu, A., Mihailescu, C.N., Purcarea, C., Boukherroub, R., Szunerits, S., Vasilescu, A.: Flow injection enzymatic biosensor for aldehydes based on a meldola blue-Ni complex electrochemical mediator. Microchim Acta **187**, 550 (2020)

33. Westmacott KL, Crew AP, Doran O, Hart JP (2020) Novel, rapid, low-cost screen-printed (bio)sensors for the direct analysis of boar taint compounds androstenone and skatole in porcine adipose tissue: Comparison with a high-resolution gas chromatographic method. Biosens. Bioelectron. **150**, 111837 (2020)

34. Garcia, C.A.B., Neto, G.D.O., Kubota, L.T., Grandin, L.A.: A new amperometric biosensor for fructose using a carbon paste electrode modified with silica gel coated with meldola's blue and fructose-5-dehydrogenase. J. Electroanal Chem. **418**, 147–151 (1996)

35. Mao, L., Yamamoto, K.: Glucose and choline on-line biosensors based on electropolymerized Meldola's blue. Talanta **51**, 187–195 (2000)

36. Santos, A.S., Pereira, A.C., Duran, N., Kubota, L.T.: Amperometric biosensor for ethanol based on co-immobilization of alcohol dehydrogenase and meldola's blue on multi-wall carbon nanotube. Electrochim Acta **52**, 215–220 (2006)

37. Du, P., Liu, S., Wu, P., Cai, C.: Single-walled carbon nanotubes functionalized with poly(nile blue A) and their application to dehydrogenase-based biosensors. Electrochim Acta **53**, 1811–1823 (2007)

38. Du, P., Wu, P., Cai, C.: A glucose biosensor based on electrocatalytic oxidation of NADPH at single-walled carbon nanotubes functionalized with poly(nile blue A). J. Electroanal Chem. **624**, 21–26 (2008)

39. Nazemi, Z., Shams, E., Amini, M.K.: Construction of a biointerface for glucose oxidase through diazonium chemistry and electrostatic self-assembly technique. J. Solid. State Electrochem **20**, 429–438 (2016)

40. Ensafi, A.A., Ahmadi, Z., Asl, M.J., Rezaei, B.: Graphene nanosheets functionalized with nile blue as a stable support for the oxidation of glucose and reduction of oxygen based on redox replacement of Pd-nanoparticles via nickel oxide. Electrochim Acta **173**, 619–629 (2015)

41. Nasri, Z., Shams, E., Ahmadi, M.: A glucose biosensor based on direct attachment of in situ generated nile blue diazonium cations to the electrode surface. J. Electroanal Chem. **703**, 146–152 (2013)

42. Dong, H., Zhou, Y., Hao, Y., Zhao, L., Sun, S., Zhang, Y., Ye, B., Xu, M.: "Turn-on" ratiometric electrochemical detection of H_2O_2 in one drop of whole blood sample via a novel microelectrode sensor. Biosens. Bioelectron. **165**, 112402 (2020)

43. Silva, W., Queiroz, A.C., Brett, C.M.A.: Nanostructured poly(phenazine)/Fe_2O_3 nanoparticle film modified electrodes formed by electropolymerization in ethaline—deep eutectic solvent. Microscopic and electrochemical characterization. Electrochim Acta **347**, 136284 (2020)

44. Ju, H., Shen, C.: Electrocatalytic reduction and determination of dissolved oxygen at a poly(nile blue) modified electrode. Electroanalysis **13**, 8–9 (2000)

45. Shervedani, R.K., Amini, A.: Preparation of graphene/nile blue nanocomposite: application for oxygen reduction reaction and biosensing. Electrochim. Acta **173**, 354–363 (2015)

46. Chen, X., Wang, F., Chen, Z.: An electropolymerized nile blue sensing film-based nitrite sensor and application in food analysis. Anal. Chim. Acta **623**, 213–220 (2008)

47. Kul, D., Ghica, M.E., Pauliukaite, R., Brett, C.M.A.: A novel amperometric sensor for ascorbic acid based on poly(Nile blue A) and functionalized multi-walled carbon nanotube modified electrodes. Talanta **111**, 76–84 (2013)

48. Prance, A., Coopersmith, K., Stobiecka, M., Hepel, M.: Biosensors for the detection of DNA damage by toxicants. ECS Trans. **33**, 3–15 (2010)

49. Jin, H., Zhao, C., Gui, R., Gao, X., Wang, Z.: Reduced graphene oxide/nile blue/gold nanoparticles complex-modified glassy carbon electrode used as a sensitive and label-free aptasensor for ratiometric electrochemical sensing of dopamine. Anal. Chim. Acta **1025**, 154–162 (2018)

50. Hossain, M.D.M., Moon, J.M., Gurudatt, N.G., Park, D.-S., Choi, C.S., Shim, Y.-B.: Separation detection of hemoglobin and glycated hemoglobin fractions in blood using the electrochemical microfluidic channel with a conductive polymer composite sensor. Biosens Bioelectron **142**, 111515 (2019)

51. Gowthaman, N.S.K., Lim, H.N., Balakumar, V., Shankar, S. Ultrasonic synthesis of CeO_2@organic dye nanohybrid: environmentally benign rabid electrochemical sensing platform for carcinogenic pollutant in water samples. Ultrason Sonochem **61**, 104828 (2019)
52. Devi, C.L., Narayanan, S.S., Arumugam, S.: New electrochemical sensor for the detection of biological analytes using poly(amido amine) dendrimer and poly(nile blue)- modified electrode. J. Electroanal Chem. **855**, 113486 (2019)
53. Ahammad, A.J.S., Shaikh, A.A., Jessy, N.J., Akter, T., Mamun, A.A., Bakshi, P.K.: Hydrogen peroxide biosensor based on the immobilization of horseradish peroxidase onto a gold nanoparticles-adsorbed poly(brilliant cresyl blue) film. J. Electrochem Soc. **162**, B52–B56 (2015)
54. Tome´, L.I.N., Brett, C.M.A.: Polymer/iron oxide nanoparticle modified glassy carbon electrodes for the enhanced detection of epinephrine. Electroanalysis **31**, 1–8 (2019)